

THE PETROLOGY AND PETRO-
GENESIS OF THE BAY OF
ISLANDS OPHIOLITE SUITE,
WESTERN NEWFOUNDLAND

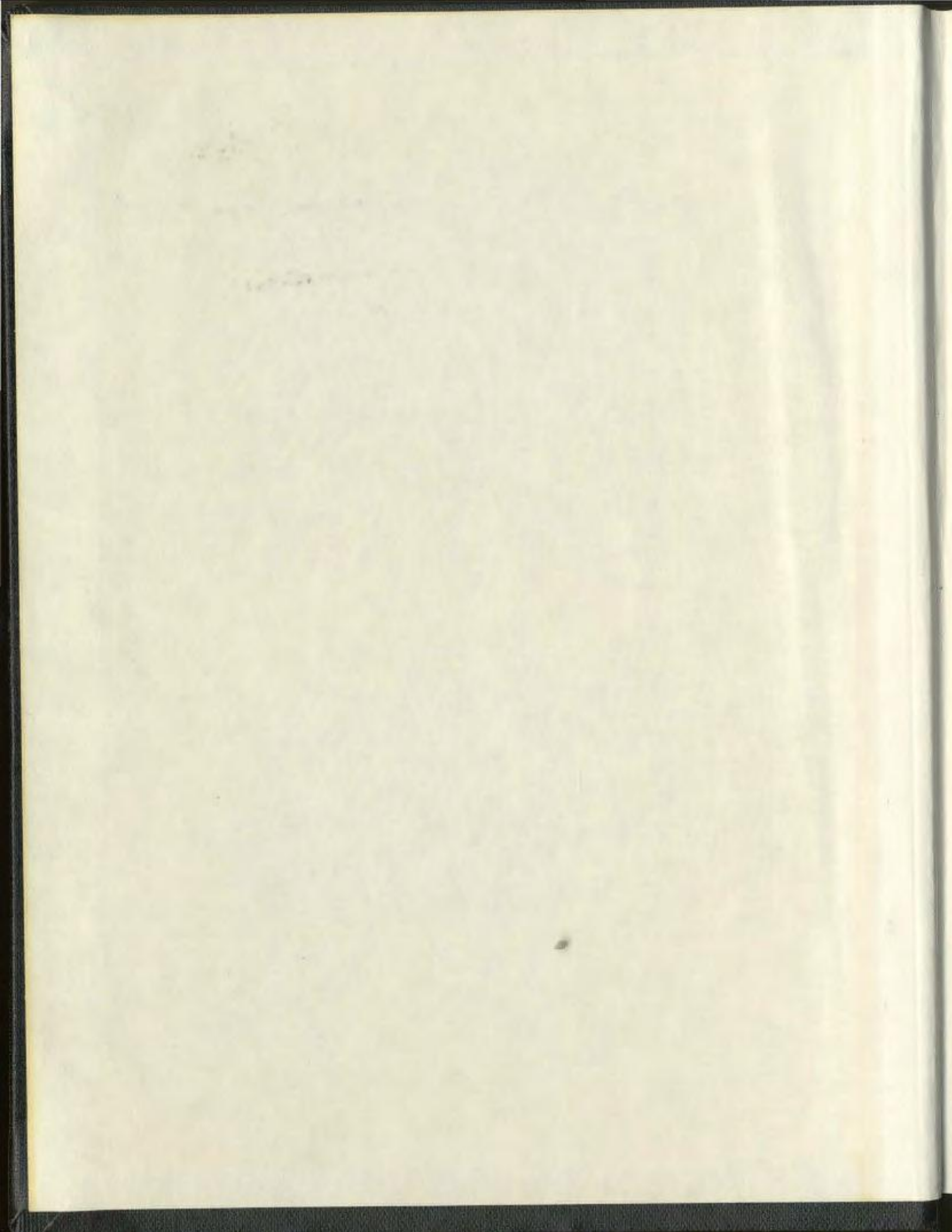
PART 1

CENTRE FOR NEWFOUNDLAND STUDIES

**TOTAL OF 10 PAGES ONLY
MAY BE XEROXED**

(Without Author's Permission)

JOHN MALPAS



INFORMATION TO USERS

THIS DISSERTATION HAS BEEN
MICROFILMED EXACTLY AS RECEIVED

This copy was produced from a microfiche copy of the original document. The quality of the copy is heavily dependent upon the quality of the original thesis submitted for microfilming. Every effort has been made to ensure the highest quality of reproduction possible.

PLEASE NOTE: Some pages may have indistinct print. Filmed as received.

Canadian Theses Division
Cataloguing Branch
National Library of Canada
Ottawa, Canada K1A 0N4

AVIS AUX USAGERS

LA THESE A ETE MICROFILMEE
TELLE QUE NOUS L'AVONS RECUE

Cette copie a été faite à partir d'une microfiche du document original. La qualité de la copie dépend grandement de la qualité de la thèse soumise pour le microfilmage. Nous avons tout fait pour assurer une qualité supérieure de reproduction.

NOTA BENE: La qualité d'impression de certaines pages peut laisser à désirer. Microfilmée telle que nous l'avons reçue.

Division des thèses canadiennes
Direction du catalogage
Bibliothèque nationale du Canada
Ottawa, Canada K1A 0N4

FOUR ARTICLES AND ONE MAP NOT MICROFILMED FOR REASONS OF COPYRIGHT.

J. Malpas and D.F. Strong. A comparison of chrome-spinels in ophiolites and mantle diapirs of Newfoundland, Geochimica et Cosmochimica Acta, 1975, Vol. 39, pp. 1045 to 1060. Pergamon Press. Printed in Northern Ireland.

D.F. Strong and J. Malpas. The Sheeted Dike Layer of the Betts Cove Ophiolite Complex does not Represent Spreading: Further Discussion, Canadian Journal of Earth Sciences, Vol. 12, No. 5, 1975. Pages 894-896. Published by The National Research Council of Canada.

Harold Williams and John Malpas. Sheeted Dikes and Brecciated Dike Rocks Within Transported Igneous Complexes, Bay of Islands, Western Newfoundland, Canadian Journal of Earth Sciences, Vol. 9, No. 9, September, 1972. Published by the National Research Council of Canada.

J. Malpas, R.K. Stevens and D.F. Strong. Amphibolite Associated with Newfoundland Ophiolite: Its Classification and Tectonic Significance, Geology, September 1973, pp. 45-47.

Map 1355 A, Paper 72-34, Geology, Bay of Islands, Newfoundland. Scale 1:125,000. Published 1973. Copies may be obtained from the Geological Survey of Canada, Ottawa.

THE PETROLOGY AND PETROGENESIS OF THE
BAY OF ISLANDS OPHIOLITE SUITE, WESTERN NEWFOUNDLAND

by



John Malpas, M.A. (Oxon), M.Sc.

A Thesis submitted in partial fulfillment
of the requirements for the degree of
Doctor of Philosophy

Department of Geology
Memorial University of Newfoundland

April 1976

St. John's

Newfoundland



Corner Brook and Blow me down Mountain from the East.



The Ultramafic Gabbro transition on Blow me down Mountain.

FRONTISPIECE

ABSTRACT

The Bay of Islands Complex, situated on the west coast of Newfoundland, forms the upper slice assemblage of a number of allochthonous slices that were emplaced on platformal carbonate rocks of the ancient North American continental margin during the lower Middle Ordovician. The Complex consists of a complete ophiolite sequence disposed in four main massifs and believed to represent obducted portions of oceanic lithosphere. During early stages of displacement from the oceanic environment, a basal dynamothermal aureole was developed and remains part of the Complex. Temperatures of metamorphism in this aureole suggest that the ophiolitic rocks were just formed and still hot when displaced. This, together with other evidence, suggests their production in a marginal basin or in the environs of a ridge, subduction zone, transform triple point.

Petrological, mineralogical and chemical data show that the Complex may be divided into a lower series of ultramafic tectonites representing mantle material, and a higher series of cumulate and extrusive rocks capped by clastic sediments which may be correlated with oceanic crust.

Examination of the tectonite series reveals a lower spinel lherzolite member overlain by harzburgites. Both rock types are cut by numerous deformed and undeformed olivine-pyroxene veins. These veins represent early crystallisation products from a picritic tholeiite magma derived at 18 kb and 1100°C by ~ 23% partial melting of a spinel lherzolite to leave a harzburgite residuum. The remainder of the magma

crystallised as differentiated cumulate and extrusive rocks under crustal conditions.

The petrogenetic model derived from the mineralogy and chemistry implies a rising diapiric body beneath an accreting centre and allows for the production of tholeiitic, transitional and mildly alkaline basalts from a similar parent. The nature of the basalt erupted depends upon rate of upwelling and rate of crystallisation within the diapir. Prolonged fractionation at pressures of 8-18 kb may explain the derivation of off ridge-axis alkaline series. Furthermore, the model places limits on the depths of melting within the rising diapir and suggests that crystallisation takes place at depths of less than approximately 60 km.

Comparison of the Bay of Islands Complex with oceanic lithosphere and other ophiolite suites suggests it is possibly the ideal type example with which to study oceanic crust/mantle relationships.

TABLE OF CONTENTS

	Page
Abstract	(i)
List of Figures	(vii)
List of Tables	(xi)
List of Plates	(xiii)

CHAPTER I

INTRODUCTION

A. Location and access	1
B. Physiography and climate	1
C. Survey control	4
D. Previous geological work	6
E. Acknowledgements	10
F. Geological Setting	
(i) Newfoundland and the Appalachian Structural Province	10
(ii) Zonal subdivision of the Appalachian Structural Province in Newfoundland	11
G. Statement of Problem	17

CHAPTER II

GEOLOGY OF WESTERN NEWFOUNDLAND

A. Introduction	20
B. Basement	20
C. The Autochthonous Succession	
(i) Lower Unit	22
(ii) Middle Unit	24
(iii) Upper Unit	24
D. The Parautochthonous Succession	25
E. Interpretation	26
F. Transported (Allochthonous) Rocks	27
(i) The carbonate succession	29
(ii) The clastic sequence	29
(iii) The ophiolites	33

CHAPTER III

THE UPPER THRUST SLICES

- A. Introduction 35
- B. Skinner Cove Formation
 - (i) Outcrop and distribution 36
 - (ii) Lithology 39
 - (iii) Mineralogy and chemistry 43
 - (iv) Significance 48
- C. The Old Man Cove Formation
 - (i) Location and outcrop 54
 - (ii) Lithology and structure 54
 - (iii) Mineralogy 55
 - (iv) Significance 57
- D. The Little Port Complex
 - (i) Location and outcrop 58
 - (ii) Lithology 58
 - (iii) Mineralogy 61
 - (iv) Chemistry 73
 - (v) Significance 78
- E. Mélange Zones
 - (i) Lithology and structure 81
 - (ii) Significance 82

CHAPTER IV

THE BASAL AUREOLE

- A. Introduction 85
- B. Lithologies
 - (i) Ultramafic rocks 90
 - (ii) Hornfelses 94
 - (iii) Amphibolites 100
 - (iv) Greenschists 105
 - (v) Phyllites and unmetamorphosed sediments 105
 - (vi) Metasomatised rocks 109
- C. Structure 112
- D. Mineralogy, Metamorphism and Mineral paragenesis
 - (i) Orthosilicates
 - a) Epidote Group 115
 - b) Garnet Group 116
 - c) Spinel 125
 - d) Zircon 126
 - (ii) Chain silicates
 - a) Amphiboles 126
 - b) Clinopyroxene 130

(iv)

	Page
(iii) Sheet silicates	
a) Biotite	132
b) Muscovite	132
c) Phlogopite	132
d) Chlorite	134
e) Prehnite	134
(iv) Framework silicates	
a) Plagioclase	135
b) Quartz	139
c) Zeolites	140
(v) Non-silicates	
a) Oxides	140
b) Carbonates	141
E. Bulk Rock Chemistry	
(i) Introduction	142
(ii) Major Oxides	
a) SiO ₂	153
b) Al ₂ O ₃	153
c) CaO	154
d) MgO	154
e) FeO and Fe ₂ O ₃	154
(iii) Minor Oxides	
a) Na ₂ O	155
b) K ₂ O	155
c) TiO ₂	155
d) MnO	155
(iv) Trace Elements	
a) Cr	156
b) Ni	156
c) Cu	156
d) Zn	156
e) Zr	156
f) Sr	157
g) Rb	157
h) Ba	157
(v) Discussion	157
F. Conditions of Formation of Aureole Rocks	159
G. Conclusions	169

CHAPTER V

THE BAY OF ISLANDS COMPLEX

A. Introduction	173
B. Lithological Cross-Sections	174

	Page
C. Lithologies	
(i) Lherzolite and harzburgite	175
(ii) Pyroxene and dunite veins and dikes	187
(iii) Origin of layering and mineral foliations	189
(iv) Origin of vein rocks	195
(v) The Main Dunite zone	198
(vi) Chromites	202
(vii) Clinopyroxenites	203
(viii) Feldspathic dunites	204
(ix) The Critical Zone: Interbanded rocks of the ultramafic-gabbro contact	206
(x) Gabbro	217
(xi) Amphibolite inclusions within the gabbro zone	225
(xii) Origin of primary textures in dunite zone, Critical Zone and gabbros	228
(xiii) Secondary structures in cumulate rocks	229
(xiv) Quartz-diorites	230
(xv) Diabases	234
(xvi) Pillow lavas	240
(xvii) Sediments	245

CHAPTER VI

CHEMISTRY AND PETROGENESIS

A. Mineral chemistry	
(i) Olivine	249
(ii) Orthopyroxenes	257
(iii) Cation distribution between coexisting olivine and orthopyroxene	261
(iv) Clinopyroxenes	264
(v) Coexisting orthopyroxene and clinopyroxene: Estimation of equilibrium temperatures	274
(vi) Spinel group	281
(vii) Coexisting olivine and chromian spinel	287
(viii) Plagioclase	288
B. Bulk rock chemistry	290
(i) Linear variation diagrams	312
(ii) FMA and CNK diagrams	317
(iii) Cr ₂ O ₃ vs. NiO wt %	320
(iv) K/Rb and Rb/Sr ratios	320
(v) Total alkalis vs. SiO ₂	323
(vi) Basalt tetrahedron	325
(vii) Rare Earth Elements	328
(viii) Strontium isotope ratios	331
C. Affinities of Mafic Suite with Oceanic Rocks	331
D. Conclusions	335

	Page
E. Petrogenesis	
(i) CMAS projections	340
(ii) Degrees of Partial Melting	351
(iii) Degrees of Fractional Crystallisation	353

CHAPTER VII

TECTONIC SETTING AND EMPLACEMENT OF THE OPHIOLITE SUITE

A. Introduction	358
B. Oceanic Crust and Mantle	358
C. The Bay of Islands Complex and other Ophiolite Suites	361
D. Orogenic History	367
E. Conclusions	374

BIBLIOGRAPHY	375
------------------------	-----

APPENDIX I	408
----------------------	-----

APPENDIX II	412
-----------------------	-----

APPENDIX III	416
------------------------	-----

APPENDIX IV	422
-----------------------	-----

APPENDIX V	427
----------------------	-----

APPENDIX VI	431
-----------------------	-----

BIBLIOGRAPHY	432
------------------------	-----

LIST OF FIGURES

	Page
Fig. Ia: Regional Location	2
Fig. Ib: Bay of Islands Region showing locations of Trout River and Cox's Cove.	3
Fig. Ic: Fault control of topography in northern massifs.	5
Fig. Id: Canadian Appalachian Region.	9
Fig. Ie: Tectono-stratigraphic zones of the Newfoundland Appalachians	12
Fig. IIa: Geology of Western Newfoundland	21
Fig. IIb: Stratigraphic sections of Western Newfoundland	23
Fig. IIc: Spatial relationships of autochthonous and allochthonous rocks prior to transport: a reconstitution of the ancient continental margin	28
Fig. IIIa: Relationships between and structural stacking order of Slice Assemblages, Humber Arm Allochthon	37
Fig. IIIb: Geological Map, Bay of Islands Region	(In pocket)
Fig. IIIc: Variation diagrams for Skinner Cove volcanics	50
Fig. IIId: Plot of alkalis vs. silica for Little Port Complex and associated rocks	72
Fig. IIIe: Variation diagrams for quartz-diorites from Little Port Complex	77
Fig. IVa: Generalised cross-section of basal aureole to show metamorphic rock types	88
Fig. IVb: Oxidation of iron (as a measure of f_{O_2}) in dynamothermal aureole.	123
Fig. IVc: Major element chemistry: Oxide vs. distance from contact	143
Fig. IVd: Trace element chemistry: element vs. distance from contact	144
Fig. IVe: Plots of clinopyroxenes from basal aureole	145
Fig. IVg: Estimation of aureole temperatures K_D^{gnt} vs. K_D^{px}	161

	Page
Fig. IVh: Estimation of aureole temperatures K_d vs. $1/T$	162
Fig. IVi: P.T. conditions for amphibole to greenschist facies transition in basaltic rocks	163
Fig. IVj: Pressures of equilibration of aureole clinopyroxenes	165
Fig. IVk: Lowering cooling gradients.	167
Fig. IVl: Schematic model for dynamothermal aureole formation.	170
Fig. Va: Stratigraphic columnar sections of Bay of Islands Complex	176
Fig. Vb: Modal plots of ultramafic rocks	178
Fig. Vc: Rock types of the Critical Zone and Dunites	212
Fig. Vd: Geology of volcanic rocks around York Harbour, Bay of Islands	242
Fig. VIa: Distribution of Fe^{2+} and Mg^{2+} in coexisting opx and olivine	265
Fig. VIb: Clinopyroxenes from Bay of Islands Complex.	271
Fig. VIc: Clinopyroxene analyses from Bay of Islands Complex plotted according to Le Bas	273
Fig. VI d: Modified Kushiro plot for cpx's from Bay of Islands Complex	275
Fig. VIe: Solubility of enstatite in diopside with increasing pressure.	277
Fig. VI f: Ca^{2+} distribution in coexisting enstatites and diopsides	278
Fig. VIg: P.T. equilibration estimates for clinopyroxenes from lherzolites.	279
Fig. VIh: Plot of spinel compositions after recalculations of end members.	286
Fig. VIIi: X-ray scans of plagioclases in gabbros.	291
Fig. VIIj: Composition of plagioclases from gabbro	293
Fig. VIIk: Major element oxides vs. M_{90}	313

	Page
Fig. VII: Trace elements vs. MgO	314
Fig. VIIm: Elements and oxides vs. FeO*/MgO	316
Fig. VIIn: F.M.A. Plot	318
Fig. VIo: CNK Plot	319
Fig. VIp: Cr ₂ O ₃ vs. NiO wt %	321
Fig. VIq: K/Rb ratios	322
Fig. VIr: Rb/Sr ratios	322
Fig. VIIs: Plot of (Na ₂ O + K ₂ O) vs. SiO ₂	324
Fig. VIIt: Projections within the basalt tetrahedron	326
Fig. VIu: Rare Earth Element Abundances	329
Fig. VIv: Ti vs. Zr and Ti/100 - Zr - Sr/2	334
Fig. VIw: Projection planes within system CaO-MgO-Al ₂ O ₃ - SiO ₂	341
Fig. VIx: Development of control plane for advanced partial melting	342
Fig. VIy: C.M.A.S. projections	343
Fig. VIz: Olivine projection onto plane CS-MS-A to show liquid lines of descent for primary melt A	345
Fig. VIaa: Model to explain increased alkalinity of off-ridge volcanics	349
Fig. VIbb: Degree of partial melting as a function of temperature	352
Fig. VIIa: A model for the oceanic crust	360
Fig. VIIb: Comparison of oceanic lithosphere and well known ophiolite suites	362
Fig. VIIc: Magmatism at spreading centre	365
Fig. VIId: Emplacement mechanisms for ophiolite suites	369

LIST OF TABLES

		Page
TABLE I:	Stratigraphy of the Curling Group.	30
TABLE II:	Modal Analyses of Little Port Rocks	62
TABLE III:	Chemical Analyses of Little Port Complex Rocks	74
TABLE IV:	Garnets from Bay of Islands Complex Aureole.	121
TABLE V:	Amphiboles from Bay of Islands Complex Aureole.	129
TABLE VI:	Pyroxenes from Bay of Islands Complex Aureole.	131
TABLE VII:	Plagioclases from Bay of Islands Complex Aureole.	138
TABLE VIII:	Aureole Rocks, Bay of Islands Complex. Chemical Analyses and Modal Analyses	146
TABLE IX:	Olivines from Bay of Islands Complex	250
TABLE X:	Orthopyroxenes from Bay of Islands Complex	258
TABLE XI:	Fo contents of olivines and En contents of orthopyroxenes from Bay of Islands Complex	262
TABLE XII:	Clinopyroxenes from Bay of Islands Complex	266
TABLE XIII:	Temperature Parameters and estimated temperatures for coexisting pyroxenes.	280
TABLE XIV:	Spinel from Bay of Islands Complex	283
TABLE XV:	Coexisting spinels and olivines	289
TABLE XVI:	Plagioclases from Bay of Islands Gabbros	292
TABLE XVII:	An contents of plagioclases from North Arm Mountain according to stratigraphic position.	293
TABLE XVIII:	Analyses of Lherzolites from Table Mountain, Bay of Islands Complex	294
TABLE XIX:	Analyses of Harzburgites from Bay of Islands Complex.	295

	Page
TABLE XX: Analyses of Dunites and Critical Zone Rocks, Bay of Islands Complex.	298
TABLE XXI: Analyses of Gabbros, Bay of Islands Complex.	301
TABLE XXII: Analyses of Diabases, Bay of Islands Complex.	307
TABLE XXIII: Analyses of Volcanic Rocks, Bay of Islands Complex.	310
TABLE XXIV: Sr ⁸⁷ /86 Isotope Data	332
TABLE XXV: Estimations of Upper Mantle Primary Composition.	338
TABLE XXVI: Compositions used for Subtraction Programme	350
TABLE XXVII: Age dates from Humber Arm Allochthon and related rocks, Western Newfoundland.	372
TABLE Aii): X-ray determination of Fo content of olivines.	411
TABLE Aiii): Time (t.my) required to produce temperature rise T at given obduction rate u	413
TABLE Aiiii): Precision of Major Element Analyses	417
TABLE Aiiiii): Accuracy of Major Element Analyses.	418
TABLE Aiiiii): Precision and Accuracy of Trace Element Analyses	420

LIST OF PLATES

	Page
FRONTISPIECE: Corner Brook and Blow me down Mountain from the East.	
The Ultramafic Gabbro transition on Blow me down Mountain.	
PLATE Ia: Well-bedded pyroclastic deposits at Skinner Cove.	40
PLATE Ib: Agglomeratic pyroclastics of possible Skinner Cove affinity just east of Trout River.	40
PLATE IIa: Pillow breccias and aquagene tuffs, Skinner Cove Formation.	41
PLATE IIb: Sedimentary rocks of Skinner Cove Formation .	41
PLATE IIIa: Poorly sorted volcanogenic deposits, Skinner Cove.	42
PLATE IIIb: Calcium carbonate cement is dominant in the volcaniclastic rocks of Skinner Cove Formation.	42
PLATE IVa: Dike with well developed chilled margins cutting agglomerates, Skinner Cove.	44
PLATE IVb: Titanaugite and plagioclase phenocrysts in basalt, Skinner Cove. X nicols, mag. x 75.	44
PLATE Va: Large resorbed olivine crystal in glass matrix, Skinner Cove olivine basalt. X nicols x 65.	45
PLATE Vb: Zoned plagioclase in Ankaramite, Skinner Cove. X nicols x 50.	45
PLATE VIa: Sieve texture in plagioclase and alteration of titanaugite phenocrysts. Skinner Cove, Ankaramite. X nicols x 50	46
PLATE VIb: Zoned titanaugite phenocrysts. Skinner Cove Basalt. X nicols x 48.	46
PLATE VIIa: Skinner Cove basalt: intersertal glass showing development of plagioclase microlites. X nicols x 150.	47

	Page
PLATE VIIb: Olivine phenocrysts completely replaced by iddingsite. Olivine basalt, Skinner Cove. X nicols x 50.	47
PLATE VIIIa: Fluidal textures in Skinner Cove trachyte. X nicols x 110.	49
PLATE VIIIb: Fragmental greenschist - fragments are commonly granulated quartz. Old Man Cove. X nicols x 100.	49
PLATE IXa: Dense fine-grained greenschist, Old Man Cove Formation. X nicols x 110.	56
PLATE IXb: Development of biotite in graphitic-hornblende schist. Old Man Cove Formation. X nicols x 190.	56
PLATE Xa: Quartz vein with granular quartz showing sutured boundaries and undulose extinction. Old Man Cove Formation. X nicols x 90.	59
PLATE Xb: Cross-bedded olivine gabbro. Little Port Complex.	59
PLATE XIa: Large poikilitic hornblende containing saussuritised plagioclase 198.71. Little Port Complex. X nicols x 30.	65
PLATE XIb: Twinned poikilitic hornblende with remnant clinopyroxene 198.71. Little Port Complex. X nicols x 80.	65
PLATE XIIa: Green biotite developed interstitially in quartz diorites, Little Port Complex. Plain light x 90.	67
PLATE XIIb: Intense granulation results in various grain sizes. Note myrmekitic growth in large grain Little Port Complex quartz-diorite. X nicols x 90.	67
PLATE XIIIa: Oxide staining developed around large crystal aggregate. Quartz-diorite, Little Port Complex. Plain light x 90.	69
PLATE XIIIb: Ultramafic pod in Little Port Complex, North of Trout River.	69
PLATE XIVa: Ultramafic mylonite. Strong cataclasis of harzburgite. Little Port Complex. X nicols x 90.	87
PLATE XIVb: Vertical splay faulting in amphibolite zone of aureole at Pond Point, North Arm.	87

	Page
PLATE XVa: Pseudo-gneissosity augening enstatite megacryst in basal lherzolite - Trout River.	89
PLATE XVb: Ultramafic mylonite basal contact. Trout River. Plain light x 10.	89
PLATE XVIa: Stretched and flattened enstatite crystal paralleling foliation in basal ultramafic mylonite. Trout River. X nicols x 20.	91
PLATE XVIb: As above, X45.	91
PLATE XVIIa: Enstatite "phenocryst" showing warped exsolution lamellae of diopside. Lamellae are rotated into plane of foliation in U.M. mylonite which shows flattening around crystal. Trout River. X nicols x 35.	92
PLATE XVIIb: Clinopyroxene disseminated throughout U.M. mylonite cpx-blue-br. Trout River. X nicols x 100.	92
PLATE XVIIIa: Hornfels with descussate textures displayed by plagioclase, pyroxene and garnet, Trout River. X nicols x 35.	96
PLATE XVIIIb: Plagioclase in hornfels showing undulose extinction. X nicols x 180.	96
PLATE XIXa: Garnet (isotropic) with inclusions of pyroxene and plagioclase. Hornfels - Trout River. X nicols x 180.	98
PLATE XIXb: Amphibole replacing pyroxene of basal hornfels - from 4 1/2 meters from basal contact, Trout River. X nicols x 150.	98
PLATE XXa: Brown pleochroic hornblende from 5 meters from basal contact, Trout River. Plain light, x 80.	99
PLATE XXb: Green pleochroic hornblende 12 meters from basal contact, Trout River. Plain light, x80.	99
PLATE XXIa: Banded amphibolite, basal aureole, North Arm Mountain.	101
PLATE XXIb: Banded amphibolite, basal aureole, Trout River.	101

	Page
PLATE XXIIa: Altered plagioclase porphyroblast containing pyroxene inclusions. X nicols x 65.	102
PLATE XXIIb: Garnet porphyroblast showing alteration to sericite. Amphibolite - basal aureole. X nicols x 80.	102
PLATE XXIIIa: Garnets in black graphitic? matrix - 1 km W. Stowbridge Head, North Head. Plain light, x 15.	104
PLATE XXIIIb: Helicitic trails (S_1) in garnets of amphibolite. S_2 commonly augens these garnets. Plain light x 50.	104
PLATE XXIVa: Laminated greenschists, North Arm aureole.	106
PLATE XXIVb: Phyllites of North Arm aureole.	106
PLATE XXVa: Clastic sediments of aureole section, North Arm. X nicols x 30	108
PLATE XXVb: Muscovite surrounding strained quartz clast in phyllite. North Arm. X nicols x 35.	108
PLATE XXVIa: Detrital garnet in sandstone from base of aureole, North Arm. Plain light, x 140.	110
PLATE XXVIb: Hornfels with original garnet/px/plag mineralogy partially replaced by Ca bearing phases in rhodinitic alteration. Trout River. X nicols x 100.	110
PLATE XXVIIa: Basal faulted contact at Winterhouse Brook. Development of calc silicates as white/grey dike in center and bleached shales below	113
PLATE XXVIIb: Pre- D_2 garnet containing S_1 inclusion trail, amphibolite, North Arm aureole. X nicols x 95.	113
PLATE XXVIIIa: Acicular crystals of clinozoisite in quartz from basal aureole sedimentary protolith, North Arm. X nicols x 150.	117
PLATE XXVIIIb: Keliphitic rim around detrital garnet in sediments, North Arm. X nicols, x 150	117

	Page
PLATE XXIXa: Large porphyroblastic garnet showing marginal alteration to sericite (?). Amphibolite, Trout River. Plain light x 35.	124
PLATE XXIXb: Aligned granules of sphene (S ₂) in amphibolite, North Arm Mountain. X 85. Plain light	124
PLATE XXXa: Green hornblende replacing brown hornblende 8 m from basal contact, Trout River. Plain light x 195.	127
PLATE XXXb: Clinopyroxene in hornfels. Trout River. X nicols x 180	127
PLATE XXXIa: Biotite aligned parallel to S ₂ schistosity in epidote amphibolite, Pond Point, North Arm. Plain light x 60	133
PLATE XXXIb: Pelite with one dominant fabric defined by muscovite, North Arm. X nicols x 150	133
PLATE XXXIIa: Phlogopite (orange-brown) with amphibole in mylonitic band in basal ultramafics. Plain light x 200.	136
PLATE XXXIIb: Twinned plagioclase from hornfels. X nicols x 90.	136
PLATE XXXIIIa: Surface features of harzburgite with orthopyroxene and spinel standing in relief against yellow weathering olivine	179
PLATE XXXIIIb: Peridotite-augen gneiss composed of enstatite eyes in a groundmass of serpentinite. From C. H. Smith ('58)	179
PLATE XXXIVa: Rhythmic banding in harzburgites, Table Mountain.	181
PLATE XXXIVb: Folding of banding in harzburgites, Winterhouse Brook, Table Mountain	181
PLATE XXXVa: Serpentinisation of margins of enstatite megacryst in harzburgite, Table Mountain. X nicols x 50	183
PLATE XXXVb: Exsolution of diopside as (100) lamellae in enstatite-harzburgite, Blow me down Mountain. x 90	183

PLATE XXXVIa:	Enstatite in mylonite band of basal ultramafics with diopside lamellae rotated into schistosity.	185
PLATE XXXVIb:	Remnant olivine kernels after serpentinisation indicating original crystal size. X nicols x 75.	185
PLATE XXXVIIa:	Yellow green spinels in herzolites mantled by magnetite, Table Mountain. Plain light x 70.	186
PLATE XXXVIIb:	Dunite veins cutting across folded veins in harzburgites, Winterhouse Brook.	186
PLATE XXXVIIIa:	Cumulate layering in dunite. Mineralogical layering of olivine and clinopyroxene . . .	200
PLATE XXXVIIIb:	"Scour and fill" structure in layered dunite.	200
PLATE XXXIXa:	Large olivine crystal from cumulate dunites - highly serpentinized along fractures. Kernels with similar extinction indicate size of crystal. X nicols x 35. .	201
PLATE XXXIXb:	Small rounded inclusion of spinel in enstatite from Main Dunite Zone, Table Mountain. Plain light x 120.	201
PLATE XLa:	Adcumulus chromite forming band in Main Chromite Zone. X nicols x 20.	205
PLATE XLb:	Feldspathic dunites showing layering enhanced by differential weathering of feldspar and olivine.	205
PLATE XLIa:	Interlocking adcumulate plagioclase crystals as aggregate in serpentinised dunite. X nicols x 95	207
PLATE XLIb:	Plagioclase showing alteration to hydrogrossular and sericite/epidote. Feldspathic dunite, Table Mountain. X nicols x 90.	207
PLATE XLIIa:	Intercumulate plagioclase surrounding early olivine cumulate crystal. X nicols x 130.	208

PLATE XLIIb:	Complex interfingering of dunite and gabbro in Critical Zone, Table Mountain.	208
PLATE XLIIIa:	Post accumulation slump folds in Critical Zone, Table Mountain	211
PLATE XLIIIb:	Branching of cumulate feldspar layers in Critical Zone, Table Mountain.	211
PLATE XLIVa:	Expansion cracks in plagioclase as a result of serpentinisation of olivine. X nicols x 85	214
PLATE XLIVb:	Anorthosite bands in Critical Zone - white, interlayered with pyroxene-dunite, North Arm Mountain	214
PLATE XLVa:	Interlocking bytownite crystals from anorthosite band. North Arm Mountain Critical Zone, X nicols x 100	216
PLATE XLVb:	Plagioclase including olivine. Troctolite, Blow me down Mountain. X nicols x 120.	216
PLATE XLVIa:	Clinopyroxene corona around olivine in reaction relationship with plagioclase. Troctolite, North Arm Mountain. X nicols x 130.	219
PLATE XLVIb:	Layering in gabbros, Table Mountain.	219
PLATE XLVIIa:	Cumulate plagioclase, intercumulus pyroxene, and olivine. Gabbro, Table Mountain. X nicols x 75.	221
PLATE XLVIIb:	Reaction rim of hornblende between clinopyroxene and plagioclase in gabbro, Blow me down. X nicols x 150	221
PLATE XLVIIIa:	Magnetite occurring along cleavage partings in clinopyroxene. Gabbro, Blow me down Mountain. Plain light x 135.	224
PLATE XLVIIIb:	Quartz diorite dike cut by basic dikes on Blow me down Mountain.	224
PLATE XLIXa:	Megacrystic hornblendites from Brighton Island, Notre Dame Bay	227
PLATE XLIXb:	Amphibole forming at the expense of clinopyroxene. Amphibolite inclusion in gabbro. North Arm Mountain. X nicols x 15.	227

	Page
PLATE La: Original igneous contact preserved in amphibolite from North Arm Mountain (C-C ₁). Plain light x 15.	231
PLATE Lb: Isoclinal post-accumulation fold folding planar fabric in critical zone rocks, Table Mountain.	231
PLATE LIa: Zoned plagioclase in quartz diorite, Blow me down Mountain. X nicols x 40.	233
PLATE LIb: Plagioclase included in poikilitic quartz - quartz-diorite. North Arm Mountain. X nicols x 45	233
PLATE LIIa: Contact between basic dike and quartz-diorite. Blow me down Mountain, X nicols x 40.	236
PLATE LIIb: Brecciated dike cutting through massive gabbro, North Arm Mountain.	236
PLATE LIIIa: Sheeted dikes - North Arm.	239
PLATE LIIIb: Plagioclase phenocrysts in diabase, North Arm Mountain. X nicols x 30	239
PLATE LIVa: Calcite filling vesicle in pillow lava, North Arm Mountain. X nicols x 80	244
PLATE LIVb: Chlorite and pyrite in vesicle in pillow lava. York Harbour, X nicols x 65	244
PLATE LVa: Plagioclase phenocrysts in basalt - York Harbour. X nicols x 95.	246
PLATE LVb: Chlorite/oxide pseudomorph after olivine, Upper Basalt, York Harbour. Plain light x100.	246

PART I

CHAPTER I

INTRODUCTION

A. Location and access.

The Bay of Islands complex forms a discontinuous north-easterly trending belt of mafic-ultramafic massifs approximately 100 km long and 25 km wide on the west coast of Newfoundland (Fig. Ia). The three northernmost massifs, Table Mountain, North Arm Mountain-Mount St. Gregory, and Blow me down Mountain, were mapped during the summers of 1971 and 1972 by the author. The fishing village of Trout River was used as a base for the reconnaissance mapping of Table Mountain and Mt. St. Gregory and may be reached by road from Deer Lake (Fig. Ib). Cox's Cove on Middle Arm was used as a base for mapping of North Arm Mountain and Blow me down Mountain, and is reached by road from Corner Brook.

Local access was attained by four-wheel drive vehicle, boat and floatplane. Travel in the mountains is of necessity by foot, and although thick growths of trees and high cliffs make climbing difficult, the mountains are flat topped, barren and easily traversed.

B. Physiography and climate.

The complex forms a distinct physiographic unit which is preserved as part of the Long Range Peneplane (Twenhofel and McClintock, 1940). The eroded remnants of the peneplane form a gently undulating highland of over 650 m, bounded to the northeast by the Long Range proper, and by a coastal lowland to the west. The highest point rises to 814.7 m in the Lewis Hills, but the peaks of North Arm Mountain and Blow me down (762.3 and 705.6 m

Figure 1a: Regional Location

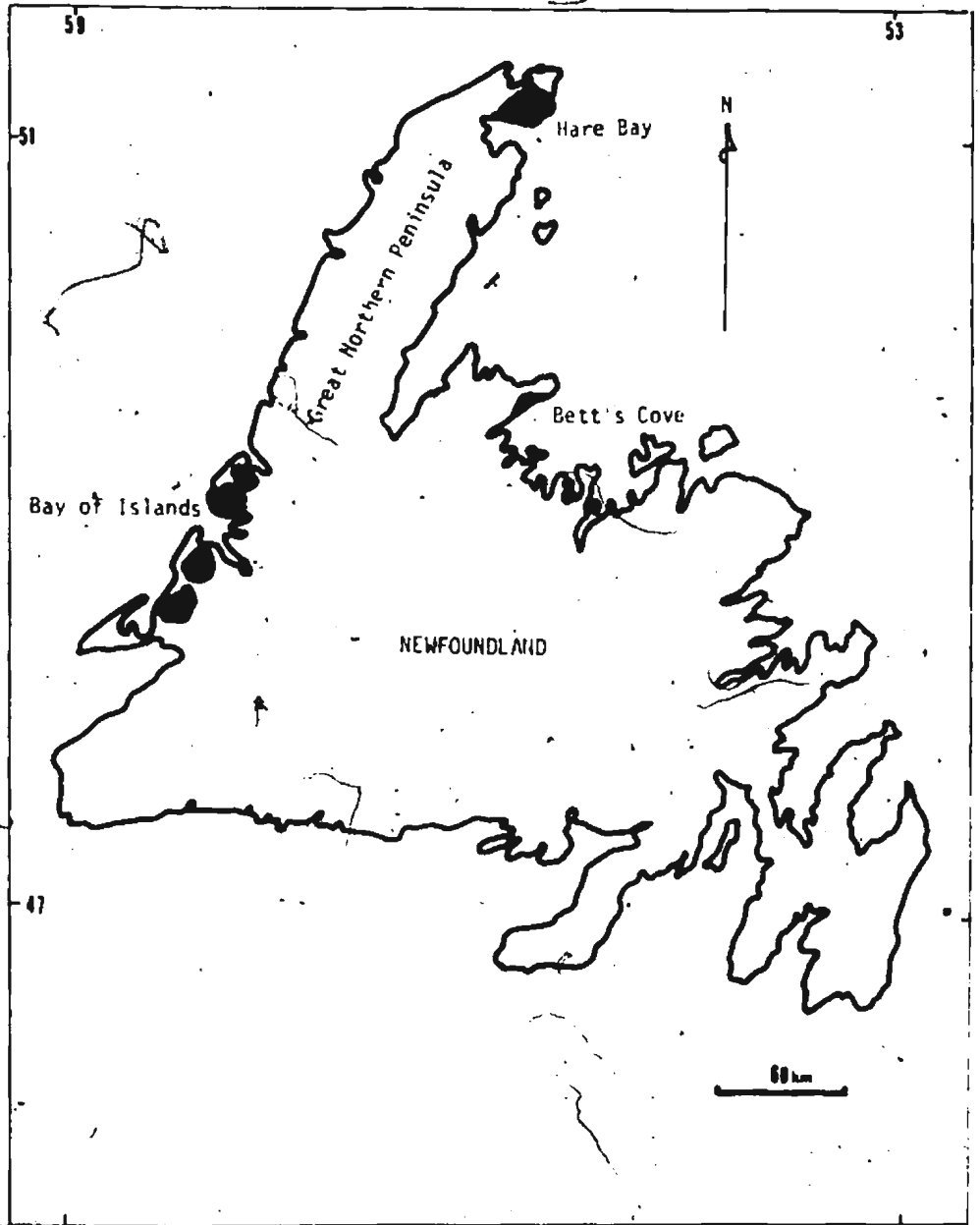
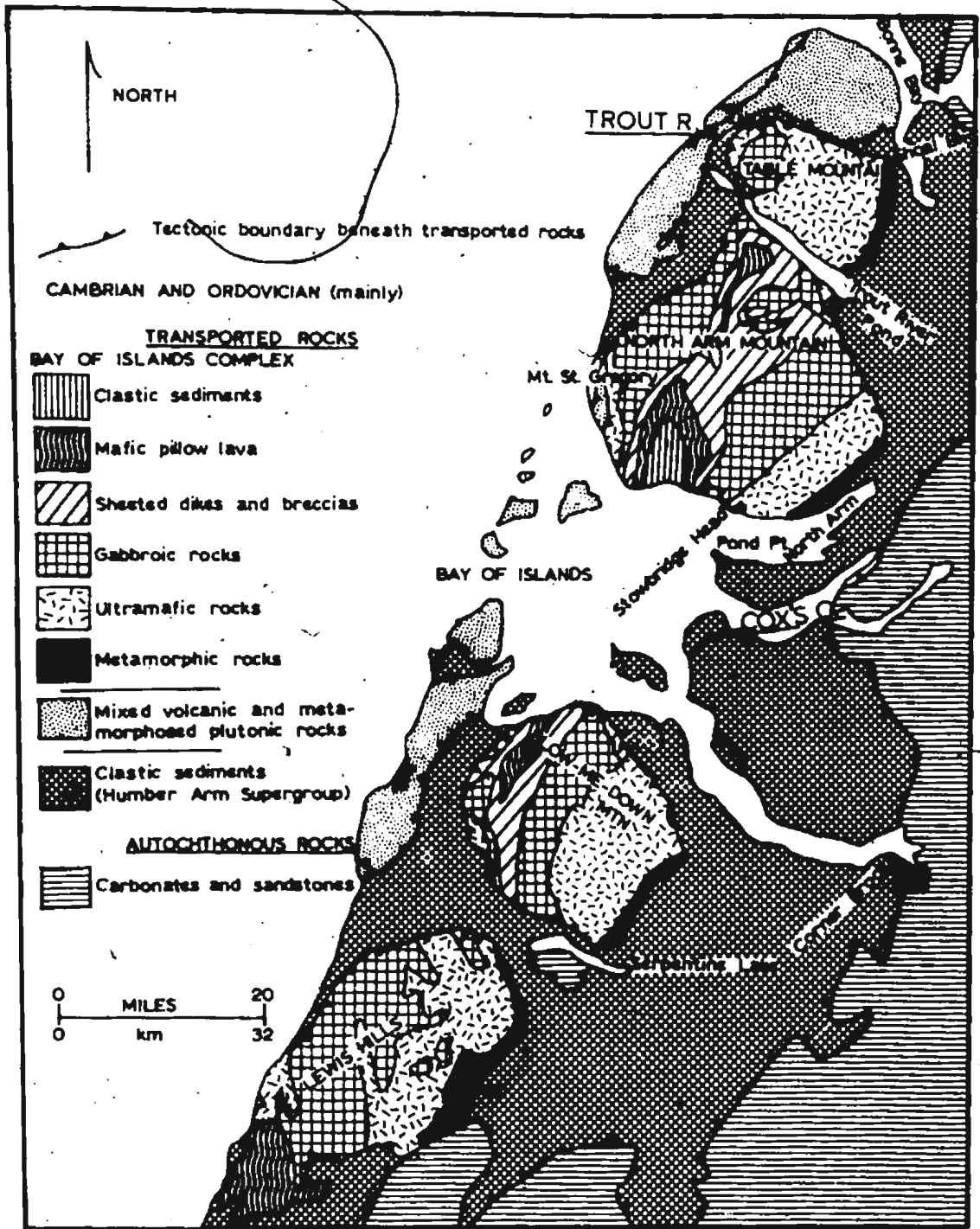


Figure 1b: Bay of Islands Region showing location of
Trout River and Cox's Cove.



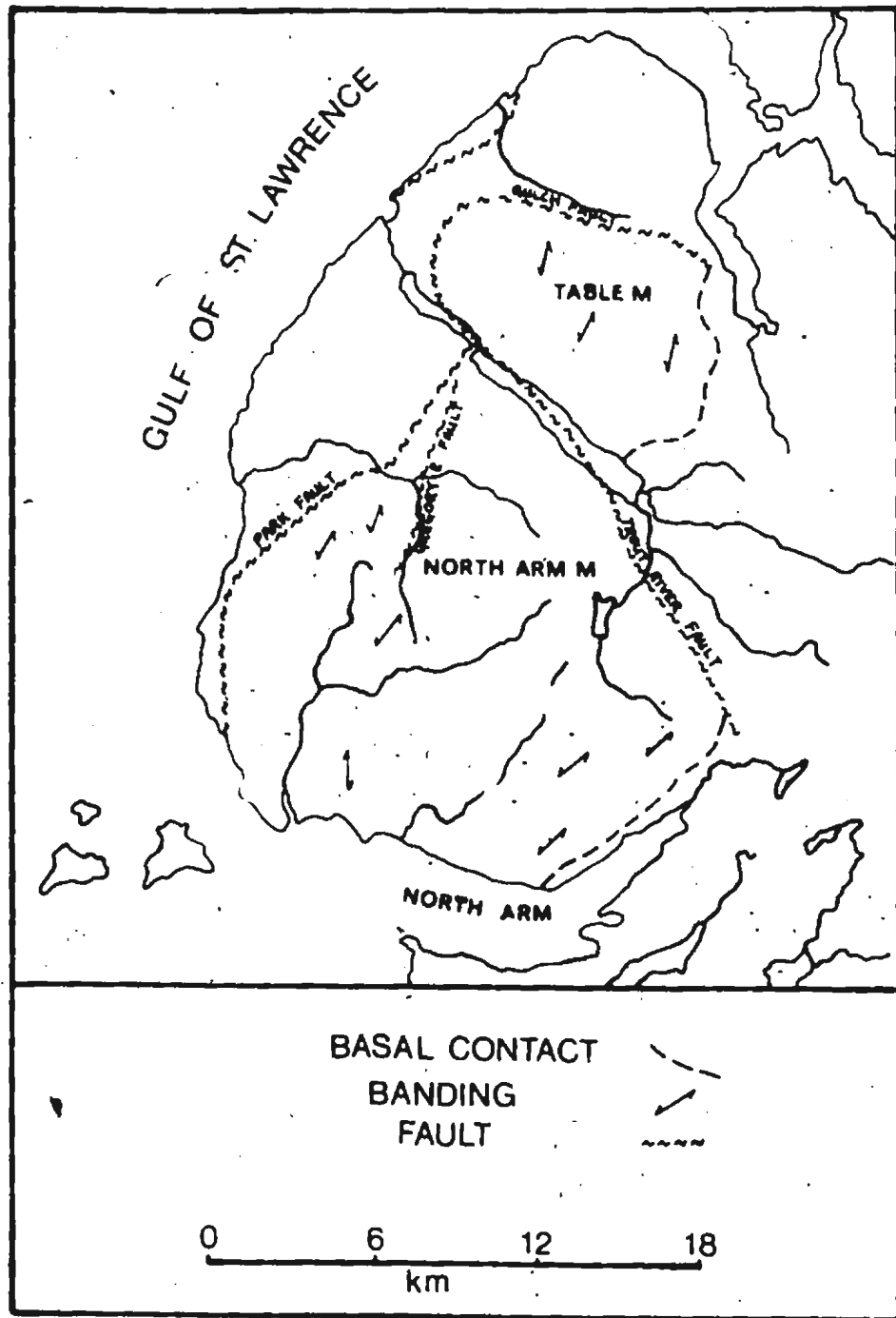
respectively) are comparable. Both regional and local topography reflect bedrock structures and lithologies. Streams run either northeastwards, parallel to the regional strike, or northwestwards, parallel to the strike of many transcurrent faults. The two Trout River Ponds are similarly structurally controlled by faults between the Table Mountain and North Arm Mountain massifs (Fig. 1c). The highlands, composed of mafic and ultramafic rocks, are bounded by fault scarps often of 300 m relief, and V-shaped canyons and cirques, and well-developed theatre-headed valleys cut the scarps and are a result of stream erosion and slumping rather than glacial action. A ridge and valley pattern is developed locally on the peneplane as a result of fine scale differential weathering. A felsenmeer is developed on the mafic and ultramafic rocks where the high magnesium content restricts the growth of trees to the boggy areas only.

The west coast of Newfoundland enjoys good summer weather with temperatures varying little from 65-70⁰ F. Rainfall is light but frequent, and the predominant wind direction is from the southwest.

C. Survey control.

Topographic base-maps (sheets of the National Topographic System: Skinner Cove E, Trout River E and W, Lomond W, Bay of Islands E and W, and Serpentine E and W) on a scale of 1:50,000, and aerial photographic coverage are available for the area from the Federal Government Department of Mines and Technical Surveys, Ottawa. Aerial photographs of 1:50,000 and 1:20,000 scales were used for the present survey. Infrared and colour photographs are being flown by the Federal Government at the present time, and are at present only available for the southern part of the study area.

Figure 1c: Fault control of topography in northern massifs.



D. Previous Geological Work.

J.B. Jukes (1842) was the first to describe the regional geology of western Newfoundland. A. Murray and J.P. Howley (1881) described the area in more detail, and the ultramafic and mafic rocks of the Bay of Islands and Hare Bay were included collectively on Howley's map of Newfoundland (1907) as 'serpentines, dolerites and diorites, etc.'

More detailed investigations did not take place until 1933, resulting in publications by Snelgrove (1934) and Snelgrove *et al.* (1934), concerned mainly with the chromite deposits, especially of the Blow me down massif. The mafic-ultramafic complexes were interpreted as a dissected, banded lopolith, and some attempt to describe the igneous stratigraphy was made. Ingerson (1935, 1937) considered the massifs to be individual layered laccoliths with domed roofs, whilst Buddington and Hess (1937) and Cooper (1936) considered them remnants of a once continuous lopolith. Troelsen (1947) studied the northern part of the area (Table Mountain and Mount St. Gregory) as part of a review of the stratigraphy and structure of the Bonne Bay-Trout River area.

Smith (1958) carried out regional mapping and petrographic studies on all four massifs of the Bay of Islands complex. He interpreted the mafic and ultramafic rocks as individual intrusions and noted that they were partially surrounded by a metamorphic aureole, and that they could be classified as intermediate between alpine peridotites and stratiform intrusions. Riley (1962) studied the southern part of the area during reconnaissance mapping of the Stephenville area, and Baird (1960) the northern part during reconnaissance mapping of the Sandy Lake (west half) area.

The general view, therefore, up until 1963 was that the igneous rocks were intruded in their present position into the surrounding clastic rocks. Johnson (1941) and Kay (1945) had argued the possibility that the clastic rocks might represent a sequence, equivalent in age to the now structurally underlying carbonates, that was transported before intrusion of the plutons. However, Rodgers and Neale (1963) interpreted the mafic-ultramafic complexes as an integral part of such a transported terrain, mainly because of their spatial association with the surrounding clastic rocks. The mafic-ultramafic rocks were still regarded as intrusive into the sediments but the intrusion now was thought to predate transport. Stevens (1970) demonstrated that the igneous and sedimentary rocks in fact formed separate thrust slices, and both these slices and several others were delineated by Williams et al. (1972) and Williams (1973). This interpretation, which implies that the igneous complexes were formed in an area separated from the transported clastics at the time of deposition, was based upon the widespread occurrence of chromite, pyroxene and serpentine grains in the upper sandstone unit of the easterly derived clastic succession (Curling Group of Stevens, 1970). Stevens interpreted the igneous rocks as a more easterly source terrain during clastic deposition, shedding material westwards into the depositional basin, at least during the latter stages of deposition of the clastics. This period of deposition may in fact have been occurring during early westward movement of the klippen rocks.

Church and Stevens (1971) and Williams (1971) delineated basal thrust contacts between plutonic rocks and underlying sedimentary rocks

and noted that the basal aureole of metamorphic rocks that had suggested an intrusive origin, were in fact part of the transported igneous slices, and were to be found faulted against relatively undeformed nearby clastic rocks. These authors and Williams and Smyth (1973) and Malpas et al. (1973) regarded the aureole as a product of dynamothermal metamorphism during transport.

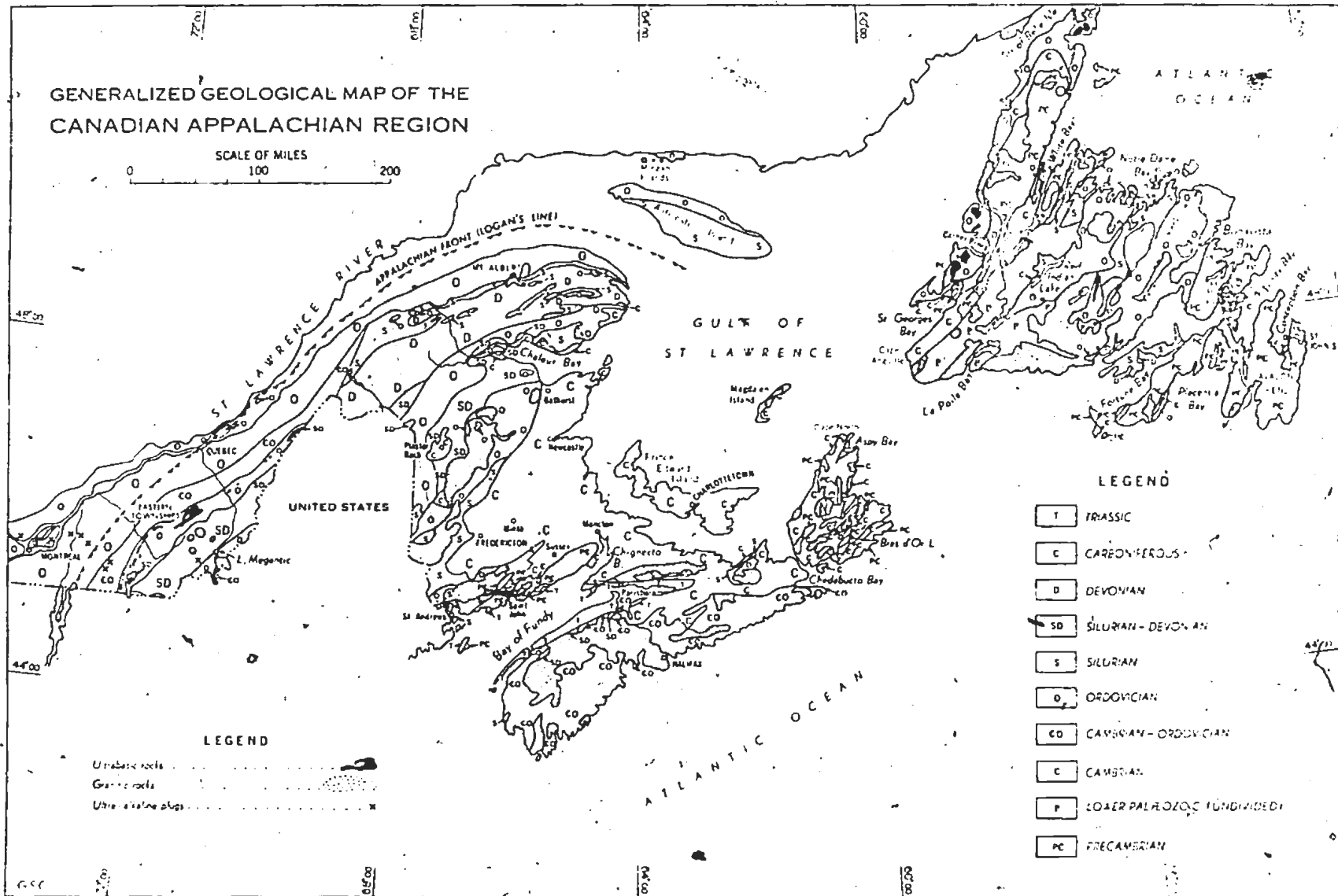
Tuke (1968) confirmed the hypothesis of Rodgers and Neale that two superimposed sequences of different lithologies but similar age existed in the Hare Bay region of northern Newfoundland (Fig. 1d). Tuke delineated three separate allochthonous slices and showed that the White Hills Peridotite Sheet occupied the highest slice. More recent work of Williams, Smyth and Stevens (1973) and Smyth (1971 and 1973) delineated a stacking order of these slices for the first time. Similar lithologies, structures and stacking orders allow close correlations to be made between the Hare Bay Allochthon and the Humber Arm Allochthon which feature in most of the recent models for the development of the Newfoundland Appalachians.

Recent interpretations have suggested the possibility that the plutonic and volcanic rocks represent oceanic crust and upper mantle now preserved on land (Stevens, 1970; Church and Stevens, 1970a & b, 1971; Bird and Dewey, 1970; Williams, 1971; Williams and Malpas, 1972; Church, 1972; Malpas, 1973) and that they fit a model based upon an opening and closing proto-Atlantic ocean as envisaged by Wilson (1966). These interpretations are discussed further in Chapter VII.

Figure 1d: Canadian Appalachian Region

GENERALIZED GEOLOGICAL MAP OF THE CANADIAN APPALACHIAN REGION

SCALE OF MILES
0 100 200



LEGEND

- T TRIASSIC
- C CARBONIFEROUS
- D DEVONIAN
- SD SILURIAN-DEVONIAN
- S SILURIAN
- O ORDOVICIAN
- CO CAMBRIAN-ORDOVICIAN
- C CAMBRIAN
- P LOWER PALEOZOIC UNDIVIDED
- PC PRECAMBRIAN

LEGEND

- Uplastic rocks
- Granite rocks
- Ultra-alpine plugs

E. Acknowledgements.

The writer was supported by a National Research Council of Canada post-graduate scholarship with additional field support from D.F. Strong (N.R.C. Operating Grant A7975). Thanks are expressed to D.F. Strong, H. Williams, and M.J. Kennedy for their supervision and guidance; to W.J. Wadsworth, A.C. Dunham and G.D. Nichols of Manchester University for their hospitality and aid in obtaining rare earth and microprobe data; to F. Frey of Massachusetts Institute of Technology for supplementary rare earth analyses and R. Cormier of St. Francis Xavier University for Sr isotopes. D.B. Clarke of Dalhousie University aided in microprobe data reduction. G. Andrews and J. Vahtra gave invaluable assistance in obtaining chemical analyses and B. Sheppard and E. Hussey proved excellent field assistants. Finally the writer wishes to express thanks to R.K. Stevens (M.U.N.), R.G. Cawthorne (M.U.N.) and A.P. Taylor (Manchester) for stimulating discussions of ophiolite geology, and especially to B. St. Croix and G. Woodland for their patience in typing the manuscript.

F. Geological Setting.

i) Newfoundland and the Appalachian Structural Province

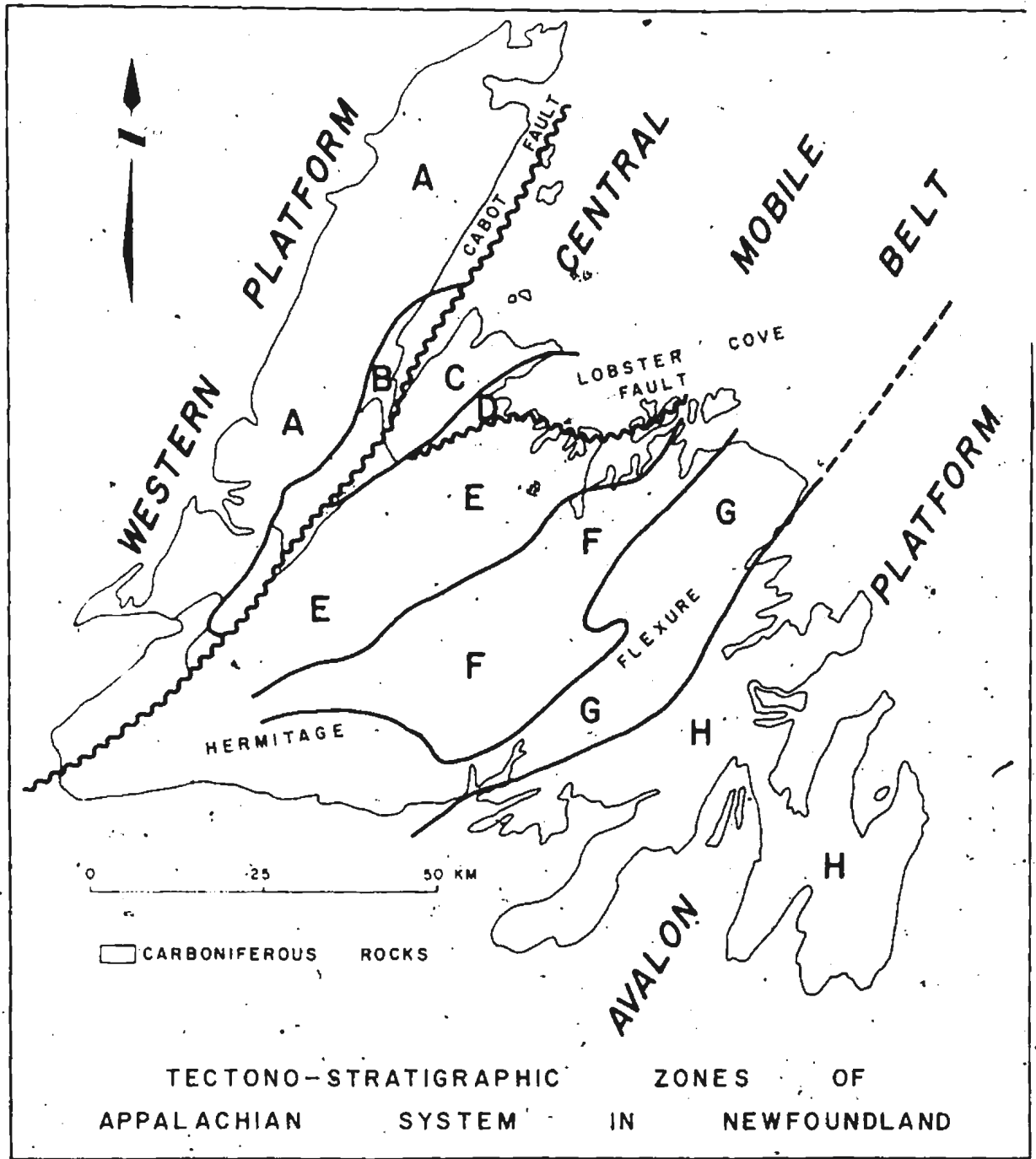
The Appalachian Structural Province (A.S.P.), lying to the south-east of the Canadian Shield, has an exposed area of some 280,000 square kilometres in Canada. Newfoundland lies at the northern extremity of the Province and exhibits a cross section of the Palaeozoic orogen (Fig. 1d). This orogen is composed chiefly of Precambrian and Palaeozoic rocks which contrast sharply with the cover rocks of the Shield in structure and facies.

Williams (1964) described the two-sided symmetry of the A.S.P. in Newfoundland and thus argued against the process of its formation by continental accretion. More importantly, however, his fundamental division of Newfoundland into three zones delineated central Newfoundland as distinctly different in geological evolution to the adjacent 'platformal' rocks. Following this dismissal of the Hall-Dana geosynclinal concept of Appalachian development, Wilson (1966) proposed that the present western and eastern parts of the Appalachian system (in Newfoundland, the Western platform and Avalon platform of Williams, 1964), had been separated by a 'proto-Atlantic ocean' which closed in the Lower Palaeozoic and brought the eastern platformal terrain into its present position relative to the North American continent. Later continental separation during the Mesozoic opened the Atlantic to the east of the Avalon Platform. Williams, Kennedy and Neale (1972) further subdivided the A.S.P. in Canada into nine zones, eight of which are represented in Newfoundland. The geological development of these zones, designated by the letters A to I (Fig. 1e), and the relationships between adjacent zones together comprise the fundamental aspects of the development of the Appalachians. Within this zonal framework, zone A and B are equivalent to the Western Platform, zones C to G, equivalent to the Central Mobile Belt and zone H equivalent to the Avalon Platform of Williams.

ii) Zonal subdivision of the Appalachian Structural Province in Newfoundland.

The westernmost zone of the system, Zone A, is underlain by continental basement of Grenvillian age. The basement crops out as the

Figure 1e: Tectono-stratigraphic zones of the Newfoundland Appalachians.



TECTONO-STRATIGRAPHIC ZONES OF APPALACHIAN SYSTEM IN NEWFOUNDLAND

gneisses of the Long Range mountains and anorthosites of the Indian Head Range and is unconformably overlain by a basal clastic sediment-plateau lava sequence, and an eastward thickening carbonate succession. The carbonates are overlain by easterly-derived, westward transgressing flysch deposits which preceded the tectonic emplacement of transported clastic and igneous rocks. Both the underlying autochthonous rocks and the transported rocks are deformed, but penetrative deformation affected some allochthonous rocks prior to their final emplacement. Upper slices of the allochthons in both the Humber Arm region and the Hare Bay region are formed of ophiolitic assemblages transported from the east, and consequently provide additional evidence for the existence of a Lower Palaeozoic ocean basin prior to Appalachian orogenesis.

In Zone B a carbonate succession overlies Grenville rocks as in Zone A. Polydeformed allochthonous rocks are also present in Zone B and are identical to the Fleur de Lys Group of Zone C. They are interpreted as transported because of the contrast in structural style and metamorphic grade where juxtaposed with relatively undeformed autochthonous Cambrian and Ordovician carbonate rocks in the southern part of this zone. The boundary between Zones A and B, where defined, is commonly faulted, but it is mostly hidden beneath Carboniferous sedimentary rocks.

The polydeformed rocks that are found in place in Zone C form a thick series of clastic sediments and volcanic rocks, all deformed in the late Cambrian or early Ordovician. They are referred to as the Fleur de Lys supergroup. These rocks were interpreted as continental margin deposits by Dewey (1969) and Zone C was described as a 'marginal crystalline

belt' by Kennedy (1973). (See also Zone G). The stratigraphic succession within this supergroup passes from a lower dominantly psammitic and semipelitic sequence overlain by a greywacke sequence into mafic and silicic volcanic rocks. A thin and discontinuous zone of ultramafic rocks separates Fleur de Lys terrain on its west side from predominantly Ordovician volcanics to its east. Dewey (1969) and Kennedy (1973) have interpreted these ultramafic rocks as part of an ophiolite sequence representing the remnant of a small ocean basin that opened within the continental rise prism of sediment. Strong et al. (1974) and Swinden and Strong (in press) prefer interpretations in which these ophiolites were overthrust in the early Ordovician and infolded during the Acadian orogeny (See Chapter VII).

Zone D is characterized by the predominance of mafic pillow lavas, associated pyroclastics and a diabase dyke terrain. Sediments, although not common are abundant locally, consisting generally of cherts, greywackes and marine limestones (Marten, 1971; Strong and Kean, 1972). Ultramafic and granodiorite rocks occur in this zone, the former being well represented by the basal portion of the Bett's Cove ophiolite assemblage (Upadhyay et al., 1971) in the west. This ultramafic member is overlain by a thin gabbroic member which itself gives way upwards to a dyke complex consisting of nearly 100% mafic dykes, which decrease in density upwards as more volcanic screens appear. Above this transition is a four kilometre thick pile of pillow lavas. The general lithological succession therefore compares favourably with that of other ophiolite suites which have been interpreted as sections of oceanic crust and upper mantle. The excessively thick sequence of pillow

lavas may be attributed to island arc volcanism, built upon oceanic crustal 'basement'. Similar island arc volcanism has been suggested throughout Zone D (Stevens et al., 1974) from Long Island (Kean, 1973), Pilley's Island (Strong, 1973) to the Twillingate-New World Island area (Strong and Payne, 1973). However, the effect of compressional stresses of such an environment (leading plate margin) have been disputed by H. Williams (personal communication, 1974). Several lines of evidence suggest that Zone D represents the source area for the transported rocks of Western Newfoundland. Ophiolitic rocks are present but, more importantly, similar relationships exist between older deformed granitic rocks and diabase dykes which cut them in both zones. Specific lithologic correlations can be made between this assemblage on Twillingate or Long Island and similar assemblages of the Little Port Complex which forms part of the allochthon.

All boundaries of Zone D are faulted.

In the lower part of the succession in Zone E, pyroclastic mafic volcanic rocks are dominant. These are overlain by sedimentary rocks, greywackes and conglomerates, which give way upwards to terrestrial and fluvial deposits. A chaotic mélange, 30 km in length and 8 km wide, is found in the northeast of Zone E. This has been interpreted by Horne (1969) as gravity slide deposits, but more recently has been argued as characteristic of an oceanic trench and subduction zone environment (Dewey and Bird, 1971; Kay, 1972). If this latter interpretation is correct then Zone E contains the remnants of an early Ordovician consuming plate margin and is most probably underlain by oceanic crust.

Most of Zone F is composed of Ordovician slates overlain by a thick sequence of arenaceous sediments of Silurian age. Although some volcanic horizons exist in the latter, both Ordovician and Silurian volcanic rocks are of minor importance in Zone F. However, a discontinuous belt of mafic volcanic rocks and associated gabbros and ultramafic rocks occurs along the margin with Zone G in the east. This contact may itself be unconformable since middle Ordovician greywackes in Zone F here contain metamorphic detritus presumably derived from Zone G (Kennedy and McGonigal, 1972). Mélange deposits have also been observed along this contact at Carmanville and near the head of Bay d'Espoir (Kennedy, 1973) and a basal conglomerate of Zone F has been reported from Gander Lake (M.J. Kennedy, personal communication, 1974).

Zone G consists of a belt of metamorphic rocks in an 'S' shaped configuration extending across Newfoundland and truncated in the west by faulting (Brown, 1973). The flexure of the belt has been attributed to tectonic bending rather than an original depositional trend since the same form of folding is seen on a smaller scale throughout central Newfoundland (Williams et al., 1970). Basement gneisses intruded by granites, and younger sedimentary cover rocks occur in northeastern Newfoundland, and similar types have been noted along the south coast (Colmann-Sadd, 1974; Brown, 1975). Devonian plant remains locally occur in ~~the~~ ~~stones~~ and slates exhibiting low grade metamorphism. The similarity in metamorphism and style of deformation between the metasedimentary cover rocks of Zone G, and the psammites and semipelites of the Fleur de Lys supergroup of Zone C has led Kennedy (1973) to suggest that Zone G is also a 'marginal crystalline belt' of similar origin to Zone C. Strong et al. (1974a, b) have suggested

that rocks of the Gander Lake metamorphic zone resulted from metamorphism of continental margin rocks along a subduction zone, the existence of which might explain the wide age span of the granites that occur in the zone.

Zone H, the easternmost of the structural zones to be represented in Newfoundland, consists of a basal assemblage of subaerial acid and basic volcanic rocks predominantly overlain by and partially interbedded with an assemblage of siliceous slates and marine greywackes. These locally have Precambrian fossils preserved in tuffaceous horizons (Anderson, 1972). They are overlain by an assemblage of sedimentary rocks, some with volcanics at the base, but everywhere containing arkoses and red sandstones of shallow water origin. The basal volcanics are intruded by granites of varying petrography and overlain unconformably by Lower Paleozoic rocks.

Hughes and Brueckner (1971) suggest that the environment in which Zone H rocks were developed was a series of volcanic islands. Further evidence suggests that some, if not all of the volcanics were originally calc-alkaline in nature (Malpas, 1972). Whether this necessarily implies an island arc situation is a matter of debate, as is the presence or absence of continental basement beneath the Avalon. Strong *et al.* (1974) have interpreted the volcanic rocks as calc-alkaline in character, produced in a Basin and Range type of environment.

G. Statement of Problem.

The importance of the development of ophiolite suites and their interpretation as fossil oceanic crust and mantle incorporated into continental margin sequences during tectonic episodes or orogenesis, has

been made clear by several workers (Dewey and Bird, 1971; Bird and Dewey, 1970; Coleman, 1971; Moores, 1973).

If ophiolites are to be interpreted as such, a study of them can give valuable insight into the genesis of oceanic crustal rocks and their relationship to the mantle. More important, a direct observation of the lithology, petrology, structure and chemistry of mantle rocks can be made without the inevitable cost of drilling contemporary mantle or relying on random sampling of the mantle in the form of xenoliths brought to the surface in basalt flows.

Many ophiolite sequences have been well documented in the literature in the last decade. These include those from the Mediterranean (Gass, 1968; Moores, 1969; Moores and Vine, 1971; Hynes, 1972; Menzies, 1973; Montigny et al., 1973; Pamic, 1971; Bezzi and Piccardo, 1971; Spooner and Fyfe, 1973); those from Turkey and the Oman (Bailey and McCallieu, 1952; Reinhardt, 1969); the Pacific (S.W.) (Davies, 1971; Guillon and Routhier, 1971); and North America (Thayer and Himmelberg, 1968; Upadhyay et al., 1971). Studies of lithological relation in many of these complexes is hampered by the degree of deformation, amount of repetition and dissection of rock types by faulting, or incomplete exposure. The Bay of Islands complex, by comparison, provides an excellent opportunity to study what appears to be a complete ophiolite suite, with little or no removal of stratigraphy or dissection by faulting. The complex is extremely well preserved, access is relatively easy and exposure is extremely good especially in critical areas.

In order to provide some answers to questions concerning the properties of and relationships between the various ophiolitic lithologies; to determine relationships between the ophiolite suite and the surrounding rocks; and to apply such relationships to models for the development of the Appalachian belt in Newfoundland; a programme of regional mapping and sampling and subsequent petrochemical analyses was carried out.

Some results of this work have already been published (Williams and Malpas, 1972; Malpas, 1973; Williams, 1973) and others are in press (Malpas and Strong, 1975). During study of the Bay of Islands complex, direct comparisons were made with type ultramafic complexes elsewhere. Field and laboratory work have been carried out on rocks from the Lizard, Cornwall, a classic high temperature peridotite intrusion (Green, 1964); the Troodos Complex and associated rocks on Cyprus (Gass, 1968), a classic ophiolite sequence; and on the layered sequence of Rhum, Scotland (Brown, 1956). Such comparisons have led to reinterpretations of the geology of these areas and in the nature of the genesis of ophiolite suites (Malpas, Stevens and Strong, 1973; Strong et al., in press).

CHAPTER II

GEOLOGY OF WESTERN NEWFOUNDLAND

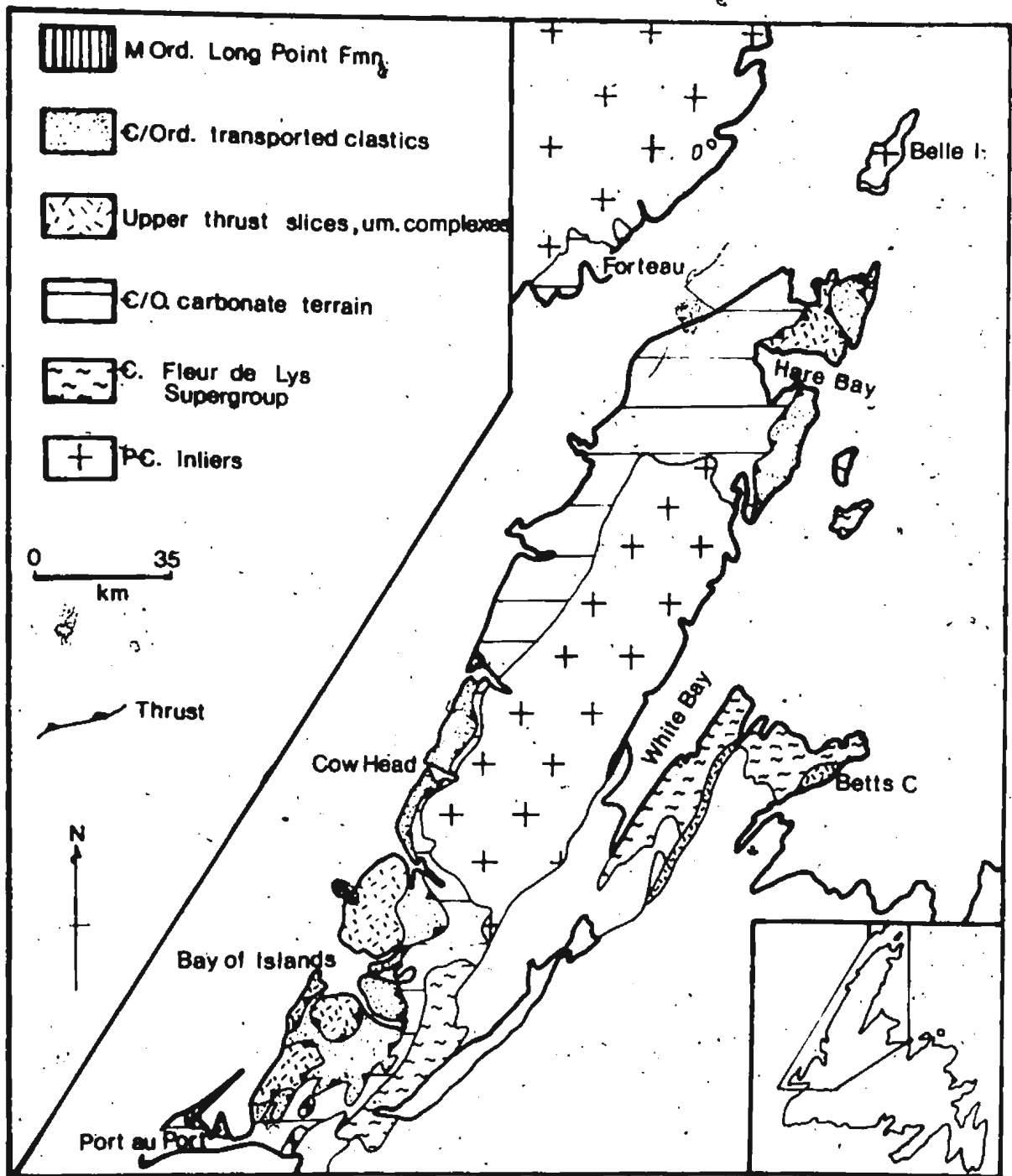
A. Introduction.

Precambrian basement inliers in western Newfoundland are overlain by autochthonous Palaeozoic cover rocks which are themselves locally overlain by allochthonous sequences or klippen of Palaeozoic clastic sedimentary and igneous rocks (Fig. IIa).

B. Basement.

Grenvillian basement rocks in western Newfoundland are referred to the Long Range and Indian Head Range Complexes. Generally the poly-deformed gneisses and schists and associated anorthosites and foliated granites on the Northern Peninsula occur in domes or faulted blocks, which appear to have acted as stable blocks during Appalachian orogenic events. Pringle et al. (1971) obtained a Rb:Sr whole rock age of 1130 ± 90 million years, and a K:Ar biotite isochron age of 840 ± 20 million years, for the foliated granite plutons. These dates fit into the Grenville pattern suggested by the geology. The basement was intruded by a north-trending tholeiite diabase dyke swarm which acted as feeders to the Eocambrian Lighthouse Cove Formation on Belle Isle and the Cloud Mountain basalts of the Northern Peninsula, with which they show petrographic and chemical similarity (Williams and Stevens, 1969; Strong and Williams, 1971; Strong, 1975). A K:Ar date of 805 ± 35 million years for the diabase dykes led Pringle et al. (1971) to suggest that a nonsequence existed between the Lighthouse Cove Formation and the overlying lower Cambrian sediments. Stukas (1973), however, stated that this conventional age was a result of

Figure IIa: Geology of Western Newfoundland.



contamination with significant quantities of radiogenic argon, and obtained an age of 621 ± 6 million years for the dykes, using the $^{40}\text{Ar}/^{39}\text{Ar}$ technique, a result more in accord with the stratigraphic interpretations of Williams and Stevens (1969).

C. The Autochthonous Succession.

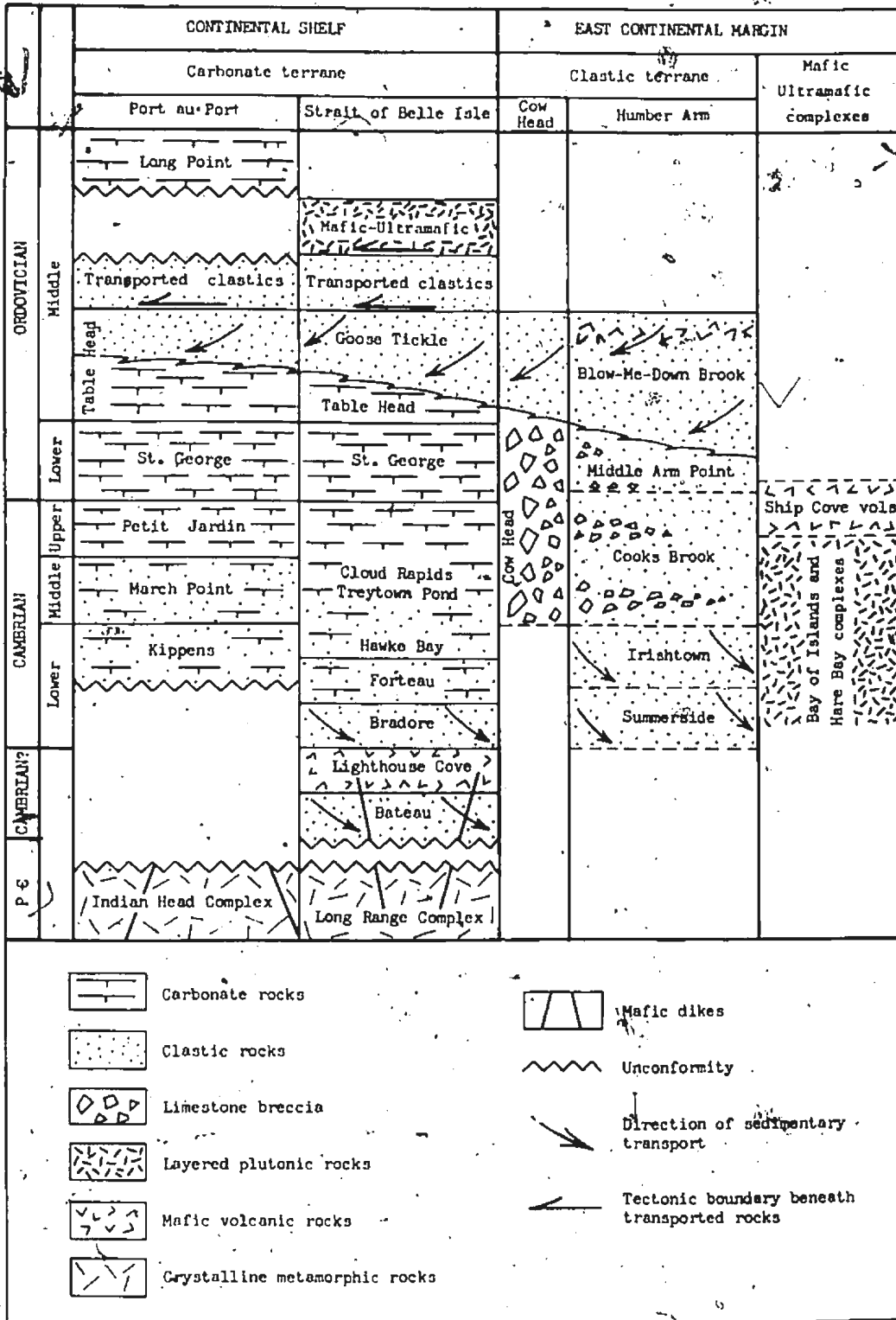
The autochthonous cover to the Grenvillian basement, ranging in age from early Cambrian to middle Ordovician, can be broadly divided into three units. The bottom unit of mainly sandstone and shale is succeeded by a middle limestone unit, and an upper unit consisting mainly of flysch deposits. A generalised section of the Cambro-Ordovician autochthonous sequence in western Newfoundland is shown in Fig. IIB.

i). Lower Unit

At the base of the lower unit are rocks of the Bradore Formation, consisting of conglomerates and quartzites overlain by cross-bedded, ripple-marked, iron-rich arkoses and mafic volcanics (Williams and Stevens, 1969). These sediments are scolithid bearing. In northern Newfoundland these successions unconformably overlie the Precambrian basement and thicken eastward. The Forteau Formation, composed of limestones, shales and silty dolostones, overlies the Bradore Formation conformably. Silty dolostones of the lower Forteau formation grade upward into oolitic limestones containing 'reeflike' Archaeocyathid masses (Fong, 1967).

Current bedded quartz-arenites of the Hawke Bay Formation conformably overlie the Forteau Formation, and are succeeded by shales, limestones and dolostones characterised by desiccation cracks and intraformational conglomerates, which have been assigned to the Cloud Rapids and

Figure Iib: Stratigraphic sections of Western
Newfoundland (after Williams, 1971).



Traytown Pond Formations. The upper contact of this series is not defined. In northwest Newfoundland these formations are in faulted contact with the Lower Ordovician St. George Formation. On the Port au Port Peninsula, the March Point Formation, composed of current-bedded, sub-arkosic sandstones, overlain by interbedded shales and limestones, is of probable age equivalence to the Hawke Bay formation (Swett and Smit, 1972). The limestones are oolitic and contain algal stromatolites and flake conglomerates.

ii) Middle Unit

The upper Cambrian and overlying lower Ordovician rocks are lithologically identical, and can be defined only on palaeontological differences. Even this is difficult since fossils are sparse, especially in the St. George Formation.

The March Point Formation is overlain by limestones, dolomitic limestones and dolostones of the Petit Jardin and St. George Formations. The Cambrian-Ordovician boundary is considered to lie in the lower part of the St. George Formation (Swett and Smit, 1972). Trilobite remains (Norwoodia sp.) and cryptozoa identify the upper Cambrian, whilst graptolites (Staurograptus sp.), cephalopods and brachiopods are present in the lower Ordovician (Schuchert and Dunbar, 1934). Limestones and dolomites predominate throughout the middle unit, the top of which is marked by about 350 metres of rubbly limestone, turbidites and shales of the middle Ordovician Table Head Formation.

iii) The Upper Unit

The upper unit of the autochthonous sequence is composed of a flysch deposit conformably overlying the Table Head Formation. It was

interpreted by Stevens (1970) as a distal turbidite sequence in its basal portion, being predominantly well-bedded and fine grained, but it passes upwards into coarser grained and thick bedded greywackes, interpreted as proximal turbidites. These represent an easterly derived, westward transgressing deposit which preceded emplacement of the transported masses. The flysch, which immediately underlies the Humber Arm Allochthon, was intensely deformed during emplacement of the allochthon. Since flysch deposits occur within the allochthonous rocks, confusion often arises in distinguishing autochthonous and allochthonous flysch. In the Port-au-Port area, however, the autochthonous greywacke is relatively well preserved. Most of the lithic fragments within this greywacke can be matched with rocks in the Humber Arm allochthon, detritus from the ophiolites being particularly prominent. It is thus postulated that the transported masses formed the source of the flysch deposits, during their emplacement.

A similar situation exists in northern Newfoundland where the autochthonous flysch under the Hare Bay allochthon is referred to the Goose Tickle Formation (Cooper, 1937; Tuke, 1968) and is of Llanvirn age. Again, the source of most lithic fragments can be found in the allochthon but the occurrence of shallow water limestone clasts is a puzzling feature since they have no apparent source in the Hare Bay Allochthon.

D. The Parautochthonous Succession.

Slices of carbonate rock, flysch and chert which are intercalated between the autochthonous flysch and the base of the transported rocks were interpreted by Stevens (1970) as parautochthonous 'scales' dragged under

the allochthon. Most of these are relatively small and have not been investigated in detail. Perhaps the largest and best described is the Penguin Hills Klippe (Lilly, 1963) made up of 150 metres of carbonate rock resembling autochthonous carbonates.

E. Interpretation.

The clastic sedimentary rocks of the basal portion of the autochthonous succession contain pebbles of metamorphic rock, granite and blue quartz derived from the basement to the west. The succeeding carbonate succession represents part of a broad bank that flanked the western margin of the proto-Atlantic ocean and shows stages of development in Scotland and Greenland as well as in western Newfoundland (Swett and Smit, 1972). This bank began to sink at the end of the lower Ordovician when deeper water shales and limestones were deposited. The sinking of the bank was roughly contemporaneous with the first easterly appearance of the transgressing flysch wedge.

Several correlations can be made between beds within the autochthonous sequence and in the transported succession. For example, clastic sedimentary rocks containing abundant metamorphic fragments are found in the klippen. Similarly the development of the carbonate bank coincides with a reduced or starved offshore facies in the transported sequence which can be interpreted as caused by a cut off in the western source terrain by the bank (Stevens, 1970).

F. Transported (Allochthonous) Rocks.

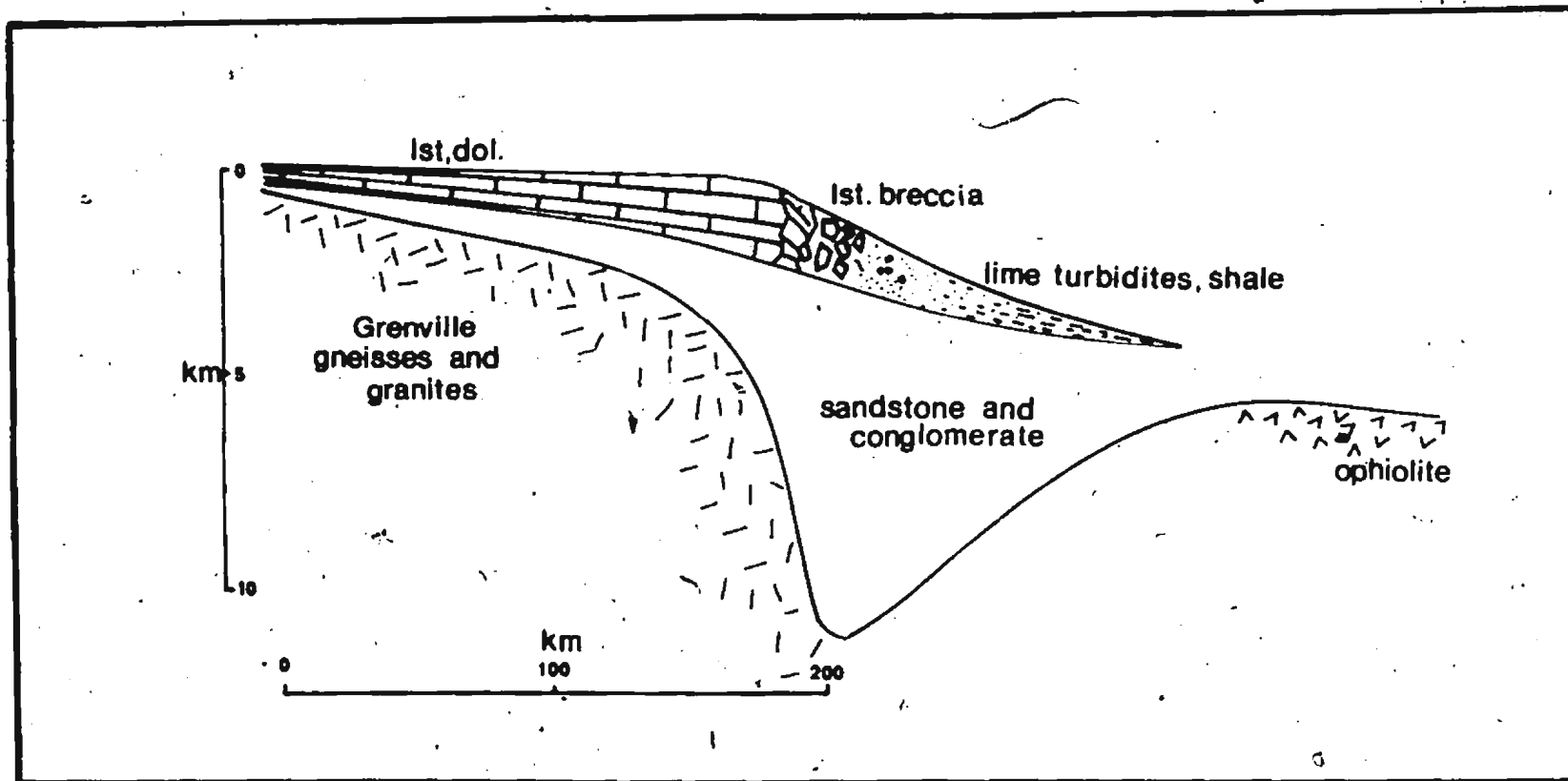
The discovery that part of the stratigraphic sequence in the Palaeozoic of western Newfoundland consisted of transported rocks was made relatively recently and a brief review of the stratigraphic nomenclature is therefore justified.

Schuchert and Dunbar (1934) described the Humber Arm Series as part of the continuous sequence of Lower Palaeozoic rocks lying to the west of the Long Range. The older part of the series was found to contain Middle Ordovician fossils whilst the youngest part was assumed to be Upper Ordovician in age. The Humber Arm Series was interpreted as a sequence (1,500 metres) of generally clastic rocks of deltaic origin with intercalated volcanic and intrusive rocks of varying types at its top. These igneous rocks were named the Bay of Islands Complex by Cooper (1936).

Palaeontological evidence showing that some of the beds of very different lithologies were contemporary (Johnson, 1941; Kindle and Whittington, 1958, 1963) led to the suggestion that much of the Humber Arm Series had been thrust from the east, over the carbonate bank which was essentially of the same age (Rodgers and Neale, 1963).

The allochthonous series, both the Humber Arm Allochthon and the Hare Bay Allochthon to the north, are now broadly classified into three sequences. These are; i. a condensed limestone-conglomerate and shale sequence, ii. a clastic succession, and iii. an ophiolitic sequence. It is thought that all are mostly contemporaneous, both with one another and with the underlying autochthon (Williams, 1971). Their spatial relationships before transportation are shown in Figure IIC.

Figure Iic: Spatial relationship of autochthonous and allochthonous rocks prior to transport: a reconstitution of the ancient continental margin.



i) The carbonate succession

The transported carbonate succession consists of coarse limestone-conglomerates and breccia beds with interbedded limestones and shales of Middle Cambrian to Middle Ordovician age, referred to the Cow Head Group. Because the sequence is relatively thin compared to nearby autochthonous successions of the same age span, and because the clasts in the conglomerate appear coeval with interbedded shales containing a trilobite fauna equivalent in age to graptolites of the shales, Stevens (1970) suggested that it represents a deposit formed at the edge of the carbonate bank, the latter being the persistent source of the clasts (see also Kindle and Whittington, 1958 and Baird, 1960).

ii) The clastic sequence

Stevens (1970) included most of the allochthonous clastic rocks of western Newfoundland in his Curling Group. He delineates a type section along Humber Arm noting a three-fold division of the Group. These divisions are; a) a lower quartzofeldspathic flysch and shale unit, b) a condensed middle unit of limestone conglomerate, carbonate flysch and shale, and c) an upper quartzofeldspathic flysch unit. His interpretation of the stratigraphy of the Curling Group is compared with previous accounts in Table 1.

a) The lower quartzofeldspathic flysch unit includes the Summerside, Meadows and Irishtown Formations of the Humber Arm Allochthon, and the Maiden Point and Canada Head Formations of the Hare Bay Allochthon. Green and red sandstones and conglomerates are overlain by green and red slates in both allochthons. The green and red rocks grade upwards into dark

TABLE I

Stevens' Divisions	Estimated thickness in feet	Stevens (1965)	Lilly (1963)	McKillop (1963)	Weitz (1954)	Walthier (1949)	Schuchert Dunbar (19			
H5 H4 H3 H2 H1	400 200 400 400 250	Woods Island Fm.	Western Sandstone Fm.	Not Studied	McIver's Fm.	Not Studied	HUMBER ARM SERIES UNDIVIDED			
G6 G5 G4 G3 G2 G1	10 80 300 30	Transition								
F2 F1	400 500	Middle Arm Point Fm.								
E2 E1	500 100	Cooks Fm.	Penguin Arm Limestone Fm.					calci-rudites	Upper and Lower Members	Upper Clastics Cooks Limestone tongue
D	300	Transition								
C6 C5 C4 C3 C2 C1	400 200 200 600 50 50	Meadows Fm.	Penguin Arm Irishtown and Summerside Quartzites					Upper and Lower shales and Quartzites		Lower Clastics
B	50	Transition								
A2 A1	50 250	Summerside Fm.			Top of the Lower Member		Cow Head Breccias			
Σ	5500-ft.		6000+ ft.		12,000+ ft.	4,000-8,500 ft.	5000+			

coloured shales, ankeritic greywackes, white quartzites and pebbly mudstones. Clasts within the lower flysch unit are mainly metamorphic rock fragments and blue quartz grains and appear to have been derived from Grenvillian basement rocks. Some rock fragments, such as quartzites, limestones and mafic volcanics may be matched with lower parts of the autochthonous succession. The sedimentary rocks in the Hare Bay Allochthon are locally interbedded with volcanic flows and cut by minor mafic intrusions chemically similar to those of the Lighthouse Cove Formation, which are unknown in the Humber Arm Allochthon.

The interpretation of the lower clastic division of the Curling Group as a deltaic deposit (Schuchert and Dunbar, 1934; Stevens, 1965; Lilly, 1963) was revised by Stevens (1970). It is more probable that the rocks represent deposits of deep sea turbidity currents. The conglomerates may thus represent lenticular deposits fed from submarine canyons. Analogous sediments are found on the present day Atlantic continental rise and are termed flysch by Dietz (1963).

b) In Humber Arm, the middle division of the Curling Group includes the Cook's Brook Formation, the Cook's limestone and the Middle Arm Point Formation. Only one unit of the carbonate flysch division has been recognised in the Hare Bay Allochthon, where it is known as the Northwest Arm Formation.

The division consists primarily of a predominantly lime-breccia unit overlain by platy, grey limestone with black shale and rare limestone breccia. The youngest part of the division is made up of green and black laminated shales. It is of Middle Cambrian to Late Arenig age and contains

a trilobite fauna characteristic of the outer detrital facies of a carbonate bank (Palmer, pers. comm. in Stevens, 1970). The succession differs from the Cow Head Group in the paucity of carbonate conglomerate, but it exhibits similar slump and resedimentation structures resulting in platy limestone fragments chaotically dispersed in a friable matrix. The major part of this middle division probably represents a period of slow sedimentation. The regular alternation of shale and limestone and current bedding suggest a deposition from turbidity currents, although no grading and bottom markings have been recognized. The source of these turbidity currents was most probably a distant site of shallow water carbonate sedimentation.

c) The quartzofeldspathic flysch unit forming the upper part of the Curling Group has been recognized only in the Humber Arm Allochthon. The unit overlies the carbonates and shales diachronously, older basal deposits being found to the west. The contact is generally marked by up to 350 metres of siliceous green shale with silty interbeds (Stevens, 1965), or red-green or dark brown cherts. Volcanic rocks of the Wood's Island Member occur towards the base of the sequence in places and associated dykes are known to cut the Humber Arm sedimentary rocks to the northeast of Trout River Pond. Above the basal rocks a thin-bedded sequence of greywackes and shales gives way to massive, coarse-grained arkoses, in places with striations, flute marks and load casts. The flysch mineralogy suggests several major sources of the detritus. Microcline granite and soda granophyre fragments must have been derived from a silicic intrusive terrain; chrome spinel and gabbroic and ultramafic rock fragments

were most probably derived from an ophiolitic terrain and thus may define a minimum age for the uplift and erosion of the ophiolites to the east; and sedimentary clasts representative of the lower quartzofeldspathic flysch unit of the allochthon are also found (Stevens, 1970). The uppermost 130 meters of clastic material, below the contact with the ophiolites, are separated from the flysch by a thick and significant mélangé zone. In some sections the upper flysch unit may be completely replaced by this mélangé which then rests directly on the middle division of carbonate flysch. Stevens (1970) interprets this mélangé as an olistostrome derived from an oversteepened delta front which was subsequently deformed by the overriding ophiolites and cut by a regional cleavage.

The upper quartzofeldspathic flysch unit occupies an important position regionally in that it indicates a transition between eastward sediment transport from craton to eugeosyncline and westward transport from uplifted eugeosynclinal material towards the craton.

iii) The ophiolites

Thick ophiolite slices and associated rocks were thrust westward over the transported clastics and form the Upper division of the Humber Arm and Hare Bay Allochthons. These slices are considered in more detail in Chapter III.

A stratigraphic analysis of the superposed successions described above suggests their interpretation as integral parts of a continental terrace wedge, and continental rise prism (Stevens, 1970). According to this model, the ophiolitic slices represent oceanic crust and mantle that

originally ~~by~~ east of the continental rise and were later transported westwards (Fig. IIC).

Following the emplacement of the allochthons, deposition in Zone A was continued, but is represented only by the Middle Ordovician Long Point Formation, the Upper Silurian-Lower Devonian Clam Bank Formation, and local occurrences of Mississippian limestone and sandstone. Although it is difficult in places to distinguish between autochthonous and allochthonous flysch, in Port au Port the Long Point Formation clearly overlies the allochthon unconformably, whilst further to the west similar rocks overlie autochthonous flysch. These relationships define a Middle Ordovician upper time limit for the emplacement of the allochthons.

CHAPTER III

THE UPPER THRUST SLICES

A. Introduction:

The 'Upper Thrust Slices' are a number of individual sheets constituting the 'ophiolite sequences' described by Stevens (1970) as forming the upper parts of the allochthonous terrains in Humber Arm and Hare Bay. The slices are made up of Lower Ordovician and possibly older igneous and metamorphic rocks, only some of which are clearly ophiolitic. In Humber Arm a complete ophiolite sequence is preserved in the highest slice. At Hare Bay, the highest slice is composed of peridotite and represents the remnants of an ophiolite sequence.

In Humber Arm, rocks of the Upper Thrust Slices can be subdivided into four distinct rock groups. These are: (i) the Skinner Cove Formation, (ii) the Old Man Cove Formation, (iii) the Little Port Complex, and (iv) the Bay of Islands Complex; and each is represented in a separate slice (Williams, 1973). Structural slices that are composed of the same rock group have been referred to as slice assemblages by Williams (1973). Thus the four rock groups above define four slice assemblages, and in each case the slice assemblage is designated by the same name as the rock group that constitutes it. The Skinner Cove, Old Man Cove, Little Port and Bay of Islands slice assemblages in most places lie directly upon transported sedimentary rocks of the Curling Group, but locally they lie upon one another, everywhere maintaining a consistent structural stacking order. This stacking order is from top to bottom:

TOP: The Bay of Islands slice assemblage
The Little Port slice assemblage
The Old Man Cove slice assemblage
BOTTOM: The Skinner Cove slice assemblage

and the relationships between the assemblages can be depicted diagrammatically as in Fig. IIIa. Thus, the Skinner Cove slice assemblage everywhere lies on Humber Arm sediments; the Old Man Cove slice assemblage lies upon the Skinner Cove slice assemblage; the Little Port slice assemblage lies upon the Old Man Cove slice assemblage (or structurally lower slice assemblages); and it is clear that if the Bay of Islands slice had been transported a little further west it would lie locally upon the Little Port slice assemblage (e.g. near Trout River). There are no known reversals of this stacking order in the map area.

B. The Skinner Cove Formation.

i) Outcrop and distribution

The Skinner Cove Formation contrasts sharply with the other rocks of the area and defines a slice assemblage which occurs west of the main ophiolite assemblage at three major localities. The slice assemblage is the lowest in the stacking order of the 'upper thrust slices'. The type outcrop area of the Skinner Cove Formation is at Skinner Cove (Fig. IIIb; Plate Ia) where rock types of the assemblage crop out over an area approximately 9 kms long and 1 km wide. Other occurrences are at Chimney Cove and Beverly Head to the south. Whether the three occurrences represent the remnants of a once continuous single slice, or a number of separate slices at the same structural level, is debatable. Outcrops of

Figure II.1a: Relationships between and structural stacking order of Slice Assemblages, Humber Arm Allochthon.

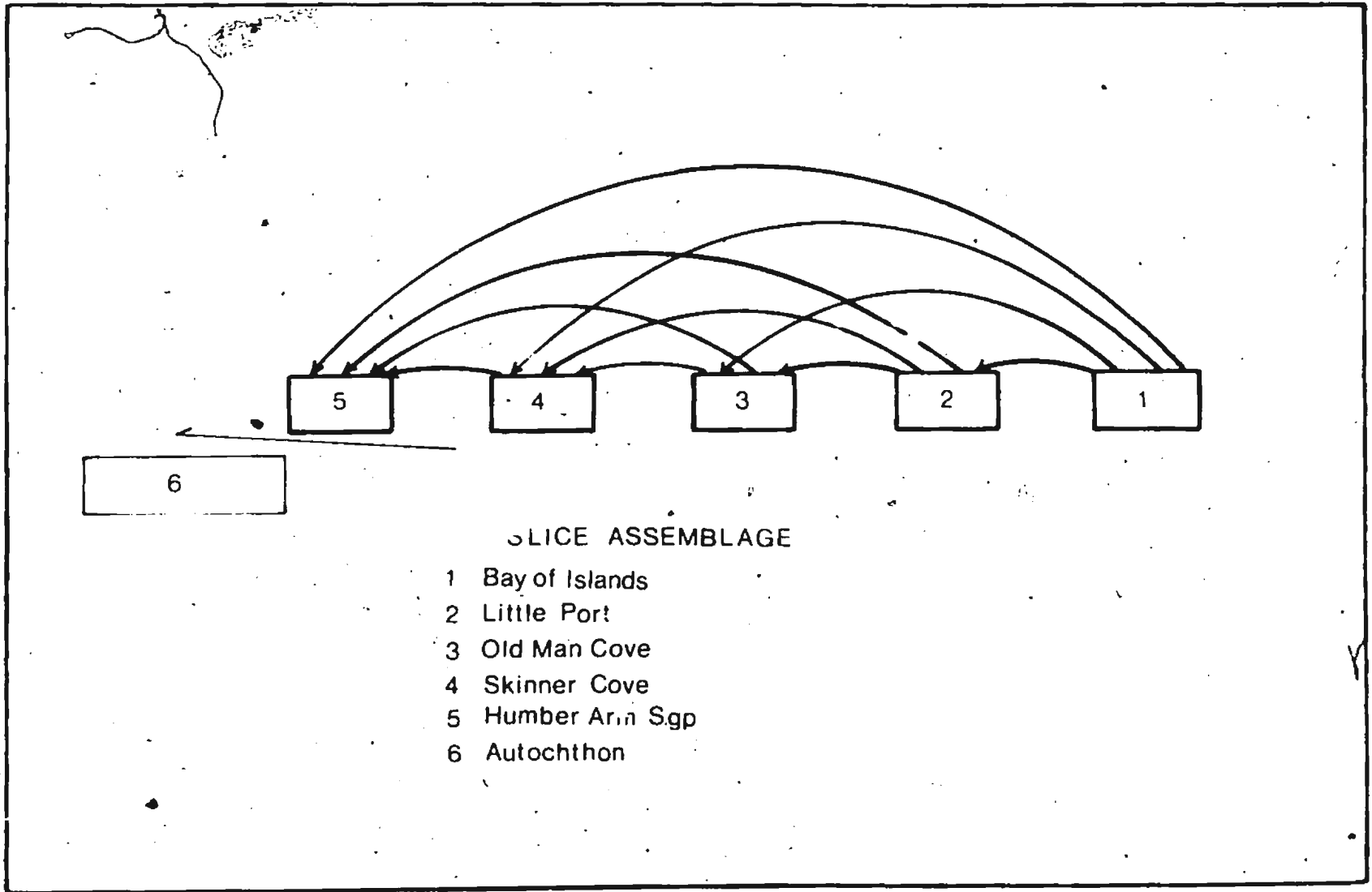


Figure IIIb: Geological Map, Bay of Islands
Region (In pocket).

volcanic rocks just east of Trout River (Plate Ib) and east of Chimney Cove suggest a possible continuation of the Skinner Cove Formation under the overriding slice. Alternatively, these may be detached blocks deposited in chaotic sediments of the transported clastic sequence by the overriding Skinner Cove slice, during emplacement.

ii) Lithology

The Skinner Cove Formation consists of steeply dipping pillow lavas, with interbedded basaltic pillow breccias, agglomerates, aquagene tuffs and red and green laminated siltstones and shales (Plates IIa and IIb). The tuffs and sediments exhibit graded bedding and slump features in places, but the agglomerates are relatively poorly sorted and there is a considerable range in the size of fragments and blocks (Plate IIIa). Fossils recently discovered by A. R. Berger (Acrothretaceans cea) in the sedimentary sequence indicate a Tremadocian age for these rocks. Calcium carbonate cements the coarser tuffs and pillow breccias and also fills vesicles and interstices in the pillow lavas and scoria (Plate IIIb). The presence of this calcite, in some cases forming up to 90% of the pillow breccia often defines bedding within the pyroclastic rocks (Plate IIa). It also makes the Skinner Cove volcanics quite distinct from volcanic rocks of the main ophiolite sequence, and suggests a different (shallower?) environment of deposition. In places the volcanics are cut by massive diabase dikes with well developed chilled margins (Plate IVa). Both the volcanics and the dikes which cut them appear to be very fresh in comparison with the other rocks of the higher structural slices.



Plate Ia: Well-bedded pyroclastic deposits at Skinner Cove.



Plate Ib: Agglomeratic pyroclastics of possible Skinner Cove affinity just east of Trout River.



Plate IIa: Pillow breccias and aquagene tuffs, Skinner Cove Formation.

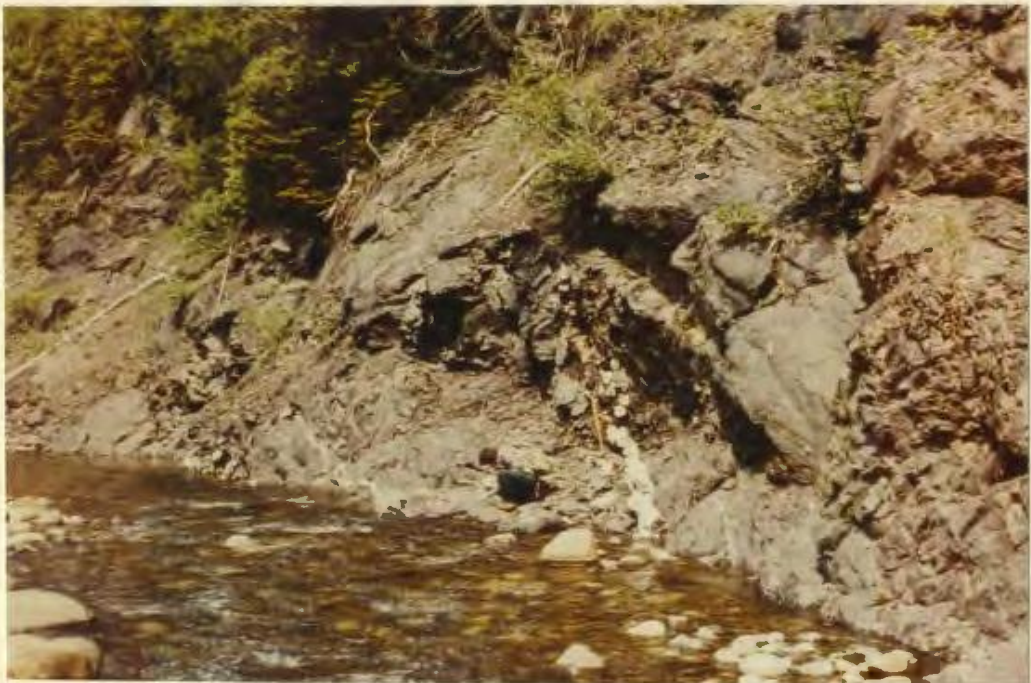


Plate IIb: Sedimentary rocks of Skinner Cove Formation.



Plate IIIa: Poorly sorted volcanogenic deposits, Skinner Cove.



Plate IIIb: Calcium carbonate cement is dominant in the volcanoclastic rocks of Skinner Cove Formation.

iii) Mineralogy and chemistry

Although apparently fresh in hand specimen, in thin section the volcanic rocks range from extremely altered to almost unaltered.

a) Porphyritic basalts: These contain between 35% and 45% euhedral to subhedral phenocrysts of plagioclase and titaniferous augite (average dimensions - 1 mm long axis) in equal amounts, and lesser amounts of olivine set in an aphanitic matrix (Plates IVb and Va). The plagioclase in most cases averages An_{43} (andesine) in composition, although it may be zoned from a core of approximately An_{45} to rims of approximately An_{32} (Plate Vb). Crystals of plagioclase which are fractured and exhibit sieve textures and chequerboard twinning are not uncommon (Plate VIa). The titanaugite is pale-pink to dark-pink pleochroic and commonly zoned, being more titanium-rich towards the rims (Plate VIb). Olivines are of high magnesium content (Fo_{90} from 2V measurements) and no zoning has been recognised. On the basis of this mineralogy, the rocks have been classified as ankaramites (Strong, 1974).

The matrix consists of plagioclase microcrysts, some augite and olivine and dusty magnetite which in places forms well developed euhedral microcrysts. In some sections (Plate VIIa) intersertal glass, rich in opaque oxides, is preserved and shows a development of plagioclase crystallites. Segregation vesicles are filled with secondary calcite, pumpellyite and rarely clinozoisite, and quartz occurs as growths along fractures. Where alteration has proceeded to a considerable degree, chlorite replaces pyroxene, serpentine and iddingsite replace olivine, and clinozoisite and sericite replace feldspars. The olivine is generally



PLATE IVa: Dike with well developed chilled margins cutting agglomerates, Skinner Cove.

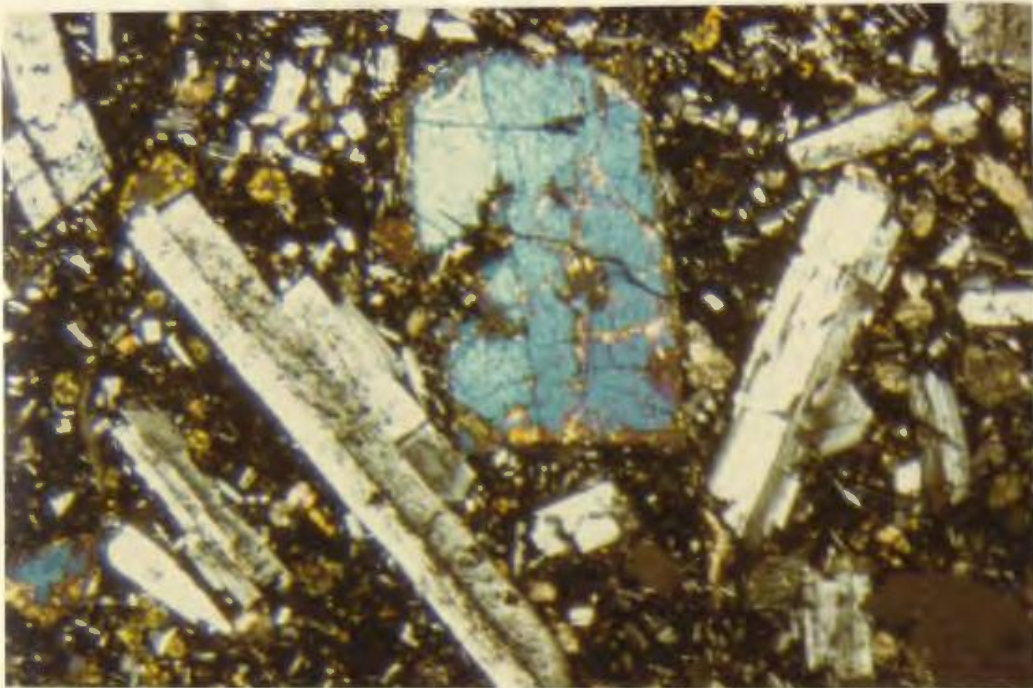


PLATE IVb: Titanite and plagioclase phenocrysts in basalt, Skinner Cove. X nicols, mag. x .75.

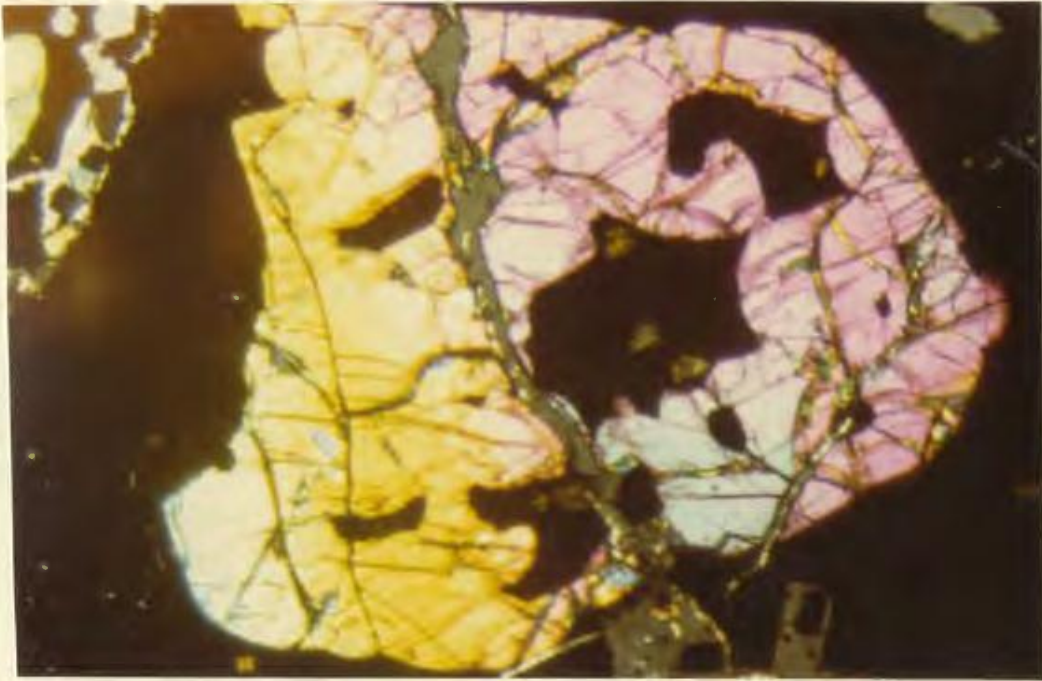


PLATE Va: Large resorbed olivine crystal in glass matrix.
Skinner Cove olivine basalt. X nicols x 65.

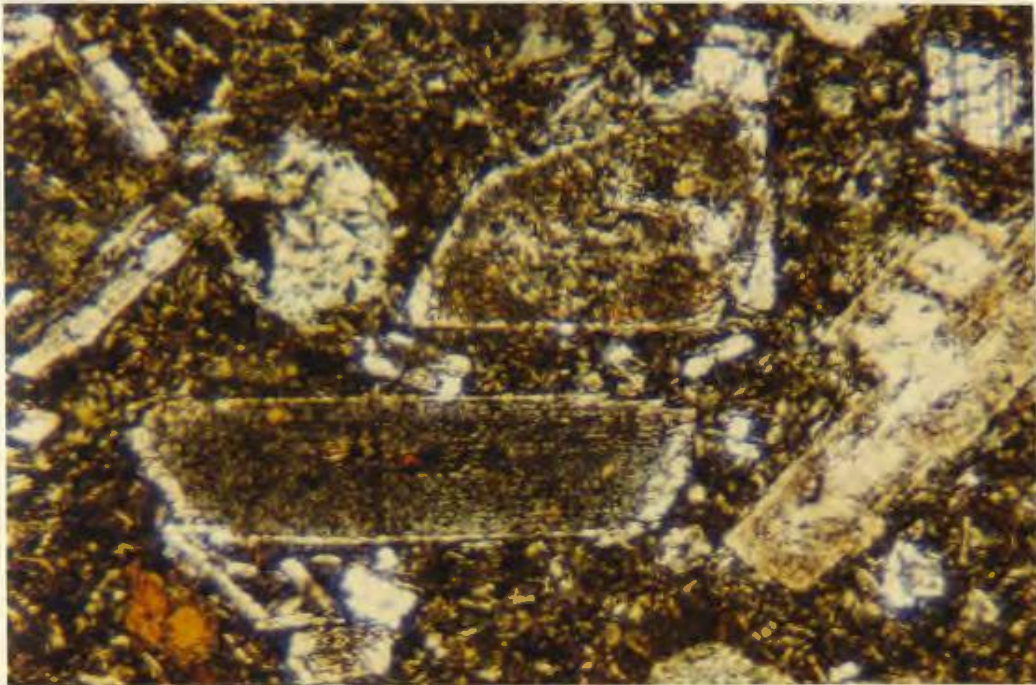


PLATE Vb: Zoned plagioclase in Ankarinite, Skinner Cove.
X nicols x 50.

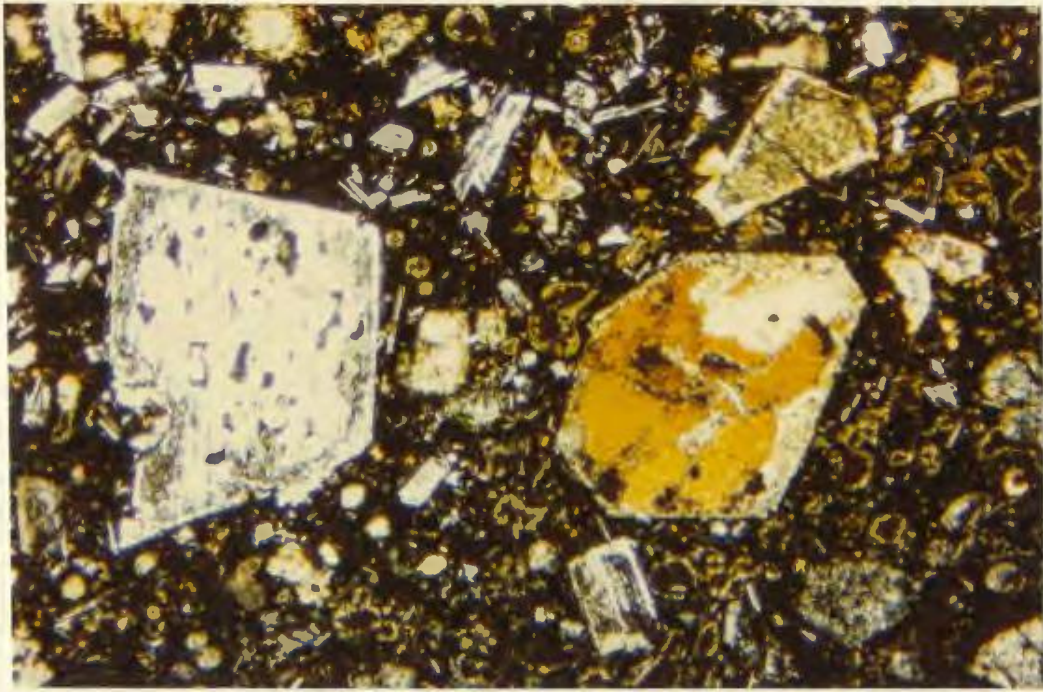


PLATE VIa: Sieve texture in plagioclase and alteration of titanite phenocrysts. Skinner Cove, Ankaranite. X nicols x 50.

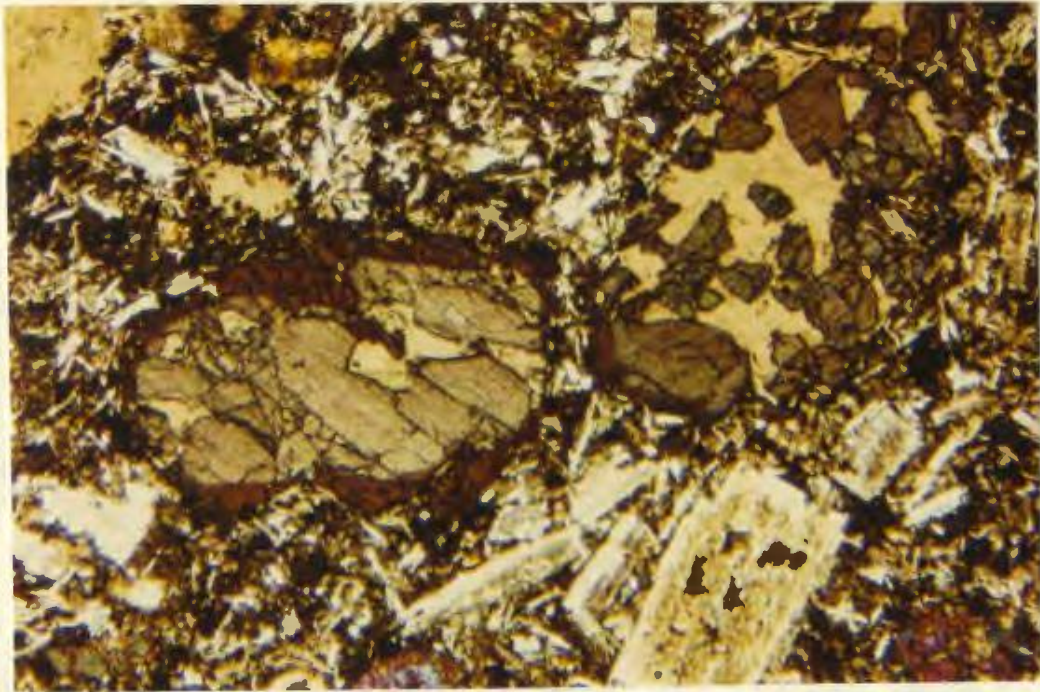


PLATE VIb: Zoned titanite phenocrysts. Skinner Cove Basalt. X nicols x 48.

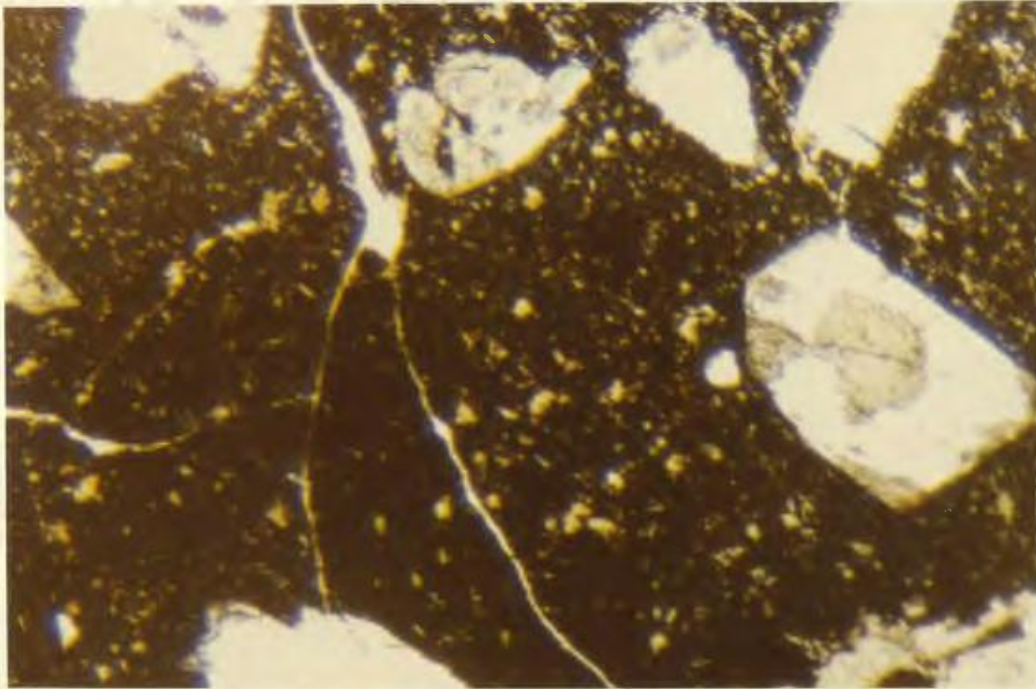


PLATE VIIa: Skinner Cove basalt; intersertal glass showing development of plagioclase microlites. X nicols x 150.

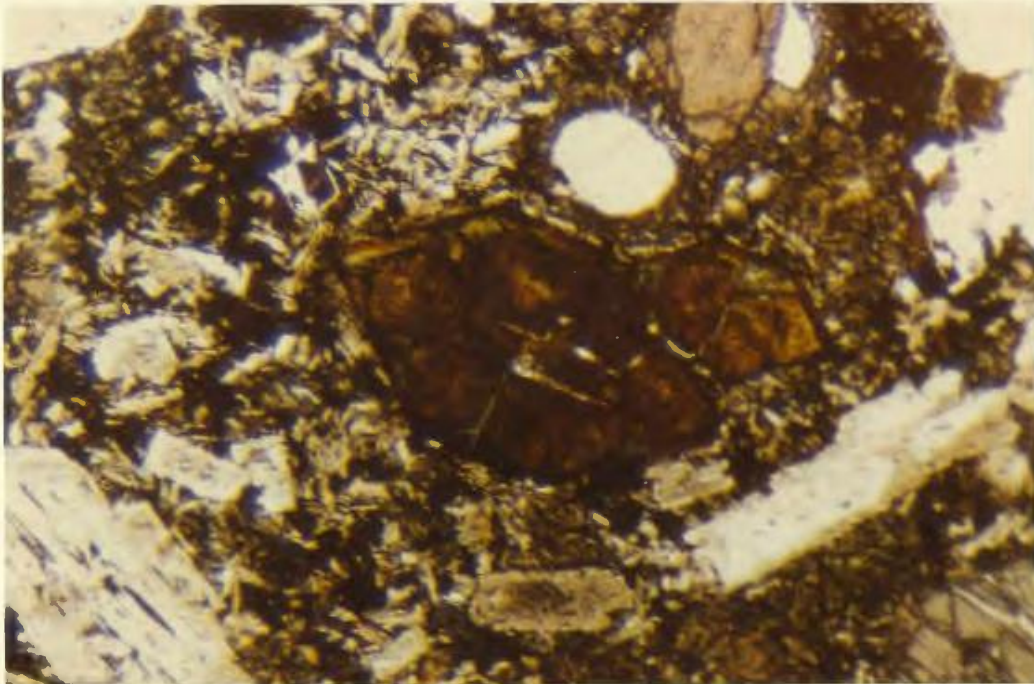


PLATE VIIb: Olivine phenocrysts completely replaced by iddingsite. Olivine-basalt, Skinner Cove. X nicols x 50.

completely pseudomorphed by iddingsite (Plate VIIb).

Basalts and basaltic scorias have been collected, both containing amounts of brown-black glass with plagioclase crystallites. A considerable number of the vesicles in the scoria contain calcite, and quartz and pumpellyite are also present.

b) Non-porphyrific flows: Non-porphyrific or sparsely porphyritic flow rocks composed almost entirely of plagioclase, but with some rare K-feldspar phenocrysts, titaniferous magnetite and olivine microphenocrysts, and displaying well-developed fluidal plagioclase textures (Plate VIIIa), have been termed trachytes (Strong, 1974). Fine grain size makes the composition of the plagioclase optically indeterminate.

Strong (1974) presented analyses for a series of samples which indicated the strongly alkalic nature of the Skinner Cove volcanics (Fig. IIIc). The chemical analyses, which show a high concentration of large cation trace elements, support an interpretation of a continuous petrogenetic series from ankaramite to trachyte. Although it could be argued that secondary calcium carbonate has contributed to the under-saturated nature of the norms (in that CaO was used to calculate part of the normative augite) CO₂ contents are not particularly high and there appears to be no direct correlation between CO₂ and CaO contents of analysed specimens, suggesting little contamination by vein or vesicular carbonate (Strong, personal communication, 1974).

iv) Significance

The fossil evidence suggests that the Skinner Cove volcanics were formed at the time inferred for the formation of the ophiolites.

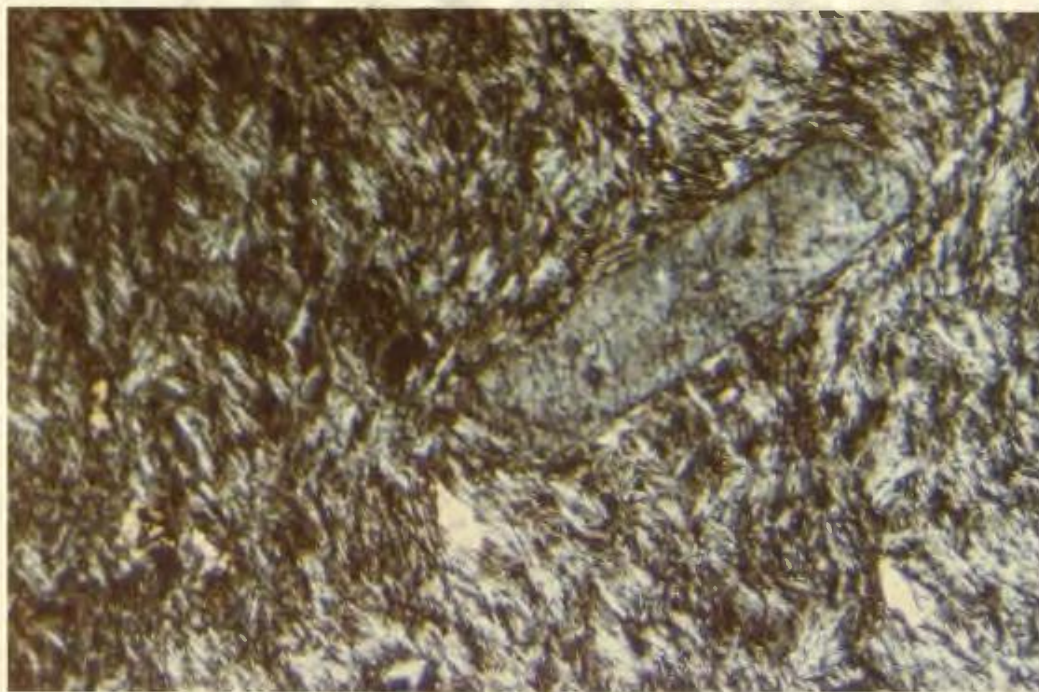


PLATE VIIIa: Fluidal textures in Skinner Cove trachyte.
X nicols x 110.

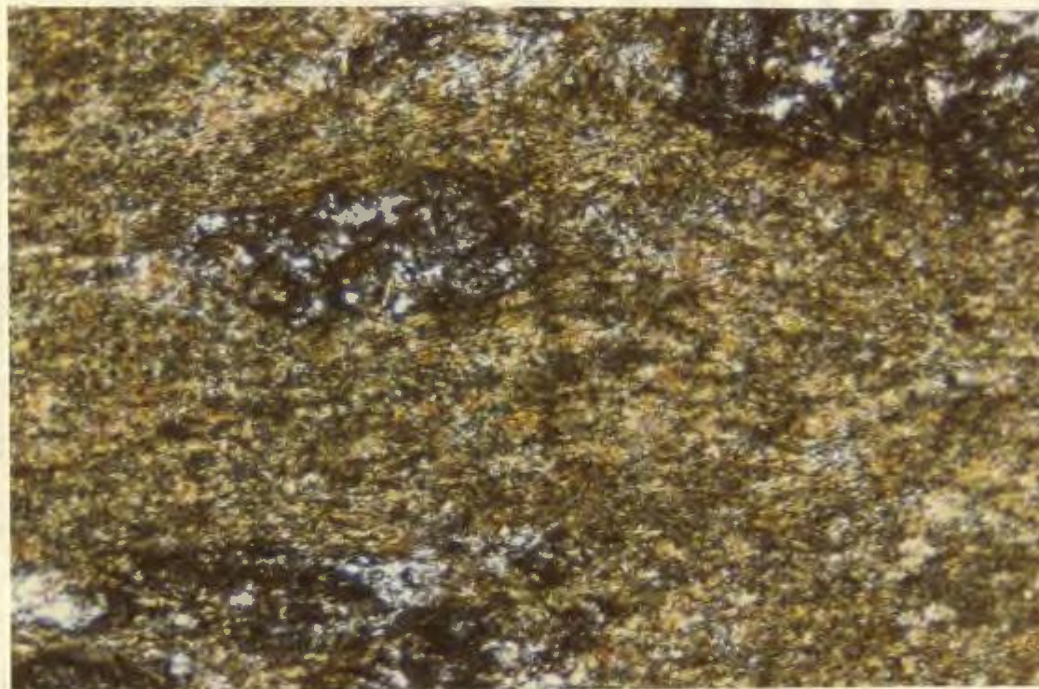
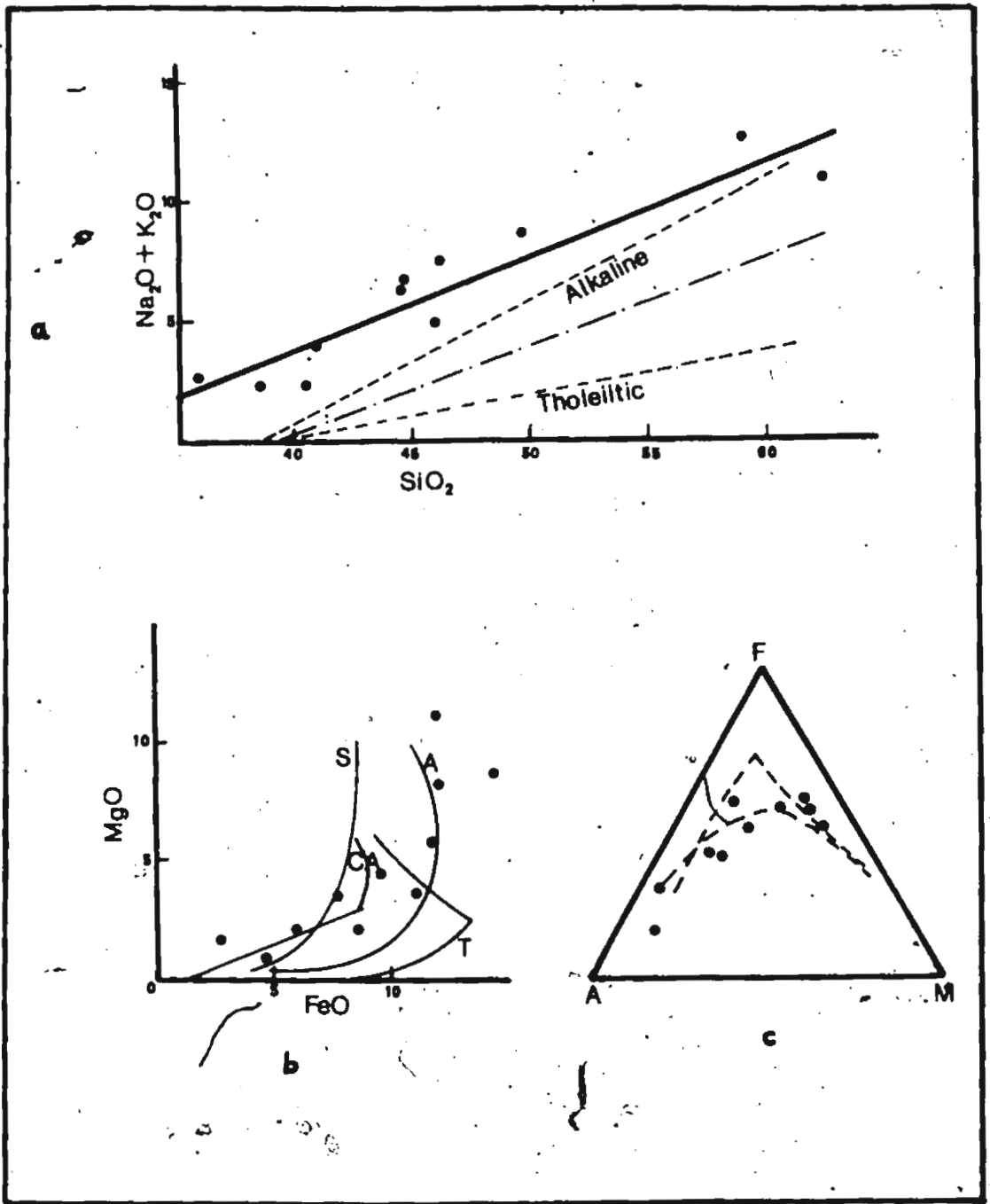


PLATE VIIIb: Fragmental greenschist - Fragments are dominantly
granulated quartz. Old Man Cove, X nicols, x 100.

Figure IIIc: Variation diagrams for Skinner Cove volcanics (after Strong, 1974).

- a) Total alkalis vs silica (Hawaiian alkaline and tholeiitic trends indicated. Solid line - Skinner Cove regression).
- b) MgO vs FeO S - Shoshonite
 CA - Calc-Alkaline
 A - Alkaline
 T - Tholeiitic
- c) F.M.A. (Hawaiian alkaline - tholeiitic trends indicated).



However, it is clear that the Skinner Cove basic rocks are chemically distinct from the Bay of Islands ophiolite suite. Also outstanding is the total lack of deformation, and the extreme freshness of the volcanics when compared to the polyphase deformation and amphibolite facies metamorphism of the tectonically overlying Little Port Complex, and the burial metamorphism evident in the ophiolites.

There are a number of explanations and subsequent arguments which may be suggested for the origin of the Skinner Cove Formation and its relationship with the Little Port and Bay of Islands Complexes.

These are:

a) The Skinner Cove volcanics represent an off-ridge axis suite comparable to those found on the flanks of modern ridges.

b) The Skinner Cove volcanics are a result of alkaline volcanism that took place at the site of subduction of oceanic crust.

c) The Skinner Cove volcanics represent alkaline volcanism produced during continental rifting and break up. In this case it would be likely that peralkaline rocks formed part of the Skinner Cove suite (W. R. Church, written communication with D. F. Strong, 1974).

Strong (1974) concluded that "the [available] evidence is best interpreted as indicating an 'off-axis' origin for the Skinner Cove sequence, produced after the [burial] metamorphism and migration of the ophiolite away from the central ridge axis" and "... such an interpretation is of local importance in that it implies that the metamorphic and tectonic features of the Bay of Islands and Little Port Complexes were

produced before eruption of the Skinner Cove sequence, presumably at the ocean ridge."

The implication that the burial metamorphism of the ophiolites took place immediately after their formation at an ocean ridge seems plausible since rocks metamorphosed to similar grades are dredged from present ocean ridges (Melson and van Andel, 1966; van Andel and Bowin, 1968; Aumento and Loncarevic, 1969). Highly deformed and mylonitised ultramafic and mafic rocks from St. Paul's Rocks, equatorial Atlantic, have been described by Melson et al. (1972) as forming during emplacement at the mid-Atlantic Ridge. Whether the complex intrusive, metamorphic and tectonic history of the Little Port Complex could have taken place in a similar environment, is debatable. If it did, then the deformed Little Port Complex might be expected to have fresh, unmetamorphosed dikes of Skinner Cove cutting it and similar volcanics associated with it. If however, the Skinner Cove volcanics predate the deformation of the Little Port Complex, then metamorphosed equivalents of the Skinner Cove volcanics may actually form part of the Little Port Complex. The relatively fresh dikes and pillow lavas that cut older foliated rocks of the Little Port Complex are remarkably similar in mineralogy and petrography to Skinner Cove rocks (see page 42) which would support the former argument.

If the Skinner Cove volcanics represent a stage in the early formation of an island arc, they presumably arose by partial melting of upper mantle material at depths in the order of 80 kms, and intrusion

in local tensional zones. Such volcanism has been described for the early formation of the Lesser Antilles island arc (Siggurdson, et al.; 1973) and Japan (Miyashiro, 1974). However, the Tremadocian age of the Skinner Cove Formation from fossil evidence is in conflict with the age of earliest recognisable island arc volcanism in central Newfoundland. The upper part of the Snooks Arm Formation (Arenig) was identified as island arc tholeiites by Upadhyay (1973) and lies directly upon ophiolitic rocks that are interpreted as obducted oceanic crust. Thus not only do the Skinner Cove volcanics appear to be older than the apparent initiation of subduction, but are also of distinctly different affinities (i.e. alkaline vs. tholeiitic) to those rocks that date the earliest subduction in central Newfoundland.

Similarly, the age of the Skinner Cove Formation is not correlatable with either of the major periods of rifting and tensional tectonics proposed in models of the development of Newfoundland. The formation of the Proto-Atlantic ocean during the lower Cambrian predated the volcanics and that of the present Atlantic during the Mesozoic clearly postdates their formation.

Church (personal communication with D.F. Strong) has mentioned a comparison of the Skinner Cove volcanics with other late Cambrian alkaline volcanics in the North Atlantic region including Spain and North Africa. His closest analogues are the Reddits Cove gabbro and associated dikes of the Burlington Peninsula and the Tayvallich lavas in the Dalradian of Scotland. This correlation, however, does not correspond with Graham's (1974) interpretation of the Tayvallich lavas as tholeiitic flood basalts.

more comparable to the flood basalts of western Newfoundland, of lower Cambrian age.

On the basis of available evidence, the writer therefore agrees with Stroffg (1974) in his interpretation of the Skinner Cove volcanics as an off-ridge axis suite, and suggests that they do probably post-date the metamorphism and deformation of the Little Port Complex, and almost definitely post-date the burial metamorphism of the ophiolites. Further arguments are discussed together with the significance of the Little Port Group on page 79.

C. The Old Man Cove Formation.

i) Location and outcrop

Polydeformed greenschists and minor amphibolites form a slice assemblage at Trout River (Fig. IIIb). This slice assemblage structurally overlies the Skinner Cove Formation and is itself overlain to the east by amphibolite and foliated gabbros of the Little Port slice assemblage. Only two areas of outcrop are known, and both are fault-bounded and relatively small in areal extent. To the immediate north of Trout River, greenschists form a thin strip about 2.5 km long and 500 m wide. The other area, probably once continuous with the first, lies to the south of Trout River and on the coast, and is approximately half that size. The two areas are now separated by coastal erosion.

ii) Lithology and structure

The Old Man Cove Formation consists of polydeformed, grey-green coloured schists. Actinolite-chlorite-albite schists are dominant and have variable amounts of epidote, carbonate and biotite. Interbeds of

graphitic-biotite schist and albite-muscovite-chlorite psammites occur and small lenses of amphibolite, with not more than 10 to 20 cm dimensions have been recorded. Some rocks are fragmentary, although generally only on the microscopic scale. The schists probably represent the metamorphosed equivalents of mafic tuffs. They have been compared in metamorphic grade and style of deformation to the Birchy Schists of the Fleur de Lys Supergroup (Williams, 1973).

Tight isoclinal folds are the prominent structural feature in the greenschists and affect at least one earlier schistosity. Tension gashes are common cutting across the fold axes and quartz and calcite occur in stringers and knots in the fold hinges. The tension gashes are probably related to strain-slip schistosesities, crenulation-cleavages and kink-bands which are numerous. The strain-slip schistosesities and crenulations are late stage structures and the kink-bands represent the youngest fold structures in the rocks. The amphibolitic pods all have schistose margins representing retrogression of the amphibolite to chlorite and biotite during the strain-slip fabric development.

Although no original lithological features are preserved, it seems that the schists were originally volcanic or tuffaceous in nature. Rocks with a fragmental appearance in thin section are rare (Plate VIIIb) and most greenschists are extremely dense and fine-grained (Plate IXa).

iii) Mineralogy

The greenschists consist dominantly of albite, chlorite and actinolite. Variable amounts of epidote, zoisite, quartz and opaques

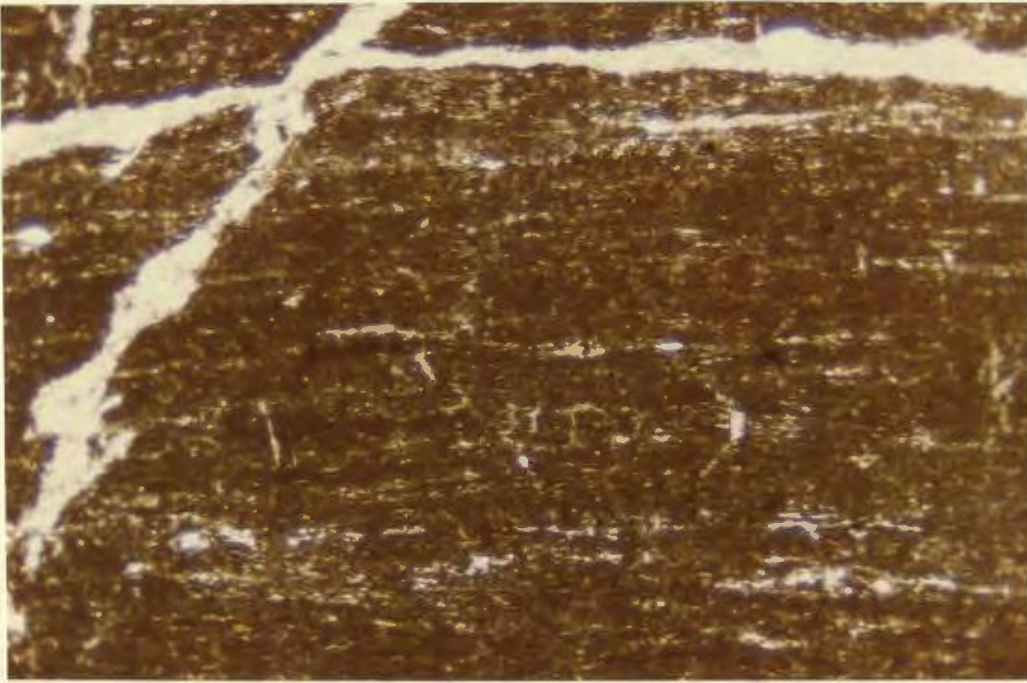


PLATE IXa: Dense fine-grained greenschist, Old Man Cove Formation. X nicols x 110.

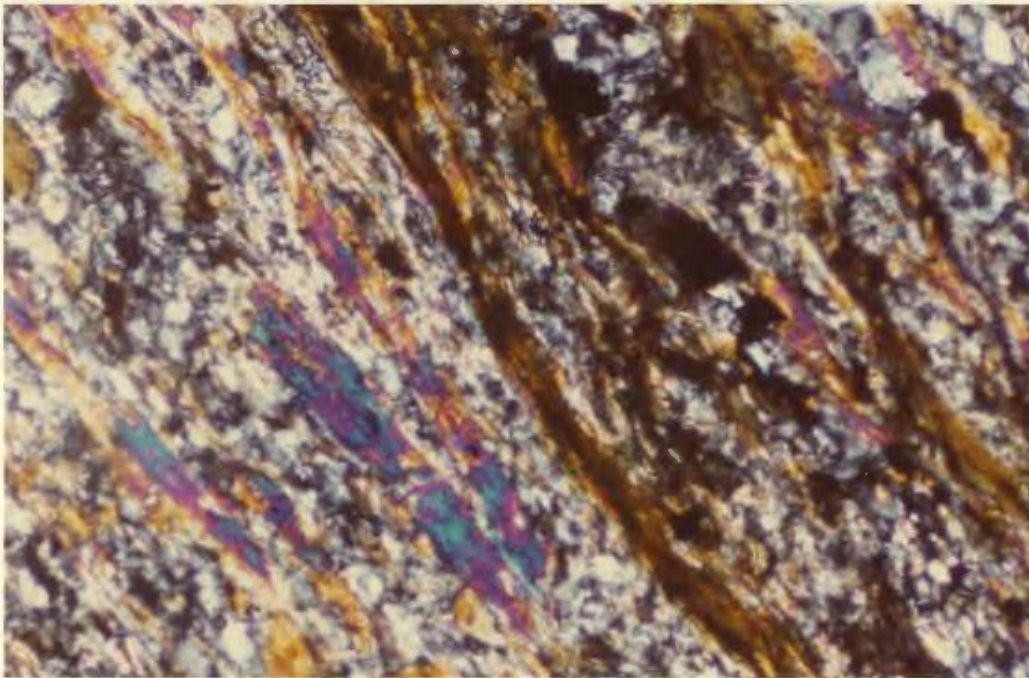


PLATE IXb: Development of biotite in graphitic-hornblende schist. Old Man Cove Formation. X nicols x 190.

are also present, and biotite occurs rarely in graphitic rocks (Plate IXb). Grain size is generally small (less than .02 mm). Variations in grain size are unlikely to represent original sedimentary bedding features since flattening and recrystallisation during deformation is intense.

Albite and quartz forming veins and segregations display lobate sutured grain boundaries and undulose extinction (Plate Xa). Other minerals are finely intergrown and in the case of platy or long prismatic forms may parallel the main schistosity.

iv) Significance

Within the slice groups, greenschists are only found in the Old Man Cove Formation, and forming part of the aureole of the Bay of Islands Complex. The resemblance of these two occurrences to one another in metamorphic and structural style suggests that the Old Man Cove greenschists might represent aureole rocks that became detached from the ophiolite slice during transportation and incorporated in the stacking order as a slice assemblage of their own. Their position directly beneath the Little Port Complex slice suggests that they may alternatively represent a basal aureole of that slice, which became effectively detached during a late stage of emplacement. The lack of a mélangé zone between these two slices could indicate a small relative distance they must have travelled.

As an alternative to their derivation as dynamothermal aureole rocks, the greenschists may be transported equivalents of part of the Fleur de Lys Supergroup. In this case, the rocks may or may not have been deformed by processes related to the obduction of the transported ophiolites. Kennedy (1973) has suggested that the deformation of the

Fleur de Lys sediments and volcanics took place in the late Cambrian to Tremadocian during closing of an early Cambrian marginal ocean basin. Swinden and Strong (in press), Bursnall and Dewit (1975), and Smyth (1973), however, suggest that the Fleur de Lys was deformed in the early Ordovician during the first stages of obduction of the ophiolites. In this case, transported equivalents of the Fleur de Lys, i.e. the Old Man Cove Formation, may be considered part of an accretion mélange as described by Karig (1971, 1972). The respective models are discussed further in Chapter VII.

D. The Little Port Complex.

i) Location and outcrop

The Little Port Complex structurally overlies sedimentary rocks of the Humber Arm sequence in most places. From Bonne Bay, south to Chimney Cove, the complex is represented by a single slice. In the Lark Harbour area, a number of superposed slices exist within the complex, separated by mélange zones, and small detached masses overlie quartzitic sandstones just east of Little Port. The complex is known to continue south of the map area as far as the mouth of Serpentine River.

ii) Lithology

Generally rocks of two different, although not necessarily widely separated, ages are represented in the Little Port Complex. The first group consists of gabbros, amphibolites and quartz-diorites, which are all highly deformed and metamorphosed. These are cut by dikes which feed volcanics, both of which are relatively unmetamorphosed and do not exhibit tectonic fabrics.

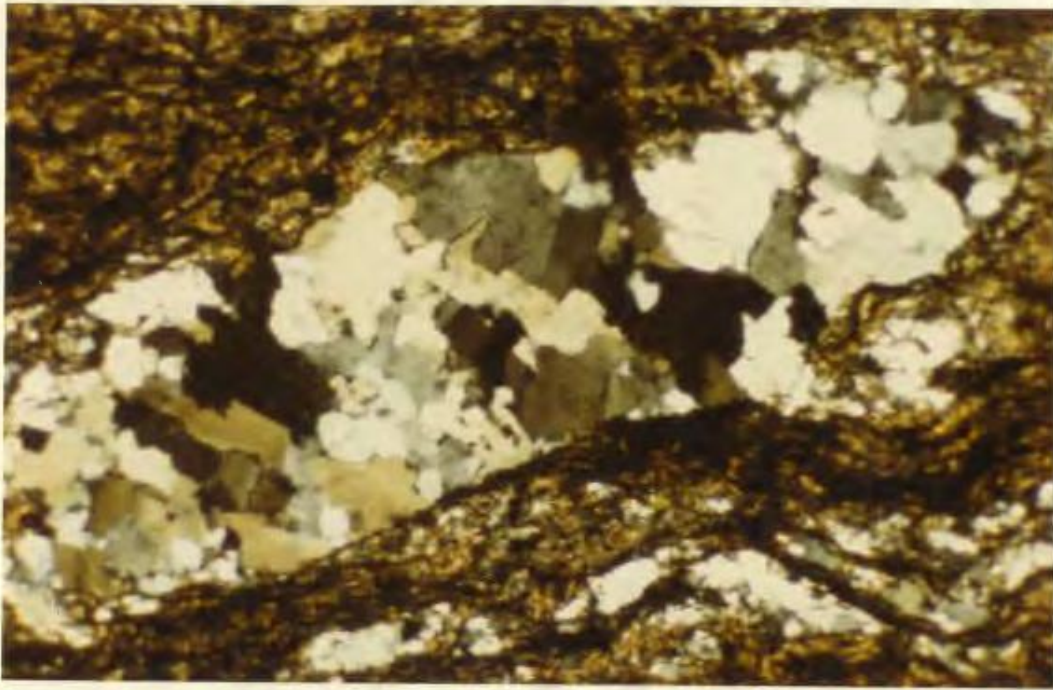


PLATE Xa: Quartz vein with granular quartz showing sutured boundaries and undulose extinction. Old Man Cove Formation. X nicols x 90.



PLATE Xb: Cross-bedded olivine gabbro. Little Port Complex.

Gabbros and amphibolites have tectonic fabrics which are nearly everywhere well developed. However, the tectonic fabric, although generally parallel to original layering in the gabbros, does not always obliterate it. Similar gabbros in the area display 'sedimentary structures' such as mineral grading and cross-bedding (Plate Xb). The tectonic fabric has also been observed clearly cross-cutting early igneous lamination and may itself show signs of refolding. Poly-deformed amphibolites are well developed in some regions (e.g. Big Cove, Fig. IIIb) but no regular pattern in the intensity of deformation has been identified.

Ultramafic rocks occur sporadically in the Little Port Complex as small masses and pod-like bodies which in some cases are definitely intrusive into surrounding rocks. The ultramafic rocks range from dunitic to wehrlitic in composition, and may exhibit mineralogical banding. This banding is generally parallel to the major tectonic fabric where the latter is best developed close to the margins of the bodies.

Quartz-diorites cut amphibolites, and intrusion breccias are developed on their margins. Major outcrops of the quartz-diorites occur north of Trout River, east of Chimney Cove and in the Lark Harbour region. The quartz-diorites are deformed together with the amphibolites and form bodies with long axes parallel to the regional strike of the Little Port Complex, and to the orientation of the major fabric in the gabbros. The bodies are intensely brecciated in places, especially where cut by late basic dikes.

The diabase dikes are locally sheeted, with chilled margins against adjacent dikes. They appear always to be post-tectonic, and

cut foliated gabbro, foliated quartz-diorites and mafic volcanics with which they are associated. However, they are almost always altered and internally brecciated (Williams and Malpas, 1972). Concentrations of sheeted dikes occur along marginal outcrops of amphibolite northeast and southeast of Trout River village.

The dikes feed tuffs, breccias and pillow lavas, which are juxtaposed with the deformed rocks. Although the volcanics are generally mafic, some quartz-porphyritic rhyolites are exposed south of Trout River. The mafic volcanics, like the dikes that feed them, may be quite altered.

iii) Mineralogy

Modal analyses for the major rock types found in the Little Port slice assemblage appear in Table II.

a) Amphibolites: The amphibolites are of variable grain size and composition. They are primarily composed of hornblende and plagioclase. Other common minerals include sphene, quartz, calcite, chlorite, sericite, epidote, zoisite, magnetite, apatite and rarely garnet.

Most amphibolites contain 50-60% amphibole, but some, especially in mylonitic zones, contain up to 90%. The amphibole is invariably green-pleochroic hornblende showing the following pleochroic scheme:

α straw-yellow; β yellow-green; γ olive-green.

An average $2V_{\alpha}$ of 90° suggests that it is magnesium-rich (Deer *et al.*, 1963). The hornblende defines the major fabric in the schistose rocks which has locally been folded into symmetrical folds with amplitudes restricted to a few cm. The feldspars have generally straight boundaries especially where in contact with the hornblendes. Generally they tend

TABLE II

Modal Analyses of Little Port Rocks

#	%	Ol	Opx	Cpx	Plag	Ch	Kfd	Qtz	Hb	Sp	Ox
UM	12-71	58	33	2						5	2
AMP	15-71			3	23	9			62		3
	295A-71				27	5			64		4
VOL	25	4		47	42	3					4
	18	2		28	56	12					2
	18A			27	58	13					2
Q. D.	2WP		1		40	2	2	34	16		5
	3WP				43	3	1	41	12		
	2271		1		46	1		42	6		4
AMP	198 71		2	3	30	5		2	52		6

towards a polygonal triple-point texture and are relatively fine grained. Large 'porphyroblasts' of plagioclase are locally present and have granulated borders and display 'shadow pressure recrystallisation' (Comeau, 1972). The plagioclase is of composition $An_{50}-An_{55}$.

Zoisite is quite widely developed as a matrix mineral and forms by alteration of the feldspar. Calcite and sericite are widespread and common matrix minerals, and calcite is also found in late veinlets.

b) Gabbros: Gabbros are commonly banded and often display a penetrative tectonic fabric. Massive, non-banded varieties are relatively rare, but where they occur, they range from medium to coarse grained, with average crystal sizes from 1 to 3 mm. Locally, however, very coarse grained pods and stringers attain crystal sizes of 6-12 cms.

The gabbros range in composition from troctolite to almost pure anorthosite in the banded varieties. Locally rare quartz-gabbros are present. Density grading, slump-structures and cross-bedding features reflect the cumulate nature of the gabbros, and cumulate textures are observed in some thin sections. The main constituents of the gabbros are plagioclase ($An_{67}-An_{80}$), and diagenic clinopyroxenes, both of which show varying degrees of alteration. Amphiboles, apatite and magnetite are important accessories and minor olivine and orthopyroxene have been recorded. The orthopyroxene generally occurs as exsolution lamellae in the clinopyroxene although individual crystals of primary orthopyroxene have been reported by Comeau (1972).

The banding in many gabbros is the result of the different relative proportions of the major minerals. The anorthositic bands

generally have less than 10% ferromagnesian minerals and the most mafic bands have up to 60% ferromagnesian. In the banded varieties a parallel alignment of the plagioclase is common, suggesting a primary igneous lamination. However, since a penetrative tectonic fabric is also often developed, the igneous lamination is generally masked. The plagioclases in this case tend to develop a polygonal or pseudo-polygonal fabric when in contact with one another. In the most highly deformed varieties, the plagioclases are flattened and form augen around the amphibolitised pyroxenes. Complete recrystallisation is evident in the mylonitic varieties.

In the ophitic varieties clinopyroxenes are generally much larger than the plagioclases they surround and exhibit well developed diallage parting. The clinopyroxene is often altered to amphibole, this alteration taking the form of complete replacement by hornblende or actinolite, or partial replacement along partings and around rims, leaving partially unaltered cores. In one massive non-banded sample (19871 in Table III) located south of Trout River, large poikilitic hornblendes from 1 to 3 mm in size include saussuritised plagioclase crystals (Plate XIa). The hornblende exhibits good cleavage traces in basal sections, but these sections display shapes typical of pyroxenes. The hornblendes are often twinned and show undulose extinction. In one case, remnant clinopyroxene has been noted in the hornblende (Plate XIb). It is therefore likely that the hornblende has replaced pyroxene, although it cannot be ascertained if this was a deuteritic or later, static metamorphic process.



PLATE XIIa: Green biotite developed interstitially in quartz-diorites, Little Port Complex. Plain light x 90.

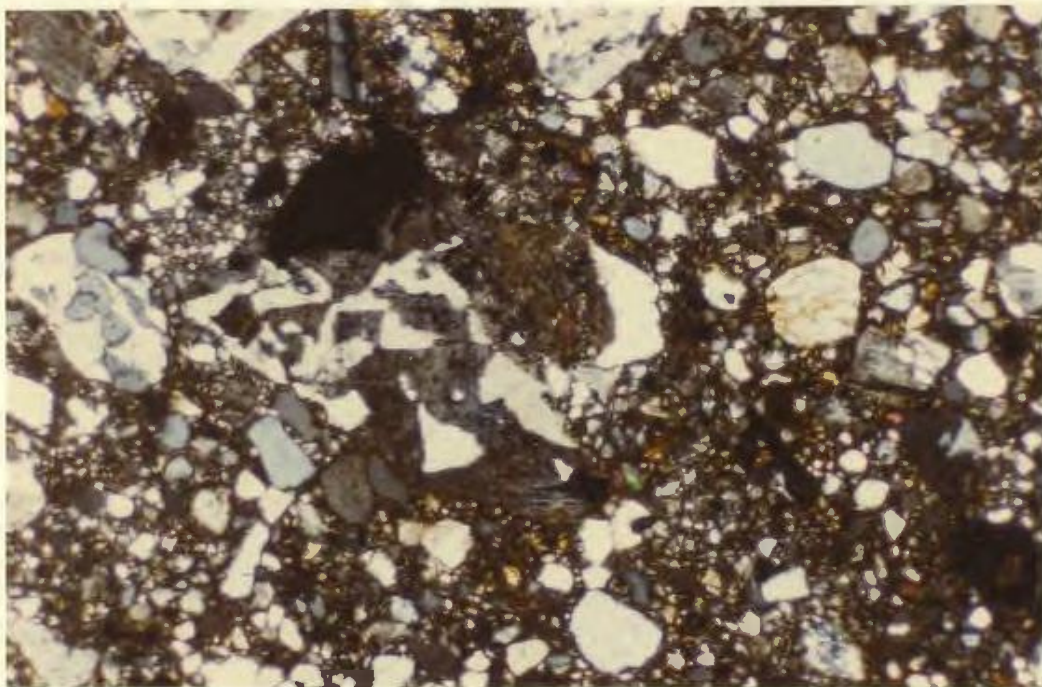


PLATE XIIb: Intense granulation results in various grain sizes. Note myrmekitic growth in large grain Little Port Complex quartz-diorite. X nicols x 90.

Olivine, where present, is relatively fresh, with only marginal alteration to iddingsite, and displays good polygonal fabrics when in contact with other olivine crystals.

Magnetite is clearly present as both a primary cumulate phase and as a secondary mineral. The cumulate magnetite is often contained in plagioclase and elsewhere forms layers parallel to the banding. Where an alteration product, the magnetite shows symplectic intergrowth textures around clinopyroxenes.

c) Quartz-diorites: The quartz-diorites are dull pinkish-white in colour on fresh surfaces and weather a chalky white. In the larger masses they are generally medium to coarse grained but in small stringers within amphibolite may be pegmatitic. Locally the quartz-diorites are crushed and fragmented to a much finer grain size. Pink aplite dikes are common.

The quartz-diorites are composed of quartz, albite/oligoclase, and minor K-feldspar, and mafic minerals include brown or green hornblende and brown or green biotite (Plate XIIa). Apatite and magnetite are common accessory minerals. Almost all plagioclases are soda-rich ($An_{10}-An_{30}$) and are normally euhedral. Twinning and oscillatory zoning evident in some crystals may be almost completely destroyed by alteration and fracturing in others. Crystals are of 1-2 mm average dimensions, although there is considerable variation in size where granulation is more intense (Plate XIIb). Quartz crystals are generally the same size as the feldspars. Stressed quartz crystals are characterised by fracture zones, especially where internal expansion of chloritic



PLATE XIIa: Green biotite developed interstitially in quartz-diorites, Little Port Complex. Plain light x 90.

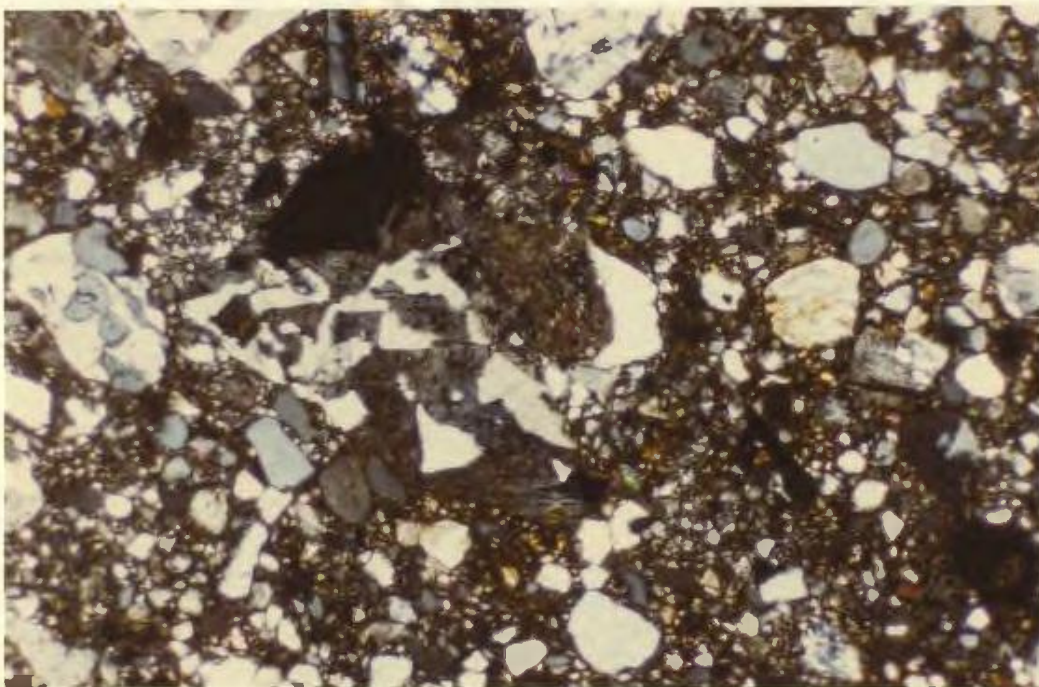


PLATE XIIb: Intense granulation results in various grain sizes. Note myrmekitic growth in large grain Little Port Complex quartz-diorite. X nicols x 90.

inclusions has taken place. Lobate quartz grains are intergrown and exhibit contact solution features. In some cases the brecciated diorites are indistinguishable from arkosic sediments. In these deformed varieties the quartz and plagioclase exhibit undulose extinction, and the products of the breakdown of the larger crystal boundaries form a fine-grained groundmass. The boundaries of the larger crystals and crystal aggregates are often marked by oxide staining (Plate XIIIa).

Feldspars and ferromagnesian minerals show appreciable alteration. The alteration of the feldspars is mainly saussuritisation, reflected in the development of fine grained epidote and zoisite. This alteration may mask original zoning and twin planes. The ferromagnesians are generally altered to light-green/colourless pleochroic chlorite.

d) Ultramafic rocks: Ultramafic rocks occur as small pods and dike-like masses within the amphibolites and mylonitised amphibolites of the Little Port Complex. The largest exposure is 150 metres wide and occurs at 1400 Brook in the O'Dwyer Mountain slice near Lark Harbour (Comeau, 1972). Smaller dike-like masses also occur in this slice. In every case the ultramafic rocks either intrude or abut against mylonitic gabbros or amphibolites. Small ultramafic pods occur along the coast just north of Trout River (Plate XIIIb). These appear to intrude amphibolitised gabbros, and markedly cross-cut a mineral banding in the basic rocks.

Primary mineral banding is present in most of the ultramafic rocks and individual bands vary from a few centimetres to tens of centimetres thick. The outer parts of the ultramafic bodies are

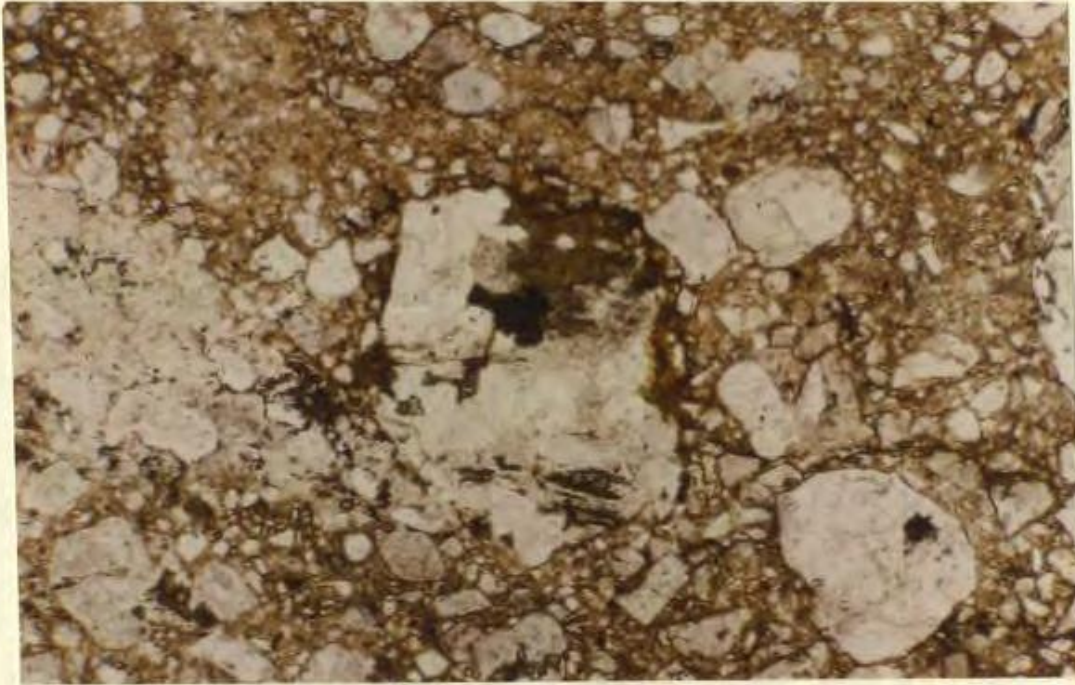


PLATE XIIIa: Oxide staining developed around large crystal aggregate. Quartz-diorite, Little Port Complex. Plain light x 90.



PLATE XIIIb: Ultramafic pod in Little Port Complex, North of Trout River.

generally deformed and scaly serpentine and talc are developed. Tectonic fabrics decrease in intensity from the margins towards the centres of the bodies and, where developed, parallel the 'igneous' banding.

The ultramafic rocks may be classified as wehrlites with minor dunitic patches. In thin section, olivine and clinopyroxene are seen to be the major constituents. Diopside clinopyroxenes locally form augen and are broken and granulated. Diopside partings are warped and rotated into the tectonic fabric. In some areas granulation is intense and ultramafic mylonites are formed (Plate XIVa). However, complete recovery textures are rarely seen, and irregular grains of olivine with magnetite in fractures are common. Green spinel forms an important accessory mineral in the ultramafics.

e) Dikes and volcanics: The Little Port Complex contains mafic dikes that in many places are brecciated. The dikes are apparently most abundant at steep contacts between the foliated gabbros and quartz-diorites and mafic volcanics. Brecciation of the dikes is intense along these zones, and makes it difficult to distinguish between dike rock and volcanic breccia. Locally, the dikes are sheeted and occur in sets of five to ten. They vary in width from 1.5 metres to 6 metres and have well developed chilled margins (Williams and Malpas, 1972).

In thin section, the diabase dikes of the Little Port Complex appear relatively fresh and unaltered. They exhibit well preserved subophitic or diabasic texture. Augite partially encloses plagioclase, and shows some alteration to chlorite and rarely actinolite. Generally

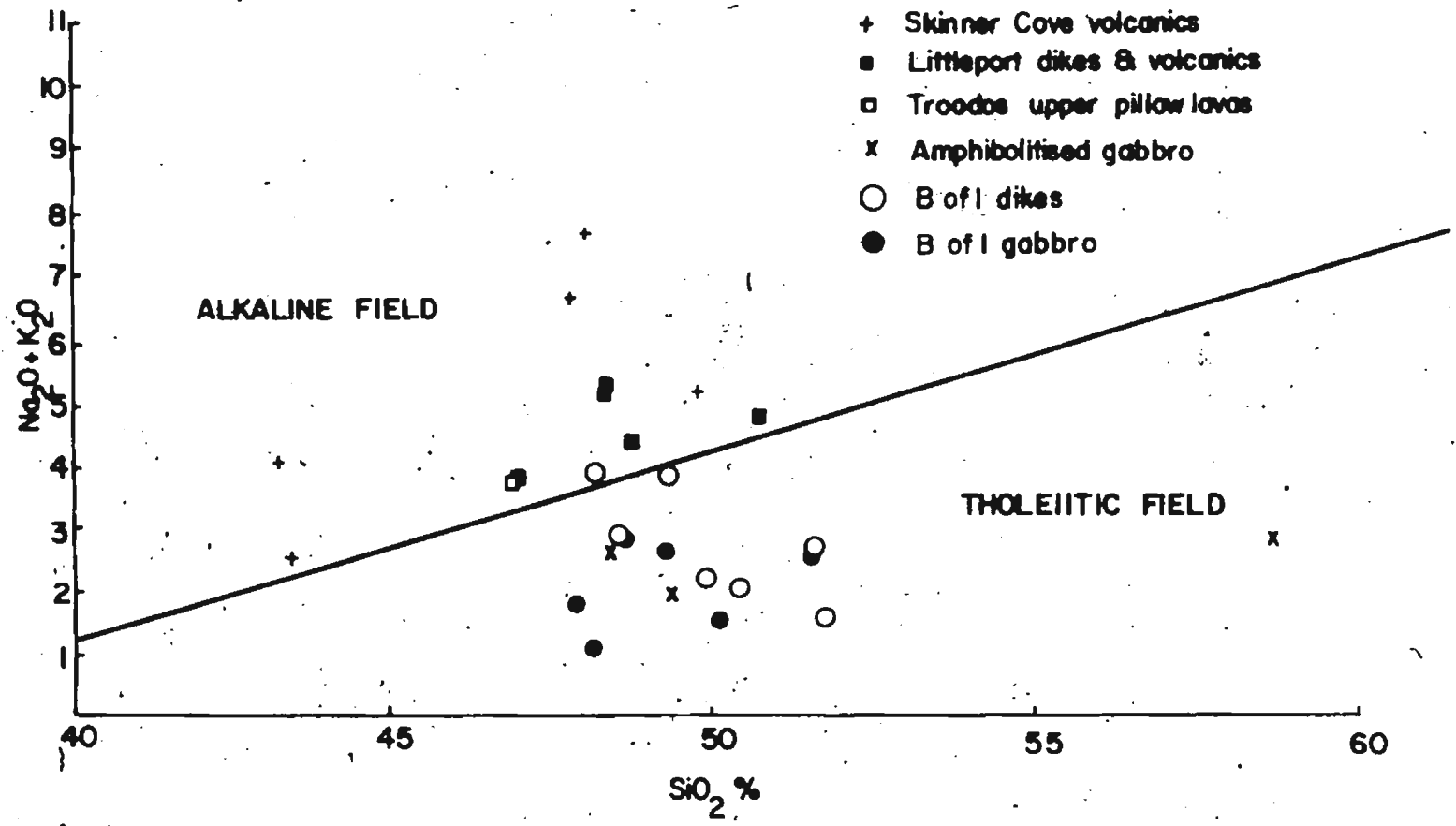
the pyroxene crystals are 0.5 mm maximum dimension. Plagioclase (An_{45-55}) occurs as lath-shaped crystals which are generally clear and unaltered. Epidote inclusions have rarely been noted. Porphyritic varieties occur with equidimensional plagioclase phenocrysts generally 3 to 4 mm in size, in a medium-grained matrix of plagioclase and chloritised augite.

The volcanic rocks of the Little Port slice assemblage are mainly basalts, basaltic andesites and mafic pyroclastics. More acidic rocks, in the form of rhyodacites, have been found in only one locality, south of Trout River village.

Flow rocks are generally basaltic andesites, and exhibit pillow features. They may be massive and aphanitic or porphyritic, and contain various proportions of amygdules. The scorias and pyroclastics are generally more basic and contain significant amounts of glass.

In thin section, the volcanics exhibit intergranular, or rarely ophitic, textures. Augite and plagioclase occur in roughly equal amounts, and olivine, sphene, magnetite and pyrite are common accessories. The pyroclastics may be considerably rich in olivine (10% of mode) and also often have aggregations of clinopyroxene. Advanced saussuritisation of the feldspars and chloritisation of the clinopyroxenes makes mineral compositions difficult to estimate. Olivine is everywhere altered to iddingsite. Prehnite, calcite and chlorite fill cracks and the vesicles of amygdaloidal varieties. These vesicles may be stretched indicating flow of the lava during vesiculation.

Figure IIIId: Plot of alkalis vs. silica for Little Port Complex and associated rocks.



Comeau (1972) has mentioned the presence of trachytic textures in many volcanics although these have not been observed by the present writer. It seems, therefore, that similarities between these volcanics in the Little Port Complex, and those of the Skinner Cove Formation are extremely strong with regards to mineralogy and textures.

iv) Chemistry

A number of rock types from the Little Port Complex have been analyzed and the results are presented in Table III.

a) Basic Rocks: Representative samples of the older foliated gabbros, amphibolitised gabbros and of the younger dikes and volcanics are compared on a plot of alkalis vs. SiO_2 in Fig. IIIId. Although too few analyses are available to make a statistically valid statement, the following tentative conclusions may be drawn.

(i) The younger dikes and volcanics are more alkaline in nature than the older foliated rocks which they cut. They appear to be chemically similar to members of the Skinner Cove series. They are also comparable with the average analysis of Troodos Upper Pillow Lavas.

(ii) The older foliated amphibolitic gabbros fall clearly in the tholeiitic field of MacDonald and Katsura (1964) and are therefore probably not related magmatically to the younger volcanics. They are, however, comparable to gabbroic and diabasic members of the Bay of Islands ophiolite complex.

(iii) The anomalously high SiO_2 content of 198-71 compared with other gabbros is due to the presence of secondary quartz disseminated in the matrix.

TABLE 111 Chemical analyses of Little Port
Complex Rocks

%	12-17	15-71	295A71	19971	2271	2571
SiO ₂	36.93	49.25	47.71	57.14	77.36	46.07
TiO ₂	0.00	0.09	1.26	0.03	0.20	1.15
Al ₂ O ₃	0.94	14.40	16.33	12.40	12.10	17.90
Fe ₂ O ₃	3.77	1.61	2.42	1.80	0.07	0.98
FeO	2.70	4.38	6.64	5.83	1.75	6.29
MnO	0.11	0.13	0.15	0.17	0.04	0.14
MgO	41.00	9.40	7.80	4.00	0.04	7.74
CaO	0.00	14.40	10.75	6.40	0.77	10.50
Na ₂ O	0.01	1.92	2.06	1.61	5.52	2.78
K ₂ O	0.00	0.02	0.61	1.50	0.72	0.86
P ₂ O ₅	0.00	0.20	0.26	0.05	0.08	0.20
Ign	15.30	4.60	2.50	7.10	1.70	3.60
TOTAL	100.76	100.40	98.49	98.03	100.35	98.21

ppm						
Zr	nd	19	99	122	77	99
Sr	nd	133	278	276	15	285
Rb	nd	5	8	33	11	13
Zn	48	54	67	90	32	72
Cu	nd	34	139	21	nd	75
Ni	2173	115	92	18	nd	80
Co	95	37	42	32	37	50
V	1945	653	235	35	9	245
Y	87	53	72	54	71	67
Ba	nd	46	68	38	101	104

wt%						
Qtz	0.00	2.47	0.00	21.82	41.51	0.00
Or	0.00	0.12	3.72	9.75	4.31	5.37
Ab	0.10	8.13	25.51	14.99	47.28	22.43
An	0.00	36.65	29.95	24.40	3.34	35.73
Re	0.00	0.00	0.65	0.00	0.00	-1.31
Cn	1.03	0.00	0.00	0.00	1.04	0.00
Wo	0.00	15.27	9.75	4.25	0.00	7.49
Di	(En	0.00	10.93	5.94	2.06	0.00
	(Fs	0.00	2.99	3.27	2.12	0.00
Hy	(En	16.96	16.11	0.00	8.90	0.10
	(Fs	1.27	4.40	0.00	9.14	0.00
Fo	72.06	0.00	9.88	0.00	0.00	10.80
Fa	5.97	0.00	5.99	0.00	0.00	4.82
Mg	2.55	2.27	2.24	2.39	1.05	2.30
Ilm	0.00	0.00	0.00	0.00	0.80	0.00
Ilm	0.00	0.18	2.47	0.06	0.33	2.31
Ap	0.00	0.49	0.62	0.13	0.19	0.49
TOTAL	99.99	100.01	99.99	100.01	100.00	100.00

Fe₂O₃ calculated as 1.5 for normative analysis.

nd: not detected
- : not determined

TABLE III (Continued)

	1871	19471	28P	29P
SiO ₂	47.70	47.70	71.80	71.60
TiO ₂	1.39	1.40	0.23	0.15
Al ₂ O ₃	15.50	15.60	12.80	12.70
Fe ₂ O ₃	2.69	2.70	3.00	2.58
FeO	5.34	5.30	3.00	2.58
MnO	0.16	0.20	0.09	0.11
MgO	6.06	6.10	0.86	0.63
CaO	9.41	9.40	2.35	2.19
Na ₂ O	4.00	4.00	4.44	5.32
K ₂ O	1.21	1.20	1.32	0.95
P ₂ O ₅	0.11	0.10	0.03	nd
Ign	4.90	4.90	1.45	1.76
TOTAL	98.47	98.60	101.37	100.57

ppm				
Zr	209	187	80	62
Sr	227	258	63	106
Rb	10	6	28	17
Zn	83	83	50	209
Cu	72	93	-	-
Ni	50	37	-	-
Co	37	43	-	-
Cu	162	91	-	-
V	86	60	-	-
Ba	1952	1982	163	-

	wt		
	Qtz	0.00	0.00
	Or	7.65	7.58
	Ab	27.36	27.25
	An	22.22	22.51
	He	4.80	4.83
	Cn	0.00	0.00
Di	Ho	11.26	11.12
	Ens	6.81	6.73
	Fs	3.85	3.78
Hy	Ens	0.00	0.00
	Fs	0.00	0.00
	Fo	6.55	6.66
	Fa	4.03	4.12
	Mg	2.33	2.32
	Hm	0.00	0.00
	Ilm	2.82	2.84
	Ap	0.27	0.25

TOTAL 100.00 99.99

Fe₂O₃ calculated as 1.5% for narrative analysis

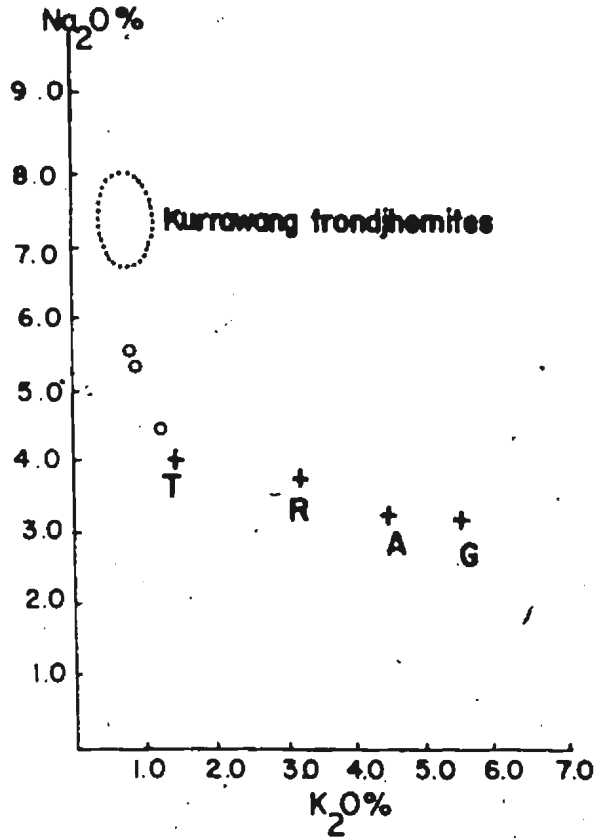
nd: not detected
- : not determined

(iv) The suggestion that the fresh dikes and volcanics of the Little Port Complex are coeval and consanguineous with the sheeted diabase dikes of the Bay of Islands Complex (Williams and Malpas, 1972) now seems unfounded. Instead, a comagmatic relationship between the Little Port Complex dikes and volcanics and the Skinner Cove volcanics is a more likely probability. This is supported partially by trace element contents, especially barium. The Little Port dikes and volcanics and Skinner Cove volcanics both have Ba concentrations ranging from 100 ppm to 2000 ppm, significantly higher than the 24 ppm to 78 ppm Ba in the foliated gabbros of the Little Port Complex and the Bay of Islands Complex gabbros.

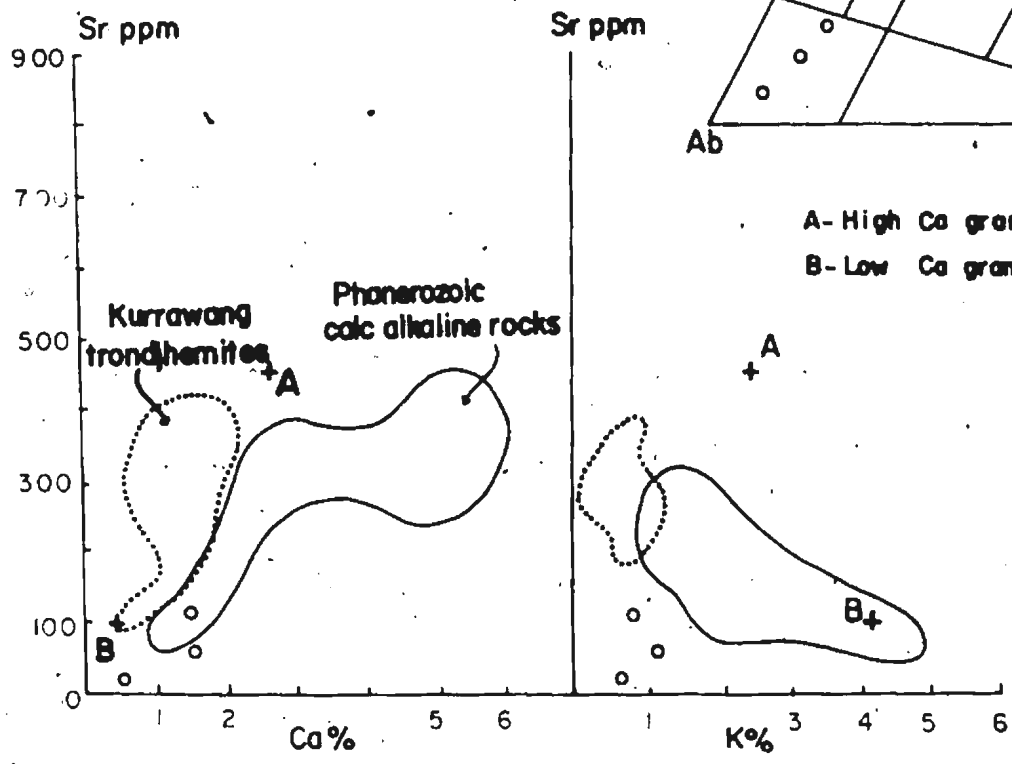
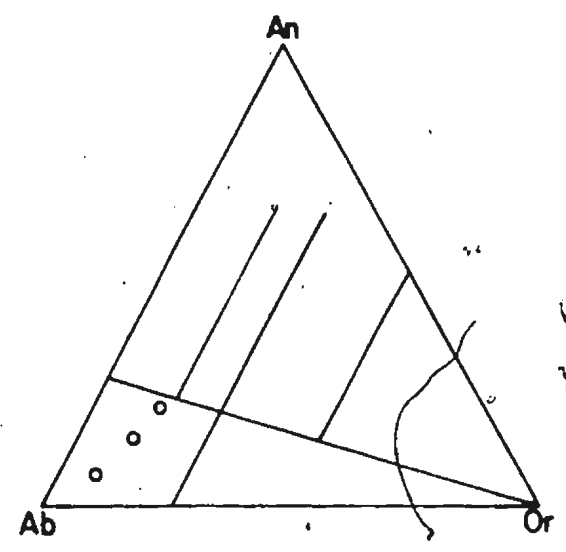
b) Ultramafic Rocks: Only one sample of peridotite from the Little Port Complex has been analysed. A modal analysis of this rock shows it to be harzburgitic, and the lack of clinopyroxene is reflected in the analysis as a lack of CaO and normative clinopyroxene. The high loss on ignition reflects the high degree of serpentinisation (58%) characteristic of the peridotites in the Little Port Complex. Comparison of the Ni/Cr ratio with ultramafic rocks from the Bay of Islands Complex suggest that the rock is not of a cumulate origin (Fig. VIp). The Mg/Fe ratio of 5.2 is also more consistent with those of the harzburgitic tectonites of the Bay of Islands Complex (av. 5.0) than with the lower ratio of about 4.2 for the cumulus dunites.

c) Quartz-diorites: The three quartz-diorites analysed (22-71, 2WP and 3WP) can be classified as trondhjemites on the basis of their normative feldspar compositions (Fig. IIIe). However, plots of

Figure IIIe: Variation diagrams for quartz-diorites from Little Port Complex.



T = AVERAGE TONALITE
 R = AVERAGE GRANODIORITE
 A = AVERAGE ADAMELLITE
 G = AVERAGE CALC-ALKALINE GRANITE
 (NOCKOLDS 1954)
 O = LITTLEPORT COMPLEX QTZ. DIORITES



Na_2O vs. K_2O and Sr vs. Ca or K (Fig. IIIe), although showing an enrichment in sodium over average siliceous igneous rocks, indicate a deficiency of sodium and strontium when compared with the Kurrawang trondhjemites described by Glikson and Sheraton (1972).

Green and Ringwood (1968) have shown that the least differentiated acid liquids arising from relatively low degrees of melting of hydrated amphibolite are typically sodic. The amphibolites of the Little Port Complex show partial melt textures in the form of trondhjemitic veins suggesting such an origin for the associated quartz-diorites. This hypothesis is supported by a lack of associated rock-suites typical of fractionation processes, a lack of hydrous mineral phases and pegmatites and a low content of trace elements compared to granites produced by crystal fractionation or anatexis of sedimentary rocks (cf. Payne, 1973; Payne and Strong, in prep.).

v) Significance

Smith (1958) considered the igneous and metamorphic rocks of the Little Port Complex and Bay of Islands Complex together as part of one intrusive assemblage. With such an interpretation, it was difficult to reconcile the large variations in metamorphic and structural style from one part of the assemblage to another. This difficulty was no further overcome when the transported nature of the rocks was first recognised, and proved a major obstacle in interpreting the whole assemblage as oceanic lithosphere. However, the recognition of four distinct slice assemblages of igneous and metamorphic rocks (Williams et al., 1972; Williams and Malpas, 1972; Williams, 1973) removed major obstacles in the geological interpretation of the area. The definition

of the Little Port Complex as a polygenetic assemblage distinct from the Bay of Islands ophiolite suite both resolves problems in attempts to reconcile the contrasting structural styles between the two and further eases the interpretation of the Bay of Islands Complex as oceanic crust and mantle (Williams, 1971).

Williams and Malpas (1972) drew attention to the fact that the Little Port Complex could not be considered a typical ophiolite suite since the dikes and volcanic rocks are younger and bear no genetic relationship to the deformed igneous rocks that they cut. The development of relatively large volumes of acidic rocks also seemed unusual in comparison with simple ophiolite suites elsewhere. Strong (1974), however, concluded that rocks of the Little Port Complex represented oceanic lithosphere formed and deformed at or close to an oceanic ridge. This suggested, and subsequent arguments above support this view, that the fresh dikes and volcanics within the complex represented the off-axis volcanism better developed as the Skinner Cove Formation. The acid rocks were considered as products of partial melting of the amphibolites under conditions of high heat flow. That such conditions might exist at ridges is also exemplified by the high-temperature "flaser-gabbro" of the Lizard Complex, S.W. England, which has been interpreted as oceanic lithosphere by Thayer (1972), Mitchell (1974) and Strong et al. (in press).

Several workers (Comeau, 1972; Williams and Malpas, 1972; Kennedy, m.s.) considered that the deformed rocks of the Little Port Complex represented older crustal remnants caught up in the spreading episode that resulted in the formation of the ophiolites and during which the younger

dikes and volcanics that surround the deformed Little Port Complex were produced. All of these workers pointed out the lithological, structural and age similarity of the Little Port Complex with rocks of Twillingate and New World Island in Notre Dame Bay. The analogy is so strong, in that the deformed trondhjemitic Twillingate granite and associated amphibolites are cut by Ordovician dikes and volcanics, that Williams and Payne (1975) suggest that the Little Port Complex could represent a sampling of the geology of the Twillingate area.

Both the Little Port Complex and Twillingate sequence have since been reinterpreted by Malpas et al. (1973), Strong and Payne (1973) and Williams and Payne (1975). The juxtaposition of intensely deformed amphibolites with fresh volcanic rocks is compared with situations in present day island arcs where fresh volcanics overlie amphibolitic basement (Shiraki, 1971; Coleman, 1970; Hutchinson and Dhonau, 1969; Tobisch, 1968). In this case the peridotites and gabbros of the Little Port Complex are presumably part of the oceanic lithosphere which formed the basement to the island arc assemblage. Stevens (personal communication) considers that the Complex represents part of an accretionary mélangé formed in the arc-trench gap, where it was subsequently deformed above the subduction zone (Karig, 1971, 1972). In such a case it is difficult to ascertain the significance of the younger alkaline volcanic rocks. Alkaline rocks generally occur at a distance from the subduction zone and most often during later stages in the development of an arc.

The genetic position of the Little Port Complex is thus, at this stage, enigmatic to say the least. Further petrological and structural

studies are at present in progress, and radiometric age determinations will soon be completed, in attempts to resolve problems unearthed during this and previous reconnaissance studies.

E. Mélange Zones.

Contacts between the upper thrust slices and the underlying transported clastics are well exposed in many coastal sections. All contacts are tectonic and generally marked by extensive mélange zones. These mélange zones consist of chaotic masses of blocks of various sizes, randomly set in a matrix of either black and green shale or serpentinite. The nature of the matrix allows a division of most mélanges into two parts. For example, a thick mélange zone, typical of most occurrences, is developed between gabbroic rocks of the Little Port Complex and the underlying transported sedimentary rocks at Bear Cove (Fig. IIIb). The upper part of the mélange is dominantly serpentinite, consisting of serpentinised gabbro and ultrabasic blocks lying in a friable serpentine matrix. However, the lower part is a sedimentary mélange consisting mainly of sedimentary blocks, but with a few igneous blocks, randomly distributed in a black-green shaly matrix. The sedimentary mélange grades downwards into the relatively undeformed sedimentary rocks.

Similar sequences of shaly mélange overlain by serpentinite mélange are found along the western edge of the Lewis Hills massif, and the leading edge of the Table Mountain massif. Serpentine mélanges also occur between the separate slices of the Little Port Complex just west of Lark Harbour. The number of separate small slices of Little Port Complex

rocks, separated by mélangé zones in this area suggest that the leading edge of the thrust slice was beginning to break up as it was finally emplaced.

i) Lithology and structure

The mélangé zones vary in thickness from a few metres to 100 metres thick at Wild Cove Brook (Fig. IIIb). The clasts in most cases make up between 10 and 30 percent of the mélangé and themselves range in size from pebbles of a few centimetres dimensions to boulders up to 20 or 30 metres long. There is no internal grading and clasts of all sizes are chaotically mixed. The bigger clasts or 'knockers' are generally found in the sedimentary mélanges where they sit in a shaly matrix that displays a well developed cleavage. The larger blocks tend to be angular and tabular and lie with their long axes parallel to the major (first) cleavage in the matrix (S_1). Many sandstone slabs can be traced into broken angular boulders. Rounding of many clasts has apparently taken place by the abrasive action of the matrix during formation, and the splitting of boulders by matrix injection under high hydrostatic pressure is evident. Many clasts exhibit slickensides on their surfaces.

In the serpentinite mélanges, ultramafic and gabbro boulders predominate. The ultramafic rocks are completely serpentinised and have contributed to the matrix by shearing and comminution of the serpentine during the formation of the mélangé.

Most mélanges possess a tectonic fabric (S_1) realized as a cleavage that crudely parallels their upper and lower contacts. This fabric is folded by open folds (F_2) with an associated weak crenulation

cleavage (S_2). Very often the S_1 fabric forms clear augen around the clasts, and in many cases this is accompanied by the flattening of the clasts. In these cases the S_1 fabric is recognised as a slaty cleavage.

ii) Significance

The origin and significance of mélangé zones has been variously discussed (e.g. Hsu, 1968; Stevens, 1970).

Brueckner (1966 and personal communication) suggests that mélangés represent a regolith after subaerial mass wasting of uplifted blocks, pointing out the lack of subaqueous sedimentary structures, the lack of sorting and a chaotic structure reminiscent of talus slopes. He equates mélangés with a form of 'molasse' and suggests that the deposits represent the precursors of flysch which is laid down subaqueously at greater distances from the source. The blocks were slumped into unconsolidated shales and the chaotic structure was thus derived before overriding by thrust slices. The origin of the shale matrix of the sedimentary mélangés must have been in an area that was traversed by the thrust slices. The only possible source of similar lithology in the Humber Arm region seems to be the Lower Ordovician Middle Arm Point Formation which consists dominantly of black and green shale and argillite and buff-weathering siltstone.

Smyth (1973) suggested that the base of the slices of the Hare Bay Allochthon bear no genetic relationship to the mélangé they overlie. This is probably true in the case of the sedimentary mélangés, with a variety of clasts, but the serpentinite mélangés are obviously much more restricted beneath igneous, and generally peridotite, masses. This supports

Stevens' (1970) conclusion that there are two types of mélangé; namely a sedimentary olistostrome developed in front of the allochthon (possibly analogous to Brueckner's 'tallus'), and a tectonic mélangé developed between the thrust slices. The tectonic fabric, presence of slickensides and the penetration of matrix into cracks in the clasts, all indicate deformation and high hydrostatic pressures, probably during overriding by the thrust slices. During the formation of this tectonic mélangé, pieces of overriding slice were ripped off and incorporated into the earlier formed olistostrome which was being traversed by the advancing thrust slice. The result is an early sedimentary olistostrome overlain by a more serpentinous tectonic mélangé derived primarily from the sole of the overriding slice.

CHAPTER IV

THE BASAL AUREOLE

A. Introduction.

Metamorphic rocks occur at the base of all the ophiolite masses forming the Bay of Islands Complex. These metamorphic rocks are considered part of the transported Bay of Islands slice assemblage and are commonly referred to as the 'basal aureole' (Church and Stevens, 1971; Malpas et al., 1973; Williams and Smyth, 1973). They crop out as the most easterly exposures of the slice assemblage and dip approximately west-northwest beneath the peridotites. From a distance the aureole rocks are best recognized by a high irregular topography and an increase in vegetation cover compared to the structurally overlying ultramafic rocks. Sections through the aureole are most easily accessible at the east end of Trout River Ponds, and at Pond Point on North Arm (Fig. IIIb). Along the eastern margin of the Lewis Hills massif, south of the map area, the aureole rocks form a wider outcrop belt than elsewhere, generally in excess of 1 km. This, together with other aspects of the outcrop pattern of the massif, suggests a more horizontal disposition of the ophiolitic and aureole rocks in the Lewis Hills than in the other massifs. Thus, within this wide zone of aureole rocks, the ultramafic outcrops which are locally present are readily interpreted as outliers of the overlying peridotites.

Aureole rocks occupy a constant level at the stratigraphic base of the exposed ophiolite sequences and are not related to the present structural base of the slices which are marked by serpentinite mélanges.

The absence of aureole rocks along the western margins of the individual massifs is probably the result of structural omission since the lowest ultramafic members are also missing. Smith (1958) mapped a narrow amphibolite band in an anomalous position on Mount St. Gregory, east of the main gabbro mass, and correlated it with aureole rocks elsewhere. Recent mapping has, however, failed to detect any rocks in this area which could be so interpreted.

The sequences of aureole rocks on the southeast side of North Arm Mountain, along North Arm, are accessible through stream valleys draining the mountain and at the coastal outcrop at Pond Point (Fig. IIIb). Here the aureole has an overall structural thickness of approximately 130 metres and grades downwards from a foliated pyroxene amphibolite at the contact, through garnetiferous amphibolite, greenschist, garnetiferous phyllite into an argillite (Fig. IVa). At Pond Point the actual contact zone is not seen and splay faulting repeats the greenschist-phyllite sequence (Plate XIVb).

At the east end of Trout River Ponds, amphibolites of the aureole are in structural contact with pillow lavas and agglomerates on the southside and with sandstone on the north side. No greenschists or phyllites are seen and have probably been removed by vertical faulting. Rodingites are especially well developed on the south side of the pond. The following petrographic and geochemical analyses are of specimens collected from all three localities.

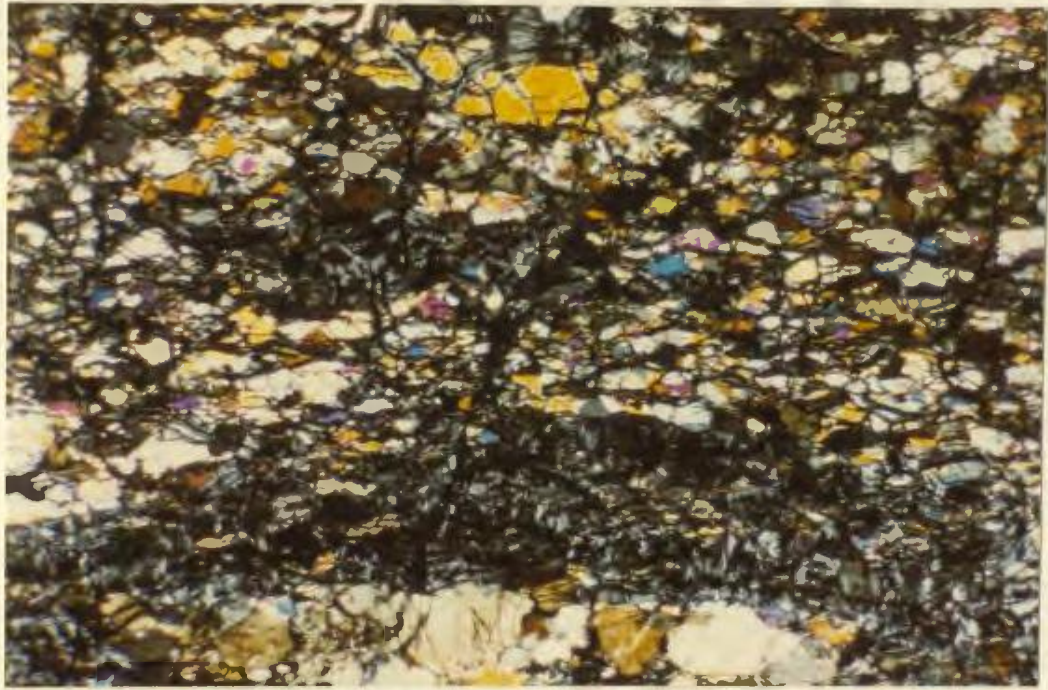


PLATE XIVa: Ultramafic mylonite. Strong cataclasis of harzburgite. Little Port Complex. X nicols x 90.



PLATE XIVb: Vertical splay faulting in amphibolite zone of aureole at Pond Point, North Arm.

Figure IVa: Generalised cross-section of basal aureole to show metamorphic rock types.

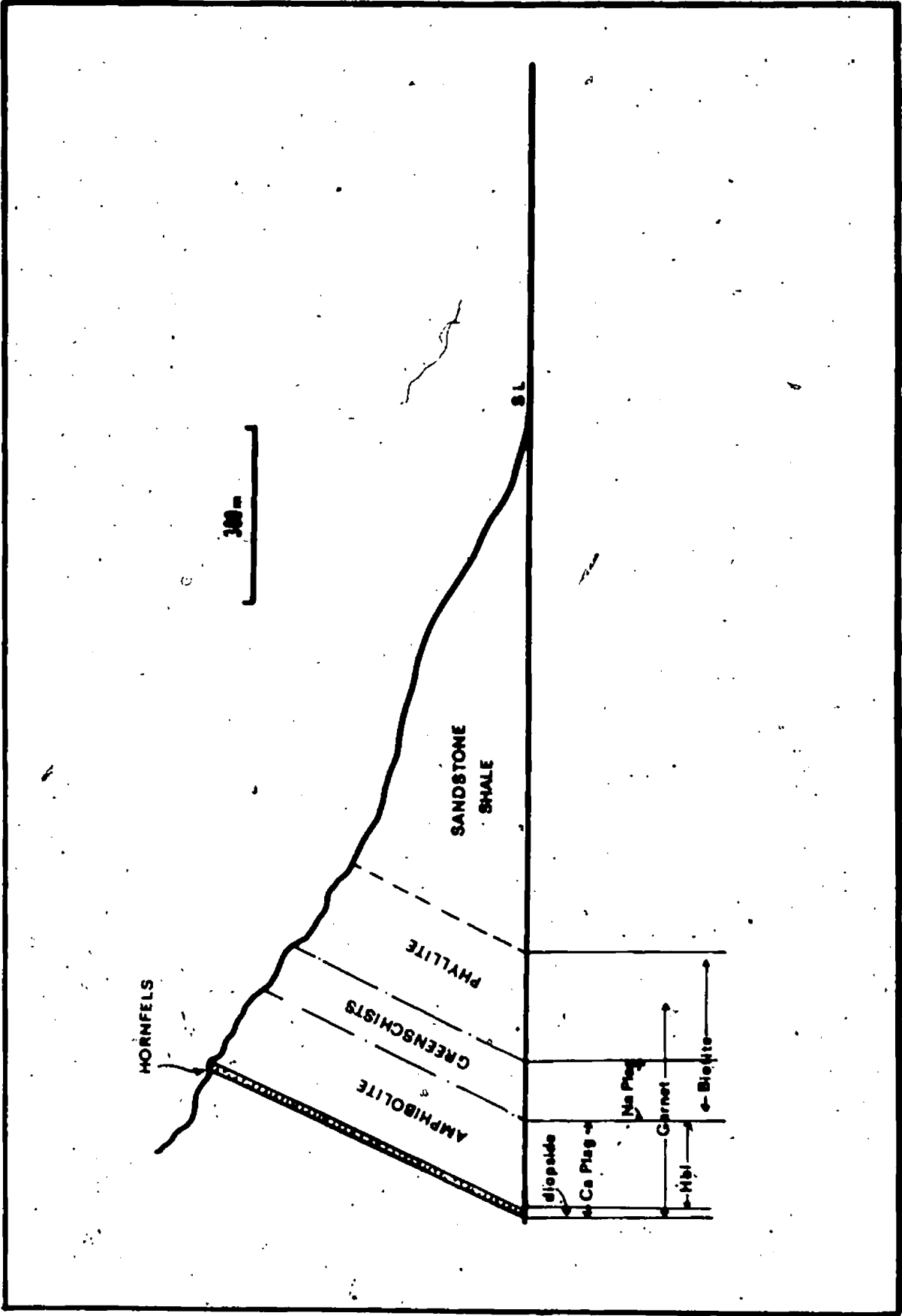




PLATE XVa: Pseudo-gneissosity augening enstatite megacryst in basal lherzolite - Trout River.

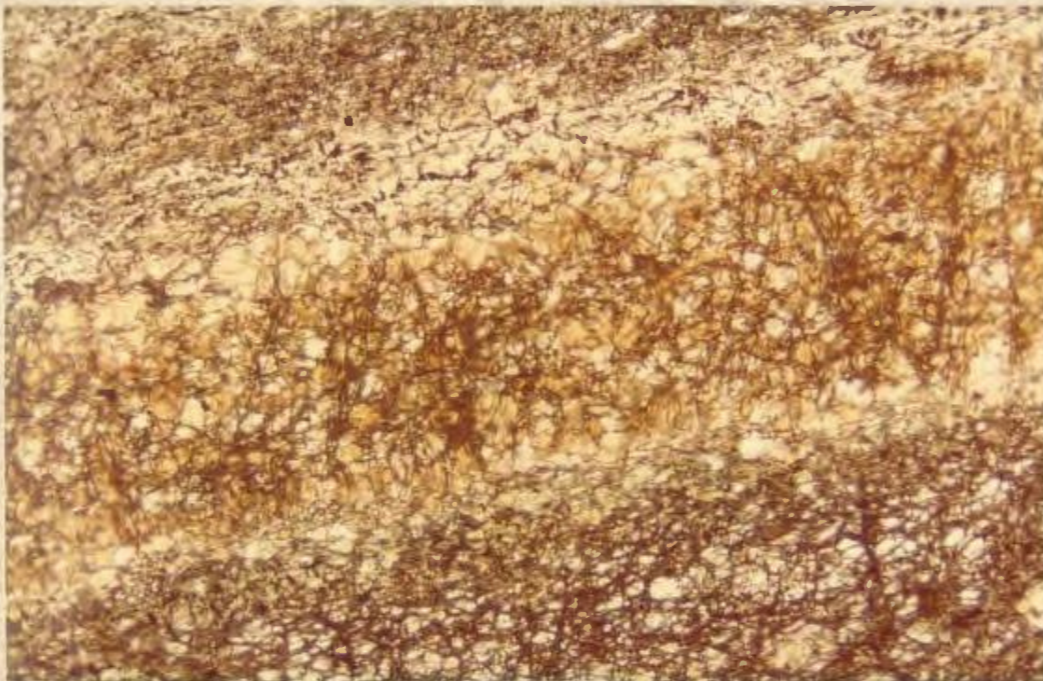


PLATE XVb: Ultramafic mylonite, basal contact. Trout River. Plain light x10.

B. Lithologies.

i). Ultramafic rocks

When considering the genesis of the aureole, it is most important to realize that the structure and petrology of the lowermost ultramafic rocks in the succession form an integral part of the assemblage.

Harzburgites overlie the amphibolites on North Arm Mountain and Blow me Down Mountain, but lherzolites are present at the base of the Table Mountain massif. Only at Trout River Pond is the actual contact seen since an exposure gap of several metres invariably separates ultramafics and aureole on North Arm and Blow me Down Mountains. These basal ultramafic rocks everywhere exhibit a well developed schistose fabric, which in hand specimen resembles a gneissosity augening enstatite megacrysts (Plate XVa). This foliation is accentuated on weathered surfaces where it appears sinuous, with enstatite augen standing out in relief. In some bands the rock is completely broken down and an ultramyylonite developed. These mylonitic bands are generally of the order of a few centimetres wide (Plate XVb), and at the contact at the southeast end of Trout River Pond, where they occur within a few feet of the amphibolite, are visibly accompanied by rodingitisation.

In thin section the schistosity is delineated mainly by recrystallised olivine and orthopyroxene. The enstatites show considerable stretching and flattening, the effect of which is to produce attenuated phenocrysts with their long axes, often of the order of 1 cm in length, parallel to the schistosity (Plate XVIa). The associated minimum dimension

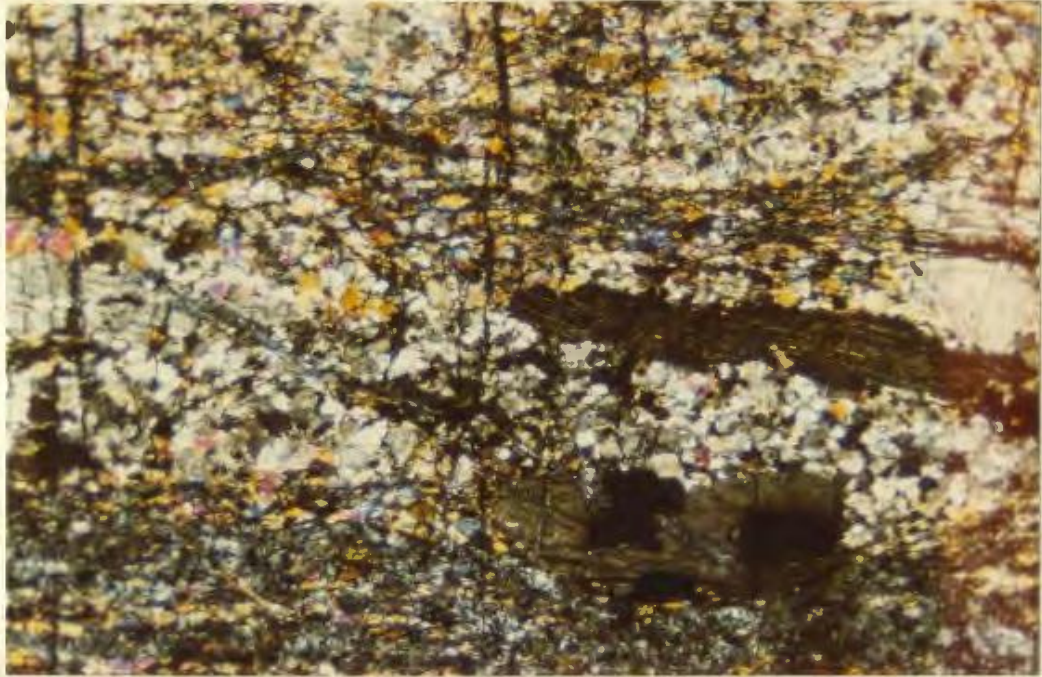


PLATE XVIa: Stretched and flattened enstatite crystal paralleling foliation in basal ultramafic mylonite - Trout River. X nicols x 20.

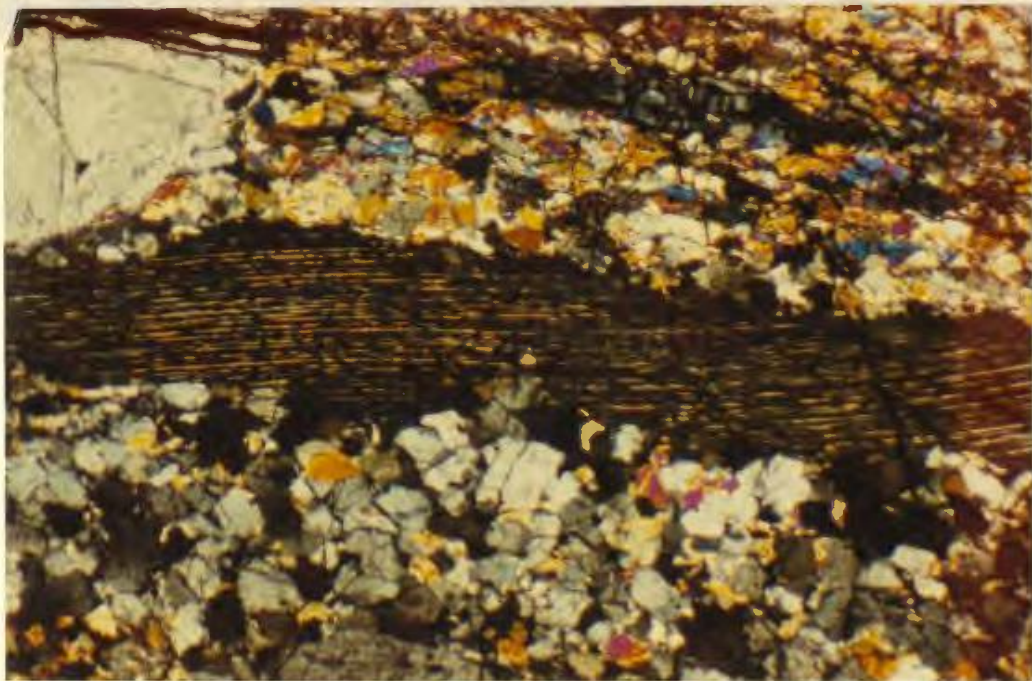


PLATE XVIb: As above: x 45.

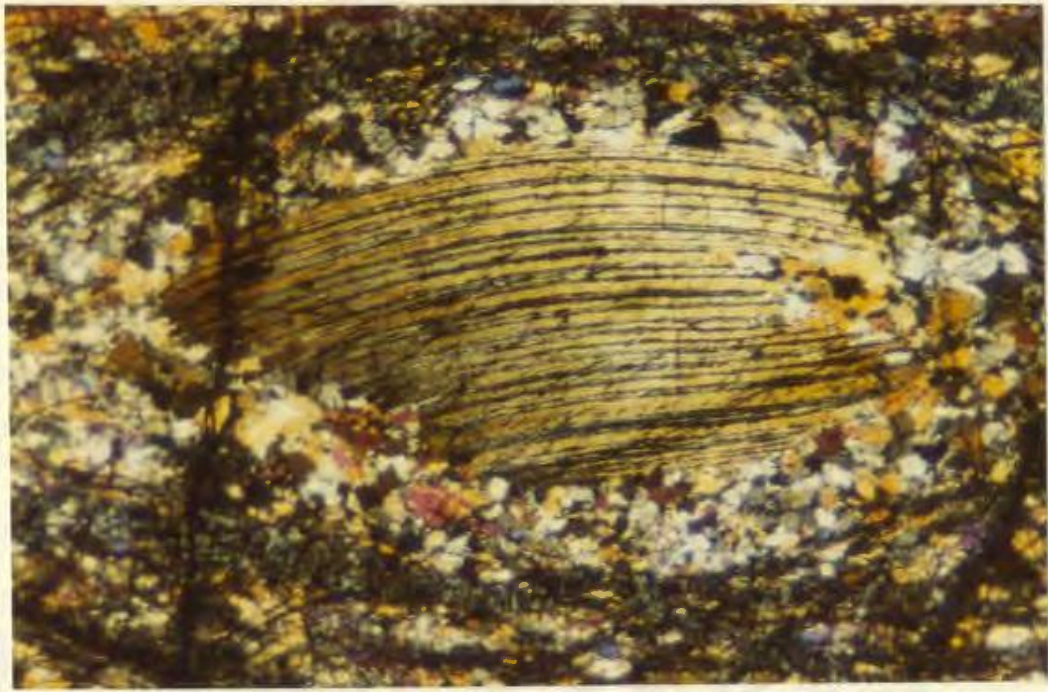


PLATE XVIIa: Enstatite 'phenocryst' showing warped exsolution lamellae of diopside. Lamellae are rotated into plane of foliation in U.M. mylonite which shows flattening around crystal. Trout River. X nicols x 35.

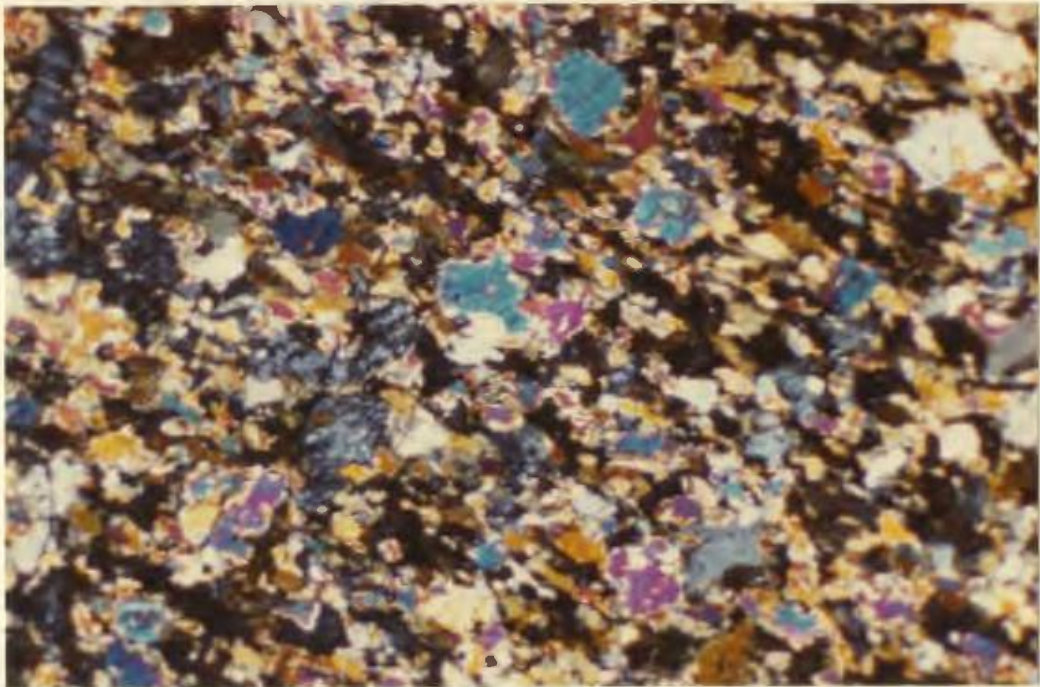


PLATE XVIIb: Clinopyroxene disseminated throughout U.M. mylonite, cpx-blue br. Trout River. X nicols x 100.

perpendicular to this may be as little as 0.1 mm. Exsolution lamellae of diopside parallel to (100) appear to have acted as planes of dislocation during the flattening of the enstatite. Such exsolution lamellae are generally warped and are invariably rotated into the schistosity to some extent (Plates XVIb, XVIIa). Serpentine forms up to 60% of a typical rock, generally as a network replacing olivine of which only kernels remain or as bastite after enstatite. Some coarser ribbon-like bands of serpentine replace original pyroxene layers. Since serpentine appears always cutting sutured grain boundaries, it is presumably formed after the major deformation.

The mylonite bands show well developed cataclastic textures and various degrees of annealing and recrystallisation. Serpentinised granulated olivine is commonly interlayered with brown amphibole bands on a millimetre scale. Green spinels, petrographically identified as ceylonite or pleonaste varieties, occur in olivine rich bands, while garnet and phlogopite are ubiquitous in the amphibole bands. Enstatite has been recognised in the olivine bands only, but aluminous clinopyroxene occurs in both (Plate XVIIb). The amphiboles form crystals up to 5 mm long, are orientated parallel to the major flattening fabric and show signs of strain and recovery (undulose extinction and the weak development of triple points). The garnets often appear to have been granulated during mylonitisation, are small and equidimensional but have irregular outlines. Serpentine cuts the mylonite fabric also. The fabrics developed in the ultramafic rocks and those of the mylonite bands are undoubtedly related to the same tectonic event.

The garnets and amphiboles were considered by Church (1972) to be part of a high pressure mineral assemblage (garnetiferous amphibole ariegite) indicating that this part of the ultramafic mass crystallised at depth within the mantle. The restriction of the amphibole-phlogopite-garnet assemblage to mylonite zones within a few metres of the basal aureole contact, and within the mylonites to discreet bands, would apparently argue against this but support an interpretation of such assemblages as related to the production of the mylonite, which itself seems inseparable from the production of the aureole in general.

Similar mylonitic zones are recognised at the base of the ultramafic pile in Hare Bay, northern Newfoundland, where they are generally better developed and more clearly exposed than in the Bay of Islands. Here, however, garnet is not ubiquitously developed in the amphibole bands. Other occurrences of amphibole in ultramafic peridotites are relatively rare. The occurrence of secondary amphibole (pargasite) within peridotites has been mentioned by Wiseman (1966) and Melson *et al.* (1972) for the mylonites of St. Paul's rocks, and amphibole is known to occur in some peridotite nodules; e.g. from Gran Canaria, Canary Islands (Frisch and Schmincke, 1968) and Tahiti (McBirney and Aoki, 1968) although they are defined as primary in the latter case, and are sufficiently rich in TiO_2 to be termed kaersutites.

ii) Hornfelses

Pyroxene-garnet hornfelses are found immediately below the foliated ultramafics at the Trout River Pond locality. The hornfelses

zone is restricted to the four metres of aureole rock nearest the contact and it has not been identified elsewhere. At a distance of about 4 metres, brown amphibole replaces both the pyroxenes and the garnets of the hornfels, often showing a preferred orientation that becomes the major schistosity in the underlying amphibolites. In the field, the hornfels appears as a dense, light grey-green, fine-grained rock in which no banding is visible. In thin section the hornfels consists dominantly of plagioclase and pyroxene with subsidiary garnet, and all minerals display decussate textures (Plate XVIIIIa). An average modal analysis of the hornfels is given in Table III.

Plagioclase, forming up to 65% of the rock, occurs as grains of variable size between 0.1 and 0.3 mm. Extinction angles suggest a composition around An_{75} and this is confirmed by electron probe microanalysis (Table VII). Some feldspars exhibit pericline twinning that is sometimes bent, but undeformed albite twins are the commonest. Some sections that do not show twinning show undulose extinction that suggests a certain amount of strain during recrystallisation (Plate XVIIIb).

Clinopyroxene ($Ca_{0.9} Mg_{0.8} Fe_{0.15} Al_{0.15} Si_2O_6$ - Table VI) forms approximately 25-35% of the rock. Equidimensional grains of about 0.3 mm are commonest but may range up to 0.8 mm in size. The clinopyroxene is non-pleochroic, colourless, has a $2V_{\gamma}$ of 55° and is optically positive. Some hypersthene ($2V_{\alpha}$ $56-58^{\circ}$ and optically negative) forms crystals up to 0.5 mm long.

Garnet with symplectite rims also occurs in the hornfels. The symplectite rims are apparently mixtures of hydrogrossular and alteration.

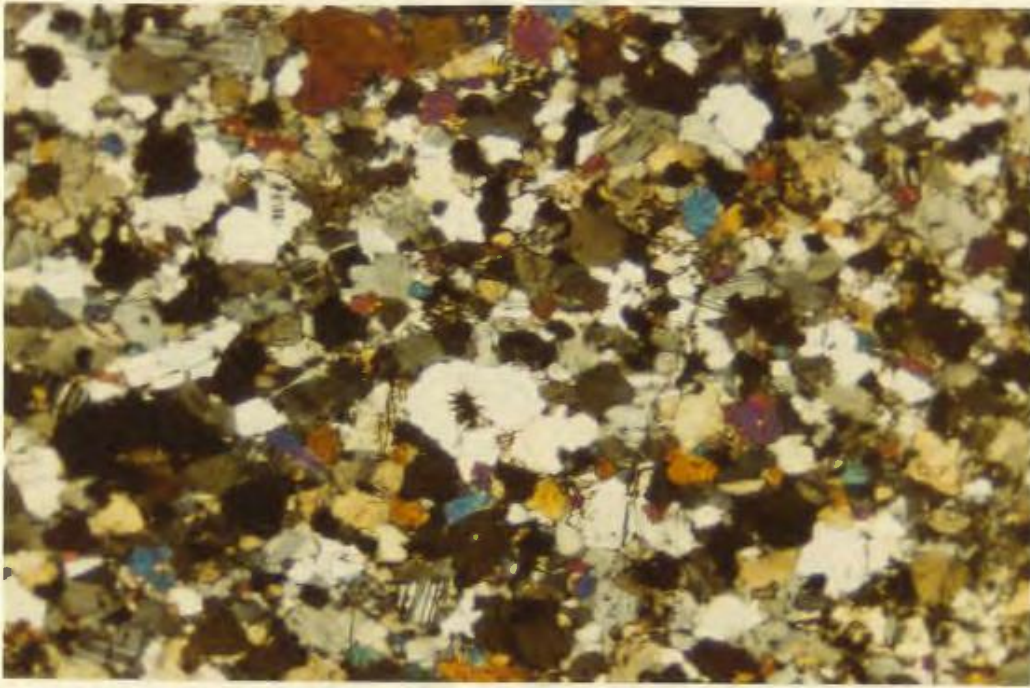


PLATE XVIIIa: Hornfels with descussate textures displayed by plagioclase, pyroxene and garnet, Trout River. X nicols x 35.

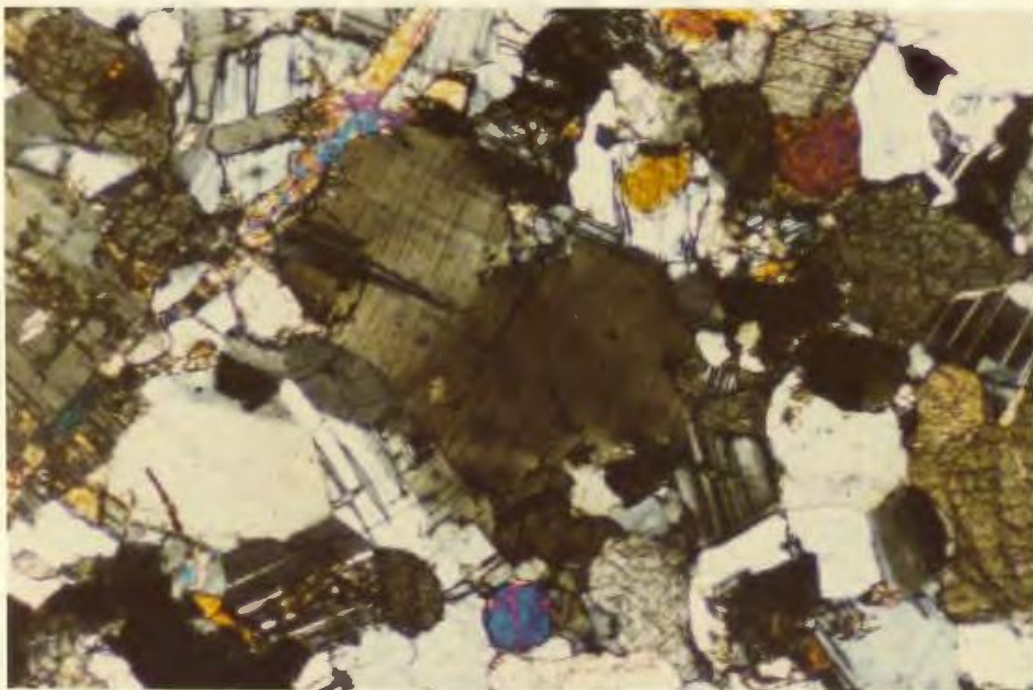


PLATE XVIIIb: Plagioclase in hornfels showing undulose extinction X nicols x 180.

products such as chlorite. The garnet itself is of the pyralspité series with a considerable proportion of grossularite, and has the composition $Mg_{1.7} Fe_{0.8} Ca_{0.5} Al_2 Si_3 O_{12}$. (Table IV). It occurs throughout the hornfels as crystals up to 0.5 mm in size and in general appears to have grown synchronously with the clinopyroxene. Rarely, however, the garnet contains randomly orientated pyroxene and plagioclase inclusions (Plate XIXa).

Similar pyroxene-garnet hornfelses have been described by Challis (1965a and b) from the western margin of the Red Hills ultramafic intrusion, New Zealand. Challis suggests that the hornfelsing is a result of thermal metamorphism produced by the intrusion of ultramafic rocks at a temperature of about 1200°C. A similar assemblage was also described by Hunahashi (1948) for an ultramafic intrusion contact aureole in Hokkaido, Japan. MacGregor (1964) has described granular garnet-clinopyroxene amphibolite within 200 feet of the contact of the Mount Albert peridotite, Gaspé, Quebec. Although composing part of an aureole originally described as a result of intrusion of hot peridotite by MacGregor, recent work (Laurent, personal communication, 1975) indicates that a dynamothermal origin similar to that of the Bay of Islands aureole is probable. Karamata (1968, 1974) has explained the origin of aureoles of ophiolite suites from the Dinarides in the same way. In some cases granulite facies rocks are developed close to the contacts.

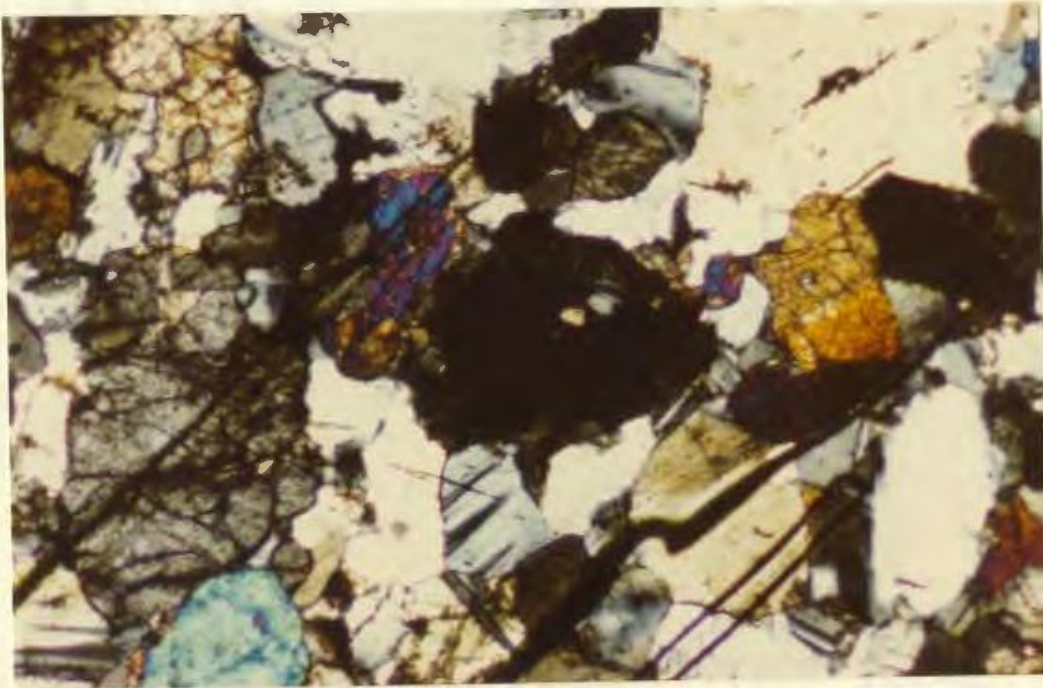


PLATE XIXa: Garnet (isotropic) with inclusions of pyroxene and plagioclase. Hornfels - Trout River. X nicols, x 180.

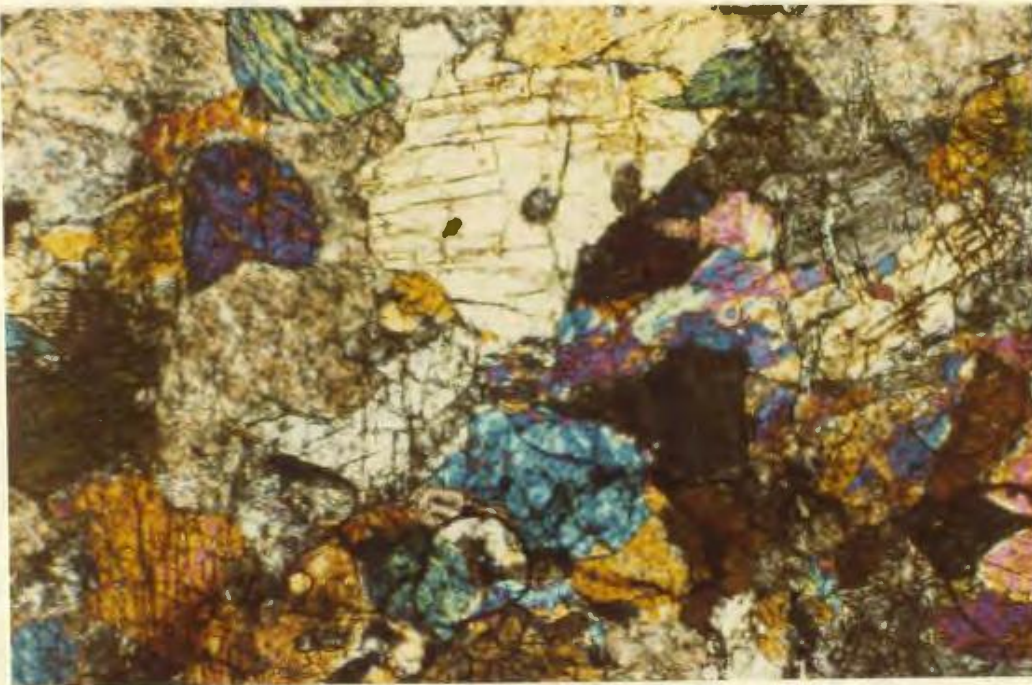


PLATE XIXb: Amphibole replacing pyroxene of basal hornfels - from 4 1/2 metres from basal contact, Trout River. X nicols x 150.

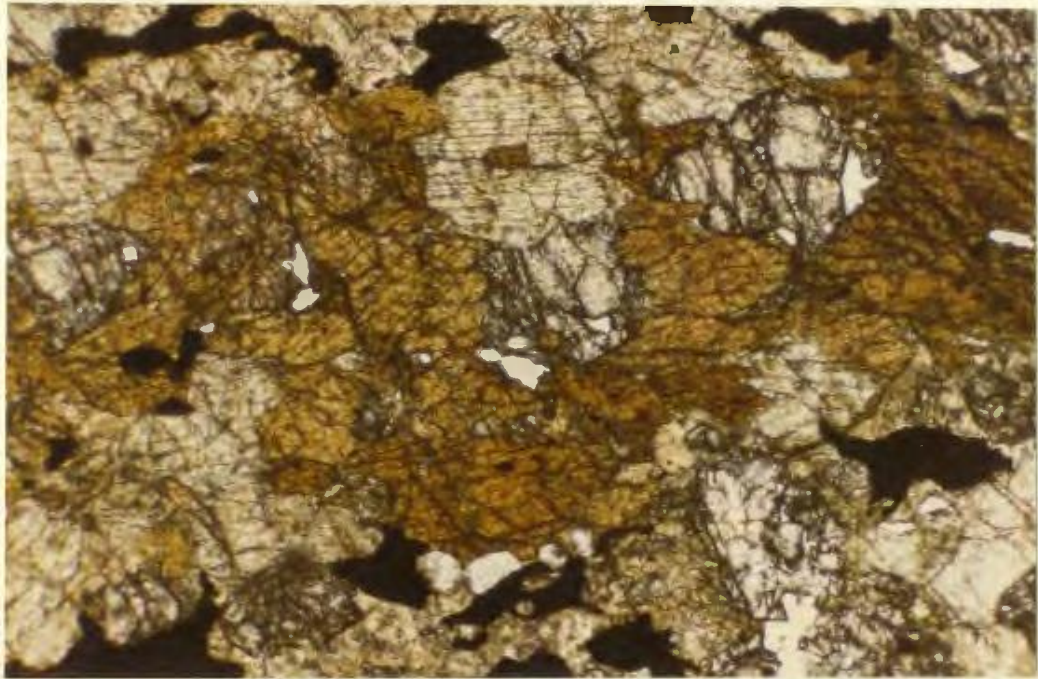


PLATE XXa: Brown pleochroic hornblende from 5 metres from basal contact, Trout River. Plain light x 80.

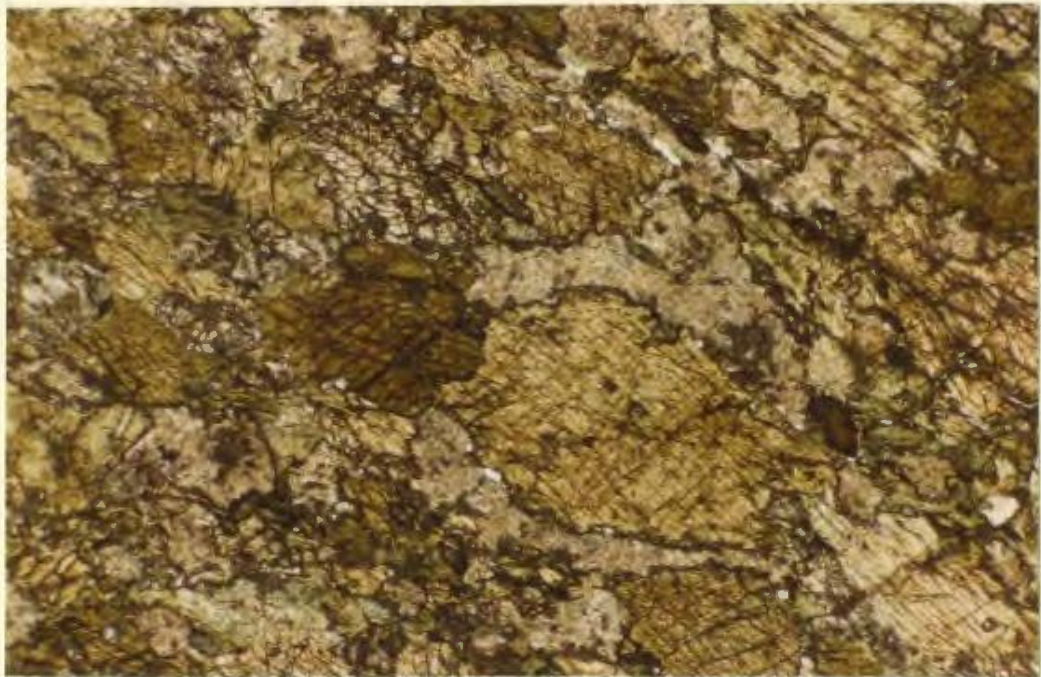


PLATE XXb: Green pleochroic hornblende 12 metres from basal contact, Trout River. Plain light x 80.

iii) Amphibolites

Except where the hornfels is developed, amphibolites occur in direct contact with the ultramafic rocks. Where a hornfels is developed, amphibole replaces the pyroxene of the hornfels at about 4 metres from the contact (Plate XIXb). The amphibolite is almost universally pyroxene-bearing at the contact and where fully developed grades downwards into garnetiferous amphibolite and black amphibolite to a distance of about 70 metres from the contact. At Pond Point on North Arm, the amphibolites grade at this point into greenschists.

In thin section the amphiboles are variably coloured. In general, brown pleochroic hornblende is more common closer to the contact and green pleochroic varieties more abundant further away (Plates XXa, XXb). The hornblende may form up to 70% of the rock (Table III), generally as elongate crystals approximately 0.5 to 1 mm in length, with their z axes usually defining a schistosity. Alternating bands of more or less amphibole content give the rock a distinctive overall banded appearance in which garnets appear quite often as large pinkish knots, and in which the alignment of the amphibole produces a well defined L-S fabric (Plates XXIa, XXIb).

The plagioclases are almost totally altered to a fine-grained intergrowth of sericite and epidote, and carbonate is present in some cases. Where twinning is still visible it does not appear strained. Some plagioclase is porphyroblastic but the inclusions, which are pyroxenes and amphiboles, give rise to sieve textures and do not define trails (Plate XXIIa).



PLATE XXIa: Banded amphibolite, basal aureole. North Arm Mountain.



PLATE XXIb: Banded amphibolite, basal aureole. Trout River.

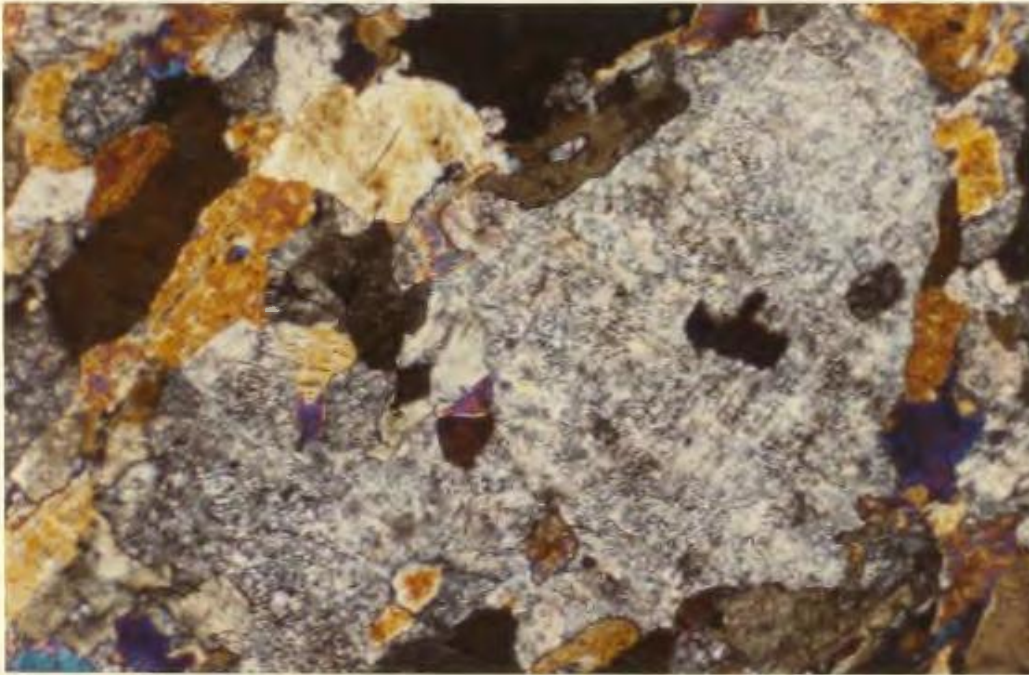


PLATE XXIIa: Altered plagioclase porphyroblast containing pyroxene inclusions. X nicols x 65.

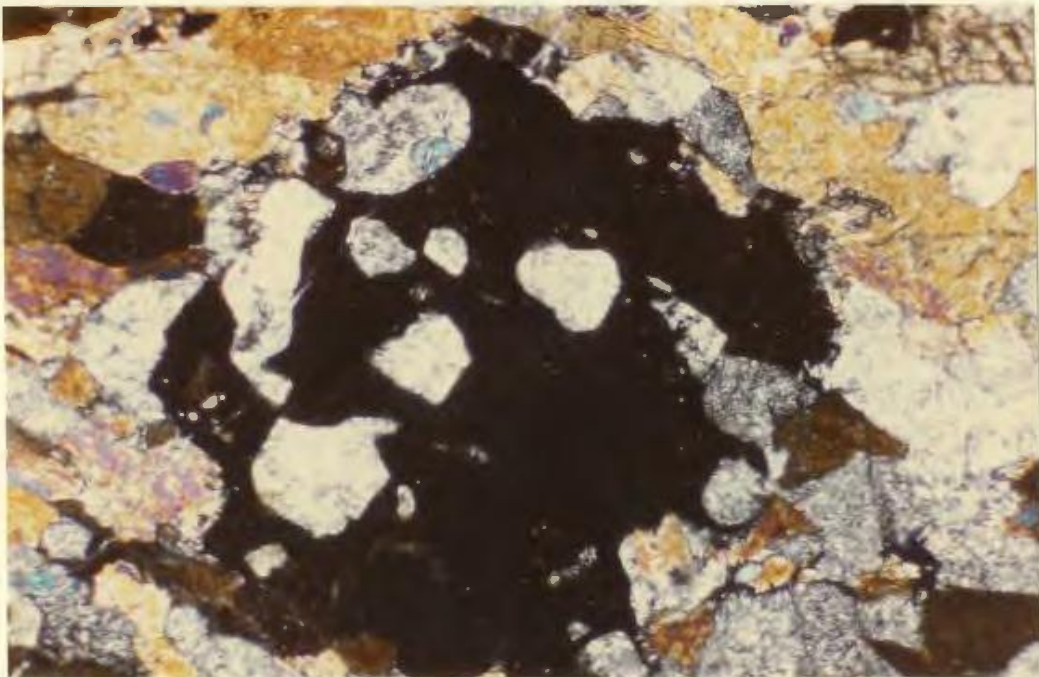


PLATE XXIIb: Garnet porphyroblast showing alteration to sericite. Amphibolite-basal aureole. X nicols x 80.

Garnet porphyroblasts generally decrease in abundance away from the contact. They are sometimes helicitic and also show embayed and altered margins. The alteration in many cases has almost completely destroyed the garnets and has penetrated far into fractures (Plate XXIIb). Even so, the garnets are quite visible in hand specimen and are as much as 5 mm in diameter. One kilometre west of Stowbridge Head on North Arm, the garnetiferous amphibolite is completely broken down and schistose at the contact with serpentinised ultramafic rock, and consists of about 50% pale red garnet porphyroblasts in a black indiscernible matrix (Plate XXIIIa).

The pyroxene-bearing amphibolites are thought to be a garnet-pyroxene hornfels which has undergone retrogressive metamorphism. Pale green pleochroic hornblende can be seen replacing both pyroxene and garnet of the hornfels at the head of Trout River Ponds. Although no pyroxene exists in the aureole rocks at a distance of greater than 6 metres from the contact, it cannot be definitely said that this marks the limit of the original hornfels because of the intensity of obliteration of the pyroxenes by amphibole further from the contact.

Within the pyroxene-free amphibolites a strong foliation is invariably developed. Where replacing the hornfels, this foliation is reasonably well developed about 4 metres from the contact, but elsewhere it may be noticeable right up to the contact. The foliation augens the helicitic garnets, which themselves contain traces of an earlier foliation (Plate XXIIIb). These garnets are therefore of a younger age than the original garnets of the hornfels.

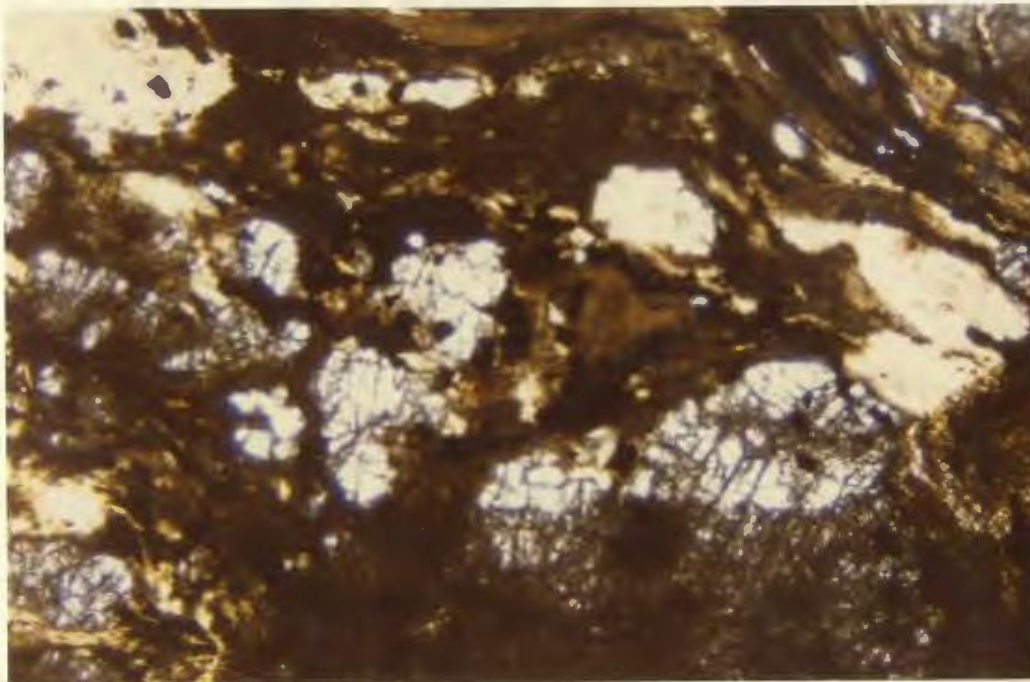


PLATE XXIIIa: Garnets in black graphitic? matrix - 1 km
W. Stowbridge Head, North Arm. Plain light x 15.

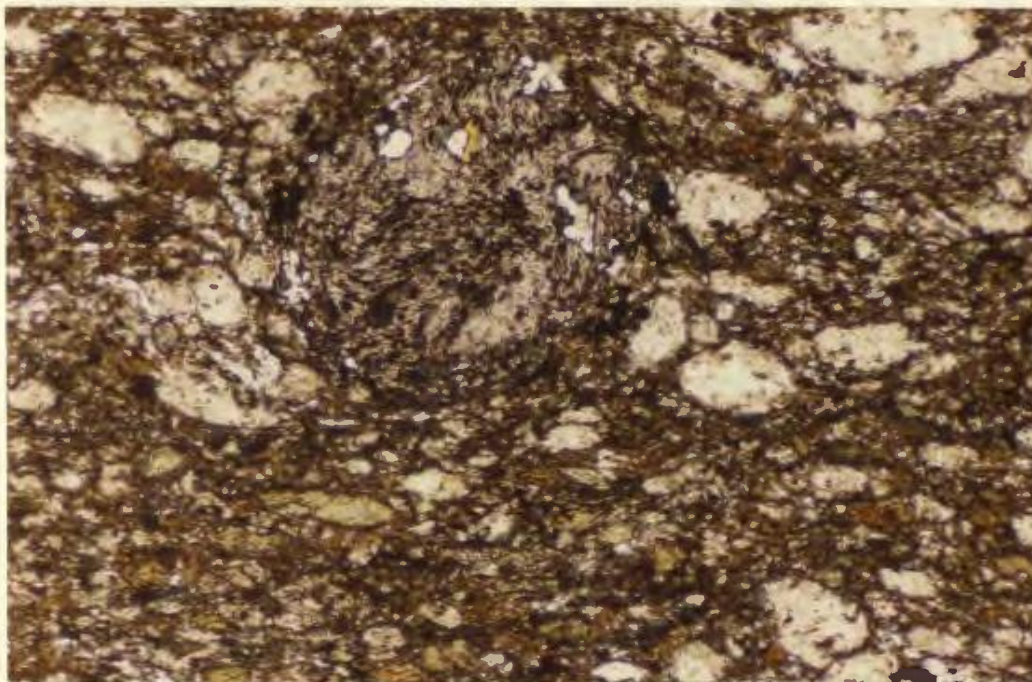


PLATE XXIIIb: Helicitic trails (S_1) in garnets of amphibolite.
 S_2 dominantly augens these garnets. Plain light x 50.

At Pond Point, underlying amphibolites consist of dark grey to black foliated rocks composed of altered plagioclase and hornblende. Garnets are not very common in these rocks, but biotite is present especially in the region of gradation into the greenschists.

iv) Greenschists

The amphibolites of the North Arm Mountain aureole are gradational over a few metres into underlying greenschists. This gradation generally takes the form of a decrease in abundance and grain size of the amphibolite and an increase in the amount of chlorite. The mineral assemblage that coincides with the lithological subdivision of the aureole rocks includes chlorite-albite-quartz-epidote-muscovite-biotite-actinolite, thus defining greenschist facies metamorphism. In hand specimen the greenschists appear finely laminated (Plate XXIVa) with thin alternating dark-green and light-green laminae. The extensively chlorite rich bands are everywhere foliated and schistose and fine grained chlorite, actinolite, biotite and epidote both define schistosity and appear to reflect periods of regenerated growth.

v) Phyllites and unmetamorphosed sediments

At Pond Point, the greenschists grade stratigraphically downwards into a phyllite zone. The phyllite zone is characterised by fine-grained dark-grey or green schistose rocks in which garnet and quartz porphyroblasts are visible in hand specimen. Such rocks are themselves gradational into unmetamorphosed argillites and sandstones



PLATE XXIVa: Laminated greenschists, North Arm aureole.



PLATE XXIVb: Phyllites of North Arm Aureole.

(Plates XXIVb, XXVa). Remnants of similar protoliths are seen in the semi-schistose rocks of the greenschist zone in the form of recrystallised quartz and feldspar rich bands in fine-grained mica rich rocks.

In thin section, the garnets of the phyllites are often poikiloblastic and have symplectite rims. Muscovite is common and augens the garnets and clasts of strained quartz (Plate XXVb). Opaques form a considerable portion of the modal mineralogy in some samples. Later-stage minerals include epidote and chlorite replacing the garnet, and calcite and rare prehnite in veins.

The sedimentary rocks are relatively unmetamorphosed but have undergone considerable cataclasis, which is especially noticeable in the coarser sandy sediments (Plate XXVa). In these, the quartz and feldspar grains are subangular to subrounded, poorly sorted and occur in a calcite, epidote and muscovite rich matrix. The grains, almost without exception, have undulose extinction, but are rarely fractured. Detrital chlorite and garnet, possibly derived from lithologies similar to those of overlying rocks, have been recognised in the sandstones (Plate XXVIa). The argillites are generally rich in opaques with additional muscovite, feldspar and secondary calcite and chlorite. In addition, they also contain small clasts of recrystallised quartz, although these are relatively rare. The composition of the argillites suggests that they may be volcanic in origin. If so, then these rocks are the only volcanic rocks that are in contact with the aureole in the Bay of Islands, except for those pillow lavas juxtaposed with amphibolites at the southeast end

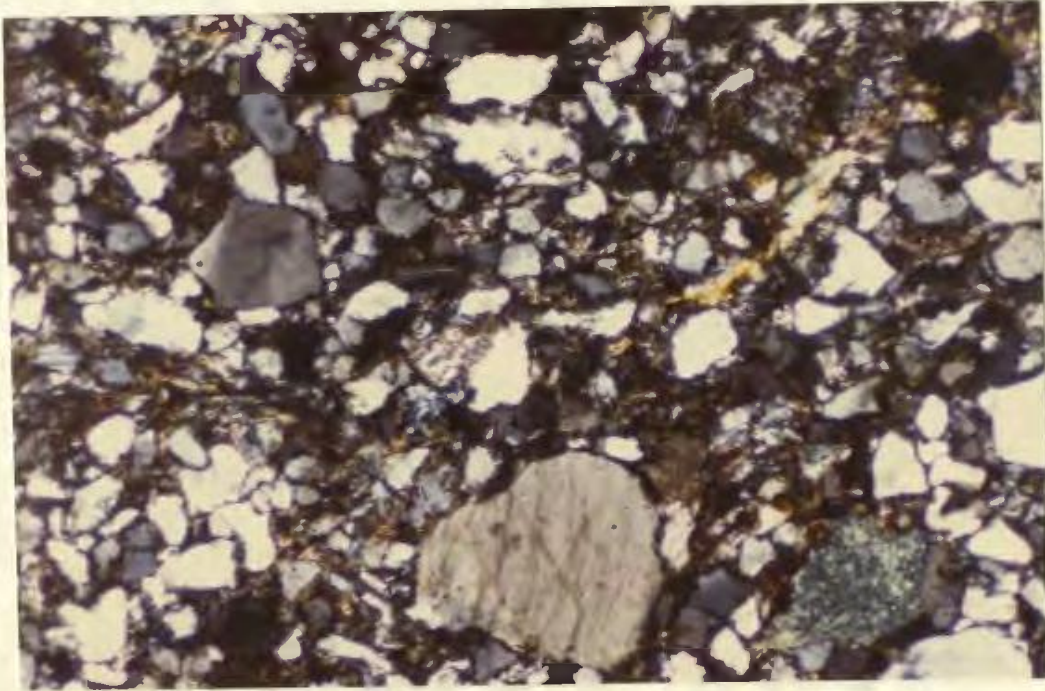


PLATE XXVa: Clastic sediments of aureole section, North Arm.
X nicols x 30.

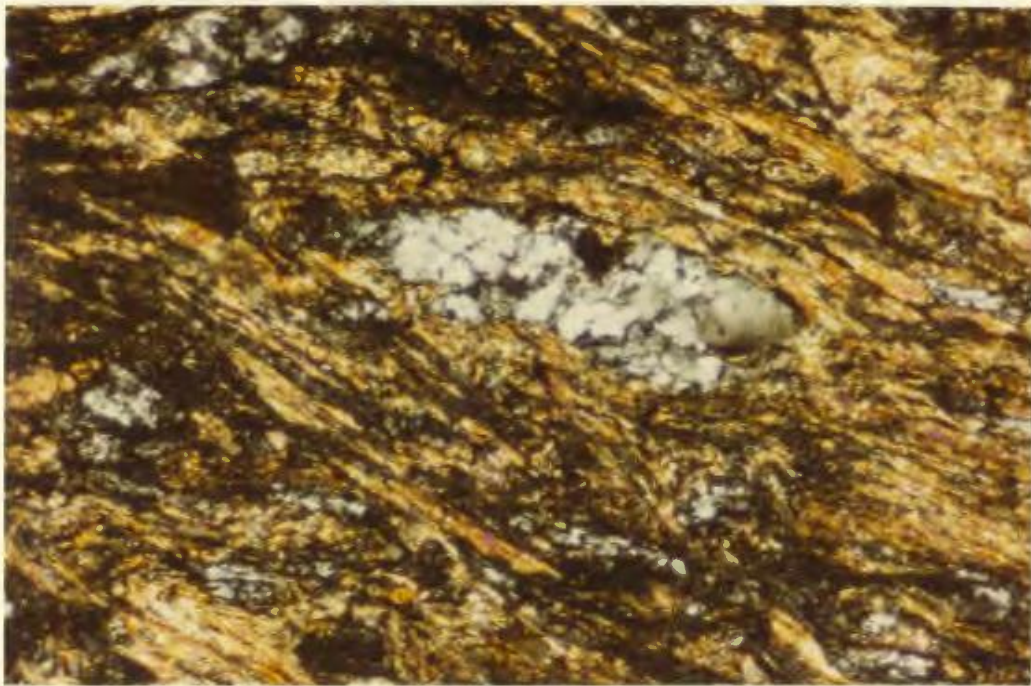


PLATE XXVb: Muscovite surrounding strained quartz clast in
phyllite. North Arm. X nicols x 35.

of Trout River Pond. This latter contact is demonstrably a fault contact and thus the volcanic rocks cannot be shown to be the certain protolith of the aureole at this locality. However, the aureole beneath the Hare Bay (White Hills) ultramafic slice has definite volcanic protoliths (Williams and Smyth, 1973; Malpas et al., 1973) and resembles that of the Bay of Islands both in structure and mineralogy. The presence of a volcanic protolith lessens the problem of appealing to metasomatic processes to account for the chemistry of the aureole (cf. Smith, 1958).

vi) Metasomatised rocks.

Hornfelses at the base of the North Arm Mountain massif are altered in places to rodingitic assemblages, which appear in hand specimen to have a gabbroic texture. Secondary calcium bearing minerals, prehnite, xonotlite, calcite and clinozoisite are present, and calcite veinlets are ubiquitous. Diopside, hornblende, plagioclase and almandine garnets are present as part of the original mineral assemblage, but the large poikilitic garnets are replaced by hydrogrossular and chlorite (Plate XXVIb). Development of fine-grained clinozoisite and epidote in the rock makes identification of plagioclase difficult. The hydrogrossular and xonotlite have been identified by x-ray diffraction (Appendix I).

Rocks of dominantly calc-silicate mineral assemblages have been recognised at the base of North Arm Mountain, near fault contacts on Winterhouse Brook and near first Trout River Pond. These metasomatic

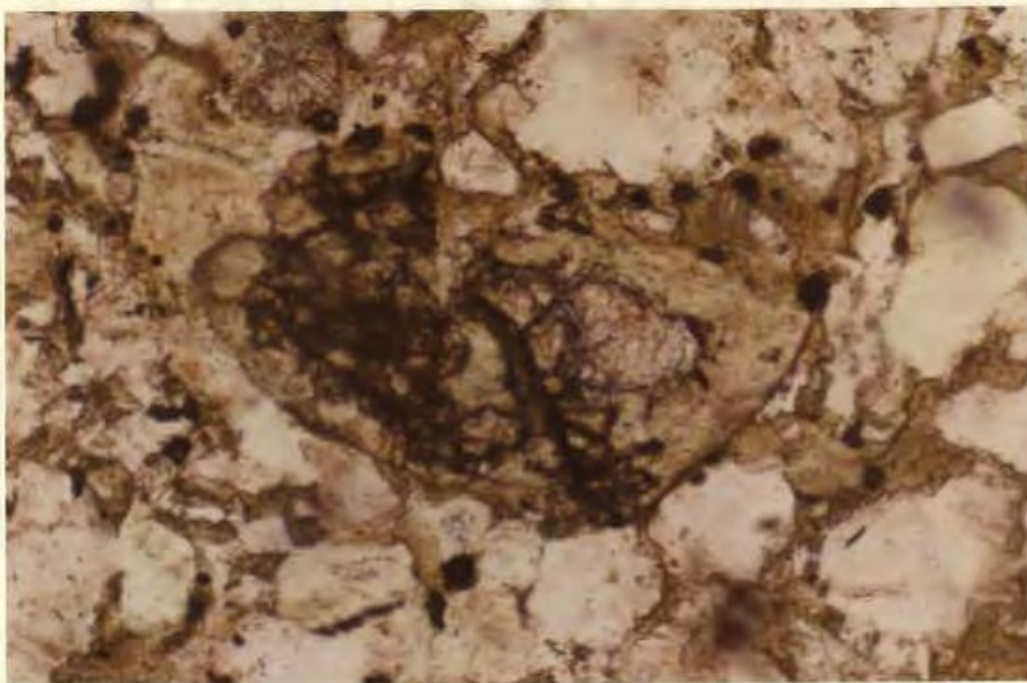


PLATE XXVIa: Detrital garnet in sandstone from base of aureole, North Arm. Plain light x 140.

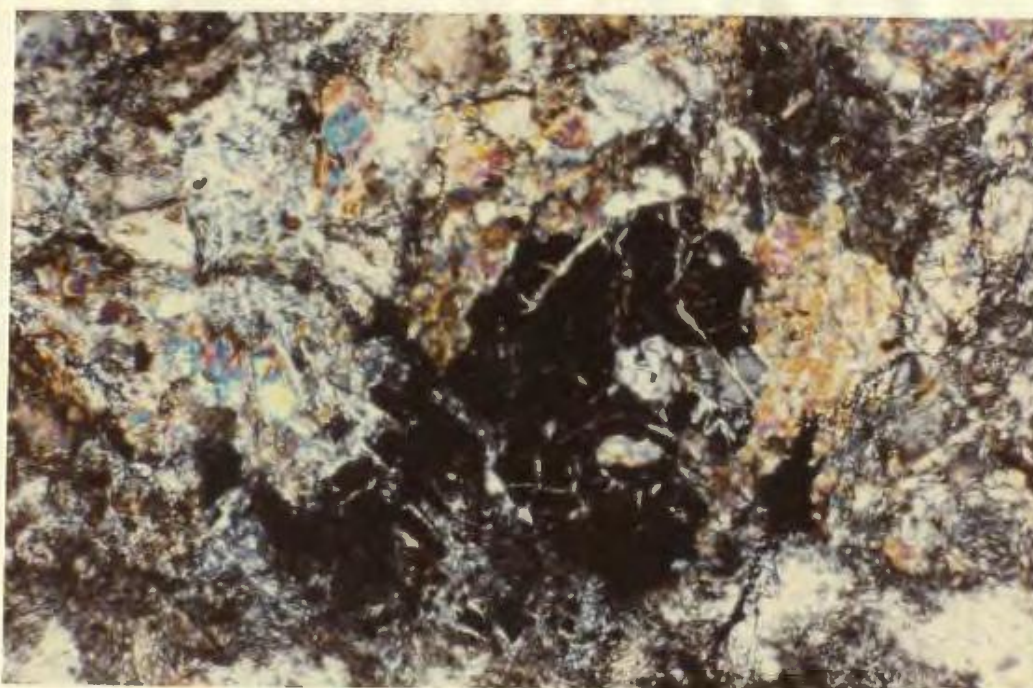


PLATE XXVIb: Hornfels with original garnet/px/plag mineralogy partially replaced by Ca bearing phases in rhodinitic alteration - Trout River. X nicols x 100.

assemblages are accompanied by a colour change in rocks adjacent to the ultramafic rocks, especially at Winterhouse Brook (Plate XXVIIa) where the assemblages are best developed and the shales juxtaposed with the ultramafics appear bleached. Here, and elsewhere, the calc-silicates form hard, resistant, white to pink veins that clearly cross-cut and therefore post-date both the development of the aureole amphibolites and the serpentinisation of the ultramafic rocks.

Mineral assemblages include prehnite, calcite, wollastonite, xonotlite, pectolite, hydrogrossular and other secondary calcium-bearing minerals. The xonotlite was reported by Smith (1954) as the first occurrence in Canada. It occurs as both amorphous, massive, pink aggregates and fibrous forms (Appendix I).

The origin of the metasomatised rocks, which can be loosely termed rodingites is probably hydrothermal, but it cannot be determined whether the metasomatism took place during a late stage of emplacement of the ophiolite, or much later during subsequent faulting. The only source of lime existing in the ultramafic rocks now exposed at the contacts is in the small amounts of clinopyroxene. It is more probable that the necessary lime was derived from the calcium-rich rocks of the aureole, possibly by the circulation of water trapped in the underlying sediments during thrusting.

G. Structure.

The deformation of the aureole rocks took place prior to the final emplacement of the ophiolite slices. The evidence for this is similar to that described by Smyth (1973) for the White Hills slice of the Hare Bay Allochthon.

i.e. 1) Aureole rocks displaying composite schistosity are truncated by black and green shales of mélangé along the coast of North Arm.

and 2) Boulders of polydeformed schist and amphibolite originating from the aureole are found in mélangé zones beneath the Table Mountain massif and the Blow me down massif.

Most of the aureole rocks are polyphase deformed, but the deformation is most evident in the greenschists and amphibolites. No folds or schistosity are observed in the pyroxene hornfels of the contact zone, but where the pyroxenes and garnets are replaced by amphiboles, then a crude alignment of these amphiboles defines a schistosity. No accompanying folds have been observed in these pyroxene amphibolites, but since the schistosity parallels axial planes of second phase (F_2) developed lower in the aureole, it has been recognised as a second phase composite schistosity.

Evidence of the first deformation (D_1) is well preserved as a strong schistosity (S_1) in the metavolcanic rocks of the greenschist member, and is defined by a preferred orientation of chlorite, tremolite-actinolite and flattened plagioclase phenocrysts. In the phyllites the



PLATE XXVIIa: Basal faulted contact at Winterhouse Brook. Development of calc silicates as white/grey dike in centre and bleached shales below.

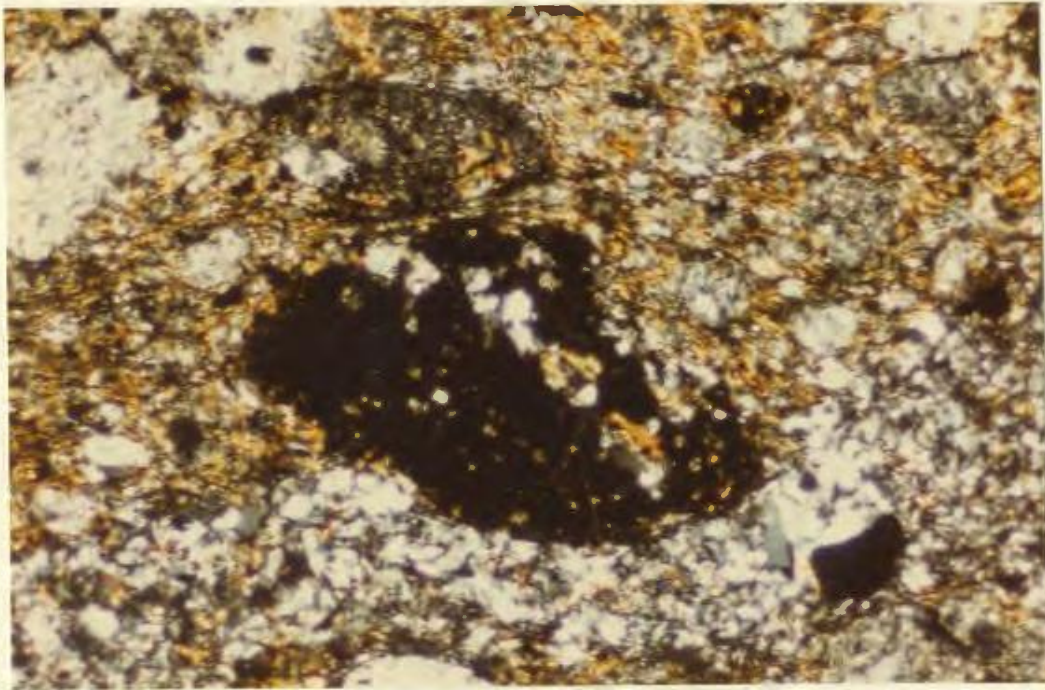


PLATE XXVIIb: Pre-D₂ garnet containing S₁ inclusion trail, amphibolite, North Arm Aureole. X nicols, x 95.

S_1 muscovite-chlorite fabric is crenulated by the S_2 schistosity in places, and on the fold limbs is transposed into the S_2 planes. S_1 is only rarely preserved in the amphibolites. It is defined by aligned hornblendes, biotites and opaques and is only recognised as an included fabric in post- D_1 garnet porphyroblasts (Plate XXVIIb).

The second deformation (D_2) produced recumbent folds with an associated axial planar cleavage in the greenschist member, and the dominant schistosity, S_2 , in the amphibolites. F_2 folds are difficult to recognise in the amphibolites. S_2 in the greenschists is represented by a closely spaced crenulation cleavage with little metamorphic growth restricted mainly to development of chlorite and sericite. S_2 completely transposes S_1 in the amphibolites and is marked by growth of biotite and amphibole. This composite fabric is the same as that found in the pyroxene amphibolites. Garnets concentrated in the higher parts of the amphibolites are augened by the composite S_2 fabric and their inclusion trails are both helicitic and straight indicating in the former case growth of garnet syntectonically with the development of S_1 (rotational) and in the latter, the static growth of garnet over the pre-existing S_1 schistosity. In no place has garnet been observed clearly cutting amphibole or biotite fabrics although Williams and Smyth (1973) report small garnet overgrowth phases including parts of the S_2 schistosity.

In a simplified view then, the structural development of the aureole appears to fall into two main dynamic phases (D_1 and D_2) separated by a period of static mineral growth. However, this simplification must not be taken to preclude the continuous metamorphic development of the aureole.

D. Mineralogy, Metamorphism and Mineral Paragenesis.

i) Orthosilicates

a) Epidote Group: Epidote group minerals occur both within the metamorphic aureole, sometimes as a major phase, and in the relatively unmetamorphosed country rocks where they form only a minor phase. Although there is no clearly definable variation in the modal percentage of these minerals with distance from the contact, their absence from the amphibolite zone is noticeable.

In the sandstones beneath the aureole, colourless, non-pleochroic, inclusion-free epidote appears as fine-grained ragged crystals intergrown with clay minerals. The mineral has characteristic high relief and the crystal outlines are enhanced by rims of dusty oxides. Rarely six-sided euhedral cross-sections may be observed. Concentrations of acicular crystals of colourless clinozoisite are more common than epidote. The clinozoisite generally exhibits anomalous birefringence, is optically positive and has a high $2V_{\gamma}$ (c. 70° but variable). It is both distributed throughout the matrix and is found growing within quartz grains which themselves show considerable recrystallisation microstructures (Plate XXVIIIa).

Epidote group minerals are finely dispersed and relatively rare in the fine grained tuffaceous rocks. In phyllites derived from these tuffs, the epidote is also rare and is generally associated with chlorite vugs.

Epidote is extremely common in the greenschists where it exhibits the following pleochroic scheme:

α colourless β pale green-yellow γ pale green

Where weak schistosity is developed the epidote crystals are often elongate with their b axes parallel to the schistosity, and in intimate association with blue-green to pale-green pleochroic ferroactinolite. In many cases, however, epidote within the greenschists defines distinct bands which are folded about small scale tight folds with attenuated limbs. Within the noses of these folds, the epidote is totally recrystallised into equidimensional crystals (c. 0.08 mm) exhibiting triple point junctions. In the nomenclature of Williams and Smyth (1973) these folds are second phase folds and the paragenesis of the epidote is related to an earlier D_1 deformation that produced the main schistosity S_1 in the greenschists. Subsequent recrystallisation of the epidote took place during D_2 and some epidote crystals cut and therefore post-date the S_1 schistosity. These later epidotes rarely contain small unidentifiable inclusions.

Epidote is absent from the amphibolites, probably as a result of the reaction:



This reaction (Liou, 1973) may be used to define P-T conditions during formation of the greenschists, as described below (Section F).

b) Garnet Group: Garnet appears as a primary phase only in the aureole rocks, but also as a detrital mineral in the sandstones underlying the aureole.

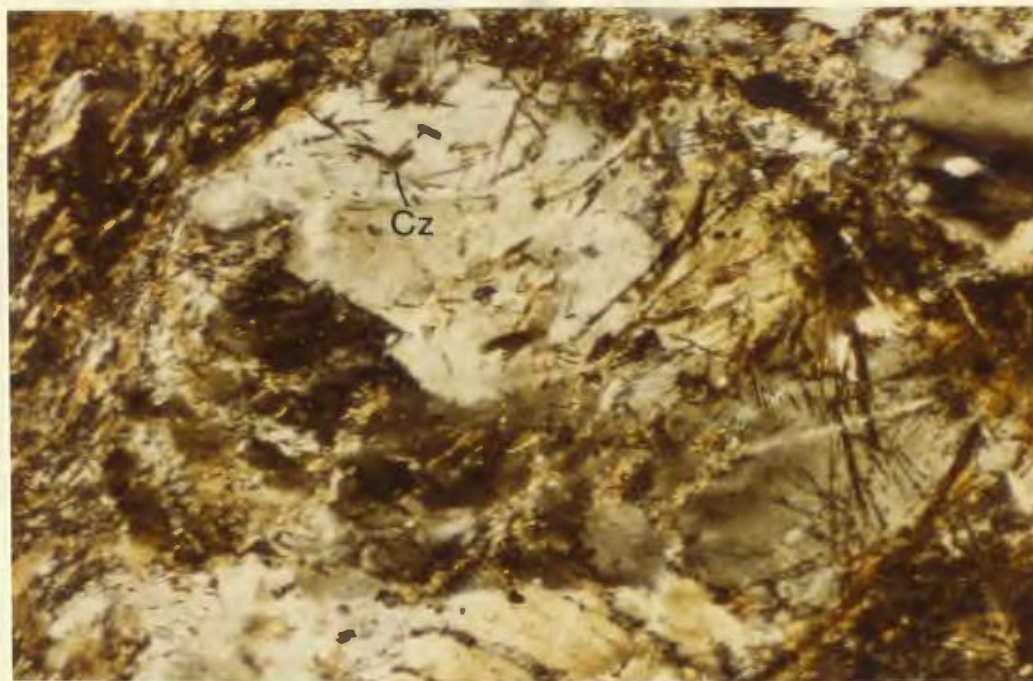


PLATE XXVIIIa: Acicular crystals of clinozoisite in quartz from basal aureole sedimentary protolith, North Arm. X nicols x 150.

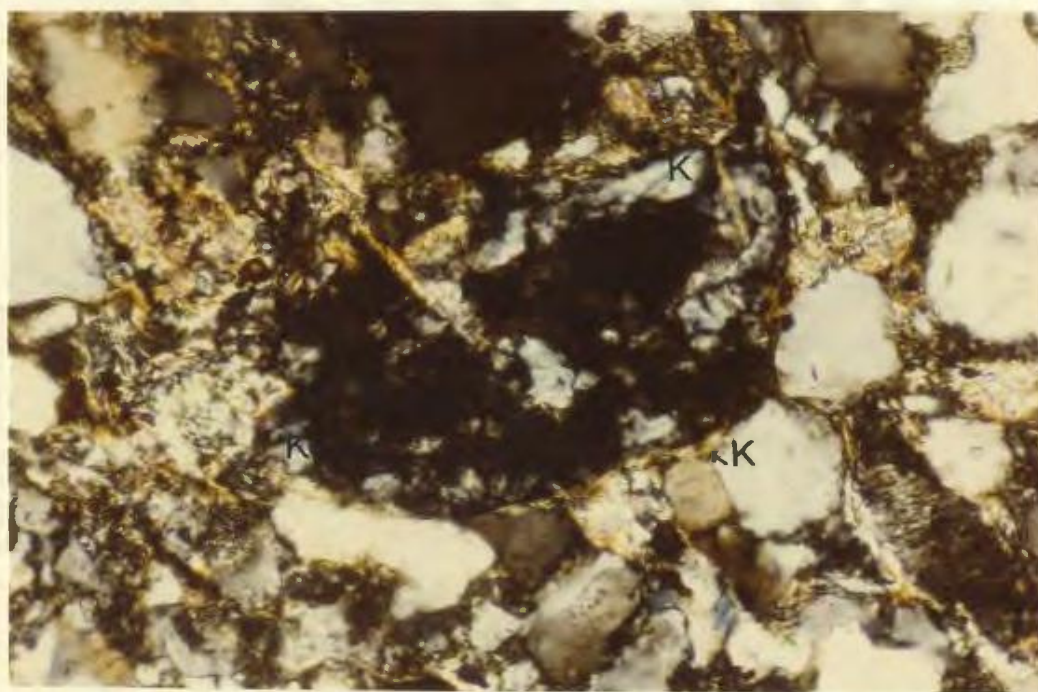


PLATE XXVIIIb: Kelyphitic rim around detrital garnet in sediments, North Arm. X nicols x 150.

The detrital garnet in the sandstones is extremely rare. It occurs as small (0.2 - 0.4 mm) subrounded crystals, although the degree of roundness is obscured by the presence of symplectite rims of mainly chlorite and epidote (Plate XXVIIIb). Ubiquitous fractures in the garnets are filled with the same minerals. If this detrital garnet was derived from aureole rocks, then the relative age and provenance of the sandstones, which lie below the aureole, becomes an important question and is discussed further below.

Primary garnet is found dominantly in the amphibolites, hornfelses, rodingites and basal ultramafic rocks, while in the greenschists and phyllites it is relatively rare and forms minute euhedral crystals less than .002 mm in diameter.

Garnets form approximately 3% of the amphibolites although they are not evenly developed throughout these rocks. Some amphibolites may be completely garnet free, whilst others contain large pink garnets up to 0.5 cm maximum dimension. It has not been determined what causes this irregular distribution of the mineral but a possibility is an original compositional difference of the protoliths. The mean size of the garnets is 1 - 1.5 mm in diameter and they are subhedral, often fractured and partly altered to hornblende, chlorite, and minor biotite (Plate XXIXa).

The garnets contain inclusion trails of two general types:

- 1) Those mimicking the crystal outline of the garnet in a number of circular trails indicating fast static growth of the garnet after an earlier deformatory phase.

2) Those defining this earlier phase of deformation in the form of an included schistosity, S_1 , in some cases indicating a rotation of the garnets.

Thus the garnets seem to be generally post-tectonic with respect to an earlier phase of deformation (D_1 of Williams and Smyth, 1973), but are pre-tectonic to a later phase (D_2 of Williams and Smyth, 1973) since the associated schistosity (S_2) outlines augen around them.

Where post- D_1 garnets do not possess inclusion trails, they may be difficult to distinguish from earlier garnets associated with the formation of the pyroxene hornfels, especially in the transition zone between hornfels and amphibolite where the pyroxenes and garnets of the former are replaced by amphibole.

e.g. GARNET \longleftrightarrow HORNBLLENDE + PLAGIOCLASE (MacGregor, 1964)
and/or GARNET \longleftrightarrow HORNBLLENDE + EPIDOTE

Garnets within well defined hornfels are clearly pre-tectonic with regard to any schistosity (including S_1). They have well developed alteration rims and do not contain inclusions. Garnets only form approximately 1% of the hornfels and are generally quite small (0.02 mm) and somewhat irregular in shape. They are marginally altered to hornblende which itself defines a schistosity with increasing distance from the contact.

Rodingitised and altered rocks at the contact contain large, irregular and fractured pink garnets. These are associated with hydrogrossular of lower refractive index, but both are colourless in thin section. The garnets include pyroxene, but no metamorphic fabrics are

identifiable, and they appear to be almandine in composition although there is a significant amount of CaO substitution, a metasomatic effect resulting from the rodingitisation. Hydrogrossular has also been recognised by x-ray diffraction methods in the calc-silicate assemblage from the base of North Arm Mountain and from Winterhouse Brook (Appendix I). The development of this calc-silicate assemblage is considered to result from processes similar to those which produced the rodingites, namely a calcium metasomatism during the emplacement of the ophiolites.

Garnet occurs within the mylonite zones in the ultramafic rocks, associated with pyroxene and brown hornblende. The garnet may form up to 20% of a single mylonite band, is generally of the order of 0.05-0.08 mm in diameter and equidimensional, subhedral and colourless. Light green spinels occur in the hornblende bands and were reported by Church (1972) to have garnet rims. No such textures were observed in this study. The garnets are pyrope in composition having an FeO/MgO mole ratio of 1.0 and 5.5 wt. % CaO (Church, 1972).

Microprobe analyses and calculated structural formulae of some aureole garnets are given in Table IV.

Approaching the basal ultramafic contact the garnets have increasing contents of magnesium and associated decreasing contents of iron, manganese and calcium. The trends are systematic and unlike those reported by Challis (1965), MacGregor (1964) and Pamic *et al.* (1973) for garnets from aureoles of other ultramafic complexes, where a relatively wide range of compositions show no systematic variation with distance from the contacts.

TABLE IV

GARNETS FROM BAY OF ISLANDS COMPLEX AUREOLE
towards contact

		→					
	Spec. #	B1	B2	B4	B5(1)	B5(2)	VII
wt %	SiO ₂	39.16	39.46	41.38	41.75	41.16	37.41
	TiO ₂	0.19	0.12	0.06	0.03	0.06	0.00
	Al ₂ O ₃	21.88	21.59	22.93	23.86	24.05	22.53
	Cr ₂ O ₃	0.00	0.09	0.11	0.05	0.00	0.12
	FeO	21.86	21.24	14.46	12.41	11.91	22.94
	MnO	1.59	0.75	0.46	0.35	0.31	0.63
	MgO	5.58	8.41	15.14	16.39	15.98	6.87
	CaO	11.66	9.27	6.24	6.18	5.83	8.81
	Na ₂ O	0.01	0.00	0.01	0.01	0.00	0.00
	K ₂ O	0.01	0.02	0.01	0.02	0.02	0.02
	RECALCULATED FORMULA UNITS	Si	5.957	5.984	6.008	5.98	5.978
Al Tet		0.043	0.016	0.008	0.02	0.022	0.178
Al Oct		3.882	3.844	3.934	4.01	4.096	3.956
Ti		0.022	0.014	0.007	0.003	0.007	0.0
Cr		0.00	0.011	0.013	0.006	0.0	0.015
Fe ²		2.782	2.694	1.756	1.487	1.447	2.986
Mn		0.205	0.096	0.057	0.042	0.038	0.083
Mg		1.265	1.901	3.277	3.499	3.459	1.594
Ca		1.901	1.506	0.971	0.949	0.907	1.469
Na		0.003	0.0	0.003	0.003	0.0	0.0
K		0.002	0.004	0.002	0.004	0.004	0.004
Octahedral Occupancy		10.061	10.069	10.018	10.002	9.958	10.106
Tetrahedral Occupancy		6.000	6.000	6.000	6.000	6.000	6.000

STRUCTURAL FORMULAE AND ROCK TYPE

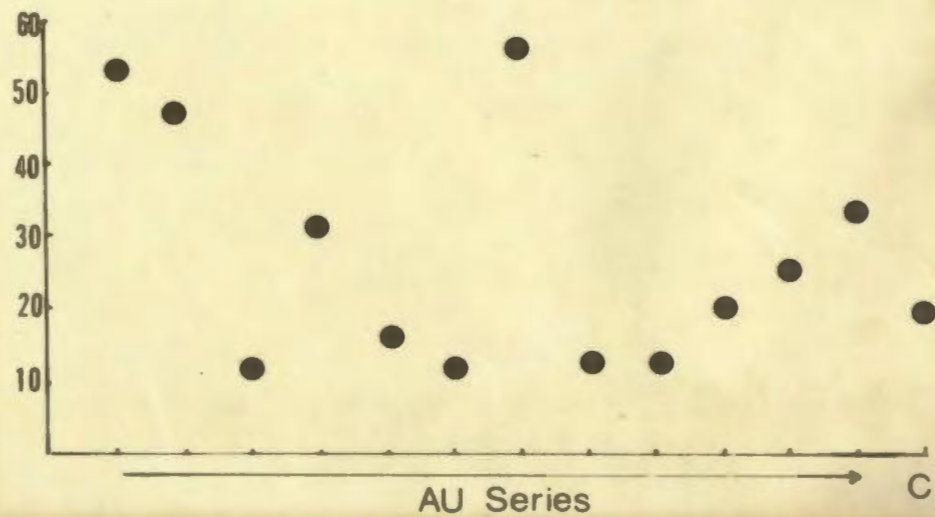
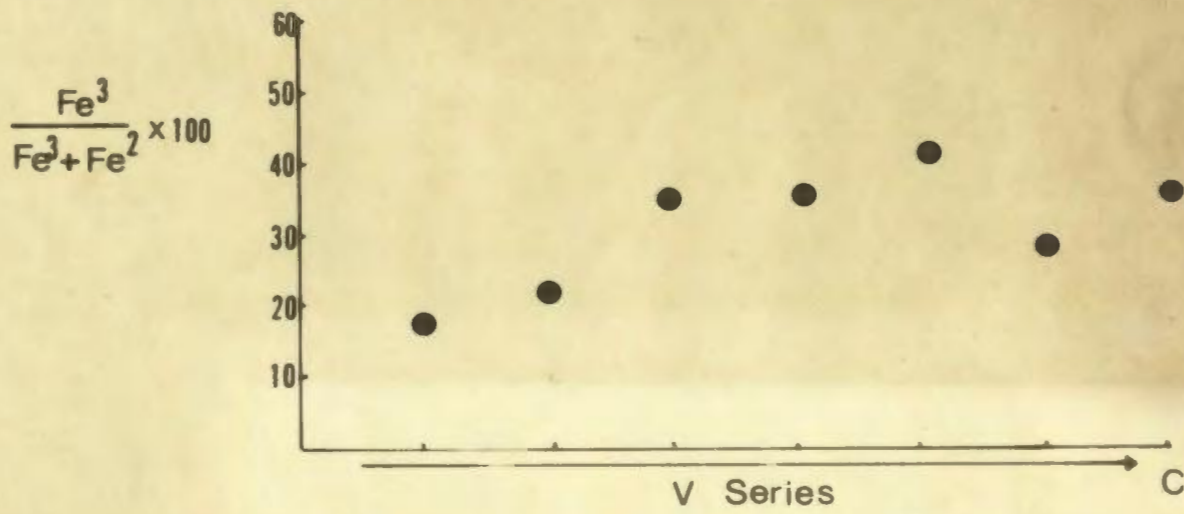
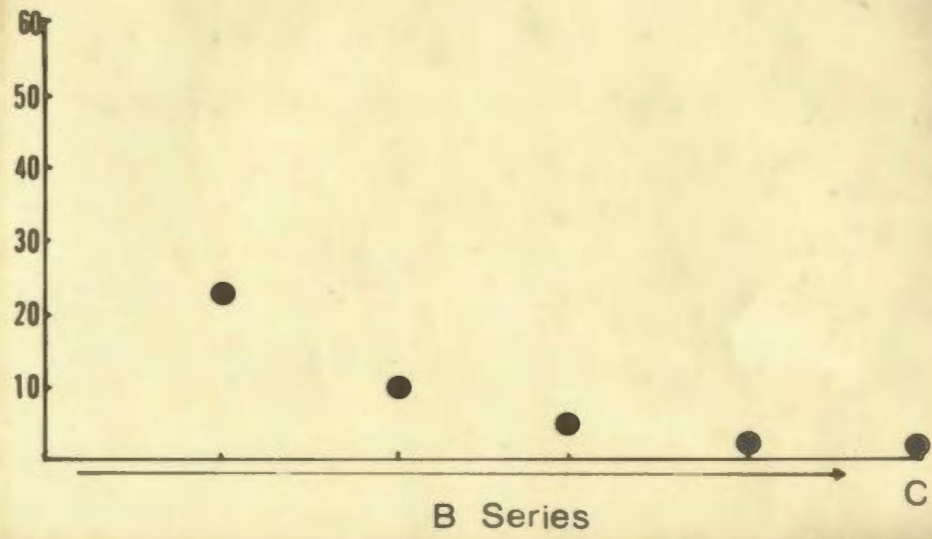
B1	(Fe _{2.5} Mg ₁ Ca ₂ Mn _{0.5}) (Al _{3.97} Ti _{0.03}) Si ₆ O ₁₂ .	Amphibolite, Trout River Po	
B2	(Fe _{2.5} Mg ₂ Ca _{1.5}) (Al _{3.99} Ti _{0.01}) Si ₆ O ₁₂ .	"	"
B4	(Mg _{3.5} Fe _{1.5} Ca ₁) (Al ₄) Si ₆ O ₁₂ .	"	"
B5(1)	(Mg _{3.5} Fe _{1.5} Ca ₁) (Al ₄) Si ₆ O ₁₂ .	Hornfels	"
B5(2)	(Mg _{3.5} Fe _{1.5} Ca ₁) (Al ₄) Si ₆ O ₁₂ .	"	"

Yoder and Chinner (1960) and Green and Ringwood (1967) have shown that the pyrope content of pyrospite garnets is a measure of pressures of equilibration. In an isochemical system pyrope content of the garnets should increase with increasing pressure. Estimates from Yoder and Chinner's (1960) work suggest that the inverse is true for increasing temperature at constant pressure. Over the relatively short distance from the contact that garnets in Table IV represent, temperature gradients were likely to have been more important than pressure gradients. With this controlling factor, iron-rich garnets are to be expected closer to the contact.

Other factors should be taken into account, such as variations in oxygen fugacity and bulk rock chemistry. The effect of increasing oxygen fugacity would be to crystallise magnetite at the expense of the almandine molecule in the garnets, resulting in more pyrope-rich garnets. However, indications are that oxygen fugacity increased away from the contact (Fig. IVb) in a manner similar to that described by MacGregor (1964) for the Mount Albert aureole. Under such conditions the more iron-rich garnets would again be expected closer to the contact.

Troger (1959), Green and Ringwood (1967), Miller (1970) and Pamic et al. (1973) have all pointed out the importance of bulk rock chemistry in controlling garnet composition. Clearly from Figs. IVc and IVd, this is the case in the aureole at Trout River Pond. Whilst bulk rock magnesium remains fairly constant throughout the aureole rocks, both ferric and ferrous iron decrease rapidly towards the contact. Calcium

Figure IVb: Oxidation of iron (as a measure of F_{O_2}) in dynamothermal aureole.



C = CONTACT

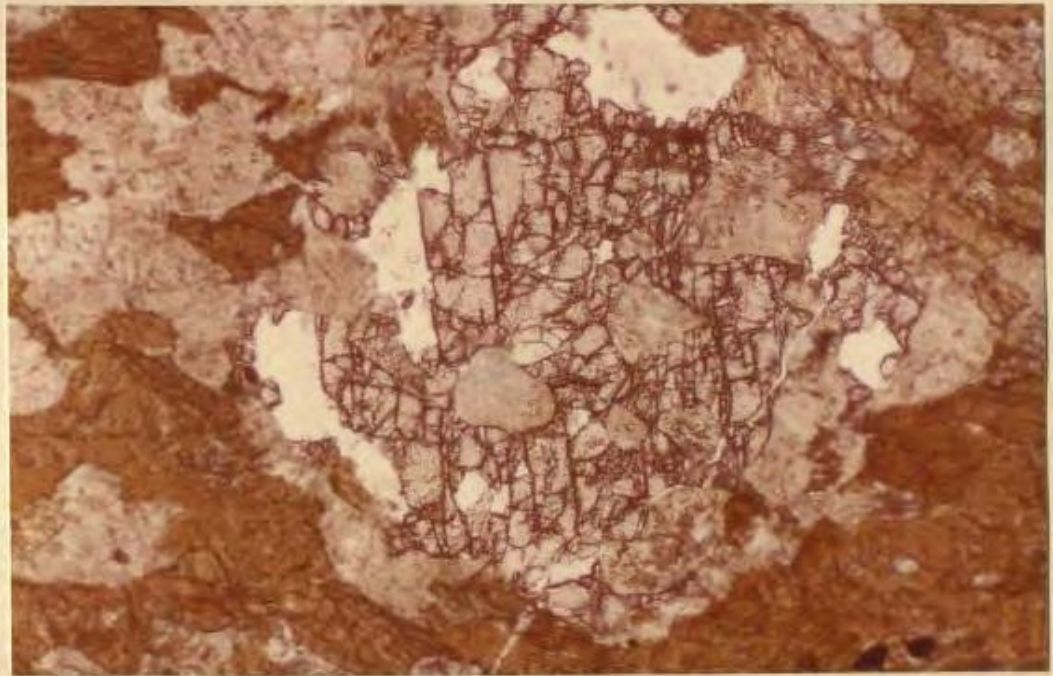


PLATE XXIXa: Large porphyroblastic garnet showing marginal alteration to sericite (?). Amphibolite, Trout River. Plain light x 35.

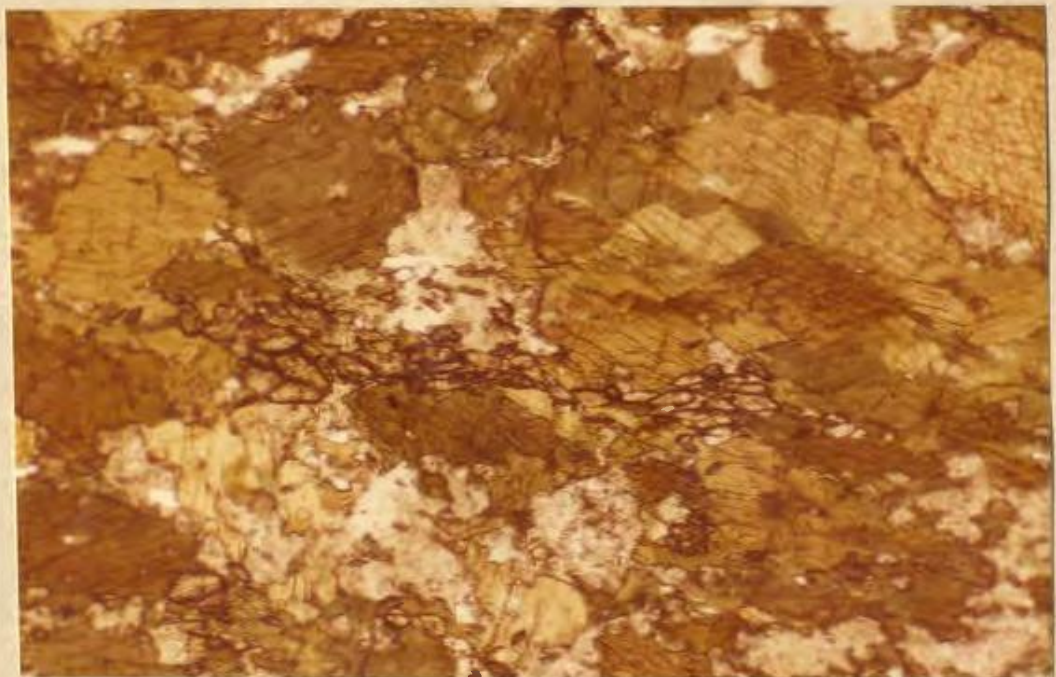


PLATE XXIXb: Aligned granules of sphene (S_2) in amphibolite - North Arm Mountain. Plain light x 85.

increases very slightly. The decrease in total iron cannot be readily explained as an original chemical feature of the amphibolites which appear lithologically similar and have a common protolith. Therefore on the assumption of an original chemical similarity of the rocks within the contact aureole at this location, both garnet compositions and trends shown by bulk rock total iron suggest a chemical redistribution in response to contact metamorphism (Section E).

c) Spene: Small, euhedral, wedge-shaped to elliptical crystals of spene have been observed throughout the aureole rocks. However, they significantly increase in abundance towards the contact and form as much as 5% of the amphibolites. Where present in the sedimentary rocks spene is probably detrital and is not believed to be authigenic because of its irregular shape and extremely rare occurrence.

In the amphibolites the spene crystals are aligned in short trails parallel to the foliation S_2 (Plate XXIXb). Individual crystals generally have their long axes orientated also, although this may not apply to the larger crystals. Crystals vary in size from 0.02 mm to 0.1 mm maximum dimension with the average approximately 0.04 mm. The larger crystals exhibit good (110) cleavage traces, and all crystals have a high relief, $2V_\gamma$ approximately 30 and are pleochroic with the following scheme:

α colourless β yellow-brown γ brown

features indicating a relatively high iron content (Deer et al., 1963)

d) Zircon: Zircon is a minor accessory as a detrital product in some of the coarser sedimentary rocks. It occurs as fine, euhedral crystals throughout the rocks.

ii) Chain silicates

a) Amphiboles: Amphiboles are the most abundant mineral group within the aureole and occur throughout the more highly metamorphosed parts. In the greenschists, amphiboles of the tremolite-actinolite series are present. Green hornblende is dominant in the amphibolite facies but gives way to brown hornblende typical of upper amphibolite facies closer to the contact.

The pleochroic scheme of some of the aluminium poor amphiboles of the greenschists:

α yellow-green; β green; γ greenish-blue suggests that they are rich in iron and may be classified as ferro-actinolites. This actinolite occurs as small prismatic crystals which together with chlorite and epidote show a preferred orientation and define the major schistosity within the greenschists (S_1 of Williams and Smyth, 1973). The crystals rarely reach dimensions of more than 0.2 mm long axis and extinction angles ($\gamma : z$) of between 12° and 16° support their identification as ferroactinolites. The larger crystals rarely contain small plagioclase and oxide inclusions. In some greenschists, pale-yellow to colourless tremolitic amphibole is present and it is therefore clear that the composition of the aluminium poor amphiboles is dependent upon the bulk composition of the rock.

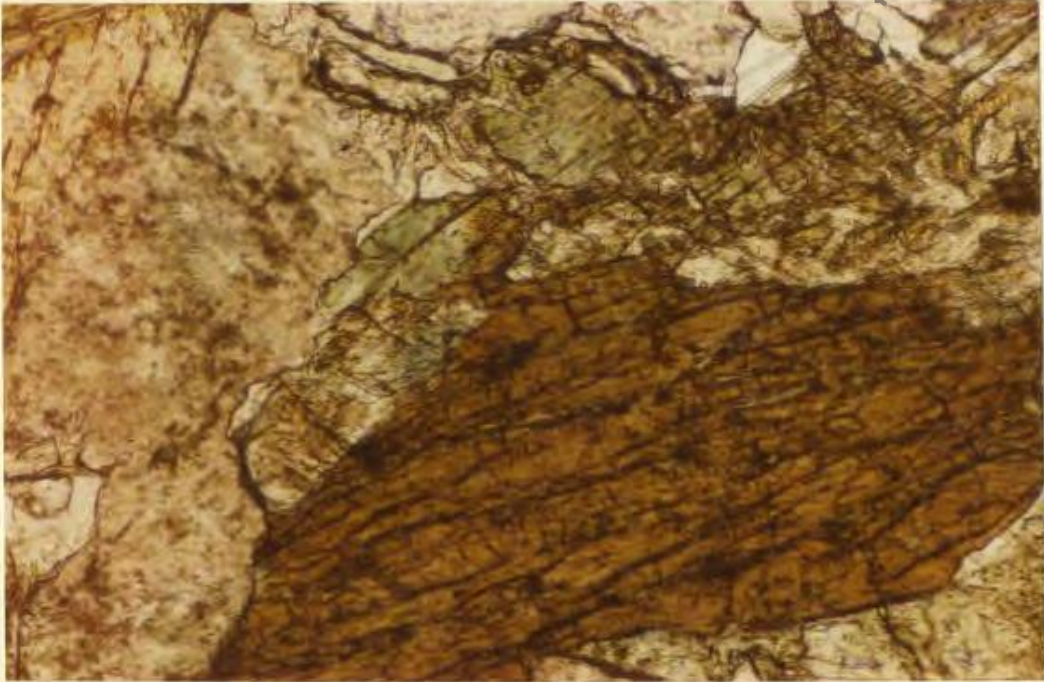


PLATE XXXa: Green hornblende replacing brown hornblende
8 m from basal contact, Trout River. Plain
light x 195.

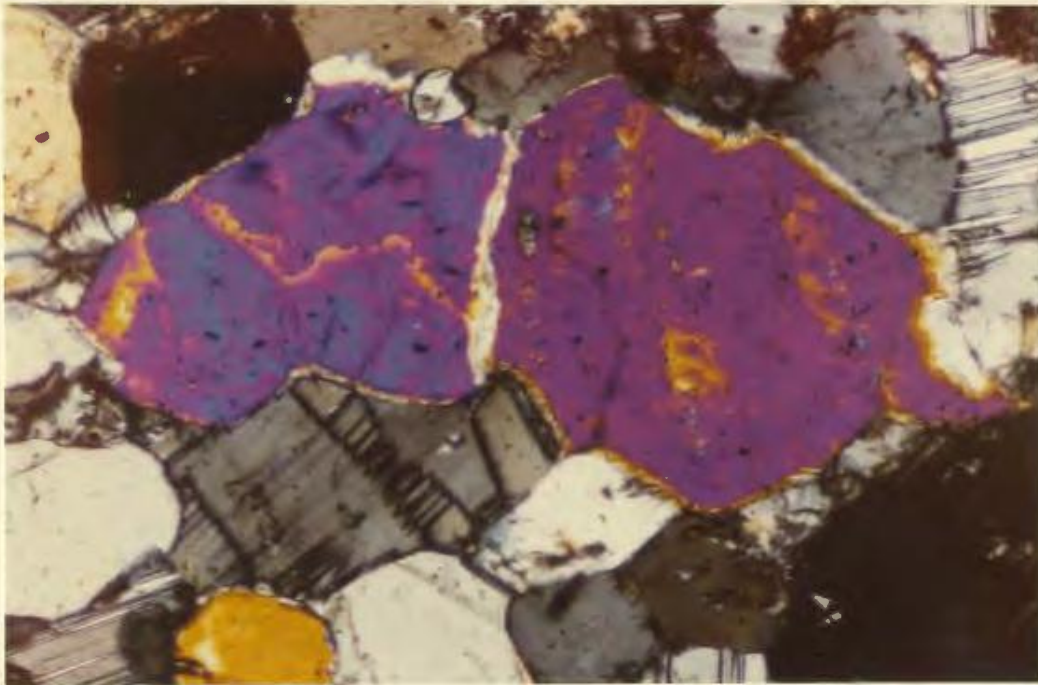


PLATE XXXb: Clinopyroxene in hornfels. Trout River. X nicols
x 180.

In the outer part of the amphibolite zone, two amphiboles are present together, one an actinolite, the other green hornblende. Similar associations of aluminium poor and aluminium rich amphiboles have been noted by Miyashiro (1958), Shido (1958) and MacGregor (1964) and interpreted by Shido and Miyashiro (1959) as the result of a miscibility gap in the actinolite-hornblende series.

An increase in grain size is noticeable at the amphibolite-greenschist boundary, and grain size increases gradually throughout the amphibolites towards the contact. The modal distribution of hornblende shows a general increase towards the contact from amounts in the 40-60% range to amounts as much as 90%. Close to the contact, green-hornblende is replaced by brown pleochroic varieties (Plate XXXa). Colour zoning is generally absent, although it does occur in brown hornblendes near the contact especially in oxide rich rocks.

The hornblendes are generally quite fresh and most are inclusion free although some crystals contain altered feldspar and magnetite. Some alteration to aggregates of irregular epidote and minor chlorite have been noted. The hornblendes show a preferred orientation with (001) concentrated in the plane of schistosity, and are strongly lineated. A variety of dips of this lineation occur, but no systematic studies have been carried out.

Microprobe analyses of four hornblendes from aureole rocks are presented in Table V. The analyses show no major differences except for the higher titanium content of the amphibole from the ultramafic mylonite. This amphibole cannot, however, be defined as kaersutite (5-10% TiO_2) as suggested by Church (1972). A general increase in calcium towards

TABLE V

AMPHIBOLES FROM BAY OF ISLANDS COMPLEX AUREOLE

towards contact

Spec. #		→			
		B2	B1	VII	V10
wt. %	SiO ₂	44.32	43.69	43.18	40.87
	TiO ₂	1.35	1.69	1.11	3.48
	Al ₂ O ₃	12.21	10.53	13.39	14.94
	Cr ₂ O ₃	0.21	0.0	0.19	0.01
	FeO	11.16	14.26	11.94	6.80
	MnO	0.10	0.16	0.0	0.03
	MgO	14.13	12.84	14.54	14.98
	CaO	11.56	11.42	11.74	11.92
	Na ₂ O	2.31	1.68	1.74	2.62
	K ₂ O	0.01	1.57	0.11	1.49
	H ₂ O	2.64	2.16	2.06	2.86
	Si	6.748	6.782	6.562	6.219
	Al Tet	1.252	1.218	1.438	1.781
	Al Oct	0.940	0.710	0.961	0.900
	Ti	0.155	0.196	0.127	0.398
	Cr	0.025	0.0	0.023	0.001
	Fe ²⁺	1.421	1.852	1.518	0.866
	Mn	0.013	0.021	0.0	0.004
	Mg	3.207	2.971	3.293	3.398
	Ca	1.886	1.900	1.912	1.944
	Na	0.682	0.506	0.513	0.773
	K	0.002	0.311	0.021	0.289
	Octahedral Occupancy	6.995	6.997	7.174	6.864
	Tetrahedral Occupancy	8.000	8.000	8.000	8.000
	A site	0.655	0.783	0.512	1.018

ROCK TYPES:

B2	Amphibolite, Trout River Pond
B1	Amphibolite, Trout River Pond
VII	Rodingite, Trout River Pond
V10	Ultramafic mylonite, Trout River Pond.

the contact, accompanied by an irregular increase in alkalis, is also noticeable and accompanies a corresponding decrease in the modal abundance of plagioclase, similar to the case described by MacGregor (1964) for the aureole of the Mount Albert intrusion, and considered a result of advanced metamorphism.

b) Clinopyroxene: Clinopyroxene occurs up to 20 metres from the contact where the aureole is fully developed. Retrograde replacement of the clinopyroxene by amphibole occurs 1.5 metres from the contact and increases in development away from it.

Clinopyroxene is well developed in the hornfels and relatively unaltered. It forms crystals ranging in size from 0.08 mm to 0.8 mm although most average 0.5 mm. The crystals are equidimensional and have generally straight grain boundaries (Plate XXXb). Optical properties ($2V \gamma$, 56°) suggest that the clinopyroxenes are diopsidic.

Microprobe analyses of eight clinopyroxenes from aureole rocks are given in Table VI and plotted in Figure IVe. All are diopsidic or salitic. Fe^{2+} and Fe^{3+} were recalculated from the analyses after the method of Cawthorn and Collerson (1974). Although Shido (1958) and others have suggested that the $(Mg^{2+} + Fe^{2+})/Ca^{2+}$ ratio of clinopyroxene increases with increasing temperature of metamorphism, a result of the increased solubility of enstatite in clinopyroxene, this is not apparent in the clinopyroxenes analysed here, probably because the initial metamorphic grade was not variable in the restricted distance from the contact from which the specimens were taken.

TABLE VI

PYROXENES FROM BAY OF ISLANDS COMPLEX AUREOLE

		towards contact →								
		cpx	cpx	cpx	cpx	cpx	cpx	cpx	cpx	opx
Spec. #		B1	B2 _A	B2 _B	B4 _A	B4 _B	B5 _A	B5 _B	V ₁₁	V ₁₀
wt. %	SiO ₂	49.63	51.28	51.05	52.52	50.70	51.79	51.19	50.59	54.72
	TiO ₂	0.74	0.40	0.27	0.23	0.32	0.25	0.28	0.00	0.14
	Al ₂ O ₃	4.91	4.28	4.08	2.61	5.64	6.55	6.64	2.74	4.01
	Cr ₂ O ₃	0.02	0.09	0.00	0.11	0.16	0.40	0.35	0.07	0.52
	Fe ₂ O ₃	2.75	1.37	2.31	0.52	2.18	--	1.21	3.00	--
	FeO	8.37	6.27	5.78	4.07	3.18	2.774	2.94	5.59	7.23
	MnO	0.23	0.11	0.17	0.14	0.11	0.06	0.05	0.00	0.14
	MgO	11.88	13.53	13.53	15.25	14.53	14.36	14.47	12.78	32.44
	CaO	21.24	21.93	21.93	23.25	22.18	22.10	22.49	23.09	0.47
	Na ₂ O	0.64	0.65	0.66	0.36	0.68	0.79	0.82	0.53	0.04
	K ₂ O	0.20	0.02	0.02	0.05	0.05	0.02	0.02	0.03	0.02
(Fe ₂ O ₃ recalculated according to Cawthorn & Collerson, 1974.)										

RECALCULATED FORMULA UNITS	Si	1.856	1.899	1.895	1.942	1.862	1.884	1.858	1.915	1.904
	Al Tet	0.144	0.101	0.105	0.058	0.138	0.116	0.142	0.085	0.096
	Al Oct	0.072	0.086	0.074	0.056	0.106	0.164	0.142	0.037	0.069
	Ti	0.021	0.011	0.008	0.006	0.009	0.007	0.008	0.00	0.004
	Cr	0.001	0.003	0.00	0.003	0.005	0.011	0.010	0.002	0.014
	Fe ³	0.007	0.038	0.065	0.015	0.060	0.00	0.033	0.086	0.0
	Fe ²	0.262	0.194	0.179	0.126	0.098	0.111	0.089	0.177	0.210
	Mg	0.662	0.747	0.749	0.840	0.795	0.778	0.783	0.721	1.682
	Mn	0.007	0.003	0.005	0.004	0.003	0.002	0.002	0.00	0.004
	Ca	0.851	0.870	0.872	0.921	0.873	0.861	0.875	0.937	0.018
	Na	0.046	0.047	0.048	0.026	0.048	0.056	0.058	0.039	0.003
	K	0.001	0.001	0.001	0.002	0.002	0.001	0.001	0.001	0.001
<u>Mg²⁺ + Fe²⁺</u>		1.09	1.08	1.06	1.05	1.02	1.03	.997	.959	
Ca ²⁺										

Jadeite	4.241	4.328	4.399	2.586	4.661	5.274	5.407	3.643
Acmite	0.0	0.0	0.0	0.0	0.0	0.0	0.0	0.0
Ti-tscher	2.194	1.192	0.806	0.691	0.955	0.750	0.830	0.0
Ferritscher	4.766	2.538	4.001	1.114	4.063	0.730	2.717	5.398
Ca-tscher	6.188	5.761	5.660	3.623	8.747	10.625	10.506	4.009
Wollastonite	37.443	40.744	40.342	45.869	39.244	39.782	39.232	44.194
Enstatite	29.450	33.707	33.753	38.316	36.270	35.999	35.849	32.330

iii) Sheet Silicates

a) Biotite: Biotite is restricted to the metasedimentary rocks of the contact aureole. It makes up 2 to 10 percent of the rock and is best developed at the greenschist-amphibolite transition. It occurs in distinct bands as flaky crystals with lengths up to 0.1 mm, growing parallel to the foliation (Plate XXXIa) and forming augen around plagioclase and garnet porphyroblasts. Slight variations are noticeable in pleochroic schemes as follows:

α	colourless straw-yellow	β	grey or olive brown, red brown	γ	golden brown deep red brown
----------	----------------------------	---------	-----------------------------------	----------	--------------------------------

n_x indices range from 1.618 to 1.634 with the lower refractive indices belonging to the paler coloured biotites.

b) Muscovite: Muscovite is present in the metasediments and meta tuffs. It occurs both within and outside the contact aureole. It is generally coarser within the aureole itself and occurs as flaky crystals that parallel the foliation. It may comprise as much as 40 modal percent in some pelitic rocks which exhibit one dominant schistosity. (Plate XXXIb). Sericite is developed as fine grained aggregates in the matrix of many of the metasediments and is found as a replacement product of some feldspars:

c) Phlogopite: Phlogopite, distinguished from biotite by lower R.I.'s (α 1.55; β 1.61; γ 1.60), occurs in significant amounts in the mylonitic bands in the basal ultramafic rocks. Church (1972) reports that this phlogopite is relatively titanium rich (c. 5% TiO_2 by weight) which is supported by its pleochroic scheme.

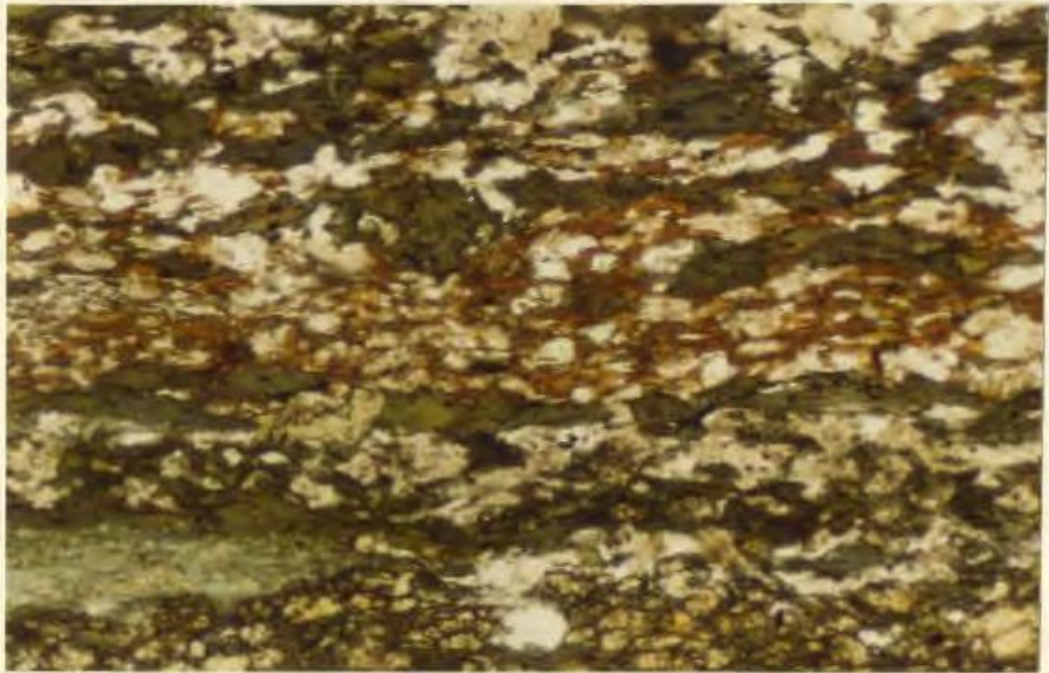


PLATE XXXIa: Biotite aligned parallel to S2 Schistosity in epidote-amphibolite Pond Point, North Arm. Plain light x 60.

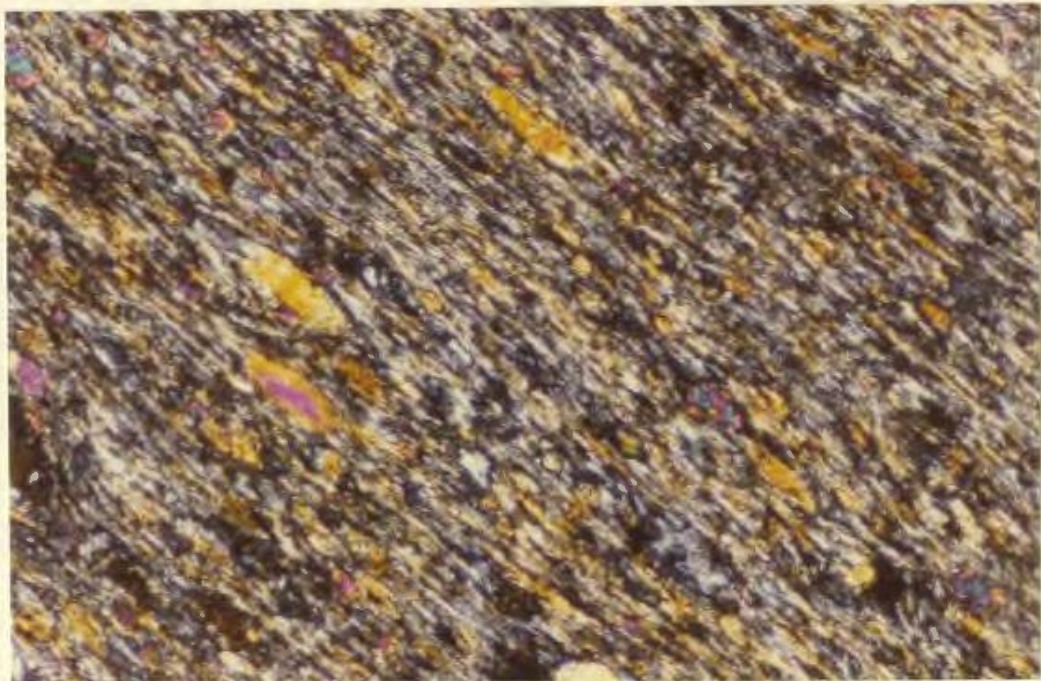


PLATE XXXIb: Pelite with one dominant fabric defined by muscovite. North Arm. X nicols x 150.

α straw yellow $\beta = \gamma$ brownish red

The phlogopite only occurs in the amphibole rich bands as small (~ 0.1 mm) flaky crystals which show no preferred orientation except when aggregates occur elongated parallel to the mylonite banding (Plate XXXIIa).

Because of its restricted occurrence, the writer feels that it is a metamorphic mineral produced during emplacement of the ophiolite slice, and not a primary mantle mineral as suggested by Church (1972).

d) Chlorite: Chlorite is ubiquitous in the greenschists and phyllites. In the greenschists it defines the major S_1 schistosity and is crenulated by F_2 . Chlorite also occurs together with quartz in late veins which cut these rocks. Along with their forms of growth, these chlorites exhibit different pleochroic schemes. The metamorphic chlorite which defines schistositities generally shows a blue-green pleochroic scheme in contrast with the grass-green scheme of the vein chlorite. In some samples the platy blue-green matrix chlorite is partially replaced by a fibrous amphibole.

Minor amounts of chlorite observed in the higher grade amphibolite facies rocks are due to the retrogression of amphibole and biotite.

e) Prehnite: Prehnite is extremely common in some samples where it occurs in coarse veinlets which cross-cut the schistositities and are not apparently deformed. It also occurs in minor quantities as an alteration product of plagioclase.

iv) Framework silicates

a) Plagioclase: Plagioclase occurs throughout the aureole in all rocks and is a constituent in some of the country rocks. Tuffaceous rocks generally contain more plagioclase than the sediments, but this appears to be the only systematic variation in plagioclase content.

In the sedimentary country rocks, plagioclase is relatively uncommon forming only 2-8 percent of the clastic particles. These grains average 0.05-0.1 mm in size and are generally subrounded. Many are deformed as indicated by bent twin lamellae, but where measurement of extinction angles are possible their composition appears to be andesine ($\sim \text{An}_{35}$). Marginal alteration to sericite and zoisite is evident in most grains. Small aggregates of these minerals may represent highly altered plagioclase.

In the phyllites and greenschists plagioclase occurs as small laths and flakes, generally too small for optical determination of composition. In the tuffaceous and volcanic protoliths where up to 40% of the rock is plagioclase, these crystals are often broken and shattered and highly altered to zoisite, sericite and calcite. Where optical determinations are possible they indicate albitic compositions. In all these rocks the plagioclase laths are aligned parallel to the major S_1 schistosity, but may show degrees of recrystallisation in the hinges of tight F_2 folds.

Plagioclases in the amphibolites are all highly altered and original grain boundaries are indiscernible. The main alteration

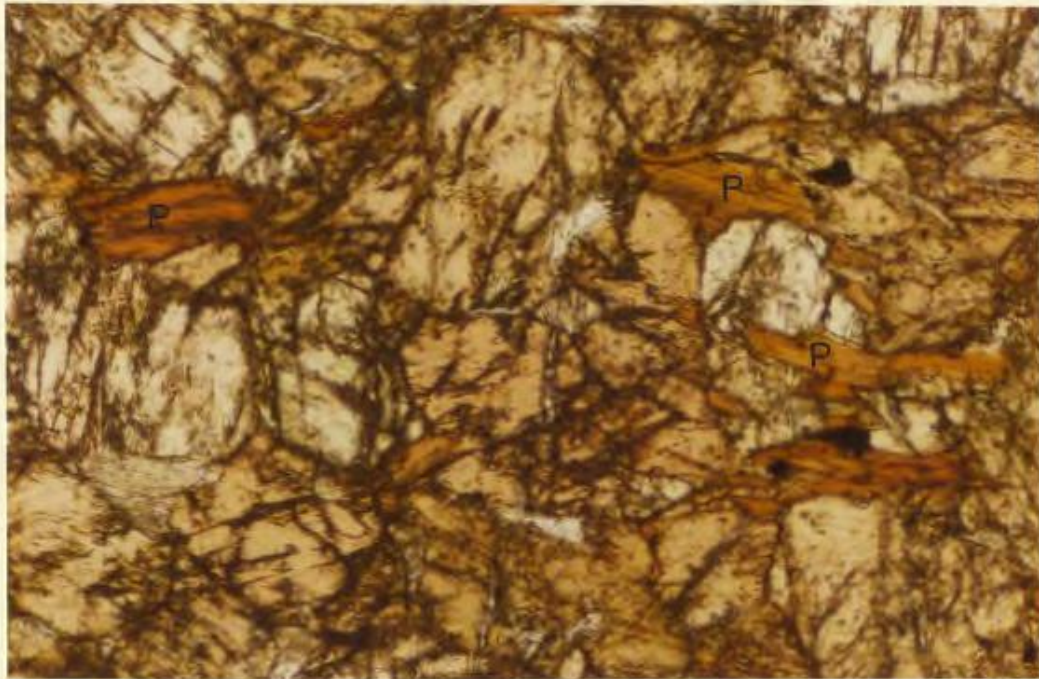


PLATE XXXIIa: Phlogopite (orange-brown) with amphibole in mylonitic band in basal ultramafics. Plain light x 200.

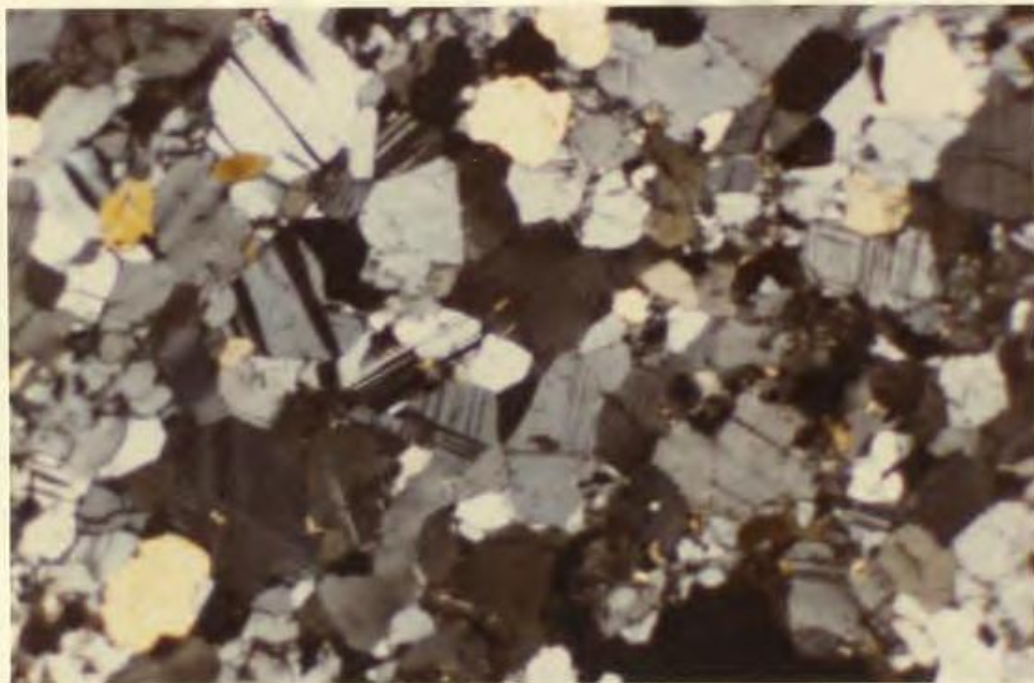


PLATE XXXIIb: Twinned plagioclase from hornfels. X nicols x 90.

products are zoisite, sericite and calcite, although some hydrogarnet and thompsonite replace plagioclase closer to the contact. The plagioclase forms granular to lens-like crystals interstitial to hornblende and epidote. Optical determinations on crystals which still show twinning indicate compositions of approximately An_{60} (Smith, 1958, also reports compositions An_{55} - An_{60} from the amphibolites). The altered plagioclases form distinct bands with more amphibole rich bands.

In the hornfelses the plagioclases are relatively fresh by comparison with those in other rocks of the aureole where they seem to have been the mineral most susceptible to alteration. The plagioclase occurs as euhedral crystals with relatively straight, unsutured grain boundaries and triple joint junctions. Most crystals are equidimensional (~ 0.5 mm diameter). They show complex twinning on Manebach and albite laws (Plate XXXIIb). An analysis of relatively fresh plagioclase from Trout River Pond is given in Table VII. The composition of An_{80} is the most calcic recognised in the aureole. Most optical determinations (U.-stage) of plagioclase from these rocks give an average composition of An_{72} . However, sodic plagioclases are found where the hornfelses have undergone metasomatic alteration. For example, Sample VII, an altered hornfels containing hydrogarnet and amphibole as well as diopside, contains albitic plagioclase (Analysis VII, Table VII). A substitution of sodium for calcium has taken place in the crystals, as is typical for metasomatic processes accompanying low grade, in this case retrogressive, metamorphism.

Table V11

Plagioclases from Bay of Islands Complex Aureole

Specimen #	V11	B5		
wt% SiO ₂	67.06	47.69		
TiO ₂	0.00	0.02		
Al ₂ O ₃	20.93	33.20		
Cr ₂ O ₃	0.01	0.00		
Fe ₂ O ₃	0.00	0.00		
FeO	0.00	0.16		
MnO	0.00	0.01		
MgO	0.00	0.00		
CaO	0.34	16.77		
Na ₂ O	9.69	2.19		
K ₂ O	0.36	0.01		
Recalculated Formula Units				
Si	11.847	8.752		
Ti	0.00	0.003		
Al	4.36	7.184		
Cr	0.001	0.00		
Fe ³	0.00	0.00		
Fe ²	0.00	0.025		
Mn	0.00	0.002		
Mg	0.00	0.00		
Ca	0.064	3.298		
Na	3.320	0.779		
K	0.081	0.002		
Composition of feldspar wt prop.	95.55 2.48 1.97	Ab Or An	18.20 0.06 81.74	Ab Or An

The plagioclase compositions that are available compare closely in their general increase in An content towards the contact, with the type of variation demonstrated by MacGregor (1964) and Compton (1958) for other metamorphic aureoles, and are notably different from variations observed in regional metamorphic terranes.

b) Quartz: Quartz occurs in both metasedimentary and metavolcanic rocks. It is a major constituent of (and forms up to 80 percent) the metasedimentary rocks and serves to distinguish them from the meta-volcanic rocks in which it is relatively rare, forming only 12 per cent or less.

Where quartz occurs in the phyllites and greenschists it is generally in small stringers that are elongated parallel to the foliation, and are generally recrystallised although many crystals show undulatory (strain) extinction. It also occurs in the hinges of some folds where triple point junctions between the crystals are common. The quartz is generally inclusion-free and although grain size is variable, many grains are of the order of 0.1 - 0.2 mm in size and are the result of the deformation, breakdown and recrystallisation of originally larger grains.

Later quartz filling veins and associated with prehnite and calcite is quite common in all the rocks. Many of these are themselves deformed, although they clearly cut earlier fabrics. In the amphibolites, the occurrence of augen around quartz knots may represent original cross-cutting veins. The absence of quartz from the matrix of the amphibolites may indicate that their origin was from a volcanic, tuffaceous protolith.

c) Zeolites: Zeolites are commonly found as an alteration product of plagioclase. Thompsonite appears to be the most important zeolite, although stilbite has also tentatively been identified. The zeolites are generally more common towards the contact since it is here that the plagioclases are most altered..

v) Non-silicates

a) Oxides: Oxides are present in most of the rocks of the aureole, the major ones being magnetite, haematite, ilmenite and minor rutile. Oxides generally occur as minor accessories, although in some rocks may be much more important. They are generally evenly scattered throughout the rocks although in some cases distinct bands of oxides, especially magnetite, are common.

Magnetite occurs as small euhedral crystals of dimensions 0.05 mm to 0.1 mm, or as much finer particles forming dusty patches. The euhedral magnetite is found mainly in the phyllites and is rarely present in the amphibolites and hornfelses. In the phyllites, the composite fabric forms augen around some magnetite octahedra, but others clearly lie in stringers parallel to the foliation. In some of the phyllites, magnetite and associated ilmenite may form up to 50% of the rock. This magnetite is often extremely fine grained and may form distinct folded layers, suggestive of original bedding. In the sediments, magnetite occurs in amounts up to 5% as small subrounded detrital grains.

Haematite occurs generally as patchy irregular crystals intergrown with or surrounding magnetite and ilmenite crystals, and

sometimes as small cross-cutting veinlets. It has also been rarely seen as an alteration product of amphibole. Because of its texture it is believed to be secondary or retrograde in origin and formed by oxidation reactions.

Rutile is relatively rare and has only been recognised in rocks of volcanic origin. It occurs as rod-like, yellow to yellow-brown crystals scattered throughout the rock. Very often alteration of ilmenite is associated with rutile and haematite development.

b) Carbonates: Calcite is the dominant carbonate mineral in the aureole and is always secondary. It is present as cross-cutting veinlets and irregular patches. It is also found rarely associated with the alteration of plagioclase. Rare patches of dolomite, tentatively identified by twinning patterns, have been observed in the altered hornfels near the contact.

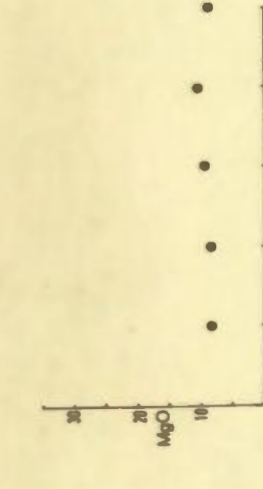
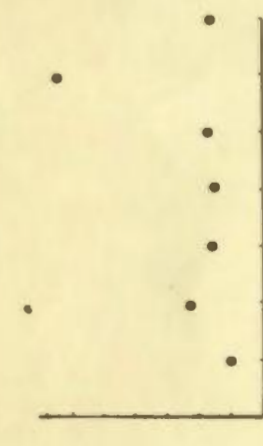
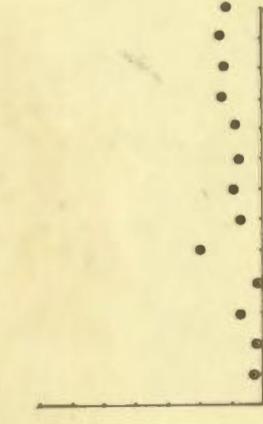
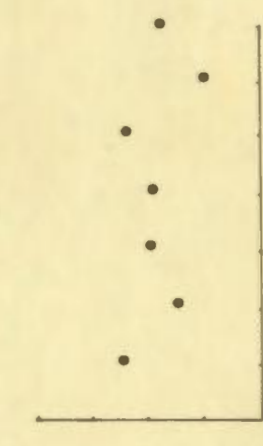
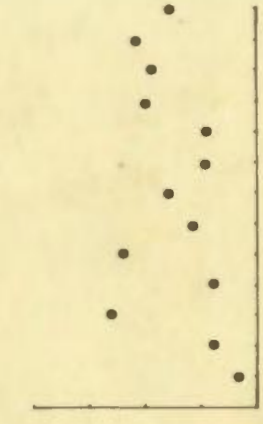
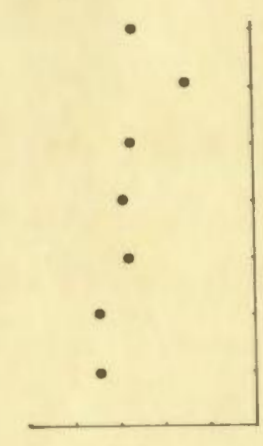
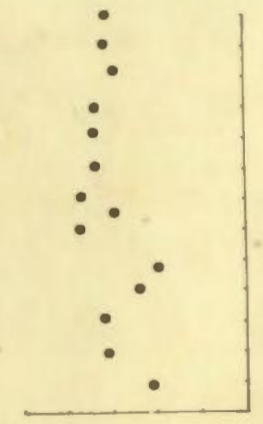
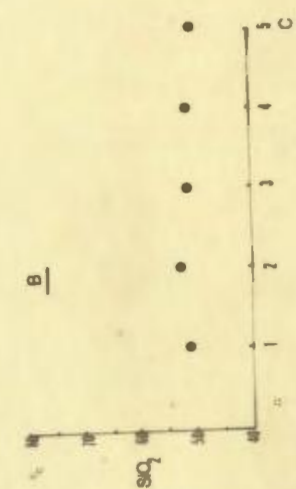
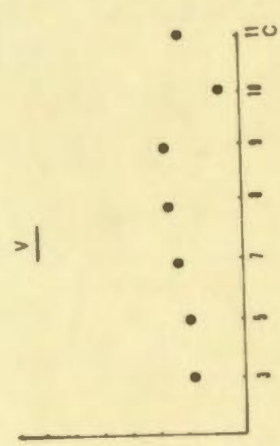
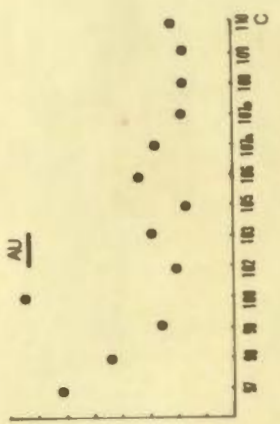
E. Bulk Rock Chemistry

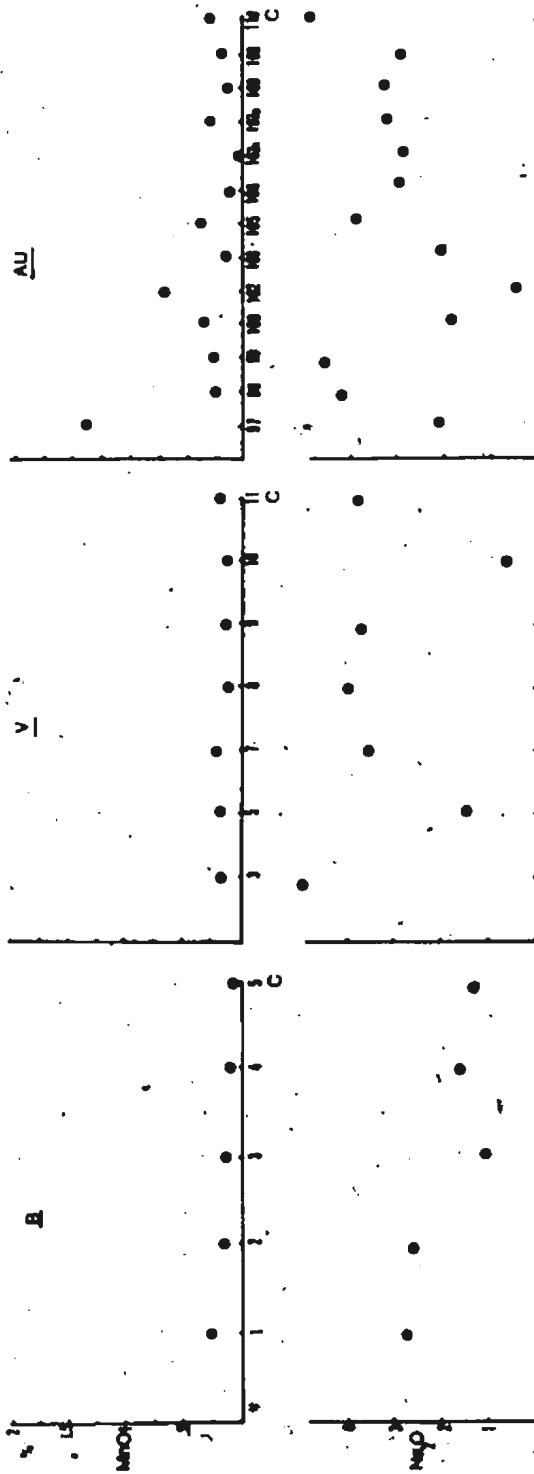
i) Introduction

Bulk rock analyses have been carried out on a series of samples from three sections of the aureole rocks. Two of these sections are on the second Trout River Pond, one on the north side and one on the south, and the third section is on North Arm, at Pond Point. Only the section at Pond Point is complete and representative rocks from the amphibolite, greenschist, phyllite and metasediment zones have been analysed. The other sections represent partial sections dominantly through the amphibolites and hornfelses, although two unmetamorphosed volcanic 'country' rocks are represented in the V series by V3 and V5. The analyses for major and minor element oxides and for trace elements are presented in Table VIII, with calculated C.I.P.W. norms. They have been represented diagrammatically in Figures IVc and IVd where they are plotted against distance from the contact for each of the three sections.

Petrographic study of the aureole rocks suggests that different units consisting of intercalated metasedimentary and metavolcanic rocks occur in the aureole. It is important to know how different the chemistry of these units is, in order to determine how much the stability of the different metamorphic phases present may depend on bulk chemistry. Similarly it is important to understand the degree of element transfer that may have taken place during metamorphic processes. In the following paragraphs, the distribution of elements is examined across the aureole in each section.

Figure IVc: Major element chemistry: Oxide vs. distance
from contact.





R

R

Handwritten scribble

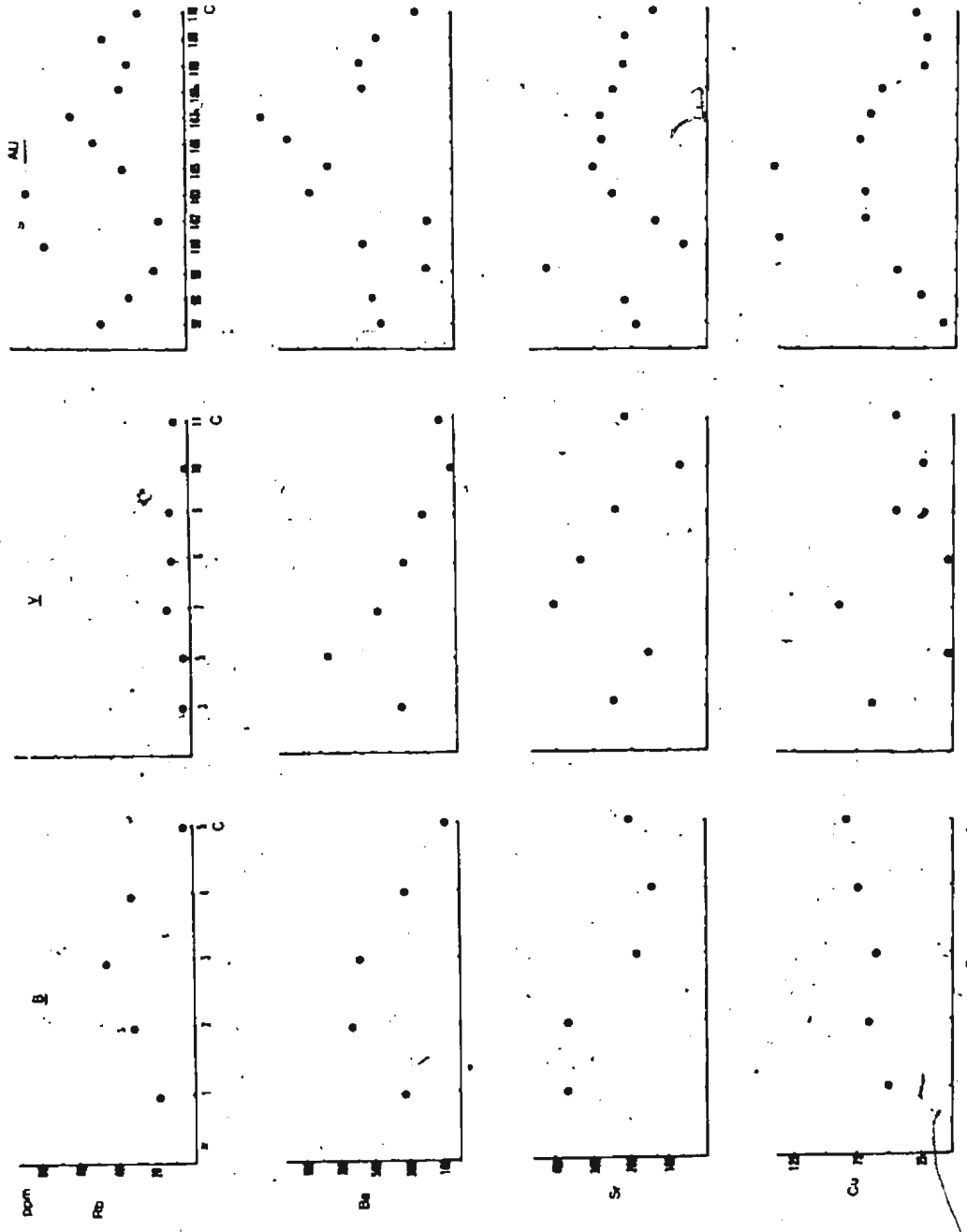
Handwritten scribble

A

Handwritten scribble

11

Figure IVd: Trace element chemistry: element vs. distance from contact.



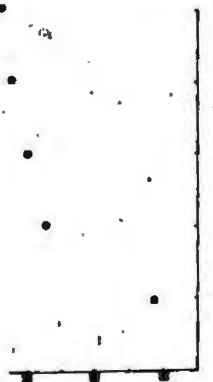
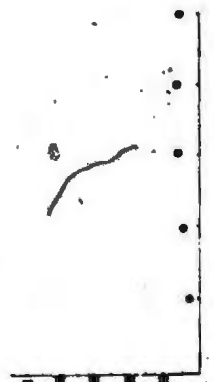
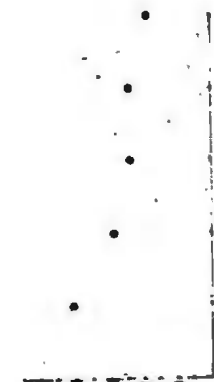
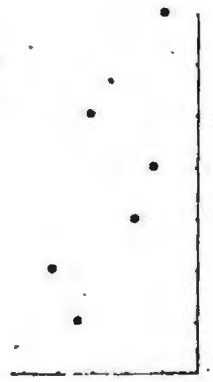
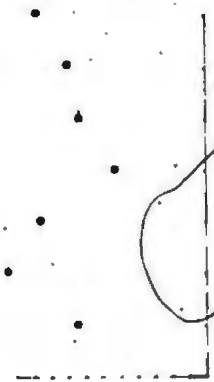
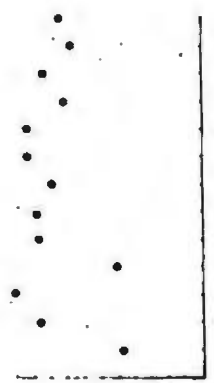
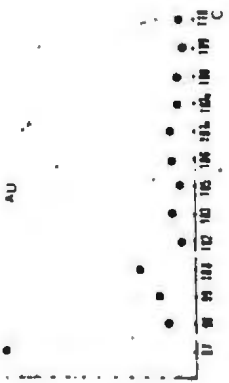
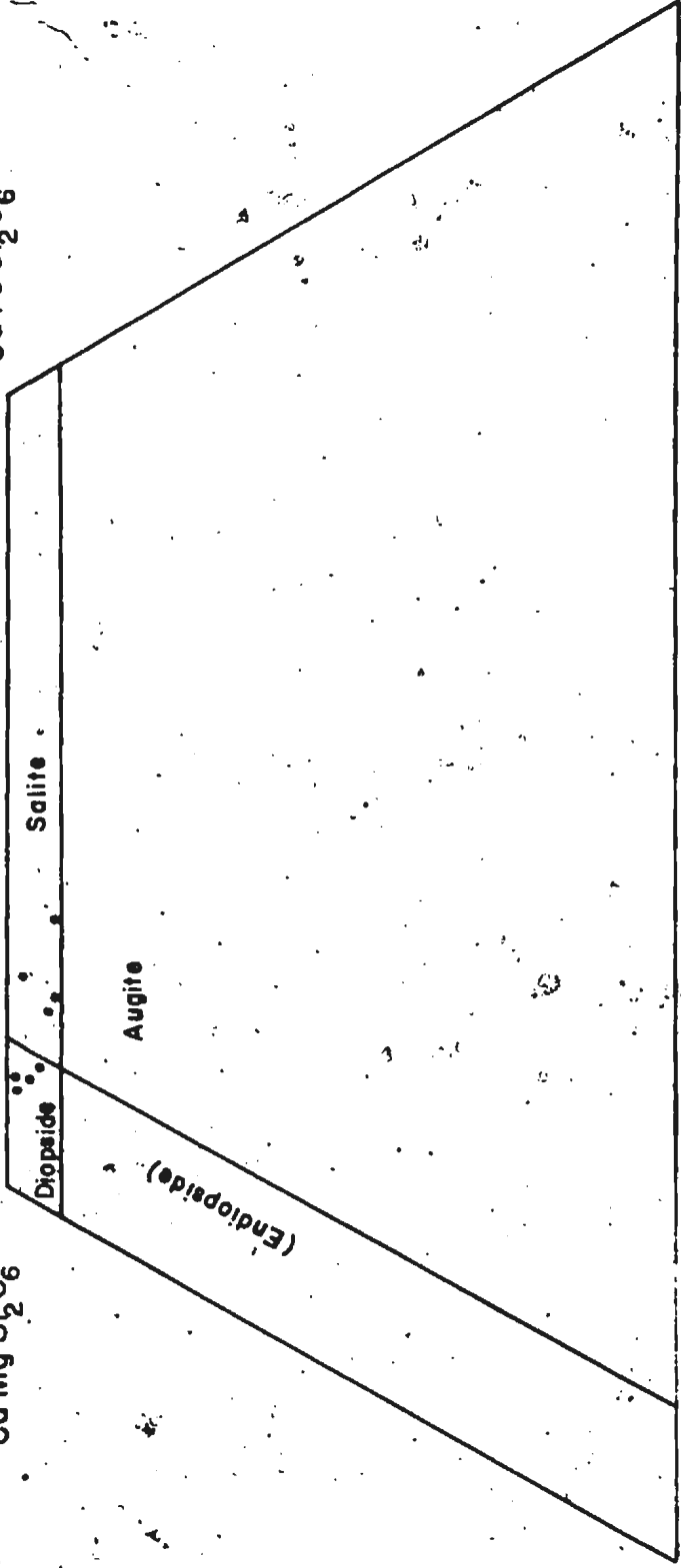


Figure IVe: Plots of clinopyroxenes from basal aureole.

$\text{Ca Fe Si}_2\text{O}_6$

$\text{Ca Mg Si}_2\text{O}_6$



Salite

(Endiopside)

Augite

Diopside

$\text{Mg}_2\text{Si}_2\text{O}_6$

$\text{Fe}_2\text{Si}_2\text{O}_6$

TABLE VIII - Anreole Rocks, Bay of Islands Complex

V Series, Table Mountain

	JMV3	JMV5	JMV7	JMV8	JMV9
SiO ₂	47.02	45.28	50.69	52.24	52.80
TiO ₂	1.13	1.76	1.20	1.53	0.54
Al ₂ O ₃	16.62	15.90	13.97	13.85	13.57
Fe ₂ O ₃	1.69	2.40	4.44	3.95	3.27
FeO	7.91	7.93	7.38	6.49	4.15
MnO	0.13	0.19	0.22	0.14	0.17
MgO	4.58	10.00	7.81	7.65	8.46
CaO	11.87	6.70	9.77	9.57	11.90
Na ₂ O	4.70	1.55	3.48	3.97	3.64
K ₂ O	0.23	0.02	0.78	0.51	0.66
P ₂ O ₅	nd	0.10	nd	nd	nd
Ign	5.14	6.87	0.83	1.08	1.73
TOTAL	101.10	98.70	100.57	100.98	100.89

ppm					
Zr	87	270	103	110	49
Sr	240	155	404	332	243
Rb	5	4	13	11	11
Zn	75	115	96	53	75
Cu	63	nd	89	4	43
Ni	182	223	55	63	72
Co	49	45	50	45	38
Cr	347	421	189	128	307
V	68	75	63	60	55
Ba	320	24	458	312	192

	wt%				
Qtz		1.77			
Or	1.42	0.13	4.63	3.02	3.94
Ab	20.50	14.30	29.61	33.71	30.37
An	24.20	35.53	20.31	18.53	18.93
Ne	11.57				0.41
Wo	15.53		11.87	12.16	17.00
Di	7.46		6.37	7.02	11.17
Fs	7.83		5.11	4.59	4.63
Hy		27.14	0.43	2.87	
		13.36	0.34	1.88	
O1	3.10		8.94	6.47	7.09
Fa	3.59		7.91	4.66	3.23
Mq	2.77	2.37	2.19	2.18	2.20
Ilm	2.24	3.64	2.29	2.92	1.04
Ap		0.25			
Cr		1.51			

V Series, Table Mountain B Series, Table Mountain

	JMV10	JMV11	B1	B2	B3
SiO ₂	39.00	49.93	49.29	50.51	49.32
TiO ₂	0.45	1.61	0.20	0.33	0.25
Al ₂ O ₃	6.93	12.72	14.94	15.62	17.01
Fe ₂ O ₃	2.72	5.10	2.82	0.84	0.24
FeO	5.98	3.20	8.16	6.38	4.93
MnO	0.16	0.23	0.22	0.13	0.11
MgO	28.65	7.83	8.21	8.31	9.12
CaO	4.52	8.88	10.72	12.26	12.80
Na ₂ O	0.62	3.75	2.77	2.50	1.06
K ₂ O	0.05	0.24	1.23	1.50	2.93
P ₂ O ₅	nd	nd	nd	nd	nd
Ign	9.02	0.75	1.44	1.50	2.93
TOTAL	98.10	98.24	100.00	99.79	100.75

ppm					
Zr	41	126	81	47	23
Sr	68	216	363	357	179
Rb	2	9	19	33	48
Zn	79	98	81	59	49
Cu	25	44	50	55	61
Ni	1163	47	60	90	124
Co	76	49	42	39	30
Cr	600	95	123	445	513
V	77	65	63	58	58
Ba	nd	96	333	633	591

	wt%				
Qtz					
Or	0.33	1.46	7.38	10.89	12.71
Ab	5.90	32.67	21.17	17.49	9.14
An	17.96	17.62	25.09	26.35	36.10
Ilc			1.43	2.13	
Wo	3.02	11.56	12.08	14.71	14.06
Di	2.33	5.93	6.54	9.53	10.22
Fs	0.37	5.33	5.12	4.19	2.53
Hy	7.66	0.50			2.86
	1.22	0.45			0.71
Ol	49.20	9.56	9.97	8.00	7.05
Fa	8.60	9.48	8.60	3.87	1.92
Mg	2.44	2.24	2.21	2.20	2.22
Plm	0.96	3.15	0.39	0.63	0.48
Ap					
Cr					

V Series, Table Mountain B Series, Table Mountain

	B4	B5	97AU	90AU	99AU
SiO ₂	49.17	48.79	68.8	56.00	43.5
TiO ₂	0.22	nd	1.41	2.11	1.79
Al ₂ O ₃	16.10	20.62	10.1	15.10	14.2
Fe ₂ O ₃	0.01	nd	4.27	5.62	1.30
FeO	4.92	3.11	4.99	5.01	9.24
MnO	0.11	0.06	0.31	0.21	0.24
MgO	10.30	7.87	1.08	1.08	3.54
CaO	13.39	17.15	1.76	4.05	11.82
Na ₂ O	1.50	1.27	2.04	4.23	4.44
K ₂ O	2.81	1.00	1.58	1.84	0.20
P ₂ O ₅	nd	nd	0.01	1.93	0.56
Ign	2.81	1.00	2.97	20.6	9.84
TOTAL	101.34	100.87	99.32	99.24	100.67

ppm

Zr	14	23	1200	188	235
Sr	136	197	186	222	424
Rb	35	4	44	30	14
Zn	49	37	47	96	110
Cu	75	84	9	28	49
Ni	136	119	19	89	103
Co	45	34	nd	nd	nd
Cr	557	585	59	77	124
V	56	53	nd	nd	nd
Ba	326	83	420	465	168

wty

	Qtz		40.79	34.05	17.47
	Or	0.95	9.64	11.10	1.30
	Ab	10.84	10.01	21.00	2.03
	An	50.51	8.95	7.77	42.01
	Ne				
	Wo	14.65			7.75
Di	Ens	10.97			3.17
	Fs	2.21			4.64
	En	0.37	2.78	2.74	6.53
Hy	Fs	0.07	16.43	11.92	9.55
	Fn	10.48			
Ol	Fa	2.33			
	Mg	2.23	2.25	2.22	2.39
	Ilm	0.43	2.77	4.09	3.74
	Ap		0.02	4.58	1.43
	Cr		2.38	0.53	

Al Series, North Arm Mountain

	100AU	102AU	103AU	105AU	106AU
SiO ₂	73.0	47.1	53.5	47.4	55.3
TiO ₂	0.64	1.27	1.11	1.23	1.11
Al ₂ O ₃	11.1	13.2	17.9	17.5	16.1
Fe ₂ O ₃	1.27	1.72	1.25	7.90	1.50
FeO	2.15	8.16	8.80	5.48	9.24
MnO	0.31	0.65	0.13	0.35	0.12
MgO	0.60	9.30	3.81	4.83	4.05
CaO	3.82	11.46	5.68	7.89	4.60
Na ₂ O	1.80	0.32	2.06	3.88	2.88
K ₂ O	1.11	0.16	3.35	1.59	2.00
P ₂ O ₅	Trace	Trace	0.02	Trace	0.07
Ign	3.97	6.90	2.17	1.57	2.10
TOTAL	99.77	100.24	99.96	96.62	99.07

ppm

Zr	348	80	132	94	152
Sr	67	139	252	299	279
Rb	73	13	81	32	47
Zn	49	97	98	88	104
Cu	9	71	72	146	79
Hf	32	56	94	254	97
Co	nd	nd	nd	nd	nd
Cr	55	102	205	649	182
V	nd	nd	nd	nd	nd
Ba	512	141	835	707	931

wt%

	Qtz	57.97	6.80	5.65		9.40
	Or	13.10	1.65	20.24	9.65	12.20
	Ab	9.01	1.02	17.82	23.83	24.62
	An	12.90	37.86	27.49	26.32	23.08
	Ne				5.35	
	Wo		9.69		5.79	
Di	En		5.84		2.34	
	Fs		3.33		3.50	
Hy	En	1.57	19.03	9.70		10.41
	Fs	1.94	10.87	13.20		14.57
Ol	Fo				7.01	
	Fa				11.58	
	Mg	2.28	2.34	2.22	2.23	2.24
	Ilm	1.23	2.59	2.16	2.40	2.18
	Ap			0.48		0.17
	Cr			1.06		1.13

AU Series, North Arm Mountain

	107AU	108AU	109AU	109AU	110AU
SiO ₂	53.1	47.9	48.3	48.8	50.8
TiO ₂	1.26	1.33	1.81	1.09	1.60
Al ₂ O ₃	16.8	16.2	14.5	15.7	15.2
Fe ₂ O ₃	1.54	2.38	3.71	3.88	2.69
FeO	9.77	8.42	9.35	7.03	9.31
MnO	0.24	0.28	0.17	0.21	0.32
MnO	4.21	6.62	6.35	6.87	5.36
CaO	4.78	10.02	9.44	10.69	7.68
H ₂ O	2.82	3.13	3.21	2.97	4.60
K ₂ O	2.52	1.27	1.16	1.46	0.82
P ₂ O ₅	0.28	0.16	0.18	0.22	0.18
Ign	2.19	1.98	1.15	1.11	0.95
TOTAL	99.51	99.69	99.33	100.03	99.51

ppm					
Zr	156	106	141	80	98
Sr	287	248	221	225	143
Rb	59	34	30	41	23
Zn	105	83	94	79	85
Cu	68	62	26	41	34
Ni	47	72	65	63	33
Co	nd	nd	nd	nd	nd
Cr	141	170	133	208	96
V	nd	nd	nd	nd	nd
Ba	1097	527	535	431	221

	wt%				
Qtz					
Or		7.69	7.00	8.74	4.92
Ab		22.86	26.53	21.36	37.95
An		27.05	22.18	25.53	18.46
Ne		2.31	0.65	2.22	1.08
Wo		9.53	10.20	11.18	7.95
Di		5.00	4.86	5.92	3.62
Fs		4.25	5.20	4.91	4.28
En					
Hy					
Fs					
Ol					
Fo		8.33	7.91	8.00	6.96
Fa		7.79	9.32	7.31	9.07
Mg		2.23	2.22	2.20	2.21
Ilm		2.59	3.51	2.10	3.09
Ap		0.58	0.43	0.52	0.42
Cr					

NOT CALCULATED

Modal Analyses

	Qtz	Plag	Biot	Ms.	Cpx	Opx	Hbl
V3		57					
V5	2	51			3		
V7		31	1		3		61
V8	1	9					63
V9		33	1		1		57
V10							
V11		27			1		67
B1		31					50
B2	1	41			4		42
B3		45	2				30
B4		33			10		29
B5		55			21		
97AU	85	8			22		
98AU	5	40		2			
99AU	3	20					
100AU	85	2		1			
102AU	1	5					
103AU	8	20	3	5			44
105AU	1	15	10				48
106AU	5	60	30	2			20
107AU	5	10	15				30
107BAU	2	10					45
108AU		15		2			80
109AU	1	40					50
110AU	4	30					45

Modal Analyses

	Epid	Sph.	Opa.	Ol/Calcite	Ch/Act	Grt.
V3				5 Calc.	35 Ch	
V5	3		2	3	36	
V7		3	4			
V8		5			1 Ch	
V9		4	1			4
V10	1		10	8301		
V11		2				4
B1		2	3			10
B2			4			12
B3			7			6
B4			1			10
B5				1		12
97AU	2		3	5 Cal	2 Ch	
98AU			45		8 "	
99AU			2	35 "	40 "	
100AU	2			10 "		
102AU	30	2	1	1 "	60 Act	
103AU		4	3	3 "		10
105AU	20	3	2		1 "	
106AU			10			5
107AU			15	3 "		2
107BAU		3	10			15
108AU		2	1			
109AU		3		2 "		4
110AU		2		3 "	1 Ch	5

ii) Major Oxides

a) SiO_2 : The silica content of the aureole rocks is fairly constant in the B and V series which consist dominantly of metavolcanics. In these sections the silica content averages around 50%, representative of a protolith of basaltic composition. V10, however, has a lower silica content consistent with it being an ultramafic mylonite consisting dominantly of enstatite and olivine with minor amphibole bands. In the AU series, the silica content is variable, but in general the higher values occur at a distance from the contact and are representative of the metasediments that are dominantly quartz-bearing. The amphibolites of the AU series have silica contents comparable with those of the B and V series, as does one recognisable basaltic protolith - Sample 98.

b) Al_2O_3 : The distribution of Al_2O_3 throughout the aureole is fairly uniform. Aluminium will be fixed in plagioclase, amphibole, and epidote group minerals. In the B series, the increased amount of aluminium in B5, a calcic hornfels, is probably due to the higher aluminium content of the calcic plagioclase.

V10, the ultramafic mylonite, is naturally relatively poor in alumina. No systematic variation of alumina with rock type or distance from the contact is noted in the AU series, where values average approximately 15%.

c) CaO: The calcium content of the B series correlates directly with the alumina content, suggesting that the calcium enrichment in the hornfels, B5, is represented as more calcic plagioclase. A similar, although not so marked correlation, exists between CaO and Al_2O_3 in the V series.

Calcium is variable in the AU series. This is possibly due to contamination from secondary calcite veins in some rocks. There is no particular difference between CaO contents of greenschists and amphibolites, the lime substituting in the amphiboles and plagioclases of the amphibolites and the epidote of the greenschists.

d) MgO: The magnesia content in the aureole rocks is fairly constant. Sample V10 has a high MgO content reflecting its ultramafic mineralogy, but otherwise contents are fairly low (5-10%). There does not appear to be any noticeable magnesium metasomatism in rocks close to the contact.

e) FeO and Fe_2O_3 : There is only small variation in total iron and this does not appear systematic in series V and AU. In general, total iron is constant in these series. However, in series B, there is a gradual increase in total iron away from the contact which is reflected as an increase in Fe^{2+} and Fe^{3+} . This is difficult to explain on the basis of original rock type since all specimens in the B series are amphibolites and appear to be derived from similar protoliths. The decreased iron at the contact therefore could be a result of metasomatism.

The variation of FeO and Fe₂O₃ is reflected in the oxidation ratio (Fig. IVb) which is systematically variable only in series B where it increases away from the contact. This may indicate that oxygen fugacity probably increased away from the contact as described by MacGregor (1964) for the Mount Albert aureole.

iii) Minor Oxides

a) Na₂O: Na₂O content is not systematically variable across the aureole. High contents are generally associated with a high modal amount of albitic feldspar in the greenschists. This is especially clear in the basaltic protolith - sample AU 98.

b) K₂O: The K₂O content shows no systematic variations across the aureole. The high (3.5%) value in sample AU 103 reflects the presence of approximately 25% matrix biotite.

c) TiO₂: TiO₂ content shows no systematic variation across the aureole in series B and series V. In series AU, the sedimentary protoliths are on average a little poorer in TiO₂ than the volcanic protoliths.

d) MnO: MnO shows no definite systematic variation across the aureole, although in section B there is indication that manganese content is correlative with total iron content and decreases towards the contact.

iv) Trace Elements

a) Cr: The distribution of Cr across the aureole shows no simple pattern. In series V and AU the only trend visible is a slight increase in Cr towards the contact in the AU series. The increase in Cr towards the contact is more marked in series B. Absolute values show the same range in each series.

b) Ni: The distribution of Ni follows that of Mg and does not show any systematic variations across the aureole. Although the general range of values is relatively small, volcanic protoliths have generally higher Ni contents than sedimentary protoliths, and the highest value in the ultramafic mylonite V 10 is much above the general trend.

c) Cu: The variation of Cu across the aureole in the three series shows no significant trend.

d) Zn: The concentration of Zn is relatively uniform in all series and across the aureole. A slight decreasing trend towards the contact is seen in series B amphibolites. The total range of zinc is from 40 to 120 ppm.

e) Zr: Zirconium values are relatively constant across the aureole in all series, averaging less than 200 ppm. The exception is AU 97, a sandstone containing detrital zircon which accounts for its concentration of 1200 ppm Zr.

f) Sr: No definite trends are apparent in strontium concentrations, although there is a suggestion in all series that strontium may decrease towards the contact.

g) Rb: No systematic trends are seen in Rb contents which show a large range. The correspondence between Rb and K_2O is, however, very marked and clearly the Rb is substituting in potassium minerals.

h) Ba: No significant trend is noted in Ba concentrations. However, there is a marked correlation between Ba and K_2O contents, especially in the B series. The large Ba ion is expected to substitute for potassium (Mason, 1958).

v) Discussion

Since each of the three aureole sections cover different distances and represent different parts of the aureole, they may be expected to show overall differences in their chemistry. The chemistry of the metamorphic rocks quite clearly depends in the first instance on the nature of the protolith, and this is most obvious in the AU series which represents the most complete section of the aureole and contains both sedimentary and volcanic protoliths. On the other hand, the amphibolites of series B were collected within a short distance from the contact and are generally petrographically identical. It is reasonable to suppose that they were derived from a common protolith. Their differences in chemistry might be a result of metasomatic processes, close to the contact. With this in mind the following subdivision of the elements previously discussed may be made.

1. Those elements which show little or no variation across the aureole:

SiO₂, Al₂O₃, MgO, MnO, Zr, Ni

2. Those which show an increase in concentration towards the intrusive contact:

Cr, CaO

3. Those which show a decrease in concentration towards the intrusive contact:

Total Fe, Ba, Sr, Zn

Other elements show strong but not systematic variations.

Two processes may have operated to produce the apparent redistribution. Firstly metasomatic changes in the aureole as a result of losses or addition to the ultramafic rocks. Secondly, large scale metamorphic differentiation within the aureole as a result of the heat produced an obduction of the ultramafics. Both processes would presumably produce identical results.

If metasomatism was the direct cause it might be expected that an increase of elements most abundant in the peridotites might occur in the aureole with a corresponding decrease of elements most abundant in the peridotites, i.e. one would expect increases of Mg, Cr, Ni, Co and decreases of Na, K and Si. Similarly a sympathetic variation should be found in

the peridotites. The results of metamorphic differentiation would be systematic variations in chemistry away from the intrusive contact with no variations within the intrusion. Clearly there has been some redistribution of elements such as calcium, titanium and sodium such that amphibolite bands have been formed in the basal ultrabasic rocks, rodingitic and calc-silicate rocks formed at the contact, and a general increase in Cr in the contact zone of the aureole. However, other elements such as Mg and Si show very little variation.

Thus, there is ample evidence to indicate metasomatism, but the overall effect is restricted to the localised areas of calc-silicate formation and development of amphibolitic mylonites in the ultramafic rocks, and some variations within the aureole itself are still possibly the result of metamorphic differentiation in response to the thermal gradient.

F. Conditions of Formation of Aureole Rocks.

For the different metamorphic facies present in the Bay of Islands aureole rocks, Turner (1968) and Hyndman (1972) estimate the following approximate temperatures and pressures:

Greenschist facies: 300° - 500° C; 3000-8000 bars

Garnet/amphibolite facies: 550° - 750° C; 4000-8000 bars

Granulite facies: 700° - 800° C; pressure variable.

More specific figures may be obtained by calculation of the temperatures of equilibration of various mineral assemblages within the aureole.

i) The equilibrium existence of clinopyroxene and garnet can be used as a geothermometer according to the methods of Banno (1970) and Mysen and Heier (1972). Banno showed that K_D values for coexisting garnets and clinopyroxenes are dominantly temperature dependent and Mysen and Heier calibrated their geothermometer by comparing K_D values with experimentally determined temperatures of formation. The functions, K_D^{gnt} and K_D^{px} are plotted on Figure IVg with these temperature estimates and the function $K_d (K_D^{gnt}/K_D^{px})$ plotted against temperature in Figure IVh. K_D values for coexisting garnets and clinopyroxenes have been calculated from electron-microprobe analyses (Tables IV and VI) with the Fe^{2+} of the pyroxene recalculated according to the method of Cawthorn and Collerson (1974). These analyses are of minerals from B5, B1 and V11. Sample B5 is a two-pyroxene garnet hornfels collected from the contact zone of Table Mountain. Sample B1 shows a development of amphibole which overprints the pyroxene and garnet and was collected from the same area but approximately 12 metres from the contact. Sample V11 is an altered hornfels, nominally called a rodingite also from Table Mountain. The temperature estimates obtained for these rocks are 850°C, 720°C, and 760°C respectively. Similar temperatures are obtained on both plots.

ii) The transition from greenschist to amphibolite facies in a basaltic system has been investigated by Liou et al. (1974). The PT diagram for this transition under various conditions of oxygen fugacity defined by QMF and NNO buffers is reproduced in Figure IVi. If the

Figure IVg: Estimation of aureole temperatures
 K_D^{gnt} vs. K_D^{px} (Banno, 1970).

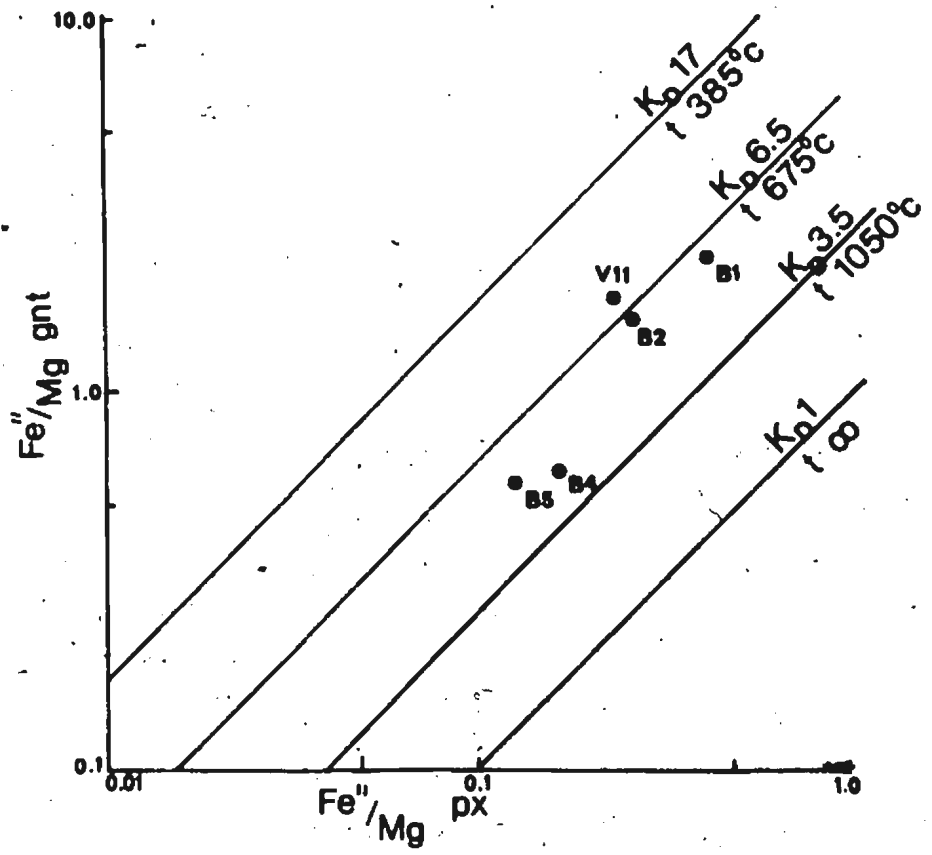


Figure IVh: Estimation of aureole temperatures
 K_d vs. $1/T$ (Mysen and Heier, 1972).

2

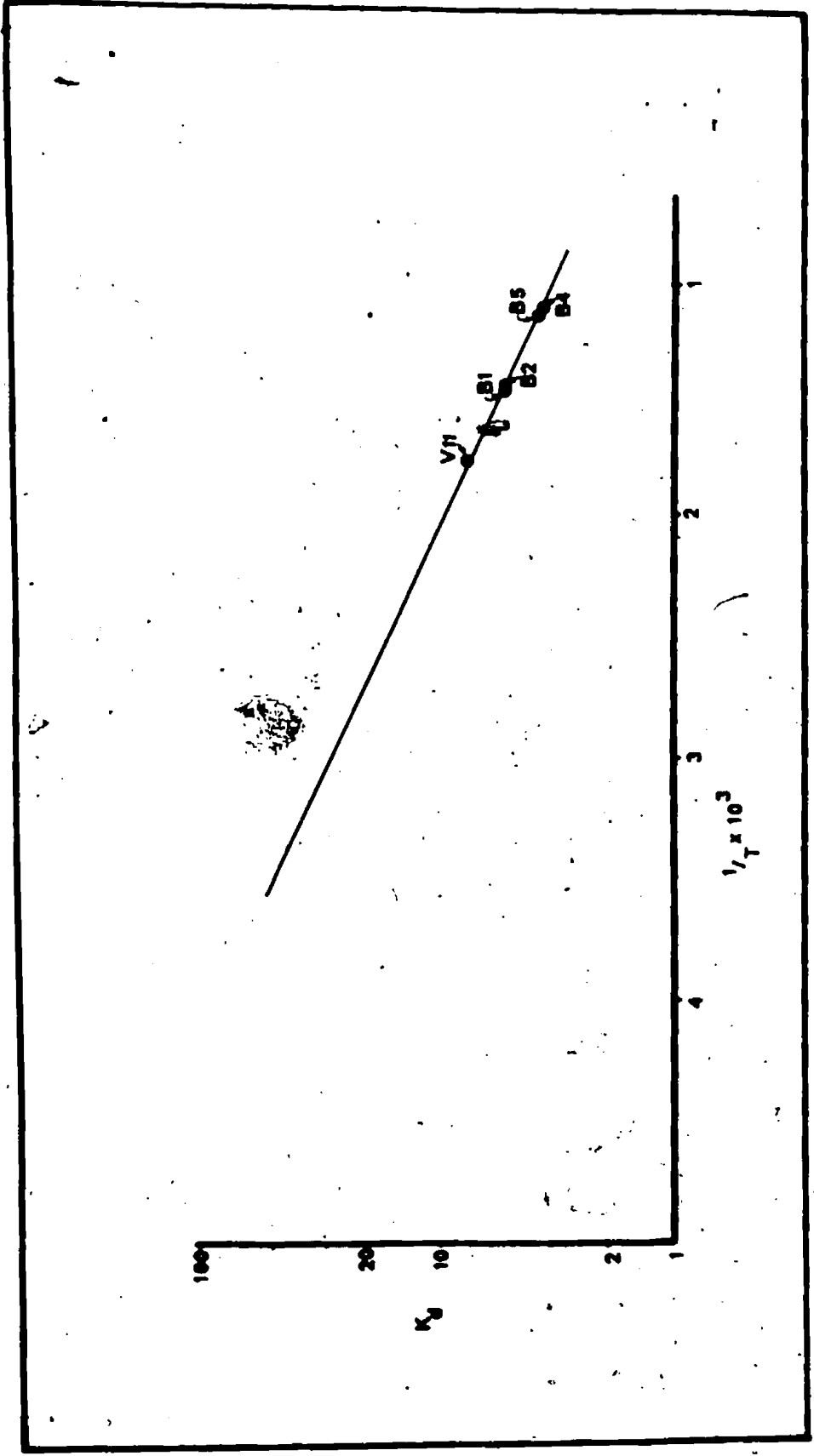
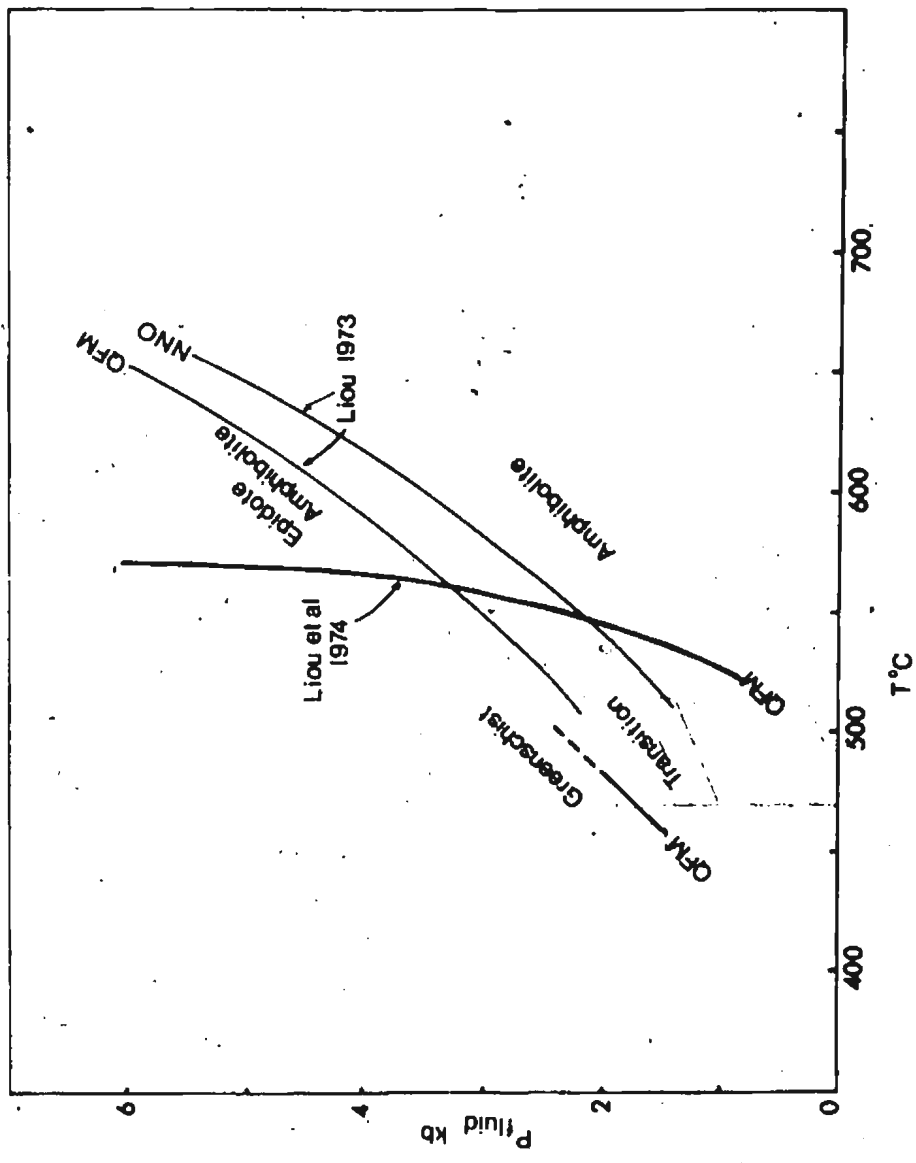




Figure IVi: PT conditions for amphibole to greenschist facies transition in basaltic rocks (Liou, et al., 1974).



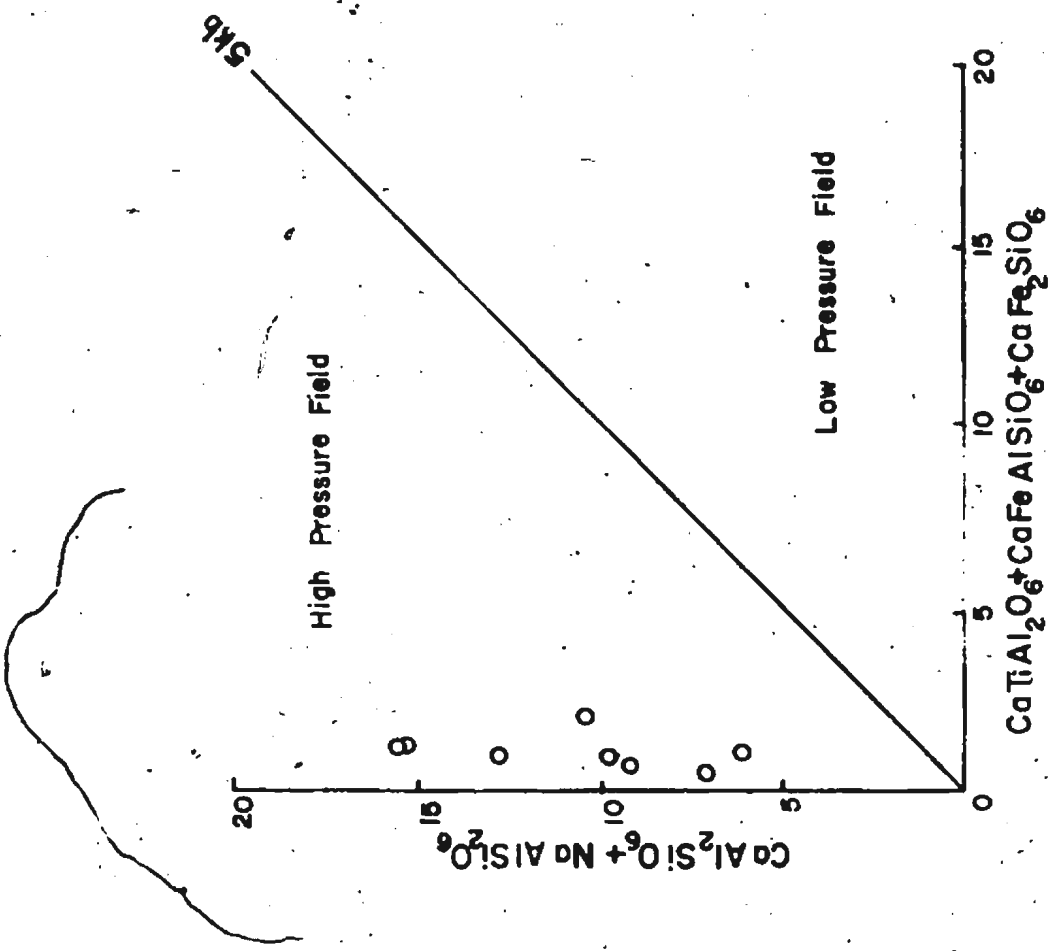
8

fluid pressure in the aureole rocks at the time of formation can be assumed as approximately equal to the hydrostatic pressure beneath the overriding thrust slice, then a temperature for this transition, recognisable by the disappearance of chlorite, can be estimated.

Assuming an overall density of 2.9 gms/cc^2 for the ophiolite slab, of maximum thickness 5 kms, then the hydrostatic pressure at the base of the slab would have been 1.4 kb. At 1.4 kb, the amphibolite-greenschist transition takes place at approximately 500°C (range 470°C - 500°C) both according to Liou (1973) using NNO buffer and Liou et al. (1974) using the QFM buffer. Thus at a distance of approximately 70-90 metres from the contact, according to the location, equilibration temperatures were of this order. It must be noted, however, that no tectonic overpressures have been accounted for in this calculation. There is indication that higher pressures were operative in the aureole. Plotted according to the scheme of Munoz and Sagredo (1974) the clinopyroxenes of the hornfels appear to have equilibrated at pressures in excess of 5 kb (Fig. IVj), although the validity of using titanium content as a barometric indicator in pyroxenes is still arguable (Thompson, 1974).

These pressures are more in accord with those estimated by Turner (1968), etc. At pressures of 5 kb, the transition from greenschist to amphibolite facies takes place at approximately 570°C . With these temperatures a gradient can be constructed of temperature versus distance from the contact for the aureole rocks. A number of workers have attempted to define the rates of conductive heat loss from igneous intrusions of different sizes

Figure IVj: Pressures of equilibration of aureole
clinopyroxenes (Munoz and Sagredo, 1974).



and shapes (Lovering, 1935; Ingersoll and Zobell, 1948; Jaeger, 1957, 1959, 1961 and MacGregor, 1964). Although none of these models effectively reproduce the situation of heat loss from the base of an overriding thrust slice, they are informative of the restrictions in the amount of country rock heating that can occur with igneous intrusions of various temperatures. For example, Lovering's curves show that an igneous mass with an initial temperature of 1075°C can produce maximum temperatures of 700°C in the contact zone which drop rapidly below 325°C one hundred metres from the contact. A number of these cooling gradients shown in Figure IVk indicate that in order to attain the temperatures observed in the aureole, the overriding ultramafic rocks had to be at temperatures in excess of 1000°C unless another heat source was available.

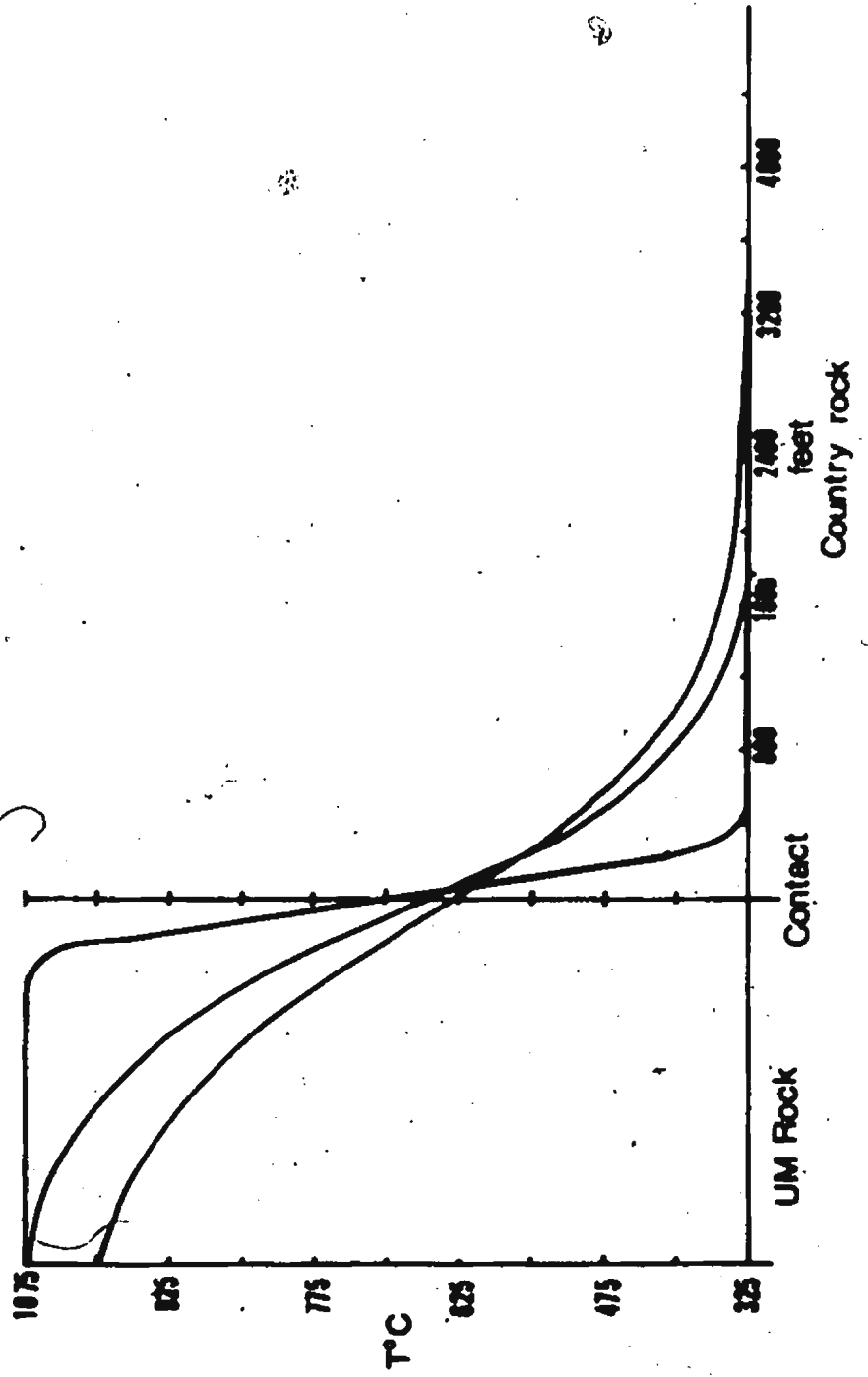
There is a possibility of heat contribution by the process of serpentinisation. Serpentinisation is an exothermic process and in the reaction



the heat evolved is 33.7 K cal/mole of serpentine (Bennington 1956). However, this heat can only be supplied at a temperature of 500°C (approximate upper stability limit of serpentine) and will not affect the country rocks down to this temperature.

More likely heat is produced by fractional heating. Reitan (1968) arrived at a number of mathematical models relating depths, stresses, rates of heat generation and size of heat production zone. His models

Figure IVk: Lowering cooling gradients.



suggest that temperature increases of the order of 100°C can be produced in periods of 0.1 my at depths of about 12 kms using variable strain rates and rates of generation. Using equations for frictional heating in solids, developed by Carslaw and Jaeger (1959) temperature increases can be related to duration and rate of obduction (Appendix II). With a maximum reasonable time span of about 10 my and reasonable rates of thrusting of 5-8 cm/year, temperature increases of up to 300°C may be expected. These calculations are made without accounting for the presence of water in the thrust zones, which would tend to increase specific heats and thus reduce temperature increases. Although with frictional heat the temperature at contact zone could be raised to $850-900^{\circ}\text{C}$ this still implies that the ultramafic rocks had to be extremely hot, probably in the order of 1000°C .

Dynamic considerations: It is clear from the structural and metamorphic history of the aureole that its development was complex and involved several stages. Although the structural history of Williams and Smyth (1973) and the nomenclature used here (Section C, p.112) serves to delineate the major deformatory phases, it oversimplifies the continuity of the development of the aureole.

It is probable that the folds and fabrics were produced during movement of the thrust slices over underlying rocks and that successive stages of movement were taken up at different levels whilst static mineral growth overprinted fabrics developed at other levels earlier. Later movements along these zones produced overprinting fabrics. Since these later fabrics are more intense lower in the aureole it might be supposed

that after initial production, rocks in the contact zone became annealed to the sole of the thrust slices and effectively became part of the slices, the whole then moving on lower dislocation surfaces. The latest periods of emplacement were dominated by gravity sliding on soft sediment mélanges, indicating insufficient temperatures to produce annealing metamorphism (Figure IVI).

G. Conclusions.

Earlier views on the origin and emplacement of Alpine peridotites were partially governed by the presence of metamorphic aureoles that related to the ultramafic plutons. With more recent views that incorporate the hypothesis of ophiolites representing oceanic crust and mantle it has been difficult to reconcile the aureole rocks in the light of plate tectonic models.

In the Bay of Islands it is clear from the lack of intrusive features at the contact zone, the considerable recrystallisation of the ultramafic rocks, the structures developed within the aureole rocks and the continuity of the aureole only around the effective base of the ophiolite thrust slice, that the aureole was not produced simply by intrusion of hot masses of igneous rock, but is related directly to the emplacement of the thrust slices (see also Williams and Smyth, 1973). It has therefore been called a dynamothermal aureole (Malpas, et al., 1973). The development of this aureole, although considered a continuous event, has been shown to have had a number of phases. These can be shown diagrammatically as in Figure IVI. The earliest fabric (S_1) seen in

Figure IV1: Schematic model for dynamothermal aureole formation.

ULTRAMAFICS

HORNFELS:
AMPHIBOLITES:

GREENSCHISTS:

MÉLANGE

Thrusting initially takes place
at ub./cr. contact - early fabric, S_1 formed (amphibolite grade?)



Thrusting halted: static H.T.
metamorphism - hornfels formed
overprinting & recrystallising
 S_1 at contact.



Thrusting continues at lower level:
Second stage fabrics formed
(amphibolite & greenschist?)



Final emplacement on soft sediment
melanges.



the aureole was produced during early dynamic movement. This movement took place along a thrust zone represented now by the ultramafic-aureole contact.

Subsequent to this early movement, a period of no movement occurred, during which static hornfelsing took place. This hornfelsing obliterated by recrystallisation all traces of the earlier dynamic phase close to the contact whilst further away S_1 fabrics remained.

Further thrust movement took place along a zone lower in the aureole, since the hornfelses were effectively annealed to the ultramafic rocks, and imparted the later (D_2) fabrics partially overprinting the hornfels. The latest periods of movement of the thrust slice are represented lower in the sequence still by *mélange* zones representing a cold cataclastic process as a result of progressive heat loss from the system.

The rate of movement of the thrust slice during the dynamic stages of emplacement cannot be determined but calculations using velocities of overthrusting within reasonable limits have indicated that frictional heating cannot raise the temperature of the aureole rocks more than 200°C . This suggests that to produce the contact hornfels and the temperature gradient indicated through the aureole, the ultramafic rocks had to be at a temperature of the order of 1000°C or greater.

A temperature of 1000°C is to be expected at a depth of approximately 55 km below the Moho on a normal oceanic geotherm. However, estimates of the depth of the basal ultramafic rocks in the mantle before displacement are not more than 5 km. The ophiolite suite was therefore

obviously not displaced from an environment in which a normal oceanic geotherm was operative. High heat flow in oceanic type mantle and crust is to be expected in the following regions:

- a) at a spreading centre
- b) in association with hot spots
- c) in marginal basins where igneous activity associated with remelting of the subducted plate raises heat flow.

A further discussion of these models is given in Chapter VII.

PART II

CHAPTER V

THE BAY OF ISLANDS COMPLEX

A. Introduction.

The Bay of Islands Complex (Williams and Malpas, 1972; Williams, 1973) forms four massifs, each part of the highest slice assemblage of the transported sequence and named from north to south as (a) Table Mountain, (b) North Arm Mountain - Mount St. Gregory, (c) Blow-me-Down Mountain and (d) the Lewis Hills (Fig. IIb). In outcrop area the ophiolite slices comprise approximately 600 square kilometres and vary in structural thickness from about 1100 to 1300 metres. Each ophiolite slice has a subhorizontal base marked by a thick serpentinite mélangé which is best displayed on the western, leading edges of the slices. This subhorizontal base does not differ very much from present sea-level. Trailing edges are less apparent and commonly affected by post emplacement high-angle faults along which the overlying slice is down-thrown. Table Mountain and Blow-me-down Mountain are bounded by tear-faults that mark the sides of the northwestwards-transported massifs and which are not continuous to the coast (Fig. 1c and Williams, 1973). The three northernmost massifs are broadly synclinal in form with similar orientations (i.e. fold-axes striking NNE). This folding was attained before the final emplacement of the slices since it is truncated by the subhorizontal thrust at the base of the slices. It does, however, involve the basal aureole and therefore post-dates initial development of the overthrust. The thinness of the western synclinal limbs on Table Mountain, Mt. St. Gregory, and Blow-me-down

Mountain is due to structural omission rather than a stratigraphic wedging-out. The Lewis Hills appears to have been rotated 90° with respect to the northern massifs (Williams and Malpas, 1972) and does not have the synclinal form of the latter. Here the ophiolite slice appears to be almost flat lying, giving rise to wide exposures of restricted stratigraphic horizons.

Since all the massifs occupy the same structural level, it has been postulated that they were emplaced as a single sheet (Cooper, 1936; Smith, 1958; Williams and Malpas, 1972). However, the different levels of exposure of each cross-section would then imply a considerable amount of post-emplacment faulting. The fact that the structural bases of all slices appear to be relatively close to sea level (Williams, 1973) would, however, suggest relatively little vertical displacement of the massifs with respect to each other. Since the Lewis Hills massif does not fit the overall structural picture, one must assume that it, at least, was emplaced as a separate entity. The different lithologies at the base of the ultramafic pile (see below) suggests that the slices were separate and exhibited different cross-sections during emplacement.

B. Lithological Cross-sections.

Two of the massifs (Blow-me-down and North Arm Mountains) display a completely developed ophiolite suite. Each of the massifs has a basal portion composed of ultramafic rocks. These basal ultramafics vary from approximately 2.5 km thick on North Arm Mountain to nearly 5 km thick on Table Mountain and are immediately underlain by the basal

aureole except where this has been removed by later faulting. Gabbroic rocks lie above the ultramafic rocks and an interbanded zone separates these two rock types. This zone has been called the 'critical zone' by Smith (1958) and Irvine and Findlay (1972) and reaches thicknesses in the order of 400 m. The gabbros are not present on the Lewis Hills, where rocks of the critical zone are the highest preserved. On Table Mountain the gabbros are not complete, but where the full sequence is developed on North Arm Mountain and Blow-me-down Mountain, they reach an approximate thickness of 4 km. On the latter two massifs diabase dikes increase in quantity at the top of the gabbro, and higher up they become 'sheeted' (100% diabase dikes) and feed overlying pillow lavas. The diabases and pillow lavas reach a total thickness of about 2.5 km where they are overlain by siltstones and silty sandstones between Crab Point and Birch Head on North Arm (Fig. IIIb).

Stratigraphic columnar sections of the three northernmost massifs are presented in Fig. Va.

C. Lithologies.

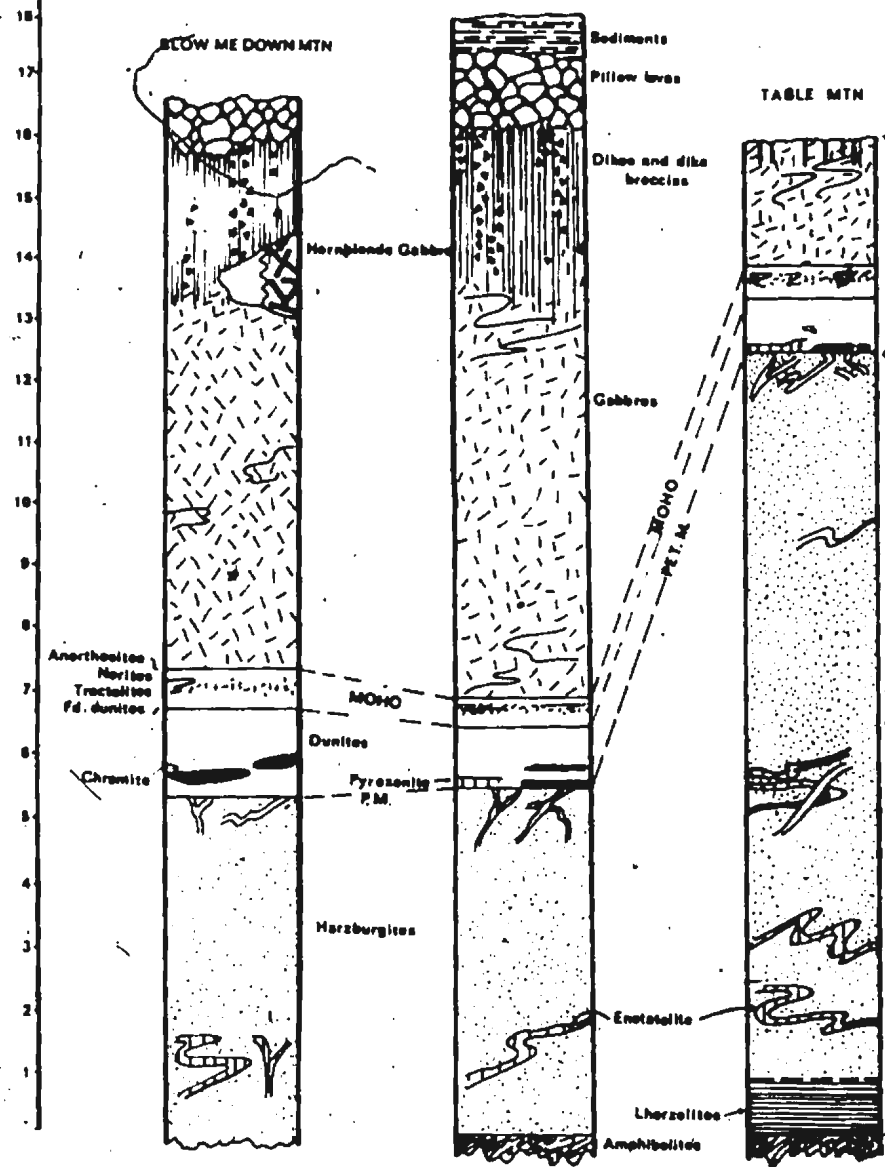
i) Lherzolite and harzburgite

Lherzolites (olivine-clinopyroxene-orthopyroxene rocks) occur at the base of the Table Mountain massif and are most easily accessible near Winter House Brook and on Trout River Pond. Elsewhere (North Arm Mountain and Blow-me-down Mountain) no lherzolites have been found and harzburgites (olivine-orthopyroxene rocks) immediately overlie the basal dynamothermal aureole. The rocks are defined according to the classification of Coleman (1971) and modal analyses are plotted in Figure Vb.

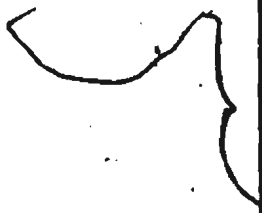
Figure Va: Stratigraphic columnar sections of Bay of Islands Complex.

ft x 10³

NORTH ARM MTN



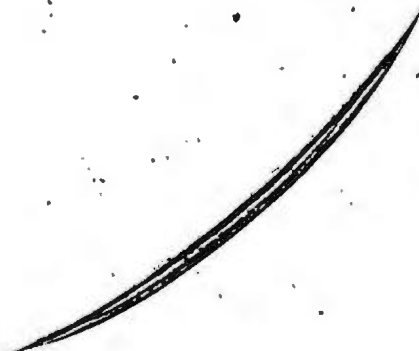
A



The lherzolites of Table Mountain grade into harzburgites about 200 metres above the basal aureole by a loss of clinopyroxene. In the field, lherzolites and harzburgites are difficult to separate since the clinopyroxenes are not clearly discernible. However, the lherzolites generally weather an olive-brown colour compared to the orange-brown of the harzburgites. This weathering occurs to depths of 4 or 5 cms and causes the more resistant light-green or bronze enstatite and black spinel to stand in relief, causing a stucco-like surface (Plate XXXIIIa). In the lherzolites the spinels appear as glassy green crystals compared with the black chromite of the harzburgites. Both rock types appear porphyritic on fresher surfaces, consisting of green bastitised enstatite crystals set in a dark aphanitic matrix. The ultramafic rocks are affected by a conjugate joint pattern. One joint set strikes generally NNE and dips moderately to the west; the other is at right angles and dips more steeply to the south.

Two types of banding occur in both the lherzolites and harzburgites. The gneissic banding described above (page 90) occurs in either rock type immediately adjacent to the aureole. In general, this banding appears to post-date some serpentinisation and was imparted during early thrusting of the ophiolites. It parallels the basal contact with the aureole, and overprints a primary mineral layering. A similar foliation is developed locally along strike-slip faults that affect the ultramafics. On North Arm Mountain, within 6 to 8 metres from the basal contact, deformed peridotites resemble augen-gneiss with sinuous foliation

Figure Vb: Modal plots of ultramafic rocks.



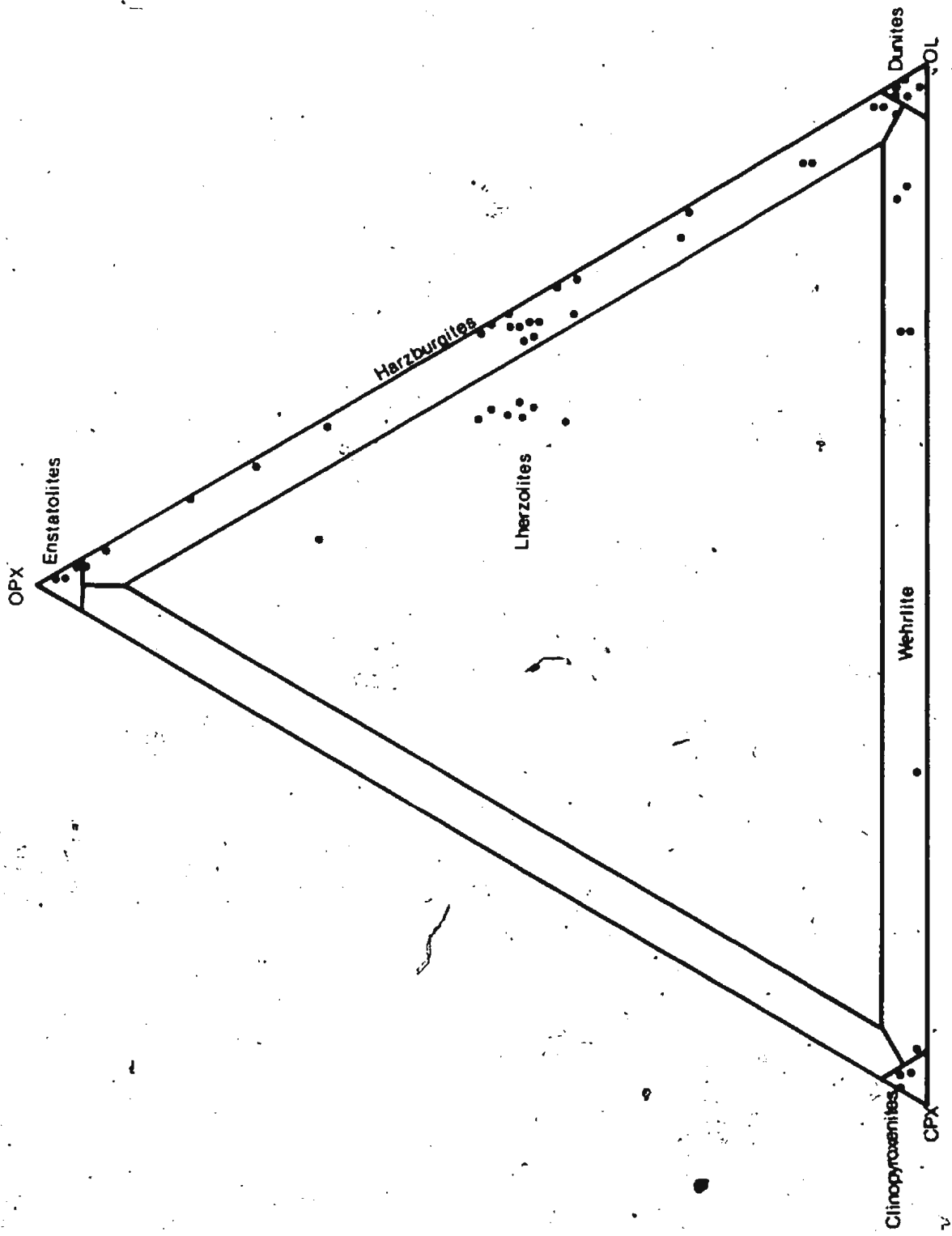




PLATE XXXIIIa: Surface features of harzburgite with enstatite and spinel standing in relief against yellow weathering olivine.

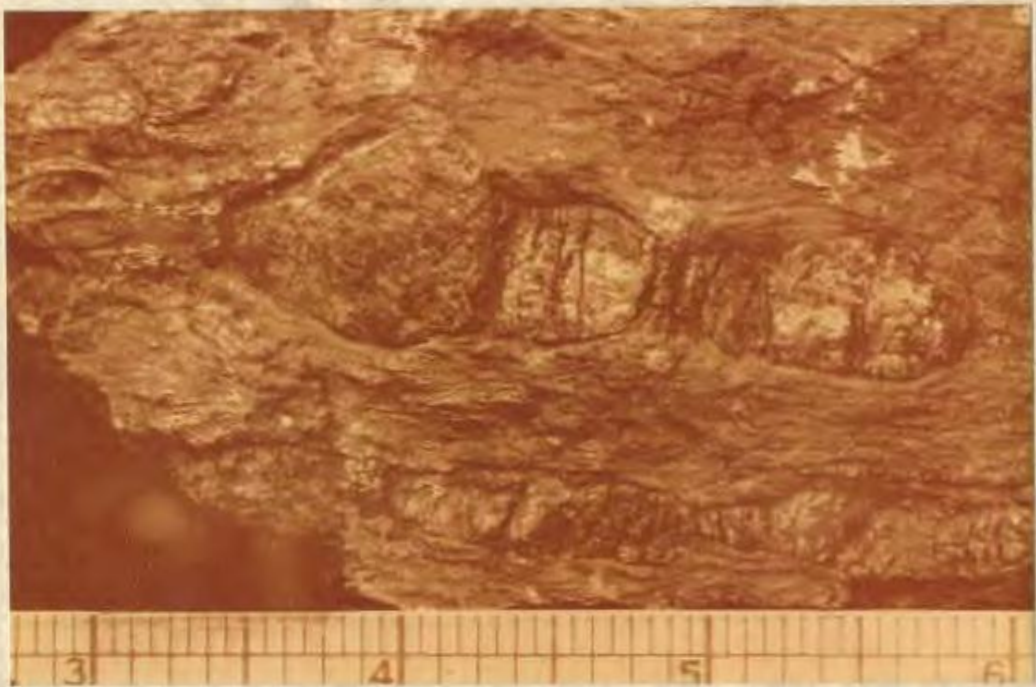


PLATE XXXIIIb: Peridotite augen-gneiss composed of enstatite eyes in a groundmass of serpentine. From C. H. Smith (1958).

and enstatite 'augen' (Plate XXXIIIb). Differential weathering accentuates the structure. In more olivine-rich layers a distinct fissility is imparted.

A primary rhythmic banding in the lherzolites and harzburgites is caused mainly by a variation in the enstatite/olivine ratio. Adjacent bands may range from olivine-rich dunites to peridotite and enstatolite (90% opx). In general, individual bands have gradational contacts and range in thickness from fractions of a centimetre to a hundred metres or so. The banding is emphasized both by differential weathering and more rarely by small concentrations of spinel (Plate XXXIVa). On an individual outcrop scale most bands seem fairly uniform in width. However, individual bands do not continue laterally for any distance but pinch out and pass into other lithologies. Maximum distances over which individual bands have been traced are in the order of 500 metres for the thickest ones, whilst the thinner ones may be only a few metres long. Therefore no distinct stratigraphy is apparent. Bands are often folded and show thinning and attenuation on fold limbs. Smith (1958) suggested that this was a result of plastic flowage due to pre-consolidation movements of a magma. The folds are restricted to small zones and are paralleled by non-folded bands (Plate XXXIVb). They show no preferred orientation although many are flat-lying and fairly tight.

The enstatite content of both the lherzolites and harzburgites cluster around 10-15% but there is a distinct separation produced by modal clinopyroxene. Spinel forms up to 4% of the mode and is variable



PLATE XXXIVa: Rhythmic banding in harzburgites - Table Mountain.



PLATE XXXIVb: Folding of banding in harzburgites - Winterhouse Brook, Table Mountain.

from lherzolite to harzburgite. Despite a considerable degree of serpentinisation (up to 60%) the original mineralogy and textural features are readily identifiable. Strained augen of enstatite, and more rarely forsterite are set in a finer grained matrix of interlocking, unstrained anhedral forsterite and spinel and, in the lherzolites, diopside. Veins of serpentine cut across the strained crystals indicating that a certain amount of recrystallisation predated serpentinisation.

Inclusions of both olivine and spinel are rarely found in enstatite. The enstatite shows varying degrees of serpentinisation and may be totally replaced by light yellow-green bastite in which the (100) parting of the original pyroxene is well preserved. Cross-cutting veins of serpentinite and associated magnetite up to 0.1 mm thick are common and thus post-date the initial serpentinisation of the orthopyroxene. The enstatite crystals generally have relatively sharp, clean boundaries with the surrounding matrix, although in some cases the crystal outlines are blurred by granulation and recrystallisation at the margins, or serpentinisation, especially around stretched enstatite crystals with ragged terminations (Plate XXXVa). Enstatite augen also contain abundant exsolution lamellae parallel to (100) which have, in most cases, been identified as diopside (Plate XXXVb). In the lherzolites there also appears to be minor exsolution of spinel along similar planes. The (100) planes have also acted as glide lamellae, especially in rocks near the basal contact (see page 93), where the enstatite augen are elongated generally parallel to these planes which

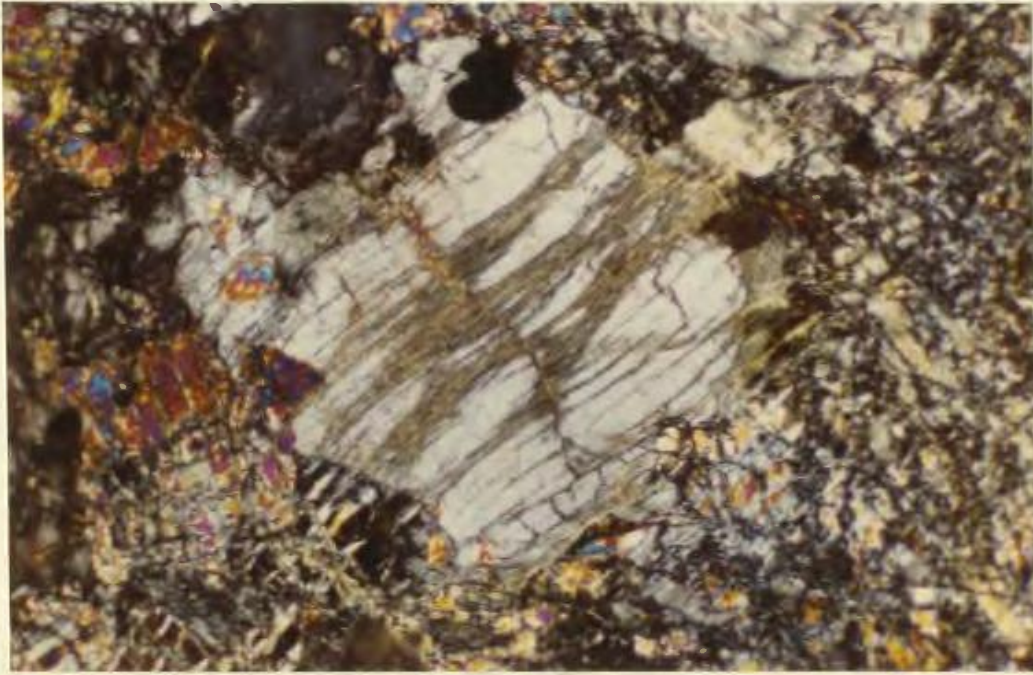


PLATE XXXVa: Serpentinisation of margins of enstatite megacryst in harzburgite - Table Mountain. X nicols x 50.

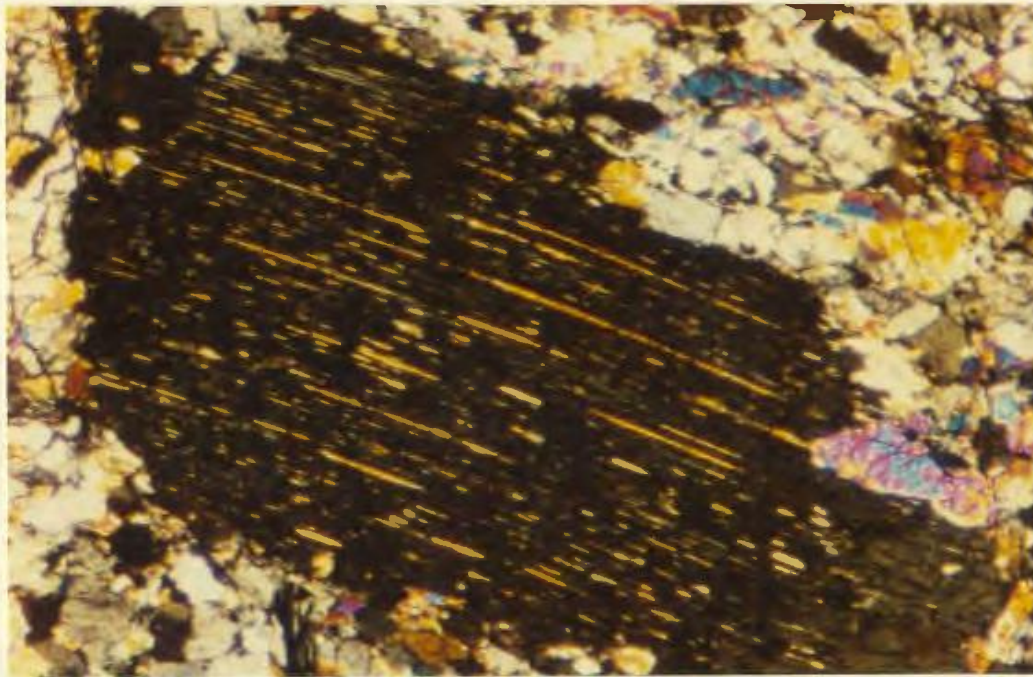


PLATE XXXVb: Exsolution of diopside as (100) lamellae in enstatite - Harzburgite, Blow me down Mountain. x 90.

lie in the foliation of the rock (Plate XXXVIa). As discussed above, this is probably an effect of deformation during the early emplacement of the ophiolites. Further from the aureole no preferred orientation of the (100) parting and exsolution lamellae occurs but they do indicate a distortion and bending of the crystals.

Olivine (Fo_{91-94}) is extensively replaced by mesh-like serpentine (lizardite and minor chrysotile). However, olivine kernels remain and extinction patterns indicate that original grain size was of the range 0.5 - 2 mm and that crystals were equidimensional (Plate XXXVIb). Triple point junctions between olivine crystals with straight boundaries and kink banding of some crystals indicate a certain amount of recrystallisation during a 'penetrative deformation' (cf. Bezzi and Piccardo, 1971). This recrystallisation clearly predated serpentinisation.

Spinel is present in both lherzolites and harzburgites. The spinel in the lherzolites has undergone some alteration during serpentinisation, the main effect of which is to produce magnetite which rims the crystals (Plate XXXVIIa) and fills expansion cracks. It is translucent and green-brown or grass-green in colour. All crystals have irregular outlines and range in size from 0.3 to 1.2 mm. Spinel forms generally only 2-3% of the lherzolite and is found both interstitial to and enclosing olivine, and rarely included in enstatite. In the harzburgites, the spinel is red-brown translucent except where secondary magnetite is developed and the spinels are almost opaque. The spinel is disseminated and generally interstitial to olivine, which it rarely includes. The maximum size of the crystals may be as much as 3 mm but these crystals are extensively shattered.

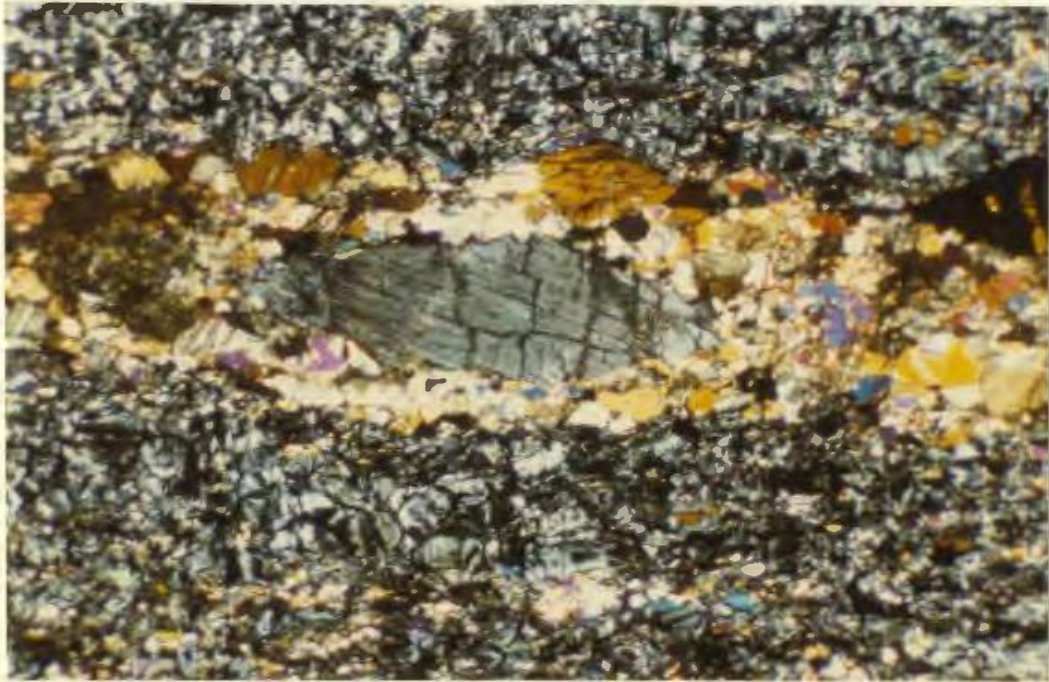


PLATE XXXVIa: Enstatite in mylonite band of basal ultramafics with diopside lamellae rotated into schistosity.

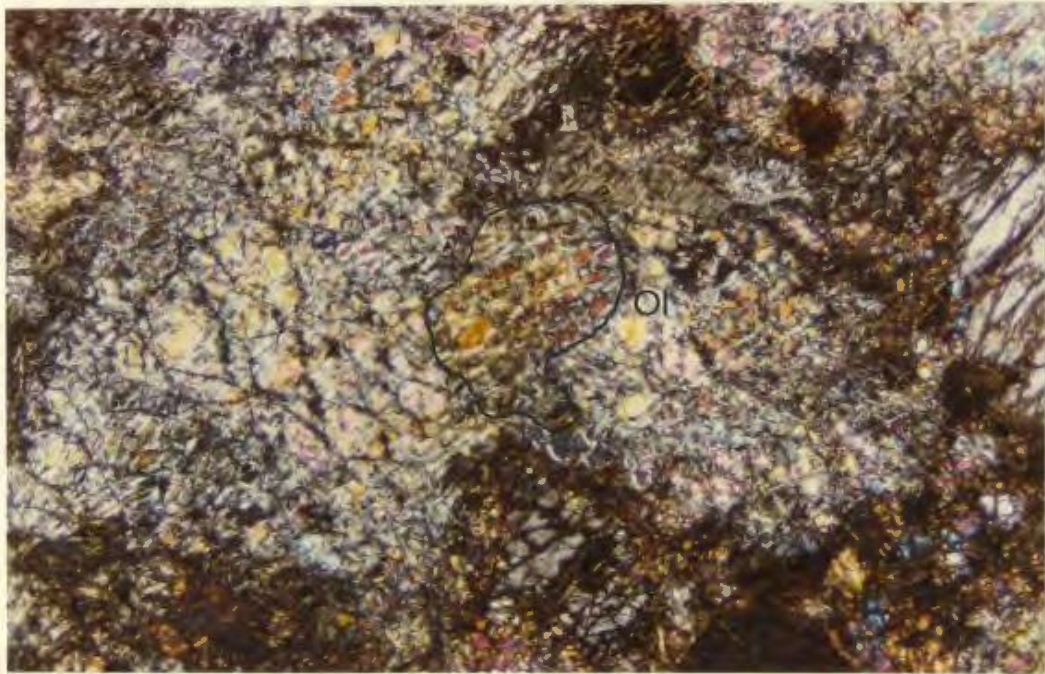


PLATE XXXVIb: Remnant olivine kernels after serpentinisation indicating original crystal size. X nicols x 75.

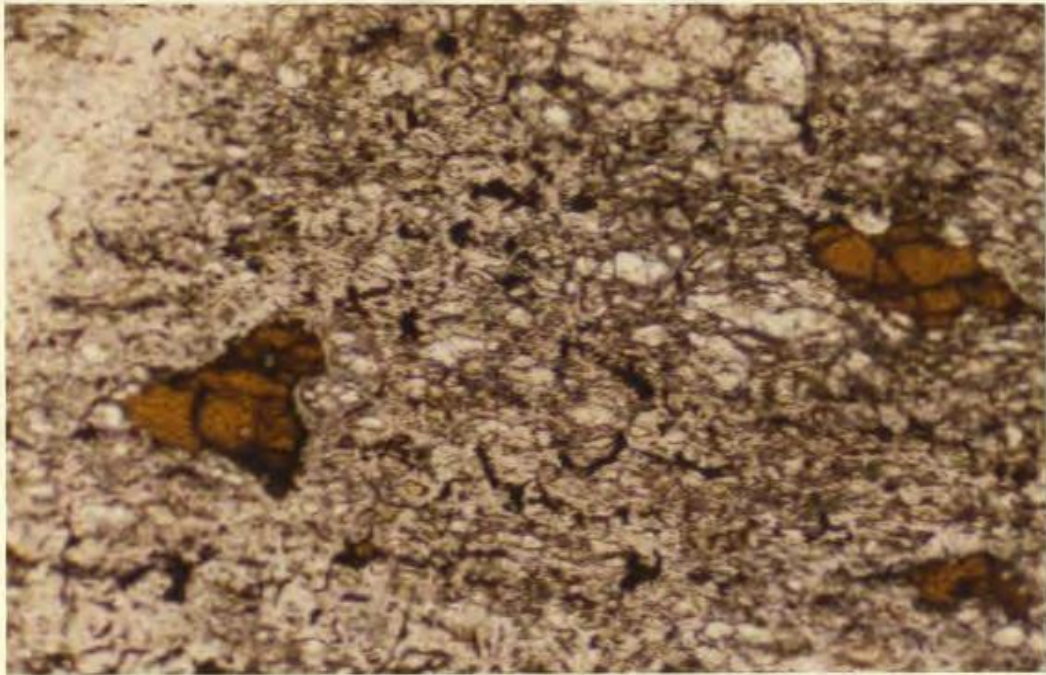


PLATE XXXVIIa: Yellow-green spinels in lherzolites mantled by magnetite, Table Mountain. Plain light x 70.



PLATE XXXVIIb: Dunite veins cutting across folded veins in harzburgites, Winterhouse Brook.

The differing colours of the spinels reflect the fact that those of the lherzolites are relatively aluminium-rich and those of the harzburgites chrome-rich, as supported by microprobe analyses (Chapter VI).

Clinopyroxene occurs ubiquitously as grains in the lherzolites interstitial to olivine and enstatite. It is also present as exsolution lamellae parallel to (100) in the enstatite augen. No exsolution lamellae have been recognised in the groundmass clinopyroxene, and optical properties suggest it is diopsidic augite. The harzburgites contain rare clinopyroxene as interstitial crystals, totalling less than 1% of the rock, but exsolution lamellae of diopside are present in enstatite augen.

ii) Pyroxene and dunite veins and dikes

The peridotite layering is cut by a number of veins and dikes that range from pyroxenite to olivine pyroxenite and dunite in composition. Pyroxenite veins are common towards the base of the pile, dunites more so at the top. The veins stand out because of differential weathering and exhibit both sharp and more irregular contacts with the host peridotite. They range in width from 3-4 mm to 1-2 metres. Although best seen cutting across the mineral layering, some also clearly run parallel to the layering for some distance before branching or linking laterally with similarly orientated veins, and may often be confused with the layering. Some pyroxenite and dunite veins are folded into open folds together with the host peridotite, others clearly cut across these folds and appear undeformed (Plates XXXIVb and XXXVIIb).

Many pyroxenite veins have zones of pure dunite adjacent to their margins, and enstatite gradually increases in abundance in the host peridotite at distances of 1 or 2 cms from the veins. Challis (1965) has described similar pyroxenite veins with long axes and prismatic cleavages of enstatite at a high angle to the walls of the veins. Pyroxene crystals in the pyroxenite veins in the Bay of Islands peridotites rarely seem to have similar orientations. However, in some coarser veins where the larger crystals reach several centimetres in length, there is often an orientation similar to that noted by Challis.

The veins consist of enstatite, diopside and forsterite in varying proportions. The pyroxenites consist of enstatite (40-50% of the vein), diopside (35-40% of the vein) and forsterite (10-15% of the vein); chrome spinel may also be present. An increase in forsterite at the expense of enstatite gives olivine-pyroxenites.

The enstatite has a positive $2V_{\alpha}$ of 85° indicating an $Mg^{2+}/Mg^{2+} + Fe^{2+}$ ratio of about 0.9. Several thin sections of the pyroxenites indicated that much of the enstatite contains exsolution lamellae of diopside parallel to (100) and these lamellae are invariably deformed. Micro-kink bands are not uncommon in enstatites with no visible exsolution lamellae and in intergranular clinopyroxenes. Larger enstatites may be partially serpentinised and represented by bastite pseudomorphs.

Diopside ($2V_{\gamma} \sim 60^{\circ}$, + ve) occurs as small anhedral (0.2 - 0.8 mm) crystals interstitial to the enstatite. Twinning has been observed in some basal sections and twin planes are often bent and distorted. Olivine occurs in small quantities as generally well formed crystals often included in the enstatite.

Dunite veins are generally thicker and more continuous than the pyroxenite veins. Their mineralogy consists of olivine (Fe_{90-93}), enstatite and chromite. Olivine forms 95% of these veins and the enstatite is subordinate. The olivine occurs as interlocking anhedral and often shows minor kinking. The chromite is dark-red, translucent to opaque and often forms strings or 'layers' up to 1 mm thick in the central region of the veins. These layers parallel the sides of the veins and can be traced for several metres before they thin out and disappear.

iii) Origin of layering and mineral foliations

The mineral layering caused by variations in the relative proportions of olivine and orthopyroxene is present throughout the peridotites of the Bay of Islands Complex. This mineral layering must be clearly distinguished from the cataclastic foliation in the harzburgites and lherzolites at the base of the ophiolite slice, which overprints it, and was imparted during the early stages of ophiolite emplacement (Chapter IV).

Several hypotheses for the origin of this layering may be considered, based on examples from alpine-type ultramafic bodies throughout the world. These are: (a) an origin through crystal settling with the aid of convection currents; (b) an origin by preconsolidation flow; and (c) an origin by post-consolidation penetrative deformation and recrystallisation.

Challis (1965) recognized a size difference between the enstatites and olivines of the harzburgites of Dun Mountain, New Zealand, and those

of the dunites, recording that those minerals were larger in the harzburgites, and also that the dunite always showed more deformation (crushing) and serpentinisation. From both a crystal size and petrofabric analysis, Challis also suggested that the origin of the layering in the ultramafic rocks was comparable to the development of bedding in sedimentary rocks and in support of this noted: the presence of well developed poikilitic textures and euhedral crystals in the harzburgites, a dimensional orientation of olivine crystals suggesting a settling on their broad faces, and a transition to feldspathic peridotites and gabbros similar to sequences shown by differentiated layered intrusions.

Thayer (1963) noted that various stages of mechanical disruption have affected primary textures which appear to have resulted from variations of the crystal settling mechanism. He states (p. 56), 'These relict features imply that the alpine complexes essentially are partially refused and remobilised parts of huge settled complexes formed deep in the crust or mantle'.

Raleigh (1965) concurs with this view, suggesting that the peridotites of Cypress Island, Washington, had a primary origin by crystal settling, since relict cumulus features are preserved, but that there had been subsequent plastic deformation.

The greatest argument against a crystal settling mechanism as an origin for the layering in the Bay of Islands peridotites is the lack of cryptic variation among the olivines and enstatites, both of which maintain a relatively constant composition throughout the peridotites

(cf. Loney et al., 1971). Such a variation if present would characterise the layering as being a result of fractionation and crystal settling and has been taken by Jackson (1961) and Wager and Brown (1967) as an indication of the mode of origin of stratiform intrusions.

Significant differentiation by crystal settling requires that a significant difference in specific gravity exist between the mineral components involved, or that there are continued renewed injections of magma (Ingerson, 1935). The two major minerals, enstatite and forsterite, that are the major components of the peridotites, have very similar specific gravities (~ 3.29) and thus equal settling rates. It is also difficult to envisage renewed injections of magma causing many thousands of alternating bands through thicknesses of up to 5 km. If the total ultrabasic complex (and associated mafic rocks) represented derivatives from one magma chamber, then the magma would have been extremely picritic, if not ultrabasic, and consequently would have required an enormously high and anomalous degree of partial melting of mantle rock for its production.

Church (1972) recorded cumulate features in the Betts Cove ophiolite and in some dunites of the Bay of Islands Complex. He therefore ascribed the origin of all peridotite material of these ophiolites to crystal settling. However, it is presumed here that the cumulates he observed were in the higher dunite zone since no relict cumulus textures have been observed in the lherzolites and harzburgites from the Bay of Islands Complex. However, it is arguable that these textures have been obliterated by later events (cf. Thayer, 1963).

Smith (1958) proposed that the banding in the peridotites was a result of preconsolidation flow. However, solid flow is only possible in the presence of interstitial fluids under restricted conditions. Hubbert and Rubey (1959) suggest that shearing stresses can only be transmitted across grain boundaries if 'effective' stress is equal to the yield stress for solid flow. Therefore, the interstitial liquid must not be distributed to prevent solid contacts between most olivine grains. It is possible that plastic deformation could have taken place when the liquid pressure was less than in the solids, i.e. when the liquid was removed by filter pressing (Raleigh, 1965) and concentrated in low-pressure environments during deformation.

Smith (1958) suggested a late stage reaction of SiO_2 -rich vapours with olivine to produce the enstatite of the peridotites. These vapours, streaming through an olivine-rich mush, under stress, would produce bands and pockets of enstatite realised later as a rhythmic mineral layering. The enstatite would therefore be almost a deuteric product. Although such an interpretation may account for the enstatite veins, which show cross-cutting relationships and sharp contacts with the layered sequence, it seems unlikely that it can account for the multitude of rhythmic bands many of which show diffuse contacts at which there is no clear sign of enstatite-olivine reactions.

Medaris (1972) describes petrofabrics in peridotites from S.W. Oregon, in which strained augen of forsterite, enstatite and diopside are set in a fine-grained matrix. He suggests that an episode of recrystallisation took place during which the 'matrix minerals' formed

at the expense of the 'augen' or 'coarse-grained minerals'. These textures are similar to those observed in the Bay of Islands peridotites.

Dickey (1970) describes 'tectonic-type' layers from the Serrania de la Ronda peridotite as a "foliation manifested by layers, boudins and schlieren of spinel pyroxenite". Further, "these layers are common in alpine-type peridotites; they resist weathering and highlight the structure of the peridotite", and "they may be formed during deformation of the peridotite as the more easily deformed olivine is segregated from the pyroxenes and spinel."

Ave Lallement (1967) and Ave Lallement and Carter (1970) have shown that tectonite fabrics, resembling depositional fabrics, are of metamorphic origin and are due to syntectonic recrystallisation. Petrofabric analyses further indicated that the fabric must have originated during folding and was associated with simultaneous deformation of olivine and enstatite grains. Den Tex (1969) also interpreted olivine fabrics from alpine peridotites as being a result of metamorphic deformation rather than primary igneous layering or deformation of a crystal mush.

It seems likely that the formation of the layering, the deformation of olivine and enstatite crystals, and the folding of layers and intrusive veins in the Bay of Islands peridotites can be related to an ongoing penetrative deformation. The deformation of the enstatite crystals is clearly related to the development of the layering since the deformed crystals and their internal glide planes are often orientated parallel to the layering.

Most workers have agreed on a mantle origin for alpine peridotites (see Wyllie, 1970). de Roever (1957) considered the fabrics common in such rocks to be due to deformation of upwelling mantle. Medaris (1972) concluded similarly that the peridotites of southwestern Oregon show effects of high temperature recrystallisation that took place as they moved upward in the mantle from depths of approximately 20 to 60 kms. Bezzi and Piccardo (1971) noted textures in Ligurian ophiolites that show strong similarities to those of the Bay of Islands peridotites. They conclude that "it seems reasonable to suppose that lherzolites and related rocks may represent more or less recrystallised primary material from the upper mantle, deformed and re-equilibrated during its tectonic evolution."

Although many authors have described and studied the deformation and recrystallisation processes by which rocks with primary cumulate layering are affected during tectonic evolution until they obtain a tectonite texture which obliterates the pre-existing cumulus features (Thayer 1963, 1969; Ayrton, 1968; Raleigh, 1965); rocks which show transitional features between tectonite and cumulus have never been seen in the Bay of Islands Complex and a sharp boundary exists between the two types. It seems reasonable that the petrofabrics including the strong foliation, recrystallisation and strain features in olivine and enstatite and the isoclinal folding of layers and veins, represent deformation of material in the upper mantle, and are comparable to fabrics described by Nicolas, et al. (1971), especially in the light of present

interpretations of ophiolite suites as slices of ancient oceanic upper mantle and crust (Church and Stevens, 1971; Dewey and Bird, 1971; Upadhyay, et al., 1971; etc.).

iv) Origin of vein rocks

Bowen and Tuttle (1949) suggested an explanation for the origin of initially cross-cutting bodies of dunite and pyroxenite in peridotite. They related the origin of pyroxenite to the streaming of silica-saturated hydrous vapour through cracks and along planes of weakness in the peridotite, resulting in the replacement of olivine by the more siliceous enstatite. Similarly, they noted that olivine might be produced by a streaming of silica undersaturated gasses through peridotite, replacing enstatite by olivine. The mutual cross-cutting of these bodies was thus a result of the gaseous transfer of components through the host peridotite. This model explains the dunitic margins to many enstatolite veins, by removal of silica from wall rock peridotite and its concentration in the central part of the veins.

However, there are a number of difficulties in accepting this interpretation. The first is obvious and involves the origin of the hydrous vapours. In most peridotite bodies, and the Bay of Islands Complex is no exception, there is a lack of hydrous minerals. The only hydrous minerals present in the Bay of Islands peridotites are phlogopite and hornblende associated with the basal aureole, and which crystallised much later in the tectonic history of the peridotites. Serpentine was obviously not stable at the temperatures suggested for the formation of

the veins by coexisting enstatite and exsolved diopside. It therefore appears that if hydrous vapours were present they must have been introduced and were not magmatic in origin. Secondly, although such a model can account for the replacement of forsterite by enstatite, it cannot account for the presence of clinopyroxene in the vein rocks, nor for the high CaO content of enstatites indicated by the exsolution of diopside, especially since calcium is rarely concentrated in vapour phases.

An alternative hypothesis to that of in situ replacement involves direct crystallisation from a magmatic liquid(s). This is the origin implied by the apparent intrusive relationships of the veins, both to one another and to the host peridotite. However, the origin of the magma can vary.

Raleigh (1965) suggested that pyroxenite veins represent segregated liquid fractions of residual magma, filter-pressed out and crystallised towards the end of the intrusion process. He therefore advocated the origin of the peridotites by a crystal settling mechanism. Arguments presented above suggest that the layering of the peridotites cut by the veins was related not to crystal settling, but to subsolidus flow in the mantle. It is probable that rest liquids did not exist at this advanced stage. It is also unlikely that pyroxenite and especially dunite veins represent relatively late stage fractionation products unless the original magma was extremely ultrabasic.

However, it is possible that the vein rocks represent early fractionation products of a basic magma produced by fusion of mantle material. Most 'magmatic-type' bodies (Dickey, 1970) in alpine peridotites are gabbroic or lherzolithic in composition. These veins

which both cut and parallel earlier 'tectonic layers' (Dickey, 1970) have been related to the production of basic magmas by partial melting of ultramafic mantle material (Dickey, 1970; Menzies, 1973). The vein rocks in the Bay of Islands peridotites may result from early fractionation of such basic magmas with the residual less mafic liquid being removed to shallower levels where it formed the mafic gabbros, diabbases and volcanics.

Megacrysts and xenoliths of aluminous clinopyroxene, orthopyroxene, olivine-poor lherzolites, harzburgites and orthopyroxenites have been reported in alkali-basalts from southern Australia by Irving (1974a, b). These are thought to represent cumulates from basanitic and related magmas in the pressure range 13-23 kb, and textures such as a partial development of crystal faces on most megacrysts, suggest they represent disaggregated parts of coarse grained polycrystalline aggregates, possibly veins (see also Ishibashi, 1970 and Strong, 1972). Similar fractionation from an olivine tholeiite is unlikely to involve orthopyroxene as the earliest crystalline phase (O'Hara, 1968). O'Hara showed that olivine is the first mineral to crystallise at high pressure (> 5 kb) from basaltic melts produced by fusion of mantle material. Olivine is succeeded by orthopyroxene and clinopyroxene respectively. Dunitic veins in the peridotites might thus represent olivine fractionation from a basaltic melt at pressures of 10-15 kb (Chapter VI). Lherzolites and olivine pyroxenites would similarly result from the coprecipitation of olivine, orthopyroxene and finally clinopyroxene. Re-equilibration of the pyroxenes at lower pressures resulted in exsolution textures.

Such a model might also explain the marginal enrichment of olivine in some veins. The petrogenesis of the veins according to such a scheme is discussed further in Chapter VI.

v) The Main Dunite zone

Although dunitic rocks are present throughout the ultramafic pile, generally in the form of cross-cutting vein rocks, and to a lesser extent interbanded with peridotite, a thick zone of dunites is found above the harzburgites and is here called 'The Main Dunite Zone'. This zone is developed on all the massifs but is especially noticeable on Blow-me-down Mountain. Smith (1958) noted the increase in dunite veins and bands towards the top of the harzburgites and made a three part division of the Blow-me-down ultramafics into a lower peridotite zone (here harzburgites with pyroxenite veining), and intermediate peridotite and dunite zone (here harzburgites with increasing dunite bands and veins) and an upper dunite zone (here the Main Dunite Zone). It is not possible to make an accurate determination of the thickness of the Main Dunite zone since the upper contact is interbanded with more feldspathic rocks, and in the field its base is gradational from harzburgites. However, the general trends of these contacts are mappable and, on average, the thickness of the zone may reach 700 metres on Blow-me-down Mountain, and generally slightly less on Table Mountain and North Arm Mountain (~400 metres). Although the zone is composed almost entirely of monomineralic dunite, other rock types including clinopyroxenite and chromitite are included, since they seem to be confined to this horizon within the ophiolite slices as a whole.

As with the dunite veins found in the harzburgites, the rock weathers to a bright-yellow, smooth, even-grained surface on which black, lustrous chromite grains are emphasized by positive relief, and is thus easily distinguished from peridotite in the field. Concentrations of chromite and clinopyroxene occur at the base of the zone and feldspar becomes a major phase towards the top. Orthopyroxene is relatively rare away from the harzburgites.

Although highly altered, and properly called a serpentinite, enough original mineralogy is available, and textures of serpentine aggregates derived from olivine are distinctive enough, to estimate the original assemblage and to allow rock names to be applied on the basis of pre-serpentinisation composition of the rock. The dunite is a monomineralic rock composed almost entirely of olivine. Minor amounts of clinopyroxene and orthopyroxene may be present and chrome spinel may form up to 1% of the rock (Fig. Vc). An increase in these minerals gives rise to pyroxene dunites or olivine pyroxenites and chromitite respectively. Tectonite fabrics are rarely present in the main dunite zone and the major features are a result of crystal settling and accumulation (Wager et al., 1960; Jackson, 1961). In hand specimen these cumulate features are only recognisable where other minerals in addition to olivine are present in the rock. Thus pseudosedimentary features such as layering, graded-bedding, mineral-grading, cross-bedding, scour and fill structures and slump structures are emphasized by the presence of chromite, clinopyroxene, or feldspar (Plates XXXVIIIa and b). The mineral layering differs in scale from the banding in the peridotites, being generally much thinner, more continuous and more constant in



PLATE XXXVIIIa: Cumulate layering in dunite. Mineralogical layering of olivine and clinopyroxene.



PLATE XXXVIIIb: 'Scour and fill' structure in layered dunite.

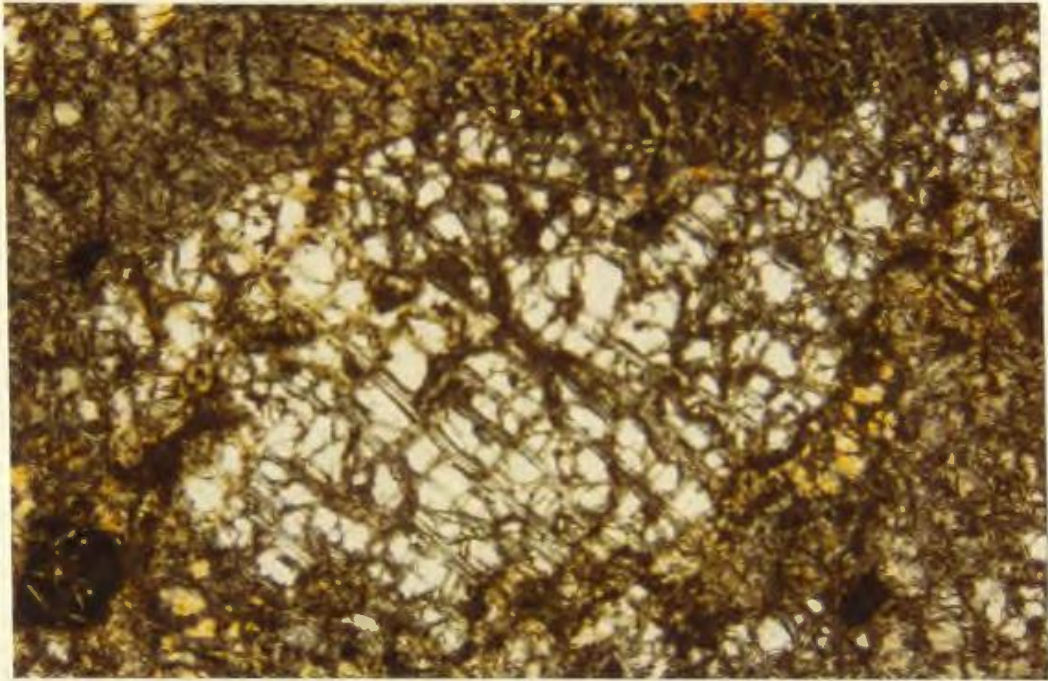


PLATE XXXIXa: Large olivine crystal from cumulate dunites - highly serpentinized along fractures. Kernels with similar extinction indicate size of crystal. X nicols x 35.

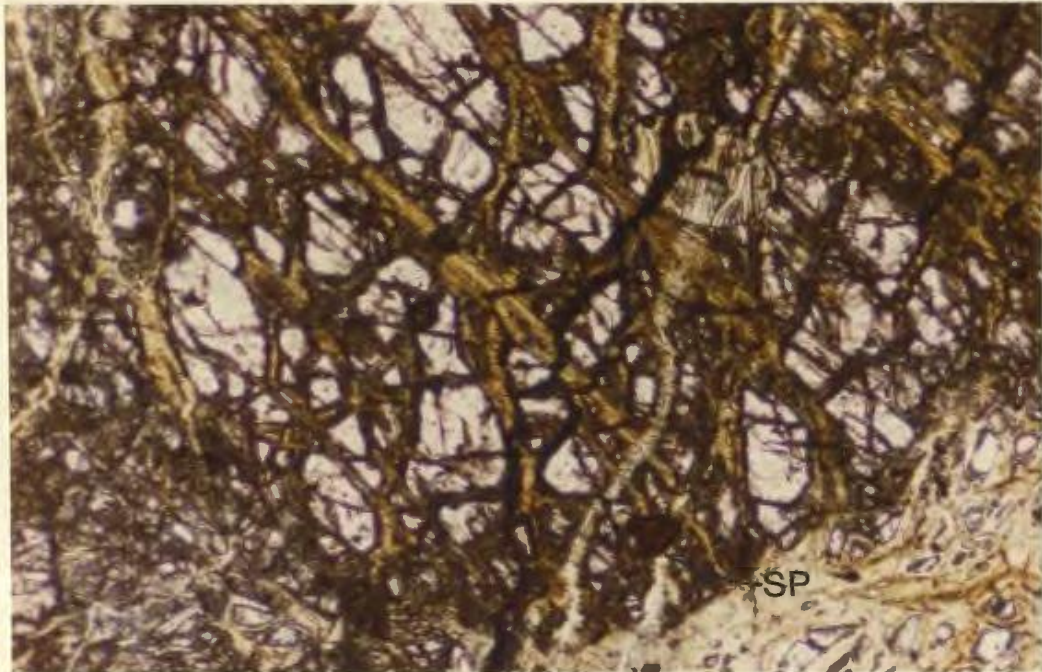


PLATE XXXIXb: Small rounded inclusion of spinel in enstatite from Main Dunite Zone, Table Mountain. Plain light, x 120.

thickness. The layers generally trend and dip parallel to the main contact with the underlying harzburgites, although the latter is not easily discernible everywhere as explained above.

Olivine grains are euhedral to subhedral and highly fractured (Plate XXXIXa). The average size of crystals is 3 to 4 mm, and can be determined by the uniform extinction position of adjacent relics of olivine. Such patterns also indicate the lack of post-serpentinisation deformation. The olivine is colourless with a large positive axial angle ($2V_{\gamma} \sim 87^{\circ} - 89^{\circ}$). Indices of refraction indicate forsterite contents of the order of Fo₈₉ ($N_{\beta} = 1.654 \pm .001$, $N_{\gamma} = 1.670 \pm .001$). Euhedral or partially rounded olivine grains (.06 - .40 mm) occur as small inclusions in chromite and rarely enstatite. Intercumulate chromite may form up to 1% of the dunite. It is disseminated throughout the main dunite zone. It occurs as translucent red, anhedral grains filling interstices between olivines. Magnetite rims occur as a result of oxidation. Where enstatite is present, small rounded chromites are rarely seen as inclusions (Plate XXXIXb). Clinopyroxene ($Ca_{48} Mg_{49} Fe_3$) also occurs as a disseminated intercumulus mineral forming 0.5 to 1% of the average rock. However, both chromite and clinopyroxene occur as cumulus minerals towards the base of the main dunite zone.

vi) Chromites

Layers of cumulate chromite may reach several centimetres in thickness but are not laterally continuous for more than 1-2 metres. In many places, post-accumulation slumping (possibly lubricated by trapped liquids) has slightly deformed these layers. Such concentrations of

cumulus chromite have not yet been recognized on Table Mountain, but are present on North Arm Mountain, Blow-me-down Mountain and the Lewis Hills (Malpas and Strong, 1975). In the Stowbridge Head area of North Arm Mountain the chromite concentrations occur in the main dunite zone just above its contact with the harzburgites and about 500 metres stratigraphically below the interbanded upper boundary. The chromite occurs in lenses within the serpentinitised dunite, which strike and dip parallel to the general trend of the layering in the ultramafic rocks. Although some harzburgites are found near the chromite deposits, none have been found in direct association. Small concentrations in a similar setting are found on Blow-me-down Mountain and are noticeably affected by post-accumulation deformation (see also Smith, 1958). Two major chromite deposits are also known from the Lewis Hills.

The chromite is opaque black to slightly translucent red in thin section. The crystal form is modified by adcumulus growth which cements crystals together (Plate XLa), and the individual grain size is thus difficult to determine. On average, however, it appears to be in the order of 0.5 to 1 mm.

Grading of chromite-rich layers exhibiting sharp bases and an upward decrease in chromite from approximately 90% to less than 15% occurs over thicknesses of 10 to 40 cm.

vii) Clinopyroxenites

Small lenses of clinopyroxenite are exposed both at the base of the dunite zone, and towards its top. Elsewhere in the zone,

clinopyroxene occurs as a minor intercumulus phase. The more massive lenses of clinopyroxene are found on North Arm Mountain and Table Mountain and have been reported from the Lewis Hills (Smith, 1958). On North Arm Mountain a number of discontinuous lenses, slightly discordant with the main cumulate layering, stretch over 4 km at the base of the dunite zone. The lenses attain a maximum thickness of 50 metres, but are rarely more than 200 to 300 metres in length. The pyroxene weathers to a grey-green granular appearance. In thin section, euhedral cumulate crystals with well developed (100) parting are relatively unaltered, but may be modified by adcumulus growth. Optical properties ($2V_{\gamma} \sim 56^{\circ}$, extinction angle $\gamma \sim 40^{\circ}$, $n_x = 1.669$) suggest that the pyroxene is almost pure diopside. Small amounts of forsterite are also present. With an increase in modal forsterite the rocks can be called olivine clinopyroxenites.

viii) Feldspathic dunites

Feldspar becomes a major mineral in the dunites towards the top of the zone. Thus by an increase in feldspar, feldspathic dunites grade into troctolites, and eventually anorthosites. However, as well as this vertical gradation, variations in rock types along strike also occur and it is not unusual to find feldspathic dunite wedging quite rapidly into dunite or even clinopyroxenite.

Feldspar stands out as small, white, resistant knobs on the smooth yellow dunite surface, greatly enhancing the cumulate textures (Plate XLb). Apparent inverted grading due to increase in modal feldspar upwards (i.e. a mineralogical grading), and cross-bedding and slumping have been recorded from exposures on Table Mountain (Plates XXXVIIIa, XXXVIIIb).

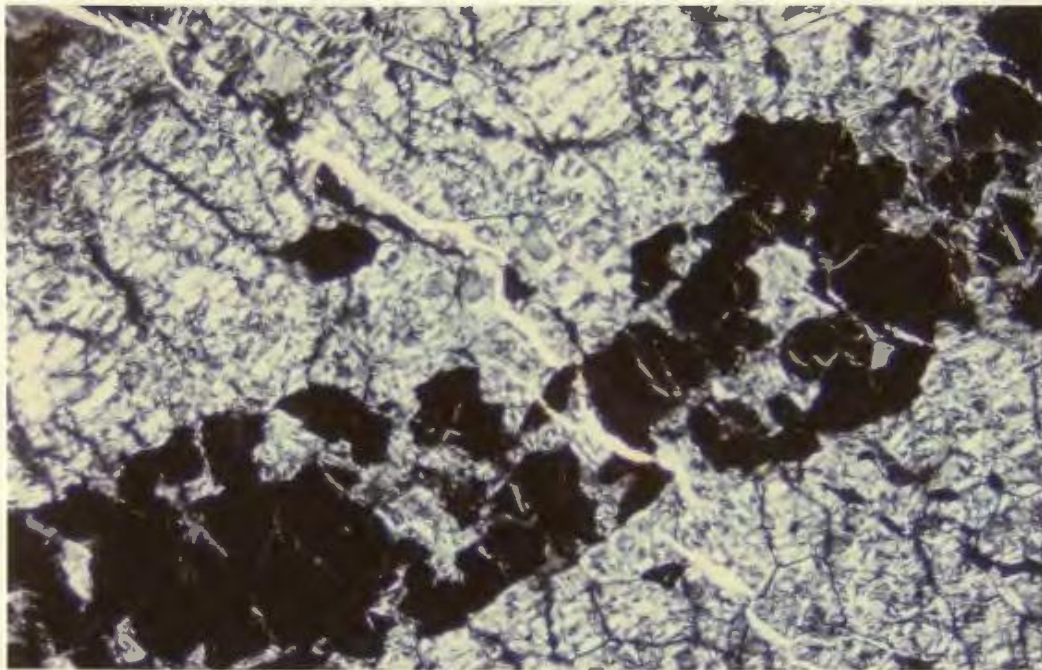


PLATE XLa: Adcumulus chromite forming band in Main Dunite Zone.
X nicols x 20.



PLATE XLb: Feldspathic dunites showing layering enhanced by differential weathering of feldspar and olivine.

In thin section, original euhedral olivine and feldspar crystals have been modified by adcumulus growth (Plate XLia). Interstitial clinopyroxene is not uncommon, especially towards the critical zone. Calcic plagioclase forms on average 5% of the rock although it may reach as much as 40% at the base of some graded layers. A large proportion is altered to a hydrogarnet (R.I. $N = 1.59-1.68$; Smith, 1958), although enough remnants of the plagioclase can still be seen to make optical determinations (Plate XLib). Cumulus plagioclase (An_{75-80}) occurs very often in aggregates with crystal sizes of about 1 to 1.5 mm. Intercumulus plagioclase (An_{70-77}) partially or totally encloses rounded olivine grains (Plate XLIIa) and is very often highly altered.

Clinopyroxene ($Ca_{47} Mg_{47} Fe_6$) occurs as an intercumulus phase and may include both olivine and euhedral feldspar.

ix) The Critical Zone: Interbanded rocks of the ultramafic-gabbro contact

A zone of extremely well-layered rocks marks the contact between the ultramafic and gabbroic zones. It has been called the 'Critical Zone' by Ingerson (1935), Cooper (1936), Smith (1958), and Irvine and Findlay (1972). The Critical Zone is not always completely preserved; for example, much is removed by faulting on the northern slopes of Table Mountain, and even where it is present, variable thicknesses have been recorded. On North Arm Mountain, the zone strikes generally northeast and is relatively thin (150 metres) although much might be covered by talus deposits on the

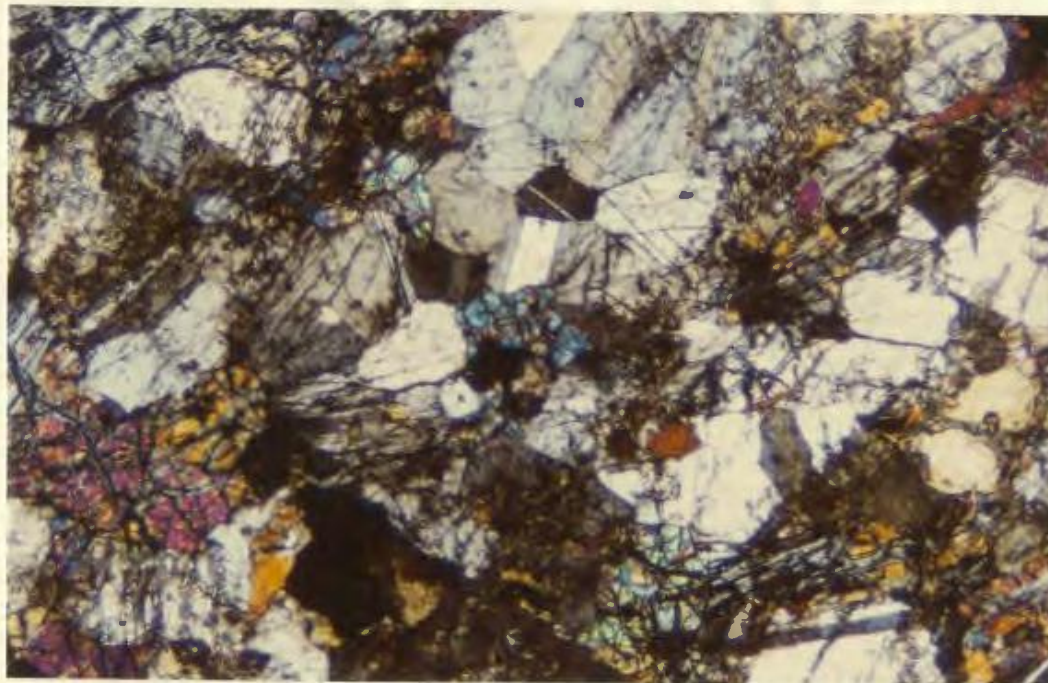


PLATE XLIa: Interlocking adcumulate plagioclase crystals as aggregate in serpentinised dunite. X nicols x 95.

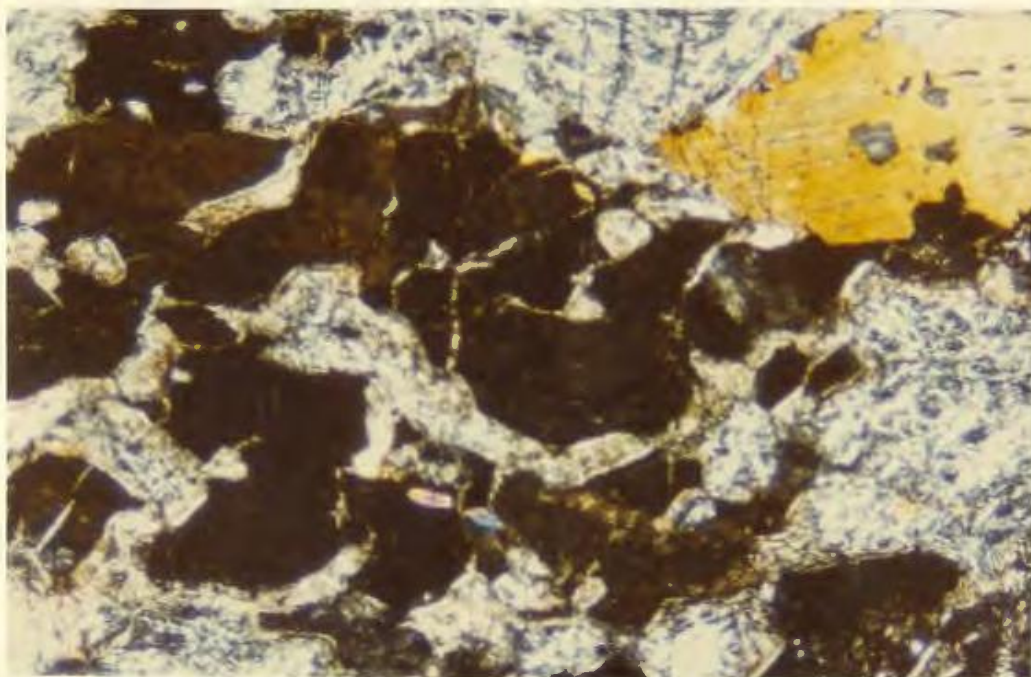


PLATE XLIb: Plagioclase showing alteration to hydrogrossular and sericite/epidote. Feldspathic dunite, Table Mountain. X nicols x 90.



PLATE XLIIa: Intercumulate plagioclase surrounding early olivine cumulate crystal. X nicols x 130.



PLATE XLIIb: Complex interfingering of feldspathic dunite and gabbro in Critical Zone, Table Mountain.

Liverpool Brook gorge. Similarly on Blow-me-down Mountain, the drainage system has cut down along the strike of the zone, and much is obscured. The best exposures therefore occur on the eastern margin of the Table Mountain gabbro, and on Mount St. Gregory, where the critical zone defines the western edge of the North Arm Mountain massif. Some of the gabbroic areas of the Lewis Hills, mapped by Smith (1958) are composed entirely of interbanded rocks, and the Lewis Hills also appears unique in that interbanding of gabbro and ultramafics appears at a number of different horizons, some quite low down in the main cumulate dunite zone (A.R. Berger, pers. comm., 1974).

Individual layers within the critical zone are of variable thickness from 1-2 cm up to several tens of metres and have been called gabbro, anorthositic gabbro, anorthosite, clinopyroxenite, olivine gabbro, troctolite and feldspathic dunite. Comparisons were made by Smith (1958) with harrisites and allivalites as defined by Harker (1909), but because of the textural reinterpretation of these terms, especially harrisite (Wadsworth, 1961), they are not used here.

The layers appear to be simply cumulates consisting of variable proportions of cumulate plagioclase, pyroxene and olivine, and differ from the underlying dunites in their overall finer scale of layering and rapid changes in mineralogy.

In general there is an increase in feldspar-rich bands away from the main ultramafic body, but complex interfingering of rock types is common and there is a small amount of post-accumulation deformation (Plates XLIIB and XLIIIa). Abrupt alternation between white feldspar, black

pyroxene and brown serpentinitised olivine bands make such changes distinctive in the field (Plate XLIIIb). Dips of the layering are highly variable and reversals are not uncommon, related to both pre- and post-consolidation deformation. The interfingering accounts for the lack of a well-defined 'stratigraphy' in the Critical Zone and the layers are essentially a series of elongate lenses rather than continuous bands. These lenses may be slightly discordant to the general contact trend of the dunites and gabbros. The layering and repetition of rock types is reminiscent of typical stratiform intrusions (Wager and Deer, 1939; Jackson, 1961; Findlay and Smith, 1965; Brown, 1956). By analogy, the critical zone sequence probably formed by accumulation of olivine, clinopyroxene and plagioclase precipitated in different proportions by fractional crystallisation of basaltic magma at shallow depths during periods of repetitive introduction of fresh magma (Irvine, 1970). The distinctive fine-scale layering in the zone may be related to these influxes setting up temperature gradients and turbulence in the body of mixed magmas (Wager, 1963). Forsterite, where present, is always an early cumulate phase, and may be associated with cumulate clinopyroxene and/or plagioclase. Both clinopyroxene and plagioclase also occur as intercumulus phases.

Rocks containing feldspar include feldspathic dunites, feldspathic wehrlites, troctolites, anorthositic troctolites, anorthosites, feldspathic pyroxenites and gabbros. The distinction between these types is arbitrary but can be based upon Fig. Vc (Smith, 1958). Plagioclase of composition An_{74-79} (optical and x-ray determination) occurs as crystals of 2-4 mm maximum dimension. The plagioclase varies in amount but is always



PLATE XLIIIa: Post accumulation slump folds in Critical Zone, Table Mountain.

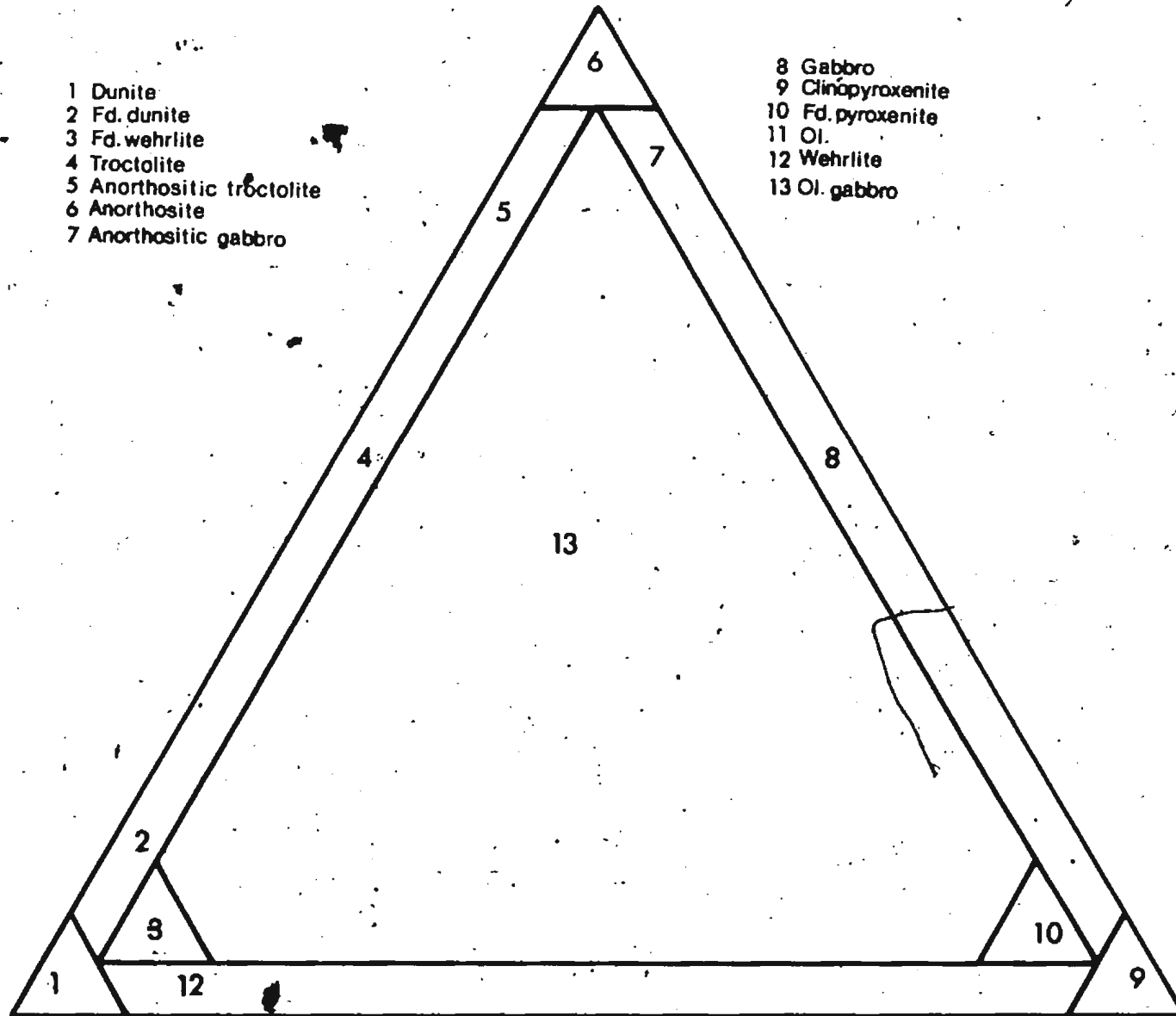


PLATE XLIIIb: Branching of cumulate feldspar layers in Critical Zone, North Arm Mountain.

Figure Vc: Rock types of the Critical Zone and Dunites
(Smith, 1958).

- 1 Dunite
- 2 Fd. dunite
- 3 Fd. wehrlite
- 4 Troctolite
- 5 Anorthositic troctolite
- 6 Anorthosite
- 7 Anorthositic gabbro

- 8 Gabbro
- 9 Clinopyroxenite
- 10 Fd. pyroxenite
- 11 Ol.
- 12 Wehrlite
- 13 Ol. gabbro



a cumulate phase, although may be present as adcumulus or heteradcumulus growths in addition. Imperfect alignment of plagioclase laths is not uncommon. No plagioclase zoning has been optically identified in any of the above rocks, but minor normal zoning has been determined in plagioclases from the gabbros by microprobe traverses (Appendix I). Small euhedral cumulate crystals of plagioclase are often enclosed in intercumulate clinopyroxenes in gabbros and anorthositic gabbros. Alteration of feldspar to epidote and sericite is not uncommon, especially in rocks where pyroxenes are altered to amphibole. Expansion fractures are ubiquitous in troctolitic rocks where olivine has undergone serpentinisation (Plate XLIVa). Saussuritisation has taken place preferentially along these cracks and may be associated with growth of light brown pleochroic amphibole. This would suggest that the serpentinisation began as a relatively early automorphic effect.

Anorthosites occur where mineralogical grading results in a rock that is almost 100% plagioclase. Thus anorthositic bands are really the upper parts of graded layers which show plagioclase increase and ferromagnesian mineral decrease (Plate XLIVb). The layers are relatively thin but fairly abundant towards the top of the critical zone away from the main ultramafic body. The anorthosite is made up of relatively large (1.5 mm) interlocking crystals of bytownite of composition An_{74-78} (optical determination) (Plate XLVa).

Clinopyroxene is a major constituent in clinopyroxenites, wehrlites and gabbros. In the clinopyroxenites and most olivine clinopyroxenites, it is a cumulate phase. Where plagioclase is present, and in some wehrlites, clinopyroxene often occurs as an intercumulate

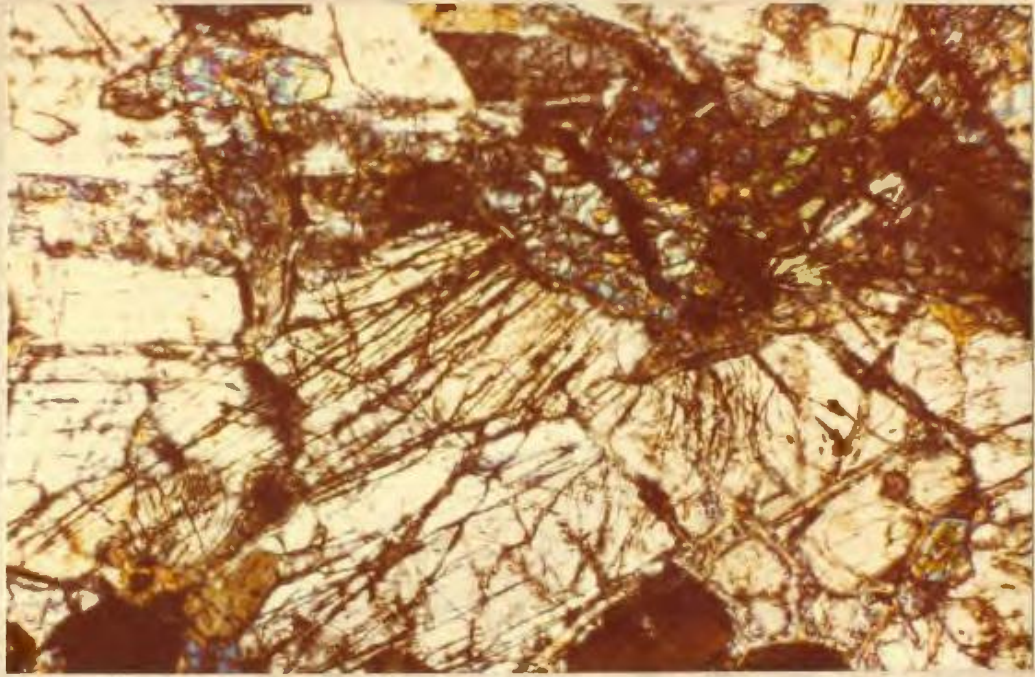


PLATE XLIVa: Expansion cracks in plagioclase as a result of serpentinisation of olivine. X nicols x 85.



PLATE XLIVb: Anorthosite bands in Critical Zone -- white, interlayered with pyroxene-dunite, North Arm Mountain.

phase. In gabbros, clinopyroxene occurs as individual grains or aggregates of grains interstitially to plagioclase laths.

Poikilitic grains of considerable size (2-3 mm) enclose rounded plagioclase laths and exhibit uniform extinction. The clinopyroxene is generally colourless or may be slightly pink-brown pleochroic.

Diallage parting is well developed and optical properties suggest compositions of $Ca_{44} Mg_{47} Fe_9$ ($N_x 1.674 \pm .002$, $N_y 1.703 \pm .002$).

Irregular coronas of brown amphibole rim the clinopyroxene in places suggesting a reaction relationship between it and plagioclase. In some rocks, especially where a tectonic fabric has been superimposed, clinopyroxene may be totally replaced by pale green actinolite with a marked fibrous habit.

Olivine is a major constituent in dunites, feldspathic dunites and troctolites in which it always appears as a cumulate phase. As in the main cumulate dunite zone, the olivine is more iron rich than that from peridotite tectonites and optical properties ($2V_y 87-89^\circ$) indicate forsterite contents of about 87-89. Smith (1958) suggested that olivine in the troctolites crystallised as a late phase interstitial to plagioclase. However, since olivine is obviously enclosed in plagioclase (Plate XLVb) and because of the subhedral shape of equidimensional olivine crystals, it appears that most, if not all, olivine is an earlier precipitate, probably crystallising simultaneously with plagioclase. Coronas of pyroxene occur regularly around olivine in contact with plagioclase (Plate XLVIa). Whether this is clinopyroxene or orthopyroxene cannot be determined since alteration to tremolite, chlorite

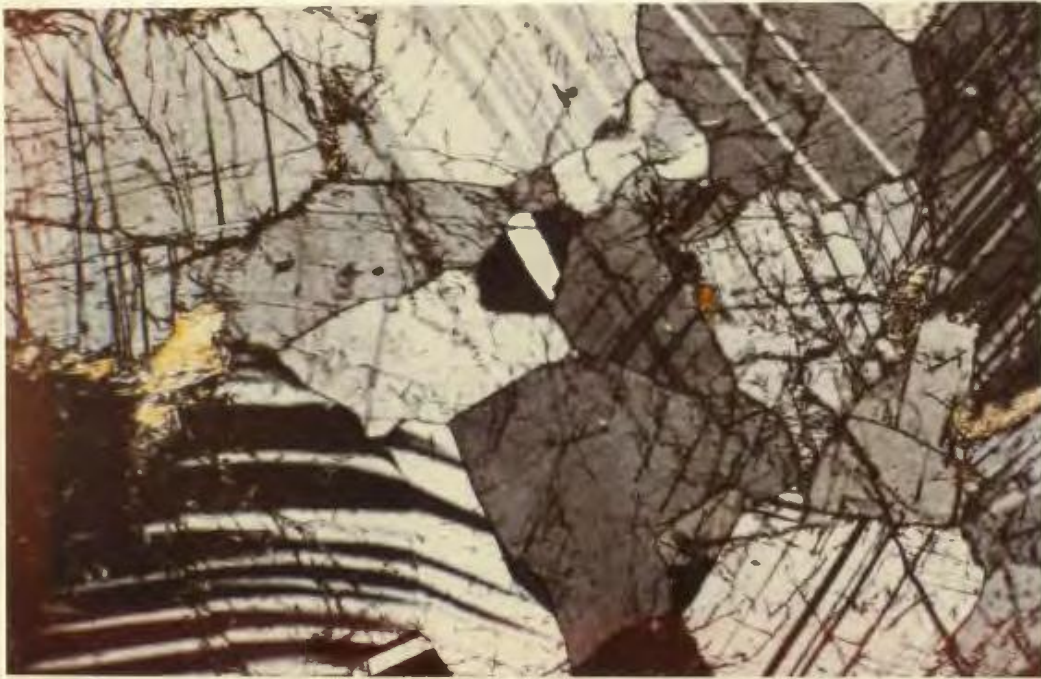


PLATE XLVa: Interlocking bytownite crystals from anorthosite band. North Arm Mountain Critical Zone. X nicols x 100.

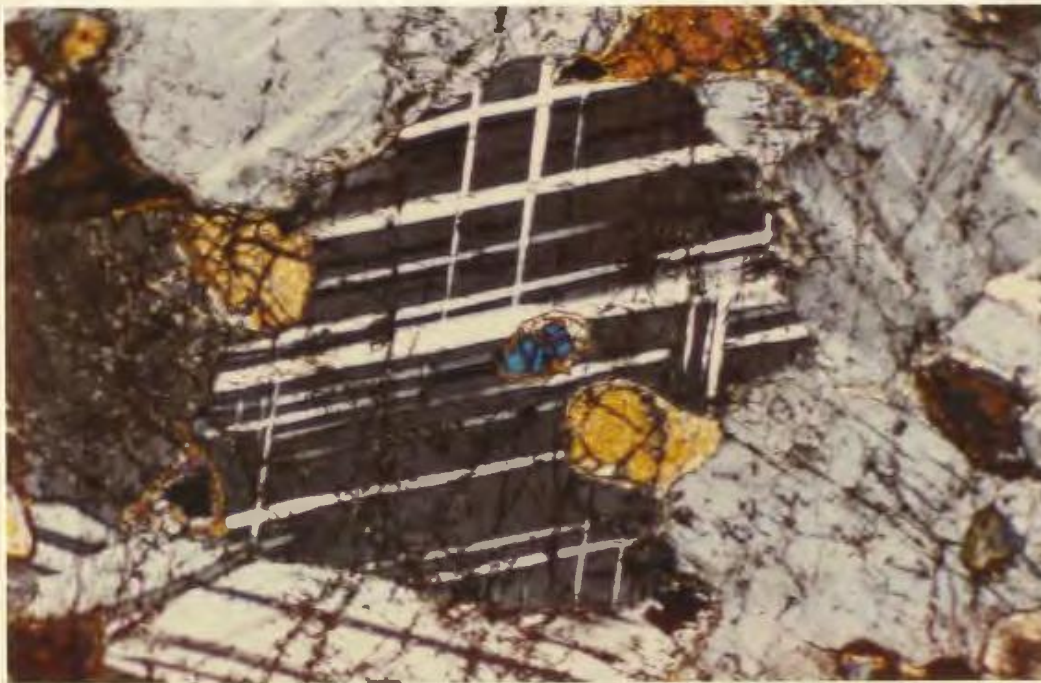


PLATE XLVb: Plagioclase including olivine. Troctolite, Blow me down Mountain. X nicols x 120.

and serpentine is fairly widespread. Thus much pyroxene is replaced by colourless, fibrous intergrowths, especially where associated with serpentinitised olivine.

Orthopyroxene is an extremely rare mineral in the critical zone. It occurs rarely in dunites and gabbros but is of restricted distribution. Chromite occurs in some dunite bands as an accessory mineral. Magnetite occurs as a secondary mineral by serpentinitisation of olivine and oxidation of chromite. The development of this magnetite might explain the magnetic anomaly which marks the critical zone and reported by Hodych (pers. comm., 1974).

x) Gabbro

Gabbro forms a major zone up to 2 km thick above the Critical Zone on Table Mountain, North Arm Mountain and Blow-me-down Mountain. Gabbros are not present to any extent on the Lewis Hills where the highest exposed parts of the section appear to be in the Critical Zone. The gabbro zone is most fully developed in the North Arm Mountain massif, where complete sections are present on both levels of the synclinal structure. On Blow-me-down Mountain, the gabbro zone is faulted at the leading edge of the thrust slice on the western synclinal limb, but is complete on the eastern limb. The gabbro is not entirely preserved on Table Mountain, the upper parts of the zone having been removed by erosion. Several downfaulted blocks of gabbro are preserved on the southern slopes of Table Mountain close to Trout River Pond.

Many varieties of gabbroic rocks are found in the zone. These vary from anorthositic gabbro, to melagabbro, and from relatively

fine-grained varieties to pyroxene or amphibole bearing pegmatites. The most common type is a medium to coarse-grained leucogabbro. This commonly grades into a melagabbro by increase in clinopyroxene, or anorthosite by an increase in plagioclase.

The leucogabbro, melagabbro and anorthositic gabbro are generally massive and poorly banded. The banding is variable in orientation and most often discordant with the banding in the Critical Zone. This may be a result of slumping, cross-bedding and winnowing action which have been described in other stratiform intrusions (e.g. Wager and Brown, 1968). However, in some cases, mineral lineations are clearly a result of post-consolidation deformation. Layering is generally of a fine scale, varying between a few centimetres and several metres thick (Plate XLVIb). It is enhanced by the pitted surface weathering due to differential erosion of white feldspar and green-brown clinopyroxene.

Plagioclase is generally randomly orientated except where a secondary fabric has been imparted. Good cumulate and adcumulate textures are preserved, but crystal size is variable. On average crystals reach 2-3 mm in size, but may be considerably smaller or much larger (Plate XLVIIa). For example, an equant, fine-grained, 'sugary' leucogabbro occurs at the head of Liverpool Brook on North Arm Mountain (Fig. IIIb) in which plagioclase crystals do not get larger than 0.5 mm. Optical properties suggest the plagioclase is bytownite (An_{70-78}) in composition although the average is generally more sodic higher in the zone. However, no definite correlation exists between plagioclase

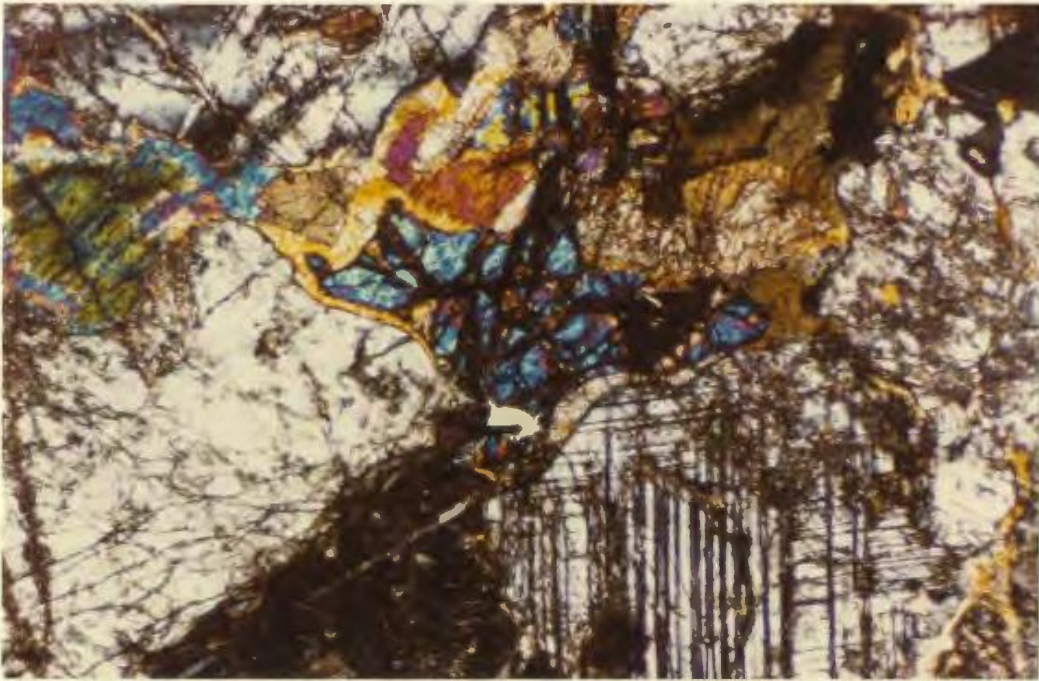


PLATE XLVIa: Clinopyroxene corona around olivine in reaction relationship with plagioclase. Troctolite. North Arm Mountain. X nicols x 130.



PLATE XLVIb: Layering in gabbros, Table Mountain.

composition and position in the zone. Triple point junctions are fairly common between adjacent plagioclase grains, but may be masked by alteration. Various stages of alteration exist from fresh plagioclase to grains which are almost completely replaced by fibrous sericite and some epidote. This saussuritisation is especially prevalent in rocks where olivine is present and has caused expansion fractures during serpentinisation.

Augite generally occurs as an intercumulate phase as poikilitic crystals up to 2-3 mm maximum dimension. The augite contains both plagioclase and olivine as rounded grains with which reaction relationships are visible. The pyroxene crystals are pinkish pleochroic suggesting a high titania content, and exhibit good diallage parting. $2V_{\gamma}$ varies from 50° to $55^{\circ} + ve$. Extinction angles ($Z \searrow C$) vary between 45° and 48° . Smith (1958) suggests a composition of $Ca_{40} Mg_{40} Fe_{20}$ for the augite on the basis of optical properties, but it seems that compositions are variable. However, it is quite clear that iron contents are significantly higher than in clinopyroxenes from the peridotites. Irregular reaction rims of brown pleochroic amphibole occur between clinopyroxene and plagioclase (Plate XLVIIb) and the clinopyroxene in some gabbros may be partially or completely altered to prismatic or fibrous actinolite or rarely chlorite. The degree of alteration does not appear to be dependent on position in the zone, but is correlatable with sericitisation of plagioclase and the development of expansion fractures.

Olivine is found as major mineral in the lower gabbros, but may occur sporadically throughout much of the zone except for the highest

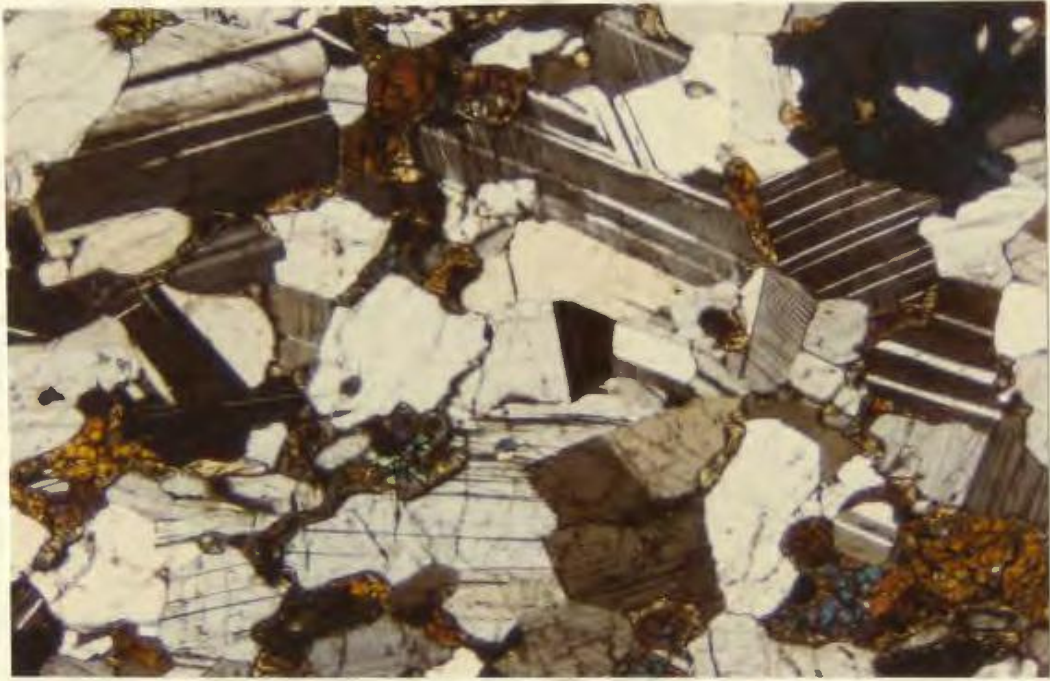


PLATE XLVIIa: Cumulate plagioclase, intercumulate pyroxene and olivine - Gabbro, Table Mountain. X nicols x 75.

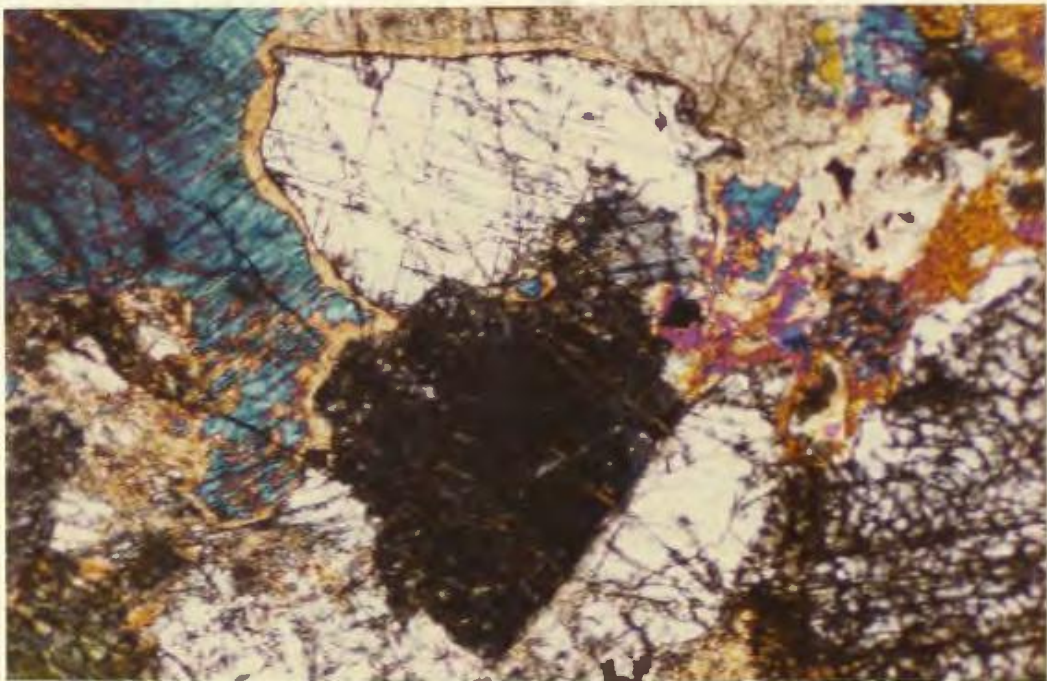


PLATE XLVIIb: Reaction rim of hornblende between clinopyroxene and plagioclase in gabbro, Blow me down. X nicols x 150.

parts. On average, olivine disappears 800 metres above the critical zone. It is locally serpentinised with well developed magnetite rims but generally much better preserved than in the ultramafic rocks. Generally the olivine appears as an intercumulate phase, but in some lower troctolitic gabbros, it may be preserved included in plagioclase, and is an early crystallisation product. Reaction coronas between olivine and plagioclase are fairly common; they are sometimes identifiable as clinopyroxene but are more generally altered to aggregates of tremolite and serpentine. Magnetite is a major accessory phase in some rocks. It appears as a late intercumulate phase generally, although in the same rock it may occur as inclusions in pyroxene, amphibole or plagioclase. It is seen developed along partings or cleavage in some pyroxenes (Plate XLVIIIa). Magnetite shows reaction rims of brown hornblende in contact with plagioclase.

Pegmatitic gabbros are of two major types. On Table Mountain, pyroxene-plagioclase pegmatites occur as boulders in the felsenmeer, but have not been found as outcrops in place. Pyroxene crystals reach several centimeters in dimension and grow interlocked with tabular plagioclase of similar sizes. The pyroxene appears to have originally been augitic in composition, but is almost totally replaced by actinolite. The plagioclase is altered to sericite and its composition is not determinable.

On Blow-me-down Mountain an area of hornblende gabbro has been mapped (Fig. IIIb), apparently lying as a 'blind pocket' or lens at the top of the gabbro zone. The gabbro is made up of a number of phases which show intrusive relationships with one another so that blocks of

coarse pegmatite are often seen 'floating' in a matrix of finer hornblende gabbro or diorite (Plate XLVIIIb). Typically the pegmatite contains up to 50% brown pleochroic hornblende, 40 to 45% plagioclase and accessory opaques, usually magnetite. Minor augite has been recorded but is usually totally replaced by chlorite. Hornblende is the major amphibole in all phases of the gabbro. It is often altered marginally to biotite and chlorite. Crystals may reach 5 or 6 cm in length and show no preferred orientations. Twinning is often evident.

Plagioclase is very often completely saussuritized although remnant twinning indicates an original composition of An_{40-45} (Andesine).

No tectonic fabrics are present and amphibole does not appear to be replacing any earlier ferromagnesian mineral. Together with the crystal habits, this suggests that the amphibole is of a primary igneous origin and that it crystallised directly from pockets of hydrous basic magma. Quite probably, the water was derived as percolating sea-water, but this hypothesis may only be substantiated by oxygen isotope determinations now in progress (see also Spooner, 1974; Spooner and Fyfe, 1973; and Spooner, et al., 1974).

On Blow-me-down Mountain the hornblende gabbros are cut by a number of basic and intermediate dikes which are traceable into the overlying sheeted dike complex. The latest period of igneous activity appears to have been intrusions of quartz diorites which cut the basic dikes at a shallow angle (Plate XLVIIIb).

Similar hornblende gabbros to those described above are known to be associated with ophiolite suites in Oregon (Dott, pers. comm., 1974),

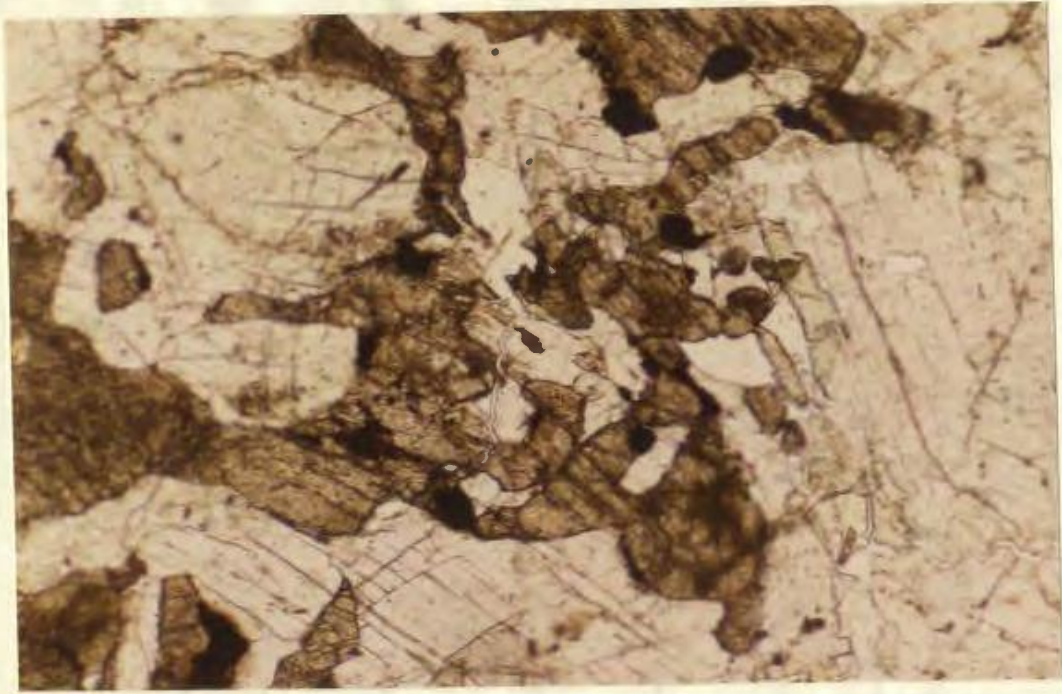


PLATE XLVIIIa: Magnetite occurring along cleavage partings in clinopyroxene. Gabbro - Blow me down Mountain. Plain light x 135.



PLATE XLVIIIb: Quartz-diorite dike cut by basic dikes on Blow me down Mountain.

the Lizard Complex and Cyprus (Malpas, et al., 1973). However, the best examples yet observed by the writer are found on Brighton Island, Notre Dame Bay, Newfoundland, where these rock types form late intrusions into the dikes and gabbros of ophiolite suites and possibly represent off-ridge axis volcanics (Plate XLIXa) (Strong, 1972, 1973; Hussey, 1974). In all cases the amphibolitic pegmatites appear to be in pockets and veins close to the upper gabbro contact immediately below the sheeted diabase zone.

Sulphide mineralisation within the gabbros is confined to shear zones which are not uncommon. For example, on Jumbo Head at the narrows of Trout River Pond, chalcopyrite and pyrite are associated with sheared and brecciated gabbros and quartz veins. Pyrrhotite has been reported from shear zones on the northern flank of North Arm Mountain (Lilly, 1957 and Figure IIIb).

xi) Amphibolite inclusions within the gabbro zone

In the Sandy Lake area of North Arm Mountain, fine to medium-grained black amphibolites crop out over an area of approximately 6 square km. Similar rock types are found in a small body on the South side of Trout River Pond (Fig. IIIb). In hand specimen these amphibolites are reminiscent of some amphibolites of the Little Port Complex found on the coast at Big Cove. The rocks appear to have a complex structural history and are not simply a more deformed part of the main gabbro which clearly surrounds the amphibolites and transects any schistosity within them.

In thin section amphibole is seen to form as much as 50-60 percent of the rock, and in many cases is clearly forming at the expense of clinopyroxene (Plate XLIXb). In other cases, clinopyroxene is absent or has been completely replaced. The amphibole displays pleochroic schemes of generally green, yellow-green and green-brown, but may in cases have distinct blue tinges. Extinction angles ($\gamma:Z$) of about 16° and $2V_\alpha$ of 90° suggest that most amphibole is common hornblende. Straight crystal boundaries and triple point junctions suggest considerable annealing of the rock. The amphibole occurs as small grains around the margins and in the cleavage traces of some large clinopyroxene phenocrysts. These phenocrysts may reach as much as a centimetre in maximum dimension, but are entirely replaced in finer-grained rocks. Where a well developed mineral lineation occurs, it may cut shallowly across a mineral banding between amphibole and plagioclase. The plagioclase occurs as small equigranular grains of approximately 0.1 mm dimension, which exhibit straight grain boundaries and well developed triple point junctions. This would suggest relatively intense conditions producing annealing. The small grains are formed at the expense of original larger lath-shaped crystals (up to 1 cm long axis) which often show bent twin lamellae, undulose extinction, and granulation along their margins. The plagioclase has compositions varying between An_{50} and An_{54} .

Original igneous features are preserved in the amphibolites. The schistosity often cuts across contacts between rocks of different grain size and these varying grain sizes of the original rocks obviously



PLATE XLIXa: Megacrystic hornblendites from Brighton Island, Notre Dame Bay.

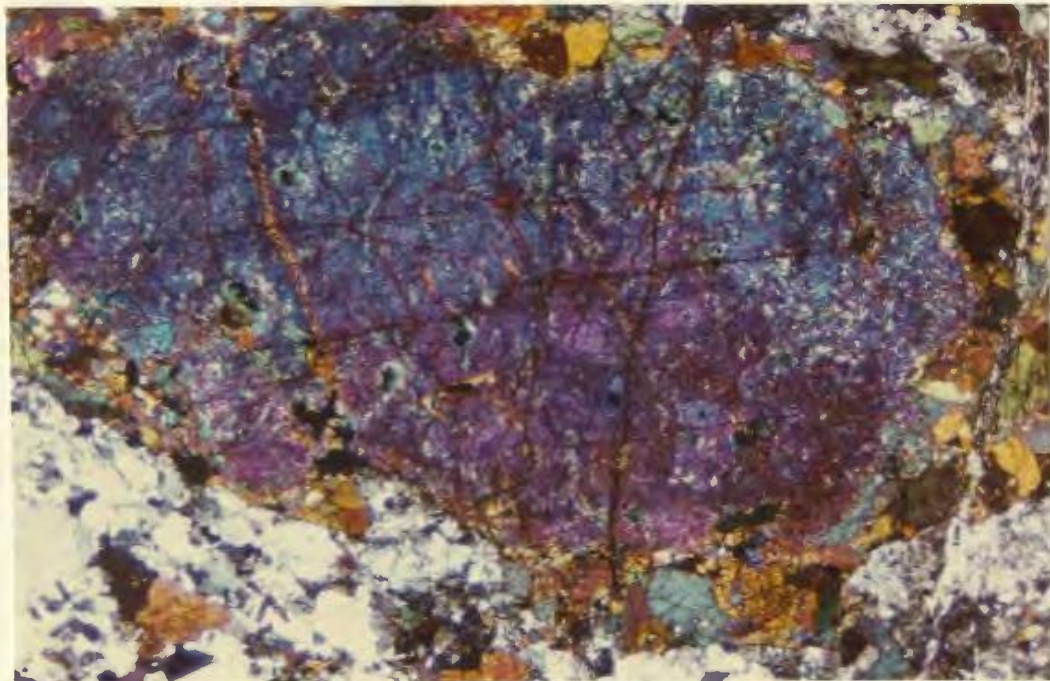


PLATE XLIXb: Amphibole forming at the expense of clinopyroxene. Amphibolite inclusion in gabbro, North Arm Mountain. X nicols x 15.

determine the intensity of the tectonic foliation and the degree of replacement of pyroxenes by amphiboles (Plate La). The mineralogy of the amphibolites suggests that the rocks were originally gabbros. Smith (1958) concluded that the amphibolites formed part of the roof zone of intrusions and that this zone included metagabbros, metadiabases and metavolcanics. However, several other origins may be proposed. Clearly the basic rocks were metamorphosed and deformed prior to inclusion in unmetamorphosed gabbro. They could therefore represent rocks produced and metamorphosed at an oceanic spreading centre before inclusion in younger gabbros produced during subsequent intrusion and extension, as suggested by Strong (1974). The metamorphism may, in this case, take place under dominantly horizontal shear stresses during lateral spreading (Strong and Malpas, 1975), or under dominantly vertical shear stresses along transform faults (Malpas, et al., 1973). Alternatively, the amphibolites could represent much older crustal remnants caught up in a new spreading episode, either in a marginal or major ocean basin. It seems probable, however, that they are closely related to amphibolites of the Little Port Complex, the origin of which has been argued above (Chapter III).

xii) Origin of primary textures in dunite zone, Critical Zone and gabbros

(Rocks of the main dunite zone, Critical Zone and gabbro zone may be classified together on the basis of primary textures. Unlike the peridotites, they still exhibit features which suggest they accumulated

after primary precipitation from a liquid melt, with additional interstitial minerals crystallising from trapped rest liquids. Such 'cumulate', 'adcumulate' and 'intercumulate' textures have been described by Hess (1960), Wager and Deer (1939), Jackson (1961), Wager, et al. (1960), Wager and Brown (1968), and Wadsworth (1973). In the field the crystallisation history of these rocks is manifested by pseudosedimentary features such as layering, mineral-grading, size-grading, cross-bedding, slump-structures and scour and fill structures (Wadsworth, 1973). Crystal settling is a highly efficient mechanism of separating early formed crystals from remaining liquid and thereby producing a variety of igneous rock types from an initially homogeneous magma. The order in which various minerals appear 'stratigraphically' in the pile is used as an indication of the order of crystallisation from the magma, although settling velocities of minerals should be taken into account. The repetitive nature of the layering (rhythmic layering) in some gabbroic intrusions has been taken to indicate repetitive intrusion of fresh magma coupled with the action of turbidity currents set up by differential thermal gradients in the magma body (Brown, 1956).

xiii) Secondary structures in the cumulate rocks

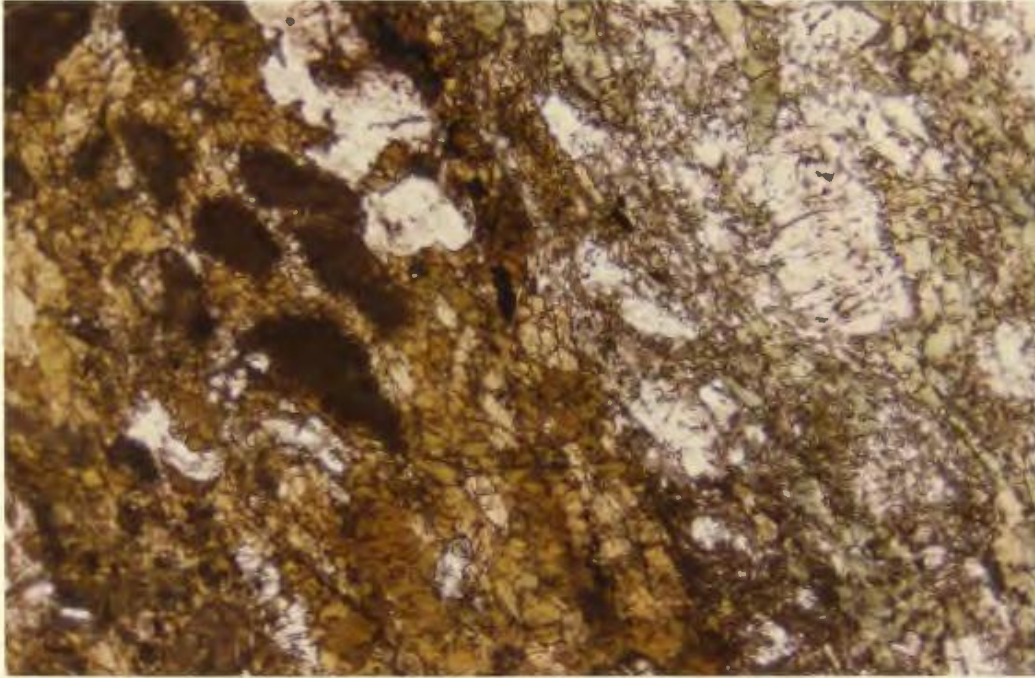
Parts of the Critical Zone and some gabbros have been affected by post-consolidation deformation. This secondary deformation appears confined to the lower cumulate rocks and is particularly apparent where rocks of contrasting mineral composition and possibly competence are

juxtaposed. Its effects are recognisable as a strong mineral foliation, especially of the plagioclases, and isoclinal folds with fold axes parallel to the regional layering, i.e. originally flat-lying (Plates XLIIb and XLIIIa). The mineral foliation is found as an axial planar fabric to some folds, although later folds obviously fold this fabric (Plate Lb). The deformation is particularly well developed on the Lewis Hills (A.R. Berger, J.F. Dewey, pers. comms., 1974). Some layers are amphibolitised and hornblende and pyroxene augen are a common feature in some gabbroic rocks in the transitional zones of the Lewis Hills. Both there and on Table Mountain and North Arm Mountain where the deformation occurs to a much lesser extent, the deformed zones are restricted to narrow horizons and are underlain and overlain by undeformed cumulate rocks. The writer suggests that the cause of the deformation is a lateral shearing and translation within the intrusion in which the competency of the rocks is affected by their degree of consolidation. Remnant interstitial magmatic liquids may lubricate some zones whilst the lack of it in more consolidated zones relatively close by may cause deformation to proceed in a more brittle fashion. Thus the deformation would have taken place soon after the intrusion of the magma bodies, possibly during lateral movement away from a spreading centre.

xiv) Quartz-diorites

Rocks of quartz-dioritic composition cut gabbros and diabases on North Arm Mountain and Blow-me-down Mountain. No such intrusions are

C



C'

PLATE La: Original igneous contact preserved in amphibolite from North Arm Mountain (C-C'). Plain light x 15.



PLATE Lb: Isoclinal post-accumulation fold folding planar fabric in critical zone rocks, Table Mountain.

recorded in the ultramafic rocks. A body of quartz-diorite cuts the basal parts of the sheeted diabase unit on Blow-me-down Mountain and small bodies of similar rocks occur near the Gregory copper deposits on Mount St. Gregory in the form of dikes and the amphibolites on North Arm Mountain as small stocks (Fig. IIIb). In the latter case inclusions of amphibolite are partially resorbed and contaminate the diorite. The outcrop areas of quartz-diorite rarely exceed 1 square kilometre, and they volumetrically form an almost insignificant part of the intrusive sequence. They are considered to be the most fractionated portion of the mafic magmas that crystallised as the cumulate rocks (Coleman, 1971). This origin contrasts with that of trondhjemites and quartz-diorites associated with ophiolitic amphibolites as partial melting products of the amphibolites during metamorphism (Payne and Strong, in prep. and page this work).

Altered plagioclase and quartz form together 90 percent of the rocks as interlocking grains up to 2.5 mm dimensions. The plagioclase varies from andesine to albite in composition and is generally highly altered. The most common type is zoned, untwinned albite in which rims are relatively fresh whilst cores are highly saussuritised. Plagioclase laths are sometimes enclosed in poikilitic quartz. The quartz has undulose extinction and forms up to 45% of the rock. Although the quartz crystals are equidimensional, they are variable in size from 0.25 mm to 2.5 mm in diameter (Plates LIa and LIb).

Amphibole forms up to 10 percent of the rock. It is green-brown pleochroic and optical properties suggest it is hornblende.

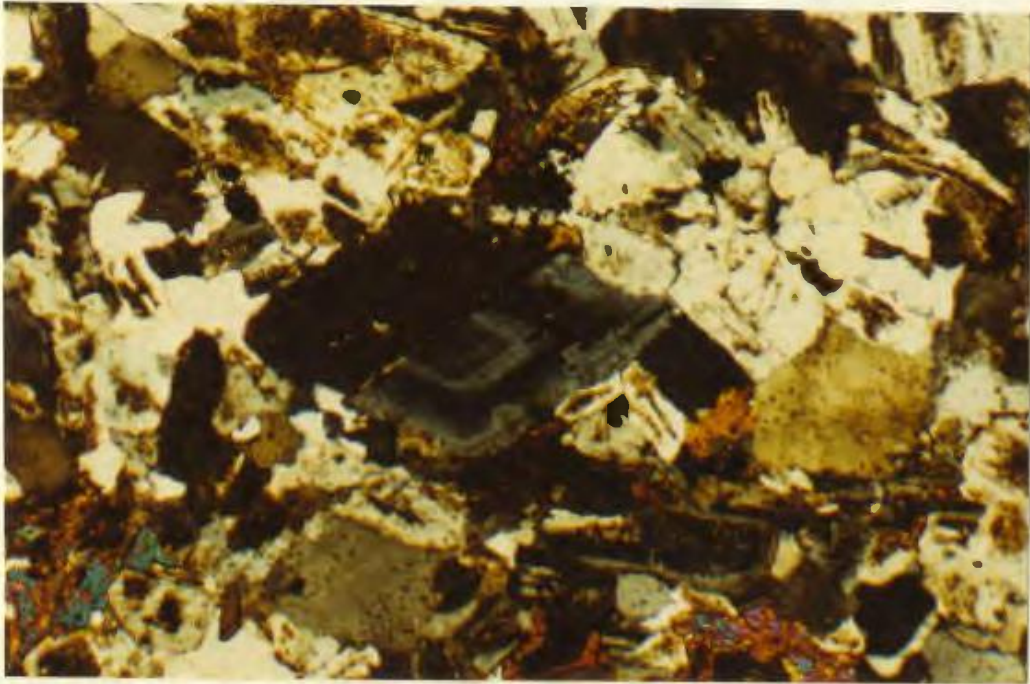


PLATE LIa: Zoned plagioclase in quartz diorite, Blow me down Mountain. X nicols x 40.

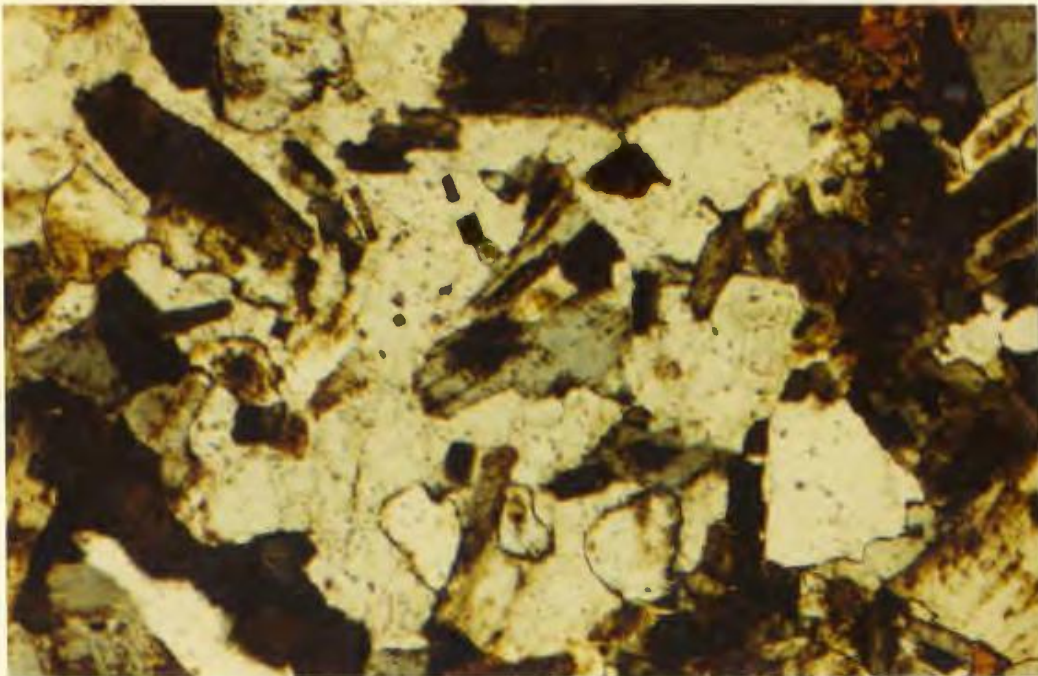


PLATE LIb: Plagioclase included in poikilitic quartz - quartz diorite, North Arm Mountain. X nicols x 45.

Chlorite often forms alteration rims around the amphibole. In the quartz-diorites intruding amphibolites, resorption of xenoliths may lead to apparently higher contents of amphibole close to the intrusive contact (Plate LIIa).

Epidote, zircon, apatite and magnetite are accessories and late stage cross-cutting prehnite veins are common. Since potash feldspar is completely lacking, the rocks could be classified as 'trondhjemites'. They are probably equivalent to trondhjemites reported from the Troodos Complex, Cyprus (Wilson, 1959) and silicic rocks noted by Upadhyay (1978) from Betts Cove, Newfoundland.

xv) Diabases

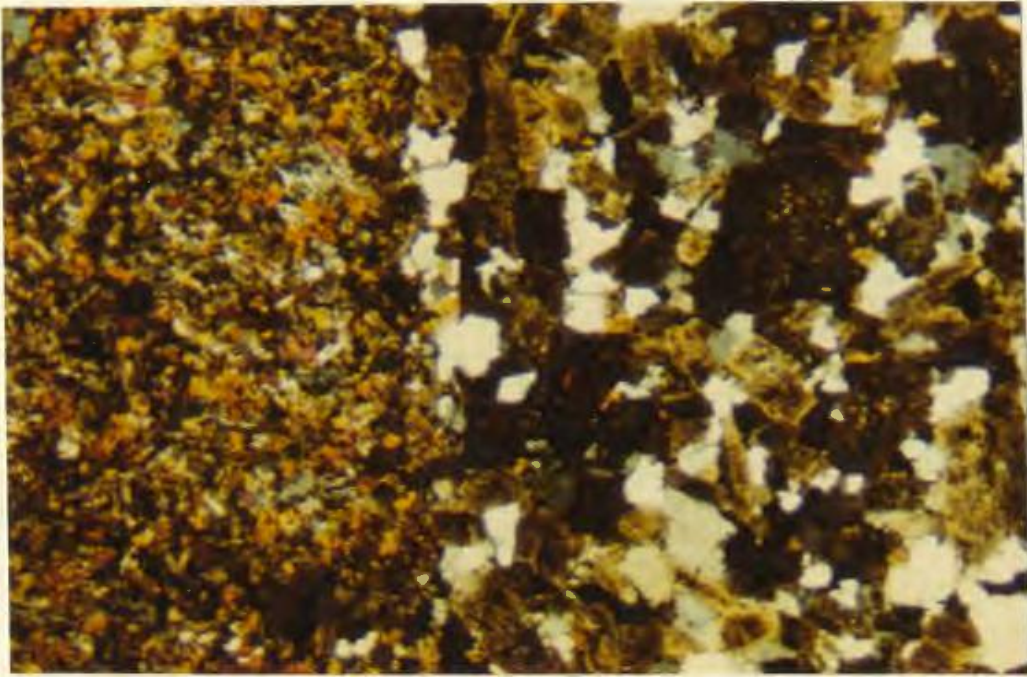
Sheeted diabase dikes and brecciated dike rocks have been recognised forming a zone between the gabbro and overlying pillow lavas. The most regular and extensive development of the dikes is on Blow-me-down Mountain, and dike breccias are also found underlying approximately 65 square kilometres of North Arm Mountain (Fig. IIIb). Diabase dikes have also been recognised on the Lewis Hills although they are generally single and not sheeted (Williamson, 1954). On the basis of lithology and the extent of brecciation, the dikes of the Bay of Islands Complex were correlated with similar rocks in the Little Port Complex (Williams and Malpas, 1972). Further studies (Chapter III) have shown this to be an unlikely correlation and the dikes of the ophiolite suite are treated separately here.

Brecciated diabases are as abundant as planar dikes in the ophiolites, and occur more so on North Arm Mountain. The breccias

consist of angular diabase fragments of varying sizes, generally close-packed in a matrix of more finely comminuted material of the same composition. The brecciation appears generally restricted to the dike horizon in the ophiolites; the only other rocks being affected is a small area of gabbros just north of Stowbridge Head on North Arm Mountain. Brecciated diabase dikes often cut fresh-looking unbrecciated gabbros and chilled margins are partially preserved (Plate LIIB). It is therefore apparent that brecciation took place after consolidation, but was restricted to the diabases.

The distribution, petrology and significance of the diabases has been discussed by Williams and Malpas (1972). On Blow-me-down Mountain, mafic dikes appear low down in the gabbro zone; for example in the region immediately south-west of Mad Dog Lake. They generally increase in abundance upwards to eventually form a sheeted dike swarm. The dikes feed pillow lavas higher in the pile and may cut and extend well up into the volcanic sequence.

Sheeted diabases and breccias occur on both limbs of the major syncline on Blow-me-down Mountain, although planar dikes are much better developed to the east. Their attitude is essentially at right angles to both the synclinal axis and the trends of contacts of the major zones within the succession, i.e. ESE. On the western limb of the syncline the dike rocks are essentially brecciated and most planar aspects are destroyed. The dike complex is approximately 1.5 km wide on the east limb of the syncline and extends about 18 km perpendicular to the strike of the dikes. Their dip is invariably steep to the northeast or southwest.



D

QD

PLATE LIIa: Contact between basic dike and quartz-diorite, Blow me down Mountain. X nicols x 40.



DIKE

GABBRO

PLATE LIIb: Brecciated dike cutting through massive gabbro - North Arm Mountain.

On North Arm Mountain few planar features are retained. Dike breccias are preserved on each limb of the major syncline, but the western limb is much narrower than the eastern. What planar features are present have an orientation similar to those on Blow-me-down Mountain, and these are best seen along the coast of North Arm near Crabb Point (Plate LIIIa). Relationships suggest that the dike rocks do not form a uniformly thick continuous zone either along or across their strike.

Individual mafic dikes are common at the southwest extremity of the Lewis Hills massif where they cut rocks of the transitional zone and overlying gabbros. They appear to be hornblende bearing (A.R. Berger, pers. comm., 1974) and may represent lower levels of a sheeted complex (Williams and Malpas, 1972). However, unlike the orientation of sheeted dikes in the more northerly plutons, the Lewis Hills examples trend northeast suggesting a rotation of this massif relative to the others.

Sheeted dikes are generally dark green-grey massive rocks. On some surfaces they weather to a buff colour and a granular 'peppery' appearance. Most are equigranular but others are plagioclase porphyritic, especially in the central portions of wide sheets. The dikes vary in width from about 10 cms to sometimes a metre or so, and can be traced for some hundred metres along strike. Chilled margins are conspicuous from a few centimetres to ten centimetres wide, with perpendicular jointing, and exhibit a complete gradation from medium-grained portions to fine-grained aphanitic portions close to the contact. Although most dikes are fairly constant in orientation, some late dikes cut across earlier ones at shallow angles. These include felsic varieties.

Massive dike rocks consist of equal amounts of altered plagioclase and actinolite or uralite after clinopyroxene. The plagioclase occurs as lath-shaped crystals and actinolite as intersertal platy or prismatic crystals. Thus sub-ophitic textures are preserved. The actinolite is yellowish-green to light-green pleochroic and rarely contains colourless cores of clinopyroxene. Epidote and chlorite are abundant accessories and sphene and minor iron oxides (mainly ilmenite?) and cross-cutting prehnite veins are common. Zoisite and zeolite facies assemblages (pumpellyite) have been reported (Williams and Malpas, 1972).

Porphyritic varieties of the diabases contain aggregates of altered equidimensional plagioclase phenocrysts set in a fine to medium grained matrix of plagioclase and actinolite. Plagioclase is the only mineral to occur as phenocrysts in the diabases (Plate LIIIb). Various stages of alteration are encountered, and in some rocks the pyroxenes appear unaltered or only slightly chloritised. On the other hand, there may be no remnant pyroxene, and actinolite may make up 45 percent of some rocks. Plagioclase is always highly altered and some rocks contain as much as 25 percent epidote. Such mineral assemblages are indicative of greenschist or low amphibolite facies metamorphism which in this case is considered a hydration process rather than a regional affect accompanying deformation. The metamorphism is probably related to the movement of water, possibly sea-water, through the rocks (cf. Christensen and Salisbury, 1972; Aumento, 1972; Spooner and Fyfe, 1973).

Fragments in the dike breccias vary in size from a metre or so down to 3 mm or less. The average size is approximately 2.5 cms. Various



PLATE LIIIa: Sheeted dikes - North Arm.

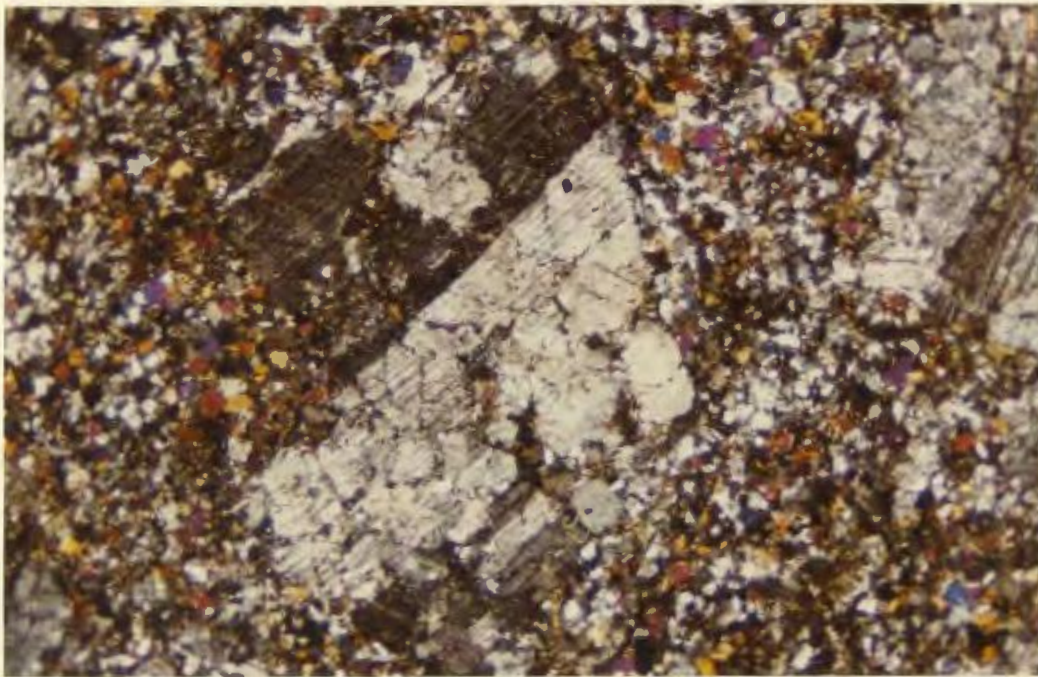


PLATE LIIIb: Plagioclase phenocrysts in diabase, North Arm Mountain.
X nicols x 30.

degrees of roundness of the fragments suggest abrasion, and the fragments in any one outcrop may be mixed so that porphyritic varieties occur with non-porphyritic aphanitic fragments suggesting a certain amount of transport. However, original positions of chilled margins for example are preserved in many cases, indicating that transport is only minimal.

The localisation of the brecciation to the diabase zone of the ophiolite succession and its regional extent suggest that it is genetically linked to the development of the ophiolite suite and was not developed after emplacement of the slices. Metamorphism of the diabase was probably synchronous with brecciation since actinolite fragments are often broken, although some alteration obviously post-dates the brecciation. The prehnite occurs as a result of retrogressive metamorphism and is found as veinlets cutting all other minerals. Textures are reminiscent of tuffisites developed in high-level intrusive bodies (Reynolds, 1954; Hughes, 1960, 1971) and are thus tentatively interpreted as fluidisation phenomena related to the passage of water vapour. However, it is quite probable that at depths that could be envisaged for the intrusion of the diabasés, water would have been in a supercritical state and that brecciation, and vesiculation in the pillow lavas, was a result of the passage of other gases such as CO₂ or liquid water.

xvi) Pillow Lavas

Volcanic rocks form the upper parts of the ophiolites of North Arm Mountain and Blow-me-down Mountain and were originally thought to be part of the roof assemblage into which gabbros and peridotites were

intruded (Smith, 1958; Church and Stevens, 1970). They are now interpreted as an integral part of the ophiolite suite (Williams and Malpas, 1972; Duke and Hutchinson, 1974). Pillow lavas and less abundant pillow breccias occur in the central axis of the syncline of North Arm Mountain in a discontinuous band running NNE/SSW almost the total length of the massif (Fig. IIb). Their thickest exposure reaches approximately 250 metres in the area immediately south-east of Mt. St. Gregory where they are overlain by sedimentary rocks. Pillow lavas from the stratigraphically highest parts of Blow-me-down stretch southwards from an area between Blow-me-down Head and Bluff Head. Because of the synclinal nature of both massifs, the central zone of pillow lava horizons is transected basally by the horizontal thrusts marking the bottom of the slices.

Duke and Hutchinson (1974) have subdivided the pillow lavas and pillow breccias of the York Harbour area (Fig. Vd) into a lower volcanic unit and an upper volcanic unit. Mineralisation occurs in brecciated and altered volcanic rocks as massive sulphide lenses in the upper portion of the lower volcanic unit. Similar mineralisation occurs at the dike-pillow lava junction on Mt. St. Gregory, and it has been pointed out by Upadhyay and Strong (1973) that sulphide deposits of most ophiolite suites are concentrated at this stratigraphic position.

The basis for subdivision is the degree of alteration of the pillow units. The lower unit consists of light grey to green fine-grained basalts containing disseminated pyrite (2-3%). In the lower part, dikes are common with numerous pillow lava screens. Such intrusive relationships are well-preserved in road cuts on the York Harbour road at Bluff Head, and


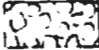



Figure Vd: Geology of volcanic rocks around York Harbour,
Bay of Islands (after Duke and Hutchinson, 1974).

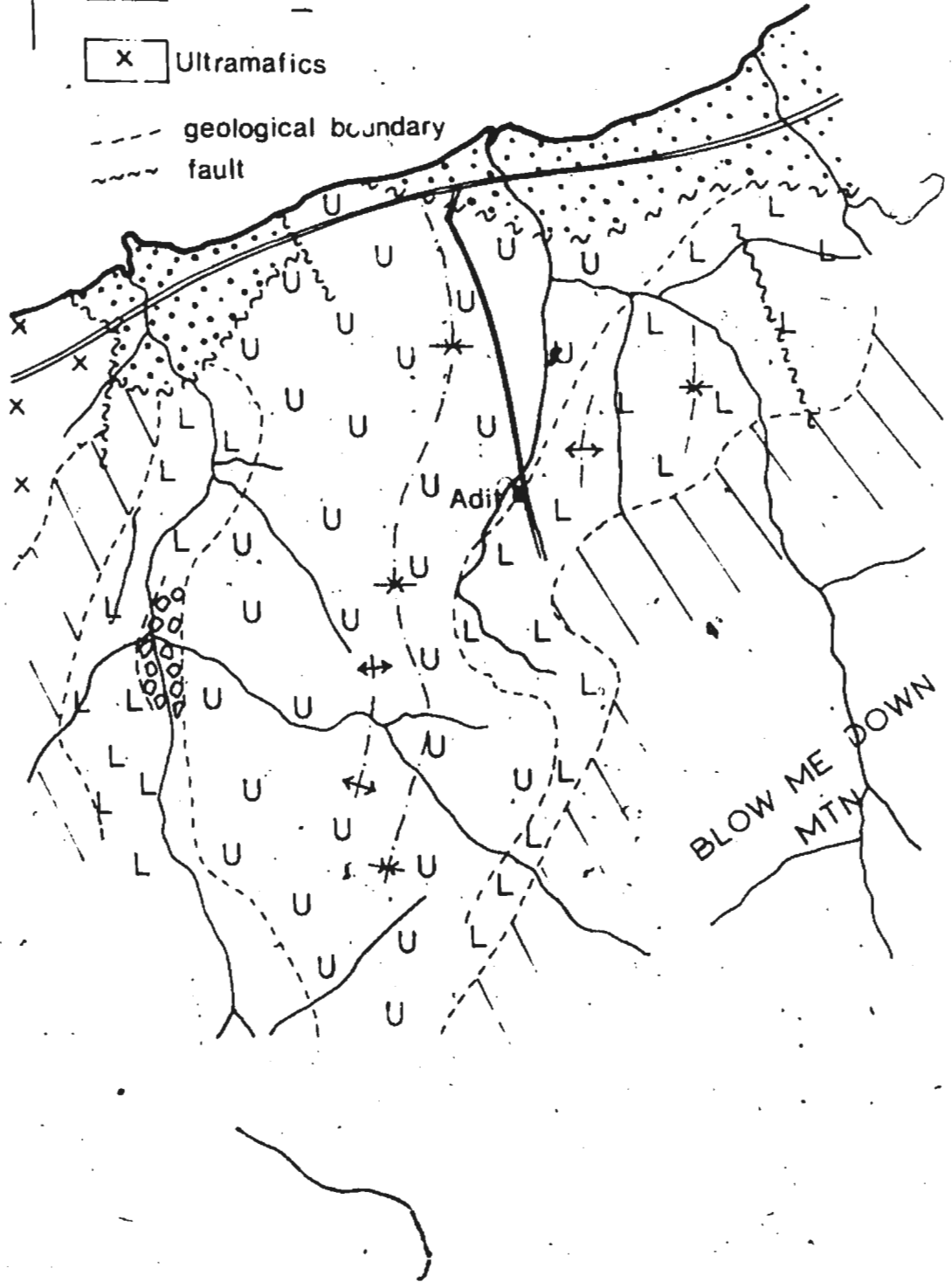
LEGEND

- U Upper volcanic unit
- L Lower volcanic unit
- / Intrusive mafic rocks
- x Ultramafics
-  Pyroclastics
-  Sediments



0 feet 2000

- - - geological boundary
- ~ ~ ~ fault



are reminiscent of the Basal Group of the Troodos Complex, Cyprus (Wilson, 1959). Chlorite is a common alteration product and is visible on local shear surfaces and forms a dense chlorite rock in the immediate vicinity of the mineralised zone. Breccias occur sporadically with zeolites and epidote filling fractures, together with sulphides closer to the ore bodies.

The upper zone volcanics are darker olive to black aphanites with a preponderance of magnetite. Dike rocks are scattered and the lavas are generally more vesicular.

Both groups are pillowed with pillows ranging from 15 cms to 1 metre in diameter. Radial and concentric jointing and selvedges are well preserved and tops are determinable in many outcrops. Vesicles are common, especially in the upper zone lavas (Plate LIVa) and are generally filled with calcite and epidote (Plate LIVb). They are always small (1-2 mm in diameter) but may indicate tops by preferential elongation. Interpillow hyaloclastites formed by spalling of glassy selvedges are found rarely and many pillows are surrounded by a chloritic shale. Jasperous chert has been noted between some pillows but is not common.

A distinction between upper and lower unit volcanics has not been made on North Arm Mountain.

In thin section, textures of the lower pillow lavas from Blow-me-down Mountain, and pillow lavas from North Arm Mountain range from intersertal to hyalophitic. Normally zoned plagioclase laths are albitic in composition (optical determination) and labradorite/andesine phenocrysts have not been

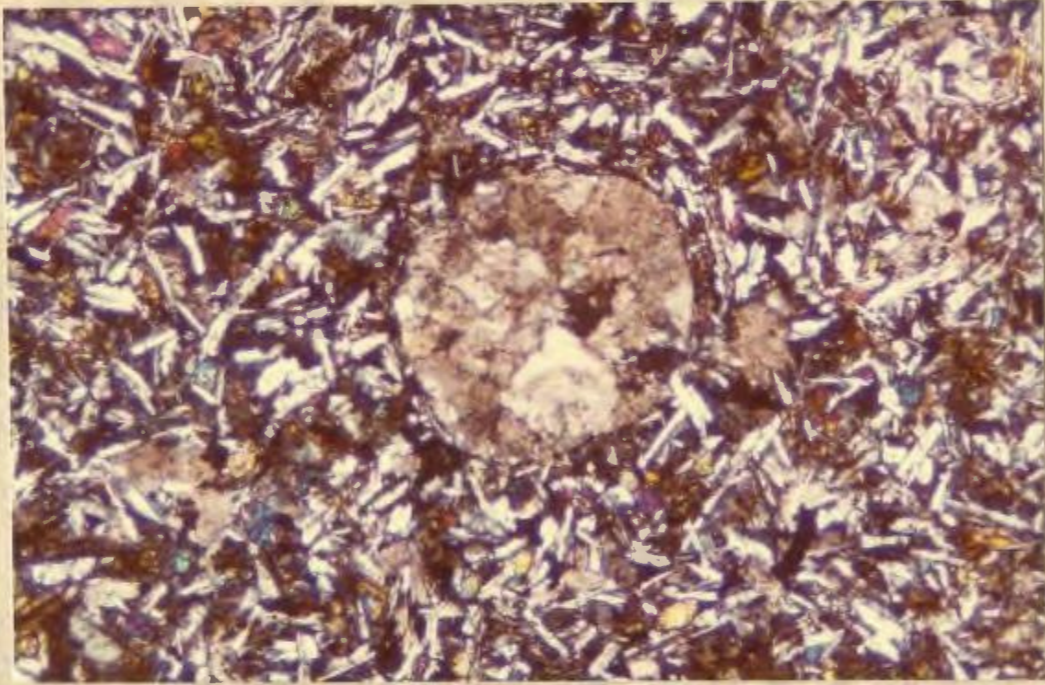


PLATE LIVa: Calcite filling vesicle in pillow lava, North Arm Mountain. X nicols x 80.

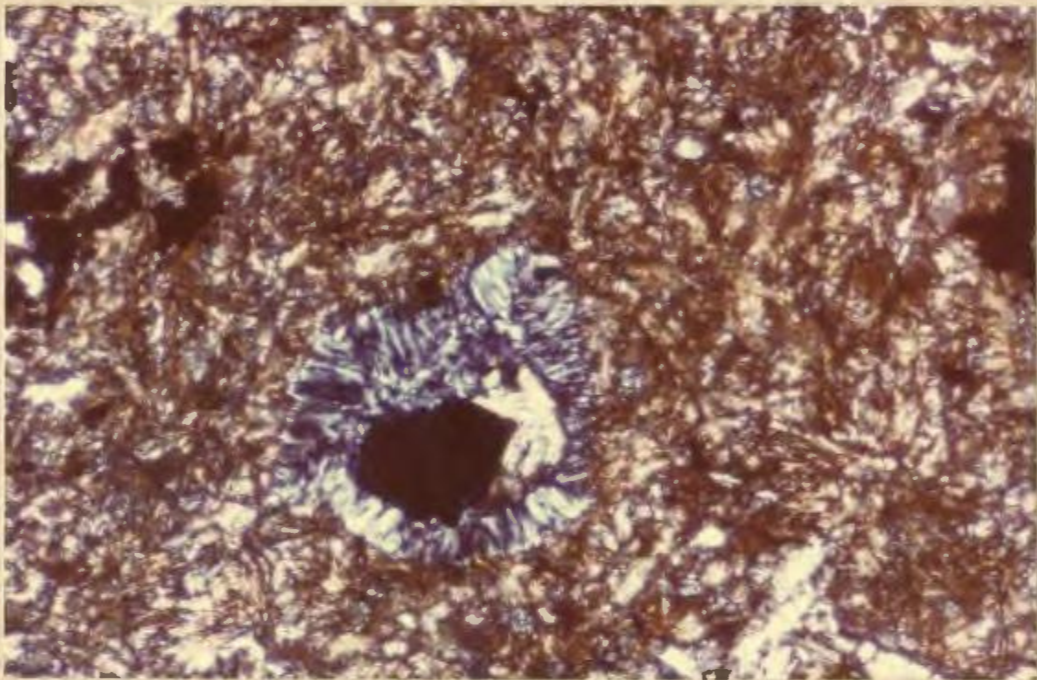


PLATE LIVb: Chlorite and pyrite in vesicle in pillow lava - York Harbour. X nicols x 65.

recorded by the writer although reported by Duke and Hutchinson (1974). Alteration of the plagioclase to chlorite and epidote is common and widespread. Clinopyroxene is partially altered to actinolite and chlorite, although in some cases appears fresh. Ophitic textures are common. Rare pigeonite phenocrysts are present particularly in the lower parts of the volcanic pile. Chlorite, palagonite and oxide dust form the matrix and by its association with sphene, the oxide is most probably ilmenite. Amygdules are filled with epidote and possibly clinocllore.

The upper lavas on Blow-me-down Mountain may often show trachytic textures. Subparallel laths and microlites of albite are in subophitic intergrowth with clinopyroxene and rarely phenocrysts of normally zoned plagioclase are also present (Plate LVa). Chlorite pseudomorphs after possible olivine have been recognised (Plate LVb). Pyroxene is generally unaltered, or only marginally altered to chlorite. The matrix consists of chlorite, calcite, ~~epidote~~ and ilmenite. Euhedral magnetite octahedra are widespread and are considered a primary crystallisation product rather than a result of alteration.

xvii) Sediments

Purple to red-brown sandstones, grey to green and red shale and siltstone and rare pebble conglomerates overlie the pillow lavas between Buck Head and Crabb Point on North Arm (Fig. IIIb). Green laminated siltstones and ribbon cherts and intraformational breccias are interbedded with pillow lavas in the Gregory River area. A maximum thickness of approximately 200 metres of sediment is estimated in the synclinal axis on North Arm.

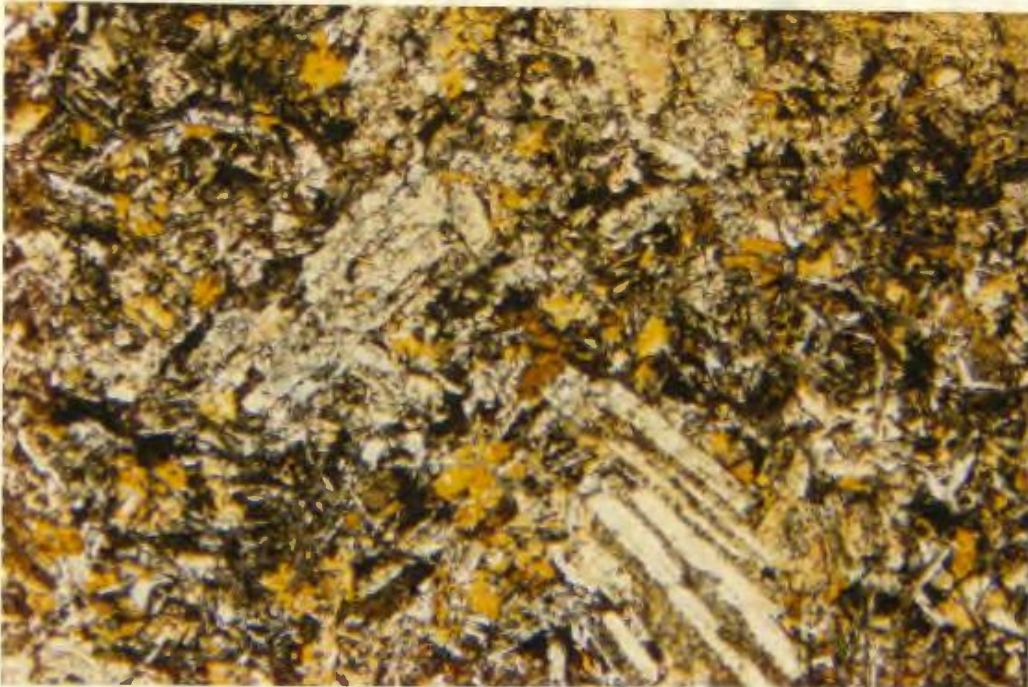


PLATE LVa: Plagioclase phenocrysts in basalt - York Harbour.
X nicols x95.

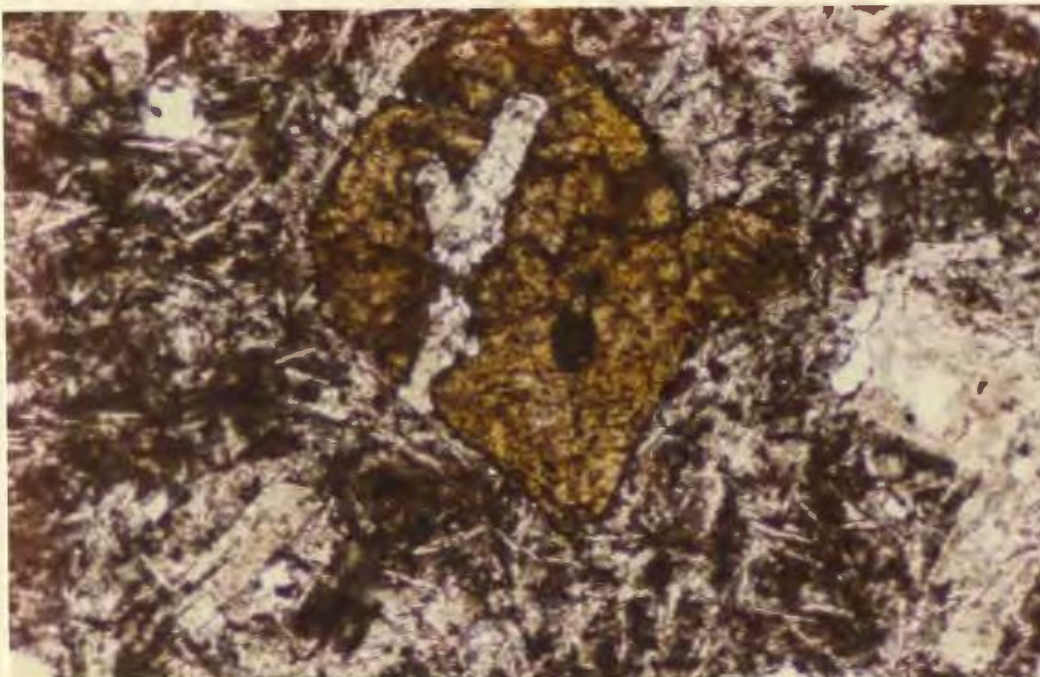


PLATE LVb: Chlorite/oxide pseudomorph after olivine, Upper Basalt,
York Harbour. Plain light x 100.

The sediments are interpreted as overlying the volcanics because

a) the contact between the sediments and volcanics is of variable relief and does not resemble a subhorizontal thrust surface,

b) high gravity anomalies suggest that basic rocks exist beneath the sediments (Weaver, 1967), and

c) the position of the sediments surrounded by volcanic rocks suggests that they lie in the axial zone of a syncline above the volcanics and thus form the highest stratigraphical unit of the succession (Williams, 1973).

The sediments are generally well sorted and well bedded. Tops are determinable from minor ripple drift lamination in the sandy-silts and load structures in the siltstones. Units exhibiting graded-bedding are not uncommon and are of the order of 3 to 4 metres thick. Coarser sands are dominantly quartzo-feldspathic, although lacking potash-feldspar, and contain numerous basic volcanic fragments. The lack of potash-feldspar and the presence of the basic volcanic fragments makes these coarser sediments lithologically distinct from the sandstones underlying the thrust slices.

The sediment lithologies do not resemble closely any sedimentary associations found presently on oceanic abyssal plains or in troughs associated with oceanic ridges. Contemporaneous sedimentation in the ocean basins is generally of calcareous (coccolithophorial or foraminiferal) muds, partially silicified turbidites and deep-sea muds. Likewise, although manganese-rich sediments are known to be associated with other ophiolite

suites (Upadhyay and Strong, 1973) and are recorded from the ocean-floor (Bonatti, et al., 1972; Scott, et al., 1976) no manganiferous sediments have been found associated with the Bay of Islands ophiolites. The presence of detrital quartz and plagioclase feldspars in some coarser units suggests a relatively proximal source of possibly granodioritic or granitic nature for the sediments. Possibly their deposition took place in a marginal basin, or at least close to an island-arc terrane or continental margin. It is unlikely that, if the sediments are to be considered as directly associated with the formation of the ophiolites, and not as a much later superposition, the ophiolites could have formed at a simple spreading centre in the middle of a large ocean basin.

CHAPTER VI

CHEMISTRY AND PETROGENESIS

A. Mineral Chemistry.

Chemical analyses have been obtained for a number of minerals of the Bay of Islands Complex by electron microprobe analyses. Details of analytical methods are given in Appendix III.

i) Olivine

Chemical analyses of olivines from lherzolites, harzburgites, dunites and gabbroic rocks are given in Table IX. Fo contents (mole percent) vary from 75.1 to 90.8 in the cumulate rocks, with the lower values representative of the gabbros above the dunites. Olivines from the lherzolites V12 and V13 have Fo contents of 89.4 and 89.7 respectively. The average Fo content of olivines from the harzburgites is slightly higher (91.1) and the range is very small (90.5-91.6). A number of these analyses have been supplemented by determination of olivine composition by X-ray methods using the determinative curve based on the olivine (130) spacing (Yoder and Sahama, 1957). This X-ray method has an accuracy of ± 3.5 mole percent in the range of values measured, but noticeably all values determined by X-ray methods are lower than chemical analyses of the cumulate rocks, and higher in the case of tectonites. The effect of varying amounts of trace elements on the X-ray determinative curve is not known. The dunitic olivines appear to contain more manganese and nickel, and in some cases more chromium than those from the harzburgites. As Jackson (1960, p. 433) points out, it is advisable to use X-ray determinative curves only for olivines with similar trace element contents as those used to calibrate the curves. The electron microprobe analyses of olivines show

Table IX: Olivines from Bay of Islands Complex

	Lherzolites				Harzburgites	
	V12	V13	181 A	181 B	182	184
SiO ₂	39.95	41.05	37.92	40.53	37.89	42.40
Al ₂ O ₃	0.00	0.02	0.00	0.00	0.02	0.00
TiO ₂	0.00	0.00	0.02	0.02	0.01	0.00
Cr ₂ O ₃	0.00	0.00	0.00	0.00	0.00	0.00
FeO	10.10	10.08	8.54	8.41	8.49	8.55
MnO	0.00	0.00	0.00	0.00	0.00	0.00
MgO	47.62	49.26	51.22	50.54	50.32	48.09
CaO	0.00	0.02	0.08	0.06	0.05	0.06
Na ₂ O	0.02	0.00	0.04	0.04	0.04	0.00
K ₂ O	0.00	0.01	0.00	0.00	0.00	0.00
NiO	0.00	0.00	0.39	0.39	0.41	0.45
Fo	Analy: 89.4 Xray:	89.7	91.6	91.6	91.4	91.0
Si	0.998	1.001	0.949	0.989	0.957	1.034
Ti	0.000	0.000	0.000	0.000	0.000	0.000
Al	0.000	0.001	0.000	0.000	0.001	0.000
Cr	0.000	0.000	0.000	0.000	0.000	0.000
Fe ₃	0.000	0.000	0.000	0.000	0.000	0.000
Fe ₂	0.213	0.206	0.179	0.172	0.179	0.174
Mn	0.000	0.000	0.000	0.000	0.000	0.000
Mg	1.791	1.791	1.911	1.839	1.895	1.748
Ca	0.000	0.001	0.002	0.002	0.001	0.002
Na	0.001	0.000	0.002	0.002	0.002	0.000
K	0.000	0.000	0.000	0.000	0.000	0.000
Ni	0.000	0.000	0.008	0.008	0.008	0.009
SiO ₂	40.756	40.815	41.128	41.131	41.112	41.038
FeO	10.367	10.054	8.384	8.369	8.469	8.863
MgO	48.877	49.131	50.488	50.501	50.419	50.099

TABLE IX (Continued)

Harzburgites

	185	186	187	188	189	190 A
SiO ₂	40.88	40.39	40.51	40.96	40.30	40.53
Al ₂ O ₃	0.00	0.00	0.00	0.00	0.00	0.00
TiO ₂	0.00	0.00	0.00	0.00	0.00	0.00
Cr ₂ O ₃	0.00	0.00	0.00	0.00	0.00	0.00
FeO	9.34	9.47	9.42	9.05	9.44	8.72
MnO	0.00	0.00	0.00	0.00	0.00	0.00
MgO	49.86	49.67	49.88	51.00	49.73	50.30
CaO	0.02	0.04	0.03	0.00	0.04	0.03
Na ₂ O	0.00	0.00	0.02	0.00	0.00	0.00
K ₂ O	0.00	0.00	0.00	0.00	0.00	0.00
NiO	0.33	0.32	0.37	0.37	0.38	0.32
Fo	Analy: 91.0 Xray:	90.5 93.5	90.5 93.1	91.0	90.8 92.9	91.2
Si	0.996	0.991	0.990	0.988	0.989	0.991
Ti	0.000	0.000	0.000	0.000	0.000	0.000
Al	0.000	0.000	0.000	0.000	0.000	0.000
Cr	0.000	0.000	0.000	0.000	0.000	0.000
Fe ₃	0.000	0.000	0.000	0.000	0.000	0.000
Fe ₂	0.190	0.194	0.193	0.183	0.194	0.178
Mn	0.000	0.000	0.000	0.000	0.000	0.000
Mg	1.821	1.816	1.818	1.834	1.819	1.833
Ca	0.001	0.001	0.001	0.000	0.001	0.001
Na	0.000	0.000	0.001	0.000	0.000	0.000
K	0.000	0.000	0.000	0.000	0.000	0.000
Ni	0.006	0.006	0.007	0.007	0.008	0.006
SiO ₂	40.959	40.932	40.947	41.039	40.939	41.072
FeO	9.287	9.431	9.349	8.854	9.390	8.681
MgO	49.754	49.637	49.704	50.104	49.671	50.247

TABLE IX (Continued)

	Harzburgites			Dunites		
	190 B	192 A	192 B	193	E2A	E2B
SiO ₂	40.32	38.83	39.65		40.25	40.17
Al ₂ O ₃	0.00	0.01	0.01		0.06	0.05
TiO ₂	0.00	0.00	0.00		0.00	0.00
Cr ₂ O ₃	0.00	0.00	0.00		0.08	0.05
FeO	8.83	8.63	8.66	No probe	9.74	9.66
MnO	0.00	0.00	0.00		0.12	0.16
MgO	50.18	50.90	50.44		49.45	49.40
CaO	0.03	0.05	0.06		0.12	0.02
Na ₂ O	0.00	0.00	0.00		0.00	0.00
K ₂ O	0.00	0.00	0.00		0.00	0.00
NiO	0.34	0.00	0.36		0.44	0.41
Fo	Analy: 91.1 Xray:	91.4	91.3	93.0	89.5	89.6
Si	0.989	0.966	0.978		0.987	0.988
Ti	0.000	0.000	0.000		0.000	0.000
Al	0.000	0.000	0.000		0.002	0.001
Cr	0.000	0.000	0.000		0.002	0.001
Fe ₃	0.000	0.000	0.000		0.000	0.000
Fe ₂	0.181	0.180	0.179		0.200	0.199
Mn	0.000	0.000	0.000	No probe	0.002	0.003
Mg	1.834	1.887	1.855		1.807	1.810
Ca	0.001	0.001	0.002		0.003	0.001
Na	0.000	0.000	0.000		0.000	0.000
K	0.000	0.000	0.000		0.000	0.000
Ni	0.007	0.000	0.007		0.009	0.008
SiO ₂	41.051	41.099	41.087		40.864	40.868
FeO	8.794	8.530	8.604		9.793	9.771
MgO	50.155	50.362	50.309		49.343	49.361

TABLE IX (Continued)

Dunites, Critical Zone, Gabbros

	321 A	321 B	321 C	321 D	321 E	321 F
SiO ₂	39.91	39.56	39.65	39.79	39.67	39.20
Al ₂ O ₃	0.04	0.06	0.04	0.02	0.07	0.03
TiO ₂	0.00	0.00	0.00	0.00	0.00	0.00
Cr ₂ O ₃	0.02	0.04	0.10	0.10	0.16	0.11
FeO	9.52	9.67	9.44	9.59	9.53	9.51
MnO	0.14	0.12	0.15	0.16	0.14	0.12
MgO	50.63	50.29	50.08	50.21	50.75	50.52
CaO	0.02	0.02	0.00	0.00	0.01	0.00
Na ₂ O	0.00	0.00	0.00	0.00	0.00	0.00
K ₂ O	0.00	0.00	0.00	0.00	0.00	0.00
NiO	0.44	0.44	0.43	0.45	0.43	0.00
Fo Analy: Xray:	89.9	89.6	89.4	89.2	89.7	89.4
Si	0.974	0.972	0.976	0.976	0.969	0.968
Ti	0.000	0.000	0.000	0.000	0.000	0.000
Al	0.001	0.002	0.001	0.001	0.002	0.001
Cr	0.000	0.001	0.002	0.002	0.003	0.002
Fe ₃	0.000	0.000	0.000	0.000	0.000	0.000
Fe ₂	0.194	0.199	0.194	0.197	0.195	0.196
Mn	0.003	0.002	0.003	0.003	0.003	0.003
Mg	1.842	1.842	1.837	1.836	1.848	1.860
Ca	0.001	0.001	0.000	0.000	0.000	0.000
Na	0.000	0.000	0.000	0.000	0.000	0.000
K	0.000	0.000	0.000	0.000	0.000	0.000
Ni	0.009	0.009	0.009	0.009	0.008	0.000
SiO ₂	40.932	40.901	40.926	40.905	40.934	40.926
FeO	9.429	9.593	9.459	9.572	9.419	9.459
MgO	49.639	49.505	49.615	49.523	49.647	49.615

TABLE IX (Continued)

Dunites, Critical Zone, Gabbros

	194	195 A	195 B	196	198	276 A
SiO ₂	40.36	41.34	40.99	40.44	38.03	41.47
Al ₂ O ₃	0.00	0.02	0.02	0.01	0.00	0.00
TiO ₂	0.01	0.00	0.00	0.00	0.01	0.02
Cr ₂ O ₃	0.00	0.00	0.00	0.00	0.00	0.00
FeO	10.36	9.77	9.81	12.11	17.85	8.31
MnO	0.00	0.00	0.00	0.00	0.00	0.19
MgO	49.81	49.23	49.91	48.48	43.13	49.81
CaO	0.23	0.26	0.25	0.26	0.08	0.01
Na ₂ O	0.00	0.00	0.00	0.27	0.00	0.00
K ₂ O	0.00	0.00	0.00	0.00	0.00	0.00
NiO	0.00	0.00	0.00	0.34	0.00	0.51
Fo	Analy: 89.1 Xray: 86.9	89.5	89.7 86.1	87.5	81.1	91.3
Si	0.985	1.005	0.994	0.986	0.979	1.007
Ti	0.000	0.000	0.000	0.000	0.000	0.000
Al	0.000	0.001	0.001	0.000	0.000	0.000
Cr	0.000	0.000	0.000	0.000	0.000	0.000
Fe ₃	0.000	0.000	0.000	0.000	0.000	0.000
Fe ₂	0.211	0.199	0.199	0.247	0.384	0.169
Mn	0.000	0.000	0.000	0.000	0.000	0.004
Mg	1.812	1.784	1.805	1.761	1.655	1.803
Ca	0.000	0.007	0.006	0.007	0.002	0.00
Na	0.000	0.000	0.000	0.013	0.000	0.000
K	0.000	0.000	0.000	0.000	0.000	0.000
Ni	0.000	0.000	0.000	0.007	0.000	0.010
SiO ₂	40.788	40.864	40.879	40.476	38.374	41.097
FeO	10.195	9.793	9.712	11.861	17.747	8.548
MgO	49.016	49.344	49.409	47.663	42.880	50.355

TABLE IX (Continued)
Dunites, Critical Zone, Gabbros

	276 B	274 A	274 B	272 A	282
SiO ₂	40.36	41.28	41.08	40.13	40.17
Al ₂ O ₃	0.00	0.02	0.01	0.03	0.14
TiO ₂	0.00	0.02	0.03	0.00	0.01
Cr ₂ O ₃	0.00	0.00	0.00	0.00	0.00
FeO	8.49	8.71	8.76	9.47	21.01
MnO	0.17	0.17	0.20	0.00	0.41
MgO	50.73	48.63	49.23	49.20	37.71
CaO	0.02	0.00	0.01	0.03	0.04
Na ₂ O	0.00	0.00	0.00	0.00	0.00
K ₂ O	0.00	0.00	0.00	0.00	0.00
NiO	0.47	0.43	0.39	0.52	0.30
Fo	Analy: 91.3 Xray: 91.3	90.7	90.8	90.3	75.1
Si	0.985	1.014	1.005	0.991	1.032
Ti	0.000	0.000	0.00	0.000	0.000
Al	0.000	0.001	0.000	0.001	0.004
Cr	0.000	0.000	0.000	0.000	0.000
Fe ₃	0.000	0.000	0.000	0.000	0.000
Fe ₂	0.173	0.179	0.179	0.196	0.471
Mn	0.004	0.004	0.004	0.000	0.009
Mg	1.844	1.780	1.796	1.811	1.443
Ca	0.001	0.000	0.000	0.001	0.001
Na	0.000	0.000	0.000	0.000	0.000
K	0.000	0.000	0.000	0.000	0.000
Ni	0.009	0.008	0.003	0.010	0.006
SiO ₂	41.096	40.998	41.002	40.920	38.419
FeO	8.555	9.076	9.054	9.491	22.838
MgO	50.350	49.926	49.944	49.589	38.742

them to be chemically homogeneous; there are no significant differences from grain to grain within any one sample and no zoning within individual grains.

A number of workers (e.g. Jackson, 1961; Smith, 1962) have suggested that olivines of alpine-type intrusions are generally more magnesian than those from layered intrusions. Challis (1965) has pointed out that data on olivine compositions do not really allow conclusions to be drawn on the origin of ultramafic rocks. The suggestion by Green (1964) that Fo_{89} marks the upper limit of compositions derived from a basaltic magma seems unfounded. However, if the rock types from the Bay of Islands Complex are classified on the basis of texture as cumulate or tectonite, then a slight difference in Fo content of the olivines is noted, the tectonite olivines being generally more magnesian, although there is an overlap in compositions (Table XI). Irvine and Findlay (1972) report olivine compositions for the Table Mountain and North Arm Mountain plutons, but have not analysed feldspar-free dunites. Nevertheless a distinct break in olivine compositions is noticeable between the tectonites and cumulates. It appears that the Fo values in the tectonites ('peridotites' of Irvine and Findlay) are relatively constant, whereas in the dunites and gabbros the values range between 90.0 and 83.4. The Cr_2O_3 content of the dunitic olivines is relatively high (up to 0.16% wt) possibly indicating relatively low fO_2 during crystallisation. Such conditions might be expected to result in exsolution of Ni metal in the olivines, but in sections examined at this stage none has been identified.

ii) Orthopyroxenes

Analyses of 21 orthopyroxenes from harzburgites, lherzolites and dunites are given in Table X. Calculation of the structural formulae gives a deficiency of tetrahedrally coordinated ions in three of these pyroxenes. Partial serpentinisation, visible in thin section, could account for this deficiency, although it is noted that Hess and Phillips (1938) reported a deficiency in silica in enstatites from olivine-bearing rocks, and this has been substantiated by Boyd and England (1960).

The orthopyroxenes analysed are all enstatites with En values between 88.5 and 92.1 and no marked difference in En value occurs between harzburgitic, lherzolititic and dunitic pyroxenes. This is typical of the compositional range of orthopyroxenes from alpine peridotites (Ross, et al., 1954; Green, 1964; Page, 1967; Himmelberg and Coleman, 1968). Although Hess (1960) indicated that the Ca^{2+} content of orthopyroxenes was representative of the magma type from which the pyroxene had crystallised, further evidence (Jackson, 1961; Rothstein, 1958; Challis, 1965) seems to dispute this. The work of Atlas (1952), however, suggests that Ca^{2+} content may be dependent on crystallisation or equilibration temperature. Atlas found that in the synthetic system $\text{MgSiO}_3\text{-CaMgSi}_2\text{O}_6$, the maximum number of Ca^{2+} atoms accepted into the enstatite was 0.115 at $1,100^\circ\text{C}$; 0.050 at 1000°C ; and 0.030 at 700°C (calculated on the basis of 6 oxygens). Values for many of the pyroxenes analysed here exceed 0.050 (maximum 0.072 in 187A) possibly suggesting equilibration temperatures in excess of 1000°C . If this is the case then i) other pyroxenes in these rocks have not accepted

Table X: Orthopyroxenes from Bay of Islands Complex

	Lherzolite				Harzburgite		
	V12A	V13A	V13B	V13C	182	183A	183B
SiO ₂	56.20	56.76	56.60	55.32	56.24	57.83	56.37
TiO ₂	0.06	0.00	0.00	0.00	0.02	0.03	0.04
Al ₂ O ₃	4.21	5.38	4.83	5.65	3.02	1.76	2.00
Cr ₂ O ₃	0.38	0.64	0.74	0.74	0.63	0.60	0.65
FeO	7.41	6.26	6.40	6.22	5.77	5.30	5.59
MnO	0.00	0.00	0.00	0.00	0.00	0.00	0.00
MgO	32.38	31.38	32.03	30.82	32.76	32.29	32.13
CaO	0.58	1.41	0.52	1.21	1.29	1.08	1.72
Na ₂ O	0.05	0.06	0.07	0.08	0.03	0.00	0.00
K ₂ O	0.00	0.00	0.01	0.00	0.00	0.00	0.00
NiO	0.00	0.00	0.00	0.00	0.11	0.10	0.11
Ca	1.13	2.82	1.04	2.47	2.51	2.15	3.38
Mg	87.62	87.39	88.98	87.61	88.74	89.61	88.04
Fe	11.25	9.78	9.98	9.92	8.75	8.24	3.58
Si	1.921	1.920	1.926	1.907	1.942	2.000	1.983
Al ⁴	0.079	0.080	0.094	0.093	0.058	0.000	0.017
Al	0.091	0.135	0.120	0.137	0.065	0.074	0.064
Ti	0.002	0.000	0.000	0.000	0.001	0.001	0.001
Cr	0.010	0.017	0.020	0.020	0.027	0.016	0.018
Fe ³	0.000	0.000	0.000	0.000	0.000	0.000	0.000
Fe ²	0.212	0.177	0.182	0.179	0.167	0.153	0.162
Mg	1.650	1.582	1.624	1.584	1.686	1.666	1.655
Mn	0.000	0.000	0.000	0.000	0.000	0.000	0.000
Ni	0.000	0.000	0.000	0.000	0.003	0.003	0.003
Ca	0.021	0.051	0.019	0.045	0.048	0.040	0.064
Na	0.003	0.004	0.005	0.005	0.002	0.000	0.000
K	0.000	0.000	0.000	0.000	0.000	0.000	0.000
Ens.	88.62	89.02	89.92	89.83	91.02	91.58	90.19

Table X (Continued)

Harzburgite

	320	184	185	186	187A	187B	188A
SiO ₂	54.59	57.23	55.59	53.56	55.52	56.75	57.13
TiO ₂	0.00	0.00	0.02	0.00	0.00	0.00	0.02
Al ₂ O ₃	2.71	2.75	2.58	2.06	2.07	1.98	1.68
Cr ₂ O ₃	0.74	0.66	0.79	0.64	0.63	0.60	0.61
FeO	6.10	5.03	6.08	5.95	5.99	6.00	5.39
MnO	0.16	0.00	0.00	0.00	0.00	0.00	0.00
MgO	34.02	31.25	31.67	34.11	34.07	33.74	33.48
CaO	0.93	1.28	0.94	1.13	1.93	0.94	1.01
Na ₂ O	0.00	0.00	0.00	0.00	0.00	0.00	0.00
K ₂ O	0.00	0.00	0.00	0.00	0.00	0.00	0.00
NiO	0.10	0.13	0.04	0.00	0.06	0.07	0.05
Ca	1.75	2.62	1.89	2.12	3.57	1.79	1.95
Mg	89.07	89.33	88.58	89.15	87.78	89.31	89.93
Fe	9.19	8.05	9.54	8.73	8.65	8.90	8.12
Si	1.906	1.992	1.962	1.907	1.922	1.956	1.975
Al ⁴	0.094	0.008	0.038	0.086	0.078	0.044	0.025
Al	0.017	0.105	0.069	0.000	0.006	0.036	0.044
Ti	0.000	0.000	0.001	0.000	0.000	0.000	0.001
Cr	0.020	0.018	0.022	0.018	0.017	0.016	0.017
Fe ³	0.000	0.000	0.000	0.000	0.000	0.000	0.000
Fe ²	0.178	0.146	0.179	0.177	0.173	0.173	0.156
Mg	1.770	1.621	1.666	1.810	1.758	1.733	1.726
Mn	0.005	0.000	0.000	0.000	0.000	0.000	0.000
Ni	0.003	0.004	0.001	0.000	0.002	0.002	0.001
Ca	0.035	0.048	0.036	0.043	0.072	0.035	0.037
Na	0.000	0.000	0.000	0.000	0.000	0.000	0.000
K	0.000	0.000	0.000	0.000	0.000	0.000	0.000
Ens.	90.65	91.73	90.28	91.08	91.03	90.94	91.72

Table X (Continued)

	Harzburgite				Dunite		
	188B	189	272A	272B	272C	276A	276B
SiO ₂	57.26	56.15	54.29	53.27	56.75	57.27	57.76
TiO ₂	0.02	0.00	0.02	0.03	0.04	0.00	0.00
Al ₂ O ₃	1.66	1.32	1.67	1.37	1.77	1.27	1.31
Cr ₂ O ₃	0.53	0.35	0.61	0.68	0.88	0.51	0.37
FeO	5.78	6.00	6.25	7.84	6.23	5.54	5.27
MnO	0.00	0.00	0.17	0.34	0.17	0.06	0.10
MgO	34.55	34.37	35.96	35.45	33.21	34.79	35.07
CaO	1.62	1.11	1.43	0.60	1.46	0.82	0.67
Na ₂ O	0.00	0.00	0.00	0.00	0.00	0.00	0.00
K ₂ O	0.00	0.00	0.00	0.00	0.00	0.00	0.00
NiO	0.01	0.03	0.14	0.09	0.14	0.05	0.06
Ca	2.99	2.07	2.53	1.06	2.77	1.53	1.25
Mg	88.69	89.20	88.61	87.60	87.76	90.32	90.94
Fe	8.32	8.73	8.86	11.33	9.47	8.15	7.81
Si	1.950	1.952	1.884	1.879	1.954	1.965	1.971
Al ⁴	0.050	0.048	0.068	0.054	0.046	0.035	0.029
Al	0.017	0.008	0.000	0.000	0.026	0.017	0.024
Ti	0.001	0.000	0.001	0.001	0.001	0.000	0.000
Cr	0.014	0.010	0.017	0.019	0.024	0.014	0.010
Fe ³	0.000	0.000	0.000	0.000	0.000	0.000	0.000
Fe ²	0.165	0.174	0.181	0.231	0.179	0.159	0.150
Mg	1.754	1.784	1.860	1.864	1.704	1.779	1.784
Mn	0.000	0.000	0.005	0.010	0.005	0.002	0.003
Ni	0.000	0.001	0.004	0.003	0.004	0.001	0.002
Ca	0.059	0.041	0.053	0.023	0.054	0.030	0.025
Na	0.000	0.000	0.000	0.000	0.000	0.000	0.000
K	0.000	0.000	0.000	0.000	0.000	0.000	0.000
Ens.	91.42	91.09	90.90	88.54	90.26	91.72	92.09

as much calcium into their structure as theoretically possible or ii) if it was there, it has subsequently been removed. The exsolution lamellae of clinopyroxene in some enstatites support the latter conclusion. Microprobe analysis has not accounted for these lamellae nor the original calcium content of the orthopyroxenes. Possibly the irregularity of calcium content distributed in the orthopyroxene is a result of inclusion of clinopyroxene lamellae in some data points although this was avoided as far as is known.

Boyd and England (1960) have noted that, with the exception of some values from nodules, Al_2O_3 contents of orthopyroxenes from ultramafic rocks are generally low. They showed that the Al_2O_3 content is dependent upon pressure, but it is clear that the availability of aluminium is also a limiting factor. For example, Green (1964) reports that orthopyroxene with the highest Al_2O_3 (6-7%) in the Lizard peridotite coexists with aluminous diopside and spinel. The aluminium content of the herzolite spinels is clearly higher, and those of the dunites much lower than the contents of harzburgite spinels in the Bay of Islands Complex. However, since no aluminous phase is present in the harzburgites it cannot be determined how great a limiting factor pressure variation between these rock types was. However, the dunite is clearly a lower pressure crystallisation product than the basal herzolites and aluminium was apparently available for the joint crystallisation of feldspar in some rocks.

iii) Cation distribution between co-existing olivine and orthopyroxene

There is some doubt of the validity of using Mg^{2+} and Fe^{2+} partition coefficients between coexisting olivines and orthopyroxenes as

TABLE XI

Fo contents of olivines and En contents of orthopyroxenes from the Bay of Islands Complex

Stratigraphic Position	Sample #	Rock Type and Texture	Fo	En	
TOP	282	Olivine gabbro, cumulate	75.1		
	198	" "	81.1		
	196	Dunite	87.5		
	195	Dunite pyroxenite, "	89.6		
	321	Dunite "	89.5		
	194	" "	89.1		
	272	Dunite + opx "	90.3		
	274	Dunite + cpx "	90.7		
	276	Dunite + cpx + opx ?	91.3		
	E2	Dunite + chromite, cumulate	89.5		
		193	Harzburgite, tectonite	93(X-ray)	--
		192	" "	91.4	--
		190	" "	91.2	--
		189	" "	90.8	91.1
		188	" "	91.0	91.5
		187	" "	90.5	90.4
		186	" "	90.5	91.1
		185	" "	91.0	90.3
		184	" "	91.0	91.7
	183	" "	--	90.6	
	182	" "	91.4	91.0	
	181	" "	91.6	--	
	V13	Lherzolite tectonite	89.4	89.7	
BOTTOM	V12	" "	89.7	88.6	

indicators of temperature of equilibration (e.g. Wilshire and Jackson, 1975). However, partition coefficients are indicators of the degree of equilibrium reached between coexisting phases. O'Hara (1963) suggested a correlation between the nature of the igneous body in which the pyroxenes and olivines occurred and their Mg^{2+} and Fe^{2+} distribution. Pairs from large layered intrusions and nodules have a ratio near 1:1. Pairs from small layered intrusions (e.g. Rhum gabbro) have En:Fo considerably lower, and pairs from lavas even lower. The departure from the experimentally determined ratio for the smaller bodies and lavas is interpreted as a failure to reach equilibrium because of rapid cooling.

The experimentally determined and naturally occurring relationships reported in the literature are diverse. This is because these partition coefficients depend on a number of factors, of which the most important are:

- 1) temperature
- 2) fO_2
- 3) cation site distribution

Speidel and Osborn (1967) have discussed the effects of temperature and oxygen fugacity on equilibrium compositions in the system $MgO-FeO-Fe_2O_3-SiO_2$. The following points are noteworthy:

- 1) A decrease in Mg:Fe ratio in both pyroxenes and olivines takes place as temperature and oxygen fugacity decrease concomitantly.
- 2) Olivine, in equilibrium with pyroxene, magnetite and liquid is always more Fe-rich than coexisting pyroxene (a similar trend was found by Bowen and Schairer, 1935).
- 3) Olivine shows the widest variation of Fe-content of all the crystalline phases in the system.

4) At low temperatures the Fe-content of olivine increases rapidly with decreasing temperature. In the temperature interval 1165°C to 1144°C, the FeO content increases by more than 25 wt.%, at a fixed fO_2 .

The effect of cation site distribution is discussed by Grover and Orville (1969) who constructed a number of partition curves based on data from Bartholeme (1960), Ernst (1960), Mueller (1963), O'Hara (1963) and Ramberg and Devore (1951).

The curves of Grover and Orville (1969), Medaris (1969) and Nafziger and Muan (1967) are reproduced in figure VIa. The paired analyses from the Bay of Islands Complex are plotted on this figure, and none seem to be in disequilibrium.

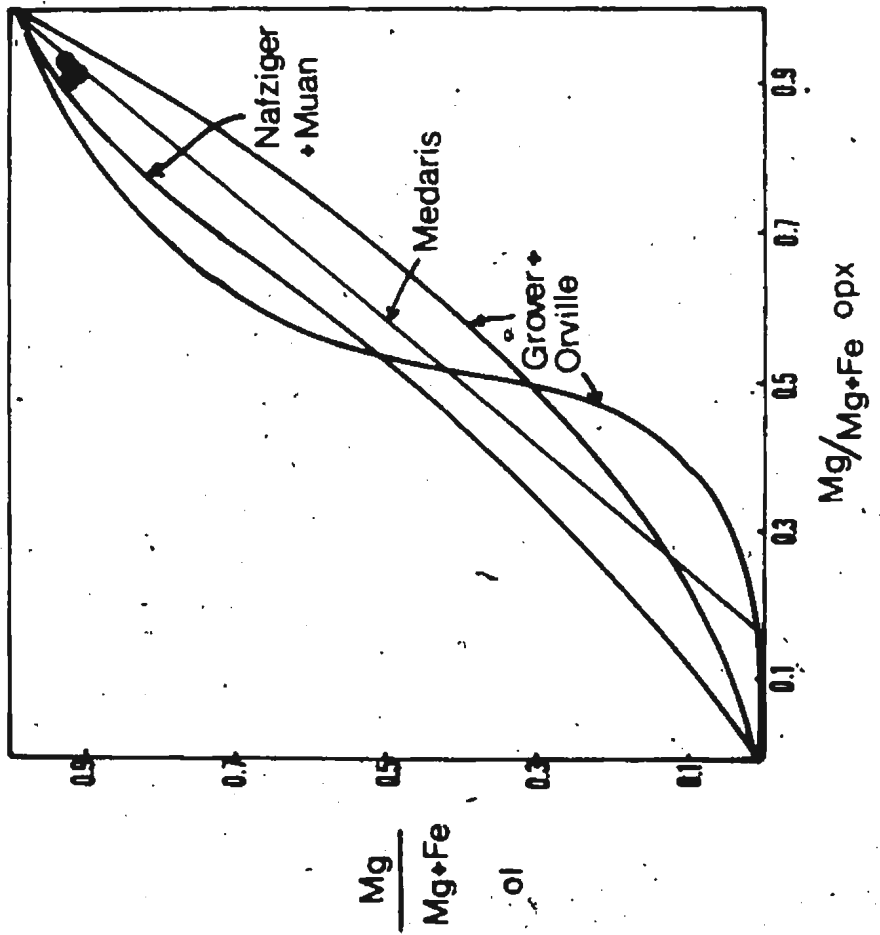
iv) Clinopyroxenes

Analyses of twenty-nine clinopyroxenes from lherzolites, harzburgites and cumulate rocks are presented in Table XII. In the harzburgites the clinopyroxene occurs as small interstitial crystals and is relatively rare. In the lherzolites the clinopyroxenes are texturally identical but are more common. In both cases, the clinopyroxene is clearly not a cumulate phase. On the other hand, in the cumulate olivine-pyroxenites and some gabbros, clinopyroxene occurs as large crystals poikilitically enclosing olivine, chromite and plagioclase, and appears in these cases to be the last mineral to crystallise.

The analyses of the clinopyroxenes are represented diagrammatically in figure VIb where they all lie in the diopside or endiopside fields (Poldevaart and Hess, 1951). The clinopyroxenes of the cumulate rocks are generally distinguishable from those of the harzburgites and lherzolites by

Figure VIa: - Distribution of Fe^{2+} and Mg^{2+} in coexisting
opx and olivine.

of



of

Table XII: Clinopyroxenes from Bay of Islands Complex

	Lherzolites				Harzburgites	
	V12A	V12B	V12C	V12 P2	V13B	320A
SiO ₂	53.46	52.79	51.23	53.13	52.54	53.82
TiO ₂	0.28	0.29	0.28	0.00	0.00	0.02
Al ₂ O ₃	6.24	6.11	6.16	6.05	5.69	2.64
Cr ₂ O ₃	0.73	0.76	0.71	1.24	0.99	0.95
Fe ₂ O ₃	2.80	2.96	1.56	2.42	1.70	2.23
FeO			1.62		1.91	
MnO	0.00	0.00	0.00	0.00	0.00	0.11
MgO	15.21	15.25	15.12	13.99	14.34	17.05
CaO	21.96	21.76	21.32	21.19	21.32	23.19
Na ₂ O	1.24	1.04	1.20	1.72	1.72	0.00
K ₂ O	0.00	0.00	0.02	0.01	0.02	0.00
NiO	0.45	0.00	0.00	0.00	0.00	0.15
Ca	48.12	48.06	46.69	49.82	48.51	47.48
Mg	47.09	46.84	46.04	45.74	45.38	48.78
Fe	4.79	5.10	5.27	4.44	6.11	3.74
Si	1.894	1.894	1.841	1.924	1.902	1.948
Al ⁴	0.106	0.106	0.129	0.076	0.098	0.052
Al ⁶	0.155	0.152	0.136	0.182	0.145	0.060
Ti	0.007	0.008	0.008	0.000	0.000	0.001
Cr	0.020	0.022	0.020	0.035	0.028	0.027
Fe ³	0.000	0.000	0.043	0.000	0.040	0.000
Fe ²	0.083	0.089	0.049	0.073	0.058	0.067
Mg	0.803	0.815	0.823	0.755	0.774	0.920
Mn	0.000	0.000	0.000	0.000	0.000	0.003
Ni	0.013	0.000	0.000	0.000	0.000	0.004
Ca	0.834	0.837	0.834	0.822	0.827	0.899
Na	0.085	0.072	0.085	0.121	0.121	0.000
K	0.000	0.000	0.001	0.000	0.001	0.000

Table XII (Continued).

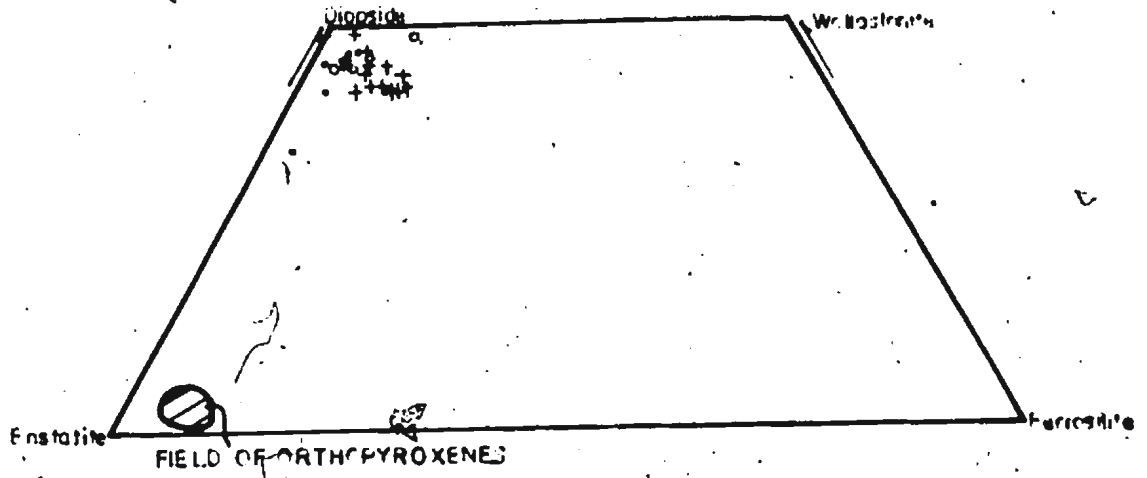
Dunites, Critical Zone, Gabbros

	205B	201A	201B	199A	199B	199C
SiO ₂	52.48	51.93	51.21	52.76	51.82	53.39
TiO ₂	0.73	0.91	0.66	0.73	0.82	0.83
Al ₂ O ₃	4.300	4.01	3.60	2.75	2.86	3.02
Cr ₂ O ₃	0.42	0.14	0.21	0.23	0.24	0.25
Fe ₂ O ₃	6.61	1.77	3.93	2.47	2.88	6.50
FeO		5.62	3.92	3.64	3.86	
MnO	0.00	0.00	0.00	0.00	0.00	0.00
MgO	15.36	15.64	16.10	15.73	15.60	16.04
CaO	21.53	21.55	21.33	23.26	22.72	21.17
Na ₂ O	0.09	0.37	0.39	0.49	0.41	0.45
K ₂ O	0.04	0.03	0.03	0.00	0.01	0.02
NiO	0.00	0.00	0.00	0.00	0.00	0.00
Ca	44.80	44.04	43.05	46.79	45.94	43.60
Mg	44.46	44.06	45.20	44.01	43.88	45.95
Fe	10.74	11.50	11.75	9.20	10.18	10.45
Si	1.900	1.877	1.862	1.902	1.888	1.928
Al ⁴	0.100	0.123	0.138	0.098	0.112	0.072
Al ⁶	0.083	0.048	0.017	0.019	0.011	0.057
Ti	0.020	0.025	0.018	0.020	0.022	0.023
Cr	0.012	0.004	0.006	0.007	0.007	0.007
Fe ³	0.000	0.048	0.108	0.067	0.079	0.000
Fe ²	0.200	0.170	0.119	0.110	0.118	0.196
Mg	0.829	0.843	0.873	0.845	0.847	0.863
Mn	0.000	0.000	0.000	0.000	0.000	0.000
Ni	0.000	0.000	0.000	0.000	0.000	0.000
Ca	0.835	0.835	0.831	0.899	0.887	0.819
Na	0.006	0.026	0.028	0.034	0.029	0.032
K	0.002	0.001	0.001	0.000	0.000	0.001

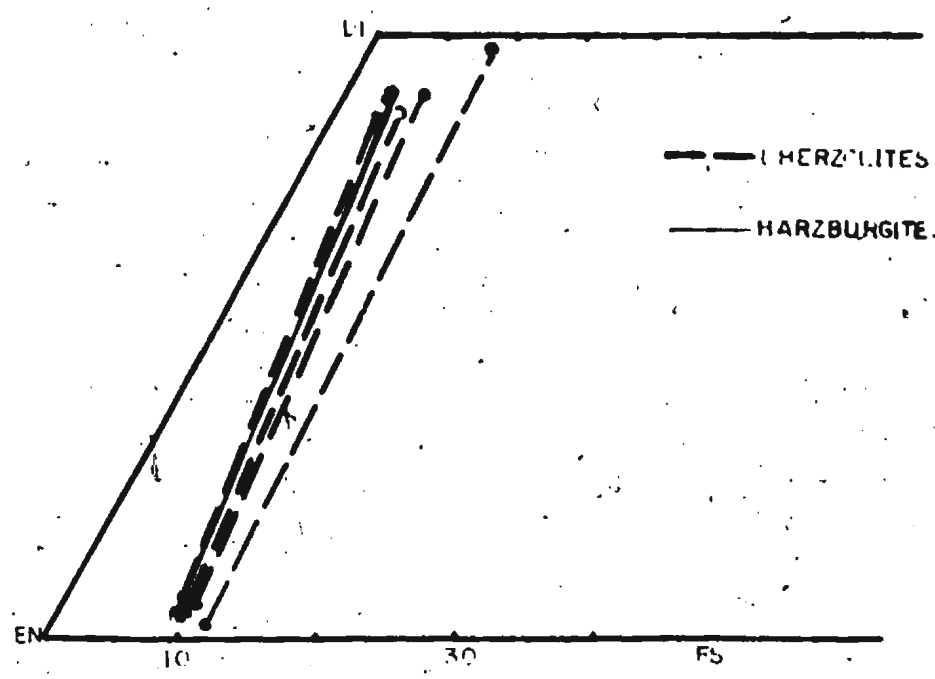
Table XII (Continued)

Dunites, Critical Zone, Gabbros			
	196	198A	198B
SiO ₂	53.25	50.48	49.19
TiO ₂	0.35	1.18	1.47
Al ₂ O ₃	2.58	3.48	3.71
Cr ₂ O ₃	0.38	0.27	0.28
Fe ₂ O ₃	2.12	2.01	4.08
FeO		3.78	1.69
MnO	0.00	0.00	0.00
MgO	16.65	15.62	15.30
CaO	25.67	21.74	22.47
Na ₂ O	0.30	0.42	0.52
K ₂ O	0.00	0.00	0.00
NiO	0.11	0.00	0.00
Ca	50.77	45.45	46.87
Mg	45.96	45.42	44.39
Fe	3.27	9.12	8.74
Si	1.919	1.874	1.834
Al ⁴	0.081	0.126	0.163
Al ⁶	0.038	0.026	0.000
Ti	0.009	0.033	0.041
Cr	0.011	0.008	0.008
Fe ³	0.000	0.056	0.115
Fe ²	0.064	0.117	0.053
Mg	0.894	0.864	0.850
Mn	0.000	0.000	0.000
Ni	0.003	0.000	0.000
Ca	0.991	0.865	0.898
Na	0.021	0.030	0.038
K	0.000	0.000	0.000

Figure Vib: Clinopyroxenes from Bay of Islands Complex.



- CUMULATES +
- HARZBURGITES •
- HERZOLITES ◦

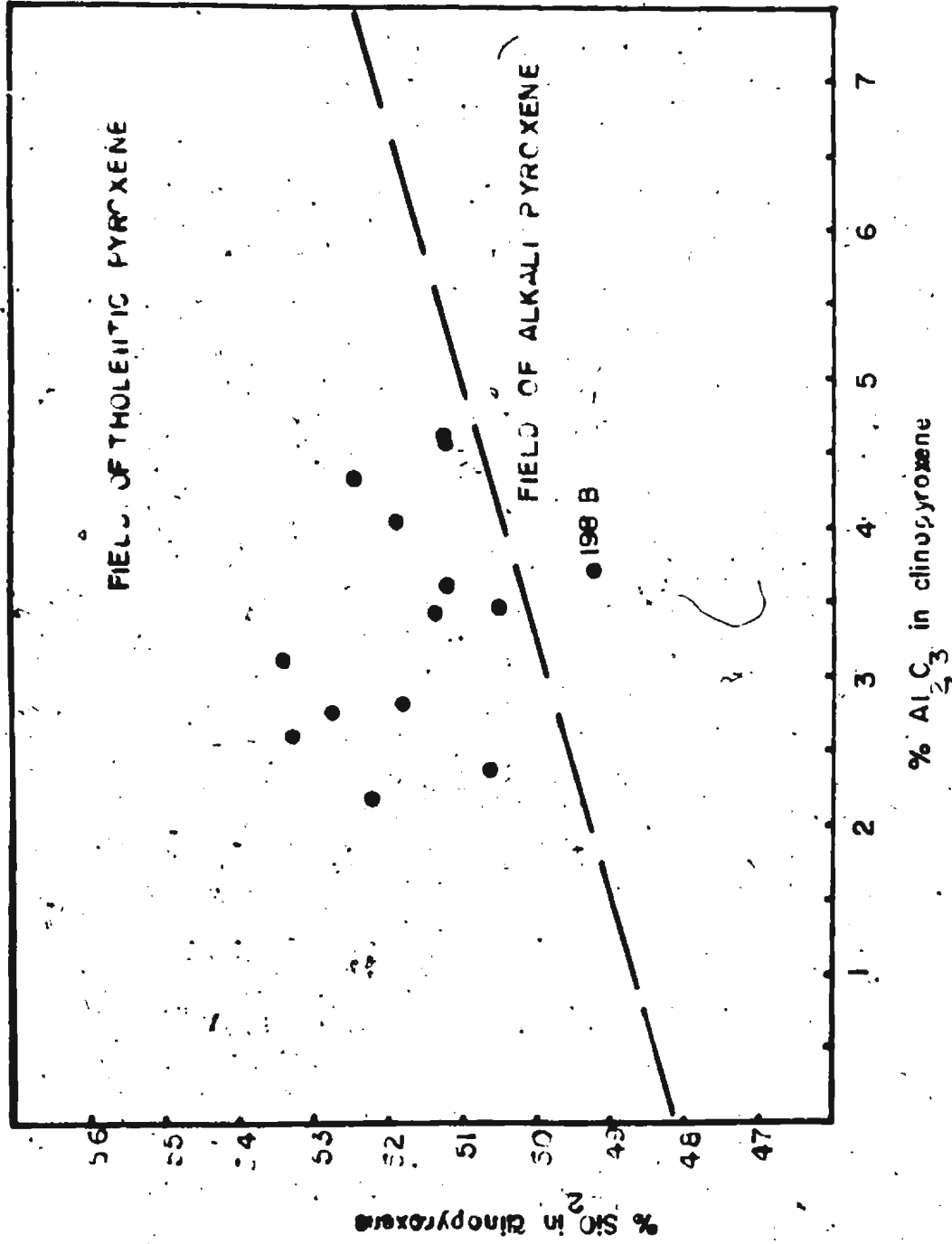


their more iron-rich compositions and a corresponding titanium enrichment, although there is some overlap in values. This titanium enrichment seems to be less dependent on pressure of crystallisation (Akella and Boyd, 1973) than on availability of titanium and its substitution for iron. The clinopyroxenes of the lherzolites and harzburgites have higher chromium contents than those from the cumulate rocks, except in one case (274A) where the pyroxene is from a chromite-rich band, and this enrichment in the Kosmochlor molecule is comparable in amount with that in the chrome-diopsides produced in the experiments of Dickey and Yoder (1972) at pressures up to 20kb.

The lherzolitic clinopyroxenes are richer in both Al_2O_3 and Na_2O compared with the harzburgitic pyroxenes. This may be taken as an effect of equilibration under higher pressures (Kushiro, 1960; Rothstein, 1962; Kuno, 1964; Green and Ringwood, 1967; Aoki and Katsura, 1968; Burns, 1969; Irving, 1974 and Munoz and Sagredo, 1974). Church (1972) recognised similar differences in Al_2O_3 contents, and divided the rocks on this basis into 'high-pressure' and 'low-pressure' associations. The present writer agrees with Church in this division but suggests that their re-equilibration need not, as he states, have involved crystallisation from a magma body (Church, 1972, p. 79).

Since diopside appears to have been the last mineral to crystallise in the gabbros and olivine pyroxenites, its composition may be expected to reflect the composition of the residual magma at this stage. Kushiro (1960), Le Bas (1962) and Rothstein (1962) have indicated that the substitution of Al for Si can indicate magma type: e.g. in the Le Bas' (1962) plot of total Al_2O_3 against SiO_2 , clinopyroxenes from tholeiitic, alkaline and

Figure VIc: Clinopyroxene analyses from Bay of Islands Complex plotted according to Le Bas (1962).



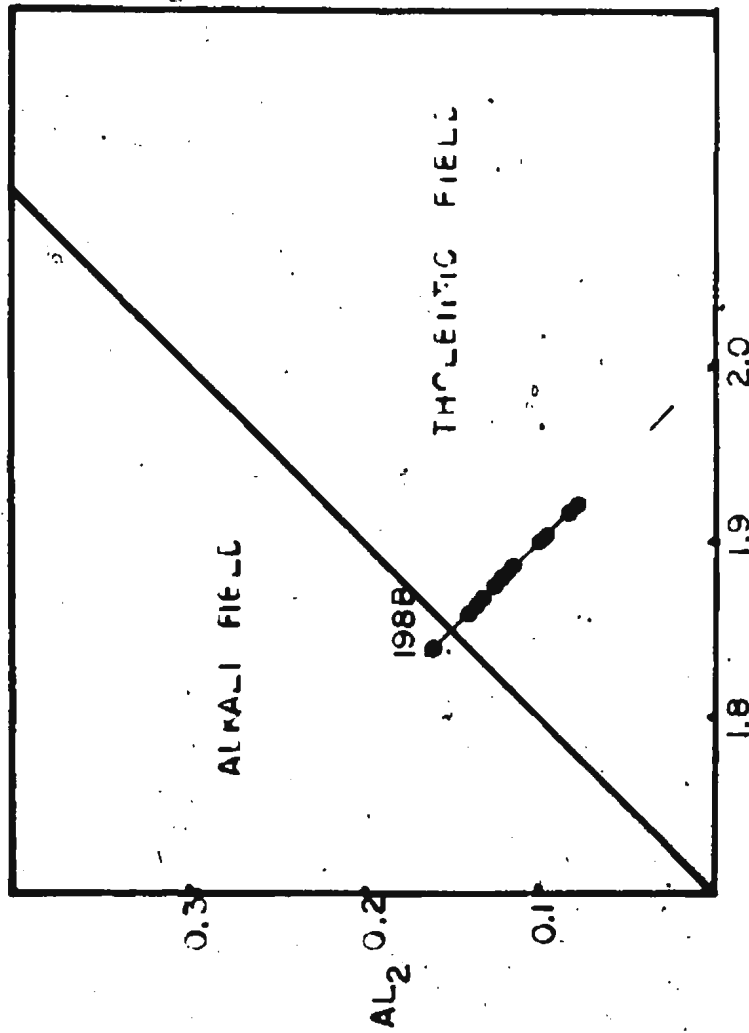
peralkaline rocks fall into three fairly well defined fields (Fig. VIc). Kushiro has obtained similar results using atomic amounts of Si and Al. Since pressure may effect the amount of total Al substitution in the pyroxenes, Kushiro's plot has been modified in figure VI d so that only substitution in the tetrahedral sites are plotted. In both diagrams, all but one of the pyroxenes plot clearly in the tholeiitic field. At first, this seems incompatible with the slightly alkaline nature of some bulk rock analyses (p. 324) but may be explained in terms of pressure of crystallisation, and an increased solubility of enstatite in diopside in pyroxenes crystallising at pressures greater than 1 atmosphere. This effect may push the clinopyroxene composition into the tholeiitic field, although the magma composition is slightly alkaline (Figure VIe).

v) Coexisting orthopyroxene and clinopyroxene; Estimation of equilibration temperatures

The clinopyroxenes from the harzburgites generally have a higher Mg: (Mg+Fe²⁺+Mn) ratio and a slightly lower Al₂O₃ content compared with the coexisting orthopyroxenes. The Al₂O₃ is present chiefly in Tschermak substitution [(Ca, Mg) Al₂SiO₆] and not as jadeite. These clinopyroxenes also have slightly more Cr₂O₃ than the orthopyroxenes; although the difference is not significant.

One method for determination of temperatures of equilibration of peridotites has been the composition of diopside coexisting with enstatite using the solvus as determined by Davis and Boyd (1966) and Boyd and Schairer (1964). The distribution of Ca²⁺ between coexisting ortho- and clino-pyroxenes from the lherzolites of the Bay of Islands Complex suggests that they last equilibrated on the pyroxene solvus at about 1000°C

Figure VI d: Modified Kushiro (1960) plot for cpx's
from Bay of Islands Complex.

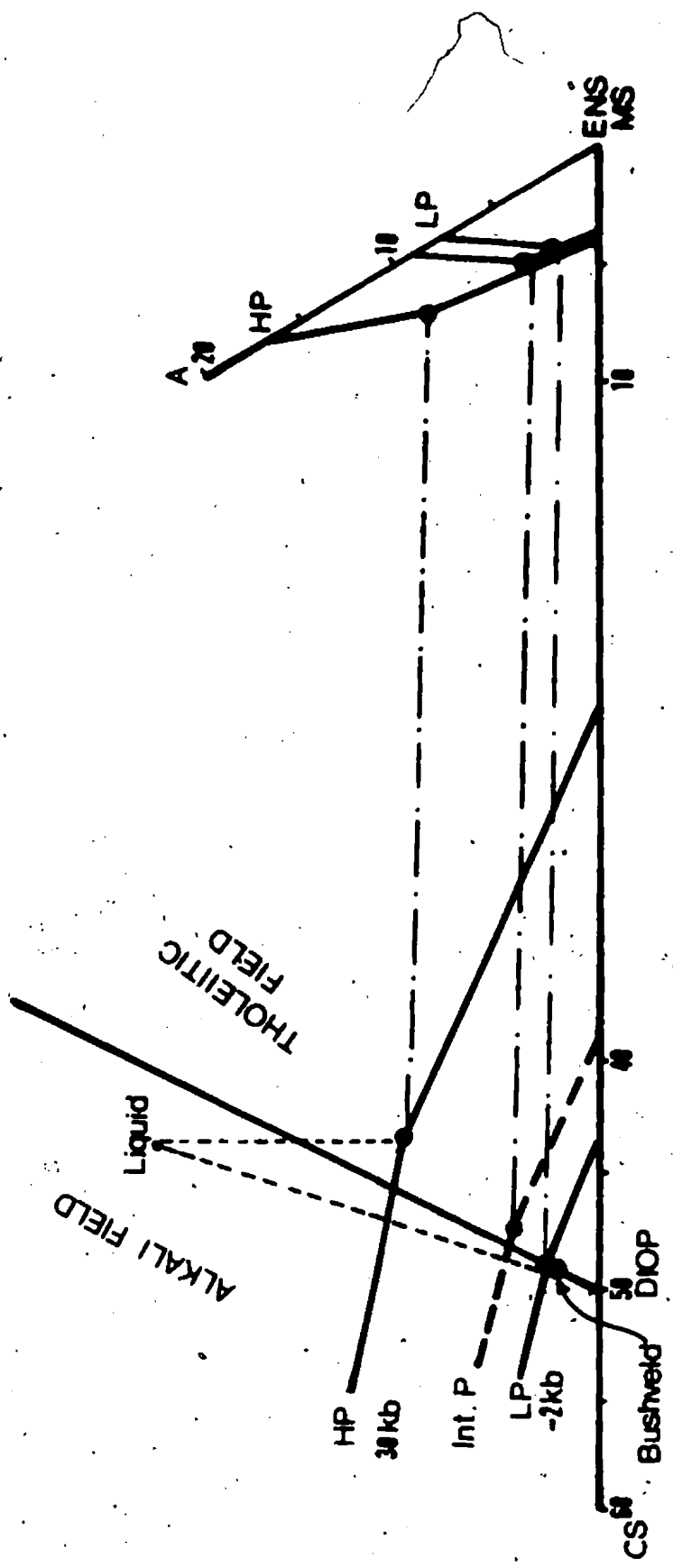


(Fig. VI f). Re-examinations of the solvus at lower temperatures (Nehru and Wyllie, 1974; Lindsley and Munoz, 1969) and higher temperatures (Howells and O'Hara, 1975; Mori and Green, 1975) indicate that the solubilities of enstatite in diopside are greater than previously thought at temperatures below 1200°C. It is probable, therefore, that temperature estimates below 1200°C might be low. The applicability of any of these solvi determined in olivine-free assemblages to olivine saturated natural assemblages is questionable in any case, since the activity of silica has a major influence upon the Ca/Ca+Mg ratio of diopside coexisting with enstatite, at least at high temperatures (Howells and O'Hara, 1975)..

Other estimates of temperature and pressure of equilibration may be obtained using the methods of O'Hara (1967), Wood and Banno (1973), Wood (1974) and MacGregor (1974). These are presented in figure VI g and Table XIII. Because most of these methods depend on the coexistence of an aluminous phase for the estimation of pressure, only clinopyroxene compositions from the lherzolites are used. In these cases, spinel is the aluminous phase. O'Hara's (1967) α and β parameters for clinopyroxenes from the lherzolites are plotted in Figure VI g and indicate temperatures of the order of 1000°C-1100°C and pressures of about 18-20 kbs. The spinel-lherzolite/garnet-lherzolite phase boundary has here been modified after O'Hara (1975, pers. comm.) and should perhaps be further modified to increase the pressure range of the spinel-lherzolite field because of the influence of Cr₂O₃ in the system on the pressure required to stabilise garnet-lherzolite (MacGregor, 1970). With these modifications the data points fall clearly within the spinel-lherzolite facies field.

Using partition coefficients of Mg²⁺ and Fe²⁺ between coexisting

Figure VIe: Solubility of enstatite in diopside with increasing pressure.



— Solid soln. limits

- - - Tie lines coexisting pxs.

Figure Vif: Ca^{2+} distribution in coexisting enstatites
and diopsides.

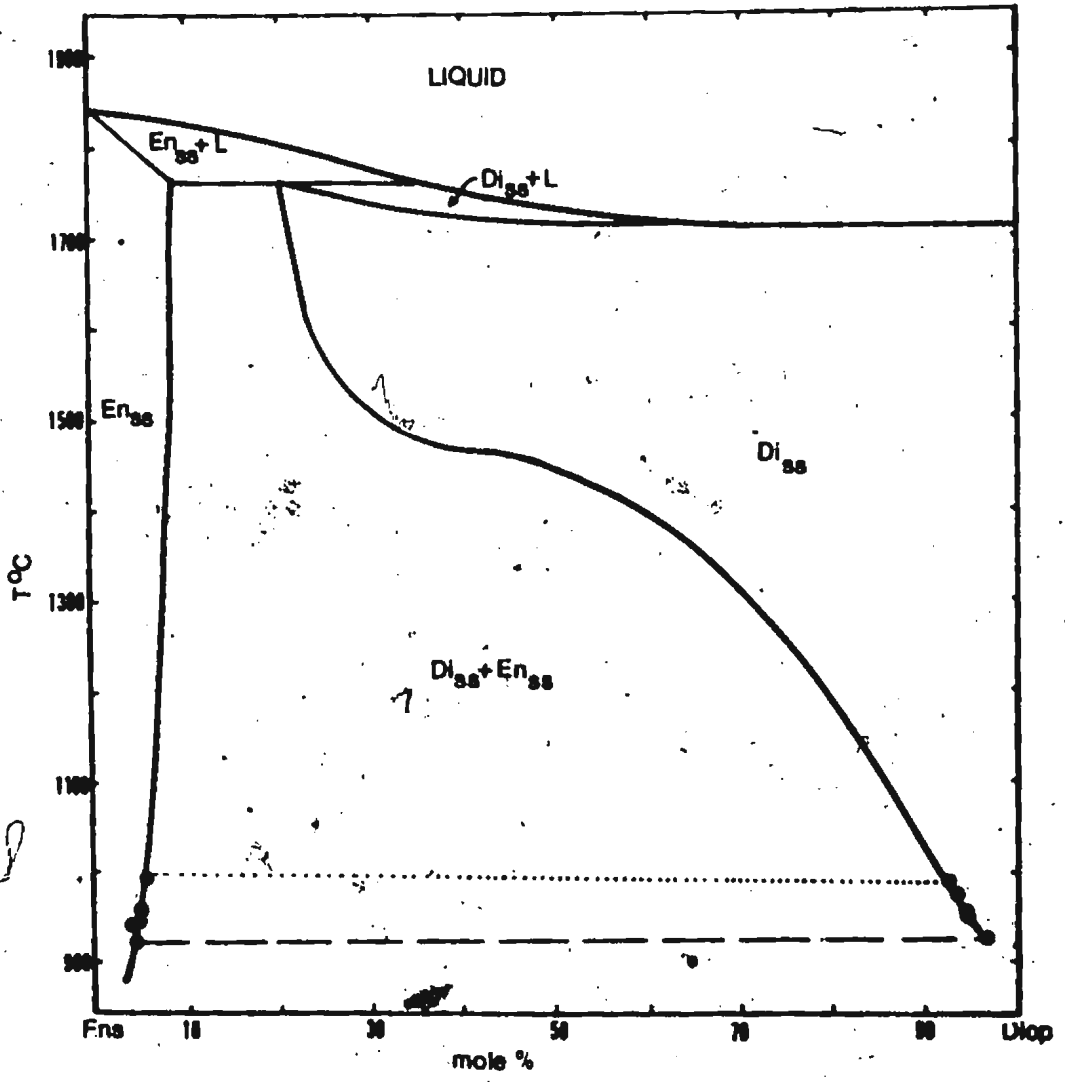


Figure VIg: PT equilibration estimates for clinopyroxenes
from lherzolites -- O'Hara (1967):

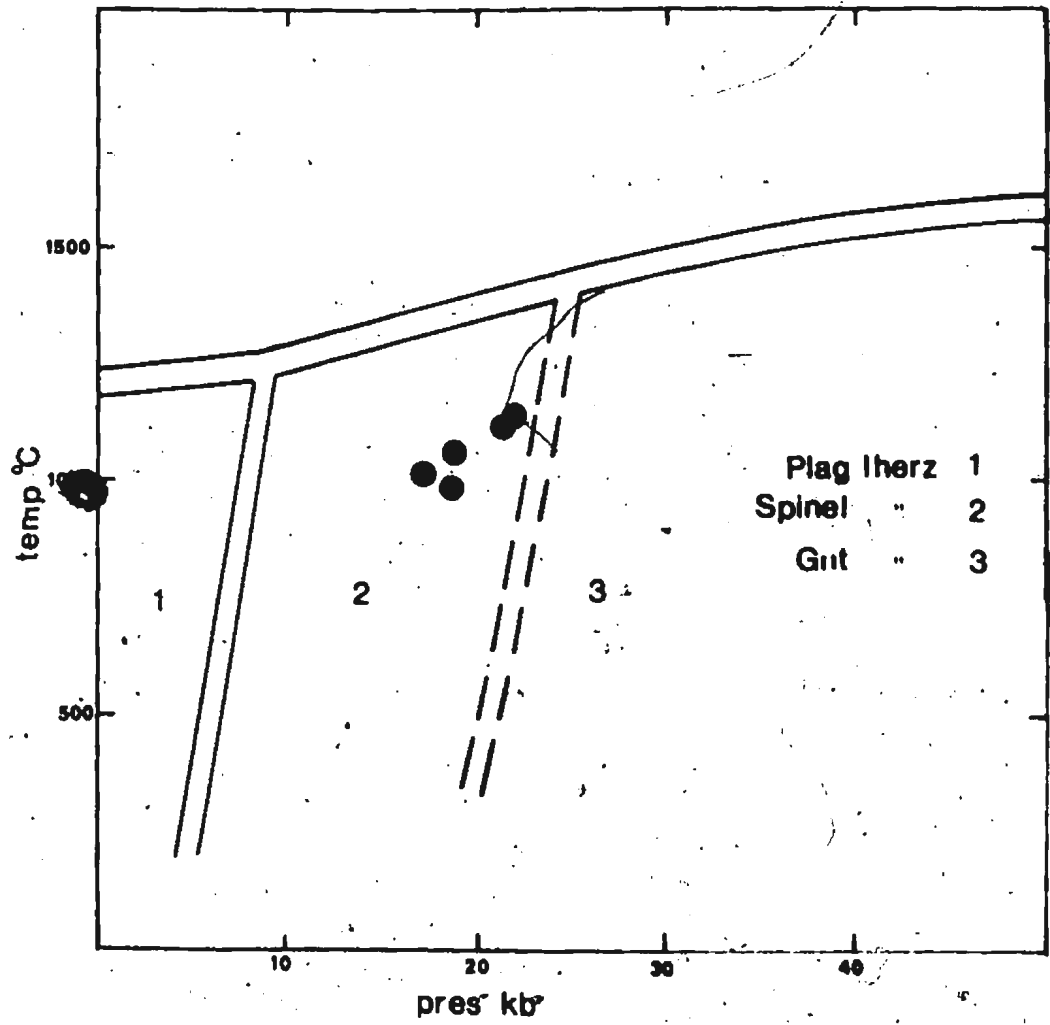


TABLE XIII

Temperature parameters and estimated temperatures
for coexisting pyroxenes (Wood and Banno, 1973)

#	a Mg ₂ Si ₂ O ₆ opx	a Mg ₂ Si ₂ O ₆ cpx	Temp°C	*Pressure
185	0.713	0.095	1120	--
186	0.781	0.064	1040	--
187	0.756	0.039	968	--
189	0.782	0.110	1140	--
320	0.764	0.075	1070	--
V12	0.687	0.054	1006	18-20 kb
V13	0.644	0.036	968	17-19 kb
V13	0.646	0.031	945	18-20 kb

* (Where in equilibrium with an aluminous phase)

Calculated after MacGregor (1974)
Wood (1974)

orthopyroxenes and clinopyroxenes (Wood and Banno, 1973) similar temperatures are indicated. Temperature estimates for the harzburgites are also possible by this method, which does not depend on an accompanying aluminous phase. With these temperatures the curves of Wood (1974) and MacGregor (1974), based on Al^{2+} substitution in M_1 sites of orthopyroxenes coexisting with an aluminous phase, give pressures of 17-20 kbs for the herzolites.

Thus all methods give relatively consistent temperatures and pressures of re-equilibration of about 1000°C and 18-20 kbs. This corroborates the textural evidence for a certain amount of subsolidus recrystallisation (Chapter V).

vi) Spinel group

Chrome spinel occurs disseminated throughout the harzburgites where it represents a residual phase, and in the dunites where it is generally an intercumulus phase forming about 1 percent of the rock. Small concentrations of cumulate chromite occur as thin streaks or layers in the dunites, but concentration is not common in the harzburgites, except possibly on the Lewis Hills (A. R. Berger, pers. comm.). On North Arm Mountain, Blow me down Mountain and the Lewis Hills, concentrated deposits of euhedral chromite have been recognised at the base of the dunite zone. In the Stowbridge deposits, the largest concentrations of chromite on North Arm Mountain, (Fig. IIIb), the chromite concentrations lie about 500 m stratigraphically below the critical zone. Similar lenses of chromite occur 300-600 m below the critical zone on Blow me down Mountain.

Chromite in the harzburgites occurs as variably resorbed to euhedral crystals. In the dunites, the disseminated chromite is rarely euhedral and

is generally found enclosing olivine as an intercumulus phase. Spinel is also found in the hercynites as subhedral to anhedral crystals which are often deformed and flattened (Malpas, 1973). The spinels not only show differences in textures but also colour differences related to chemical composition. The harzburgite spinels are red-brown or brown-green translucent. In the dunites an opaque to deep-red chromite is common and looks very much like the cumulus chromite of stratiform intrusions (Irvine and Findlay, 1972). Spinel from the hercynites are characteristically grass-green to olive-green.

Electron microprobe analyses of 17 spinels are given in Table XIV. The iron was determined as total Fe^{2+} and then recalculated on the assumption that the overall $RO:R_2O_3$ ratio is 1:1. The validity of this method has been discussed by Stevens (1944) and Irvine (1965). The spinel end members have been calculated according to the method of Irvine (1965) and end member proportions are plotted in the Johnson spinel prism in Figure VIh.

All analyses plot close to the spinel, hercynite, chromite, picrochromite plane. Projection of these data points onto the two planes expressing $Cr/(Cr+Al)$ vs $Mg/(Mg+Fe^{2+})$ and $Fe^{3+}/(Cr+Al+Fe^{3+})$ vs $Mg/(Mg+Fe^{2+})$ show a number of features. Most importantly, the spinels show a large variation in composition, especially with regards to $Cr/(Cr+Al)$. Generally the $Mg/(Mg+Fe^{2+})$ ratio increases as the $Cr/(Cr+Al)$ ratio decreases. This has been shown to be the general case for alpine peridotites (Irvine, 1967; Himmelberg and Coleman, 1968; Loney et al., 1971). The harzburgite spinels show distinctly higher Cr^{3+} than those of the dunites. They also show correspondingly (although only slightly) lower $Mg/(Mg+Fe^{2+})$. In general the dunite spinels contain more iron in the Fe^{3+} state than those of the harzburgite. Spinel

Table XIV: Spinels from Bay of Islands Complex

	Dunite				Harzburgite		
	195A D	195B D	196 D	194 D	192 H	181 H	182 H
SiO ₂	0.0	0.0	0.0	0.0	0.10	0.50	0.0
TiO ₂	0.36	0.43	0.51	0.43	0.11	0.11	0.05
Al ₂ O ₃	32.05	31.19	29.09	30.62	8.55	7.78	33.61
Cr ₂ O ₃	33.74	34.02	34.06	34.04	61.18	61.29	33.45
Fe ₂ O ₃	4.88	5.20	6.10	5.46	2.04	1.93	2.52
FeO	14.04	14.33	16.42	14.90	17.51	16.39	13.31
MnO	-	-	-	-	-	-	-
MgO	15.36	15.09	13.10	14.38	10.36	10.39	15.06
CaO	-	-	0.10	-	0.12	-	-
Na ₂ O	-	-	0.02	-	-	0.04	0.03
K ₂ O	-	-	-	-	-	-	-
NiO	-	-	0.47	0.45	0.04	0.47	0.40
TOTAL	100.44	100.27	99.79	100.29	99.82	98.46	98.44
Usp	0.79	0.95	1.13	0.95	0.24	0.28	0.11
Chr	32.71	33.34	39.03	34.97	48.24	45.75	32.66
MgChr	6.14	6.11	1.37	4.77	32.17	31.53	6.31
Sp	55.14	54.03	51.55	53.42	16.79	15.60	58.50
Her	-	-	-	-	-	-	-
Mgf	5.32	5.94	6.90	6.30	2.57	1.83	2.40
Mt	-0.32	-0.38	-0.00	-0.43	-	-	-

Usp = ulvospinel; Chr = chromite; MgChr = magnesiocromite; Sp = spinel; Her = hercynite; Mgf = magnesioferrite; Mt = magnetite. End member calculated according to the method of Irvine (1965).

Table XIV (Continued)

Harzburgite

	186 H	190 H	188 H	184 H	185 H	183 H	187 H
SiO ₂	0.0	0.03	0.10	0.08	0.06	0.07	0.04
TiO ₂	0.12	0.14	0.15	0.02	0.0	0.10	0.12
Al ₂ O ₃	27.01	13.00	18.93	25.56	25.98	18.84	21.20
Cr ₂ O ₃	42.56	54.10	50.54	45.23	43.38	51.36	47.98
Fe ₂ O ₃	1.30	0.0	1.66	0.45	1.07	0.83	1.71
FeO	15.32	20.94	15.79	13.83	15.81	15.40	14.66
MnO	-	-	-	-	-	-	-
MgO	13.36	11.34	12.49	14.28	13.04	12.49	13.25
CaO	-	0.01	-	0.03	-	0.02	-
Na ₂ O	0.08	-	-	-	-	-	-
K ₂ O	-	-	-	-	-	-	-
NiO	0.34	0.40	0.41	0.48	0.37	0.57	0.40
TOTAL	100.10	99.96	100.09	99.98	99.72	99.68	99.37
Usp	0.27	0.32	0.35	-0.00	0.0	0.20	0.28
Chr	38.39	44.24	40.15	34.50	39.90	39.72	37.33
MgChr	12.64	24.95	22.47	19.44	12.22	24.11	21.53
Sp	48.38	24.83	35.04	45.54	46.64	34.98	38.55
Her	-	-	-	-	-	-	-
Mgf	0.31	6.03	1.97	0.51	1.22	0.97	2.00
Mt	-	0.38	-	-	-	-	-0.01

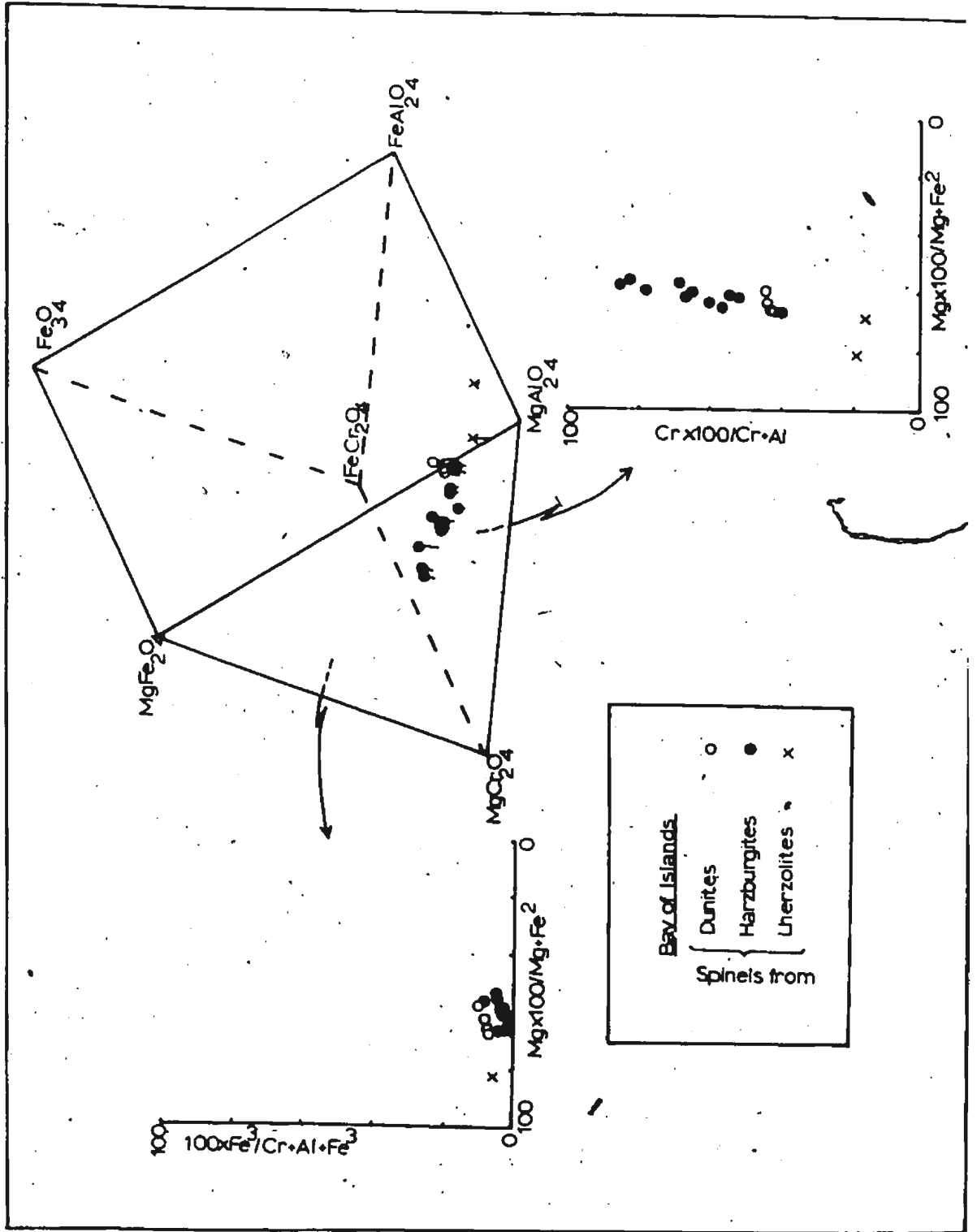
Usp = ulvospinel; Chr = chromite; MgChr = magnesiochromite; Sp = spinel; Her = hercynite; Mgf = magnesioferrite; Mt = magnetite. End member calculated according to the method of Irvine (1965).

Table XIV (Continued)

	Harzburgite	Lherzolite	
	189 H	V12 L	V13 L
SiO ₂	0.06	0.0	0.0
TiO ₂	0.14	0.10	0.0
Al ₂ O ₃	17.22	54.32	53.34
Cr ₂ O ₃	51.27	13.35	16.81
Fe ₂ O ₃	2.18	0.32	5.04
FeO	17.54	14.28	7.32
MnO	-	-	-
MgO	11.10	17.19	17.86
CaO	-	-	0.02
Na ₂ O	-	-	-
K ₂ O	-	-	-
NiO	0.38	-	-
TOTAL	99.90	99.57	100.41
Usp	0.33	0.20	-0.03
Chr	45.83	14.06	18.77
MgChr	18.80	0.0	1.47
Sp	32.42	68.34	79.78
Her	-	17.07	-
Mgf	2.64	0.0	-
Mt	-0.04	0.31	-

Usp = ulvospinel; Chr = chromite; MgChr = magnesiochromite; Sp = spinel; Her = hercynite; Mgf = magnesioferrite; Mt = magnetite. End member calculated according to the method of Irvine (1965).

Figure VIh: Plot of spinel compositions after recalculations of end members.



4

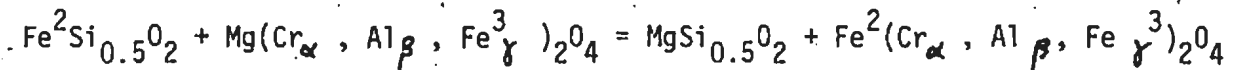
from the herzolite, V13, tentatively recognised as ceylonite by Church (1972) does not have sufficient Fe^{2+} substitution for Mg^{2+} to be considered such chemically, although that from V12 does have a $\text{Mg}/\text{Mg}+\text{Fe}^{2+}$ ratio within the limits for pleonaste spinels (Deer et al., 1962). However, these spinels are highly aluminous by comparison with other spinels from the harzburgites. It is notable that the Cr_2O_3 in the clinopyroxenes of the herzolites probably accounts for much of the bulk rock Cr_2O_3 .

Irvine and Findlay (1972) suggested a correlation between chromite cell size and calcium content of the bulk rock, as a result of a reaction between liquid and chromite to produce a more aluminous spinel and clinopyroxene. Loney et al. (1971) similarly suggest that the different compositions of the chrome spinels in alpine peridotites are not a result of different conditions of crystallisation, but reflect differences in original bulk rock composition. Malpas and Strong (1975) have suggested that differences in environment of crystallisation may, however, account for much of the variation in the Bay of Islands spinels, in as much as Cr^{3+} is concentrated in residual phases (Dickey and Yoder, 1972; Burns, 1973).

vii) Coexisting olivine and chromian spinel

Cation distribution between coexisting olivine and chromian spinel has been discussed by Irvine (1965), Jackson (1969) and Loney et al. (1971).

The Mg- Fe^{2+} exchange reaction can be written:



where $\alpha + \beta + \gamma = 1$, and are fractions of trivalent cation in chromian spinel.

Irvine (1965) and Jackson (1969) have shown that the thermodynamic equilibrium distribution coefficient (K) for this exchange reaction is given by:

$$K = \frac{x_{Mg}^{O1} \cdot x_{Fe^{2+}}^{chr}}{x_{Fe^{2+}}^{O1} \cdot x_{Mg}^{chr}}$$

where x_{Mg}^{O1} and $x_{Fe^{2+}}^{O1}$ are the mole fractions of the end members of $MgSi_{0.5}O_2$ and $FeSi_{0.5}O_2$ in olivine, and x_{Mg}^{chr} and $x_{Fe^{2+}}^{chr}$ are the fractions of divalent cations in chromian spinel.

Jackson (1969) developed the following equation for determination of temperature (in °K):

$$T^{\circ} = \frac{5580\alpha + 1018\beta - 1720\gamma + 2400}{0.90\alpha + 2.56\beta - 3.08\gamma - 1.47 + 1.987 \ln K}$$

K values and estimated temperatures for coexisting chrome spinels and olivines are presented in Table XV. Temperatures are of the order of 1300°C in the harzburgites and 1200°C in the dunites, up to 300°C higher than previous temperature estimates. The range of temperature estimates may not, however, be so significant and represents small analytical errors and estimates in recalculation of results. For temperature calculations Fe^{2+} was taken as total iron for the olivines. Jackson (1969) estimates that variations of up to $\pm 300^{\circ}C$ are possible when errors in spinel free-energies alone are considered.

viii) Plagioclase

The plagioclase of the gabbroic rocks occurs as twinned, subhedral crystals that range from 2 to 4 mm in greatest dimension. The crystals appear unaltered in thin section and are unzoned. Confirmation of the lack of zoning was obtained by scanning the crystals for Ca and Na

Table XV

Coexisting Spinels and Olivines

Specimen #	Rock type	K	T°C
196	Dunite	5	1291
195 A	"	5	1314
195 B	"	5	1318
194	"	5	1263
192 A	Harzburgite	10	1418
192 B	"	10	1408
190 A	"	9	1382
190 B	"	8	1394
189	"	8	1263
188	"	7	1336
187	"	6	1433
186	"	6	1237
185	"	7	1204
182	"	5	1140
181 A	"	9	1458
181 B	"	10	1460

(Fig. VII). Analyses of nine plagioclases from the gabbros of Blow me down Mountain and critical zone of North Arm Mountain are given in table XVI and plotted in figure VIj. The composition of these plagioclases varies from An_{66} to An_{83} and there is negligible potassium. However, the variation does not seem correlative with distance from the critical zone. This lack of correlation between composition and position within the layered gabbro sequence may indicate that rather than crystallising from a single large differentiating magma body, rejuvenation of the magma by fresh intrusions led to a number of cyclic units. Banding is not everywhere well developed in the gabbro and it is often difficult to relate mineralogical differences with position. However, with the few analyses available a tentative suggestion may be made that a number of cyclic units are represented, with compositions ranging from about An_{80} at the base of the cycles to An_{65} at the top (Table XVII). This suggestion must await confirmation by analysis of more closely spaced samples.

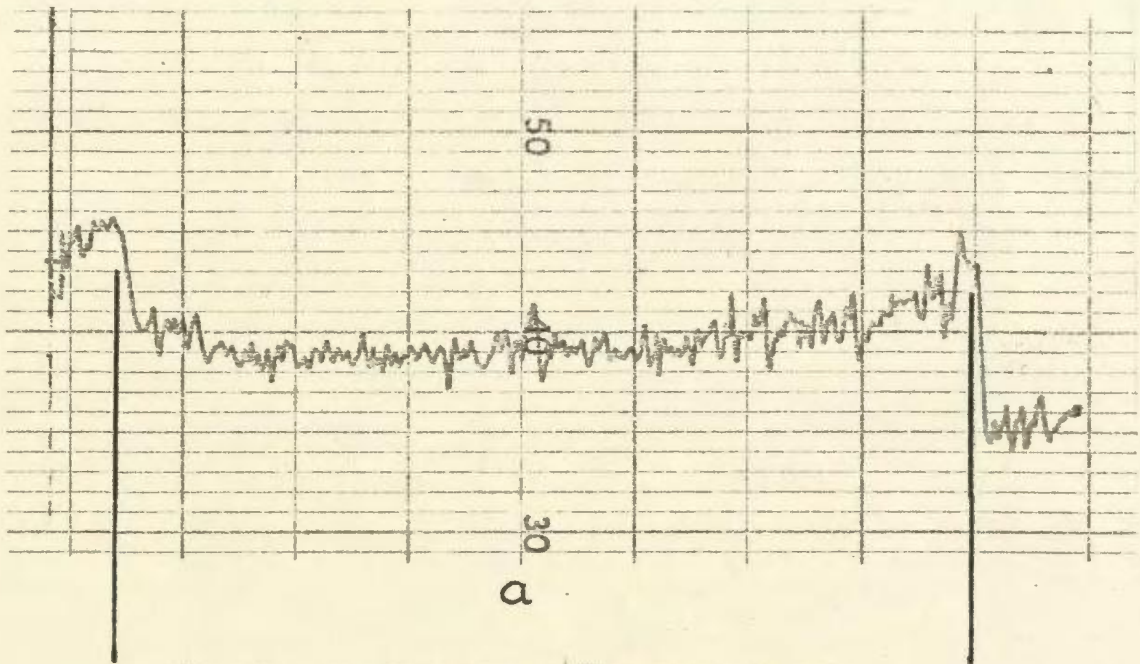
B. Bulk Rock Chemistry.

Chemical analyses of samples from the ophiolite suite are given in Tables XVIII-XXIII. The major oxides were determined by Atomic Absorption Spectrometry and the trace elements by X-ray fluorescence Spectrometry. Precision and accuracy of analyses are given in Appendix III. The variation in degree of serpentinisation of the ultramafic rocks results in variations of H_2O content which makes it difficult to compare chemical analyses. Interpretation of the analyses is also complicated by the possibility that serpentinisation may have removed major constituents. Recent literature tends to suggest, however, that this is not generally the case (Green, 1964;

Figure VII: X-ray scans of plagioclases in gabbros --

a) Na

b) Ca



CRYSTAL MARGINS. Plagioclase 206.

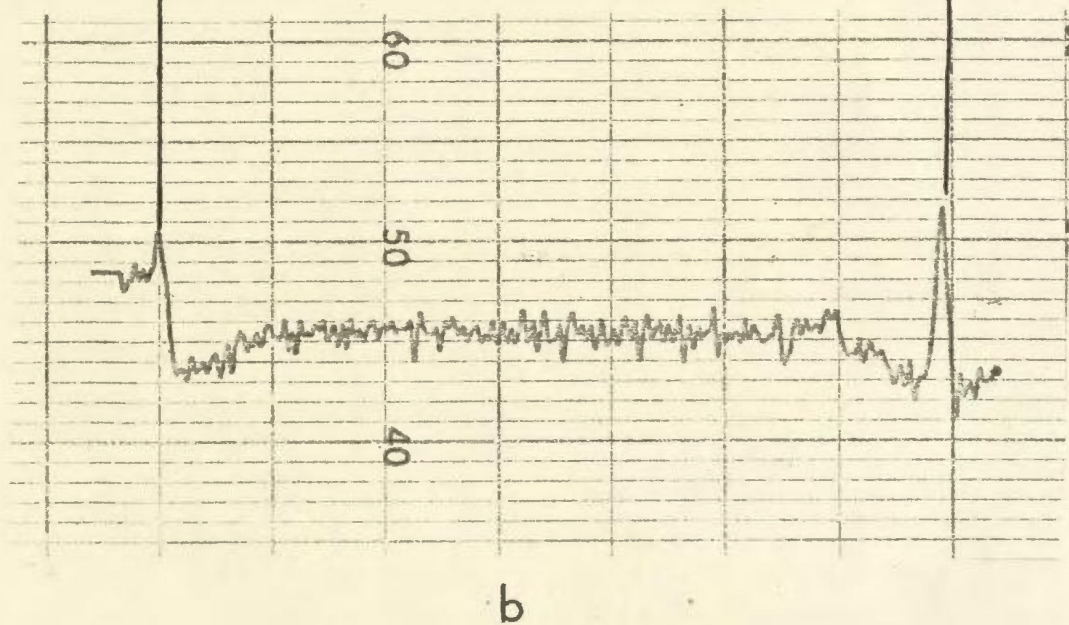


TABLE XVI

Plagioclases from Bay of Islands Gabbros

		Blow me down Mtn. Gabbros								N.A. Mtn. C.Z.
		198	199A	199B	200A	200B	201	204	205	271
	SiO ₂	47.73	51.61	53.22	48.50	47.93	48.15	52.67	51.85	45.37
	TiO ₂	0.05	0.08	0.07	0.05	0.05	0.05	0.04	0.03	0.00
	Al ₂ O ₃	33.03	30.87	31.11	33.18	32.79	33.75	30.93	32.42	33.10
	FeO	0.38	0.55	0.44	0.24	0.20	0.42	0.14	0.20	0.32
	MnO	0.00	0.00	0.00	0.00	0.00	0.00	0.00	0.00	0.03
	MgO	0.03	0.02	0.03	0.02	0.00	0.04	0.00	0.00	0.00
	CaO	16.26	13.75	13.62	16.21	16.10	16.95	13.34	14.29	19.10
	Na ₂ O	2.43	4.03	4.12	2.60	2.56	2.00	4.21	3.28	2.43
	K ₂ O	0.02	0.03	0.07	0.04	0.04	0.03	0.03	0.03	0.00
Structural Formula	Si	8.772	9.326	9.429	8.823	8.822	8.725	9.436	9.192	8.419
	Ti	0.007	0.011	0.009	0.007	0.007	0.007	0.005	0.004	0.00
	Al	7.158	6.577	6.499	7.117	7.116	7.211	6.534	6.843	7.242
	Fe ²⁺	0.058	0.083	0.065	0.037	0.031	0.064	0.021	0.030	0.050
	Mn	0.000	0.000	0.000	0.000	0.000	0.000	0.000	0.000	0.005
	Mg	0.008	0.005	0.008	0.005	0.000	0.011	0.000	0.000	0.000
	Ca	3.203	2.663	2.586	3.160	3.176	3.291	2.561	2.741	3.798
	Na	0.866	1.412	1.416	0.917	0.914	0.703	1.463	1.139	0.874
K	0.005	0.007	0.016	0.009	0.009	0.007	0.007	0.007	0.000	
Feldspar Com- position	An	79.60	66.56	65.70	78.34	78.48	83.10	64.90	71.74	82.17
	Ab	20.29	33.27	33.90	21.43	21.28	16.72	34.93	28.08	17.83
	Or	0.12	0.17	0.40	0.23	0.23	0.18	0.17	0.18	0.00

TABLE XVII

An contents of plagioclases from North Arm Mountain
according to stratigraphic position

TOP	198	An ₇₉	}	Proposed cycle 3 (?)
	199	An ₆₆		
	200	An ₇₈	}	Proposed cycle 2 (?)
	201	An ₈₃		
	204	An ₆₅	}	Proposed cycle 1 (?)
BOTTOM	205	An ₇₂		

Figure VIj: Composition of plagioclases from gabbro.

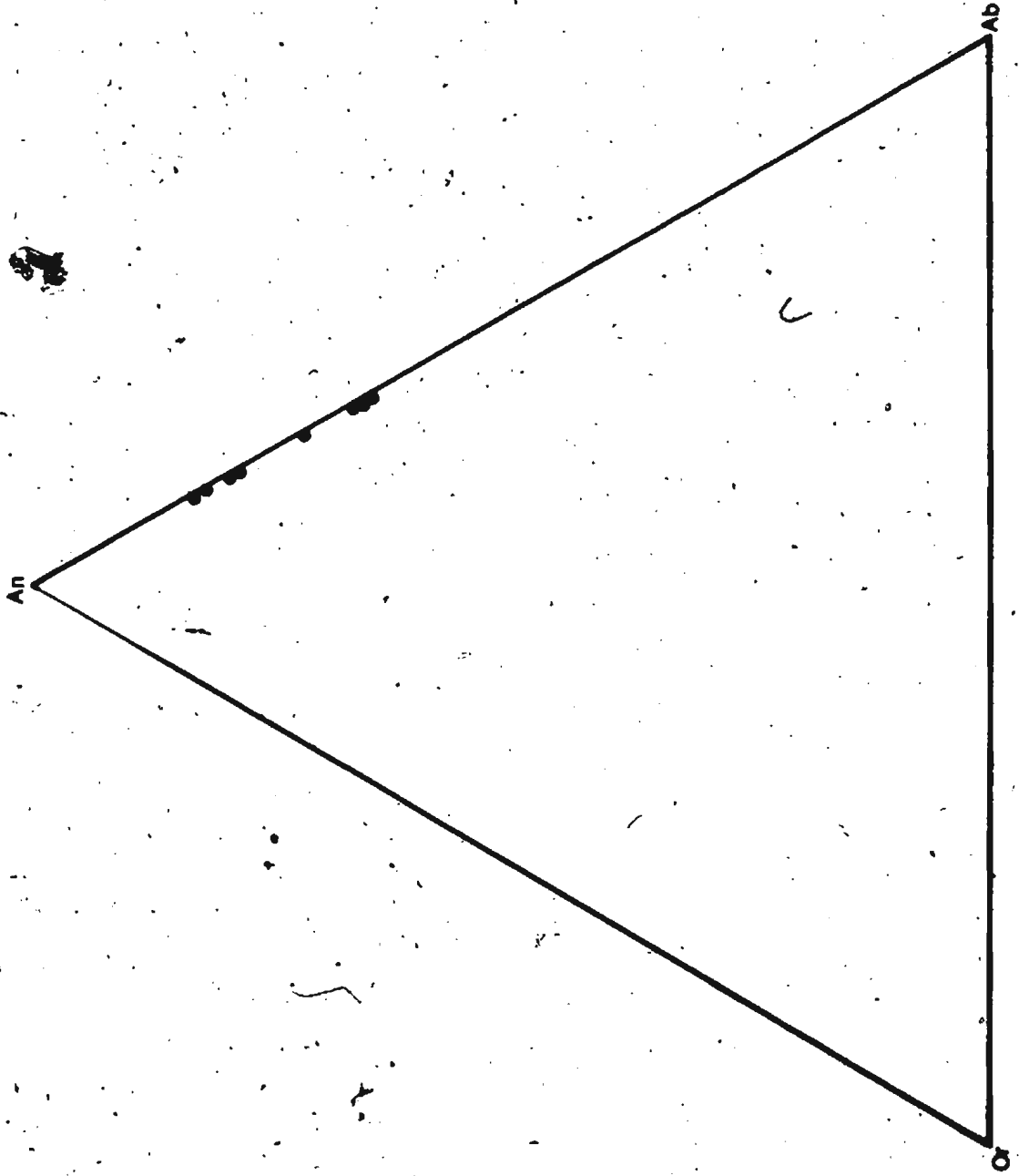


TABLE XVIII

ANALYSES OF LIHERZOLITES FROM TABLE MTH.,
BAY OF ISLANDS COMPLEX

%	V1271	V1371	V1471	V1571	V1671
SiO ₂	37.70	38.34	42.49	38.89	39.25
TiO ₂	0.00	0.21	0.30	0.00	0.31
Al ₂ O ₃	1.63	4.50	3.14	2.21	2.40
Fe ₂ O ₃	1.51	1.70	1.73	1.80	1.90
FeO	5.07	8.13	5.89	5.84	5.39
MnO	0.12	0.10	0.11	0.11	0.11
MgO	37.70	31.20	34.80	36.00	37.76
CaO	1.02	4.00	3.00	2.06	2.70
Na ₂ O	0.04	0.21	0.10	0.13	0.09
K ₂ O	0.00	0.60	0.00	0.03	0.00
P ₂ O ₅	0.00	0.05	0.05	0.00	0.05
Ign.	13.46	11.30	9.00	11.02	10.20
TOTAL	98.25	100.34	100.61	98.09	100.16

ppm					
Zr	nd	33	9	nd	2
Sr	nd	77	16	7	2
Rb	9	15	11	12	11
Zn	51	72	53	55	55
Cu	10	32	24	14	17
*Ni	0.33	0.21	0.28	0.29	0.30
*Cr	0.19	0.12	0.17	0.18	0.17
Ba	82	182	85	76	77

*Ni and Cr in %

wt. %					
Or	0.00	3.98	0.00	0.20	0.00
Ab	0.40	2.00	0.92	1.26	0.85
An	5.03	10.74	8.86	6.16	6.83
(Wo)	0.39	4.67	2.94	2.33	3.22
Di	0.32	3.55	2.34	1.86	2.59
(Fs	0.03	0.63	0.26	0.21	0.25
(Ens	19.87	3.50	2.51	17.61	12.60
Hy	1.76	0.62	3.07	2.00	2.21
(Fo	63.45	56.22	45.39	58.64	62.63
Ol	6.19	11.05	5.58	7.33	6.62
Hg	2.56	2.44	2.37	2.50	2.42
Ilm	0.00	0.45	0.62	0.00	0.65
Ap	0.00	0.13	0.13	0.00	0.13
TOTAL	100.00	99.98	99.99	100.00	100.00

For normative analyses Fe₂O₃ recalculated to 1.5%.

nd: not detected
- : not determined

TABLE XIX

Analyses of Harzburgites from Bay of Islands Complex

%	JM115	JM120	JM122	JM124	JM181	JM182	JM183
SiO ₂	35.76	40.00	56.47	39.53	34.20	38.20	35.33
TiO ₂	0.40	0.39	0.08	0.11	0.02	0.04	0.07
Al ₂ O ₃	0.38	0.38	0.49	0.60	0.20	0.60	0.40
Fe ₂ O ₃	2.15	3.04	1.10	3.10	3.13	2.93	2.61
FeO	4.30	5.73	4.10	4.80	4.22	4.80	5.01
MnO	0.10	0.10	0.06	0.10	0.11	0.12	0.11
MgO	37.50	39.00	27.20	38.40	41.50	40.80	41.50
CaO	0.80	0.80	1.00	1.30	0.00	0.70	0.00
Na ₂ O	0.01	0.01	0.01	0.02	0.00	0.00	0.00
K ₂ O	0.00	0.00	0.00	0.00	0.02	0.02	0.02
P ₂ O ₅	0.10	0.15	0.05	0.05	0.00	0.03	0.00
Ign.	16.91	11.37	9.80	12.10	14.54	11.30	13.53
TOTAL	98.41	100.97	100.36	100.11	97.94	99.54	98.58

ppm

Nb	-	-	-	-	nd	4	nd
Zr	10	nd	nd	11	11	11	14
Sr	626	613	597	681	699	635	671
Rb	10	11	10	12	7	15	6
Zn	54	50	51	55	49	61	60
Cu	nd	14	5	12	nd	nd	nd
*Ni	0.36	0.36	0.34	0.35	0.34	0.32	0.33
*Cr	0.16	0.17	0.19	0.18	0.51	0.23	0.18
La	-	-	-	-	nd	nd	35
Ba	68	69	72	70	26	9	19

*Ni and Cr in %

wt. %

Qtz	0.00	0.00	13.29	0.00	0.00	0.00	0.00
Or	0.00	0.00	0.00	0.00	0.14	0.13	0.14
Ab	0.10	0.09	0.09	0.19	0.00	0.00	0.00
An	1.22	1.11	1.43	1.76	0.00	1.80	0.00
Ne	0.00	0.00	0.00	0.00	0.00	0.00	0.00
Cor	0.00	0.00	0.00	0.00	0.21	0.00	0.45
(Wol	1.19	0.94	1.54	2.18	0.00	0.90	0.00
Di(Ens	0.97	0.74	1.25	1.74	0.00	0.73	0.00
(Fs	0.08	0.09	0.10	0.19	0.00	0.07	0.00
Hy(Ens	19.04	24.74	73.51	22.23	4.18	14.90	8.04
(Fs	1.49	2.90	6.09	2.38	0.37	1.43	0.73
(Fo	66.32	58.23	0.00	59.48	84.19	70.07	79.87
(Fa	5.70	7.52	0.00	7.01	8.24	7.41	8.04
Ol(Ln	0.00	0.00	0.00	0.00	0.00	0.00	0.00
Mg	2.67	2.43	2.40	2.48	2.62	2.47	2.57
Ilm	0.93	0.83	0.17	0.24	0.05	0.09	0.16
Ap	0.29	0.39	0.13	0.13	0.00	0.00	0.00
TOTAL	100.00	100.01	100.00	100.01	100.00	100.00	100.00

For normative analyses Fe₂O₃ recalculated to 1.5%.

nd: not detected

- : not determined

Table XIX (Continued)

%	JM184	JM185	JM186	JM187	JM188	JM189	JM190
SiO ₂	36.83	37.54	36.74	37.93	37.33	37.69	36.13
TiO ₂	0.02	0.07	0.02	0.07	0.07	0.09	0.02
Al ₂ O ₃	0.60	0.60	0.40	0.60	0.40	0.40	0.30
Fe ₂ O ₃	2.30	3.01	2.51	3.61	2.96	2.41	2.25
FeO	5.49	4.56	4.56	3.91	4.62	5.17	4.92
MnO	0.10	0.11	0.12	0.11	0.12	0.11	0.11
MgO	40.80	41.03	30.43	42.53	41.03	41.50	43.45
CaO	0.70	0.60	0.30	0.60	0.50	0.60	0.30
Na ₂ O	0.00	0.00	0.00	0.00	0.00	0.00	0.00
K ₂ O	0.02	0.02	0.02	0.02	0.02	0.02	0.02
P ₂ O ₅	0.01	0.00	0.04	0.00	0.00	0.05	0.00
Ign.	11.30	11.84	13.94	10.76	13.37	13.09	13.74
TOTAL	98.17	99.38	98.09	100.14	100.42	101.13	101.24

ppm							
Nb	-	4	3	nd	nd	nd	nd
Zr	12	11	11	13	10	16	13
Sr	671	677	663	683	687	664	704
Rb	6	5	16	2	13	13	10
Zn	49	51	52	54	52	56	47
Cu	nd	12	nd	nd	nd	6	nd
*Ni	0.42	0.31	0.33	0.33	0.33	0.31	0.31
*Cr	0.15	0.24	0.22	0.25	0.21	0.25	0.19
La	-	nd	nd	nd	13	nd	nd
Ba	22	23	16	16	20	6	24

*Ni and Cr in %

wt. %							
O ₂	0.00	0.00	0.00	0.00	0.00	0.00	0.00
Of	0.14	0.14	0.14	0.13	0.14	0.13	0.14
Ab	0.00	0.00	0.00	0.00	0.00	0.00	0.00
An	1.83	1.81	1.23	1.77	1.19	1.18	0.87
Ne	0.00	0.00	0.00	0.00	0.00	0.00	0.00
Cor	0.00	0.00	0.00	0.00	0.00	0.00	0.00
(Ho)	0.91	0.67	0.23	0.66	0.70	0.93	0.35
Di (Ens)	0.74	0.54	0.18	0.53	0.56	0.75	0.28
(Fs)	0.07	0.05	0.02	0.05	0.05	0.07	0.02
Hy (Ens)	10.23	12.92	17.68	10.08	12.99	12.48	4.07
(Fs)	0.98	1.19	1.55	0.90	1.20	1.12	0.33
(Fo)	74.67	72.66	69.61	75.83	73.05	73.39	83.95
Ol (Fa)	7.88	7.39	6.73	7.47	7.46	7.28	7.46
(Ln)	0.00	0.00	0.00	0.00	0.00	0.00	0.00
Mg	2.52	2.49	2.60	2.44	2.51	2.48	2.50
Ilm	0.04	0.15	0.05	0.15	0.15	0.20	0.04
Ap	0.00	0.00	0.00	0.00	0.00	0.00	0.00
TOTAL	100.01	100.01	100.02	100.02	100.00	100.01	100.01

For normative analyses Fe₂O₃ recalculated to 1.5%

Rd: not detected

- : not determined

TABLE XIX (Continued)

%	JM191	JM192	JM193	JMEN-V
SiO ₂	33.78	34.77	32.77	45.30
TiO ₂	0.07	0.02	0.04	0.00
Al ₂ O ₃	0.20	0.50	0.20	2.00
Fe ₂ O ₃	2.00	2.44	2.04	1.89
FeO	5.33	5.21	5.57	4.26
MnO	0.10	0.11	0.12	0.00
MgO	41.83	40.45	41.73	20.10
CaO	0.30	0.30	0.00	19.05
Na ₂ O	0.00	0.00	0.00	0.00
K ₂ O	0.02	0.02	0.02	0.00
P ₂ O ₅	0.00	0.00	0.01	0.00
Ign.	16.27	14.62	15.65	7.30
TOTAL	99.90	98.44	98.15	99.72

ppm

Hf	5	-	-	-
Zr	15	16	nd	-
Sr	18	nd	nd	-
Rb	16	7	7	-
Zr	51	56	55	-
Cu	nd	nd	127	-
*Ni	0.37	0.42	0.32	-
*Cr	0.39	0.37	0.47	-
La	nd	-	-	-
Ba	16	22	10	-

*Ni and Cr in. %

wt. %

Qtz	0.00	0.00	0.00	0.00
Or	0.06	0.14	0.00	0.00
Ab	0.00	0.00	0.00	0.00
An	0.58	1.56	0.00	6.02
Ilc	0.06	0.00	0.00	0.00
Cor	0.00	0.00	0.22	0.00
(Wo)	0.50	0.09	0.00	35.75
Di (En)	0.41	0.07	0.00	27.94
(Fs)	0.03	0.01	0.00	3.89
Hy (En)	0.00	6.55	0.00	0.00
(Fs)	0.00	0.62	0.00	0.00
(Fo)	87.40	79.95	88.72	19.12
Ol (Fa)	8.17	8.35	8.83	2.93
(Ln)	0.00	0.00	0.00	1.95
Hg	2.61	2.61	2.65	2.40
Ilm	0.16	0.05	0.09	0.00
Ap	0.00	0.00	0.00	0.00
TOTAL	99.98	100.00	100.51	100.00

For normative analyses Fe₂O₃ recalculated to 1.5%

nd: not detected
- : not determined

TABLE XX (Continued)

%	TMC1	TMC2	TMC3	TMC4	TMC5	TMC6
SiO ₂	36.79	34.61	33.90	40.81	35.30	48.90
TiO ₂	0.40	0.32	0.10	0.07	0.08	0.10
Al ₂ O ₃	4.98	4.76	4.80	14.10	7.10	5.10
Fe ₂ O ₃	3.13	4.00	3.80	2.30	2.98	1.01
FeO	4.69	4.10	4.00	4.70	4.43	4.38
MnO	0.11	0.12	0.11	0.10	0.11	0.10
MgO	34.10	36.07	36.01	18.01	34.10	18.16
CaO	3.21	2.13	2.60	8.76	2.46	14.30
Na ₂ O	0.10	0.10	0.10	0.60	0.15	0.19
K ₂ O	0.01	0.00	0.00	0.01	0.01	0.00
P ₂ O ₅	0.01	0.01	0.02	0.00	0.01	0.00
Ign	12.50	12.78	13.63	9.89	13.30	7.58
TOTAL	100.03	99.00	99.07	99.35	100.03	99.74

ppm:

Zr	nd	nd	nd	nd	nd	nd
Sr	nd	nd	nd	170	nd	nd
Rb	10	5	5	10	5	8
Zn	55	50	50	60	50	45
Cu	44	14	70	200	12	36
*Ni	0.19	0.23	0.21	0.014	0.16	0.031
Co	158	140	150	nd	53	nd
*Cr	0.31	0.46	0.58	0.032	0.47	0.37
V	60	52	40	87	70	20
Ba	nd	nd	nd	13	11	10

*Ni and Cr in %

wt%

Qtz	0.00	0.00	0.00	0.00	0.00	0.00
Or	0.07	0.00	0.00	0.07	0.07	0.00
Ab	0.97	0.98	0.00	5.68	1.47	1.74
An	15.01	12.22	14.85	40.00	14.02	14.15
Ne	0.00	0.87	0.54	0.00	2.76	0.00
(Wo	1.31	0.00	0.00	3.60	0.00	26.19
Di (Ens	1.05	0.00	0.00	2.71	0.00	20.55
(Fs	0.12	0.00	0.00	0.53	0.00	2.73
Hy (Ens	7.10	1.00	0.00	12.76	5.67	27.94
(Fs	0.80	0.12	0.00	2.50	0.63	3.72
Fo	62.40	72.44	73.77	29.33	64.76	0.35
Fa	7.79	8.99	9.02	5.25	7.91	0.05
Mg	2.49	2.53	2.55	2.43	2.51	2.36
Ilm	0.87	0.71	0.22	0.15	0.18	0.21
Ap	0.03	0.03	0.05	0.00	0.03	0.00
TOTAL	100.00	100.00	100.00	100.00	100.01	99.99

TABLE XXI

Analyses of Gabbros, Bay of Islands Complex

%	19872	19972	20072	20172	20272
SiO ₂	45.07	46.73	47.32	47.77	47.77
TiO ₂	0.72	nd	0.07	nd	0.78
Al ₂ O ₃	19.30	22.20	24.60	17.80	17.60
Fe ₂ O ₃	1.45	0.11	0.70	2.04	0.12
FeO	4.03	5.03	2.33	3.65	4.48
MnO	0.08	0.09	0.05	0.10	0.09
MgO	13.03	8.30	5.52	10.23	9.01
CaO	10.43	10.95	12.69	16.62	13.62
Na ₂ O	1.42	2.57	2.43	1.04	1.57
K ₂ O	nd	0.10	0.09	nd	nd
P ₂ O ₅	0.01	0.03	nd	nd	0.03
Ign.	3.62	3.38	2.00	1.19	2.93
TOTAL	99.16	99.49	97.80	100.44	98.00

ppm

Zr	21	21	47	27	21
Sr	211	232	293	191	138
Rb	9	11	7	12	11
Zn	47	50	42	49	48
Cu	55	51	55	21	120
Ni	548	154	169	139	256
Cr	94	130	103	252	668
Ba	nd	54	nd	6	11
Co	-	-	-	-	-
V	-	-	-	-	-

wt. %

Qtz	0.00	0.00	0.00	0.00	0.14
Or	0.00	0.61	0.55	0.00	0.00
Ab	12.58	22.60	21.45	8.87	13.96
An	48.46	50.66	58.36	44.26	43.05
Ne	0.00	0.00	0.00	0.00	0.00
Cor	0.00	0.00	0.00	0.00	0.00
(Wo	2.38	2.42	3.05	16.23	11.67
Di (Ens	1.84	1.72	2.41	11.73	8.99
(Fs	0.29	0.49	0.30	3.02	1.44
Hy (Ens	13.12	2.89	6.06	3.25	14.59
(Fs	2.03	0.82	0.75	0.83	2.33
Ol (Fo	13.32	11.82	4.11	7.50	0.00
(Fa	2.27	3.70	0.56	2.13	0.00
Mg	2.28	2.26	2.27	2.19	2.28
ILm	1.43	0.00	0.14	0.00	1.56
Hm	0.00	0.00	0.00	0.00	0.00
Sp	0.00	0.00	0.00	0.00	0.00
Ap	0.01	0.03	0.00	0.00	0.03
TOTAL	100.01	100.02	100.01	100.01	100.04

Fe₂O₃ recalculated as 1.5% for normative analyses

nd : not detected

TABLE XXI (Continued)

%	20372	20572	206A72	206B72	20772
SiO ₂	50.03	46.73	45.79	45.97	42.37
TiO ₂	nd	0.47	nd	0.47	0.20
Al ₂ O ₃	19.30	19.70	21.80	22.00	22.50
Fe ₂ O ₃	1.51	0.33	0.10	0.12	0.52
FeO	4.03	5.10	4.94	4.01	2.50
MnO	0.10	0.08	0.08	0.08	0.05
MgO	7.77	9.35	10.25	9.60	11.18
CaO	11.81	13.67	12.46	13.18	12.69
Na ₂ O	12.52	1.85	1.50	1.57	1.29
K ₂ O	nd	0.03	0.23	0.09	nd
P ₂ O ₅	nd	nd	0.01	0.03	0.06
Ign.	2.31	2.90	1.88	3.45	5.36
TOTAL	99.38	100.21	99.04	100.57	98.72

ppm

Zr	23	7	25	30	36
Sr	196	174	255	263	549
Rb	9	5	9	6	6
Zn	52	46	50	71	32
Cu	24	88	77	54	53
Ni	120	205	355	290	520
Cr	151	524	244	163	212
Ba	4	4	nd	nd	nd
Co	-	-	-	-	-
V	-	-	-	-	-

wt. %

Qtz	0.00	0.00	0.00	0.00	0.00
Or	0.00	0.18	1.39	0.54	0.00
Ab	21.97	16.07	13.02	13.52	11.20
An	42.60	46.56	53.42	54.67	59.53
Ne	0.00	0.00	0.00	0.00	0.26
Cor	0.00	0.00	0.00	0.00	0.00
(Wo	7.41	9.62	4.17	5.39	3.29
Di (Ens	5.13	7.04	3.09	4.01	2.73
(Fe	1.69	1.68	0.69	0.85	0.15
Hy (Ens	12.90	2.17	5.24	3.84	0.00
(Fe	4.24	0.52	1.16	0.81	0.00
Ol (Fo	1.34	10.29	12.52	11.55	18.98
(Fa	0.48	2.71	3.06	2.69	1.03
Mg	2.24	2.23	2.23	2.21	2.33
ILm	0.00	0.92	0.00	0.91	0.41
Hin	0.00	0.00	0.00	0.00	0.00
Sp	0.00	0.00	0.00	0.00	0.00
Ap	0.00	0.00	0.01	0.03	0.14
TOTAL	100.00	99.99	100.00	100.02	100.05

Fe₂O₃ recalculated as 1.5% for normative analyses

TABLE XXI (Continued)

	28571	JM289	301A71	301C71	31271	312A71
SiO ₂	45.22	47.69	48.15	48.40	47.40	47.70
TiO ₂	0.31	0.17	0.76	0.40	0.90	0.79
Al ₂ O ₃	22.20	15.00	16.06	16.10	20.30	20.91
Fe ₂ O ₃	1.05	1.79	0.84	0.97	2.07	2.31
FeO	4.10	5.67	5.51	4.78	4.07	3.98
MnO	0.09	0.13	0.12	0.10	0.10	0.10
MgO	8.50	5.00	8.94	8.70	6.80	6.73
CaO	13.60	15.40	13.22	13.60	11.90	11.49
Na ₂ O	0.75	1.16	2.44	2.50	3.20	3.22
K ₂ O	nd	0.02	0.06	0.10	0.50	0.48
P ₂ O ₅	nd	0.21	0.08	nd	0.10	0.10
Ign.	4.05	7.30	1.23	2.30	1.90	2.30
TOTAL	99.87	99.54	97.41	97.95	99.24	100.11

ppm						
Zr	25	85	33	37	72	62
Sr	187	268	185	201	267	183
Rb	4	6	5	nd	5	nd
Zn	55	65	59	71	56	70
Cu	105	18	141	136	35	57
Ni	112	63	57	71	90	110
Cr	391	189	111	138	178	203
Ba	63	65	35	35	62	54
Co	36	63	53	73	40	41
V	27	64	59	61	62	64

wt. %						
Qtz	0.00	5.24	0.00	0.00	0.00	0.00
Or	0.00	0.13	0.37	0.61	3.02	2.91
Ab	6.62	10.61	21.45	21.62	20.94	23.52
An	59.67	38.54	33.97	33.57	40.37	42.20
He	0.00	0.00	0.00	0.16	3.63	2.38
Cor	0.00	0.00	0.00	0.00	0.00	0.00
Wo	4.47	17.77	14.04	15.16	8.03	6.49
Di	3.25	9.45	9.86	10.30	5.25	4.40
Fs	0.80	7.76	3.00	3.68	2.21	1.59
Hy	15.56	4.00	2.58	0.00	0.00	0.00
Fs	3.83	3.28	0.78	0.00	0.00	0.00
Ol	2.29	0.00	7.49	8.51	8.43	8.95
Fa	0.62	0.00	2.51	3.35	3.92	3.56
Mg	2.27	2.35	2.26	2.25	2.22	2.23
ILm	0.61	0.35	1.50	0.79	1.74	1.54
Ilm	0.00	0.00	0.00	0.00	0.00	0.00
Sp	0.00	0.00	0.00	0.00	0.00	0.00
Ap	0.00	0.53	0.19	0.00	0.24	0.24
TOTAL	99.99	100.01	100.00	100.00	100.00	100.01

Fe₂O₃ recalculated as 1.5% for normative analyses

nd : not detected

- : not determined

TABLE XXI (Continued)

%	E672	E772	E972	E1272
SiO ₂	47.29	47.93	47.10	44.40
TiO ₂	0.20	0.13	0.06	0.20
Al ₂ O ₃	22.37	22.99	24.62	18.90
Fe ₂ O ₃	0.51	0.84	0.51	0.35
FeO	5.04	4.13	1.57	2.87
MnO	0.09	0.08	0.04	0.07
MgO	8.66	7.97	5.00	9.52
CaO	11.97	7.72	13.70	16.00
Na ₂ O	2.10	3.76	1.15	1.44
K ₂ O	0.08	0.59	0.20	0.12
P ₂ O ₅	nd	nd	0.05	nd
Ign.	1.46	4.00	7.30	4.90
TOTAL	99.77	100.14	101.30	98.77

ppm

Zr	27	74	59	18
Sr	217	642	502	233
Rb	5	17	6	12
Zn	54	51	39	46
Cu	109	75	17	54
Ni	134	143	93	212
Cr	243	205	137	833
Ba	28	45	61	65
Co	42	40	21	29
V	24	30	23	26

wt. %

Qtz	0.00	0.00	4.59	0.00
Or	0.48	3.62	1.26	0.75
Ab	18.06	33.07	10.34	7.11
An	52.21	39.81	65.28	47.62
Ne	0.00	0.00	0.00	3.17
Cor	0.00	2.21	0.00	0.00
(Wo	3.40	0.00	2.76	15.38
Di {	En	2.41	0.00	2.38
	Fs	0.69	0.00	1.02
Hy {	En	5.88	0.39	10.85
	Fs	1.70	0.10	0.00
01 {	Fo	9.55	14.18	0.00
	Fa	3.03	4.09	0.00
	Mg	2.21	2.26	2.28
	ILm	0.39	0.26	0.12
	Hm	0.00	0.00	0.00
	Sp	0.00	0.00	0.00
	Ap	0.00	0.00	0.12
TOTAL	100.01	99.99	99.98	99.99

Fe₂O₃ recalculated as 1.5% for normative analyses

nd: not detected
- : not determined

TABLE XXI (Continued)

%	E1672	E1772	E1872
SiO ₂	43.83	47.70	49.72
TiO ₂	0.08	0.16	0.10
Al ₂ O ₃	23.18	18.15	20.58
Fe ₂ O ₃	0.13	0.61	0.21
FeO	0.39	2.80	1.32
MnO	0.01	0.06	0.02
MgO	7.20	10.82	9.08
CaO	15.70	15.22	14.88
Na ₂ O	0.49	1.60	1.21
K ₂ O	0.26	0.07	0.43
P ₂ O ₅	0.05	nd	nd
Ign.	8.00	2.41	1.73
TOTAL	99.32	99.60	99.28

ppm

Zr	67	32	39
Sr	568	152	326
Rb	10	nd	9
Zn	28	43	31
Cu	1	124	3
Ni	126	137	160
Cr	85	731	549
Ba	174	75	123
Co	17	41	16
V	25	38	21

wt. %

Qtz	0.00	0.00	0.90
Or	1.68	0.43	2.60
Ab	4.54	13.92	10.48
An	65.98	43.32	50.63
Ne	0.00	0.00	0.00
Cor	0.00	0.00	0.00
(Wo	7.79	14.32	10.42
Di (Ens	6.73	11.63	9.00
(Fs	0.00	0.98	0.00
Hy { Ens	11.00	1.71	14.15
{ Fs	0.00	0.14	0.00
01 { Fo	1.33	10.06	0.00
{ Fa	0.00	0.94	0.00
Mg	0.00	2.24	0.30
ILm	0.02	0.31	0.19
Hm	0.61	0.00	1.33
Sp	0.18	0.00	0.00
Ap	0.13	0.00	0.00
TOTAL	99.99	100.00	100.00

Fe₂O₃ recalculated as 1.5% for normative analyses

nd: not detected

- : not determined

TABLE XXI (Continued)

%	12671	24471	24971	25871	28271	28471
SiO ₂	47.17	48.04	48.29	48.52	42.50	47.57
TiO ₂	0.37	1.91	0.84	0.74	0.26	1.43
Al ₂ O ₃	16.40	16.16	15.06	19.88	23.84	16.87
Fe ₂ O ₃	2.03	5.01	0.93	0.84	1.11	1.69
FeO	4.80	6.58	6.87	5.68	5.12	6.73
MnO	0.10	0.13	0.14	0.12	0.10	0.14
MgO	8.50	5.47	8.97	6.19	10.50	6.20
CaO	14.20	11.15	12.93	12.12	12.69	13.08
Na ₂ O	1.07	3.65	2.52	2.65	1.72	2.49
K ₂ O	nd	0.11	0.08	0.12	nd	0.00
P ₂ O ₅	0.05	0.12	nd	0.16	0.09	0.14
Ign.	1.91	1.40	0.92	2.60	2.30	1.30
TOTAL	99.55	99.73	97.55	99.62	100.23	97.64
PPM						
Zr	33	43	60	59	28	36
Sr	206	223	175	183	178	190
Rb	13	6	6	4	3	7
Zn	51	63	65	68	66	72
Cu	78	15	29	80	92	88
Ni	93	45	84	60	208	55
Cr	229	151	222	152	163	186
Ba	41	65	36	41	35	56
Co	-	84	47	40	46	60
V	-	74	60	61	30	69
wt. %						
Qtz	0.89	0.00	0.00	0.00	0.00	0.00
Or	0.00	0.66	0.49	0.73	0.00	0.00
Ab	9.57	28.31	22.05	23.09	7.32	21.87
An	42.21	27.95	30.56	43.25	58.52	36.19
Ne	0.00	1.74	0.00	0.00	4.08	0.00
Cor	0.00	0.00	0.00	0.00	0.00	0.00
(Wo	13.31	11.57	14.94	7.35	2.15	12.63
Di	8.93	5.66	9.80	4.70	1.53	7.48
(Fs	3.39	5.71	4.09	2.17	0.43	4.52
Hy	13.44	0.00	1.44	6.97	0.00	4.39
(Fs	5.10	0.00	0.60	3.21	0.00	2.65
O1	0.00	5.78	8.31	2.95	17.63	2.92
(Fa	0.00	6.42	3.82	1.50	5.41	1.94
Mg	2.30	2.22	2.25	2.24	2.22	2.26
ILm	0.74	3.70	1.65	1.45	0.50	2.82
Hm	0.00	0.00	0.00	0.00	0.00	0.00
Sp	0.00	0.00	0.00	0.00	0.00	0.00
Ap	0.12	0.28	0.00	0.38	0.21	0.34
TOTAL	100.00	100.00	100.00	99.99	100.00	100.01

Fe₂O₃ recalculated as 1.5% for normative analyses

TABLE XXII

Analyses of Diabases, Bay of Islands Complex

%	WF11071	WF112B71	WF12371	WF123A71	21172
SiO ₂	49.40	46.90	49.70	51.60	51.37
TiO ₂	0.80	0.70	1.00	1.30	1.37
Al ₂ O ₃	14.60	19.10	14.10	12.10	14.90
Fe ₂ O ₃	0.80	1.10	2.80	2.20	0.20
FeO	7.90	5.50	7.20	8.20	10.39
MnO	0.20	0.10	0.20	0.20	0.19
MgO	8.50	7.50	7.40	7.30	4.80
CaO	9.70	9.00	8.60	8.90	7.11
Na ₂ O	2.90	2.90	3.40	4.20	4.78
K ₂ O	0.10	1.80	0.10	0.10	0.38
P ₂ O ₅	0.10	0.10	0.10	0.10	nd
H ₂ O	2.90	4.40	3.30	3.20	1.53
TOTAL	97.90	99.10	97.90	99.40	97.02

ppm

Zr	70	132	81	88	91
Sr	170	633	119	67	220
Rb	6	10	5	4	14
Zn	76	66	68	74	93
Cu	22	81	4	5	50
Ni	120	79	42	52	28
Co	41	33	32	42	-
Cr	408	243	164	204	70
V	64	63	66	68	-
Ba	54	118	54	15	130

wt%

Qtz	0.00	0.00	0.00	0.00	0.00
Or	0.62	11.23	0.63	0.61	2.35
Ab	25.81	21.30	30.45	36.97	42.30
An	27.90	35.66	24.26	14.43	18.91
Ne	0.00	2.49	0.00	0.00	0.00
(Wo	9.20	4.50	8.44	12.87	7.51
Df (Ens	5.68	3.01	4.77	7.17	3.46
(Fs	2.99	1.16	3.32	5.20	3.99
Hy (Ens	12.61	0.00	11.58	6.15	3.75
(Fs	6.65	0.00	8.08	4.47	4.33
O1 (Fo	2.79	11.71	2.21	3.92	3.71
(Fa	1.62	4.99	1.70	3.14	4.71
Mg	2.29	2.30	2.30	2.26	2.27
Ilm	1.60	1.40	2.01	2.57	2.72
Ap	0.24	0.25	0.25	0.24	0.00
TOTAL	100.00	100.00	100.00	100.00	100.00

Fe₂O₃ recalculated as 1.5% for normative analysis.

nd: not detected
- : not determined

TABLE XXII (Continued)

%	21772	22172	22472	22572
SiO ₂	46.82	50.48	47.27	45.45
TiO ₂	0.60	0.90	0.96	0.90
Al ₂ O ₃	15.50	16.10	16.40	18.80
Fe ₂ O ₃	2.29	1.74	0.42	1.50
FeO	7.09	6.49	8.76	5.37
MnO	0.18	0.16	0.16	0.13
MgO	8.58	8.58	9.32	8.20
CaO	10.45	10.48	9.00	10.51
Na ₂ O	2.44	2.44	2.81	2.25
K ₂ O	1.04	0.16	1.05	1.46
P ₂ O ₅	0.10	0.05	nd	0.10
H ₂ O	2.89	2.10	3.42	3.72
TOTAL	97.98	99.68	99.57	98.39

ppm

Zr	96	74	91	70
Sr	352	268	423	385
Rb	17	13	17	18
Zn	78	80	80	66
Cu	69	98	103	87
Ni	112	208	158	191
Co	-	-	-	-
Cr	192	213	183	238
V	-	-	-	-
Ba	160	53	144	116

wt%

	Qtz	0.00	0.00	0.00	0.00
	Or	6.48	0.97	6.45	9.12
	Ab	20.77	21.10	23.97	15.77
	An	29.79	33.11	30.16	38.78
	Ne	0.53	0.00	0.40	2.36
Di	(Wo	10.37	9.07	6.77	6.73
	(Ens	6.21	5.80	4.22	4.57
	(Fs	3.61	2.69	2.14	1.65
Hy	(Ens	0.00	15.39	0.00	0.00
	(Fs	0.00	7.13	0.00	0.00
Ol	(Fo	11.42	0.45	13.94	11.93
	(Fa	7.32	0.23	7.79	4.75
	Mg	2.29	2.22	2.26	2.30
	Ilm	1.20	1.75	1.89	1.81
	Ap	0.25	0.13	0.00	0.24
TOTAL		99.99	100.04	99.99	100.01

Fe₂O₃ recalculated as 1.5% for normative analysis

nd: not detected
 - : not determined

TABLE XXII (Continued)

%	294B71	294C71	294E71	301B71
SiO ₂	49.57	46.89	49.38	47.64
TiO ₂	1.31	1.20	1.61	1.36
Al ₂ O ₃	16.08	14.60	15.26	15.88
Fe ₂ O ₃	2.04	3.80	1.50	2.84
FeO	6.70	8.04	6.25	6.52
MnO	0.16	0.20	0.13	0.14
MgO	9.00	7.00	8.20	8.49
CaO	11.50	10.50	11.50	12.34
Na ₂ O	1.35	1.76	0.93	2.70
K ₂ O	0.63	0.22	0.60	0.20
P ₂ O ₅	0.10	0.10	0.10	0.18
H ₂ O	1.70	4.78	4.10	0.68
TOTAL	100.14	99.09	99.56	98.97

ppm

Zr	62	71	70	47
Sr	218	223	239	187
Rb	8	8	8	6
Zn	79	78	71	59
Cu	39	40	13	12
Ni	95	95	121	88
Co	43	41	40	47
Cr	295	301	212	204
V	57	58	56	64
Ba	63	88	59	44

wt%

	Qtz	1.37	0.37	6.28	0.00
	Or	3.78	1.38	3.71	1.20
	Ab	11.61	15.83	8.24	22.34
	An	36.54	33.26	37.39	31.19
	Ne	0.00	0.00	0.00	0.50
Di	(Ho	8.86	8.95	9.06	12.52
	(Ens	5.59	4.59	6.06	7.76
Hy	(Fs	2.52	4.13	2.32	4.03
	(Ens	17.19	13.94	15.33	0.00
Ol	(Fs	7.75	12.57	5.87	0.00
	(Fo	0.00	0.00	0.00	9.66
	(Fa	0.00	0.00	0.00	5.52
	Mg	2.21	2.31	2.28	2.22
	Ilm	2.53	2.42	3.20	2.63
	Ap	0.24	0.25	0.24	0.43
	TOTAL	100.01	100.00	99.98	100.00

Fe₂O₃ recalculated as 1.5% for normative analysis.

nd: not detected
- : not determined

TABLE XXIII

Analyses of Volcanic Rocks, Day of Islands Complex

%	Avolc	Bvolc	Cvolc	Dvolc	Evolc	Fvolc	Gvolc
SiO ₂	45.97	47.77	49.13	49.01	48.65	48.01	47.10
TiO ₂	0.70	1.33	1.36	1.01	1.50	1.00	1.00
Al ₂ O ₃	15.00	13.60	15.00	14.10	13.93	14.68	12.91
Fe ₂ O ₃	4.74	5.66	5.53	1.90	2.96	2.98	2.71
FeO	4.61	4.05	3.84	9.10	6.30	4.89	4.97
MnO	0.51	0.14	0.16	0.30	0.20	0.15	0.15
MgO	6.13	5.55	5.95	8.53	8.78	8.45	8.10
CaO	12.00	11.27	10.82	8.70	5.60	11.13	10.91
Na ₂ O	3.35	2.90	2.81	4.60	4.90	3.00	3.12
K ₂ O	0.18	0.12	0.08	0.01	0.10	0.00	0.00
P ₂ O ₅	0.10	nd	0.05	0.15	0.20	0.10	0.10
Ign.	5.08	4.95	3.63	2.80	4.76	3.91	7.80
TOTAL	98.01	97.34	98.36	100.21	97.88	98.30	98.87
<u>PPM</u>							
Zr	108	103	132	140	156	138	111
Sr	173	168	175	203	216	169	173
Rb	12	15	11	6	4	12	6
Zn	87	84	89	83	87	79	67
Cu	77	84	93	94	97	87	94
Ni	49	115	58	121	63	41	110
Co	-	-	-	41	40	43	36
Cr	109	216	137	123	24	97	151
V	-	-	-	-	-	-	-
Ba	81	88	89	91	86	71	123
<u>wt. %</u>							
Qtz	0.00	0.00	1.23	0.00	0.00	0.00	0.00
Or	1.15	0.77	0.50	0.06	0.64	0.00	0.00
Ab	22.47	26.68	25.22	32.91	4.60	26.94	29.03
An	27.41	25.81	29.78	18.28	16.91	28.22	23.33
Ac	4.41	0.00	0.00	3.83	0.00	0.00	0.00
Ho	15.52	14.61	11.34	10.46	4.84	12.40	14.81
Di	8.42	7.83	6.36	5.88	3.05	8.13	9.69
{Fs	6.46	6.30	4.52	4.16	1.48	3.40	4.09
Hy	0.00	6.97	9.36	0.00	1.37	4.59	3.78
{Fs	0.00	5.61	6.65	0.00	0.67	1.92	1.60
{Fo	5.67	0.16	0.00	11.17	13.38	6.74	6.11
Ol	4.79	0.14	0.00	8.70	7.17	3.11	2.84
{Fa	2.35	2.36	2.31	2.23	2.34	2.31	2.39
{Hm	1.44	2.75	2.74	1.97	3.06	2.02	2.09
{Ap	0.25	0.00	0.10	0.36	0.50	0.25	0.26
TOTAL	100.36	99.99	100.11	100.52	100.01	100.03	100.02

Fe₂O₃ recalculated as 1.5% for normative analyses

nd: not detected
- : not determined

TABLE XXIII (Continued)

%	JM7C	Jm671S	JM671C	JM8S	JM8C
SiO ₂	49.21	49.09	46.04	48.00	45.50
TiO ₂	1.31	1.98	1.94	1.80	1.80
Al ₂ O ₃	15.81	14.70	14.70	14.70	15.00
Fe ₂ O ₃	2.21	2.71	4.91	3.10	4.70
FeO	7.10	5.91	5.46	6.10	5.90
MnO	0.16	0.13	0.13	0.10	0.10
MgO	8.53	5.06	5.84	5.00	5.90
CaO	11.14	9.16	11.67	9.20	11.20
Na ₂ O	2.71	5.28	3.38	5.40	3.40
K ₂ O	0.26	0.32	0.26	0.30	0.30
P ₂ O ₅	0.15	0.31	0.33	0.20	0.20
Ign.	1.30	5.60	5.60	4.30	4.60
TOTAL	99.98	100.25	100.26	98.20	98.40

ppm

Zr	201	148	127	209	183
Sr	193	258	181	253	163
Rb	8	6	6	10	12
Zn	90	83	90	83	86
Cu	110	93	93	72	76
Ni	38	36	40	50	52
Co	27	40	40	37	36
Cr	109	91	85	162	163
V	69	67	66	86	86
Ba	73	75	65	196	110

wt. %

Qtz	0.00	0.00	0.00	0.00	0.00
Or	1.56	2.00	1.63	1.89	1.89
Ab	23.25	37.30	25.11	33.60	24.11
An	30.63	16.36	25.63	15.99	26.45
Ilc	0.00	5.40	2.82	8.21	3.58
Wo	10.20	12.35	13.98	13.08	13.14
Dt	6.28	7.03	7.55	7.06	6.98
Fs	3.33	4.79	5.95	5.57	5.75
Hy	6.46	0.00	0.00	0.00	0.00
Fs	3.43	0.00	0.00	0.00	0.00
Ol	6.17	4.41	5.51	4.36	5.10
Fa	3.61	3.31	4.79	3.79	5.53
Mg	2.21	2.30	2.31	2.32	2.32
Ilm	2.52	3.98	3.91	3.65	3.65
Ap	0.35	0.76	0.81	0.50	0.50
TOTAL	100.00	99.99	100.00	100.02	100.00

Fe₂O₃ recalculated as 1.5% for normative analyses

nd: not detected
- : not determined

Hostetler et al., 1966; Barnes et al., 1967; Himmelberg and Coleman, 1968; Loney et al., 1971). Another major variation in the chemistry of the peridotite samples is the Fe_2O_3 content. This largely reflects the amount of magnetite present and this in turn is related to the degree of serpentinisation. Except in chrome spinels, Fe_2O_3 is not a major component of the primary minerals of the peridotites.

Calculation of C.I.P.W. norms was carried out after adjustments for hydration and oxidation (Fe_2O_3 recalculated as 1.5 wt. %).

The analyses have been compared on a number of standard variation diagrams.

i) Linear variation diagrams (Figs. VIK, VII)

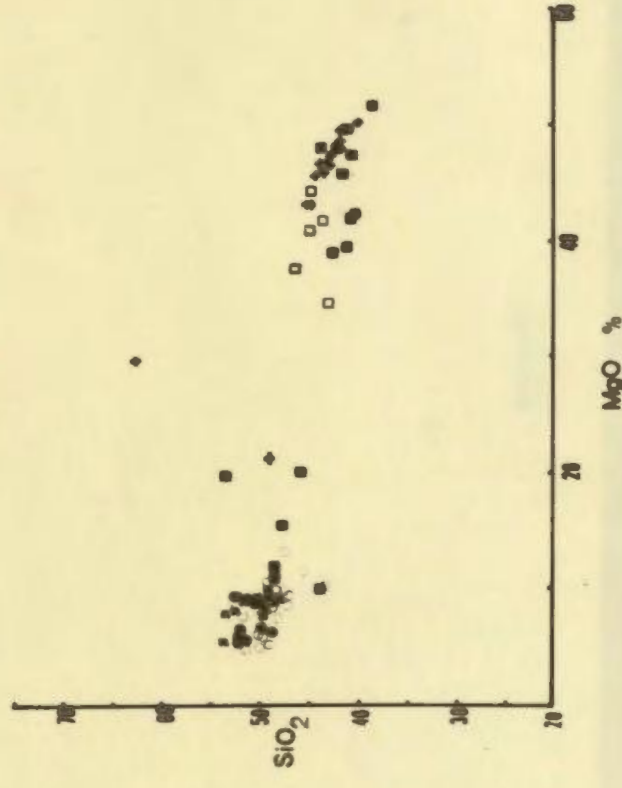
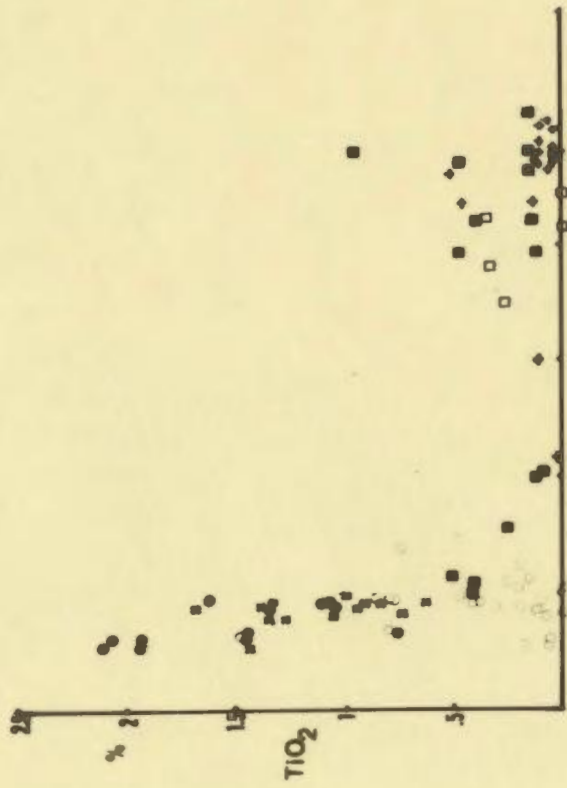
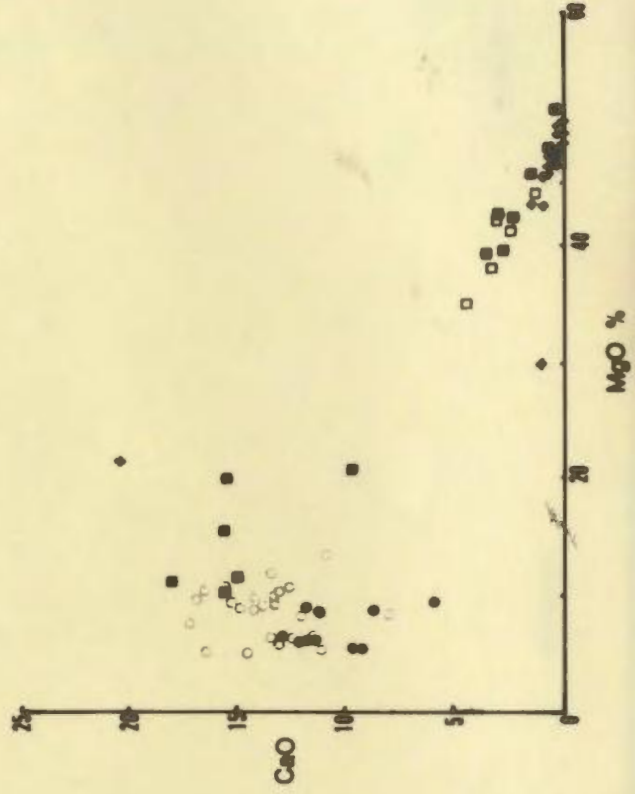
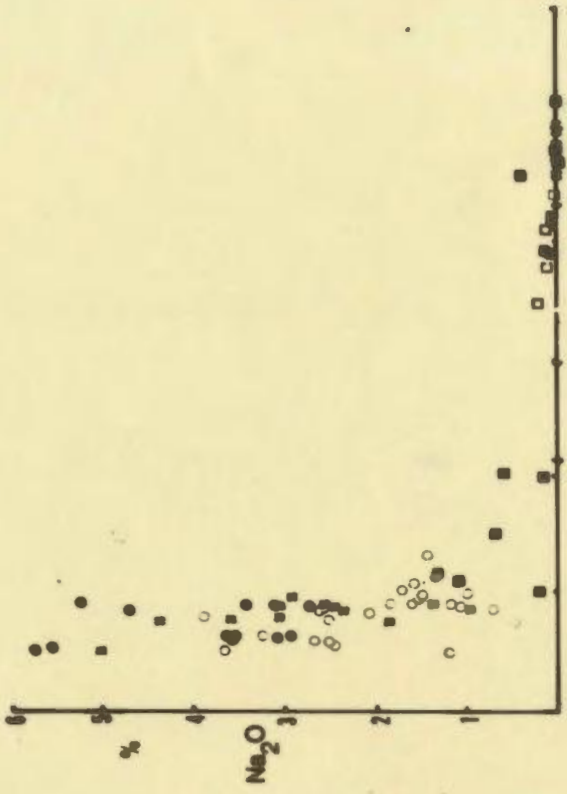
All major element oxides and trace elements have been plotted against MgO , and a number have been plotted against the value FeO^*/MgO (where FeO^* = total iron as FeO), which acts as a simple differentiation index (Miyashiro, 1973; Miyashiro and Shido, 1975).

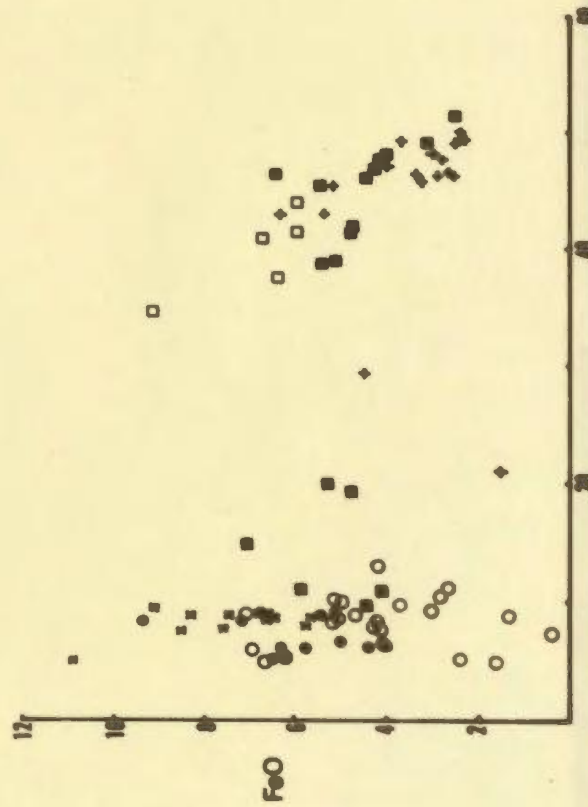
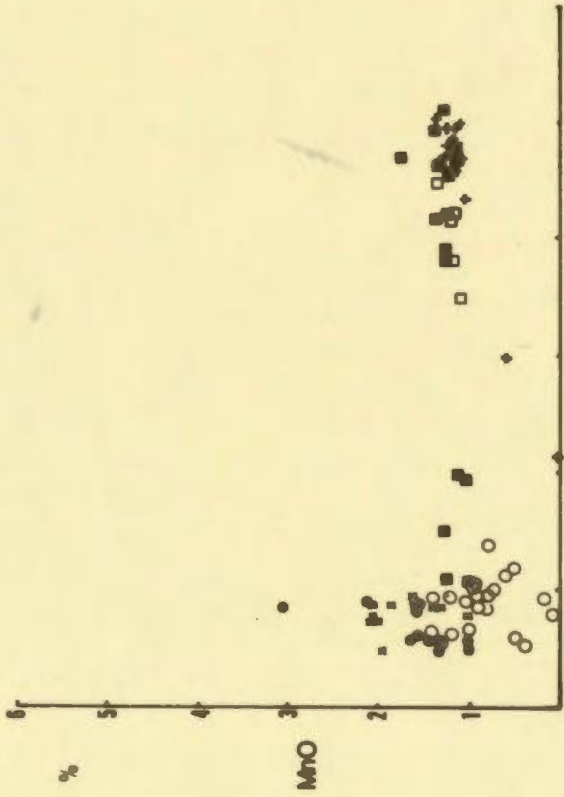
The trends of Al_2O_3 and CaO are characteristic. Both increase from the dunites and tectonite peridotites and reach a maximum in the pyroxenites and lower gabbros where plagioclase and clinopyroxene crystallisation depletes the magma. There is then a sharp decrease to a minimum in the most differentiated lavas.

Total iron, Fe^{2+} and Fe^{3+} , are generally quite low in the lower gabbros, but increase in the higher gabbros, dikes and pillow lavas. The high value of iron in the dunites and tectonite peridotites represents their concentrations of olivine and orthopyroxene, and spinel phases. Titanium content increases simultaneously with total iron, but shows no marked concentration in the peridotites. The titanium content therefore

Figure VIk: Major element oxides vs. MgO (wt %)

- Lherzolites
- + Harzburgites
- Dunites and Critical Zone
- Gabbros
- × Diabases
- Volcanics





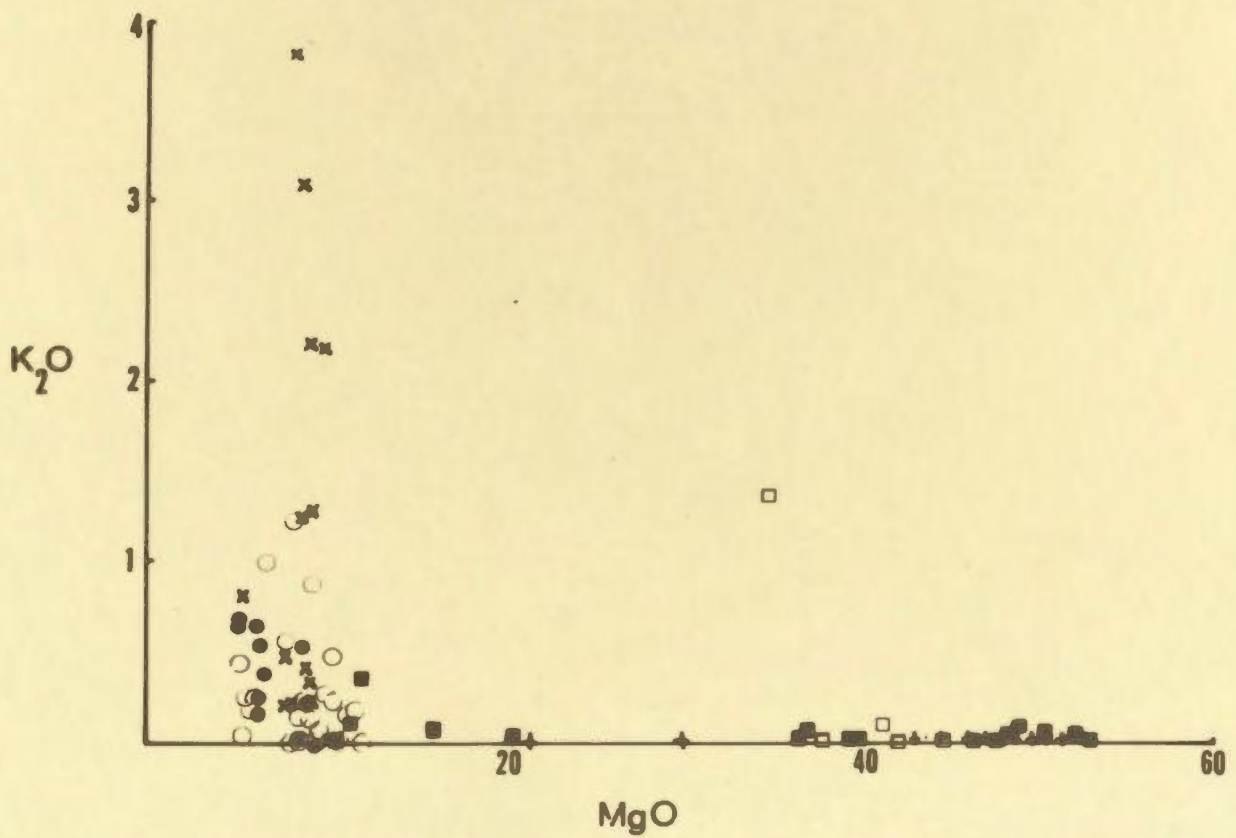
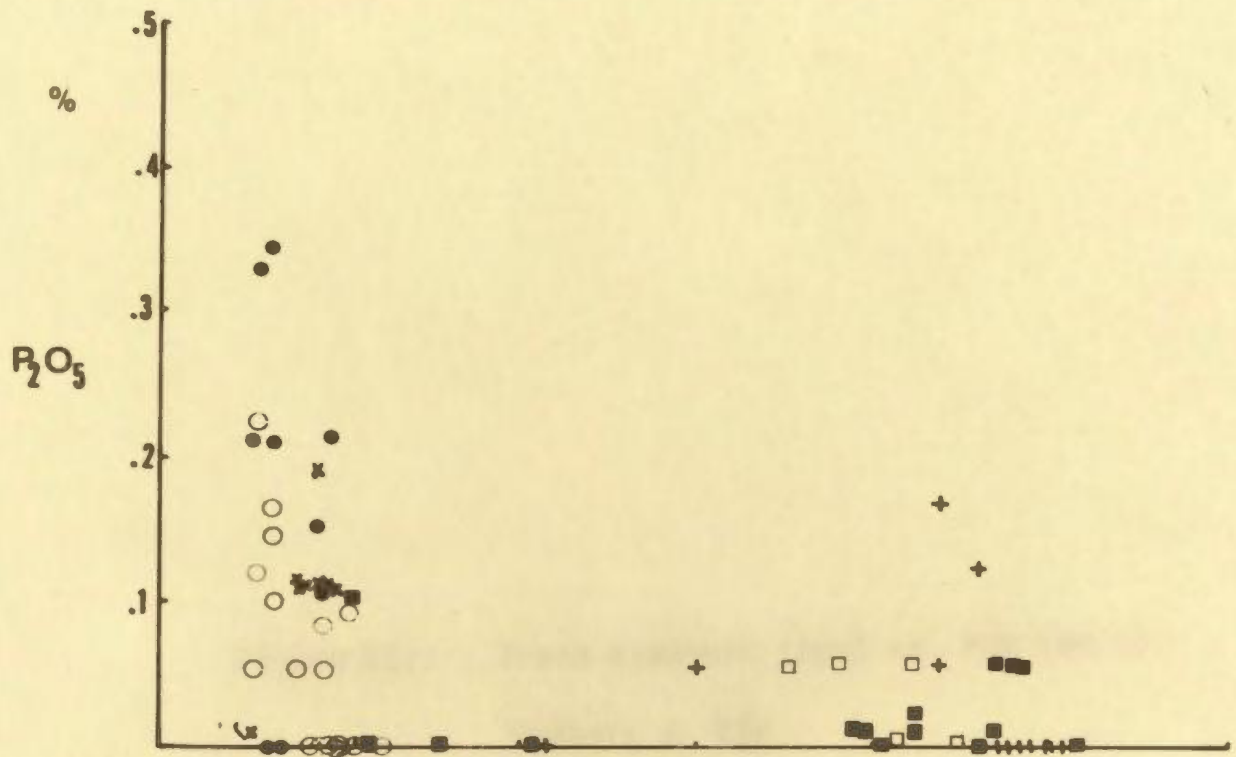
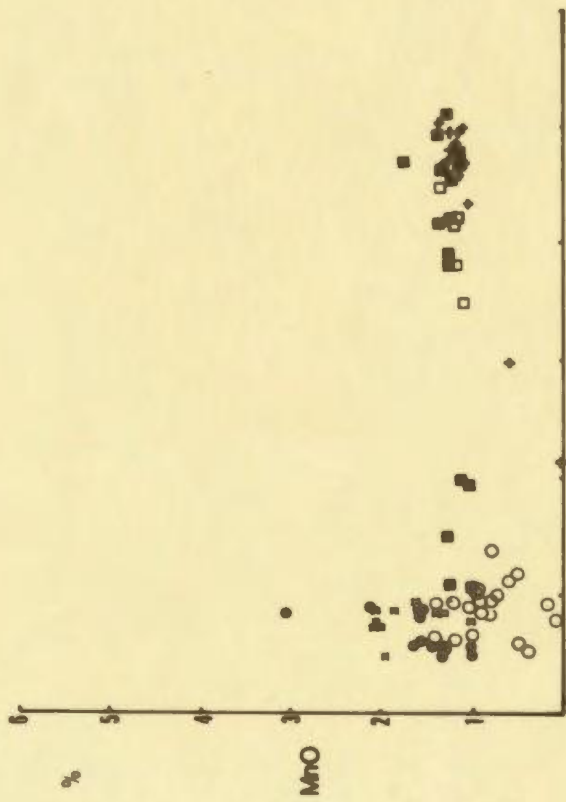
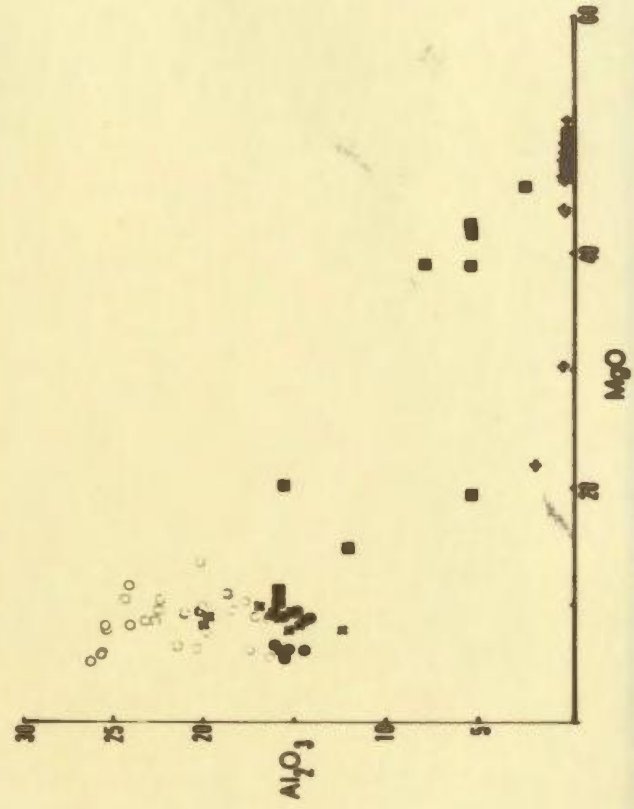
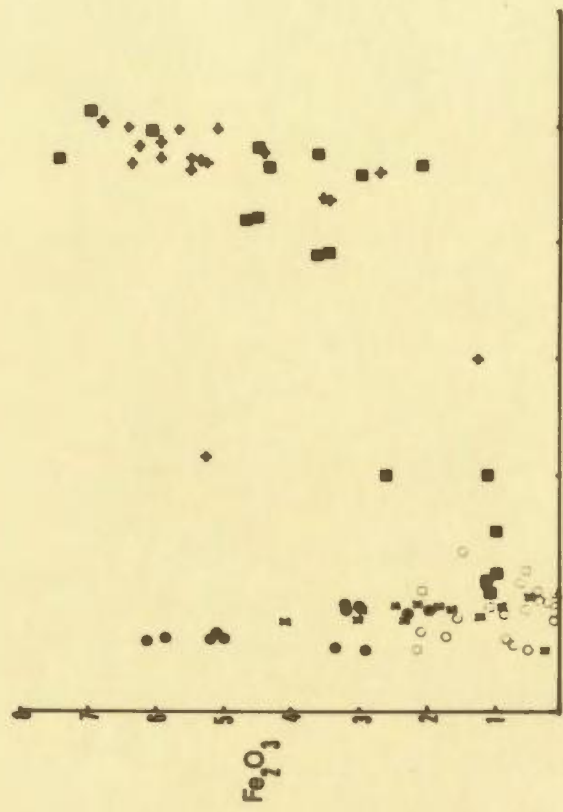
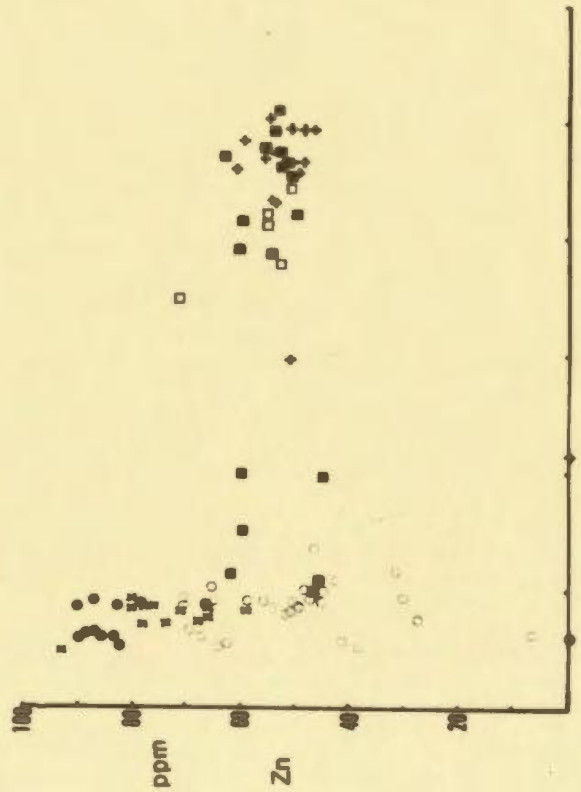
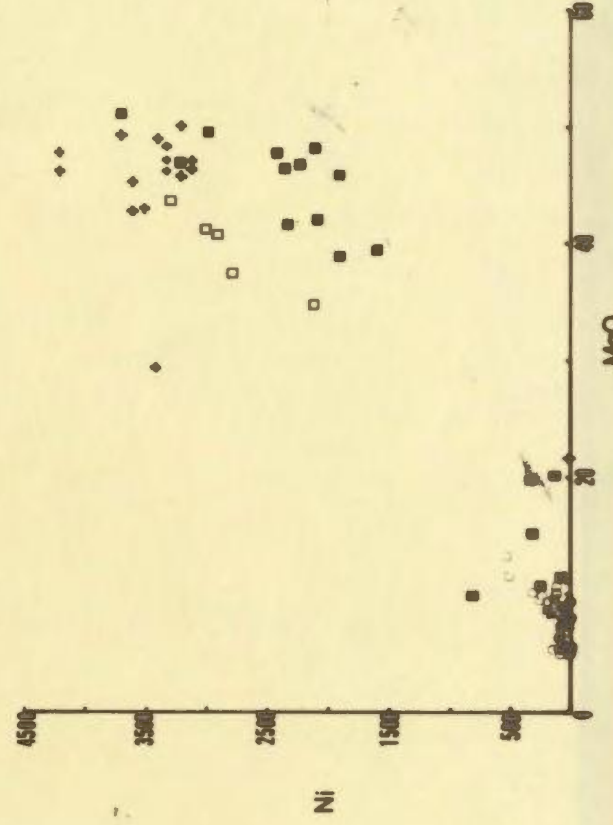
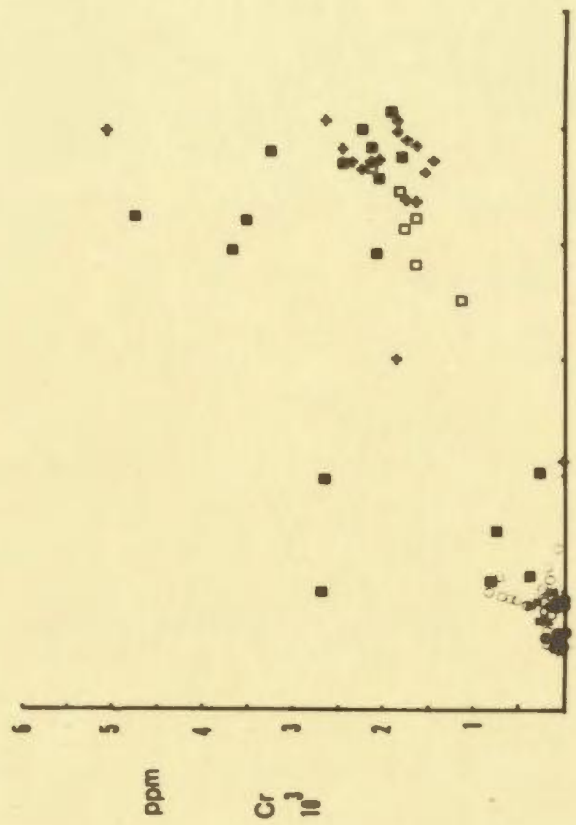
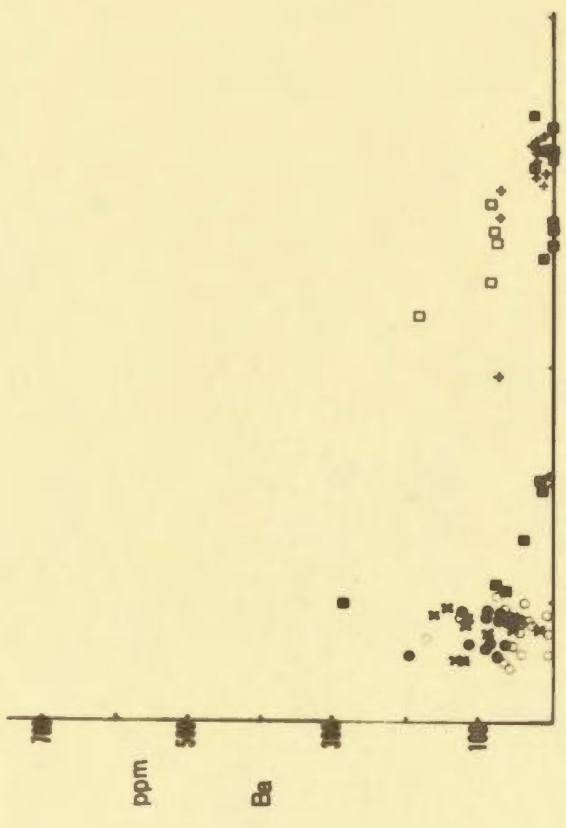
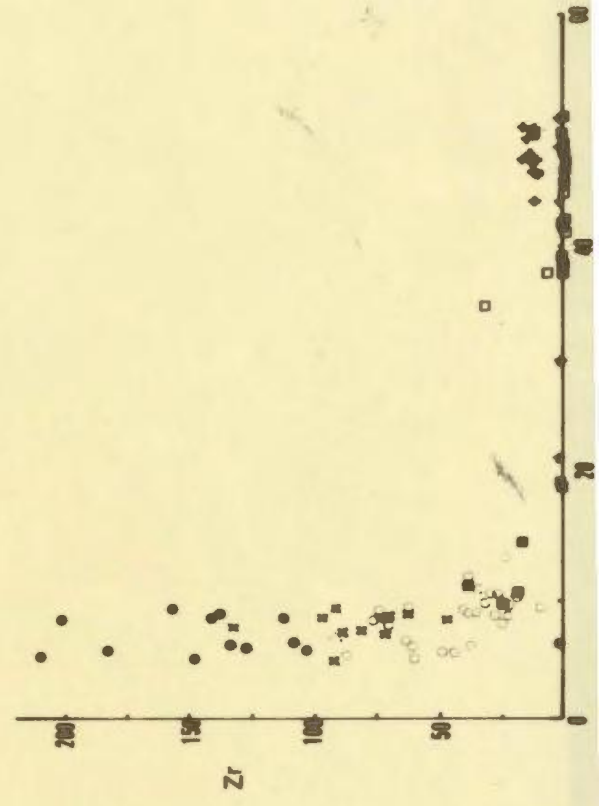
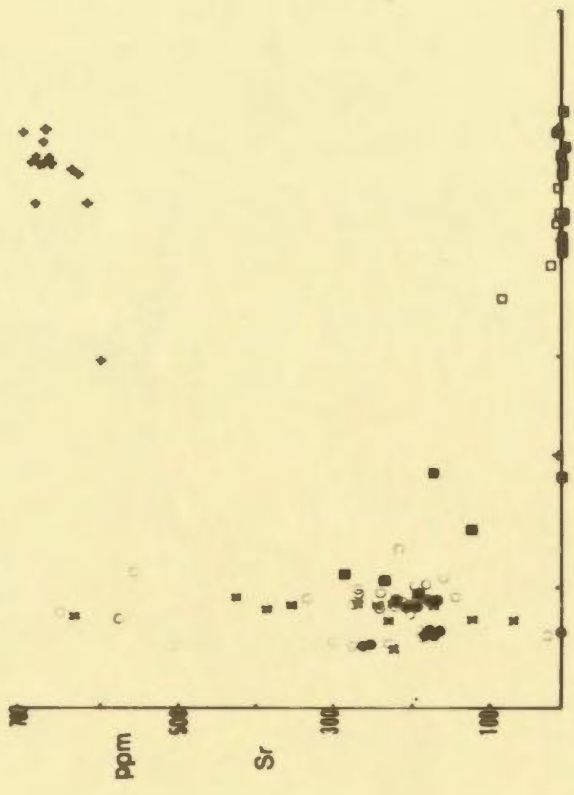


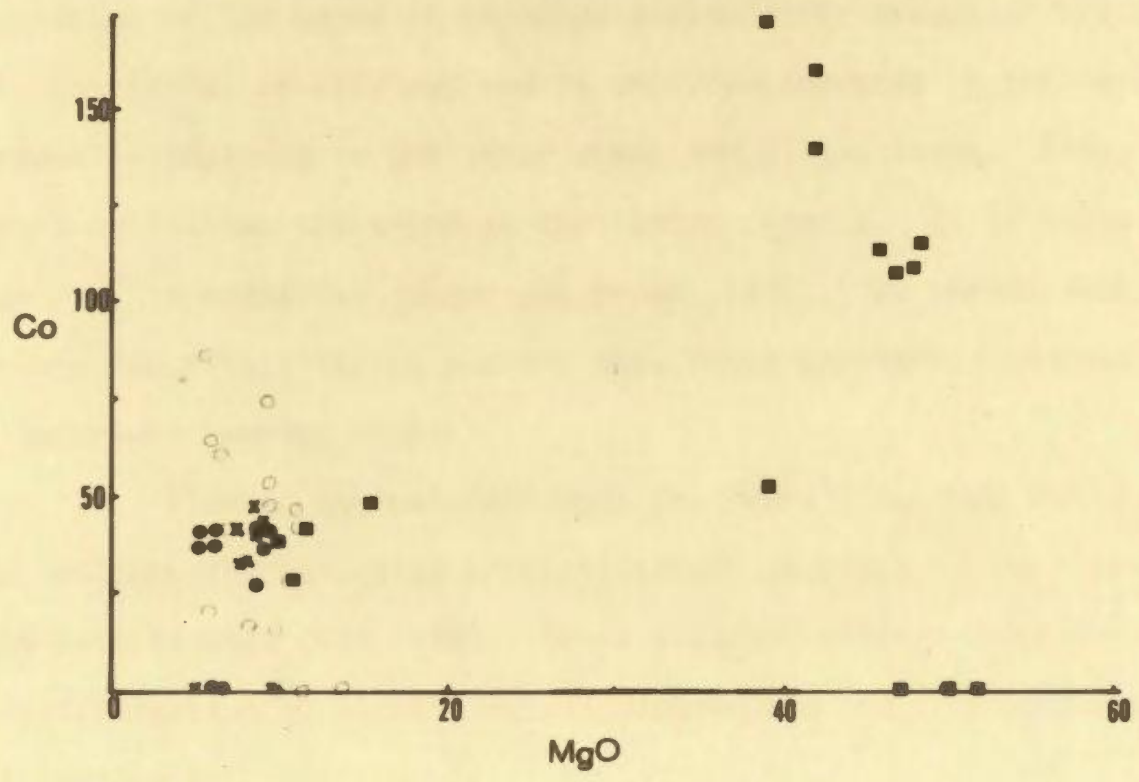
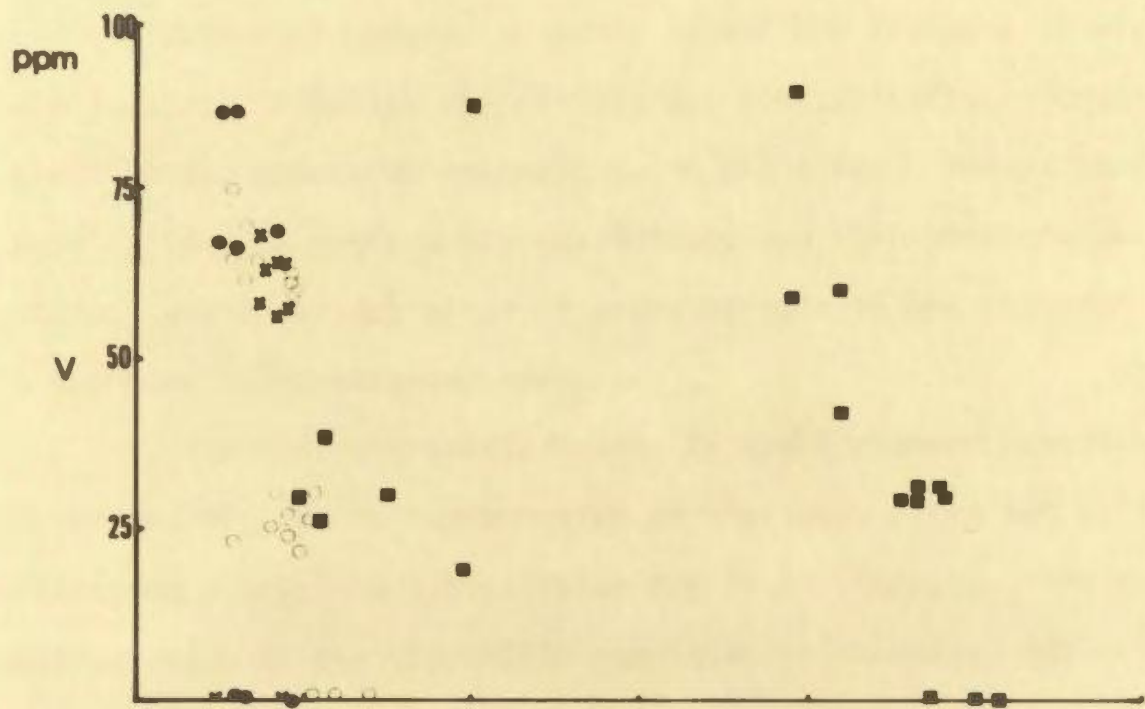
Figure VII: Trace elements (ppm) vs. MgO (wt %).

Symbols as Vik.









reflects its concentration in opaque oxides which crystallised in the late liquids resulting in their high normative ilmenite contents. This crystallisation of opaques possibly caused the increase in silica in the late liquids. Alkalies and phosphorous are typically concentrated in the late liquids, potassium markedly so in the dikes. Magnesium decreases rapidly from the peridotites and dunites and then more gradually from the gabbros, where the depletion is sympathetic with the increase in total iron in the more differentiated rocks.

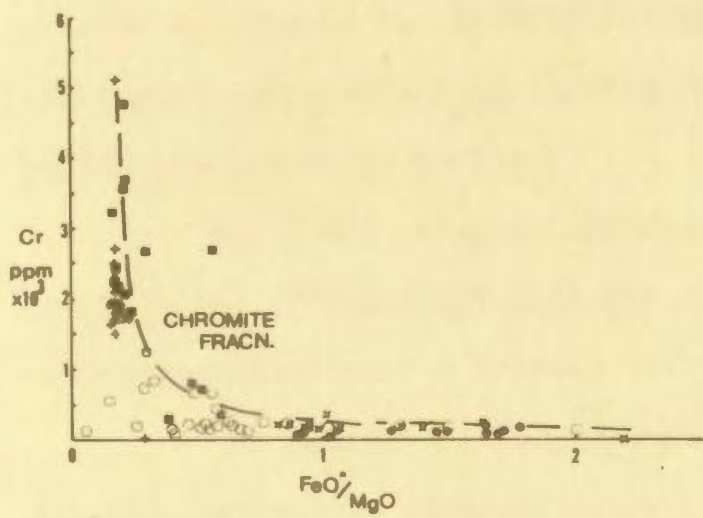
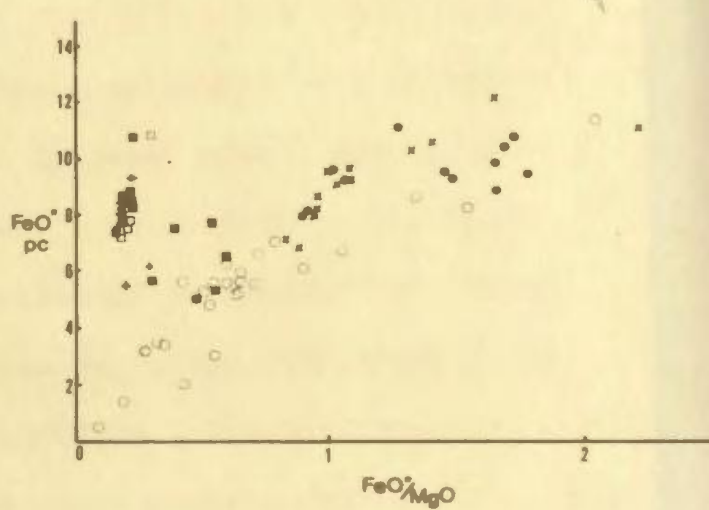
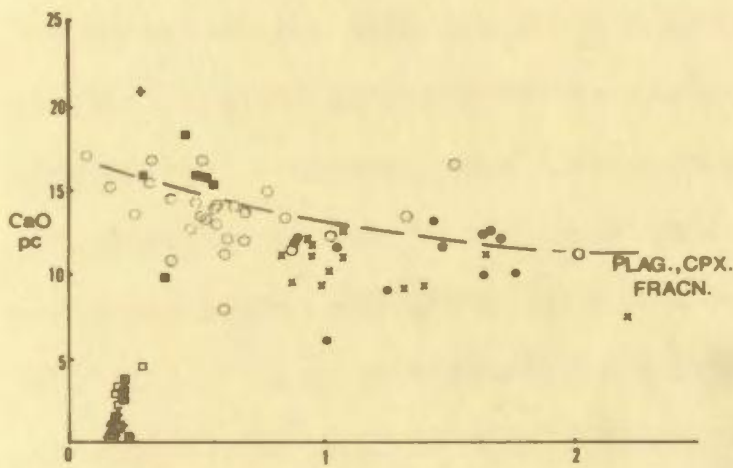
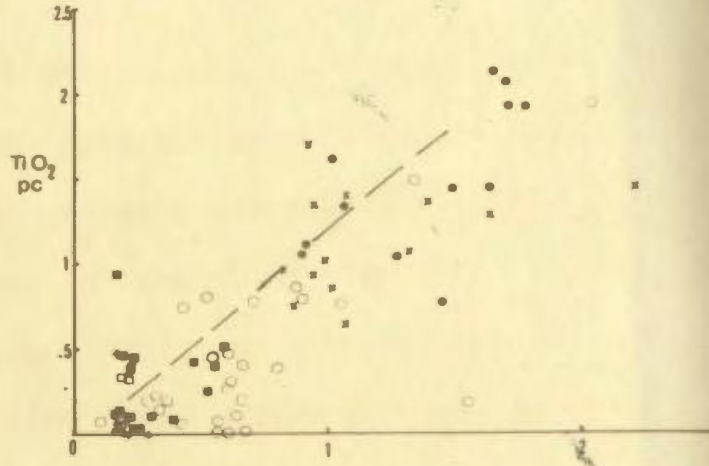
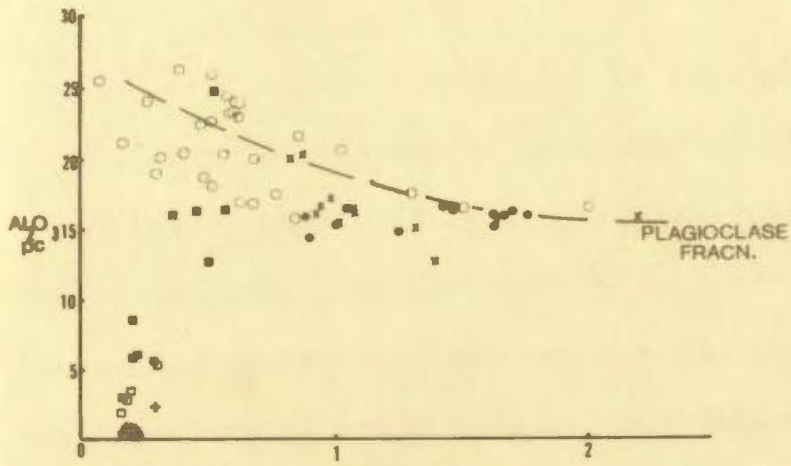
The most noticeable trends in trace element contents are those of Zr, Cr and Ni. Zr is concentrated in the later dikes and pillow lavas, reflecting a possible substitution for Ti in ilmenite. The major chrome bearing phase in the ultramafic cumulates is chromite, but Cr^{3+} is also known to substitute for Fe^{3+} in pyroxenes (Taylor, 1965). Thus there is a depletion of the magma in chromium during early stages of fractionation. Ni substitutes in olivines and is thus concentrated in the dunites and gradually depleted in the later dikes and pillow lavas. Zinc, substituting for iron follows the trend of the latter closely. It is known to substitute for Fe^{3+} in magnetite (Wager and Brown, 1968). Ba and Sr both relatively freely substitute for Ca and are thus found in highest concentrations in the plagioclase bearing rocks.

Plotted against FeO^*/MgO ; Cr, FeO^* , TiO_2 , CaO and Al_2O_3 are used to indicate the effective crystallisation sequence in the cumulate rocks and late liquids (Fig. VIIm). These diagrams clearly show the effects of crystallisation of 1) olivine, 2) plagioclase and clinopyroxene, 3) opaques, in that order.

Figure VI_m: Elements and oxides vs. FeO*/MgO.

FeO* = Tot. Fe as FeO.

Symbols as VI_k.



ii) FMA and CNK diagrams

In figure VI the Bay of Islands Complex rocks are compared with standard differentiation trends of Skaergaard and Hawaii, and trends exhibited by the recognised ophiolite suites of Papua and Oman. All the ophiolites plot along a similar trend of iron enrichment typical of tholeiitic suites (see also Norman and Strong, 1975), and are comparable with the general trend suggested by Thayer (1967) for alpine peridotites. The spread of the gabbroic rocks apparently indicating their enrichment in alkalis might be explained by their various concentration of cumulate plagioclase. However, more likely it is an apparent effect resulting from the decrease in iron in the lower gabbros which is visible on the linear variation plots, and which gives the impression of an overall enrichment in alkalis. Similar features have been noted by Norman and Strong (1975) for ophiolitic rocks of Ming's Bight, Newfoundland. The enrichment of some basalts in alkalis is possibly attributable, to a certain degree, to alteration. The quartz-diorites are apparently crystallised from the final residual liquid of the fractionation series.

The F.M.A. diagram clearly indicates that the pillow lavas are crystallised from a magma that has already undergone fractionation, and are not representative of a primary melt.

The C.N.K. diagram (figure VIo) shows an increase of sodium, possibly reflecting plagioclase composition during differentiation, but possibly also degrees of alteration, especially soda-metasomatism in the basalts. The potash contents are low and typical of oceanic tholeiites as described by Engel et al. (1965).

Figure VI: F.M.A. Plot

Key:

- Ultramafic rocks (mainly dunites)
- ▲ Critical Zone rocks
- Gabbros
- Dikes
- Pillow lavas
- Quartz diorite

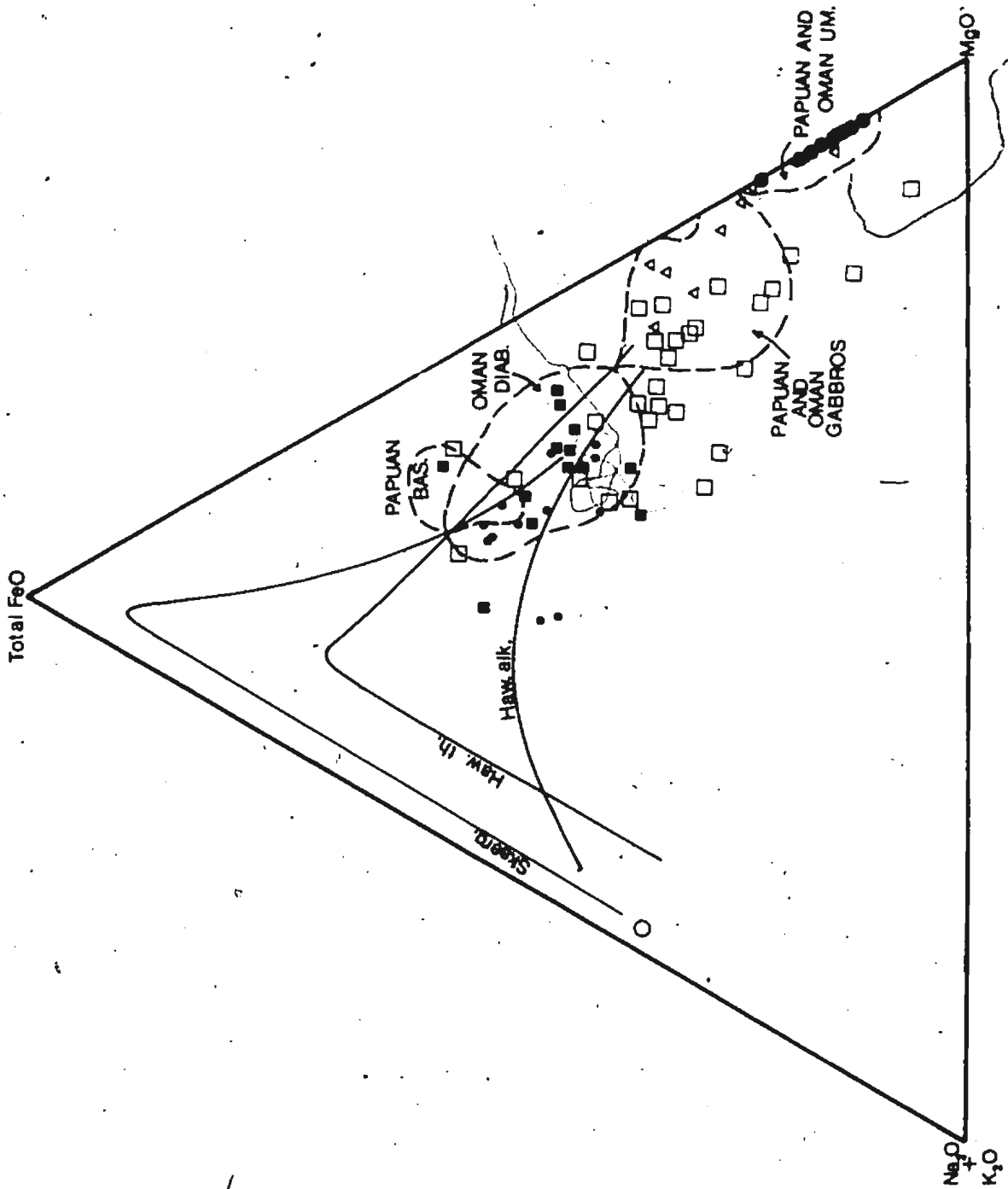
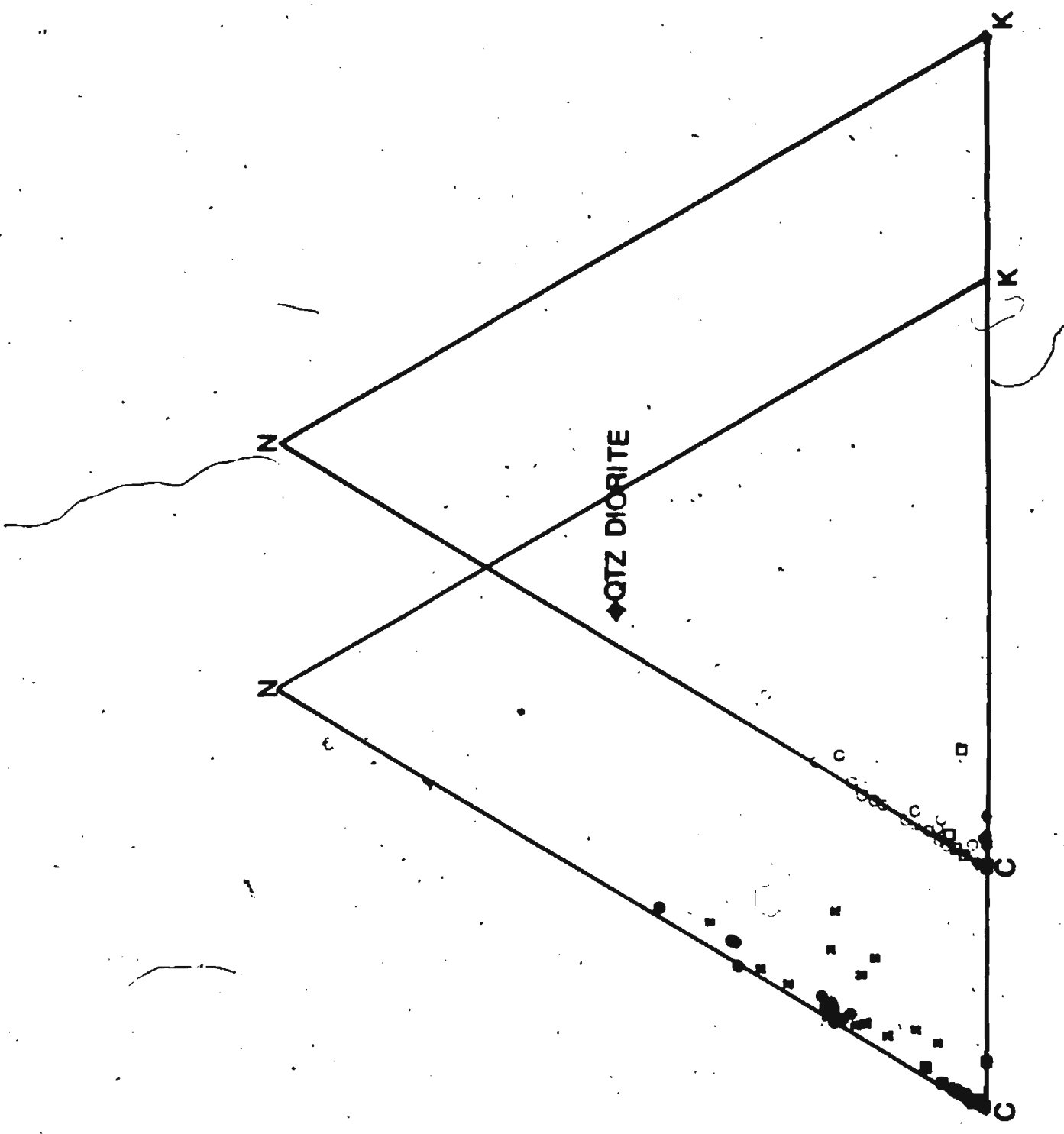


Figure VIo: C.N.K. Plot

- Key: + □ Ultramafic Rocks
■ Critical Zone Rocks
○ Gabbros
× Dikes
● Pillow Lavas
◆ Quartz diorite



iii) Cr₂O₃ vs NiO wt. % (Figure VIp)

Irvine and Findlay (1972) used Cr₂O₃ and NiO relationships to separate alpine type peridotites and cumulate rock associations. They suggested a similarity between alpine peridotites and the tectonic harzburgites and lherzolites of the Bay of Islands Complex and attributed to them a mantle origin. They distinguished rocks of the critical zone and gabbro zone from the tectonites with the suggestion that their similarity to layered intrusions indicated that they crystallised under relatively low pressures in the crust. The present study supplements this view in that rocks from the dunite zone, below the critical zone, and not specifically identified by Irvine and Findlay may also be considered of the same origin. These rocks are clearly cumulate (p. 228) and must therefore be considered as part of a low pressure fractionation series which includes the critical zone, gabbros, diabases and basalts, and which is distinct from the ultramafic tectonites which it overlies (Malpas, 1973).

iv) K/Rb and Rb/Sr ratios (Figures VIq and VIr)

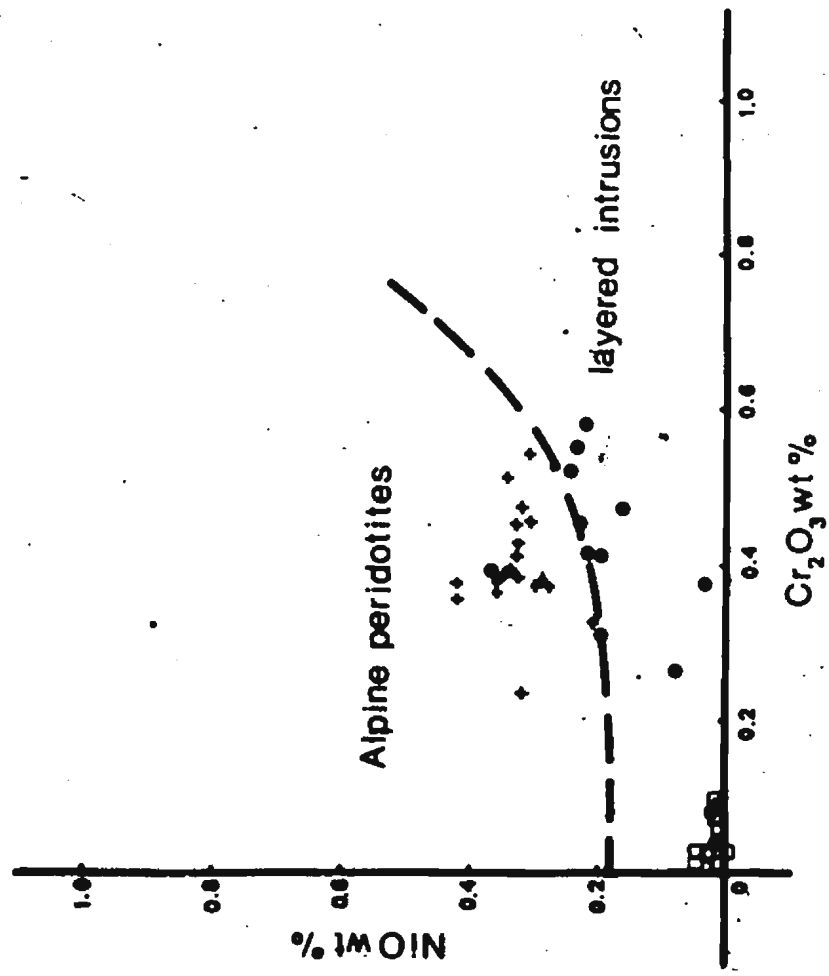
The sensitivity of the methods used for analysing for Sr and Rb do not allow for accurate determinations of K/Rb and Rb/Sr ratios in the ultramafic rocks. However, values determined for the mafic rocks may be compared with values previously reported in the literature (Engel et al., 1965; Hurley, 1967; Murthy and Steueber, 1967).

In low potassium oceanic tholeiites the K/Rb ratios reach up to approximately 1900, while lower values (< 500) are more characteristic of alkaline basalts. This relationship has been interpreted by Gast (1965) to be in accord with the behaviour of K and Rb in the crystallisation of

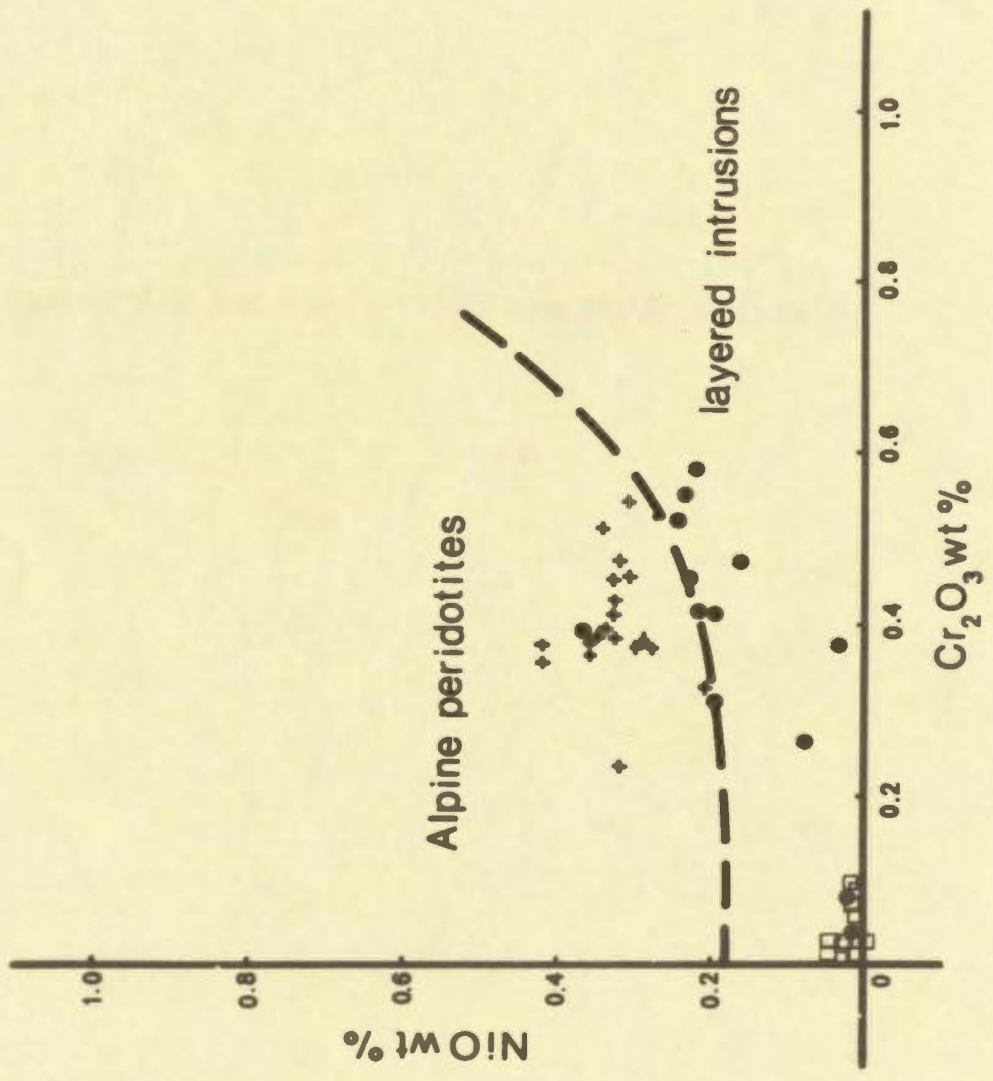
Figure VIp: Cr_2O_3 vs. NiO wt %

Key:

- + Tectonite Harzburgites
- Dunites
- Gabbros.



Figures VIq and VIr: K/Rb and Rb/Sr ratios.



basalts and requires that oceanic tholeiites are total melts of upper mantle material according to Engel et al. (1965). The K/Rb ratios in mantle-derived ultramafic rocks range from 200-500. Thus generally their K/Rb ratios are not as high as those found in oceanic tholeiites (St. Paul's Rocks, Equatorial Atlantic, prove exceptions: K/Rb 400 to 1000). K/Rb ratios are plotted against MgO content for the ophiolitic rocks of the Bay of Islands Complex to show variations of the ratio with differentiation. The K/Rb ratio in the ultramafic rocks is low and comparable to values from alpine peridotites. The ratio is very similar throughout the gabbros, diabases and basalts except for one high value of 1600 in the diabases. These values fit those expected of a more differentiated series rather than the high values of a more primitive (less differentiated) series and are in accord with the average range for alkali basalts.

The range of Rb/Sr values in the gabbros, diabases and basalts is from approximately 0.01 to 0.05 and is thus a little high compared with values from fresh oceanic abyssal basalts, and again is more comparable to alkali basalts. The Rb/Sr value increases rapidly with the crystallisation of calcium bearing phases such as plagioclase and diopside which preferentially incorporate Sr. The cumulate plagioclase-enriched gabbros, and feldsparphyric dikes have lowest Rb/Sr values amongst the differentiated series.

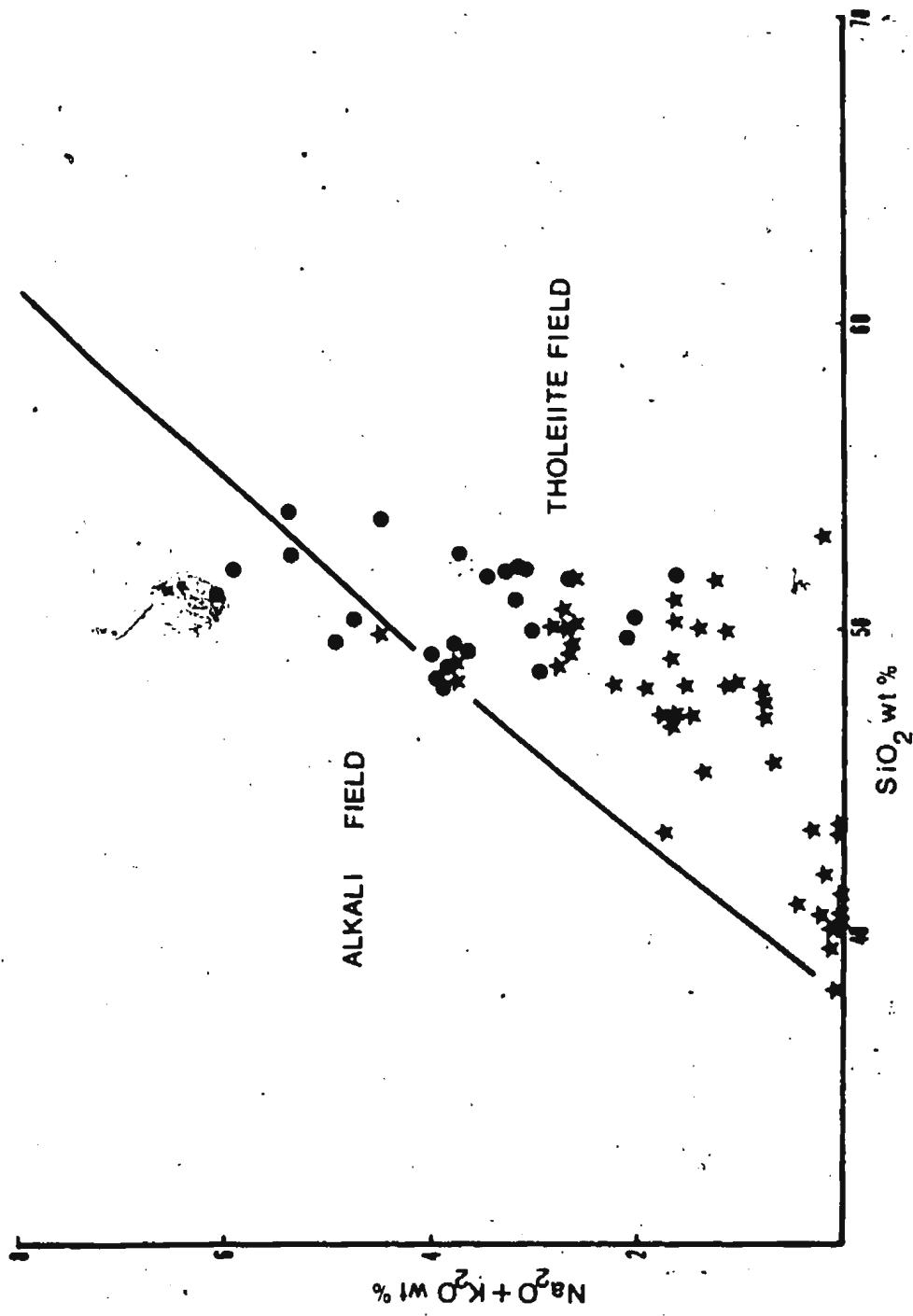
v) Total alkalis vs. SiO₂ (Figure VI)

The total alkalis versus silica diagram shows that although the majority of the rocks from the ophiolite suite can be considered tholeiitic, a number are transitional or definitely alkaline in their present chemistry. There are two possible reasons for this alkaline affinity. Firstly, the rocks are altered and the increased alkalinity is due primarily to soda-

Figure VI: Plot of $(\text{Na}_2\text{O} + \text{K}_2\text{O})$ vs. SiO_2 wt %

● Dikes and volcanics

★ Cumulate Gabbros + CZ rocks



metasomatism during low-grade metamorphism. It is notable that in this regard the two samples which plot furthest into the alkaline field are clearly metasomatised pillow-selvages. However, the cores of these pillows are themselves transitional in composition. The second alternative is that the rocks form a series that was primarily transitional in nature and which is comparable to rocks described by Aumento (1968) from Confederation Peak and Muir and Tilley (1964) from Discovery Tablemount, both in the mid-Atlantic. The importance of each of these alternatives must be considered after further evidence cited below.

vi) Basalt tetrahedron

The cumulate rocks, diabases and volcanics from the Bay of Islands Complex have been plotted as projections within the simple normative basalt tetrahedron of Yoder and Tilley (1962) in figure VI. Projections are given from the four corners of the tetrahedron and one atmosphere dry cotectics of the synthetic system Fo-Di-An-Qtz and the natural system Olivine-Cpx-Plag-Qtz shown. The differences in positioning are caused principally by the presence of Na and Fe in the natural systems which have the effect of expanding the primary phase volumes of the ferromagnesians against that of plagioclase. The natural cotectics are obtained from Clarke (1970) and based upon experimental work by Tilley et al. (1963, 1964, 1965, 1967).

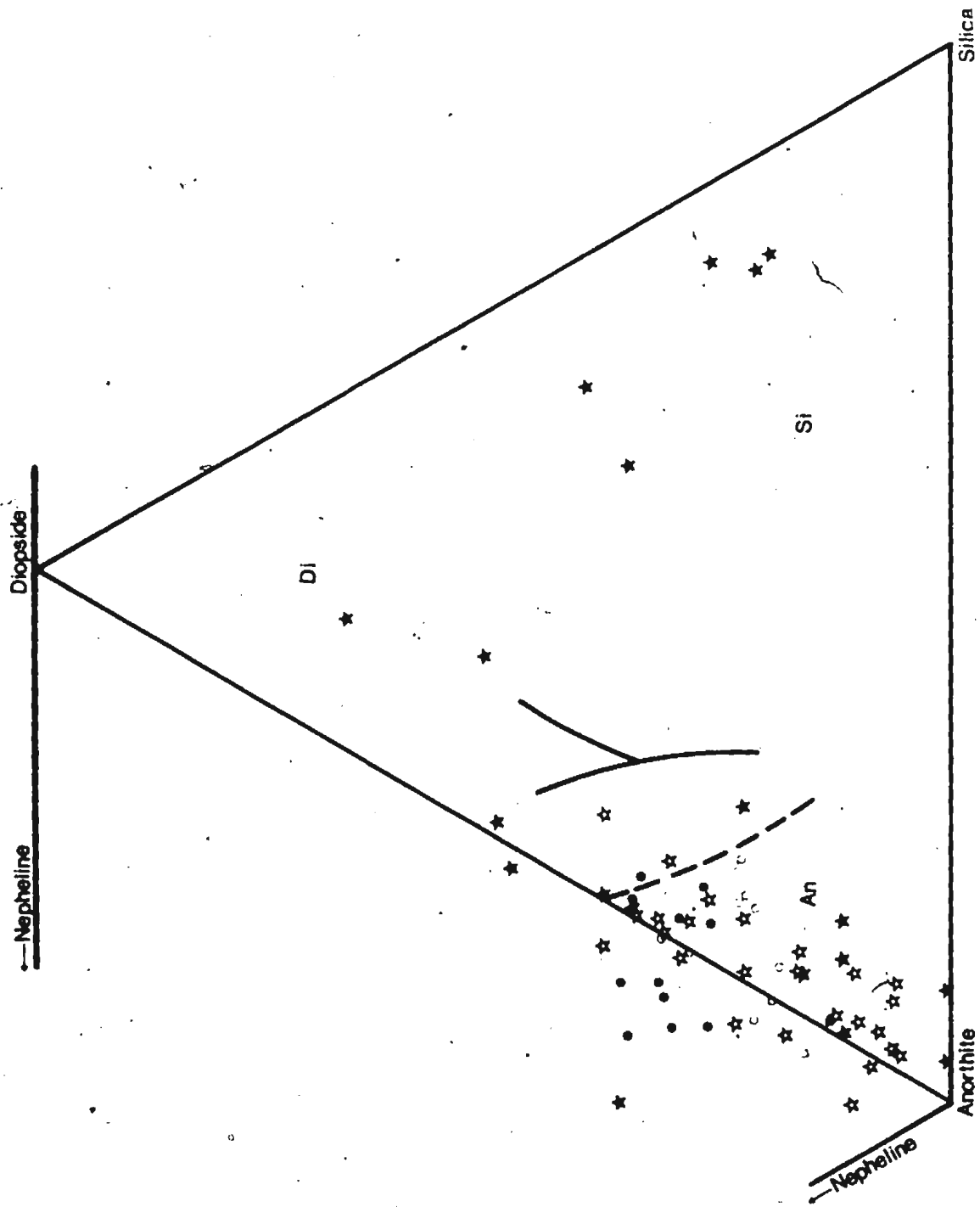
In the olivine projection a considerable spread of points from the dunite zone is a result of their close proximity to the projecting phase such that a small variation in their composition is reflected as a large spread after projection. Relative to the natural system cotectic in the olivine projection, plagioclase appears to be the second phase to crystallise

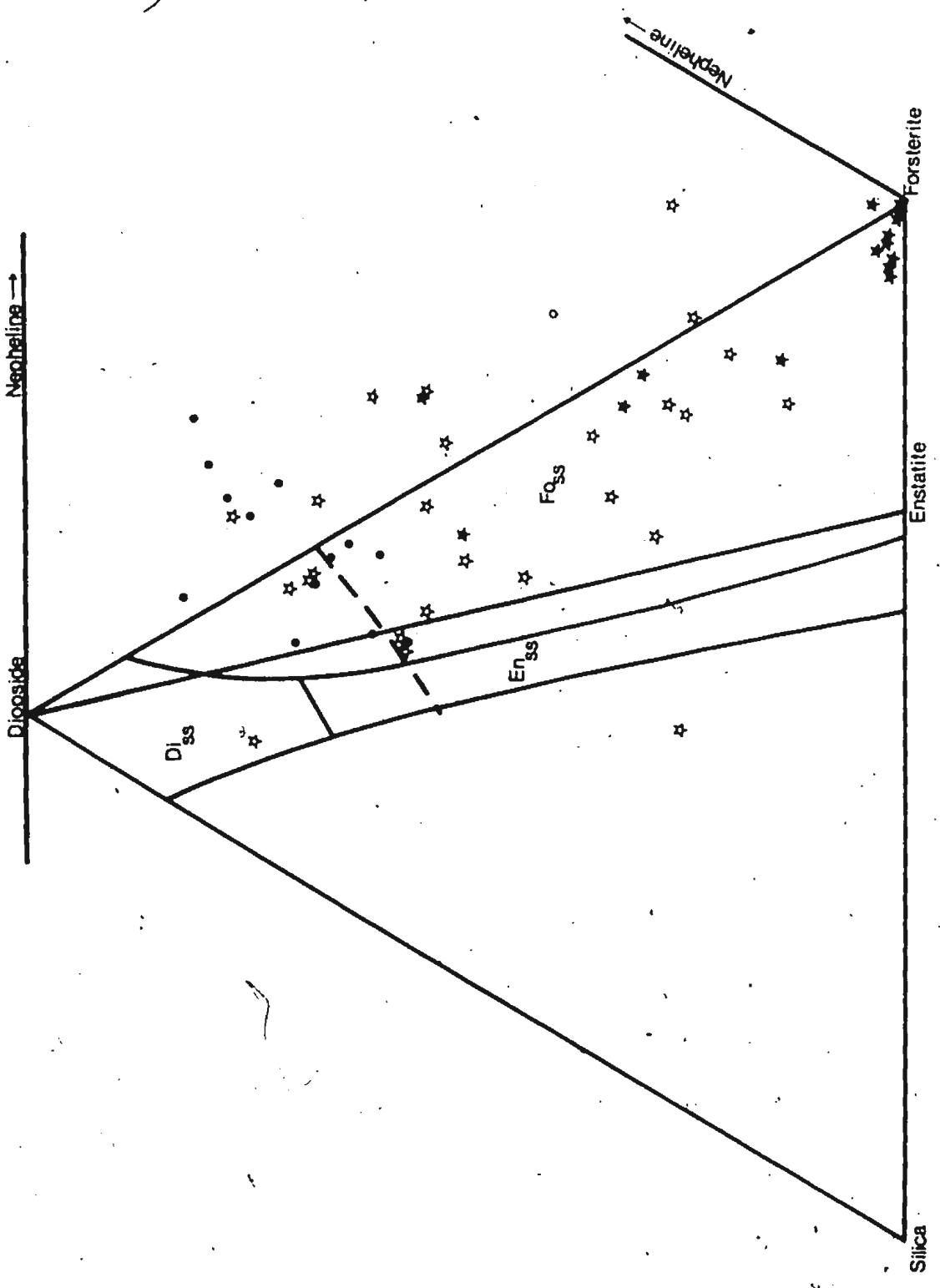
Figure VI: Projections within the Basalt Tetrahedron
(Yoder and Tilley, 1962).

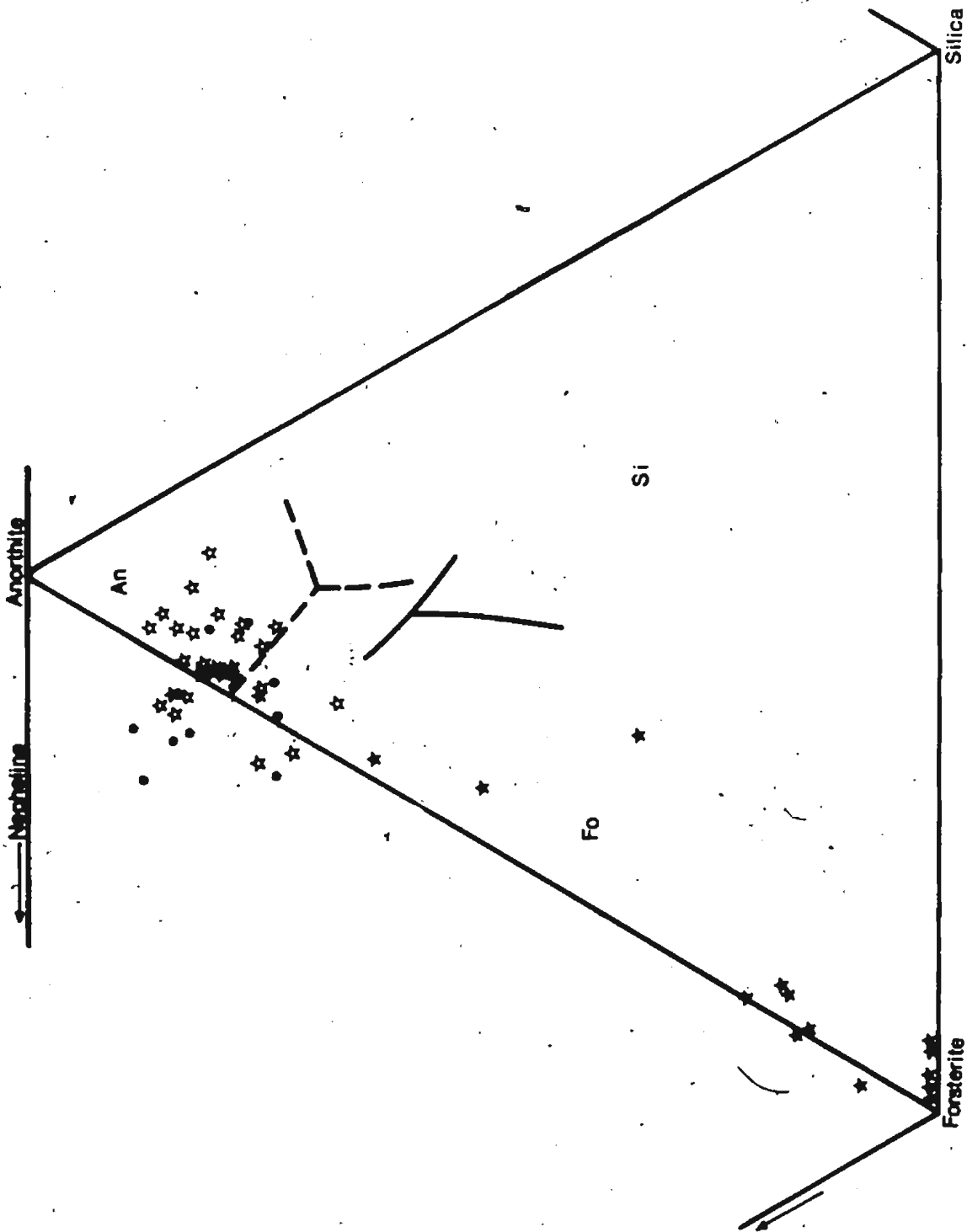
- a) From Forsterite
- b) From Plagioclase
- c) From Diopside
- d) From Quartz/Nepheline

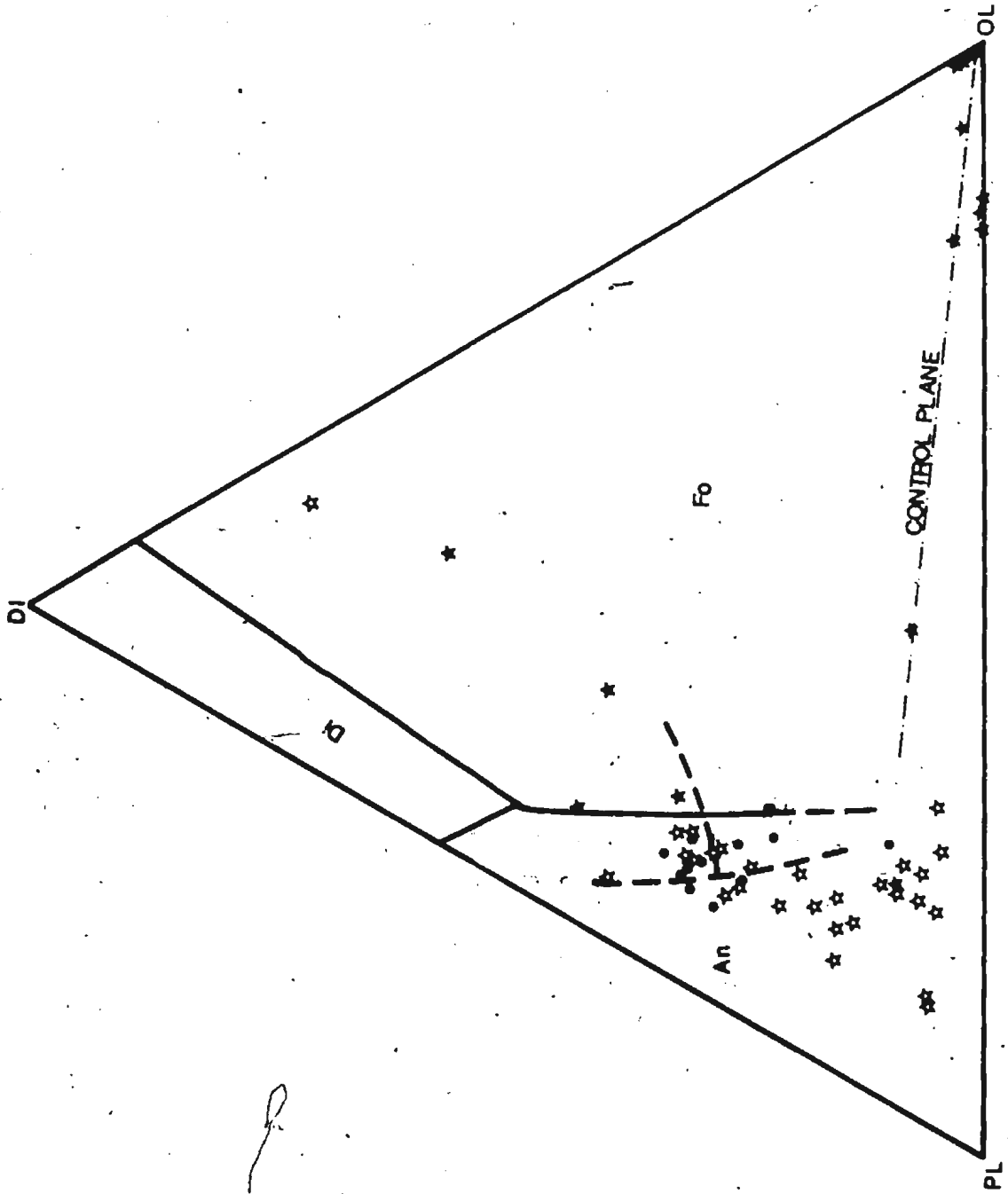
Key:

- ★ Dunites + CZ
- ☆ Gabbros
- Dikes
- Volcanics









followed by clinopyroxene:

In the plagioclase projection there is a large spread in the gabbros because of their cumulate plagioclase enrichment. The distribution of analyses in this projection suggests that the field of clinopyroxene constructed by Clarke (1970) may be a little too large.

An olivine control line is suggested in the diopside projection, with the basalts falling between the natural and synthetic system plagioclase-olivine cotectic. The gabbros are clearly enriched in cumulate plagioclase. Since all points plot at a distance from quartz or nepheline in these projections, a projection from quartz/nepheline is of some use in indicating liquid lines of descent. Such a projection clearly shows the initial olivine control and the crystallisation sequence, i.e. 1) olivine, 2) olivine + plagioclase, 3) olivine + plagioclase + clinopyroxene. This sequence is exactly that observed in the field and is upheld by textural evidence in the gabbros where olivine is found included in plagioclase and clinopyroxene is generally intercumulate. The basalts clearly plot around the low pressure natural system eutectic, and the dikes along the plagioclase-olivine cotectic in this projection.

All projections within the basalt tetrahedron indicate a spread of compositions across the critical plane of silica undersaturation. The spread observed is difficult to relate entirely to alteration, the effects of varying $\text{Fe}_2\text{O}_3/\text{FeO}$ ratio having been reduced for these plots by normalising the ratio of 0.25 for all rocks. The projections therefore substantiate other plots (Rb/Sr, K/Rb, alkalis vs. SiO_2) in suggesting that the suite is transitional in nature.

vii) Rare Earth Elements

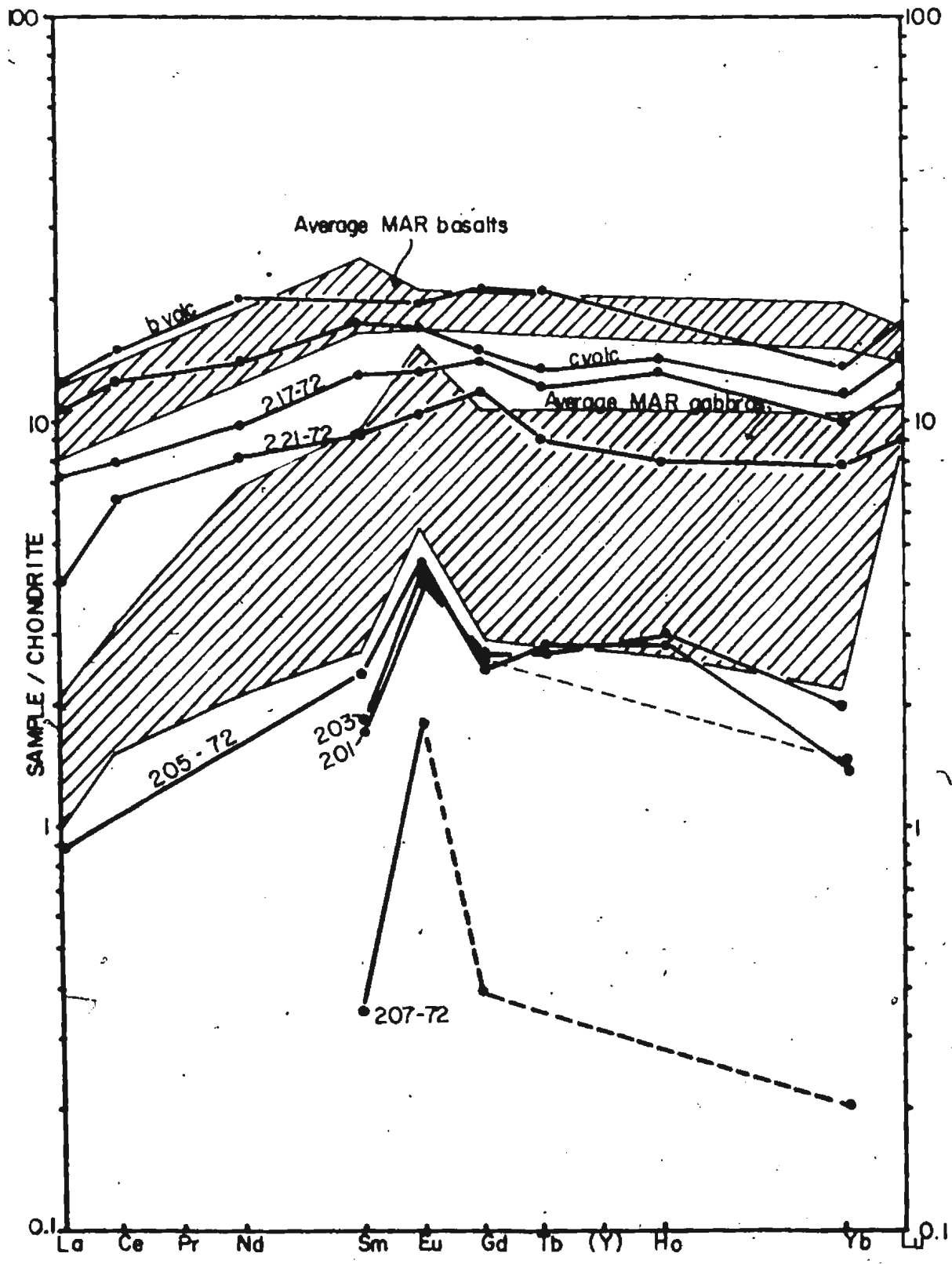
Determinations of rare earth elements (R.E.E.) and yttrium were carried out on an AEI MS7 spark-source mass spectrometer. Analytical details are given in Appendix III. The analyses were substantiated by measurements carried out by F. A. Frey using instrumental neutron activation. Results are shown diagrammatically in figure VIu where the rare earth abundances have been normalised against chondritic abundances and plotted against atomic weight. The following points are noteworthy:

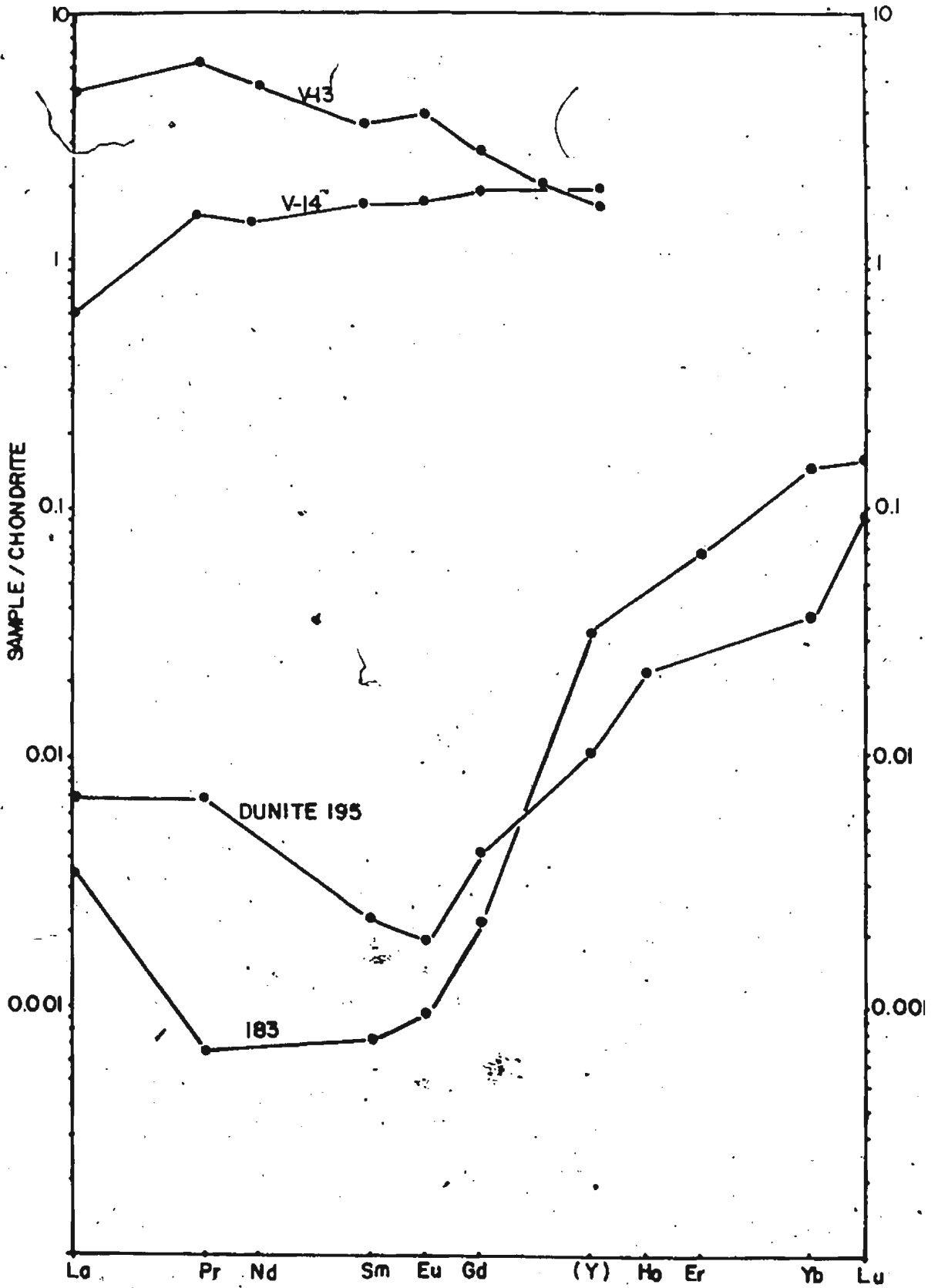
a) There is a marked similarity of the R.E.E. abundances of the pillow lavas with mid-Atlantic Ridge basalts (data from Frey et al., 1968). They show a slight depletion of the light rare earths (1.1 times chondritic L.R.E.E.) with respect to chondritic R.E.E. abundances. Oceanic alkaline basalts usually show a preferential enrichment in L.R.E.E. (Frey, 1970; Graham and Nicholls, 1969).

b) There is generally a lower R.E.E. abundance and stronger L.R.E.E. depletion observed in the diabases compared with the pillow lavas. This would indicate that the lavas are slightly more fractionated than the diabases, which agrees with the results of major element chemistry.

c) The gabbros are relatively poor in R.E.E. However, definite Eu enrichment anomalies are observed indicating a strong accumulation of plagioclase. This agrees with the conclusion from textural evidence that the gabbros are plagioclase cumulates and suggests that their crystallisation took place under conditions of low oxygen fugacity (O'Hara et al., 1975). Comparison of patterns from oceanic gabbros show that these are also plagioclase cumulates (Fig. VIu). Eu anomalies are small in the lavas and diabases.

Figure VIu: Rare Earth Element abundances.





d) The dunite 195 shows strong enrichment in H.R.E.E., but the overall pattern is V-shaped and characteristic of olivine (Frey, 1970). The enrichment in H.R.E.E. is due to the presence of clinopyroxene in the dunites, this phase preferentially incorporating the heavier atomic weights.

e) The harzburgite R.E.E. pattern is typical of residual peridotites after the removal of a tholeiitic partial melt (Frey et al., 1971; Frey and Green, 1974) showing a strong depletion of L.R.E.E. with respect to chondritic abundances. The low R.E.E. abundances are typical of rocks containing olivine and orthopyroxene and patterns are comparable with the Lizard residual peridotite (Frey, 1970). It is notable that, if the dunite (195) represents an early crystallisation product of the melt derived by partial melting leaving the harzburgite as residue, then a similarity in their R.E.E. patterns might be expected if the melt was derived under equilibrium conditions. From the data available, this seems to be the case.

f) The variability of R.E.E. patterns for lherzolitic rocks has been pointed out by Phillpotts et al. (1972), and Frey and Green (1974). The two lherzolites analysed here are similarly diverse, with V14 showing a steady although slight enrichment in heavy rare earths, indicating that it is probably partly depleted in tholeiitic melt. V13, on the other hand, shows an enrichment in light rare earths which may not be related to the process of partial melting as reflected in the resultant tholeiitic magma but can be explained as the process described by Frey and Green (1974) where lherzolites represent a mix of two geochemically distinct components. Component A is important in terms of major elements, and abundances of compatible trace elements (including H.R.E.E.). It has the characteristics of a residuum after basalt extraction from a peridotitic parent. Component B,

dominant in V13, is important in terms of minor and incompatible trace elements (including L.R.E.E.) and has the characteristics of a highly fractionated melt phase such as basanite, olivine nephelinite, olivine leucitite or other highly silica undersaturated magmas.

The two divergent patterns at least indicate the inhomogeneity of the lherzolites within even a small volume.

viii) Strontium isotopes. $Sr^{87}/86$ ratios

Isotope analyses of strontium from five Bay of Islands Complex gabbros have been made for the writer by R. Cormier (St. Francis Xavier University) and the results presented in table XXIV along with representative analyses from other basaltic suites; continental tholeiites, oceanic alkali basalts and oceanic abyssal tholeiites. Within the limits of errors associated with the analyses, the Bay of Islands rocks are clearly of mantle derivation and oceanic affinities. However, they cannot be easily distinguished as either alkaline (av. 0.7033) or tholeiitic oceanic basalts (av. 0.7024).

C. Affinities of Mafic Suite with Oceanic Rocks.

Williams and Malpas (1972) pointed out the general similarities in chemistry of pillow basalts from the Bay of Islands Complex and oceanic tholeiites as exemplified by an average composition from Engel et al. (1965) and Melson et al. (1968). This similarity is upheld by the plots of oxides vs. FeO^*/MgO after Miyashiro and Shido (1975) where the mafic rocks from the Bay of Islands Complex fall into the abyssal tholeiite fields (figure VII). The oceanic tholeiites used to define these fields are from Engel et al. (1965), Melson and Thompson (1971), Thompson et al.

TABLE XXIV

Sr^{87/86} Isotope Data

1. Continental tholeiites	2. Oceanic alkali-basalts
0.7057 Karroo tholeiites	0.7043 Reunion, I
0.7115 Tasmanian dolerites	0.7030 Easter I.
0.7112 Antarctic dolerites	0.7031 St. Helena
0.7113 E. North American diabase	0.7025 Ascension
0.7060 Nuanetsi	0.7039 Hawaii
0.7065 Skaergaard marginal gabbro	
3. Abyssal oceanic tholeiites	4. Bay of Islands Gabbros
0.7026 0.7021	JM 198 0.7028 ± 0.0011
Engel <u>et al.</u> (1965)	JM 200 0.7040 ± 0.0013
Hedge and Peterman (1970)	JM 203 0.7030 ± 0.0013
	JM 205 0.7041 ± 0.0011
	JM 207 0.7040 ± 0.0012
	Average 0.7036 ± .0012

Data from Carmichael et al., (1974).

Error given in Bay of Islands analyses is one standard deviation of the norm. Values have been normalised to 0.1194 for the ratio 87/86 in normal strontium.

(1972), Kay et al. (1970), Aumento (1968) and Campsie et al. (1973).

R.E.E. data suggest a close affinity between the two analysed basalts and mid-Atlantic ridge tholeiites. However, an examination of their major element chemistry indicates that these samples are not representative of the whole mafic suite. Neither, for example, are nepheline normative.

When plotted on the diagrams of Pearce and Cann (1973) as in figure VIv, it is clear that no definite affinities are suggested. In the Ti-Zr plot, which Pearce and Cann suggest be used for rocks that have undergone mild metamorphism, the basaltic rocks plot in a field encompassing both oceanic tholeiites and calc-alkaline basalts. The same is true in the triangular plot $Ti/100 - Zr - Sr/2$, although the effects of albitisation and greenschist facies metamorphism on strontium distribution is questionable, and the plot is not advised for altered rocks.

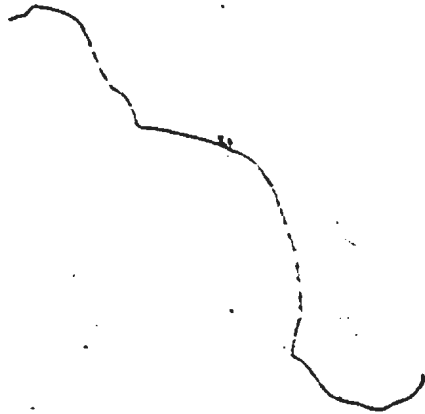
The total alkalis-silica plot, projections within the basalt tetrahedron, strontium isotope values and bulk-rock K_2O content indicate that not all rocks in the mafic suite can be considered truly tholeiitic. A number of rocks are clearly nepheline normative and others are transitional between olivine tholeiites and alkaline rocks. The bulk rock alkali content is generally higher in the basaltic rocks than expected for abyssal tholeiites, and this may not be due simply to alteration since, for example, R.E.E. data does not show the marked enrichment in L.R.E.E. usually correlatable with alteration.

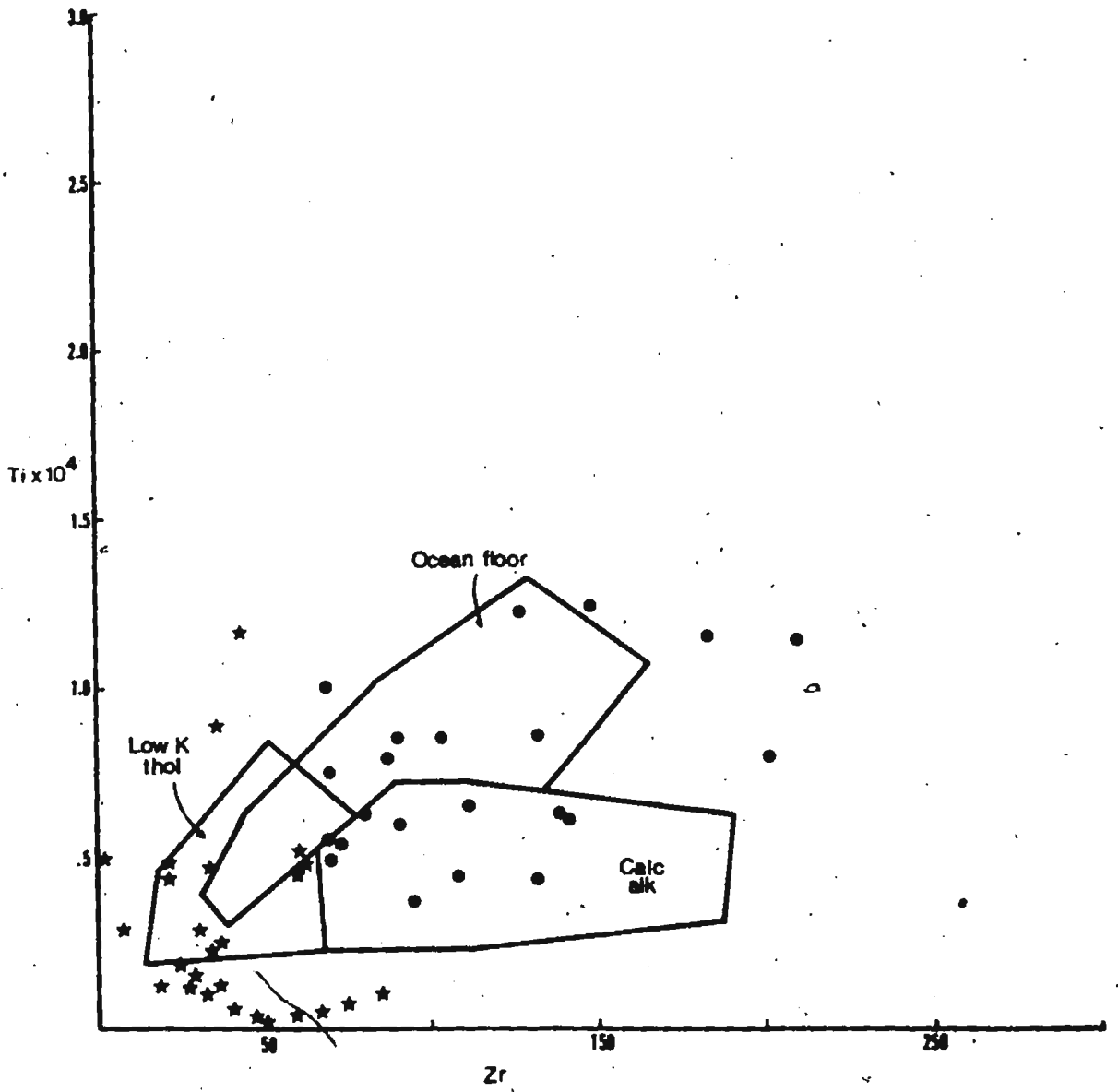
There is thus a distinct possibility that the Bay of Islands suite is in fact a transitional series from tholeiitic to mildly alkaline. It is not, in this case, directly correlatable with typical oceanic abyssal tholeiites. Such transitional suites have been collected from the mid-Atlantic

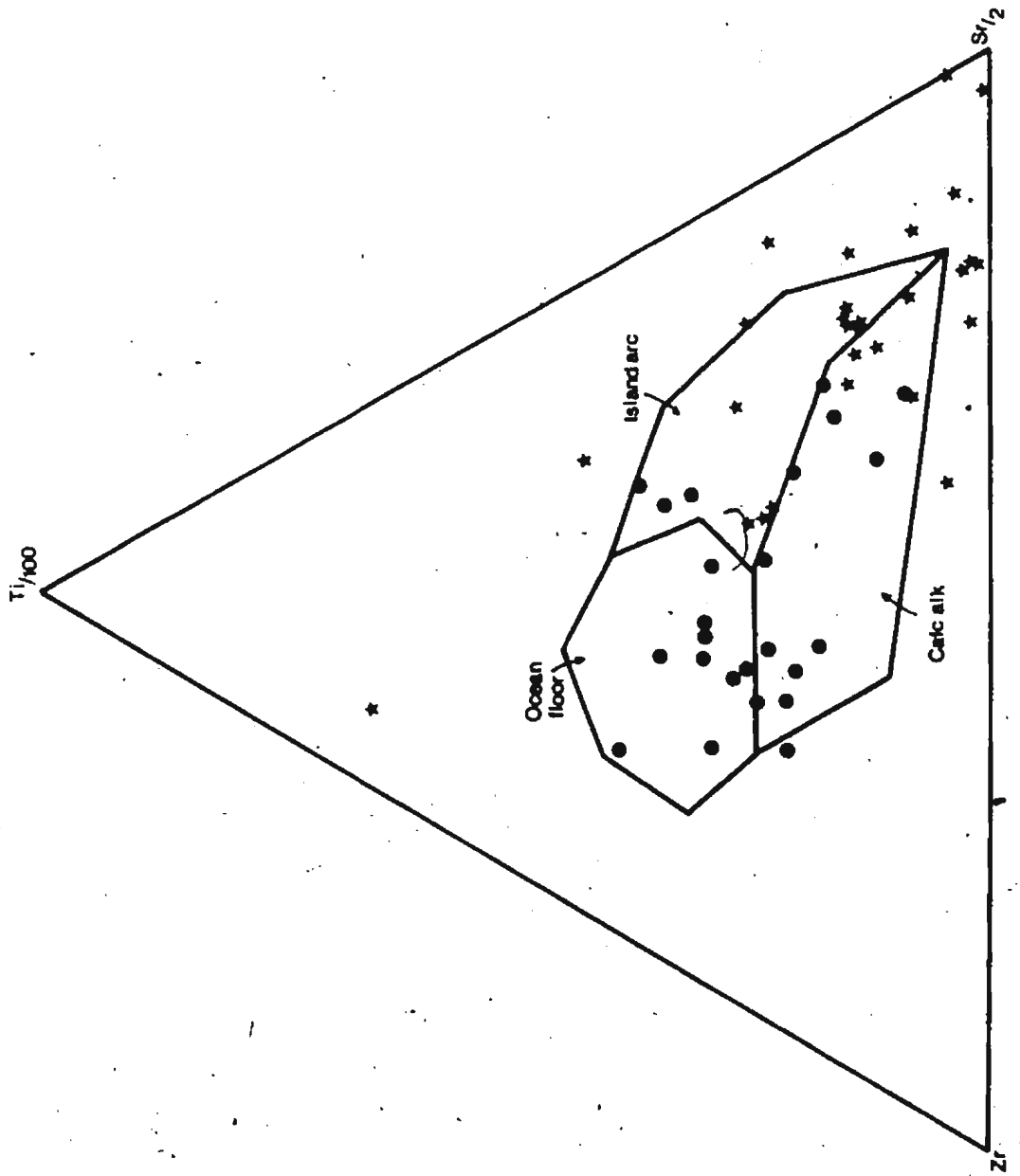
Figure VIv: (a) Ti vs. Zr (Pearce and Cann, 1973)

(b) $Ti/100 - Zr - Sr/2$

Key: ● Dikes and volcanics
★ Gabbros + CZ rocks







ridge crest by Aumento (1968) from Confederation Peak and Muir and Tilley (1964) at 45°50'N. A number of basalts in these collections are similar to some Bay of Islands Complex basalts in their high alkali content (for abyssal basalts) and their nepheline normative (or transitional) chemistry. On a recent cruise to the M.A.R. at 26°N and 11°N, the writer collected basalt samples from the central rift valley that appear mildly alkaline in nature. In the light of the above facts, some doubt is cast on the proposed constancy of composition of oceanic tholeiites as first proposed by Engel et al. (1965).

D. Conclusions.

The mineral and bulk rock chemistry support the following conclusions.

Nickel/chromium ratios, Fo contents of olivine, spinel compositions and petrographic evidence all suggest different origins for the tectonite, peridotite and cumulate mafic series. Such arguments are supported by the work of Irvine and Findlay (1972). The cumulate mafic series, diabases and pillow-lavas are genetically related. These rocks are the result of fractionation, presumably at low pressure, of olivine, clinopyroxene and plagioclase from a low-Ti and -K picritic magma derived from a mantle source. The pillow lavas are part of this fractionation series and not crystallisation products of a primary magma. There is a systematic pattern of compositional variation from basalts, through diabases and gabbros in present oceanic tholeiitic suites, suggesting that modern abyssal tholeiites likewise cannot be considered unfractionated primary magmas, but rather crystalline products of a fractionated magma at low-pressure eutectics

(O'Hara, 1968; Norman and Strong, 1975). The gabbros are clearly not melts but cumulates formed from the low-pressure crystallisation sequence a) olivine, b) olivine and plagioclase, c) olivine and plagioclase and clinopyroxene. This is supported by textural evidence. The dikes and pillow lavas are liquid compositions themselves indicating a differentiation trend. Although the suite is generally tholeiitic in composition there are strong suggestions that it is transitional to mildly alkaline in parts. This is supported by petrographic analyses which indicate the absence of orthopyroxene in most of the fractionation series.

The high proportion of harzburgite to overlying cumulates does not support any hypothesis that these peridotites formed by cumulate processes from a basaltic magma. The low pressure anhydrous (<5kb) reaction relationship between olivine and orthopyroxene, which persists to higher pressures even under low water contents (Kushiro *et al.*, 1968) prevents the simultaneous crystallisation of olivine and orthopyroxene in constant proportions as observed in the harzburgite. The harzburgites exhibit very little cryptic mineralogical or bulk chemical variation as might be expected in cumulate systems and what is observed can be attributed to interstitial liquid re-equilibrating with the harzburgite (Irvine and Findlay, 1972). The harzburgites consist of an assemblage of highly refractory chemistry with bulk Mg/Mg+Fe ratios of 0.94, alkali content and CaO and Al₂O₃ generally less than 1% and low Ti and P. Finally field evidence reveals differences in textures and structures, the harzburgites being distinctly tectonites whilst the overlying cumulates are relatively free of deformation structures. Temperatures and pressures of equilibration of the present mineralogy of the tectonites appear to be of the order of 1000°C and 18-20 kb.

The harzburgites are therefore thought to represent depleted upper mantle produced by the partial melting of aluminous upper mantle peridotite and subsequent removal of the basaltic liquid (Hamilton and Mountjoy, 1965; Himmelberg and Loney, 1973; Menzies and Allen, 1974). The further extraction of much basaltic liquid would seem impossible from the low abundance of elements that are liquid accumulative, and from the highly magnesian nature of the harzburgite mineral phases. Spinel lherzolite rocks may be modified mantle material which retain evidence of incomplete extraction processes in the form of clinopyroxene and spinel, or primary mantle compositions showing little or no partial melting.

The spinel lherzolites are compared in composition with estimated compositions of the upper mantle, both synthetic and natural, in table XXV. If the pyrolite model of Ringwood (1966) is compared it is obvious that the lherzolites are lower in contents of Na and P and possibly K and Ti. Although Green's (1970) multistage partial melt model for the origin of ocean-ridge basalts, involving the extraction of both nepheline normative melts and tholeiitic melts has been called upon to explain such depletions, it can be argued that the pyrolite composition is generally inaccurate as an estimated upper mantle composition. For example, bulk Fe/Mg ratios for the pyrolite are inconsistent with those of the tholeiitic magmas that are supposedly produced by their partial melting. Also to produce an olivine-tholeiite composition with 1-1.5% weight Na_2O would require melting of 50%, an amount too high to be plausible.

Alternative models of mantle composition compare more favourably with spinel-lherzolite compositions although generally the Fe/Mg ratio of the lherzolites is a little higher than in other naturally occurring

Table XXV

Estimations of Upper Mantle Primary Composition.

wt%							
SiO ₂	48.09	43.24	44.5	44.2	43.95	45.1	44.26
MgO	31.15	38.10	41.7	41.3	39.00	36.7	39.94
FeO	12.71	9.25	7.3	7.3	7.50	7.9	6.82
Fe ₂ O ₅	-	-	1.5	1.1	0.75	2.0	1.95
M ₂ O ₃	3.02	3.90	2.55	2.7	3.88	4.1	3.13
CaO	2.32	3.72	2.25	2.4	2.60	2.3	2.88
Na ₂ O	1.13	1.78	0.25	0.25	0.60	0.6	0.12
K ₂ O	0.13	-	0.015	0.015	0.22	0.0(2)	0.15
Cr ₂ O ₃	0.55	-	-	0.30	0.41	0.3	0.42
NiO	-	-	-	0.20	0.39	0.2	0.37
MnO	0.43	-	0.14	0.15	0.13	0.2	0.12
P ₂ O ₅	0.34	-	-	-	-	0.1	0.03
TiO ₂	0.13	-	0.15	0.1	0.57	0.5	0.18
TOTAL	100.00	100.00	100.36	100.02	100.00	100.00	100.37

1. Mason (1966)
2. Ringwood (1966)
3. White (1967)
4. Harris et al (1967)
5. Green and Ringwood (1967)
6. Nicholls (1967)
7. Lherzolite average, this work.

herzolites (Ito and Kennedy, 1967). The chemical heterogeneity of the spinel herzolites may be produced by modal fluctuations of the magmatic segregation material, some being depleted, and others indicating that they are enriched by trapped segregated liquid, with high contents of alkalis and alumina.

The bulk of the dunitic rocks in the Bay of Islands Complex lie above the harzburgites. Dunite veins and dikes within the harzburgites generally have sharp contacts with the host rock, and are believed to be the result of crystallisation of olivine and chromite from liquids trapped in the harzburgite during its convective ascent, probably below a spreading ridge axis. There is no evidence for residual 100% or 90% olivine dunites which would be expected to have a much higher Cr, Ni and lower Ti, Fe and Mn content than refractory harzburgites (Burns, 1973). A cumulate origin can be similarly argued for the main dunite zone, suggesting that it forms the basal portion of the fractionated stratiform series, and this is especially evident where it contains euhedral chromite accumulations strung out parallel to the contact with the harzburgites.

The significance of the contact between the harzburgite and overlying dunite is that it must represent the junction between rocks of mantle origin and rocks which formed under crustal conditions in relatively high-level stratiform intrusions. Irvine and Findlay (1972) have suggested a similar model but did not recognise the cumulate dunite zone. The horizon has been called the 'petrological Moho', or the genetic discontinuity between crust and mantle (Malpas, 1973). Such a discontinuity was suggested by the models of Greenbaum (1972) for the Troodos Complex, Cyprus. The Critical Zone, higher in the succession, represents the moho as defined

geophysically, since it is here that major density changes take place in the lithologies. There is some indication that the petrological moho may also be defined seismically since weak discontinuities have been noted below the present oceanic moho to depths of about 600 metres (M. J. Keen, R. Moberly; pers. comms., 1972).

E. Petrogenesis.

i) C.M.A.S. projections

One atmosphere phase relation can generally be shown adequately in the normative basalt tetrahedron. However, since its usefulness is restricted to portrayal of processes acting near the surface, phase relationships at mantle pressures, which determine the compositions of partial melts produced at depth, are more usefully shown in the system $\text{CaO-MgO-Al}_2\text{O}_3\text{-SiO}_2$ (C.M.A.S.). The projection rules for this tetrahedron are given by O'Hara (1968, pp. 86-87). Figure VIw shows the positions of the three planes of projection used in the following discussion.

The development of a hypothetical control plane for advanced partial melting is shown in figure VIx. Source rock 1 at the beginning of melting produces the liquid composition E at the quaternary eutectic. The liquid will remain at this composition with increased melting until the aluminous phase has been completely melted. Subsequently the liquid will migrate along path EA until all the clinopyroxene is melted and then along control plane A-1-En5 as the liquid becomes progressively richer in the enstatite molecule. Liquids produced at any stage along the control plane between A and the original source rock composition, 1, will leave a residue of olivine and enstatite. The control plane therefore effectively includes the original source rock composition plus the residual harzburgite composition

Figure VIw: Projection planes within the system
 $\text{CaO-MgO-Al}_2\text{O}_3\text{-SiO}_2$.

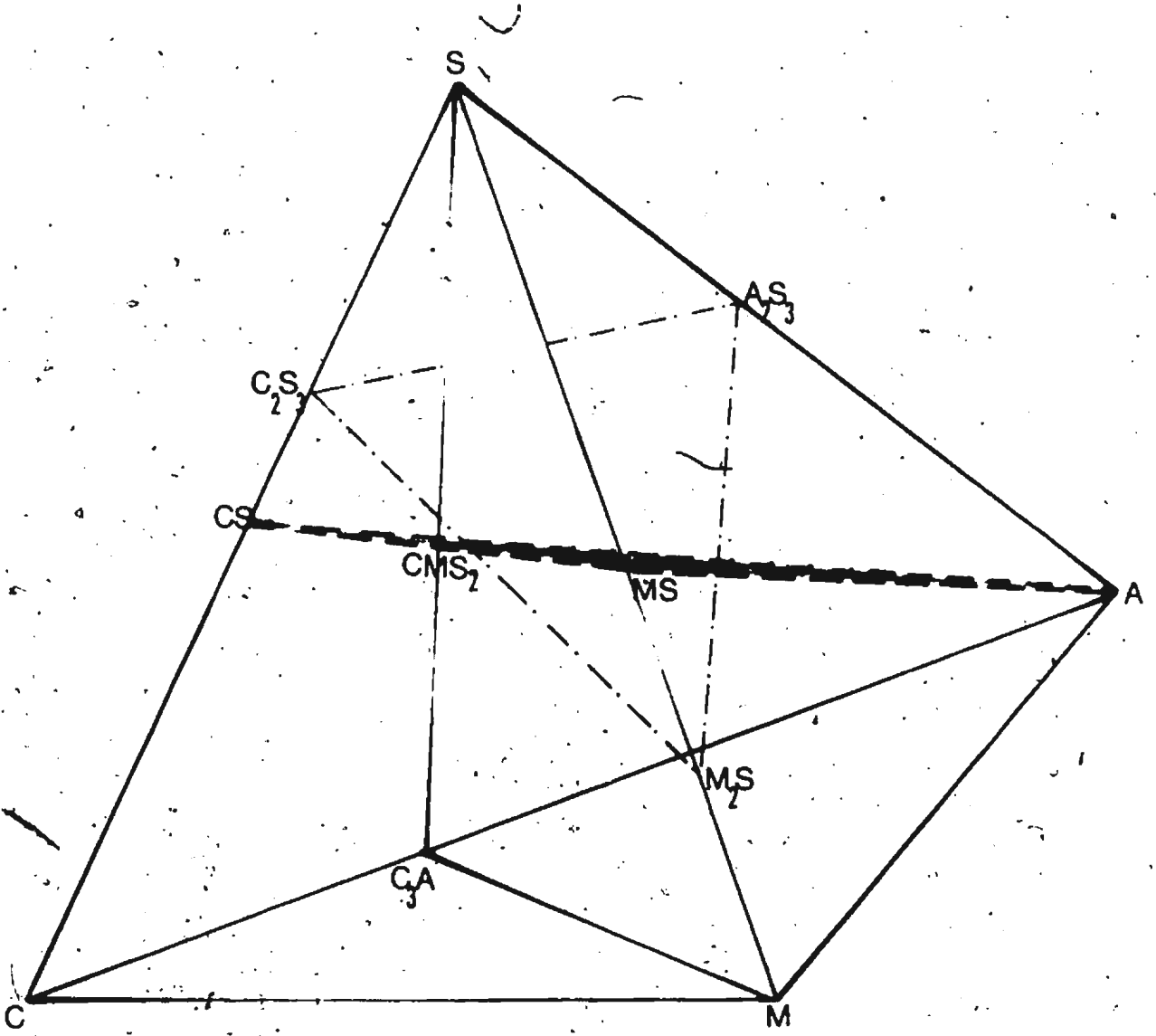


Figure Vix: Development of control plane for advanced melting.

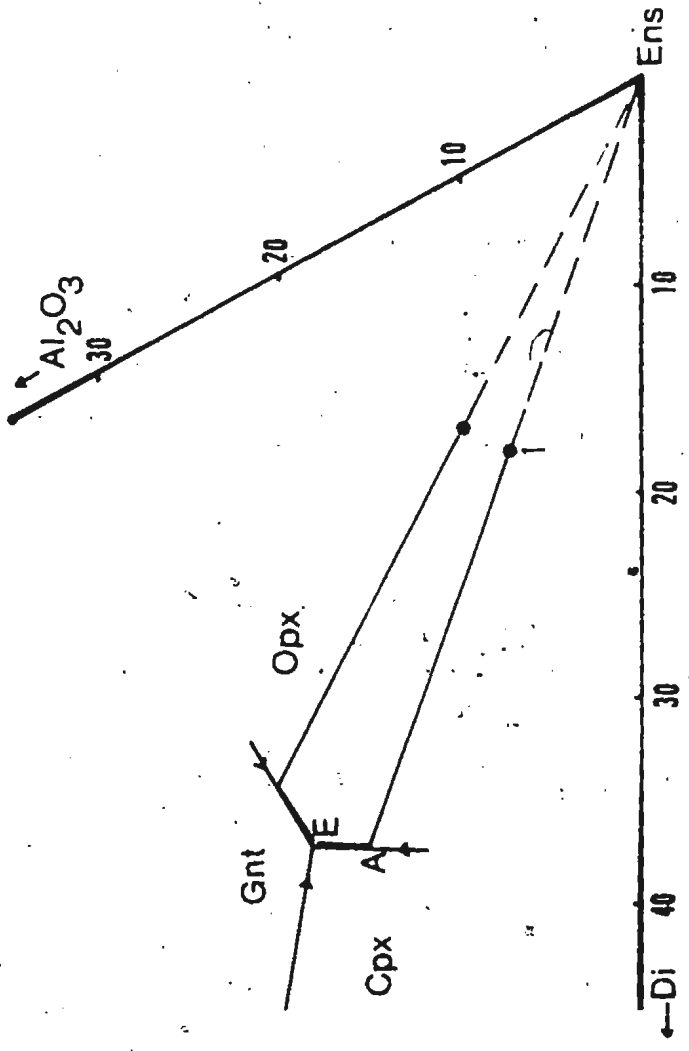
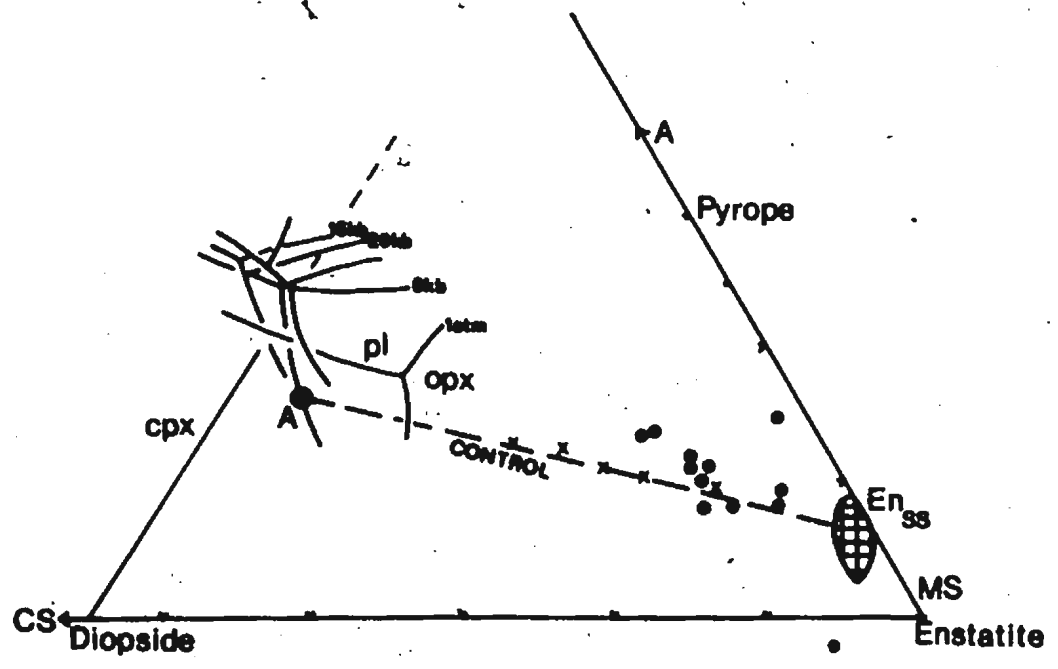
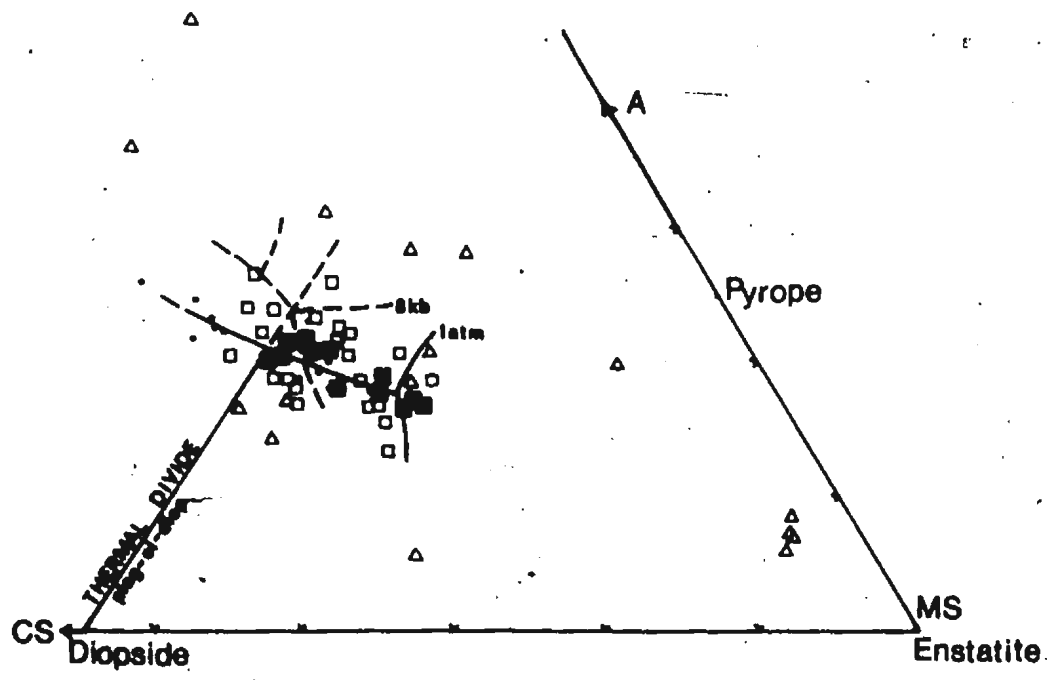


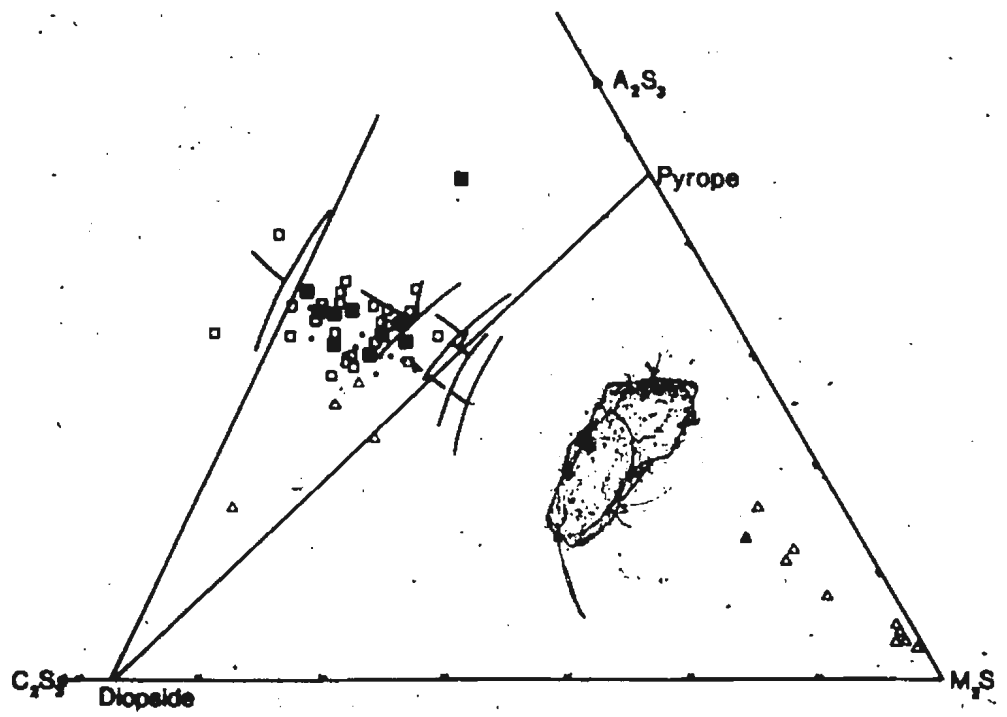
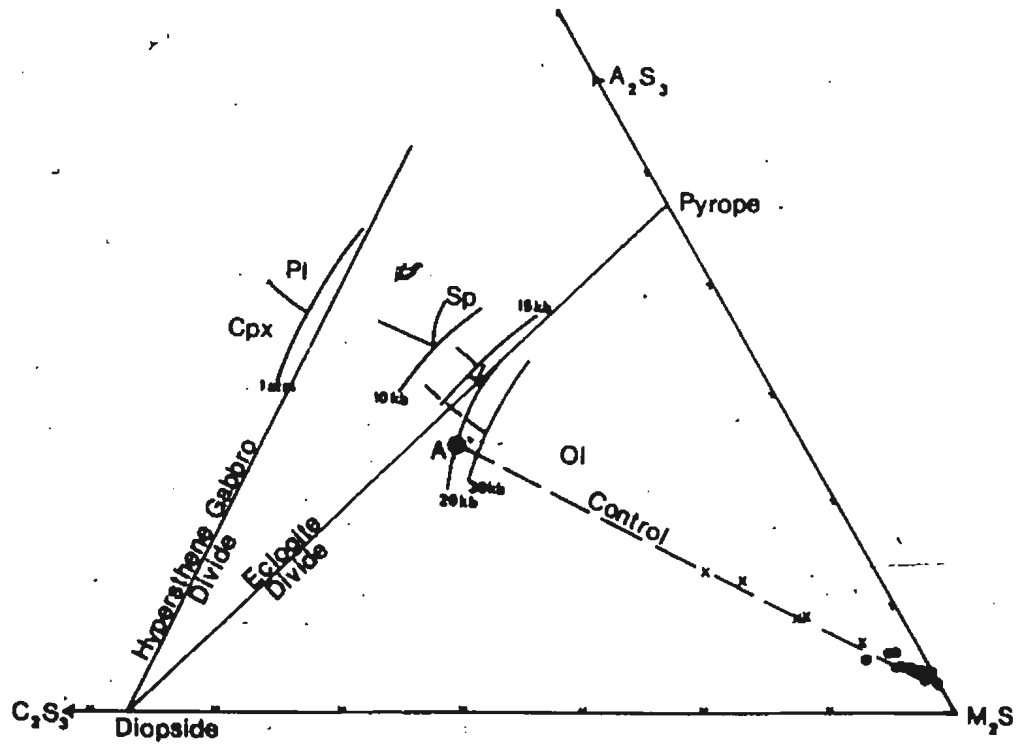
Figure VIy: C.M.A.S. Projections

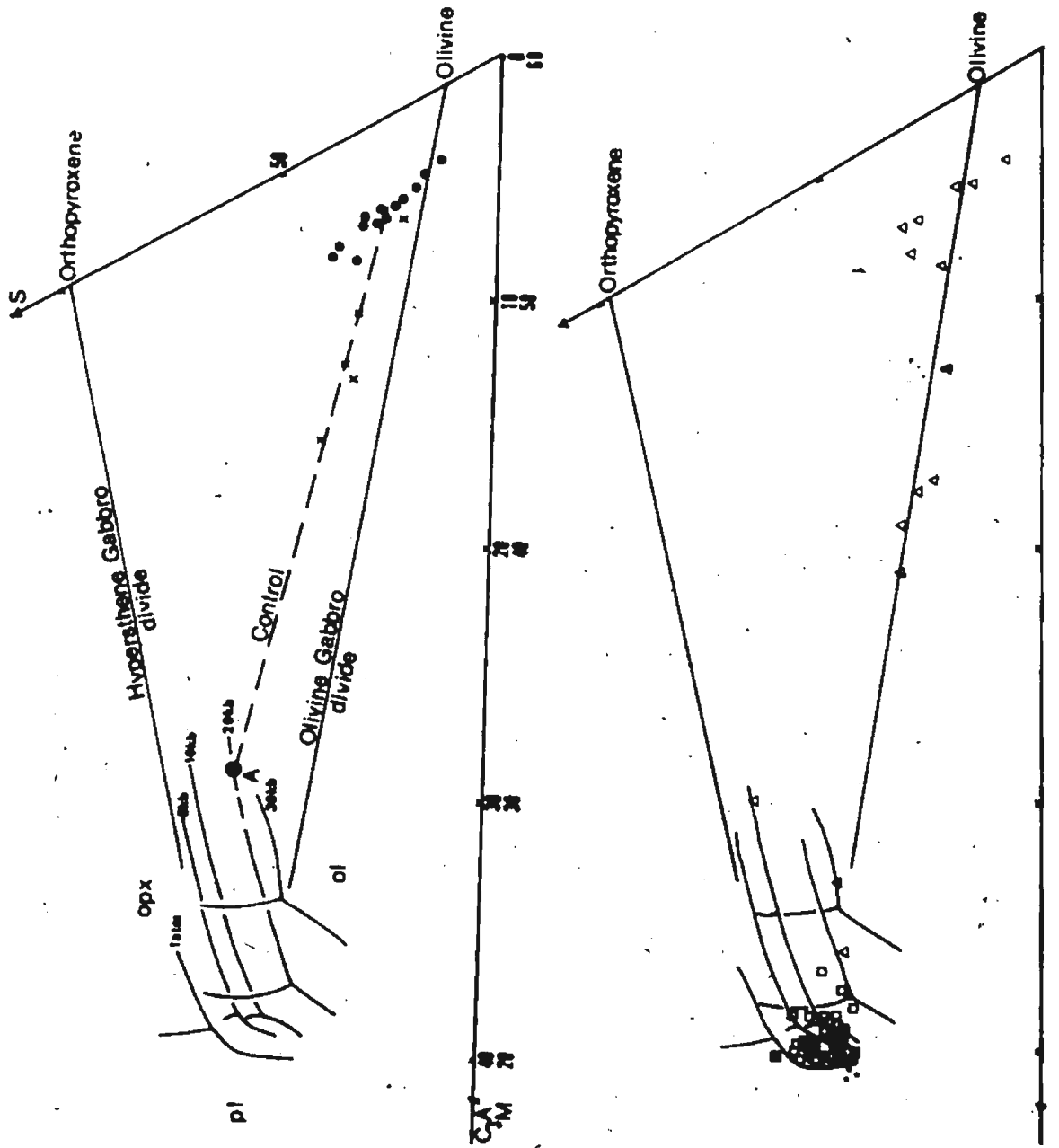
- a) From Olivine
- b) From Enstatite
- c) From Diopside

Key:

- Harzburgites
- x Lherzolites
- △ Dunites + CZ rocks
- Gabbros
- Dikes
- Volcanics





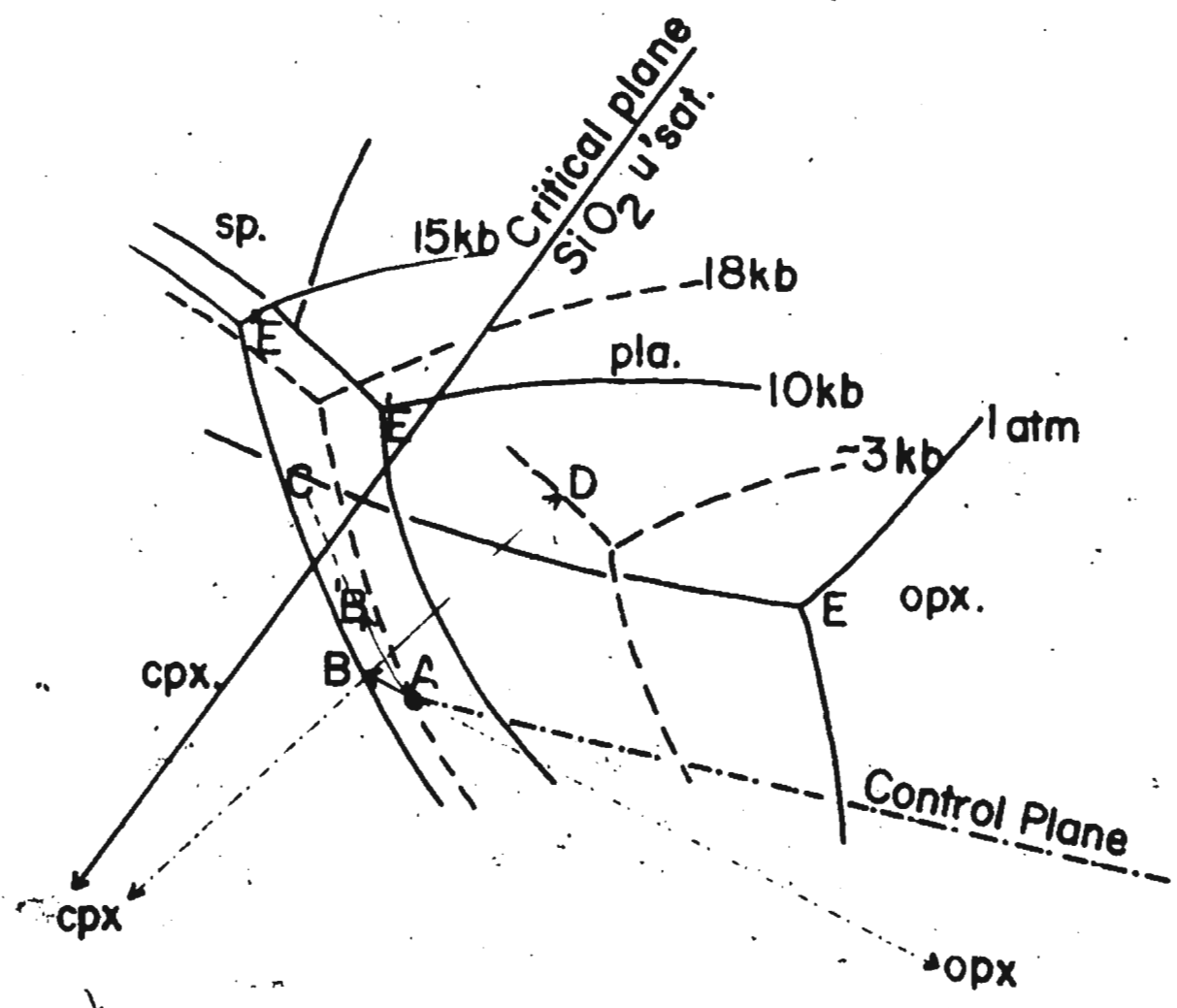


at advanced melting.

The olivine-orthopyroxene control plane during partial melting of spinel lherzolite compositions is indicated on all projections in figure VIy, but is especially evident on the enstatite and olivine projections. It is drawn through the lherzolite average composition and residual harzburgite average composition and is controlled by the solid solution compositions of olivine and enstatite. (The scatter of some harzburgite compositions in the olivine projection is a result of the projection method.) The composition of the final liquid produced during partial melting of the spinel lherzolite must also lie on these control lines, and since some small amount of clinopyroxene remains in the harzburgites, must also be on the olivine, orthopyroxene, clinopyroxene cotectic, i.e. Point A, at 18-20 kb. This pressure is chosen since it is the pressure at which the harzburgite mineralogy equilibrated during final stages of partial melting. If continued melting had taken place at any lower pressure, then presumably the harzburgite would register lower equilibrium pressures. The primary melt, i.e. composition A, has komatiitic affinities (Cawthorn and Strong, 1975).

Basalt compositions project close to low-pressure plagioclase-clinopyroxene cotectics. The spread of points in the olivine and enstatite projections is mainly resultant from the projection method. This can be seen by comparison with the diopside projection where basalts cluster around 1-5 kb plagioclase-clinopyroxene-olivine cotectics in a relatively restricted field. Some dikes, all gabbros and the cumulate rocks plot away from the cotectics indicating cumulate enrichment in plagioclase and/or olivine, but dominantly along low-pressure control planes defined by these

Figure VIz: Olivine projection onto plane CS-MS-A
to show liquid lines of descent for primary
melt A.



minerals. No rocks appear to have crystallised at the low-pressure eutectic in agreement with the absence of orthopyroxene in the basalts. The basalt compositions straddle the low-pressure thermal divide between alkaline and olivine-tholeiite fields indicating the transitional nature of the series.

The convective rise of mantle material into pressure regimes of less than 20 kb caused crystallisation of the melt that had been produced at greater pressures. This convective rise can be viewed as a diapiric upwelling of a solid/liquid mixture. The nature of the crystallisation depended upon the rate of uprise of the diapir, thence the rate of pressure reduction, and the rate of crystallisation of the liquid. With reduction in pressure the cotectics move as indicated in the projections. If reduction in pressure took place slowly, allowing the rate of crystallisation to maintain a liquid path along the olivine-clinopyroxene-orthopyroxene cotectic, then between pressures of 18-20 kb and 15 kb, the liquid path would be along a line such as A-B-C (figure VIz) such that an initially tholeiitic liquid (primary melt A) would become eventually alkaline as it crossed the low pressure thermal divide. Such would be the case if continued fractionation took place along this cotectic at any pressures between 20 and 10 kb (figure VIz). It is estimated from the projections that 25% crystallisation of melt A at such pressures would cause the transition into the alkali field. Below 10 kb continued fractionation would give a residual liquid once more in the tholeiitic field.

If pressure reduction took place relatively quickly, such that cotectic crystallisation was not maintained, then olivine alone would crystallise out initially. The olivine would be joined by orthopyroxene if the olivine-orthopyroxene cotectic was intersected (figure VIy).

Co-crystallisation of olivine and orthopyroxene would be possible down to pressures of 15 kb (i.e. path A → B, figure VIz) when movement of the cotectic to lower pressure positions would leave liquid B in the olivine-clinopyroxene field. Orthopyroxene would then be replaced by clinopyroxene in the crystallisation sequence causing liquid composition to move from B towards D (figure VIz). At any stage during such a crystallisation sequence, the residual liquid is tholeiitic in composition.

At lower pressures, clinopyroxene and olivine would be joined by plagioclase as fractionating phases (e.g. position D, figure VIz) and the sequence as explained in the one atmosphere basalt tetrahedron derived.

Clearly, if cotectic crystallisation had taken place during slow ascent of the diapir, then orthopyroxene would disappear as a crystallising phase when the path of the eutectic "E-E" passed across the path of liquid descent and intersection of the clinopyroxene-plagioclase cotectic was possible.

Any combination of these crystallisation paths can occur according to the changing rate of pressure reduction, or crystallisation rate; e.g. a period of cotectic crystallisation might be followed by an increase in rate of upward movement of the diapir causing the crystallisation of only one phase, or vice versa.

The various proportions of the three phases, olivine, orthopyroxene, clinopyroxene, that are obtained by crystallisation under polybaric high-pressure conditions explains the various modal proportions of these minerals comprising the veins in the tectonites. These veins represent early fractionation products of the primary melt as it crystallises at pressures

below 20 kb. Dunite veins represent non-cotectic crystallisation of olivine; enstatolite, crystallisation of orthopyroxene and olivine along a line such as A-B in figure VIz; and pyroxenite veins (e.g. Sample En-V, table XIX), fractionation of dominantly clinopyroxene, e.g. along line B-D in figure VIz.

Starting with a primary melt of composition A, it is possible to derive both nepheline normative alkaline liquids (e.g. composition C) and tholeiitic liquids. Release of these liquids and their subsequent eruption may explain the transitional nature of the mafic series of the Bay of Islands Complex. Release of the primary melt, or a very slightly fractionated derivative of it would give rise to picritic lavas such as described by Upadhyay (1973) and Norman (1974) found associated with other Newfoundland ophiolite suites. Control of the time and depth of release of these liquids would be dominantly controlled by the amount of liquid present and the rate of ascent of the diapir.

More significantly perhaps, the petrogenetic scheme presented may explain the increase in alkalinity of volcanics away from ridge axes in present oceans (McBirney and Gass, 1967; Strong, 1974) and support O'Hara's (1973) view that this is due to increased opportunity for crystal fractionation. Liquids erupted in off-ridge environments have progressively thicker, colder and perhaps more solid lithosphere to pass through before eruption and therefore greater opportunity for high-pressure cotectic crystallisation as their upward progress is physically impeded by the lithosphere plate. Material ascending directly beneath the ridge-axis encounters virtually no lithosphere and will be erupted after little high-pressure cotectic crystallisation (Figure VIaa). Material ascending

Figure VIaa: Model to explain increased alkalinity of off-ridge volcanics.

Low p. fractionn.
Rapid rise

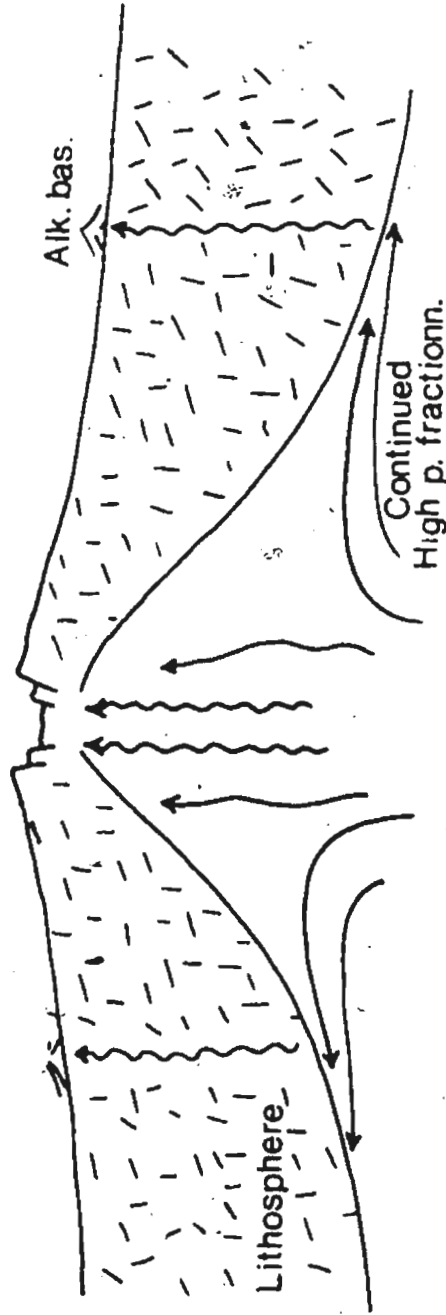


TABLE XXVI

Compositions used for Subtraction Programme

	Lherzolite	Harzburgite
SiO ₂	44.26	43.67
TiO ₂	0.18	0.02
Al ₂ O ₃	3.13	0.48
Cr ₂ O ₃	0.42	0.42
Fe ₂ O ₃	1.95	1.19
FeO	6.82	6.85
MnO	0.12	0.14
MgO	39.94	46.86
CaO	2.88	0.36
Na ₂ O	0.12	0.00
K ₂ O	0.15	0.02
P ₂ O ₅	0.03	0.00
NiO	0.37	0.39

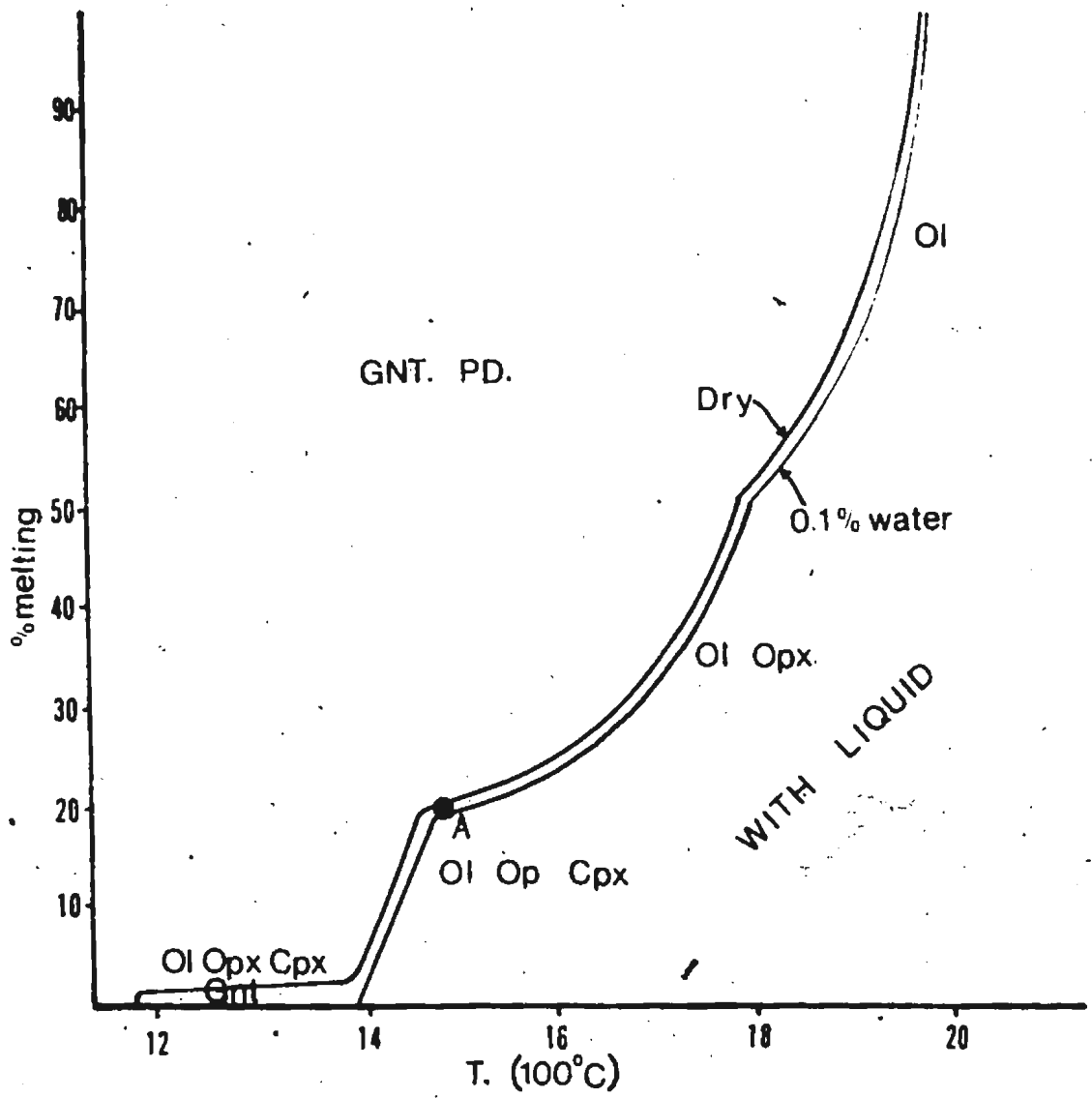
just off-axis might travel laterally and undergo further fractionation before eruption. Temperature gradients derived by Bottinger (1974) for spreading rates of 4 cm/year suggest that magma held at pressures of 20-10 kb (i.e. 60-30 kb depth) may still be fractionating (i.e. still liquid present) up to 1000 km from the ridge axis. This suggests that some oceanic island-alkali-magmatism is possibly not hot-spot related, but is rather a result of intersection of deep fault structures with zones of partially fractionated magmas.

The petrogenetic model also indicates that at pressures of less than 20 kb, no melting has taken place in the upwelling diapir. If applicable on a wider scale, this is contrary to the views of many workers which state that release of pressure and accompanied adiabatic temperature increase lead to melting at any depth, but is in accord with Cawthorn's (1975) calculations.

ii) Degrees of Partial Melting

An 'extraction programme' developed by R. G. Cawthorn (1975) has been used to calculate the degree of partial melting of the spinel lherzolites that had to take place to produce a melt of composition A (figure VIy). This programme subtracts various amounts of a given harzburgite composition from a given lherzolite composition and recalculates the residuum (in this case, the melt) composition (Appendix IV). In this case an average Bay of Islands spinel lherzolite composition was used as starting material and the most residual harzburgite composition subtracted (Table XXVI). The resultant liquid must plot at point A on all C.M.A.S. projections and should have an $Mg/Mg+Fe^2$ ratio consistent with

Figure Vibb: Degree of partial melting as a function of temperature.



it being in equilibrium with the harzburgite, i.e. 0.77-0.78. It has been found that partial melting of 23% produces a liquid composition fulfilling these requirements. This liquid composition is noticeably similar to the picritic basalts of Glarke (1970) who suggests their formation as a primary magma by partial melting of garnet peridotite at 30 kb.

According to the work of O'Hara (1968) a partial melt of 23% plots at position A (figure VIb) and should be in equilibrium with a harzburgitic residuum containing little remaining clinopyroxene. The field evidence and petrogenetic model of the Bay of Islands Complex is thus correlatable with this experimental work.

iii) Degrees of Fractional Crystallisation

The original magma, of composition A (figure VIy), produced in equilibrium with the harzburgites, must have had a $Mg/Mg+Fe^2$ ratio in equilibrium with olivine Fo_{92} (olivine composition of harzburgites). Experimentally determined partition coefficients between olivine and liquid suggest that this ratio should be 0.77-0.78 (Roeder and Emslie, 1970). Clearly, therefore, the basalts do not represent this original composition but are crystallised from a later liquid after fractionation of a certain proportion of cumulates. These proportions can be estimated approximately as follows:

(i) Assuming that only olivine is removed as cumulate material and that all olivine removed has an average content Fo_{87} (Fo_{90} is removed during early stages of fractionation and much more fayalitic compositions later), then

$$\text{wt \% MgO}_{\text{initial magma}} = \text{wt \% MgO}_{\text{basalt}} + x \text{ wt \% MgO}_{\text{Fo}_{87}}$$

$$\text{wt \% FeO}_{\text{initial magma}} = \text{wt \% FeO}_{\text{basalt}} + x \text{ wt \% FeO}_{\text{Fo}_{87}}$$

where x = % of fractionated Fo_{87}

$$\text{and } \text{Mg}/\text{Mg} + \text{Fe}^2 \text{ initial magma} = 0.78.$$

$$\text{Wt \% MgO in } \text{Fo}_{87} = 47.5$$

$$\text{Wt \% FeO in } \text{Fo}_{87} = 12.5$$

$$\text{Wt \% MgO in basalt} = 8$$

$$\text{Wt \% FeO in basalt} = 7.$$

Therefore for basalt + 20% Fo_{87}

$$\text{Wt \% MgO} = 17.5$$

$$\text{Wt \% FeO} = 9.5$$

$$\text{Mg}/\text{Mg} + \text{Fe}^2 = 0.768.$$

and for basalt + 25% Fo_{87}

$$\text{Wt \% MgO} = 19.8$$

$$\text{Wt \% FeO} = 10.1$$

$$\text{Mg}/\text{Mg} + \text{Fe}^2 = 0.779.$$

This calculation suggests that an initial magma produced in equilibrium with Fo_{92} would require fractionation of 20-25% olivine (Fo_{87}) to produce the basalt composition. Although no accurate estimate of the amount of vein material cutting the harzburgites is available, the total amount of fractionated olivine from field evidence does not appear to exceed 10 per cent of the total mafic sequence. Therefore it is necessary to take into account fractionation of gabbroic composition in addition to olivines.

The presence of cumulate gabbros in the field support this reasoning.

(ii) Assuming 10% fractionation of olivine Fo_{87} : Wt % MgO = 12.71,
Wt % FeO = 8.25
 $Mg/Mg + Fe^2 = 0.735$.

Now with further fractionation of gabbroic material (including critical zone rocks),

Wt % MgO gabbro = (approx.) 12.0
Wt % FeO gabbro = " " 4.1

Then,

Basalt + 10% Fo_{87} + 60% gabbro
Wt % MgO = 19.91
Wt % FeO = 10.65
 $Mg/Mg + Fe^2 = 0.771$

This calculation assumes 10% olivine fractionation (orthopyroxene and clinopyroxene have also been fractionated, especially in the veins, but since their Mg/Fe ratios are similar to olivine and since they crystallise in relatively small amounts, they are neglected for this approximation), followed by 60% gabbro fractionation, leaving 30% liquid. That is the primary magma, A, should give rise to

- Olivine (pyroxene) cumulates including veins - 10%
- Gabbro cumulates + some dikes + C.Z. - 60%
- Basalts + dikes - 30%

Such proportions do not seem inappropriate for the Bay of Islands Complex, from the field evidence. The proportion of ultramafic cumulates might be increased, and gabbro proportion decreased when an accurate estimate of amounts of vein material are made.

At this point it is worth noting that similar arguments applied to contemporary oceanic tholeiites indicate that they do not have an $Mg/Mg + Fe^2$ ratio in equilibrium with the mantle composition from which many authors suggest they are directly derived. Calculations made, for example, on the analyses presented by Dimitriev (1974), who explicitly states that abyssal tholeiites are primary and undifferentiated melts of the upper mantle, indicate that a 20% fractionation of olivine (Fo_{87}) is required to produce his basalt composition from a primary melt in equilibrium with upper mantle lithologies. Such arguments apply to almost all oceanic tholeiites described in the literature, and substantiate the view that oceanic tholeiites are a result of crystallisation from a differentiated magma.

CHAPTER VII

TECTONIC SETTING AND EMPLACEMENT OF THE OPHIOLITE SUITE

A. Introduction.

Ophiolite suites have been the source of controversy and discussion amongst geologists for several decades. Early workers (e.g. Benson, 1926; Steinmann, 1905, 1927) who first defined the ophiolite suite on the basis of their work in the Alps, suggested that these rocks represented intrusive and volcanic products of a eugeosynclinal environment that later became involved in the mountain building episode of the orogenic cycle. With more recent theories of plate tectonics and sea-floor spreading, ophiolites have assumed a more significant role in that they have been interpreted by a number of geologists as cross-sections of oceanic lithosphere (e.g. Dietz, 1963; Hess, 1964; Gass, 1968; Reinhardt, 1969; Moores and Vine, 1971; Dewey and Bird, 1971; Church, 1972). Williams and Smyth (1973) have summarised the evidence supporting such views.

B. Oceanic Crust and Mantle.

The probable structure and stratigraphy of oceanic lithosphere has been outlined by a number of workers (e.g. Cann, 1968, 1970; Christensen, 1970; Aumento, 1972; Vine and Moores, 1973). Almost all of the knowledge concerning thickness, composition and physical properties of the oceanic crust is derived from seismic refraction experiments and dredging in the deep sea. Constraints on the models developed from this evidence are placed by measurements of gravity and magnetic fields in the ocean basins, and proposed models of the upper mantle below the oceanic crust.

Refraction seismics have delineated three layers within the oceanic crust. Layer one has variable seismic velocities and is of variable thickness. The seismic properties suggest that this layer is made up of sediments and this has been confirmed by dredge and drill sampling. Layer two exhibits compressional wave velocities (V_p) between 4.3 and 5.8 km/s. Typically the layer is 1-2 km thick. Layer three has seismic velocities (V_p) of 6.7 ± 0.3 km/s, and is between 4.5 and 5 km thick on average. The presence of submarine volcanoes and the predominance of basaltic rocks, especially pillow lavas, in bottom photographs and dredge hauls, suggest that basaltic rocks floor the ocean basins beneath the sediments and probably comprise the major part of layer two. More recently, the results of JOIDES and other drilling programmes have confirmed beyond reasonable doubt that at least the top of layer two is basaltic in composition. The composition of layer three is more controversial. In his classic paper of 1962, Hess suggested that it consists of serpentinised peridotite. Subsequently other workers (e.g. Christensen, 1970; Cann, 1970) suggested that layer three is more likely to be comprised of amphibolite, gabbro or a combination of gabbro, diabase and their metamorphic equivalents. The fact that diorites, gabbros and anorthosites have been dredged from the ocean floor (Cann and Funnel, 1967; Aumento, 1969; Engel and Fisher, 1969; Melson and Thompson, 1970) supports this view.

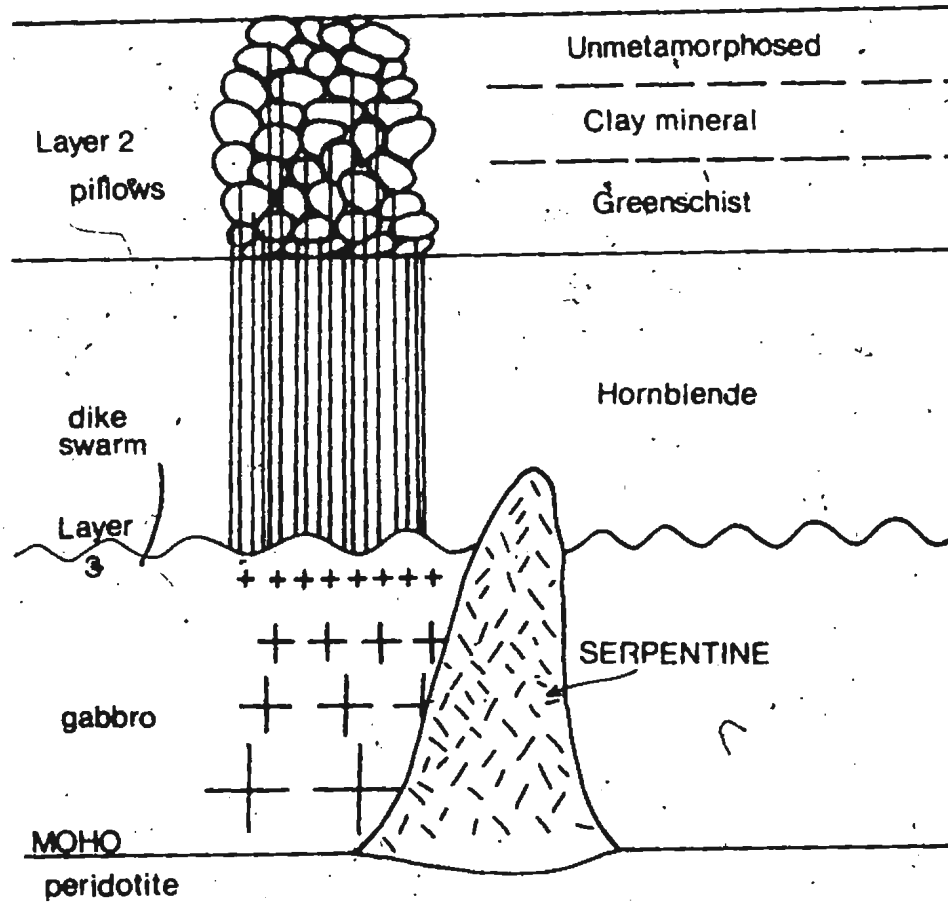
Cann (1970) constructed a model for oceanic crust entirely from the consequences of plate tectonic theory and from rocks and geophysical measurements from the ocean floor, especially at ridge-crests. The crustal structure he envisaged comprises a zone of unmetamorphosed pillow lavas overlying metamorphosed pillow lavas in two metamorphic zones. These zones show (a) the development of clay minerals and zeolites from the ferromagnesian

minerals and deeper (b) greenschist-facies metamorphism (Melson et al., 1968; Cann, 1969; Aumento, 1972). The pillow lavas are intruded by feeder dikes for the flows and beneath this is a diabase dike swarm proper which grades downwards through coarser-grained dikes to a massive layered gabbro forming the lower crust (figure VIIa). No reference was made to the ophiolite complexes of continents during the construction of this model, but when comparison is made between the model and the observed structure of ophiolite complexes, the similarities are very striking. Several ophiolite complexes, e.g. Bay of Islands Complex, Troodos Complex, South Oman Complex, have exactly the same elements as the model, and in many others only small parts of the sequence are missing.

The mantle underlying oceanic crust may be divided into three types on the basis of dredged samples and inclusions in basalts from oceanic islands. Primary or primitive mantle material has not been depleted through processes of partial melting. The composition of this material is generally typified by the lherzolitic inclusions found in oceanic basalts. Depleted mantle is material from which a basaltic, or more likely a picritic, melt has been extracted to give rise to the cumulate and extrusive members of the oceanic crust. This mantle material is generally believed to consist of harzburgite plus or minus dunite. Thirdly, cumulate ultramafic rocks have been recorded in dredge hauls from the Atlantic Ocean floor (Aumento et al., 1971; Aumento and Loubat, 1971) and are thought to have formed by fractionation from the magma produced by partial melting of the primary mantle.

Although no stratigraphy, or direct relationship between these ultramafic rocks can be recorded from ocean dredge hauls, all types occur

Figure VIIa: A model for the oceanic crust (Cann, 1970).



in the Bay of Islands ophiolite, with an apparent stratigraphy, and strengthen the correlation between this ophiolite suite and oceanic lithosphere.

C. The Bay of Islands Complex and Other Ophiolite Suites.

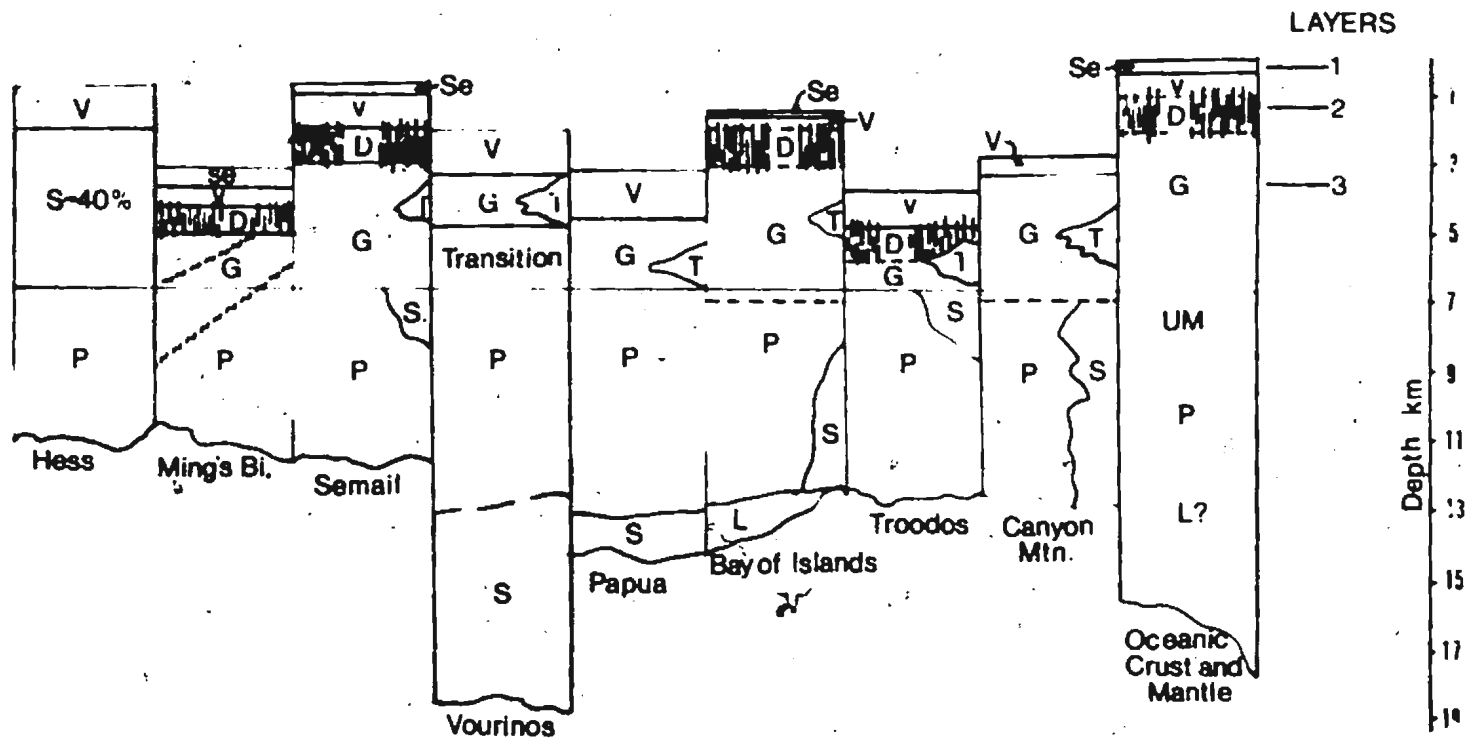
The Bay of Islands Complex is compared with proposed sections of oceanic lithosphere and other well-known ophiolite complexes in figure VIIb. Clearly many of the ophiolite suites, including the Bay of Islands Complex, are thinner overall than oceanic crust, generally as a result of a reduced gabbro section compared with layer three of the oceanic crust. Six of the ophiolite complexes show a clear development of sheeted diabases, four of these being Newfoundland examples. The Papuan ophiolite, the Canyon Mountain Complex, and the Vourinos Complex are comparable in that they show a significantly greater development of dioritic rocks in the cumulate sequence than the other complexes, and apart from the Semail Complex, Oman, they approach more closely the thicknesses implied for oceanic crust.

Perhaps the widest cited and best recognised of these ophiolite complexes is the Troodos Complex of Cyprus. Indeed, this Complex has been taken by some authors as a type example of ophiolite suites. It is therefore pertinent here to make a closer comparison between this Complex and the Bay of Islands Complex.

The Troodos Complex has been investigated by a number of workers (e.g. Wilson, 1959; Bear, 1960, 1966; Gass and Masson-Smith, 1963; Moores and Vine, 1971; Greenbaum, 1972; Vine and Moores, 1972). All have recognised a basic stratigraphy within the Troodos Complex comparable with that described here for the Bay of Islands Complex except that the exposure and preservation of ultramafic rocks is much more complete in the latter.

Figure VIIb: Comparison of oceanic lithosphere and well known ophiolite suites.





- | | | | |
|----|-----------|----|--------------|
| Se | Sediments | T | Trondhjemite |
| V | Volcanics | P | Peridotite |
| D | Diabase | L | Lherzolite |
| G | Gabbro | S | Serpentine |
| | | UM | Upper mantle |

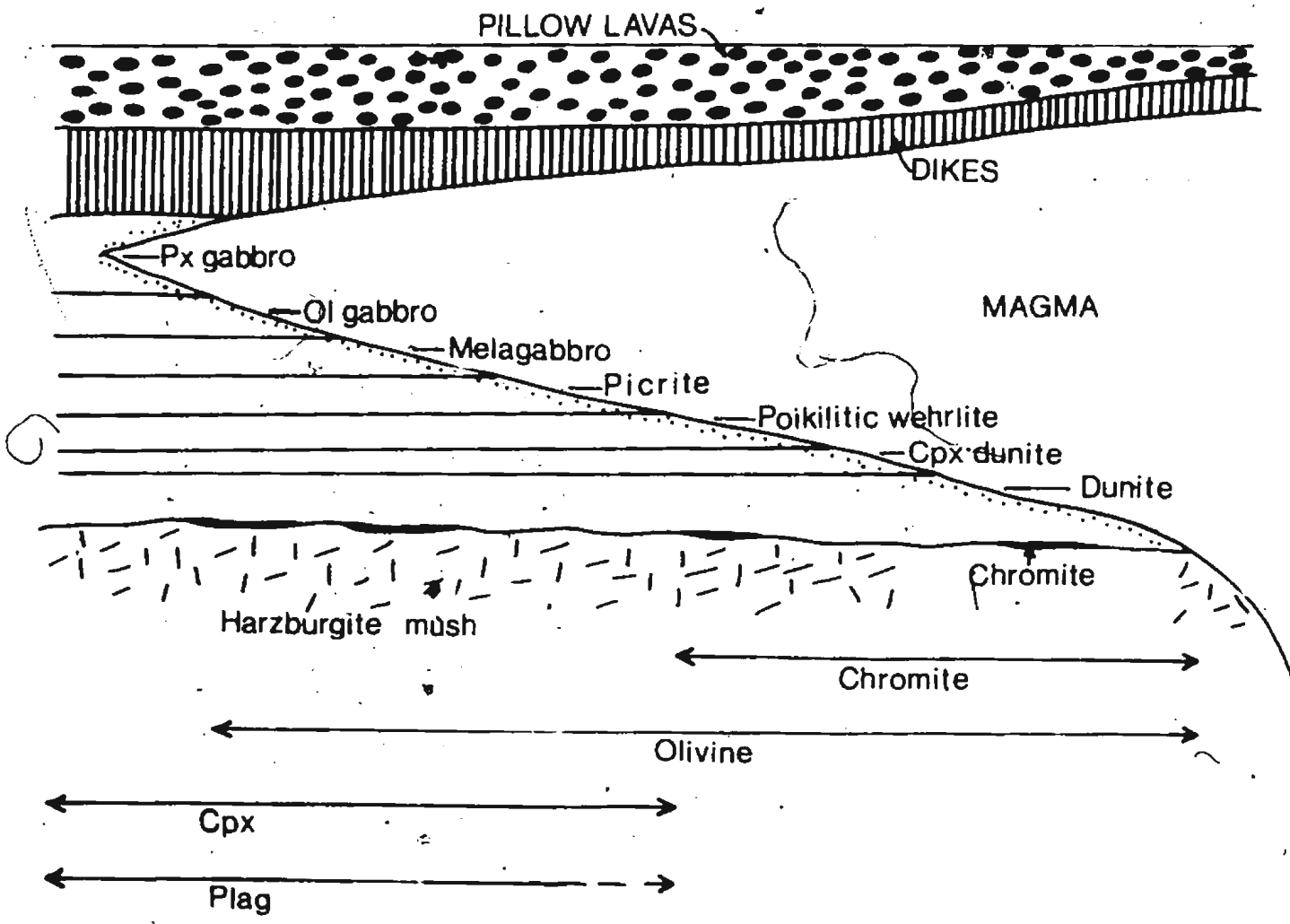
On Troodos, the ultramafic rocks are dominantly harzburgite tectonites, a residual product of mantle fusion, which form the basement for the Plutonic Complex (Bear, 1960). There is no recognised base to these rocks, such as the basal thrust zone of the Bay of Islands Complex, and gravity data suggest that they extend downwards for some considerable distance although they might be thrust at depth (Gass and Masson-Smith, 1963). No ultramafic compositions such as the high-pressure spinel lherzolites of the Bay of Islands Complex, which here are interpreted as primary mantle material, are evident in the Troodos Complex. The harzburgites, or enstatite olivinites of the Cyprus Survey geologists, are strongly foliated, display isoclinal folds especially marked by interlayered dunite bands and in thin section, show all the features of mantle tectonites. Optical determinations of mineral compositions (Böttcher, 1969) suggest that forsterite content of olivines in these rocks is between Fo_{90} and Fo_{94} . These harzburgites thus are directly comparable with the harzburgite tectonites of the Bay of Islands Complex.

The overlying Plutonic Complex consists of a layered series of unalbitised gabbro, norite, olivine-gabbro, troctolite, olivine-pyroxene and dunite with accessory chromite. It has been demonstrated by Greenbaum (1972) that the crystallisation sequence of cumulate minerals in this series is i) olivine + chromite, ii) olivine + clinopyroxene, iii) olivine + clinopyroxene + orthopyroxene, iv) clinopyroxene + orthopyroxene + plagioclase. The presence of orthopyroxene as a cumulate mineral in the later sequences is in marked contrast to the Bay of Islands plutonic rocks where this phase is absent from all but the earliest cumulate rocks. Mineralogical analyses of the plutonic complex olivines indicate forsterite contents varying between

Fo₈₇ and Fo₈₂ and there is an associated bulk rock iron enrichment trend. Thus there is a marked discontinuity between the harzburgites and rocks of the Plutonic Complex both in textures (tectonites to cumulates) and mineralogy (Fo₉₂ to Fo₈₇). This is directly comparable to the petrological Moho as already defined here in the Bay of Islands Complex.

Although both Greenbaum (1972) and Moores and Vine (1971) agree that the Troodos Plutonic Complex was produced below a slowly spreading oceanic ridge, the actual nature of the magma chamber(s) and its crystallisation is disputed. Greenbaum envisages a single, large magma chamber extending along the strike of the ridge as a trough-like pool fed centrally by a tapering conduit (figure VIIc). The magma chamber is surrounded on bottom and sides by residual mantle harzburgites whilst the cap above the reservoir is made up of dikes and extruded pillow lavas. In this model, crystallisation proceeding within the magma chamber gives rise to mafic and ultramafic cumulates according to the thermal conditions at any point. That is, high-temperature phases (e.g. chromite and olivine) crystallise in the hotter, inner regions near to the axis. Hot magma of the same composition entering the chamber serves to maintain the process. As spreading continues, crystals accumulating on the moving floor are carried slowly outwards and become buried beneath lower temperature assemblages (figure VIIc). The main argument against this model is structural. It is difficult to conceive of a mechanism to support a thin cover of diabases above a large magma chamber such that the dikes are emplaced at the spreading centre and apparently thicken away from this axial zone as a layer. Added to this is an argument which Greenbaum himself realises. This is the apparent lack of evidence for any large scale magma chamber convection that

Figure VIIC: Magmatism at spreading centre (Greenbaum, 1972).



would be expected in a reservoir in which temperature gradients were fairly dominant, in this case from the hot, central feeder zone to the cooler lateral margins.

These arguments do not arise with the model proposed by Moores and Vine (1971) which depicts the formation of the plutonic complex as a number of small fractionating magma chambers below the spreading centre. Evidence supporting this model consists of the intrusive relationships visible between gabbro bodies within the main gabbro zone (Allen, pers. comm., 1974) and the presence of diabase dikes cross-cutting gabbro cumulates and in some places the more ultramafic cumulates. In a sequence of small intrusions it would not be difficult to envisage dikes from one body extending vertically towards the surface and also laterally to cut dikes, gabbros and possibly ultramafic cumulates of an older solidified body. A similar model has been proposed for the genesis of Newfoundland ophiolites at an oceanic spreading centre by Strong and Malpas (1975).

The hypabyssal intrusive rocks and volcanics of the Troodos are comparable in many aspects with those of the Bay of Islands. The Troodos complex has an extremely well developed sheeted dike complex, much more so than the Bay of Islands, but unlike the latter does not show a development of dike breccias. Some tectonic brecciation took place during Alpine orogenic episodes but this is not restricted to the diabases. In both its areal extent and its restriction to the diabase unit, the dike brecciation in the Bay of Islands Complex does not have a parallel in Troodos.

Cyprus geologists have recognised two divisions of pillow lavas in the Troodos Complex. The Upper Pillow Lava Group consists of pillowed flows and extrusive breccia. Most pillows in this group contain olivine

phenocrysts and are chemically alkaline in nature. They lie with marked unconformity either on the lower pillow lavas or the sheeted diabases. The Lower Pillow Lavas characteristically display plagioclase and pyroxene phenocrysts. Alteration is much more marked in the Lower Series; albite and celadonite are common and vesicles are filled with quartz and chalcedony. Chilled margins are preserved in the Lower Pillow Lavas but have not been found in the upper series. Unlike the Upper Pillow Lavas, the Lower Series are characterised by high silica, low potash and variable amounts of other elements. K_2O contents group around 0.25% in contrast to a greater spread for the Upper Pillow Lavas.

The presence of the unconformity between the two series has allowed Gass and Smewing (1973) to suggest that sufficient time had elapsed for ocean-ridge metamorphism and erosion, and migration of the Lower Pillow Lavas from the ridge axis before extrusion of the Upper Pillow Lavas. They explain the Upper Series as resulting from 'off-axis' magmatic activity, probably on the ocean rise.

Although a division between upper and lower pillow lavas has been made in the Bay of Islands Complex, all the volcanics are probably correlatable with the lower pillow lavas of the Troodos Complex. If Strong's (1974) hypothesis is correct, then the Skinner Cove volcanic series and possibly the volcanics of the Little Port Complex are comparable with the Troodos Upper Pillow Lava Group.

D. Orogenic History.

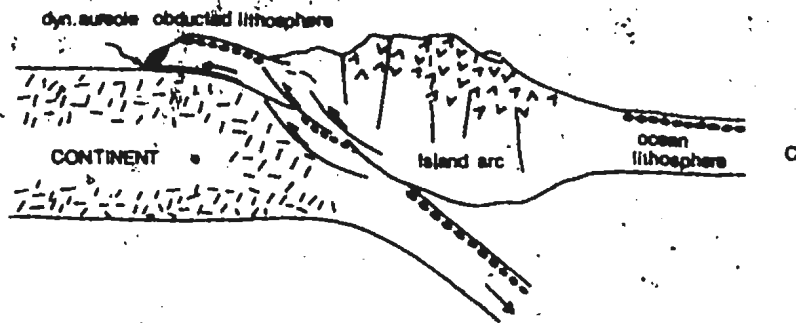
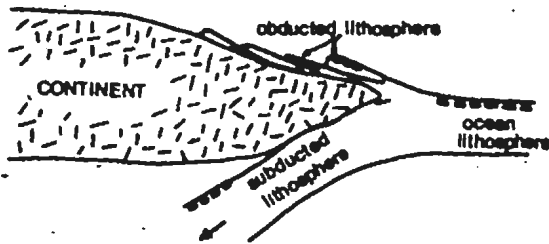
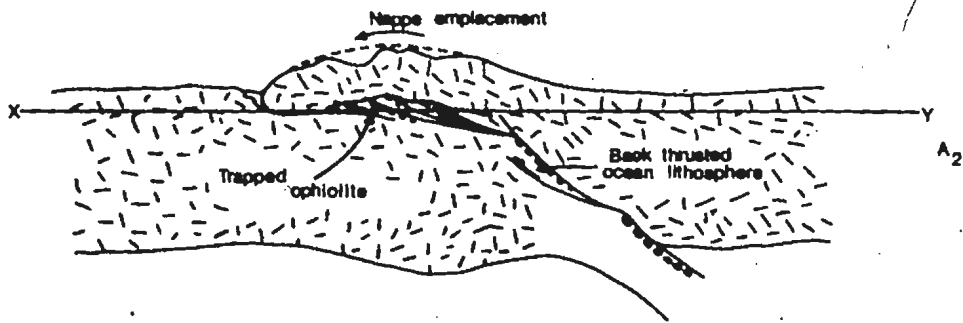
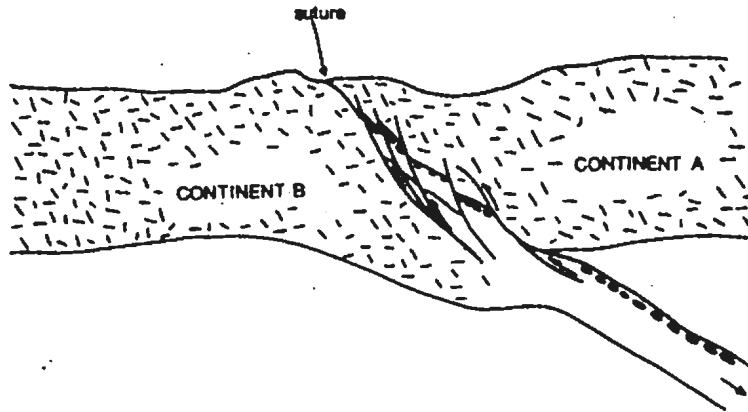
The ophiolite suite is therefore generally assigned an oceanic origin, but subsequent emplacement in fold belts is another problem about

which considerably less is known (Coleman, 1971; Church and Stevens, 1971; Moores, 1970; Moores and MacGregor, 1972; Maxwell, 1974).

Observation of a number of ophiolite terranes and accompanying literature research suggests that two major groups of models account for ophiolite emplacement in orogenic belts. Both groups involve tectonic activity at consuming plate margins but whereas one invokes the emplacement of the ophiolite suite by obduction and gravity sliding, the other involves initially the subduction of the suite and its subsequent elevation to the surface by isostatic rebound. In this case the term obduction is applied to the lithosphere plate that is overthrust during plate collision, and when only part of the lithosphere is obducted the term 'flake-tectonics' has been used (Oxburgh, 1972 and figure VIId). When emplacement takes place by obduction and gravity sliding, then the ophiolite forms the overriding slice and is more likely to be preserved as one or two thrust slices displaying a complete or nearly complete stratigraphy. Because the ophiolite is not overridden by another plate, the obducted rocks are relatively little deformed and high-pressure, blueschist-type metamorphism is rare or absent. However, amphibolitic dynamothermal aureoles formed during initial displacement of hot rocks, and local mélangé zones formed during gravity sliding or late stage emplacement are common.

On the other hand, ophiolites emplaced by subduction mechanisms might be expected to show the results of being overridden by the other lithosphere plate. They are more likely to be dismembered by thrusting in the subduction zone, so much so in some cases to produce 'ophiolite mélangé' which is of considerable aerial extent and shows no well preserved stratigraphy. High-pressure metamorphic assemblages developed as

Figure VIId: Emplacement mechanisms for ophiolite suites.



Sections A₁, A₂ - Subduction mechanisms
 X-section through X-Y after isostatic uplift would expose trapped ophiolite in window. A₁ - initial collision
 A₂ - after nappe emplacement

Section B - Flate tectonic obduction mechanism.

Section C - Whole lithosphere obduction mechanism.

underthrusting takes place are more common and may show later retrograde metamorphism developed during the isostatic rebound of the ophiolite.

If these general models are correct, then the tectonic setting and state of preservation of an ophiolite suite may indicate its mode of emplacement, e.g. the Troodos and Semail Complexes are ideal examples of the obducted ophiolites whereas the disrupted Franciscide Formation and Alpine-Zagros ophiolites display many of the characteristics of the subducted type.

Study of the Bay of Islands Complex affords an opportunity for the discussion of an emplacement model. It seems from the field evidence that the Bay of Islands ophiolite was emplaced by obduction of the flake-tectonics type. It is also apparent from temperatures of metamorphism obtained from the aureole rocks that the ultramafics were at temperatures in the order of 1000°C at the time of their initial displacement. The obducted oceanic slice appears to have been thrust at about 3 km below the critical zone, a depth by analogy equivalent to 10 km of oceanic lithosphere. According to present day geothermal gradients, temperatures of 1000°C could only occur in two oceanic environments at these depths. One is on, or very close to, a spreading centre; the second is in a marginal basin where high heat flow exists as a result of igneous activity above a subduction zone.

Naturally, the heat source, the factors controlling heat distribution and the attitude of geotherms are all recurring problems in any analysis of this sort, and whether or not a correlation of environments is valid rests largely upon these poorly understood conditions.

If the Bay of Islands Complex was formed at a major spreading centre, e.g. a mid-ocean ridge, then the strike of the sheeted dikes should

parallel that of the ridge axis. This direction would be expectedly north-east, parallel to the ancient continental margin, yet the orientation of the dikes on both Blow me down Mountain and North Arm Mountain is at a high angle to this, implying either that there was rotation of the ophiolite slices during transportation or that the ridge did not parallel the continental margin but possibly intersected it at an angle. The former case seems less likely when it is realised that the individual slices forming the massifs must have rotated in exactly the same manner to exactly the same degree.

Sediments penetrated by drill holes during the JOIDES deep-sea drilling programme are typically calcareous ooze, partially chertified turbidites or deep-sea muds. The radiolarian ribbon cherts commonly overlying basalts of ophiolite sequences are rarely formed. Pebble conglomerates and quartzofeldspathic sandstones as found in the Bay of Islands Complex have no deep-sea equivalents. It seems likely that these sediments were derived from continental or island arc terranes, suggesting that the site of formation of the ophiolites was close to an ocean margin. In some ophiolite localities, particularly the Tethyan ophiolites, the radiolarian chert may be thin or represented by either limestone or turbidite sandstones. When fossil dating is possible, the cherts and limestones associated with the uppermost basalt are of the same or only slightly greater age than the oldest flysch deposits of the orogen in which the ophiolite has been incorporated.

A summary of palaeontological and radiometric ages obtained for rocks of the Humber Arm Allochthon, and correlatable rocks in the Hare Bay Allochthon, is given in Table XXVII. The dates of formation of the Skinner

TABLE XXVII

Age dates from Humber Arm Allochthon and related rocks, Western Newfoundland

Formation etc.	Age	Type	Source	Significance
Skinner Cove	Tremadocian	Fossil	Strong (197)	Age of formation of Skinner Cove Assemblage. (Upper Slice Assemblages?)
Cape Onion (Hare Bay)	Tremadocian Grapt. Zn l.	Fossil		Age of formation of Cape Onion volcs. Upper Slice Assemblage, Hare Bay (Possibly = to aureole volcs. of Bay of Islands).
Little Port Complex	507 \pm 4 my	Zircon	Mattinson (1975)	Age of granitic intrusion in L.P.C.
Little Port Complex	469 \pm 14 my	K/Ar	Archibald and Farrar (1976)	Cooling age of L.P.C. following granite emplacement and metamorphism or displacement of L.P.C. as thrust slice.
Middle Arm Point	Lower Arenig 500 my	Fossil	Stevens (1970)	Early detritus from allochthonous rocks dates early stages of obduction?
Bay of Islands C. Aureole:	454 \pm 9 my	Ar ⁴⁰ /39	Archibald and Farrar (1976)	Age of cooling through blocking temperature for amphiboles of aureole -- post-dates initial obduction
	460 \pm 5 my	Ar ⁴⁰ /39	Dallmeyer & Williams (1975)	
Bay of Islands C. Gabbros/Dikes:	452 \pm 12 my	K/Ar	Archibald and Farrar (1976)	Age of cooling of ophiolite suite.
Gabbros:	445 my	Ar ⁴⁰ /39	Dallmeyer, pers. comm. (prelim. figure)	
Long Point Fm.	Llandeill/ Caradoc. 445 my	Fossil	Rodgers (1965)	Age of autochthonous rocks immediately overlying allochthon. Final emplacement of allochthon complete by this time.

Cove Assemblage and Little Port Complex are given as Tremadocian and 507 m.y. (Tremadocian?) respectively, although some doubt may be attached to the assignment of numerical values to the fossil ages (see below). Other radiometric ages from the allochthonous rocks are cooling ages and represent the time at which argon was effectively locked within the mineral(s) used for dating. The cooling age of 469 m.y. obtained for the Little Port Complex has been interpreted by Archibald and Farrar (1976) as the time of initial displacement of these rocks. Since it is believed that all the allochthonous rocks were displaced and assembled at the same time, ages obtained for the aureole rocks of the ophiolite slice should concur with this date. The actual dates of 454 and 460 m.y. do agree within the stated limits, and slight discrepancies might be explained by minor differences in cooling rates. Clearly the cooling ages obtained for the ophiolite suite itself are simultaneous to the displacement dates suggesting that times of formation and obduction of the ophiolite were not vastly different unless completely different cooling rates apply. Furthermore, since palaeontological and stratigraphic control is good for the Humber Arm region, the dates reported above might be used as geochronological reference points for the lower to middle Ordovician. Stevens (1970) argued that obduction of the Bay of Islands Complex was initiated in early Ordovician time since the oldest flysch containing ophiolite detritus is late Arenig in age. It therefore seems plausible that the age of 469 m.y. might be attributed to the late Arenig. For comparison, Harris et al. (1965) suggested an age of 475 m.y. for the middle Arenig and Dallmeyer and Williams (1975) have suggested an average age of 460 m.y. for late Arenig-early Llanvirn time.

E. Conclusions.

Since there is considerable evidence that the Bay of Islands ophiolite was still hot when initially displaced, it can be suggested that its formation was in a region close to the continental margin onto which it was obducted. The estimates of geothermal gradients within the ophiolite indicate that it was formed either in a marginal basin or at a major spreading centre. If this spreading centre was an oceanic ridge then it is probable that this ridge intersected the ancient continental margin as supported by the nature of overlying sediments and the orientation of sheeted dikes. The formation of the ophiolite suite was thus closely followed by its obduction as supported by available age dates.

These conclusions place several constraints on plate-tectonic models of the development of the Newfoundland Appalachians (e.g. position of major and marginal basins) and should be considered in any proposed regional synthesis.

BIBLIOGRAPHY

- AKELLA, J. and BOYD, F. R., 1973. Partitioning of Ti and Al between coexisting silicates, oxides and liquids. *Geochim. Cosmochim. Acta*, Supp. 4 (4th Lunar Sci. Conf.), v. 1, pp. 1049-1059.
- ANDERSON, M. M., 1972. A possible time span for the late Precambrian of the Avalon Peninsula, S. E. Newfoundland, in the light of world wide correlation of fossils, tillites and rock units within the succession. *Can. J. Earth Sci.*, v. 9, #12, pp. 1710-1726.
- AOKI, K. and KUSHIRO, I., 1968. Some clinopyroxenes from ultramafic inclusions in Dreiser Weiher, Eifel. *Contrib. Mineral. Petrol.*, v. 18, #4, pp. 326-337.
- ARCHIBALD, D. A. and FARRAR, E., 1976. K/Ar ages of amphiboles from the Bay of Islands ophiolite and the Little Port Complex, W. Newfoundland, and their geological implications. *Can. J. Earth Sci.*, (in press, April).
- ATLAS, L. M., 1952. The polymorphism of $MgSiO_3$ and solid state equilibria in the system $MgSiO_3 - CaMgSi_2O_6$. *J. Geol.*, v. 60, #2, pp. 125-147.
- AUMENTO, F., 1968. The Mid-Atlantic Ridge near 45°N. II. Basalts from the area of Confederation Peak. *Can. J. Earth Sci.*, v. 5, pp. 1-21.
- AUMENTO, F., 1969. Diorites from the M.A.R. at 45°N. *Science*, v. 165, pp. 1112-1113.
- AUMENTO, F., 1972. The oceanic crust of the M.A.R. at 45°N: in "The ancient oceanic lithosphere", E. Irving (ed.). *Earth Physics Branch Publ.* v. 42, #3, pp. 49-54.
- AUMENTO, F. and LONCAREVIC, B.D., 1969. The M.A.R. near 45°N. IV. Bald Mountain. *Can. J. Earth Sci.*, v. 6, pp. 1431-1440.

- AUMENTO, F., LONCAREVIC, B. D., ROSS, D. I., 1971. Hudson geotraverse: Geology of the M.A.R. at 45°N. in A discussion on the petrology of igneous and metamorphic rocks from the ocean floor. Roy. Soc. London Phil. Trans. Ser. A., v. 268, #1192, pp. 623-650.
- AUMENTO, F. and LOUBAT, H., 1971. The Mid-Atlantic Ridge near 45°N; XVI, Serpentinised ultramafic intrusions. Can. J. Earth Sci., v. 8, #6, pp. 631-663.
- AVE LALLEMENT, H. G., 1967. Structural and petrofabric analyses of an 'alpine-type' peridotite: the Iherzolite of the French Pyrenees. Leidse Geol. Med., v. 42, pp. 1-57.
- AVE LALLEMENT, H. G., and CARTER, N. L., 1970. Syntectonic recrystallisation of olivine and modes of flow in the upper mantle. Geol. Soc. America Bull., v. 81, #8, pp. 2203-2220.
- AYRTON, S., 1968. Structures isoclinales dans les peridotites du Mont Vourinos (Macedoine greque) - un exemple de deformation de roches ultrabasiques. Schweiz. Mineral. Petrog. Mitt., v. 48, pp. 101-132.
- BAILEY, E. B. and McCALLIEU, W. J., 1952. Ballantrae igneous problems; historical review. Edin. Geol. Soc. Trans., v. 15, pp. 14-38.
- BAIRD, D. M., 1960. Sandy Lake (west half), Newfoundland. Geol. Surv. Canada Map 47-1959.
- BANNO, S., 1970. Classification of eclogites in terms of physical conditions of their origin. Phys. Earth & Planet. Int., v. 3, pp. 405-421.
- BARNES, I., LaMARCHE, V. C., HIMMELBERG, G., 1967. Geochemical evidence of present day serpentinisation. Science, v. 156, pp. 830-832.
- BARTHOLEME; P., 1960. Genesis of the Gore Mountain garnet deposit, N.Y. Econ. Geol., v. 55, #2, pp. 255-277.

- BEAR, L. M., 1960. The geology and mineral resources of the Akaki-Lythrodondha area. Cyprus. geol. surv. dept. Mem. #3, 122p.
- BEAR, L. M., 1966. Ann. Rep. Geol. Surv. Dep. Cyprus for 1965, pp. 26-37.
- BENNINGTON, K. O., 1956. Role of shearing stress and pressure in differentiation as illustrated by some mineral reactions in the system $MgO-SiO_2-H_2O$. J. Geol., v. 64, #6, pp. 558-577.
- BENSON, W. N., 1926. The tectonic conditions accompanying the intrusion of basic and ultrabasic igneous rocks. Nat. Acad. Sci. Mem. 19, #1, 90p.
- BEZZI, Alfredo and PICCARDO, G. B., 1971. Structural features of the Ligurian ophiolites; petrologic evidence for the 'oceanic' floor of the Northern Apennines Geosyncline; a contribution to the problem of the alpine-type gabbro-peridotite associations. Soc. Geol. Ital. Mem., v. 10, #1, pp. 53-63.
- BIRD, J. M. and DEWEY, J. F., 1970. Lithosphere plate - continental margin tectonics and the evolution of the Appalachian orogen. Geol. Soc. America Bull., v. 81, pp. 1031-1060.
- BOETTCHER, A. L., 1969. The system $CaO-Al_2O_3-SiO_2-H_2O$ (abst.): Eos Amer. Geophys. Union Trans., v. 50, #4, p. 352.
- BONATTI, E., KRAEMER, T. and RYDELL, H., 1972. Classification and genesis of submarine Fe-Mn deposits. in Papers from a conference on Ferromanganese deposits on the ocean floor, pp. 149-166, Natl. Sci. Found. Off. Int. Dec., Ocean. Expl. Washington, D.C.
- BÖTTCHER, W., 1969. Zur Entstehung des magmatischen Troodos-Komplexes (Zypern). Neues Jb. Mineral. Abh. 110, #2, pp. 159-187.
- BOTTINGER, Y., 1974. Thermal aspects of sea-floor spreading, and the nature of the suboceanic lithosphere. Tectonophysics, v. 21, pp. 15-38.

- BOWEN, N. L. and SCHAIRER, J. F., 1935. The system $MgO-FeO-SiO_2$.
Am. J. Sci., s 5, v. 29, #170, pp. 151-217.
- BOWEN, N. L. and TUTTLE, O. F., 1949. The system $MgO-SiO_2-H_2O$.
Geol. Soc. America Bull., v. 60, pp. 439-460.
- BOYD, F. R. and ENGLAND, J. L., 1960. Apparatus for phase equilibria
measurements at pressures up to 50 kb and temperatures
up to 1750°C. J. Geophys. Res., v. 65, #2,
pp. 741-748.
- BOYD, F. R. and ENGLAND, J. L., 1960. Minerals of the mantle: Carnegie
Inst. Washington Yearbook, 1959-1960, pp. 47-52.
- BOYD, F. R. and ENGLAND, J. L., 1961. Melting of silicates at high
pressure. Carnegie Inst. Washington Yearbook, 1960-1961,
pp. 113-125.
- BOYD, F. R. and SCHAIRER, J. F., 1964. The system $MgSiO_3-CaMgSi_2O_6$.
J. Petrol., v. 5, #2, pp. 275-308.
- BROWN, G. M., 1956. The layered ultrabasic rocks of Rhum, Inner Hebrides.
Phil. Trans. Roy. Soc. London, Ser. B., 240, pp. 1-53.
- BROWN, P. A., 1973. Possible cryptic suture in S. W. Newfoundland.
Nature Phys. Sci., v. 245, # 140, pp. 9-10.
- BROWN, P. A., 1975. A structural and metamorphic history of gneissic
and supracrustal rocks in the Port-aux-Basques/Garia Bay
Area, S. W. Newfoundland. Unpub. Ph.D. dissertation,
Memorial University of Newfoundland, St. John's.
- BRÜCKNER, W. D., 1966. Stratigraphy and structure of West Central
Newfoundland. in W. H. Poole (ed.), Guidebook, Geology
of Parts of Atlantic Provinces; Ann. Meeting Geol. Assoc.
Canada, Min. Assoc. Canada, pp. 137-151.
- BUDDINGTON, A. F. and HESS, H. H., 1937. Layered peridotite laccoliths
in the Trout River Area, Newfoundland. Am. J. Sci., v. 33,
pp. 380-388.

- BURNS, R. G., 1970. Mineralogical applications of crystal field theory. Cambridge Univ. Press, 224p.
- BURNS, R. G., 1973. The partitioning of trace transition elements in crystal structures: a provocative review with application to mantle geochemistry. *Geochim. Cosmochim. Acta*, v. 37, pp. 2395-2403.
- BURNSNALL, J. T. and DEWIT, M. J., 1975. Timing and development of the orthotectonic zone in the Appalachian Orogen of N.W. Newfoundland. *Can. J. Earth Sci.*, v. 12, #10, pp. 1712-1722.
- CAMPSIE, J., BAILEY, J. C., RASMUSSEN, M., 1973. Chemistry of tholeiites from the Reykjanes Ridge and Charlie Gibb's Fracture Zone. *Nature, Phys. Sci.*, v. 244, #135, pp. 71-73.
- CANN, J. R., 1968. Geological processes at mid-ocean ridge-crests. *Roy. Astron. Soc. Geophys. J.*, v. 15, #3, pp. 331-341.
- CANN, J. R., 1969. Spilites from the Carlsberg Ridge - Indian Ocean. *J. Petrol.*, v. 10, pp. 1-19.
- CANN, J. R., 1970. New model for the structure of the ocean crust. *Nature*, v. 226, # 5249, pp. 928-930.
- CANN, J. R. and FUNNEL, B. M., 1967. Palmer Ridge: a section through the upper part of the ocean crust? *Nature*, v. 213, pp. 661-664.
- CARSLAW, H.S. and JAEGER, J. C., 1959. Conduction of heat in solids. 2nd. ed., Oxford Univ. Press., 510p.
- CAWTHORN, R. G. and COLLERSON, K. D., 1974. The recalculation of pyroxene end-member parameters and the estimation of Fe^{2+} and Fe^{3+} content from electron microprobe analyses. *Am. Mineral.*, v. 59, #11-12, pp. 1203-1208.
- CAWTHORN, R. G. and STRONG, D. F., 1975. The petrogenesis of komatiites and related rocks as evidence for a layered upper mantle. *Earth & Planet. Sci. Lett.*, v. 23, pp. 369-375.

- CHALLIS, G. A., 1965. The origin of New Zealand ultramafic intrusions. *J. Petrol.*, v. 6, pp. 322-364.
- CHALLIS, G. A., 1965. High-temperature contact metamorphism at the Red Hills ultramafic intrusion - Wairau Valley, New Zealand. *J. Petrol.*, v. 6, pp. 395-419.
- CHRISTENSEN, N. I., 1970. Composition and evolution of the oceanic crust. *Marine Geol.*, v. 8, pp. 139-154.
- CHRISTENSEN, N. I. and SALISBURY, M. H., 1972. Sea floor spreading, progressive alteration of layer 2 basalts, and associated changes in seismic velocities. *Earth Planet. Sci. Lett.*, v. 23, pp. 369-375.
- CHURCH, W. R., 1972. Ophiolite: its definition, origin as oceanic crust and mode of emplacement in orogenic belts with special reference to the Appalachians. in "The ancient oceanic lithosphere", E. Irving (ed.). *Earth Physics Branch Publ.*, E.M.R., Ottawa, v. 42, #3, pp. 71-86.
- CHURCH, W. R. and STEVENS, R. K., 1970. Mantle peridotite and the early Palaeozoic ophiolite complexes of the Newfoundland Appalachians. *Univ. Western Ontario, Dept. Geology Contributions. Prelim. Rep. #175.*
- CHURCH, W. R. and STEVENS, R. K., 1970. Mantle peridotites and early Palaeozoic ophiolite complexes of the Newfoundland Appalachians. (abst.) *Int. Symp. Mechanical Properties and Processes in the Mantle: Flagstaff, Arizona, 1970, (Abst. & Prog.)*.
- CHURCH, W. R. and STEVENS, R. K., 1971. Early Paleozoic ophiolite complexes of the Newfoundland Appalachians as mantle-oceanic crust sequences. *J. Geophys. Res.*, v. 76, #5, pp. 1460-1466.
- CLARKE, D. B., 1970. Tertiary basalts of Baffin Bay: Possible primary magma from the mantle. *Contrib. Mineral. Petrol.*, v. 25, pp. 203-224.
- COLEMAN, P. J., 1970. Geology of the Solomon and New Hebrides Islands, as part of the Melanesian Re-entrant, S.W. Pacific. *Pacific Sci.*, v. 34, pp. 289-314.

- COLEMAN, R. G., 1971. Petrologic and geophysical nature of serpentinites. Geol. Soc. America Bull., v. 82, pp. 897-918.
- COLEMAN, R. G., 1971. Plate tectonic emplacement of upper mantle peridotites along continental edges. J. Geophys. Res., v. 76, #5, pp. 1212-1222.
- COLEMAN, R. G. and KEITH, T. E., 1971. A chemical study of serpentinisation, Burro Mountain, California. J. Petrol., v. 12, #2, pp. 311-328.
- COLMAN-SADD, S. P., 1974. The geologic development of the Bay d'Espoir Area, S. E. Newfoundland. Unpub. Ph.D. dissertation, Memorial University of Newfoundland, St. John's.
- COMEAU, R. L., 1972. Transported slices of the coastal complex, Western Newfoundland. Unpub. M.Sc. dissertation, Memorial University of Newfoundland, St. John's.
- COMPTON, R. R., 1958. Significance of amphibole paragenesis in the Bidwell Bar region, California. Am. Mineral., v. 33, #9-10, pp. 890-907.
- COOPER, J. R., 1936. Geology of the Southern half of the Bay of Islands igneous complex. Nfld. Dept. Nat. Res. Geol. Sec. Bull. #4, 62p.
- COOPER, J. R., 1937. Geology and mineral deposits of the Hare Bay area. Geol. Surv. Newfoundland, Bull. #9, 28p.
- DALLMEYER, R. D. and WILLIAMS, H., 1975. Ar⁴⁰/39 release spectra of hornblende from the Bay of Islands metamorphic aureole, western Newfoundland: their bearing on the timing of ophiolite obduction at the Ordovician continental margin of eastern North America. Can. J. Earth Sci., v. 12, pp. 1685-1690.
- DAVIES, H. L., 1971. Peridotite-gabbro-basalt complex in eastern Papua, an overthrust plate of oceanic mantle and crust. Aust. Bur. Min. Res. Geol. Geophys. Bull. #28, 48p.

- DAVIES, H. L. and SMITH, I. E., 1971. Geology of eastern Papua. Geol. Soc. America Bull., v. 82, #12, pp. 3299-3312.
- DAVIS, B. T. C. and BOYD, F. R., 1966. The join $Mg_2Si_2O_6$ - $CaMgSi_2O_6$ at 30 kb pressure and its application to pyroxenes from kimberlites. J. Geophys. Res., v. 71, #14, pp. 3567-3576.
- DEER, W. A., HOWIE, R. A. and ZUSSMAN, J., 1962. The rock forming minerals, v. 1. (Ortho-and Ring Silicates.) Longmans: 333p.
- DEER, W. A., HOWIE, R. A., ZUSSMAN, J., 1962. The rock forming minerals, vol. 5. (Non-Silicates): Longmans, 371p.
- DEER, W. A., HOWIE, R. A. and ZUSSMAN, J., 1963. Rock forming minerals: v. 2. (Chain Silicates): Longmans, 379p.
- DEN TÈX, E., 1969. Origin of ultramafic rocks, their tectonic setting and history: a contribution to the discussion of the paper "the origin of ultramafic and ultrabasic rocks" by P. J. Wyllie. Tectonophysics, v. 7, pp. 457-458.
- DE ROEVER, W. P., 1957. Sind die Alpinotypen peridotitmassen vielleicht tektonisch verfrachtete Bruchstücke der Peridotitschale? Geol. Rundschau, v. 46, pp. 137-146.
- DEWEY, J. F., 1969. Evolution of the Appalachian/Caledonian Orogen. Nature, v. 222, April 1969, pp. 124-129.
- DEWEY, J. F. and BIRD, J. M., 1970. Mountain belts and the new global tectonics. J. Geophys. Res., v. 75, #14, pp. 2625-2647.
- DEWEY, J. F. and BIRD, J. M., 1970. Plate tectonics and geosynclines. Tectonophysics, v. 10, #5-6, pp. 625-635.
- DEWEY, J. F. and BIRD, J. M., 1971. Origin and emplacement of the ophiolite suite, Appalachian ophiolites in Newfoundland. J. Geophys. Res., v. 76, #14, pp. 3179-3206.

- DICKEY, J. S., 1970. Partial fusion products in alpine-type peridotites: Serrania de la Ronda and other examples. Mineral. Soc. America Spec. Pap. 3, pp. 33-49.
- DICKEY, J. S., YODER, H. S., SHAIRER, J. F., 1971. Incongruent melting of chromian diopside and the origin of podiform chromite deposits (abst.). Geol. Soc. America Abst., v. 3, #7, pp. 543-544.
- DICKEY, J. S. and YODER, H. S., 1972. Partitioning of chromium and aluminium between clinopyroxene and spinel. Carnegie Inst. Washington Yearbook, v. 71, pp. 384-392.
- DIETZ, R. S., 1963. Alpine serpentinites as oceanic rind fragments. Geol. Soc. America Bull., v. 74, pp. 947-952.
- DIMITRIEV, L. V., 1974. Petrochemical study of the basaltic basement of the mid-Indian Ocean Ridge. Leg 24 - Djibouti to Mauritius. in Fisher, R. L., Bunce, E. T. et al.; Initial Rep. D.S.D.P., v. XXIV, Washington.
- DUKE, N. A. and HUTCHINSON, R. W., 1974. Geological relationships between massive sulphide bodies and ophiolitic volcanic rocks near York Harbour, Newfoundland. Can. J. Earth Sci., v. 11, #1, pp. 53-69.
- ENGEL, A. E. J., ENGEL, C. and HAVENS, R. G., 1965. Chemical characteristics of oceanic basalts and the upper mantle. Geol. Soc. America Bull., v. 76, pp. 719-734.
- ENGEL, C. G. and FISHER, R. L., 1969. Lherzolite anorthosite, gabbro and basalt dredged from the Mid-Indian Ocean Ridge. Science, v. 166, pp. 1136-1141.
- ERNST, W. G., 1960. Diabase-granophyre relations in the Endion sill, Duluth, Minn. J. Petrol., v. 1, #3, pp. 286-303.
- FINDLAY, D. C. and SMITH, C. H., 1965. The MuskoX Drilling Project. Geol. Surv. Canada Paper 64-44, 170p.
- FONG, C. C. K., 1967. Palaeontology of the Lower Cambrian Archaeocyatha-bearing Forteau Formation in S. Labrador. Unpub. M.Sc. dissertation, Memorial University of Newfoundland, St. John's.

- FREY, F. A., 1970. Rare-earth abundances in alpine ultramafic rocks. *Phys. Earth Planet. Int.*, v. 3, pp. 323-330.
- FREY, F. A. and GREEN, D. H., 1974. The mineralogy, geochemistry and origin of lherzolite inclusions in Victorian basanites. *Geochim. Cosmochim. Acta*, v. 38, #7, pp. 1023-1059.
- FREY, F. A., HASKIN, M. A., POETZ, J. A. and HASKIN, L. A., 1968. Rare earth abundances in some basic rocks. *J. Geophys. Res.*, v. 73, #18, pp. 6085-6098.
- FREY, F. A., HASKIN, L. A., HASKIN, M. A., 1971. Rare-earth abundances in some ultramafic rocks. *J. Geophys. Res.*, v. 76, #8, pp. 2051-2070.
- FRISCH, T. and SCHMINCKE, H. V., 1968. Petrology of cpx-amph inclusions from the Roque Nublo volcanics, Gran Canaria, Canary Islands. *Intn. Symp. on Volcanology (Spain, Canary Islands, September, 1968)*.
- GASS, I. G., 1967. The ultrabasic volcanic assemblage of the Troodos massif, Cyprus; in *Ultramafic and related rocks* (ed. P. J. Wyllie). *J. Wiley & Sons*, pp. 121-134.
- GASS, I. G., 1968. In the Troodos massif of Cyprus a fragment of Mesozoic ocean floor. *Nature*, v. 220, #5162, pp. 39-42.
- GASS, I. G. and MASSON-SMITH, O., 1963. The geology and gravity anomalies of the Troodos massif, Cyprus. *Roy. Soc. London Phil. Trans.* 5A, v. 255, #1060, pp. 417-467.
- GASS, I. G. and SMEWING, J. D., 1973. Intrusion, extrusion and metamorphism at constructive margins -- evidence from the Troodos Massif - Cyprus. *Nature*, v. 242, pp. 26-28.
- GAST, P. W., 1965. Terrestrial ratio of potassium to rubidium and the composition of the earth's mantle. *Science*, v. 147, #3660, pp. 858-860.

- GLIKSON, A. Y., SHERATON, J. W., 1972. Early Precambrian trondhjemitic suites in W. Australia and N.W. Scotland and the geochemical evolution of shields. *Earth & Planet. Sci. Lett.*, v. 17, pp. 227-242.
- GRAHAM, A. L. and NICHOLLS, G. D., 1969. Mass spectrographic determinations of lanthanide element contents in basalts. *Geochim. Cosmochim. Acta*, v. 33, #5, pp. 555-568.
- GRAHAM, C. M., 1974. Petrology and tectonic significance of L. Cambrian basaltic rocks of the Scottish Dalradians. *Geol. Assoc. Canada Prog. & Abstracts, Ann. Mtg.*
- GREEN, D. H., 1964. The petrogenesis of the high-temperature peridotite intrusion in the Lizard area, Cornwall. *J. Petrol.*, v. 5, #1, pp. 134-188.
- GREEN, D. H., 1964. The metamorphic aureole of the peridotite at the Lizard, Cornwall. *J. Geol.*, v. 72, #5, pp. 543-563.
- GREEN, D. H., 1970. Peridotite-gabbro complexes as keys to the petrology of mid-oceanic ridges; discussion. *Geol. Soc. America Bull.*, v. 81, pp. 2161-2166.
- GREEN, D. H. and RINGWOOD, A. E., 1967. The genesis of basaltic magmas. *Contrib. Mineral. Petrol.*, v. 15, pp. 103-190.
- GREEN, T. H. and RINGWOOD, A. E., 1968. Genesis of the calc-alkaline igneous rock suite. *Contrib. Mineral. Petrol.*, v. 18, pp. 105-162.
- GREENBAUM, D., 1972. Magmatic processes at oceanic ridges. Evidence from the Troodos Massif, Cyprus. *Nature, Phys. Sci.*, v. 238, #80, pp. 18-21.
- GROVER, J. E. and ORVILLE, P. M., 1969. The partitioning of cations between coexisting single and multi-site phases with application to the assemblages orthopyroxene - clinopyroxene and orthopyroxene - olivine. *Geochim. Cosmochim. Acta*, v. 33, #2, pp. 205-226.

- GUILLON, J. H. and ROUTHIER, P., 1971. Les stades d'évolution et de mise en place des massifs ultramafiques de Nouvelle-Calédonie. Fr. Bur. Rech. Geol. Minieres Bull. (Ser. 2), Sect. 4, #2, pp. 5-37.
- HAMILTON, W. and MOUNTJOY, W., 1965. Alkali content of alpine ultramafic rocks. Geochim. Cosmochim. Acta, v. 29, pp. 661-671.
- HARKER, A., 1909. The natural history of igneous rocks. London.
- HARRIS, P. M., FARRAR, E., MacINTYRE, R. M., and YORK, D., 1965. Potassium-argon age measurements on two igneous rocks from the Ordovician system of Scotland. Nature, v. 205, pp. 352-353.
- HESS, H. H., 1960. The AMSOC hole to the earth's mantle. Am. Scientist, v. 48, #2, pp. 254-263.
- HESS, H. H., 1960. Stillwater igneous complex, Montana - a quantitative mineralogical study. Geol. Soc. America Mem. 80, 230p.
- HESS, H. H., 1962. History of ocean basins; in "Buddington Volume". Geol. Soc. America, pp. 599-620.
- HESS, H. H., 1964. The oceanic crust, the upper mantle and the Mayaguez serpentinitised peridotite. In: "A study of serpentine: the AMSOC Core Hole near Mayaguez, Puerto Rico." Nat. Acad. Sci. Nat. Res. Council Pub. 1188, pp. 169-175.
- HESS, H. H. and PHILLIPS, A. H., 1938. Orthopyroxenes of the Bushveld type. Am. Mineral., v. 23, pp. 450-456.
- HIMMELBERG, G. R. and COLEMAN, R. G., 1968. Chemistry of primary minerals and rocks from the Red Mountain - De Puerto ultramafic mass, California. U.S.G.S. Prof. Pap. 600C, pp. C18-C26.
- HORNE, G. S., 1969. Early Ordovician chaotic deposits in the central volcanic belt of Northeast Newfoundland. Geol. Soc. America Bull., v. 80, #12, pp. 2451-2464.

- HOSTETLER, P. B., COLEMAN, R. G., MUMPTON, F. A., and EVANS, B.W., 1966. Brucite in Alpine serpentinites. *Am. Mineral.*, v. 51, pp. 75-98.
- HOWELLS, S. and O'HARA, M.J., 1975. Palaeogeotherms and the diopside enstatite solvus. *Nature*, v. 254, #5499, pp. 406-408.
- HOWLEY, J. P., 1907 (reprinted 1925). Geological map of Newfoundland: Scale 1" to 17 miles (approx.).
- HSU, K. J., 1968. Principles of mélanges and their bearing on the Franciscan-Knoxville paradox. *Geol. Soc. America Bull.*, v. 79, pp. 1063-1074.
- HUBBERT, M. K. and RUBEY, W. W., 1959. Mechanics of fluid-filled porous solids and its application to overthrust faulting, Pt. 1. *Geol. Soc. America Bull.*, v. 70, #2, pp. 115-166.
- HUGHES, C. J., 1960. The Southern Mountains igneous complex, Isle of Rhum. *Quart. Jour. Geol. Soc. London*, v. 116, pp. 111-138.
- HUGHES, C. J., 1971. Anatomy of a granophyre intrusion. *Lithos*, v. 4, pp. 403-415.
- HUGHES, C. J. and BRÜCKNER, W. D., 1971. Late Precambrian rocks of eastern Avalon Peninsula, Newfoundland - a volcanic island complex. *Can. J. Earth Sci.*, v. 8, pp. 899-915.
- HUNAHASHI, M., 1948. Contact metamorphism associated with the pyroxene peridotite of the Horoman region in the Hidaka metamorphic zone, Hokkaido. *J. Fac. Sci. Hokkaido Univ.*, Ser. iv 8, pp. 31-63 (Japanese).
- HURLEY, P. M., 1967. Rb^{87} - Sr^{87} relationships in the differentiation of the mantle; in "Ultramafic and related rocks", P. J. Wyllie (ed.). *Pub. J. Wiley*, N.Y., pp. 372-375.
- HUSSEY, E. M., 1974. Geological and petrochemical data on the Brighton Complex, Notre Dame Bay, Newfoundland. Unpub. B.Sc. dissertation, Memorial University of Newfoundland, St. John's, 60p.

- HUTCHINSON, C. S. and DHONAU, T. J., 1969. Deformation of an Alpine ultramafic association in Darrel Bay, east Sabah, Malaysia. *Geol. Mijnbouw*, v. 48, pp. 481-493.
- HYNDMAN, D. W., 1972. *Petrology of igneous and metamorphic rocks*. McGraw-Hill Book Co., New York, 533p.
- HYNES, A. J., 1972. The geology of part of the Western Othris Mountains, Greece. Unpub. Ph.D. dissertation, University of Cambridge.
- INGERSOLL, L. R. and ZOBELL, O. J., 1948. *Heat conduction*. McGraw-Hill Book Co. Inc., N.Y.
- INGERSON, F. E., 1935. Layered peridotitic laccoliths of the Trout River Area, Newfoundland. *Am. J. Sci.*, ser. 5, v. 29, #173, pp. 422-440.
- INTERSON, F. E., 1937. Layered peridotitic laccoliths of the Trout River Area, Newfoundland: A Reply. *Am. J. Sci.*, v. 33, #197, pp. 389-392.
- IRVINE, T. N., 1965. Chromian spinel as a petrogenetic indicator. Pt. 1 - Theory. *Can. J. Earth Sci.*, v. 2, pp. 648-672.
- IRVINE, T. N., 1967. Chromian spinel as a petrogenetic indicator. Pt. 2 - Petrologic applications. *Can. J. Earth Sci.*, v. 4, pp. 71-103.
- IRVINE, T. N., 1970. Crystallisation sequences in the Muskox and other layered intrusions. 1. Sheets and Sills. *Can. J. Earth Sci.*, v. 7, pp. 1031-1061.
- IRVINE, T. N. and FINDLAY, T. C., 1972. Alpine Peridotite with particular reference to the Bay of Islands igneous complex. In: "The ancient ocean lithosphere", E. Irving (ed.). Pub. Earth Physics Branch, E.M.R., Ottawa, v. 42, #3, pp. 97-128.
- IRVING, A. J., 1974. Megacrysts from the newer basalts and other basaltic rocks of southeastern Australia. *Geol. Soc. America Bull.*, v. 85, pp. 1503-1514.

- IRVING, A. J., 1974. Pyroxene rich ultramafic xenoliths in the newer basalts of Victoria, Australia. Neues Jahrb. Mineral. Abh., v. 120, #2, pp. 147-167.
- ISHIBASHI, K., 1970. Petrochemical study of basic and ultrabasic inclusions in basaltic rocks from N. Kyushu, Japan. Kyushu Univ. Fac. Sci. Mem. Ser. D., Geology, v. 20, pp. 85-146.
- ITO, K. and KENNEDY, G. C., 1967. Melting and phase relations in a natural peridotite to 40 kb with geological implications. Contrib. Mineral. Petrol., v. 19, pp. 177-211.
- JACKSON, E. D., 1960. X-ray determinative curve for natural olivine of composition Fo_{80-90} . Art. 197 in U.S.G.S. Prof. Paper 400-B, pp. B432-B434.
- JACKSON, E. D., 1961. Primary textures and mineral associations in the ultramafic zone of the Stillwater Complex, Montana. U.S.G.S. Prof. Paper 358, 106p.
- JACKSON, E. D., 1969. Chemical variation in coexisting chromite and olivine in chromitite zones of the Stillwater Complex. Symposium on Magmatic Ore Deposits. Econ. Geol. Monograph, v. 4, pp. 41-71.
- JAEGER, J. C., 1957. The temperature in the neighbourhood of a cooling intrusive sheet. Am. J. Sci., v. 255, pp. 306-318.
- JAEGER, J. C., 1959. Temperatures outside a cooling intrusive sheet. Am. J. Sci., v. 257, pp. 44-54.
- JAEGER, J. C., 1961. The cooling of irregularly shaped igneous bodies. Am. J. Sci., v. 259, pp. 721-734.
- JOHNSON, H., 1941. Palaeozoic lowlands of western Newfoundland. Trans. N. Y. Acad. Sci. Ser. 2, v. 3, pp. 141-145.
- JUKES, J. B., 1842. Excursions in and about Newfoundland during the years 1839 and 1840. 2 vols., 322 and 354p.

- KARAMATA, S., 1968. Zonality in contact metamorphic rocks around the ultramafic mass of Brezovica (Serbia, Yugoslavia). *Intn. Geol. Cong. 23rd, Prague, Proc. Sec. 1*, pp. 197-207.
- KARAMATA, S., 1974. Dynamothermal metamorphism related to emplacement of ultramafics on examples from the Dinarides. *Annales de la Soc. Geol. de Belgique, T.97*, pp. 541-545.
- KARIG, D. E., 1971. Origin and development of marginal basins in the Western Pacific. *J. Geophys. Res.*, v. 76, pp. 2542-2561.
- KARIG, D. E., 1972. Remnant arcs. *Geol. Soc. America Bull.*, v. 83, pp. 1057-1068.
- KAY, M., 1945. Palaeogeographic and Palinspastic maps. *Am. Assoc. Petrol. Geol.*, v. 29, pp. 426-450.
- KAY, M., 1972. Dunnage melange and L. Palaeozoic deformation in N.E. Newfoundland. *24th Intn. Geol. Cong. Proc. Sec. 3*, pp. 122-133, Montreal.
- KAY, R., HUBBARD, N.J. and GAST, P. W., 1970. Chemical characteristics and origin of oceanic ridge volcanic rocks. *J. Geophys. Res.*, v. 75, #8, pp. 1585-1613.
- KEAN, B. F., 1973. Stratigraphy, petrology and geochemistry of volcanic rocks of Long Island, Newfoundland. Unpub. M.Sc. thesis, Memorial University of Newfoundland, St. John's.
- KENNEDY, M. J., 1973. Pre-Ordovician polyphase structure in the Burlington Peninsula of the Newfoundland Appalachians. *Nature, Phys. Sci.*, v. 241, #110, pp. 114-116.
- KENNEDY, M. J. and MCGONIGAL, M. H., 1972. The Gander Lake and Davidsville Groups of N.E. Newfoundland. New data and geotectonic implications. *Can. J. Earth Sci.*, v. 9, pp. 452-459.
- KINDLE, C. H. and WHITTINGTON, H. B., 1958. Stratigraphy of the Cow Head Region, West Newfoundland. *Geol. Soc. America Bull.*, v. 69, pp. 315-342.

- KINDLE, C. H. and WHITTINGTON, H. B., 1963. Middle Ordovician Table Head Formation, West Newfoundland. Geol. Soc. America Bull., v. 74, #6, pp. 745-758.
- KUNO, H., 1964. Fractionation trends of basalt magmas in lava flows. J. Petrol., v. 6, #2, pp. 302-321.
- KUSHIRO, I., 1960. Si-Al relation in clinopyroxenes from igneous rocks. Am. J. Sci., v. 258, pp. 548-554.
- KUSHIRO, I., SYONO, Y., and AKIMOTO, S., 1968. Melting of a peridotite nodule at high pressures and high water pressures. J. Geophys. Res., v. 73, #18, pp. 6023-6029.
- LE BAS, M. J., 1962. The role of aluminum in igneous clinopyroxenes with relation to their parentage. Am. J. Sci., v. 260, #4, pp. 267-288.
- LILLY, H. D., 1957. Geological report on Bonne Bay area, Newfoundland. in Report on exploration for year ending March 31, 1957. Unpub. British Newfoundland Exploration, Toronto, 36p.
- LILLY, H. D., 1963. Geology of Hughes Brook - Goose Arm area, W. Newfoundland. M.U.N. Geology Rept. #2, St. John's, 123p.
- LINDSLEY, D. H. and MUNOZ, J. C., 1969. Subsolidus relations along the join hedenbergite-ferrosilite. Am. J. Sci., v. 267-A, pp. 295-324.
- LIU, J. G., 1973. Synthesis and stability relations of epidote, $\text{Ca}_2\text{Al}_2\text{FeSi}_3\text{O}_{12}(\text{OH})$. J. Pet., v. 14, pp. 381-413.
- LIU, J. G., KUNIYOSHI, S., and ITO, K., 1974. Experimental studies of the phase relations between greenschist and amphibolite in a basaltic system. Am. J. Sci., v. 274, #6, pp. 613-632.
- LONEY, R. A., HIMMELBERG, G. R. and COLEMAN, R. G., 1971. Structure and petrology of the alpine-type peridotite at Burro Mountain, California, U.S.A. J. Petrol., v. 12, #2, pp. 245-309.

- LOVERING, T. S., 1935. Theory of heat conduction applied to geological problems. Geol. Soc. America Bull., v. 46, pp. 69-94.
- MacDONALD, G. A. and KATSURA, T., 1964. Composition and origin of Hawaiian lavas. in "Studies in Volcanology", eds. Coats, R. C., Hay, R. L., Anderson, C. A. Geol. Soc. America Mem. 116, pp. 477-522.
- MacGREGOR, I. D., 1964. A study of the contact metamorphic aureole surrounding the Mount Albert ultramafic intrusion. Unpub. Ph.D. dissertation, Princeton University.
- MacGREGOR, I. D., 1974. The system $MgO-Al_2O_3-SiO_2$: solubility of Al_2O_3 in enstatite for spinel and garnet peridotite compositions. Am. Mineral., v. 59, #1-2, pp. 110-119.
- MALPAS, J., 1972. The petrochemistry of the Bull Arm Formation (Late Precambrian) near Rantem Station, S.E. Newfoundland. Unpub. M.Sc. thesis, Memorial University of Newfoundland, St. John's.
- MALPAS, J., 1973. A restored section of oceanic crust and mantle in western Newfoundland (abst.). Geol. Soc. America 8th Ann. Mtg., N.E. Sect. (Abst. with Prog.), v. 5, #2, p. 192.
- MALPAS, J., STEVENS, R. K. and STRONG, D. F., 1973. Amphibolite associated with Newfoundland ophiolite. Its classification and tectonic significance. Geology, v. 1, #1, pp. 45-47.
- MALPAS, J. and STRONG, D. F., 1975. A comparison of chrome spinels in ophiolites and mantle diapirs of Newfoundland. Geochim. Cosmochim. Acta, v. 39, pp. 1045-1060.
- MARTEN, B. E., 1971. Stratigraphy of volcanic rocks in the Western Arm area of the Central Newfoundland Appalachians. Geol. Assoc. Canada Proc., v. 24, #1, pp. 73-84.
- MASON, B. H., 1958. Principles of geochemistry, vii -- 310p. John Wiley, N.Y., 2nd Edition.

- MAXWELL, J. C., 1974. Structural and stratigraphic cross section of Franciscan Complex, Coast Range of Northern California (abst.). Geol. Soc. America Cordilleran Sect., 70th Annual Meeting, Abst., v. 6, #3, pp. 215-216
- McBIRNEY, A. R. and AOKI, K., 1968. Petrology of the Island of Tahiti. in Studies in Volcanology, eds. Coats, R. R., Hay, R. L. and Anderson, C. A. Geol. Soc. America Mem. 116, pp. 523-556.
- McBIRNEY, A. R. and GASS, I. G., 1967. Relations of oceanic volcanic rocks to mid-oceanic rise and heat flow. Earth & Planet. Sci. Lett., v. 2, #4, pp. 265-276.
- MEDARIS, L. G., 1969. Partitioning of Fe^{2+} and Mg^{2+} between coexisting synthetic olivine and orthopyroxene. Am. J. Sci., v. 267, pp. 945-968.
- MEDARIS, L. G., Jr., 1972. High-pressure peridotites in S. W. Oregon. Geol. Soc. America Bull., v. 83, #1, pp. 41-57.
- MELSON, W. G., HART, S. R., and THOMPSON, G., 1972. St. Paul's Rocks, Equatorial Atlantic: Petrogenesis, radiometric ages and implications on sea-floor spreading. in Mem. 132, Geol. Soc. America, "Studies in Earth and Space Sciences", Hess volume, pp. 243-272.
- MELSON, W. G. and VAN ANDEL, Tj. H., 1966. Metamorphism in the M.A.R., 22°N latitude. Mar. Geol., v. 4, pp. 165-186.
- MELSON, W. G. and THOMPSON, G., 1970. Layered basic complex in oceanic crust, Romanche fracture, equatorial Atlantic Ocean. Science, v. 168, #3933, pp. 817-820.
- MELSON, W. G. and THOMPSON, G., 1971. Petrology of a transform fault zone and adjacent ridge segments. in "A discussion of the petrology of igneous and metamorphic rocks from the ocean floor". Roy. Soc. London Phil. Trans. Ser. A., v. 268, #1192, pp. 423-441.
- MELSON, W. G., THOMPSON, G. and VAN ANDEL, Tj. H., 1968. Volcanism and metamorphism in the Mid-Atlantic Ridge, 22°N lat. J. Geophys. Res., v. 73, pp. 5925-5941.

- MENZIES, M., 1973. Mineralogy and partial melt textures within an ultramafic body, Greece. *Contrib. Mineral. Petrol.*, v. 42, #4, pp. 273-285.
- MENZIES, M. and ALLEN, C., 1974. Plagioclase-herzolite-residual mantle relationships within two eastern Mediterranean ophiolites. *Contrib. Mineral. Petrol.*, v. 45, #3, pp. 197-213.
- MILLER, Ch., 1970. Petrology of some eclogites and metagabbros of the Oetztal Alps, Tirol, Austria. *Contrib. Mineral. Petrol.*, v. 28, #1, pp. 42-56.
- MITCHELL, A. H. G., 1974. Southwest England granites: magmatism and tin mineralisation in a post-tectonic setting. *Trans. Inst. Min. Metall. Sec. B.*, v. 83, pp. B95-B97.
- MIYASHIRO, A., 1958. Regional metamorphism of the Gosaisyo-Takanuki District of the Central Abukuma Plateau. *Jour. Fac. Sci. Univ. Tokyo, Sect. I*, v. 11, pp. 219-272.
- MIYASHIRO, A., 1973. The Troodos ophiolite complex was probably formed in an island arc. *Earth & Planet. Sci. Lett.*, v. 19, #2, pp. 218-224.
- MIYASHIRO, A., 1974. Volcanic rock series in island arcs and active continental margins. *Am. J. Sci.*, v. 274, pp. 321-355.
- MIYASHIRO, A. and SHIDO, F., 1975. Tholeiitic and calc-alkalic series in relation to the behaviour of titanium, vanadium, chromium and nickel. *Am. J. Sci.*, v. 275, #3, pp. 265-277.
- MONTIGNY, R., BOUJAUULT, H., BOTTINGER, Y., 1973. Trace element geochemistry and genesis of the Pindos ophiolite suite. *Geochim. Cosmochim. Acta*, v. 37, #9, pp. 2135-2147.
- MOORES, E. M., 1969. Petrology and structure of the Vourinos ophiolitic complex of Northern Greece. *Geol. Soc. America Sp. Paper*, 118, 74p.

- MOORES, E. M., 1970. Ultramafics and orogeny, with models of the U.S. Cordillera and the Tethys. *Nature*, v. 228, pp. 837-842.
- MOORES, E. M., 1973. Geotectonic significance of ultramafic rocks. *Earth Sci. Rev.*, v. 9, #3, pp. 241-258.
- MOORES, E. M., and MacGREGOR, I. D., 1972. Types of alpine ultramafic rocks and their implications for fossil plate interactions. in *Studies in Earth and Space Sciences*, *Geol. Soc. America Mem.* #132, pp. 209-223.
- MOORES, E. M. and RAYMOND, L. A., 1972. On the origin of ultramafic rocks: Discussion. *Geol. Soc. America Bull.*, v. 83, #10, pp. 3157-3160.
- MOORES, E. M. and JACKSON, E. D., 1974. Ophiolites and oceanic crust. *Nature*, v. 250, #5462, pp. 136-139.
- MOORES, E. M. and VINE, F. J., 1971. The Troodos massif, Cyprus and other ophiolites as oceanic crust; evaluation and implications. *Roy. Soc. London Phil. Trans. Ser. A.*, v. 268, #1192, pp. 443-466.
- MORI, T. and GREEN, D. H., 1975. Pyroxenes in the system $Mg_2Si_2O_6$ - $CaMgSi_2O_6$. *Earth Planet. Sci. Lett.*, v. 26, #3, pp. 277-286.
- MORRIS, R. V., HASKIN, L. A., BIGGAR, G. M., O'HARA, M. J., 1975. Measurement of the effects of temperature and partial pressure of oxygen on the oxidation states of europium in silicate glasses. *Geochim. Cosmochim. Acta*, v. 39, #3, pp. 377-381.
- MUELLER, R. F., 1963. A comparison of oxidative equilibria in meteorites and terrestrial rocks. *Geochim. Cosmochim. Acta*, v. 27, #3, pp. 273-278.
- MUIR, I. D. and TILLEY, C. E., 1964. Basalts from the northern part of the rift zone of the M.A.R. *J. Petrol.*, v. 5, pp. 409-434.

MUNOZ, M. and SAGREDO, J., 1974. Clinopyroxenes as geobarometric indicators in mafic and ultramafic rocks from Canary Islands. Contrib. Mineral. Petrol., v. 44, pp. 139-147.

MURRAY, A. and HOWLEY, J. P., 1881. Geological survey of Newfoundland. Geol. Surv. Newfoundland Publication, 536p.

MURTHY, V. R. and STEUEBER, A. M., 1967. Potassium/rubidium ratios in mantle derived rocks. in "Ultramafic and related rocks", ed. P. J. Wyllie. J. Wiley, pp. 376-380.

MYSEN, B. O. and HEIER, K. S., 1972. Petrogenesis of eclogites in high grade metamorphic gneisses, exemplified by the Hareidland Eclogite, W. Norway. Contrib. Mineral. Petrol., v. 36, #1, pp. 73-94.

NAFZIGER, R. H., and MUAN, A., 1967. Equilibrium phase compositions and thermodynamic properties of olivines and pyroxenes in the system $MgO - FeO - SiO_2$. Am. Mineral., v. 52, #9-10, pp. 1364-1385.

NEHRU, C. E. and WYLLIE, P. J., 1974. Electron microprobe measurements of pyroxenes coexisting with H_2O under saturated liquid in the join $CaMgSi_2O_6 - Mg_2Si_2O_6 - H_2O$ at 30 kb with application to geothermometry. Contrib. Mineral. Petrol., v. 48, pp. 221-228.

NICOLAS, A., BOUCHEZ, J. L., BOUDIER, F., MERCIER, J. C., 1971. Textures, structures and fabrics due to solid state flow in some European herzolites: Tectonophysics, v. 12, pp. 55-86.

NORMAN, R. E., 1974. Geology and petrochemistry of ophiolitic rocks of the Baie Verte Group exposed at Ming's Bight, Newfoundland. Unpub. M.Sc. dissertation, Memorial University of Newfoundland, St. John's.

NORMAN, R. E. and STRONG, D. F., 1975. The geology and chemistry of ophiolitic rocks exposed at Ming's Bight, Newfoundland. Can. J. Earth Sci., v. 12, pp. 777-797.

O'HARA, M. J., 1963. Distribution of iron between coexisting olivines and Ca-poor pyroxenes in peridotites, gabbros and other magnesian environments. Am. J. Sci., v. 261, #1, pp. 32-46.

- O'HARA, M. J., 1967. Mineral paragenesis in ultrabasic rocks, pp. 393-403. in Ultramafic and related rocks, ed. P. J. Wyllie, John Wiley, New York.
- O'HARA, M. J., 1968. The bearing of phase equilibria studies in synthetic and natural systems on the origin and evolution of basic and ultrabasic rocks. *Earth Sci. Rev.*, v. 4, pp. 69-133.
- O'HARA, M. J., 1973. Non-primary magmas and a dubious mantle plume beneath Iceland. *Nature*, v. 243, pp. 507-508.
- OXBURGH, E. R., 1972. Flake tectonics and continental collision. *Nature*, v. 239, pp. 202-204.
- PAGE, N. J., 1967. Serpentinisation at Burro Mountain, California. *Contrib. Mineral. Petrol.*, v. 14, pp. 321-342.
- PAGE, N. J., 1967. Serpentinisation considered as a constant volume metasomatic process - a discussion. *Am. Mineral.*, v. 52, #3-4, pp. 545-549.
- PAMIC, J. J., 1971. Some petrological features of Bosnian peridotite - gabbro complexes in the Dinaride Zone of Yugoslavia. *Tschernaks Mineral. Petrog. Mitt.*, v. 15, #1, pp. 14-42.
- PAMIC, J., SCAVNICAR, S., MEDJIMOREC, S., 1973. Mineral assemblages of amphibolites associated with alpine type ultramafics in the Dinaride ophiolite zone (Yugoslavia). *J. Petrol.*, v. 14, #1, pp. 133-157.
- PAYNE, J. G., 1974. The Twillingate granite and its relationship to surrounding country rocks. Unpub. M.Sc. dissertation, Memorial University of Newfoundland, St. John's.
- PAYNE, J. G., and STRONG, D. F., The Twillingate granite and the origin of trondjemite. Ms. in preparation.
- PEARCE, J. A. and CANN, J. R., 1973. Tectonic setting of basic volcanic rocks determined using trace element analyses. *Earth Planet. Sci. Lett.*, v. 19, #2, pp. 290-300.

- PHILPOTTS, J. A., SCHNETSLER, C. C. and THOMAS, H. H., 1972. Petrogenetic implications of some new geochemical data on eclogitic and ultrabasic inclusions. *Geochim. Cosmochim. Acta*, v. 36, #10, pp. 1131-1166.
- POLDERVAART, A., and HESS, H. H., 1951. Pyroxenes in the crystallisation of basaltic magma. *J. Geol.*, v. 59, #5, pp. 472-489.
- PRINGLE, I. R., MULLER, A., WARREL, D. M., 1971. Radiometric age determinations from the Long Range Mountains, Newfoundland. *Can. J. Earth Sci.*, v. 8, p. 1328.
- RALEIGH, C. BARRY, 1965. Crystallisation and recrystallisation of quartz in a simple piston-cylinder device. *J. Geol.*, v. 73, #2, pp. 369-377.
- RAMBERG, H. and DEVORE, G., 1951. Distribution of Fe^{2+} and Mg^{2+} in coexisting olivines and pyroxenes. *J. Geol.*, v. 59, #3, pp. 193-210.
- REINHARDT, B. M., 1969. On the genesis and emplacement of ophiolites in the Oman Mountain geosyncline. *Schweiz. Mineral. Petrogr. Mitt.*, v. 49, #1, pp. 1-30.
- REITAN, P. H., 1968. Frictional heat during metamorphism. 1. Quantitative evaluation of heat generation in time. *Lithos*, v. 1, #2, pp. 151-163.
- REITAN, P. H., 1968. Frictional heat during metamorphism. 2. Quantitative evaluation of concentration of heat in space. *Lithos*, v. 1, #3, pp. 368-274.
- REYNOLDS, D. L., 1954. Fluidisation as a geological process and its bearing on the problem of intrusive granites. *Am. J. Sci.*, v. 252, pp. 577-613.
- RILEY, G. C., 1962. Stephenville map-area, Newfoundland. *Geol. Surv. Canada Mem.* 323, 72p.
- RINGWOOD, A. E., 1966. Chemical evolution of the terrestrial planets. *Geochim. Cosmochim. Acta*, v. 30, pp. 41-104.

- RODGERS, J. and NEALE, E. R. W., 1963. Possible Taconic Klippen in Western Newfoundland. *Am. J. Sci.*, v. 261, pp. 713-730.
- ROEDER, P. L. and EMSLIE, R. F., 1970. Olivine-liquid equilibrium. *Contrib. Mineral. Petrol.*, v. 29, #4, pp. 276-289.
- ROSS, C. S., FOSTER, M. D. and MYERS, A. T., 1954. Origin of dunites and of olivine-rich inclusions in basaltic rocks. *Am. Mineral.*, v. 39, #9-10, pp. 693-737.
- ROTHSTEIN, A. A., 1962. Magmatic facies in ultrabasic igneous rocks of the tholeiitic series - a naturally occurring example in the peridotites of Dawros, Connemara, Eire, and Belhelvie, Abd. Scotland. *Akad. Nauk SSSR, Inst. Geol. Rud Mestovozh. Petrog. Miner. Geokhim. Moscow*, 44p.
- ROTHSTEIN, A. T. V., 1958. Pyroxenes from the Dawros peridotite and some comments on their nature. *Geol. Mag.*, v. 95, #6, pp. 456-462.
- SCHUCHERT, C. and DUNBAR, C. O., 1934. Stratigraphy of western Newfoundland. *Geol. Soc. America Mem.* 1, 123p.
- SCOTT, R. B., MALPAS, J., RONA, P. A., UDINSTEV, G., 1976. Duration of hydrothermal activity at an oceanic spreading centre, M.A.R. (lat 26°N). *Geology*, v. 4, #4, pp. 233-236.
- SHIDO, F., 1958. Plutonic and metamorphic rocks of the Makoso and Iritono Districts in Central Abukuma Plateau. *Jour. Fac. Sci. Univ. Tokyo, Sect. II*, v. 11, pp. 131-217.
- SHIDO, F. and MIYASHIRO, A., 1959. Hornblendes of basic metamorphic rocks. *Jour. Fac. Sci. Univ. Tokyo, Sect. II*, v. 12, pp. 1-85.
- SHIRAKI, K., 1971. Metamorphic basement rocks of Yap Islands, western Pacific: Possible oceanic crust beneath an island arc. *Earth & Planet. Sci. Lett.*, v. 13, pp. 167-174.
- SIGGURDSON, H., TOMBLIN, J. F., BROWN, G. M., HOLLAND, J. G., and ARCULUS, R. J., 1973. Strongly undersaturated magmas in the Lesser Antilles island arc. *Earth & Planet. Sci. Lett.*, v. 18, pp. 285-295.

- SMITH, C. H., 1954. On the occurrence and origin of xonotlite. Am. Mineral., v. 39, #5-6, pp. 531-532.
- SMITH, C. H., 1958. Bay of Islands igneous complex, western Newfoundland. Geol. Surv. Canada Mem. 290, 1-32p.
- SMITH, C. H., 1962. Notes on the Muskox Intrusion, Coppermine River area, District of Mackenzie. Can. Geol. Survey Pap. 61-25, 16p.
- SMYTH, W. R., 1971. Stratigraphy and structure of part of the Hare Bay allochthon, Newfoundland. Geol. Assoc. Canada Proc., v. 24, #1, pp. 47-51.
- SMYTH, W. R., 1973. The stratigraphy and structure of the southern part of the Hare Bay Allochthon, N.W. Newfoundland. Unpub. Ph.D. dissertation, Memorial University of Newfoundland, St. John's. a
- SNELGROVE, A. K., 1934. Chromite deposits of Newfoundland. Nfld. Dept. of Nat. Res. Geol. Sec. Bull. #1.
- SNELGROVE, A. K., ROEBLING, III, F. W., KAMINARA, J. L. J., 1934. The Blow me down intrusive complex. Am. Mineral., v. 19, pp. 21-23.
- SPEIDEL, D. H. and OSBORN, E. F., 1967. Element distribution among coexisting phases in the system $MgO-FeO-Fe_2O_3-SiO_2$ as a function of temperature and f_{O_2} . Am. Mineral., v. 52, #7-8, pp. 1139-1152.
- SPOONER, E. T. C., 1974. Sub-sea floor metamorphism, heat and mass transfer; an additional comment. Contrib. Mineral. Petrol., v. 45, pp. 169-173.
- SPOONER, E. T. C., BECKINSALE, R. D., FYFE, W. D., SMEWING, J. D., 1974. O^{18} enriched ophiolitic metabasic rocks from Eligrina (Italy), Prindos (Greece) and Troodos (Cyprus). Contrib. Mineral. Petrol., v. 47, pp. 41-62.
- SPOONER, E. T. C. and FYFE, W. D., 1973. Sub-sea floor metamorphism, heat and mass transfer. Contrib. Mineral. Petrol., v. 42, #4, pp. 287-304.

- STEINMIAN, G., 1905. Geologische Beobachtungen in des Alpen. II. Die Schardtsche Überfaltungstheorie und die geologische Bedeutung des Tiefseeabsatzes und der ophiolithischen Massengesteine. Ber. Nat. Ges. Freiburg I Bd. 16, pp. 44-65.
- STEINMIAN, G., 1927. Die ophiolithischen Zonen in dem mediterranen Kettengebirgen. 14th Intern. Geol. Cong. Madrid, C.R. 2, pp. 638-667.
- STEVENS, R. E., 1944. Composition of some chromites of the Western Hemisphere. Am. Mineral., v. 29, pp. 1-34.
- STEVENS, R. K., 1965. Geology of the Humber Arm Area, W. Newfoundland. Unpub. M.Sc. dissertation, Memorial University of Newfoundland, St. John's.
- STEVENS, R. K., 1970. Cambro-Ordovician flysch sedimentation and tectonics in west Newfoundland and their possible bearing on a proto-Atlantic Ocean. Geol. Assoc. Canada Spec. Paper #7, pp. 165-177.
- STEVENS, R. K., STRONG, D. F. and KEAN, B. F., 1974. Do some eastern Appalachian ultramafic rocks represent mantle diapirs produced above a subduction zone? Geology, v. 2, #4, pp. 175-178.
- STRONG, D. F., 1972. Sheeted diabases of Central Newfoundland: new evidence for Ordovician sea-floor spreading. Nature, v. 235, pp. 102-104.
- STRONG, D. F., 1972. The petrology of the lavas of Grande Comore. J. Petrol., v. 13, #2, pp. 181-217.
- STRONG, D. F., 1973. Lushs Bight and Roberts Arm Groups of Central Newfoundland: possible juxtaposed oceanic and island-arc volcanic suites. Geol. Soc. America Bull., v. 84, #12, pp. 3917-3928.
- STRONG, D. F., 1974. An off-axis volcanic suite associated with the Bay of Islands ophiolites, Newfoundland. Earth & Planet. Sci. Lett., v. 21, pp. 301-309.

- STRONG, D. F., 1975. Plateau lavas and diabase dikes of N.W. Newfoundland. *Geol. Mag.* III, v. 6, pp. 501-514.
- STRONG, D. F., DICKSON, W. L., O'DRISCOLL, C. F., and KEAN, B. F., 1974. Geochemistry of E. Newfoundland granitoid rocks. *Prov. Nfld. & Lab. Dept. Mines and Energy, Min. Dev. Div. Rep. 74-3*, 140p.
- STRONG, D. F., DICKSON, W. L., O'DRISCOLL, C. F., KEAN, B. F. and STEVENS, R. K., 1974. Geochemical evidence for an east-dipping subduction zone in Newfoundland. *Nature*, v. 248; #5443, pp. 37-39.
- STRONG, D. F. and KEAN, B. F., 1972. New fossil localities in the Lush's Bight terrain of central Newfoundland. *Can. J. Earth Sci.*, v. 9, #11, pp. 1572-1576.
- STRONG, D. F. and MALPAS, J., 1975. The sheeted dike layer of the Bett's Cove ophiolite complex does not represent spreading: Further discussion. *Can. J. Earth Sci.*, v. 12, #5, pp. 894-896.
- STRONG, D. F. and PAYNE, J. G., 1973. Early Palaeozoic volcanism and metamorphism of the Moreton's Harbour - Twillingate area, Newfoundland. *Can. J. Earth Sci.*, v. 10, #9, pp. 1363-1379.
- STRONG, D. F., STEVENS, R. K., MALPAS, J., and BADHAM, J. P. N., 1975. A new tale for the Lizard. *Proc. Usher Soc.*, in press.
- STRONG, D. F. and WILLIAMS, H., 1971. Early Palaeozoic flood basalts of N. W. Newfoundland: their petrology and tectonic significance. *Geol. Assoc. Canada Spec. Paper 25*, pp. 43-54.
- STUKAS, V., 1973. $^{40}\text{Ar}/^{39}\text{Ar}$ dating of the Long Range dikes, Newfoundland. Unpub. M.Sc. dissertation, Dalhousie University, Halifax.
- SWETT, K. and SMIT, D. E., 1972. Palaeogeography and depositional environments of the Cambro-Ordovician shallow-marine facies of the N. Atlantic. *Geol. Soc. America Bull.*, v. 83, pp. 3223-3248.

- SWINDEN, H. S. and STRONG, D. F., (in press). A comparison of plate tectonic models of metallogenesis in the Appalachians, the N.A. Cordillera and eastern Australian Palaeozoic. in Metallogeny and Plate Tectonics, Geol. Assoc. Canada Spec. Paper #14.
- TAYLOR, S. R., 1965. The application of trace element data to problems in petrology. *Phys. Chem. Earth*, v. 6, pp. 133-213.
- THAYER, T. P., 1963. Flow-layering in Alpine-type peridotite-gabbro complexes. *Miner. Soc. Amer. Spec. Pap. #1*, pp. 55-61.
- THAYER, T. P., 1967. Chemical and structural relations of ultramafic and feldspathic rocks in alpine intrusive complexes. in Ultramafic and related rocks; ed. P. J. Wyllie, John Wiley, New York, pp. 222-239.
- THAYER, T. P., 1969. Peridotite-gabbro complexes as keys to petrology of mid-oceanic ridges. *Geol. Soc. America Bull.*, v. 80, #8, pp. 1515-1522.
- THAYER, T. P., 1972. Gabbro and epidiorite versus granulite and amphibolite: a problem of the ophiolite assemblage. *Caribb. Geol. Conf. Trans.*, #6, pp. 315-320.
- THAYER, T. P., HIMMELBERG, G. R., 1968. Rock succession in the alpine-type mafic complex at Canyon Mountain, Oregon. in Intn. Geol. Cong. 23rd, Prague 1968, Proc. Sec. 1 (Upper mantle - Geol. Proc.), Prague, Academia, pp. 175-186.
- THOMPSON, G., SHIDO, F. and MIYASHIRO, A., 1972. Trace element distribution in fractionated oceanic basalts. *Chem. Geol.*, v. 9, #2, pp. 89-97.
- THOMPSON, R. N., 1974. Some high-pressure pyroxenes. *Min. Mag.*, v. 39, #307, pp. 768-787.
- TILLEY, C. E., YODER, H. S., and SCHAIRER, J. F., 1963. Melting relations of basalts. *Carn. Inst. Washington Yearbook* 62, pp. 77-84.
- TILLEY, C. E., YODER, H. S., and SCHAIRER, J. F., 1964. New relations on melting of basalts. *Carn. Inst. Washington Yearbook* 63, pp. 92-97.

- TILLEY, C. E., YODER, H. S., and SCHAIRER, J. F., 1965. Melting relations of volcanic tholeiite and alkali rock series. *Carn. Inst. Washington Yearbook* 64, pp. 69-82.
- TILLEY, C. E., YODER, H. S., and SCHAIRER, J. F., 1967. Melting relations of volcanic rock series. *Carn. Inst. Washington Yearbook* 65, pp. 260-269.
- TOBISCH, O. T., 1968. Gneissic amphibolite at Las Palmas, Puerto Rico, and its significance in the early history of the Greater Antilles island arc. *Geol. Soc. America Bull.*, v. 79, pp. 557-574.
- TROELSEN, J., 1947. Stratigraphy and structure of the Bonne Bay - Trout River area. Unpub. Ph.D. dissertation, Yale University.
- TRÖGER, E., 1959. Die Granatgnippe: Beziehungen zwischen Mineralchemismus und Gesteinsart. *Neues Jahrb. Mineral. Abh.* 93, pp. 1-44.
- TUKE, M. F., 1968. Autochthonous and allochthonous rocks in the Pistolet Bay area in northernmost Newfoundland. *Can. J. Earth Sci.*, v. 5, #3, pt. 1, pp. 501-522.
- TURNER, F. J., 1968. *Metamorphic petrology: mineralogical and field aspects.* McGraw-Hill Book Co., New York, 403p.
- TWENHOFEL, W. H. and McCLINLOCK, P., 1940. Surface of Newfoundland. *Geol. Soc. America Bull.*, v. 51, #11, pp. 1665-1727.
- UPADHYAY, H. D., 1973. The Betts Cove ophiolite and related rocks of the Snook's Arm Group, Newfoundland. Unpub. Ph.D. dissertation, Memorial University of Newfoundland, St. John's.
- UPADHYAY, H. D., DEWEY, J. F., and NEALE, E. R. W., 1971. The Bett's Cove ophiolite complex, Newfoundland; Appalachian oceanic crust and mantle. *Geol. Assoc. Canada Proc.*, v. 24, #1, pp. 27-34.
- UPADHYAY, H. D. and STRONG, D. F., 1973. Geological setting of the Bett's Cove copper deposits, Newfoundland. An example of ophiolite sulphide mineralisation. *Econ. Geol.*, v. 68, #2, pp. 161-167.

- VAN ANDEL, Tj. H., and BOWIN, C. O., 1968. M.A.R. between 22^o and 23^o north latitude and the tectonics of mid-ocean rises. *J. Geophys. Res.*, v. 73, pp. 1279-1298.
- VINE, F. J. and MOORES, E. M., 1972. A model for the gross structure, petrology and magnetic properties of oceanic crust: in *Studies in Earth and Space Sciences*. Geol. Soc. America Mem. #132, pp. 195-205.
- WADSWORTH, W. J., 1961. The ultrabasic rocks of south west Rhum. *Phil. Trans. Roy. Soc. London, Ser. B*, 244, pp. 21-64.
- WADSWORTH, W. J., 1973. Magmatic sediments. *Min. Sci. and Engin.*, v. 5, #1, pp. 25-35.
- WAGER, L. R., 1963. The mechanism of adcumulus growth in the layered series of the Skaergaard intrusion. *Mineral. Soc. America, Spec. Paper 1*, pp. 1-9.
- WAGER, L. R., BROWN, G. M. and WADSWORTH, W. J., 1960. Types of igneous cumulates. *J. Petrol.*, v. 1, pp. 73-85.
- WAGER, L. R. and BROWN, G. M., 1968. Layered igneous rocks. Oliver and Boyd, 588p.
- WAGER, L. R. and DEER, W. A., 1939. Geological investigations in East Greenland, Pt. III - The petrology of the Skaergaard intrusion, Kangerdlugssuaq, E. Greenland. *Medd. om Grønland*, 105, #4, pp. 1-352.
- WEAVER, D. F., 1967. A geological interpretation of the Bouguer anomaly field of Newfoundland. *Can. Dominion Observatory*, v. 35, #5, pp. 233-251.
- WILLIAMS, H., 1964. The Appalachians in N. E. Newfoundland - a two-sided symmetrical system. *Am. J. Sci.*, v. 262, pp. 1137-1158.
- WILLIAMS, H., 1969. Pre-Carboniferous development of Newfoundland Appalachians. in *North Atlantic: geology and continental drift*. Am. Assoc. Petrol. Geol. Mem. #12, pp. 32-58.

- WILLIAMS, H., 1971. Mafic-ultramafic complexes in western Newfoundland Appalachians and the evidence for their transportation. A review and interim report. Geol. Assoc. Canada Proc., v. 24, pp. 9-25.
- WILLIAMS, H., 1973. Bay of Islands map-area, Newfoundland. Geol. Surv. Canada Paper 72-34.
- WILLIAMS, H., KENNEDY, M. J. and NEALE, E. R. W., 1970. The Hermitage flexure, the Cabot Fault, and the disappearance of the Newfoundland central mobile belt. Geol. Soc. America Bull., v. 81, #5, pp. 1563-1567.
- WILLIAMS, H., KENNEDY, M. J. and NEALE, E. R. W., 1972. The Appalachian structural province. in Variations in Tectonic Style in Canada (ed. R. A. Price and R. J. W. Douglas). Geol. Assoc. Canada Spec. Paper 11, pp. 181-262.
- WILLIAMS, H., and MALPAS, J., 1972. Sheeted dikes and brecciated dike rocks within transported igneous complexes, Bay of Islands, W. Newfoundland. Can. J. Earth Sci., v. 9, #9, pp. 1216-1229.
- WILLIAMS, H., MALPAS, J. and COMEAU, R., 1972. Bay of Islands map-area, Newfoundland. Rep. of Activities, April-October, 1971. Geol. Surv. Canada Paper 72-1, pt. A, pp. 14-17.
- WILLIAMS, H., and PAYNE, J. G., 1975. The Twillingate Granite and nearby volcanic groups: an island arc complex in N. E. Newfoundland. Can. J. Earth Sci., v. 12, #6, pp. 982-995.
- WILLIAMS, H., and SMYTH, W. R., 1973. Metamorphic aureoles beneath ophiolite suites and Alpine peridotites: tectonic implications with west Newfoundland examples. Am. J. Sci., v. 273, pp. 594-621.
- WILLIAMS, H., SMYTH, W. R. and STEVENS, R. K., 1973. Hare Bay allochthon, Northern Newfoundland. Geol. Surv. Canada Paper 73-1, pt. A, pp. 8-14.
- WILLIAMS, H. and STEVENS, R. K., 1969. Geology of Belle Isle: northern extremity of the deformed Appalachian miogeosynclinal belt. Can. J. Earth Sci., v. 6, #5, pp. 1145-1157.

WILLIAMSON, D. H., 1954. The asbestos bearing rocks of Lewis Brook, W. Newfoundland. Geol. Surv. Newfoundland. Unpub. Rep., 49p.

WILSHIRE, H. G. and JACKSON, E. D., 1975. Problems in determining mantle geotherms from pyroxene compositions of ultramafic rocks. J. Geol., v. 83, pp. 313-329.

WILSON, J. T., 1966. Did the Atlantic close then re-open? Nature, v. 211, #5050, pp. 676-681.

WILSON, N. W., 1958. Kimberlite intrusions. Min. Mag., v. 98, #2, pp. 92-93.

WILSON, R. A. M., 1959. The geology of the Xeros - Troodos area. Geol. Surv. Cyprus Mem. #1, 175p.

WISEMAN, J. D. H., 1966. St. Paul's Rocks and the problem of the upper mantle. Royal Astron. Soc. Geophys. Jour., v. 11, pp. 519-525.

WOOD, B. J., 1974. The solubility of alumina in orthopyroxene coexisting with garnet. Contrib. Mineral. Petrol., v. 46, pp. 1-15.

WOOD, B. J. and BANNO, S., 1973. Garnet-orthopyroxene and orthopyroxene-clinopyroxene relationships in simple and complex systems. Contrib. Mineral. Petrol., v. 42, pp. 109-124.

WYLLIE, P. J., 1970. Ultramafic rocks and the upper mantle. Mineral. Soc. America Spec. Paper, v. 3, pp. 3-32.

25 YODER, H. S. and CHINNER, G. A., 1960. Gross - pyrope - H₂O system at 10,000 b. and Alm. - pyrope - H₂O system at 10,000 b. Carn. Inst. Washington Yearbook 1959-1960, pp. 78-84.

YODER, H. S. and SAHAMA, T. G., 1957. Olivine x-ray determinative curve. Am. Mineral., v. 42, #7-8, pp. 475-491.

YODER, H. S. and TILLEY, C. E., 1962. Origin of basaltic magmas: an experimental study of natural and synthetic rock systems. J. Petrol., v. 3, pp. 342-532.

ADDENDUM

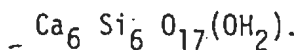
- GREEN, D. H. and RINGWOOD, A. E., 1967. The genesis of basaltic magmas. Contrib. Mineral. & Petrol., v. 15, pp. 103-190.
- HARRIS, P. G., REAY, A, and WHITE, I. G., 1967. Chemical composition of the Upper Mantle. J. Geophys. Res., v. 72, pp. 6359-6369.
- MASON, B., 1966. Composition of the Earth. Nature 211, pp. 616-618.
- NICHOLLS, G. D., 1967. Geochemical studies in the ocean as evidence for the composition of the mantle in "Mantles of the Earth and Terrestrial Planets", ed. S. K. Runcorn, Wiley, N.Y.
- RINGWOOD, A. E., 1966. The chemical composition and origin of the earth. in "Advances in Earth Sciences", ed. P. M. Hurley. M. I. T. Press, Cambridge, Mass.
- WHITE, I. G., 1967. Ultrabasic rocks and the composition of the Upper Mantle. Earth Planet. Sci. Lett., v. 3, pp. 11-18.

APPENDICES

APPENDIX I

X-Ray Methods

(a) Identification of xonotlite (Calcium Silicate Hydrate,



A white to pink, fibrous to massive mineral associated with hydrothermal alteration and rodingitisation of basal aureole rocks on North Arm Mountain and similar alteration of shales and siltstones at the basal fault contact in Winterhouse Brook, has been identified as xonotlite by X-Ray diffraction techniques.

The mineral, crushed to -325 mesh, was mounted as a dry powder pressed in an aluminium and glass holder and scanned in a Philips X-Ray diffractometer. Identification of the major peaks for xonotlite (A.S.T.M. 10-488) are as below:

The following parameters applied to this determination:

Sample: Xonotlite/Hydrogrossular

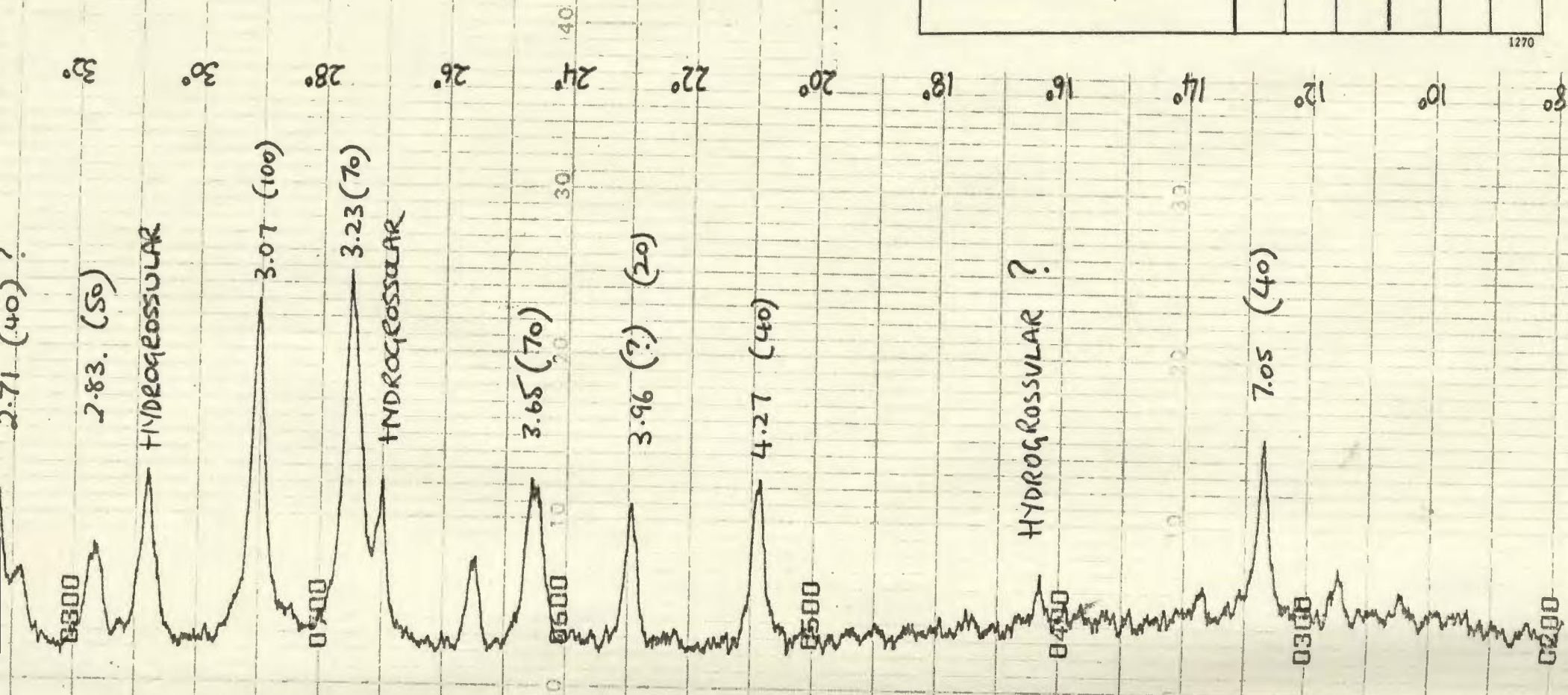
Excitation kv. 40 mA 20

Time constant: 4 sec.

Rate: 1×10^3

Chart speed: $1^\circ 20/\text{min}$.

Cu K_α radiation, Ni filter.



XONOTLITE
 $Ca_6Si_6O_{17}(OH)_2$

HYDROGROSSULAR
 $3CaO \cdot Al_2O_3 \cdot 6H_2O$

3-0568 MAJOR CORRECTION

2017 d 3-0568	3.09	1.96	2.83	7.0	$Ca_6Si_6O_{17}(OH)_2$					
3-0568	100	64	48	20	CALCIUM META SILICATE HYDRATE			XONOTLITE		
Rad. MoK α	A 0.709		Filter ZnO ₂		d Å	I/I ₁	hkl	d Å	I/I ₁	hkl
Dia. 16 INCHES	Cut off		Coll.		7.0	20	001	1.64	3	
I/I ₁ CALIBRATED STRIPS			d corr. abs.? No		4.28	28	211	1.60	3	
Ref. H ₂ (1) (2) (8)					3.64	40	020,410	1.58	2	
					3.25	32	202,021	1.52	16	
					3.09	100	302	1.43	10	
Sys. MONOCLINIC	S.G. C _{2h} - P2/A				2.83	48	321	1.39	8	
a ₀ 16.5 b ₀ 7.33 c ₀ 7.04	A 2.255 C 0.960				2.72	40	420+			
α β 90° γ	Z 2 D _x 2.79				2.52	40	022,412			
Ref. NAMEDOV AND BELOV, CHEM. ABSTR. 50	P. 16574				2.35	11	003			
ϵ d 1.579-1.583 n ₀ β 1.583	1.590-1.593		Sign +		2.27	10	203,701			
2V SMALL D 2.70 mp	Color COLORLESS TO PINK				2.04	40	INDEXED BY JVS			
Ref. WINGHELL ₂					1.96	64				
SAMPLE FROM BOILER SCALE					1.84	32				
CELL DIMENSIONS OBTAINED ON NATURAL MATERIAL					1.76	10				
FROM S. OSSETTIA, USSR.					1.72	28				

(b) Determination of Fo content of olivines by X-ray determinative curve of Yoder and Sahara (1957).

The position of the d_{130} peak for olivine was measured on peridotite samples crushed to -325 mesh using a pure silica internal standard. The quantity of olivine in the peridotites allowed whole rock crushes to be used rather than olivine separates, in order to obtain high intensity reflections.

The sample was ground in an agate mortar under acetone and about 10 mg of the powder was mixed with 1.5 mg of pure silica powder on a glass slide. Two drops of weak laquer in acetone solution were added and the powder stirred into a thin film on the slide.

Six oscillations were carried out for each specimen at $1/2^\circ$ /minute scan speed. The positions of the olivine (130) and silica (111) peaks were then measured on a backlighted vernier. The olivine reflection was corrected by the silica reflection and absolute values obtained. The average d_{130} reflection from the six oscillations was then used to determine the Fo content of the olivine in the following equation:

$$Fo \text{ (mol\%)} = 4,233.91 - 1,494.59 d_{130}$$

Results are presented in Table Aii).

TABLE Aii)

X-RAY DETERMINATION OF Fo CONTENT OF OLIVINES

Specimen #	Rock Type	Fo Content
186	Harzburgite	94.5
187	"	93.1
189	"	92.85
191	"	Not measurable
193	"	93.01
194	Dunite	85.53
195	"	86.87
196	"	86.12

APPENDIX II

Calculation of temperature changes due to frictional heating during obduction

- i. For calculation of temperature changes at a surface during frictional heating on that surface:

$$T_{o,t} = \frac{2 F_o}{K} \left(\frac{kt}{K} \right)^{\frac{1}{2}} \quad [\text{Carslaw and Jaeger, 1959}]$$

where $T_{o,t}$ = temperature change at surface during time t

F_o = rate of heat production

K = conductivity

k = diffusivity = $\frac{K}{\rho C_p}$

t = time during which heating takes place

ρ = density of heated medium

C_p = specific heat of heated medium

and assuming that during constant motion the rate of heat production is constant:

$$F_o = \frac{1}{2} u \tau$$

where u = rate of obduction in cm/year

τ = shear stress of heated medium.

In this equation the following constants are known assuming the aureole protoliths to be basic tuffs free of water: (this places severe upper limits on possible temperature increases):

$$K = 6 \times 10^{-3} \text{ cal s cm}^{-1} \text{ s}^{-1} \text{ } ^\circ\text{C}^{-1}$$

$$\rho = 2.8 \text{ gm/cc}$$

$$C_p = 0.21 \text{ cgs}$$

$$\gamma = 2.64 \times 10^8 \text{ dynes/cm}^2$$

using these constants and variable T, t and u, the following table can be constructed relating temperature increase to obduction rate and time.

TABLE AIII)

Time (tmy) required to produce temperature rise T at given obduction rate u

u(cm/yr)	1	2	5	8	10
T °C					
900	5550.0	1388.8	222.2	86.8	55.5
800	4389.1	1097.3	175.6	68.6	43.9
700	3360.4	840.1	134.4	52.5	33.6
600	2468.9	617.2	98.8	38.6	24.7
500	1714.5	428.6	68.6	26.8	17.1
400	1097.3	274.3	43.9	17.1	10.9
300	617.2	154.3	24.6	9.6	6.2
200	274.3	68.6	10.9	4.3	2.7
100	68.5	17.1	2.7	1.1	0.7

If an upper limit of obduction time (t) of approximately 15 my is taken, temperature increases on the thrust plane of up to 400°C can be attained according to the spreading rate. Spreading rates of the order of 5-8 cm/year may produce temperature increases of 200-300°C.

ii. A second approach may be taken to estimate rates of obduction.

An assumption that all the heat necessary for metamorphism is produced by frictional heating and heat content of the overriding slice is made. Then, from equations developed by Jaeger (1959), the initial contact temperature as a result of hot overriding slice is given by

$$T_0 = \sigma T_1 (1 + \sigma)$$

where T_0 = initial contact temperature

T_1 = temperature of overriding slice

$$\sigma = \frac{K_1 k_0 \frac{1}{Z}}{K_0 k_1 \frac{1}{Z}} \quad \text{and} \quad \begin{array}{l} K_1 = \text{conductivity of hot slice} \\ K_0 = \text{" of country rock} \\ k_1 = \text{diffusivity of hot slice} \\ k_0 = \text{" of country rock} \end{array}$$

For the lithologies involved in this study $\sigma = 1.10$

and $T_1 = 1200^\circ\text{C max}$

∴ contact temperature = 625°C.

This represents the temperature component produced by the heat content of the overriding slice.

It is known that temperatures of metamorphism were $\sim 850^{\circ}\text{C}$.

\therefore approximately 275°C must be supplied by frictional heating.

Such a temperature increase may be produced in 15 my at obduction rates of approximately 5 cm/year.

N.B. These calculations provide upper limits on temperatures produced by frictional heating. Movement of volatiles (esp. water) may severely change these estimates. However, the presence of granulite facies metamorphic rocks at the contact suggests that the system at this point was effectively dry.

APPENDIX III

(a) Major Element Analysis

Samples for major element analysis were prepared according to the method of Langmyr and Paus (1968). The major elements were determined on a Perkin Elmer model 303 atomic absorption spectrophotometer with chart recorder read-out.

After drying overnight at 100°C and homogenisation, exactly 0.2000 grammes were weighed in a plastic cap and placed in a polycarbonate digestion bottle with 5 cc. hydrofluoric acid. The bottles were then heated on a water bath for 30 minutes to one hour. After cooling, 50 cc. of saturated boric acid was added in order to complex undissolved fluorides. The samples were then heated again to ensure complete dissolution, cooled and diluted with 145 cc. of distilled/deionised water to yield 200 cc. of 1000 ppm solution.

For samples containing sulphides or chromite, it was necessary to add 5 cc. aqua regia, heat for 20 minutes and then follow the above procedure, diluting with 5 cc. less water.

Standards were prepared in a manner similar to that described by Abbey (1968).

Phosphorus was determined on a Bausch and Lomb Spectronic 20 colourimeter according to a modified method after Shapiro and Brannock (1962).

Loss on ignition (H_2O , CO_2 , SO_2) was determined by weighing an amount of sample in a porcelain crucible, heating to 1050°C for two hours, cooling in a dessicator, and weighing to determine the percent loss of volatiles.

Analytical precision was determined by choosing a sample of intermediate composition in the range expected and running this precision sample in each analytical batch. Results are given in Table AIIII.

TABLE AIIII)
Precision of Major Element Analyses

Element	No. of Determinations	Mean (wt %)	σ	Ci (Coeff. of vn.)
SiO ₂	10	45.97	0.73	1.59
TiO ₂	10	0.48	0.01	2.08
Al ₂ O ₃	10	22.01	0.18	0.82
Fe ₂ O ₃	10	4.12	0.10	2.43
MnO	10	0.07	0.01	14.29
MgO	10	9.70	0.01	0.10
CaO	10	13.21	0.05	0.38
Na ₂ O	10	1.55	0.02	1.29
K ₂ O	10	0.11	0.04	36.36
P ₂ O ₅	10	0.02	0.01	50.00
L.I. J	10	3.48	0.15	4.31

Accuracy of major element analyses was determined by comparison with U.S.G.S. standard B.C.R.1. The results are given in Table AIIIii.

TABLE AIIIii)

Accuracy of Major Element Analyses

Wt %	Proposed Value (Abbey, 1968)	Mean Wt %	σ	No. of Determinations
SiO ₂	54.36	55.38	0.26	6
TiO ₂	2.24	2.31	0.19	6
Al ₂ O ₃	13.56	13.52	0.25	6
Fe ₂ O ₃	13.40	13.01	0.27	6
CaO	6.94	6.82	0.06	6
MgO	3.46	3.52	0.06	6
Na ₂ O	3.26	3.26	0.04	6
K ₂ O	1.67	1.70	0.04	6
MnO	0.19	0.17	0.01	6

(b) Trace Element Analysis

Trace elements were determined by X-ray fluorescence (except for R.E.E.) on pressed powder discs using a Philips 1220-C Automatic x-ray fluorescence spectrometer. Typical precision and accuracy data for these determinations are given below in Table AIIIiii.

Rare Earth Elements were determined on an Associated Electrical Industries Ltd. (A.E.I.) M.S.7 mass spectrograph. General descriptions of this instrument are given by S. R. Taylor (1965). Electrodes were prepared by compressing mixtures of the sample under analysis and Ringsdorffwerke R.W.A. grade graphite in an electrode-forming die under a pressure of 7500 psi. Operating pressures in the analyzer region of the instrument were in the range 10^{-8} to 10^{-7} torr and in the source region 1×10^{-6} to 5×10^{-6} torr. Fifteen graded exposures of the spectrum from a sample were recorded polarographically on Ilford Q2 plates, which were subsequently processed according to the manufacturer's instructions.

In the approach adopted here to this method of analyses, a basic equation can be written, viz.

$$C_E = C_S \times \text{Exp}_S / \text{Exp}_E \times I_S / I_E \times 1/R$$

where

C_E = content of element E in electrode analysed (at parts per million)

C_S = content of a second element S (internal standard Rhenium used).

TABLE AIIIIii)

Precision and Accuracy of Trace Element Analyses

PRECISION

Element	Mean ppm.	σ	Ci (Coeff. of vn.)
Zr	201	8	4.0
Sr	193	5	2.6
Rb	8	2	2.5
Zn	90	8	8.9
Cu	110	7	6.4
Ni	38	7	18.4
Co	27	7	25.9
Cr	109	9	8.26
V	69	3	4.3
Ba	73	8	11.0

ACCURACY

Element	Proposed Value Flanagan (1969)	Mean ppm	σ	No. of Determinations
Zr	190	193	9	10
Sr	330	345	12	10
Rb	46.6	49	4	10
Zn	120	110	10	10
Cu	18.4	20	4	10
Ni	15.8	17	4	10
Co	38.	36	4	10
Cr	17.6	22	7	10
V	399	379	23	10
Ba	675	682	12	10

Exp_E = Exposure (in millimicrocoulombs) required to give a line of chosen density for a chosen isotope of E on photographic plate.

Exp_S = Exposure (same units) required to give the same chosen density for a chosen isotope of element S on the same plate.

These exposures measured by microdensitometer:

I_S = isotopic abundance of chosen isotope of S.

I_E = isotopic abundance of chosen isotope of E.

and R = a factor (relative sensitivity factor) introduced as a measure of sensitivity of total recording procedure to line of element E used to compare with sensitivity to line of element S used, arbitrarily assigned a value of unity.

Precision and accuracy of the analytical method are described by Nicholls et al. (1967).

(c) Mineral Analyses

Mineral analyses were carried out on a Cambridge Microscan 500 electronmicroprobe analyser with two spectrometers. Data output on punched cards was provided. Metal, mineral and synthetic glass standards were used. Fluorescence and absorption corrections were completed with a Rucklidge reduction programme (University of Toronto).

Supplementary olivine analyses by X.R. Diffraction are described in Appendix I.

APPENDIX IV

Petrochemical Subtraction Programme

This calculation was developed by R. G. Cawthorn at Memorial University Geology Department in 1975. To make estimates of residual liquid compositions various proportions of known phases may be added or subtracted from the known parent rock composition. The resultant calculated composition is determined and printed out.

DATA INPUT:

The following data must be supplied: the composition of the starting material and all the phases involved; the number of phases and the proportions of the individual phases to be added or subtracted.

Several sets of proportions may be listed consecutively.

PRINT OUT:

Before the calculation is performed all analyses are normalised to 100%. These normalised values are printed out, together with the proportion of each phase which is to be added or subtracted. The residual composition is also normalised to 100% and printed out. Only major elements are added together and normalised to 100%. However, concentrations of minor elements are multiplied by the same normalisation factor as the major elements and thus remain in the same proportion to the major elements in the print out.

The results of the calculations used in this work are presented below:

```

C PETROCHEMICAL SUBTRACTION PROGRAM
C   N IS NUMBER OF PHASES TO BE ADDED OR SUBTRACTED
      INTEGER TITLE(10,50)
      DIMENSION ANAL(10,20),RES(20),PROP(10)
0001      29 READ 9,K
0002      9 FORMAT (I1)
0003      IF(K.EQ.0.) GO TO 30
0004      READ 10,(TITLE(I,J),J=1,50)
0005      10 FORMAT (50A1)
0006      READ 11,(ANAL(I,N),N=1,13)
0007      11 FORMAT (13F6,2)
0008      READ 17,(ANAL(I,N),N=14,20)
0009      17 FORMAT (7F6,2)
0010      KK=K+1
0011      DO 12 L=2,KK
0012      READ 10,(TITLE(L,J),J=1,50)
0013      READ 11,(ANAL(L,N),N=1,13)
0014      12 READ 17,(ANAL(L,N),N=14,20)
0015      27 READ 13,(PROP(N),N=2,10)
0016      13 FORMAT (9F6,4)
0017      FRACT=0.
0018      DO 28 L=2,KK
0019      FRACT=FRACT+ABS(PROP(L))
0020      IF(FRACT.EQ.0.) GO TO 29
0021      DO 18 L=1,KK
0022      SUM=0.
0023      DO 19 N=1,13
0024      SUM=SUM+ANAL(L,N)
0025      SUM=SUM/100.
0026      DO 18 N=1,20
0027      ANAL(L,N)=ANAL(L,N)/SUM
0028      DO 14 N=1,20
0029      RES(N)=ANAL(1,N)
0030      DO 14 L=2,KK
0031      RES(N)=RES(N)+ANAL(L,N)*PROP(L)
0032      SUM=0.
0033      DO 15 N=1,20
0034      SUM=SUM+RES(N)
0035      SUM=SUM/100.
0036      DO 16 N=1,20
0037      RES(N)=RES(N)/SUM
0038      PRINT 20,(TITLE(I,J),J=1,50)
0039      20 FORMAT ('0', ' ALL ANALYSES ARE NORMALISED TO 100% BEFORE THE C
0040      CALCULATION IS PERFORMED',/, ' NOW I 13',115,50A1)
0041      DO 21 L=2,KK
0042      PRINT 22,L,(TITLE(L,J),J=1,50),PROP(L)
0043      22 FORMAT ('0', ' ROW',I2, ' IS',115,50A1, ' PROPORTION ADDED 13',F8,4)
0044      21 CONTINUE
0045

```

```
0046      PRINT 23
0047      23 FORMAT ('0', ' S102 T102 AL203 CR203 FE203 FEU HMO HGU CAU
1 NA2O X2O P2O5 LO2 ANY OTHER ELEMENTS YOU WISH TO ADD')
0048      DO 25 L=1, KX
0049      PRINT 24, (ANAL(L,N), N=1, 20)
0050      24 FORMAT (' ', 20F6, 2)
0051      25 CONTINUE
0052      NEG=0
0053      DO 31 N=1, 20
0054      31 IF(RES(N), LT, -0.05) NEG=NEG+1
0055      IF(NEG, GT, 0) PRINT 32, NEG
0056      32 FORMAT ('0', ' THIS CALCULATION GIVES A NEGATIVE SOLUTION FOR', I2, '
1 ELEMENTS')
0057      PRINT 26, (RES(N), N=1, 20)
0058      26 FORMAT ('0', ' COMPOSITION OF THE RESIDUAL MATERIAL IS', /, ' ', 20F6,
12)
0059      GO TO 27
0060      30 STOP
0061      END
```

ALL ANALYSES ARE NORMALISED TO 100% BEFORE THE CALCULATION IS PERFORMED
 ROW 1 IS STARTING COMPOSITION LHERZOLITES

ROW 2 IS HARZBURGITE

PROPORTION ADDED IS -0.9500

SI02	TIO2	AL2O3	CR2O3	FE2O3	FeO	MNO	MGO	CAO	NA2O	K2O	P2O5	CO2	ANY OTHER ELEMENTS YOU WISH TO ADD					
44.26	0.18	3.13	0.42	1.95	6.82	0.12	39.94	2.88	0.12	0.15	0.03	0.0	0.37	0.0	0.0	0.0	0.0	0.0
43.67	0.02	0.48	0.42	1.19	6.85	0.14	46.86	0.36	0.0	0.02	0.0	0.0	0.39	0.0	0.0	0.0	0.0	0.0

THIS CALCULATION GIVES A NEGATIVE SOLUTION FOR 2 ELEMENTS

COMPOSITION OF THE RESIDUAL MATERIAL IS

55.59	3.15	53.55	0.42	16.36	6.33	-0.23	9.62	50.86	2.48	2.87	0.68	0.0	-0.02	0.0	0.0	0.0	0.0	0.0
-------	------	-------	------	-------	------	-------	------	-------	------	------	------	-----	-------	-----	-----	-----	-----	-----

ALL ANALYSES ARE NORMALISED TO 100% BEFORE THE CALCULATION IS PERFORMED
 ROW 1 IS STARTING COMPOSITION LHERZOLITES

ROW 2 IS HARZBURGITE

PROPORTION ADDED IS -0.9000

ie 90% harzburgite composition removed from Uherzite = 10% partial melting.

SI02	TIO2	AL2O3	CR2O3	FE2O3	FeO	MNO	MGO	CAO	NA2O	K2O	P2O5	CO2	ANY OTHER ELEMENTS YOU WISH TO ADD					
44.26	0.18	3.13	0.42	1.95	6.82	0.12	39.94	2.88	0.12	0.15	0.03	0.0	0.37	0.0	0.0	0.0	0.0	0.0
43.67	0.02	0.48	0.42	1.19	6.85	0.14	46.86	0.36	0.0	0.02	0.0	0.0	0.39	0.0	0.0	0.0	0.0	0.0

THIS CALCULATION GIVES A NEGATIVE SOLUTION FOR 1 ELEMENTS

COMPOSITION OF THE RESIDUAL MATERIAL IS

49.53	1.58	26.96	0.42	8.76	6.57	-0.05	22.33	25.55	1.24	1.25	0.34	0.0	0.18	0.0	0.0	0.0	0.0	0.0
-------	------	-------	------	------	------	-------	-------	-------	------	------	------	-----	------	-----	-----	-----	-----	-----

ie melt composition

ALL ANALYSES ARE NORMALISED TO 100% BEFORE THE CALCULATION IS PERFORMED
 ROW 1 IS STARTING COMPOSITION LHERZOLITES

ROW 2 IS HARZBURGITE

PROPORTION ADDED IS -0.8500

SI02	TIO2	AL2O3	CR2O3	FE2O3	FeO	MNO	MGO	CAO	NA2O	K2O	P2O5	CO2	ANY OTHER ELEMENTS YOU WISH TO ADD					
44.26	0.18	3.13	0.42	1.95	6.82	0.12	39.94	2.88	0.12	0.15	0.03	0.0	0.37	0.0	0.0	0.0	0.0	0.0
43.67	0.02	0.48	0.42	1.19	6.85	0.14	46.86	0.36	0.0	0.02	0.0	0.0	0.39	0.0	0.0	0.0	0.0	0.0

COMPOSITION OF THE RESIDUAL MATERIAL IS

47.51	1.06	18.12	0.92	6.23	6.66	0.02	0.71	17.14	0.82	0.84	0.22	0.0	0.25	0.0	0.0	0.0	0.0	0.0
-------	------	-------	------	------	------	------	------	-------	------	------	------	-----	------	-----	-----	-----	-----	-----

ALL ANALYSES ARE NORMALISED TO 100% BEFORE THE CALCULATION IS PERFORMED
 ROW 1 IS STARTING COMPOSITION LHERZOLITES

ROW 2 IS HARZBURGITE

PROPORTION ADDED IS -0.8000

SI02	TIO2	AL2O3	CR2O3	FE2O3	FeO	MNO	MGO	CAO	NA2O	K2O	P2O5	CO2	ANY OTHER ELEMENTS YOU WISH TO ADD					
44.26	0.18	3.13	0.42	1.95	6.82	0.12	39.94	2.88	0.12	0.15	0.03	0.0	0.37	0.0	0.0	0.0	0.0	0.0
43.67	0.02	0.48	0.42	1.19	6.85	0.14	46.86	0.36	0.0	0.02	0.0	0.0	0.39	0.0	0.0	0.0	0.0	0.0

COMPOSITION OF THE RESIDUAL MATERIAL IS

46.51	0.80	13.70	0.42	4.97	6.70	0.05	12.21	12.94	0.62	0.63	0.17	0.0	0.29	0.0	0.0	0.0	0.0	0.0
-------	------	-------	------	------	------	------	-------	-------	------	------	------	-----	------	-----	-----	-----	-----	-----

ALL ANALYSES ARE NORMALISED TO 100% BEFORE THE CALCULATION IS PERFORMED
 ROW 1 IS STARTING COMPOSITION LHERZOLITES

ROW 2 IS HARZBURGITE

PROPORTION ADDED IS -0.7500

SI02	TIO2	AL2O3	CR2O3	FE2O3	FeO	MNO	MGO	CAO	NA2O	K2O	P2O5	CO2	ANY OTHER ELEMENTS YOU WISH TO ADD					
44.26	0.18	3.13	0.42	1.95	6.82	0.12	39.94	2.88	0.12	0.15	0.03	0.0	0.37	0.0	0.0	0.0	0.0	0.0

43.67 0.02 0.48 0.42 1.19 6.85 0.14 46.86 0.36 0.0 0.02 0.0 0.0 0.39 0.0 0.0 0.0 0.0 -0.0 0.0

COMPOSITION OF THE RESIDUAL MATERIAL IS

45.90 0.65 11.05 0.42 4.21 6.72 0.07 19.11 10.42 0.49 0.51 0.13 0.0 0.31 0.0 0.0 0.0 0.0 0.0 0.0

ALL ANALYSES ARE NORMALISED TO 100% BEFORE THE CALCULATION IS PERFORMED
 ROW 1 IS STARTING COMPOSITION LMERZOLITE

ROW 2 IS HARZBURGITE

PROPORTION ADDED IS -0.7000

SiO2	TiO2	AL2O3	CR2O3	FE2O3	FeO	MNO	MGO	CAO	NA2O	K2O	P2O5	CO2	ANY OTHER ELEMENTS YOU WISH TO ADD						
44.26	0.18	3.13	0.42	1.95	6.82	0.12	39.94	2.88	0.12	0.15	0.03	0.0	0.37	0.0	0.0	0.0	0.0	0.0	0.0
43.67	0.02	0.48	0.42	1.19	6.85	0.14	46.86	0.36	0.0	0.02	0.0	0.0	0.39	0.0	0.0	0.0	0.0	0.0	0.0

COMPOSITION OF THE RESIDUAL MATERIAL IS

45.50 0.54 9.29 0.42 3.70 6.74 0.08 23.71 8.74 0.41 0.43 0.11 0.0 0.32 0.0 0.0 0.0 0.0 0.0 0.0

C. Critical Zone and Dunites:

From Blow me down Mountain

271	Anorthosite gabbro.	01	5%	Cpx	10%	Plag	85%		
272	Dunite	01	90%	Cpx	7%	Spinel	3%		
274	"	01	85%	Opx	8%	Spinel	4%	Cpx	3%
275	"	01	90%	Cpx	3%	Spinel	7%		
276	"	01	92%	Cpx	2%	Spinel	6%		

From North Arm Mountain

194	Dunite	01	90%	Cpx	2%	Spinel	6%	Opx	2%
195	"	01	85%	Cpx	5%	Spinel	7%	Opx	3%
196	"	01	90%	Opx	2%	Spinel	8%		

From Table Mountain

E2	Dunite	01	80%	Cpx	15%	Spinel	5%		
E4	01. Gabbro	01	10%	Cpx	30%	Plag	55%	Spinel	5%
E5	01. Gabbro	01	15%	Cpx	35%	Plag	50%		
E8	01. Gabbro	01	10%	Cpx	35%	Plag	55%		
TMC1	Fd. Dunite	01	85%	Plag	10%	Spinel	5%	Minor cpx.	
TMC2	Fd. Dunite	01	80%	Plag	10%	Spinel	2%	Cpx	8%
TMC3	Fd. Dunite	01	85%	Plag	15%				
TMC4	Fd. Dunite	01	80%	Cpx	10%	Plag	10%		
TMC5	Fd. Dunite	01	85%	Cpx	2%	Plag	13%		
TMC6	01. Gabbro	01	22%	Cpx	30%	Plag	40%	Spinel	8%

D. Gabbros:

From North Arm Mountain

198	Gabbro
199	"
200	"
201	"
202	"
203	"
205	"
206A	"
206B	"
207	"

Average modal analysis:

Plagioclase 60%. Cpx 30%. Ol 3%.
 Oxides 2%. Amphibole 5%.
 Alteration of Cpx and Plag is variable.

Where there is significant departure from this average it is shown.

From Table Mountain

126	Gabbro
244	"
249	"
258	"

282	Gabbro	01	8%	Plag	60%	Cpx	30%	
284	"							
285	"							
289	"							
E6	"							
E7	"							
E9	"							
E12	"							
E16	"							
E17	"	01	10%	Plag	52%	Cpx	31%	Oxides 6%
			Amp. 1%					
E18	"							

From Blow me down Mountain.

301A Gabbro
 301C "
 312 "
 312A "

E. Diabases:

From Blow me down Mountain.

WF11071
 WF112B71
 WF12371
 WF123A71

From North Arm Mountain

Average modal analysis:

Plag 48%. Cpx 38%. Oxides 5%.

211
 217 Plag pheno.
 221
 224
 225 Plag pheno.
 294B
 294C
 294E Plag pheno.
 301B Plag pheno.

Plag pheno. 8%. Other 1%.

Cpx variably altered to actinolite/
chlorite.

F. Volcanics:

From Blow me down Mountain

A volc.
 B volc.
 C volc.

D volc.

E volc.

F volc.

G volc.

7c

671s. selvage

671c. core

8s selvage

8c core

Average modal analysis

Plag 43%. Cpx 36%. Chlorite 10% (inc.
Ol. pseud.). Oxides 3%. Carbonate 6%.
Sulphides 2%.

Alteration to chlorite and carbonate/sericite
is variable.



APPENDIX VI: Published papers which include results
pertinent to this thesis.

BIBLIOGRAPHY

- ABBEY, S., 1968. Analysis of rocks and minerals by atomic absorption spectroscopy. Pt. 2. Determination of Tot. Fe, Mg, Ca, Na and K. Geol. Surv. Canada Pap. 68-20, 21p.
- FLANAGAN, F. J., 1969. U. S. Geological Survey Standards II. First compilation of data for the new U.S.G.S. rocks. Geochim. Cosmochim. Acta, v. 33, pp. 81-120.
- LANGMYHR, F. J. and PAUS, P. E., 1968. The analysis of inorganic siliceous materials by atomic absorption spectrophotometry and the hydrofluoric acid decomposition technique. Pt. I. The analysis of silicate rocks. Anal. Chimica Acta, v. 43, pp. 397-408.
- NICHOLLS, G. D., GRAHAM, A. L., WILLIAMS, E. and WOOD, M., 1967. Precision and accuracy in trace element analysis of geological materials using solid source mass spectrography. Analytical Chemistry, v. 39, pp. 584-590.
- SHAPIRO, L. and BRANNOCK, W. W., 1962. Rapid analysis of silicate, carbonate and phosphate rocks. U. S. Geol. Survey Bull., 1144a.
- TAYLOR, S. R., 1965. Geochemical analysis by spark source mass spectrography. Geochim. Cosmochim. Acta, v. 29, pp. 1246-1261.





Folded pyroxenite veins in harzburgite, Table Mountain.



Bonne Bay looking east.

ENDPIECE

The field mapping carried out by the author has been published as Paper 72-34 (G.S.C., Williams, 1973) and a copy has been included to supplement Figure IIIb. Topography and structures are shown on this map.

FIG III b

BAY OF ISLANDS

GEOLOGY

1 : 125000

Humber Arm Sgrp

1 LC-MC Summerside Fmn

2 Irishtown Fmn

3 MC-LO Cooks Brook Fmn

4 LO Middle Arm Point Fmn

5 LO-MO Blow me down brook Fmn

6 undivided

7 Skinner Cove Fmn

8 Old man Cove Fmn

Little Port Complex

9 amphibolite

10 qtz diorite

diabase

12 volcanics

Bay of Islands Complex

13 amphibolite incls

14 aureole

15 Ultramafic rocks

16 Gabbros

Diabase dikes

volcanics

19 sediments

qtz diorites

Geologic boundary

Fault

21 Sample location

105

GREGORY ISLAND

North Head

Beverly Head

Lower Berth Cove

10

5

ST

Christy Cove



3 of 1

Lower Bear Cove

GREEN ISLAND

Upper Bear Cove

TWEED ISLAND

SHAG ROCKS

GUERNSEY ISLAND

BAY OF ISLANDS

MURRAY MTNS

LITTLE PORT

LARK HBR

VIRGIN MTN

GOVERNORS ISLAND

York Hbr

Bear Cove

BLOW ME DOWN MTN

201A C 16

32A 312

